AMERICAN RESEARCH PRESS

PIERRE A. MILLETTE

ELASTODYNAMICS OF THE SPACETIME CONTINUUM

SECOND EXPANDED EDITION

STCED

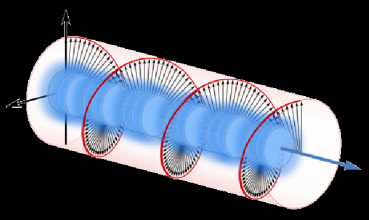

$$\rho c^2 = 4\kappa_0 \varepsilon$$

American Research Press

Pierre A. Millette

Elastodynamics of the Spacetime Continuum

SECOND EXPANDED EDITION

–STCED–

Rehoboth, New Mexico, USA
— 2019 —

Cover image: The illustration representing a spacetime continuum deformation has been prepared by the author, incorporating a helix wave from Wikimedia Commons, available at
Page URL: https://commons.wikimedia.org/wiki/File
File URL: https://upload.wikimedia.org/wikipedia/commons/d/de/
Circular.Polarization.Circularly.Polarized.Light
Attribution: By Dave3457 (Own work) [Public domain], via Wikimedia Commons.

This book was typeset using the LaTeX typesetting system.

ISBN 978-1-59973-987-8

American Research Press, Box 141, Rehoboth, NM 87322, USA
Standard Address Number: 297-5092
Printed in the United States of America

Table of Contents

Foreword

There is an old idea that the space-time background of the world can be represented as a continuous medium. Really, the modern mechanics of a continuum medium uses a similar mathematical basis as General Relativity, but applied to a three-dimensional physical medium in a flat three-dimensional space: see the famous four-volume *A Course in Continuum Mechanics* by L. I. Sedov*, or the less-comprehensive *Fluid Mechanics* by L. D. Landau & E. M. Lifshitz†. Why not use this approach in General Relativity? Namely, — if the space-time curvature is connected with such a continuous material object as the field of gravitation, why not consider the other geometric properties of the space-time background in analogy to the physical properties of a continuous medium? This approach could result in a complete geometric interpretation of classical mechanics as a result. This idea fired the minds of theoretical physicists commencing in probably that year when the General Theory of Relativity was introduced in 1915.

Many prominent theoretical physicists worked on this problem in the 1930s and 1940s. L. D. Landau and E. M. Lifshitz, A. L. Zelmanov, A. Lichnérowicz, L. I. Sedov and others were among them. For example, in 1944, Zelmanov considered the evolution of cosmological models in *Chronometric Invariants*‡, where he introduced the space viscosity, the volume deformation, and the three-dimensional curvature in analogy to the similar factors in the continuous media mechanics. However this movement had ended in the 1960s: no full representation of the space-time as a continuous medium was suggested. I asked Leonid I. Sedov, on occasion, why this occurred? He answered that there was an insurmountable obstacle along the way: many geometric properties of the space-time did not find respective analogies in the mechanics of a continuous medium; so only a very partial mathematical analogy between a continuous medium and the four-dimensional space-time exists.

In this view, this new research done by Pierre A. Millette opens very promising possibilities for further development of the General Theory of Relativity. His comprehensive study on this subject is presented here.

---

*Sedov L. I. A Course in Continuum Mechanics, Vols I–IV. Wolters-Noordhoff Publ., 1971.

†Landau L. D. & Lifshitz E. M. Fluid Mechanics. Pergamon Press, 1959.

‡Zelmanov A. L. Chronometric Invariants: On Deformations and the Curvature of Accompanying Space. American Research Press, 2006.

Because so many new developments are contained in his book, I would recommend to read it chapter-by-chapter from the very beginning.

The key idea realized by the author of this book, Pierre A. Millette, is that the space strains are somehow connected with the space-time curvature. He then has supported this idea by an elegant mathematical solution, based on a plain decomposition of any 2nd rank symmetric tensor into two parts, named the dilatation-distortion decomposition. So forth, applying the decomposition to the energy-momentum stress tensor and to the Ricci tensor, he has demonstrated how the volume dilatation results in the rest-mass energy density, while the volume deformation results in the space-time curvature and, thus, gravitation and the gravitational field energy. So forth, he actually resolved the old-time discussion that was so popular among the relativists commencing in the 1960s: whether gravitational waves are the waves of the space-time curvature or the waves of the volume deformation of space? Now, looking at Millette's results, we see that this question was an actual tautology, because the one results in the other, and vice versa.

The same decomposition is then applied to the symmetric term of the electromagnetic field tensor, thus resulting in the "strained" electromagnetic field theory, with many interesting sequences.

Among the other derived results, which are many in the book (all developed on the same basis of the aforementioned decomposition), I would emphasise the elastic volume force, the quantum mechanical volume force, the linear and rotational defects of the space-time, the space-time dislocations and disclinations, the wave function and the basics of quantum mechanics that takes the aforementioned decomposition and its sequences into account, the particle physics which, in the framework of the theory, associates known types of the elementary particles with respective defects of the space-time... All these and other problems are explained in the other chapters of the book.

As a result, I see that Pierre A. Millette has created an absolutely original extension of Einstein's version of the General Theory of Relativity. This extension, having the same Riemannian basis as the "classical" General Relativity, meanwhile provides the closest analogy between the space-time background and a continuous medium.

I therefore very much hope that the Spacetime Continuum Elastodynamics — the new extension of the "classical" General Theory of Relativity — will turn, again, the attention of scientists to the space-time analogy with a continuous medium. This new extension clearly shows that the General Theory of Relativity in its "classical form" introduced already by Einstein is not something fossilized but still is a

wide field for further development and extensions even without the use of extra-dimensions or modifications of the Riemannian mathematical basis.

Puschino, November 16, 2016

Dmitri Rabounski

Editor-in-Chief
Progress in Physics

Preface

This book is about spacetime physics, in particular as it concerns gravitation, electromagnetism and quantum physics. The purpose of this book is to lay the theoretical foundations of the Elastodynamics of the Spacetime Continuum, allowing physicists to study and perform research in this new area of spacetime physics.

This second edition of the book includes the new research results developed over the last two years:

- clarification of special relativistic concepts in Chapter 2;
- enhanced analysis of the origin of inertial mass in the spacetime continuum in Chapter 5;
- clarification of dislocation and disclination defects in Chapters 9 and 10;
- detailed analysis of quantum entanglement in Chapter 13;
- enhanced identification of quantum particles and their associated spacetime defects in Chapter 18;
- identification of the electroweak interaction in Chapter 18;
- explanation of QED mass renormalization, vacuum polarization and self-energies in *STCED* in Chapter 18.

In addition, known typos and other errata have been corrected and some figures have been improved.

As mentioned in the copyright notice, this book is published and distributed in agreement with the Budapest Open Initiative [299], as is open-access journal *Progress in Physics* which publishes papers on advanced studies in theoretical and experimental physics, including related themes from mathematics. I am grateful to *Progress in Physics* and Editor-in-Chief Dr. Dmitri Rabounski for being available to independent scientists to publish their work, independently of the pressures from academia for conformance to the mainstream of physics. This has resulted in a fruitful collaboration with the journal.

A note on continuum mechanics terminology. The subject matter covered in this book covers many fields of physics, including general relativity, electromagnetism, quantum theory, elasticity and continuum mechanics. The terminology used in the literature is in general consistent across the different fields.

However, there are some differences within continuum mechanics, in particular with respect to defect theory, where there are some inconsis-

tencies in the terminology used in the literature. This is not surprising given that the development of defect theory was initiated in the twentieth century and is still an area of active research. We will point out the inconsistencies in the relevant sections of the book as the terminology is encountered. A glossary of the self-consistent physical symbols used in this book is included at the end of the book (see page 379) to facilitate the reading of this book.

A note on spacetime continuum constants. Note that in this book, we denote the *STCED* spacetime continuum constants with a diacritical mark over the symbols (for example $\bar{\kappa}_0, \bar{\lambda}_0, \bar{\mu}_0, \bar{\rho}_0$) to differentiate them from similar symbols used in other fields of physics. This allows us to retain existing symbols such as μ_0 for the electromagnetic permeability of free space, compared to the Lamé elastic constant $\bar{\mu}_0$ used to denote the spacetime continuum shear modulus.

A note on units and constants in equations. In general relativity and in quantum electrodynamics, it is customary to use "geometrized units" and "natural units" respectively, where the principal constants are set equal to 1. The use of these units facilitates calculations since cumbersome constants do not need to be carried throughout derivations. However, the absence of constants also obscures the physics of the equations. In this book, all constants are retained in the derivations, to provide physical insight into the nature of the equations under development.

In addition, we use rationalized MKSA units (*Système International*) for electromagnetism, as the traditionally used Gaussian units are gradually being replaced by rationalized MKSA units in more recent textbooks (see for example [17]).

With these clarifications, we are now ready to tackle the Elastodynamics of the Spacetime Continuum.

Ottawa, July 30, 2019 Pierre A. Millette

Chapter 1

Strained Spacetime

§1.1 Properties of the spacetime continuum

The publication of the General Theory of Relativity (GTR) by Albert Einstein in 1915 [97] was a watershed moment in our understanding of spacetime and gravitation. This led to an ever growing cascade of research and publications that continues unabated to this day. Einstein himself spent his last forty years of research until his death in 1955 working mostly on his search for a unified field theory of gravitation and electromagnetism.

General relativity is essentially a theory of the geometry of spacetime, which is generated by the energy-momentum present in spacetime. Gravitation is then simply the effect of that geometry on the masses present in spacetime. This can be represented as

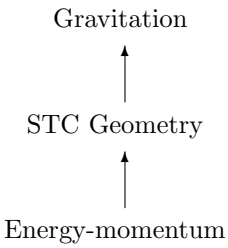

Mathematically, this is described by the deceptively compact Einstein field equations

$$G^{\mu\nu} = -\varkappa T^{\mu\nu} \tag{1.1}$$

where $G^{\mu\nu}$ is the Einstein tensor describing the geometry of spacetime, $T^{\mu\nu}$ represents the energy-momentum in the spacetime and $\varkappa = 8\pi G/c^4$ where G is the gravitational constant and c is the speed of light. The above equation actually represents 16 separate non-linear coupled partial differential equations, which belies the simplicity and elegance of (1.1).

Unlike Einstein, who was searching for a spacetime geometrical description of his unified field theory, in this book, we consider the physics of the spacetime continuum, to develop a theory that brings gravitation,

electromagnetism and quantum physics under one umbrella description providing a new theory of spacetime physics. This provides an alternate perspective to the problem of describing the dynamics of the spacetime continuum (STC), separate from the geometrical description pursued over the last one hundred years of GTR. This perspective derives from general relativity, starting with the Einstein field equations (1.1), and leads us to understand the geometrical description of GTR.

§1.1.1 *Stresses and strains in the spacetime continuum*

The first inkling that there is more to spacetime than just its geometry, is the representation of the energy-momentum in Einstein's field equations (1.1) above: $T^{\mu\nu}$ is called the energy-momentum *stress* tensor. The word *stress* implies that forces are being applied to the spacetime continuum by the energy-momentum present in its structure. At the same time, this also implies that spacetime is indeed a *continuum* that is warped by the presence of energy-momentum. From continuum mechanics, we know that the application of stresses to the spacetime continuum must result in strains in its structure, hence the terminology *strained spacetime*. We will derive this result in the next section §1.2.

The deformation of the spacetime continuum is a *physical* process, as shown by the deflection of light by the sun. Einstein in defending his theory in 1918 stated [98]:

> Whereas according to the special theory of relativity a part of space without matter and without electromagnetic field seems to be completely empty, that is to say not characterised by any physical properties, according to the general theory of relativity even space that is empty in this sense has physical properties.

More than forty years later, in 1952, Einstein wrote in Appendix V, *Relativity and the Problem of Space*, of his book on Relativity [99]:

> There is no such thing as an empty space, i.e. a space without field. Space-time does not claim existence on its own, but only as a structural quality of the field.

Einstein, throughout his search for a unified field theory of the gravitational and electromagnetic fields after the publication of his General Theory of Relativity, recognized that spacetime has physical properties of its own [204]. Hence general relativity implicitly leads us to the realization that the spacetime continuum must be a deformable continuum, where the deformations are physical in nature.

The assignment of physical dynamic properties to the spacetime of general relativity has been considered previously. For example, Sakha-

rov [312] considers a "metrical elasticity" of space in which generalized forces oppose the curving of space. Blair [27, p. 3–4] notes the very large value of the proportionality constant in the inverse of (1.1). This leads him to point out that spacetime is an elastic medium that can support waves, but its extremely high stiffness means that extremely small amplitude waves have a very high energy density. He notes that the coupling constant $c^4/8\pi G$ can be considered as a modulus of elasticity for spacetime, and identifies the quantity c^3/G with the characteristic impedance of spacetime [27, p. 45]. Tartaglia *et al* have recently explored strained spacetime in the cosmological context, as an extension of the spacetime Lagrangian to obtain a generalized Einstein equation [341, 342].

The physical properties of the spacetime continuum can be traced into other areas of physical theory. The *vacuum* of electromagnetic theory can also be identified with the spacetime continuum. This vacuum has various physical properties such as the characteristic impedance of the vacuum $Z_0 = 376.73\,\Omega$, the electromagnetic permittivity of the vacuum $\epsilon_0 = 8.854 \times 10^{-12}\,\mathrm{F\,m^{-1}}$, the electromagnetic permeability of the vacuum $\mu_0 = 12.566 \times 10^{-7}\,\mathrm{N\,A^{-2}}$ and the speed of electromagnetic waves in vacuo $c = 2.998 \times 10^{8}\,\mathrm{m\,s^{-1}}$. These are physical electromagnetic properties of the spacetime continuum observed during physical electromagnetic processes in the vacuum of space that hint at a connection between general relativity and electromagnetism via the spacetime continuum.

At the other end of the distance scale, we encounter the *vacuum* of quantum physics [30, 255, 256]. The vacuum of quantum electrodynamics is characterized by a constant creation/annihilation of (virtual) particles, corresponding to the state of constant vibration of the spacetime continuum due to its energy-momentum content. The quantum vacuum also provides a physical framework for various quantum effects such as vacuum polarization, zero-point energy, the Casimir force, the Aharonov-Bohm effect, and is the seat of physical quantum processes in the vacuum that again hint at a connection between general relativity and quantum physics via the spacetime continuum. The omnipresent quantum vacuum is in effect the spacetime continuum, seen from up close, with its microscopic properties made more evident by the microscopic scale of quantum phenomena.

In all of these cases, from the macroscopic to the microscopic, the spacetime continuum is not an empty canvas, but rather has physical properties of its own. It is understandable that physicists and mathematicians (not to mention philosophers) do not all have the same per-

spective on the emptiness of the vacuum (see [32,314]). One can always create an empty underlying mathematical structure used to "measure" the deviations of the spacetime continuum from a reference state, but there is no doubt that the spacetime continuum of physical theory is characterized by physical dynamic properties.

§1.1.2 *Deformations of the spacetime continuum*

Recognizing that the spacetime continuum of general relativity is a deformable continuum leads to a different approach to characterize the dynamics of the spacetime continuum. As seen in section §1.1.1, the energy-momentum stress tensor leads to strains in the spacetime continuum and the strains result in the displacement of the elements of the spacetime continuum from equilibrium, corresponding to the spacetime continuum (STC) deformations. The spacetime continuum itself is the medium that supports those deformations and is consequently deformed by the energy-momentum in its structure. This can be represented as

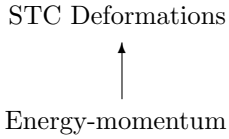

The methods of continuum mechanics applied to the spacetime continuum are used for the analysis of the STC deformations in four dimensions. This allows us to study the behaviour of the spacetime continuum at a local level, as it is being deformed by the presence of energy-momentum. The analysis can be defined both for small infinitesimal deformations and for large finite deformations.

The combination of all STC deformations generates the geometry of the spacetime continuum used in general relativity. The geometry of the spacetime continuum of general relativity resulting from the energy-momentum stress tensor can thus be seen to be a representation of the deformations of the spacetime continuum resulting from the strains generated by the energy-momentum stress tensor. And as before, gravitation is then simply the effect of that geometry on the masses present in spacetime.

The analysis of STC deformations is thus seen to be an additional layer of details in our understanding of the dynamics of the spacetime continuum. Consequently, general relativity must be used in combination with continuum mechanics for a complete description of the dy-

namics of the spacetime continuum, from the microscopic to the macroscopic. This can be represented as

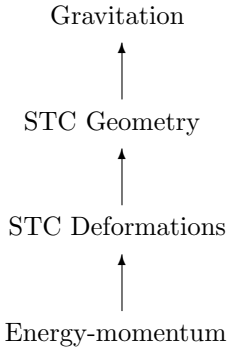

This theory is referred to as the Elastodynamics of the Spacetime Continuum (*STCED*) (see Millette [238–246]). In this theory, the spacetime continuum is analyzed within the framework of continuum mechanics and general relativity. Hence, while general relativity can be described as a top-down theory of the spacetime continuum, the Elastodynamics of the Spacetime Continuum can be described as a bottom-up theory of the spacetime continuum. *STCED* provides a fundamental description of the processes underlying the dynamics of the spacetime continuum.

Given that the combination of all deformations present in the spacetime continuum generates its geometry, *STCED* thus provides a description complementary to that of general relativity. While *GTR* is concerned with modeling the resulting geometry of the spacetime continuum, *STCED* is used to analyze the deformations generating that geometry. General relativity is thus the theory used to provide a macroscopic, large-scale description of the spacetime continuum, while *STCED* is used to provide a microscopic, small- to intermediate-scale description of the fundamental spacetime continuum processes, reaching down to the quantum level. The unification of general relativity and quantum physics is accomplished via *STCED*, the theory of the Elastodynamics of the Spacetime Continuum.

§1.2 Strained spacetime and the natural decomposition of the spacetime metric tensor

We start by demonstrating from first principles that spacetime is strained by the presence of mass. In addition, we find that this provides a

natural decomposition of the spacetime metric tensor of general relativity into a background and a dynamical part, and of spacetime tensor fields, both of which are still unresolved and are the subject of continuing investigations (see for example [60, 61, 81, 207, 334]). We find that the presence of mass results in strains in the spacetime continuum, and that those strains correspond to the dynamical part of the spacetime metric tensor.

In section §1.1.1, we noted that the energy-momentum stress tensor leads to strains in the spacetime continuum, and we mentioned that we would derive this result in this section. This we accomplish by using the time-honoured tradition in physics of analyzing such problems by introducing test objects, in this case a test mass, into a well-understood situation, and evaluating the consequences of this action. As a result, we will also solve a long-standing problem of general relativity.

There is no straightforward definition of local energy density of the gravitational field in general relativity [362, see p. 84, p. 286] [60, 181, 337]. This arises because the spacetime metric tensor includes both the background spacetime metric and the local dynamical effects of the gravitational field. No natural way of decomposing the spacetime metric tensor into its background and dynamical parts is known.

In this section, we propose a natural decomposition of the spacetime metric tensor into a background and a dynamical part. We also demonstrate that the energy-momentum stress tensor generates strains in the spacetime continuum. This is derived from first principles by introducing a test mass in the spacetime continuum described by the background metric, and calculating the effect of this test mass on the metric.

Consider the diagram of Figure 1.1. Points A and B of the spacetime continuum, with coordinates x^μ and $x^\mu + dx^\mu$ respectively, are separated by the infinitesimal line element

$$ds^2 = g_{\mu\nu}\, dx^\mu dx^\nu \tag{1.2}$$

where $g_{\mu\nu}$ is the metric tensor describing the background state of the spacetime continuum.

We now introduce a test mass in the spacetime continuum and examine the consequences of this action. This results in the displacement of point A to $\widetilde{A}$, where the displacement is written as u^μ. Similarly, the displacement of point B to $\widetilde{B}$ is written as $u^\mu + du^\mu$. The infinitesimal line element between points $\widetilde{A}$ and $\widetilde{B}$ is given by $\widetilde{ds}^2$.

By reference to Figure 1.1, the infinitesimal line element $\widetilde{ds}^2$ can be

Figure 1.1: Effect of a test mass on the background metric tensor

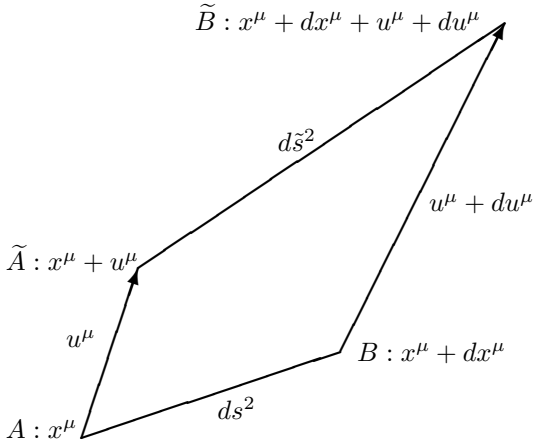

expressed in terms of the background metric tensor as

$$\widetilde{ds}^2 = g_{\mu\nu}(dx^\mu + du^\mu)(dx^\nu + du^\nu). \tag{1.3}$$

Multiplying out the terms in parentheses, we get

$$\widetilde{ds}^2 = g_{\mu\nu}(dx^\mu dx^\nu + dx^\mu du^\nu + du^\mu dx^\nu + du^\mu du^\nu). \tag{1.4}$$

Expressing the differentials du as a function of x, this equation becomes

$$\begin{aligned}\widetilde{ds}^2 = g_{\mu\nu}(&dx^\mu dx^\nu + dx^\mu\, u^\nu{}_{,\alpha}\, dx^\alpha + u^\mu{}_{,\alpha}\, dx^\alpha dx^\nu + \\ &+ u^\mu{}_{,\alpha}\, dx^\alpha\, u^\nu{}_{,\beta}\, dx^\beta)\end{aligned} \tag{1.5}$$

where the comma (,) denotes partial differentiation. Rearranging the dummy indices, this expression can be written as

$$\widetilde{ds}^2 = (g_{\mu\nu} + g_{\mu\alpha}\, u^\alpha{}_{,\nu} + g_{\alpha\nu}\, u^\alpha{}_{,\mu} + g_{\alpha\beta}\, u^\alpha{}_{,\mu} u^\beta{}_{,\nu})\, dx^\mu dx^\nu \tag{1.6}$$

and lowering indices, the equation becomes

$$\widetilde{ds}^2 = (g_{\mu\nu} + u_{\mu,\nu} + u_{\nu,\mu} + u^\alpha{}_{,\mu} u_{\alpha,\nu})\, dx^\mu dx^\nu. \tag{1.7}$$

The expression $(u_{\mu;\nu}+u_{\nu;\mu}+u^{\alpha}{}_{;\mu}u_{\alpha;\nu})$ is equivalent to the definition of the strain tensor $\varepsilon^{\mu\nu}$ of continuum mechanics. The strain $\varepsilon^{\mu\nu}$ is expressed in terms of the displacements u^{μ} of a continuum through the kinematic relation [320, see p. 149] [126, see pp. 23–28]:

$$\varepsilon^{\mu\nu} = \tfrac{1}{2}\left(u^{\mu;\nu} + u^{\nu;\mu} + u^{\alpha;\mu}u_{\alpha}{}^{;\nu}\right) \tag{1.8}$$

where the semicolon (;) denotes covariant differentiation. Substituting for $\varepsilon^{\mu\nu}$ from (1.8) into (1.7), we get

$$\widetilde{ds}^{\,2} = (g_{\mu\nu} + 2\,\varepsilon_{\mu\nu})\,dx^{\mu}dx^{\nu}. \tag{1.9}$$

Setting [126, see p. 24]

$$\widetilde{g}_{\mu\nu} = g_{\mu\nu} + 2\,\varepsilon_{\mu\nu} \tag{1.10}$$

then (1.9) becomes

$$\widetilde{ds}^{\,2} = \widetilde{g}_{\mu\nu}\,dx^{\mu}dx^{\nu} \tag{1.11}$$

where $\widetilde{g}_{\mu\nu}$ is the metric tensor describing the spacetime continuum with the test mass.

From (1.9) and (1.2), we obtain

$$\widetilde{ds}^{\,2} = ds^2 + 2\,\varepsilon_{\mu\nu}\,dx^{\mu}dx^{\nu}. \tag{1.12}$$

The change in the line element resulting from the generated strains is then given by

$$\tfrac{1}{2}\left(\widetilde{ds}^{\,2} - ds^2\right) = \varepsilon_{\mu\nu}\,dx^{\mu}dx^{\nu}. \tag{1.13}$$

Given that $g_{\mu\nu}$ is the background metric tensor describing the background state of the continuum, and $\widetilde{g}_{\mu\nu}$ is the spacetime metric tensor describing the final state of the continuum with the test mass, then $2\,\varepsilon_{\mu\nu}$ must represent the dynamical part of the spacetime metric tensor due to the test mass:

$$g^{dyn}_{\mu\nu} = 2\,\varepsilon_{\mu\nu} \tag{1.14}$$

with a corresponding line element

$$ds^2_{dyn} = 2\,\varepsilon_{\mu\nu}\,dx^{\mu}dx^{\nu}. \tag{1.15}$$

We are thus led to the conclusion that applied stresses due to the presence of energy-momentum result in strains in the spacetime continuum. Those strains correspond to the dynamical part of the spacetime

metric tensor. In addition, we obtain a natural way of decomposing the spacetime metric tensor into a background spacetime metric and a dynamical part corresponding to the local dynamical effects of the gravitational field, given by twice the strain tensor.

It is important to note that these results also apply to the spacetime of general relativity.

§1.3 Decomposition of tensor fields in strained spacetime

In this section, we consider the decomposition of spacetime tensor fields of rank 2. As opposed to vector fields which can be decomposed into longitudinal (irrotational) and transverse (solenoidal) components using the Helmholtz representation theorem [320, see pp. 260–261], the decomposition of spacetime tensor fields can be done in many ways (see for example [61, 81, 207, 334]).

The application of continuum mechanics to the spacetime continuum offers a natural decomposition of tensor fields, in terms of dilatations and distortions [126, see pp. 58–60]*. A *dilatation* corresponds to a change of volume of the spacetime continuum without a change of shape while a *distortion* corresponds to a change of shape of the spacetime continuum without a change in volume. As we will see in Chapter 2, dilatations correspond to longitudinal displacements and distortions correspond to transverse displacements of the elements of the spacetime continuum [320, see p. 260].

The strain tensor $\varepsilon^{\mu\nu}$ can thus be decomposed into a strain deviation tensor $e^{\mu\nu}$ (the *distortion*) and a scalar e_s (the *dilatation*) according to [126, see pp. 58–60]:

$$\varepsilon^{\mu\nu} = e^{\mu\nu} + e_s g^{\mu\nu} \tag{1.16}$$

where

$$e^{\mu}{}_{\nu} = \varepsilon^{\mu}{}_{\nu} - e_s \delta^{\mu}{}_{\nu} \tag{1.17}$$

$$e_s = \tfrac{1}{4}\,\varepsilon^{\alpha}{}_{\alpha} = \tfrac{1}{4}\,\varepsilon. \tag{1.18}$$

Similarly, the energy-momentum stress tensor $T^{\mu\nu}$ is decomposed into a stress deviation tensor $t^{\mu\nu}$ and a scalar t_s according to

$$T^{\mu\nu} = t^{\mu\nu} + t_s g^{\mu\nu} \tag{1.19}$$

where similarly

$$t^{\mu}{}_{\nu} = T^{\mu}{}_{\nu} - t_s \delta^{\mu}{}_{\nu} \tag{1.20}$$

*see footnote on page 26 on the terminology used.

$$t_s = \tfrac{1}{4}\, T^{\alpha}{}_{\alpha} = \tfrac{1}{4}\, T. \tag{1.21}$$

This decomposition of spacetime tensor fields of rank 2 in terms of dilatation and distortion components allows us to also decompose relations involving these tensor fields into separate dilatation and distortion relations. We will apply this decomposition to the Ricci tensor in section §2.4 once the basis of the theory of the Elastodynamics of the Spacetime Continuum has been developed in the next Chapter 2.

§1.4 The physicality of four-dimensional spacetime

Minkowski [257, 288] first introduced the concept of a four-dimensional spacetime and the description of particles in this spacetime as worldlines in 1908. This has given rise to the question whether four-dimensional spacetime is real or a mathematical abstraction. Eddington [288] considered this question in 1921:

> It was shown by Minkowski that all these fictitious spaces and times can be united in a single continuum of four dimensions. The question is often raised whether this four-dimensional spacetime is real, or merely a mathematical construction; perhaps it is sufficient to reply that it can at any rate not be less real than the fictitious space and time which it supplants.

Petkov [287, 288] provides a cogent summary of Minkowski's paper. Worldlines of particles at rest are vertical straight lines in a *space*−*ct* diagram, while particles moving at a constant velocity v are oblique lines and accelerated particles are curved lines. This provides a physical explanation for length contraction as a manifestation of the reality of a particle's extended worldline, where the cross-section measured by an observer moving relative to it (*i.e.* at an oblique line in the *space*−*ct* diagram), creates the difference in perceived length between a body at rest and one in movement. This is explored in greater detail in section §2.6.2. Minkowski's work demonstrates the physicality of four-dimensional spacetime, and that indeed, four-dimensional physics is spacetime geometry.

Chapter 2

Spacetime Continuum Elastodynamics (STCED)

§2.1 Model of the spacetime continuum

In this chapter, we derive the Elastodynamics of the Spacetime Continuum by applying continuum mechanical results to strained spacetime. Based on this model, a stress-strain relation is derived for the spacetime continuum. We apply that stress-strain relation to show that rest-mass energy density arises from the volume dilatation of the spacetime continuum. Then we apply the natural decomposition of tensor fields in strained spacetime, in terms of dilatations and distortions, to the Ricci tensor of general relativity, and conclude with a demonstration of the relation between general relativity and *STCED*.

The model of the spacetime continuum used in the theory of the Elastodynamics of the Spacetime Continuum is an extension of the general relativistic spacetime continuum based on continuum mechanics. The spacetime continuum is modelled as a four-dimensional differentiable manifold endowed with a metric $g_{\mu\nu}$. It is a continuum that can undergo deformations and support the propagation of such deformations. A continuum that is deformed is *strained*.

An infinitesimal element of the unstrained continuum is characterized by a four-vector x^μ, where $\mu = 0, 1, 2, 3$. The time coordinate is $x^0 \equiv ct$.

A *deformation* of the spacetime continuum corresponds to a state of the spacetime continuum where its elements are displaced from their unstrained positions*. Under deformation, an infinitesimal element at x^μ is displaced to a new position $x^\mu + u^\mu$, where u^μ is the displacement of the infinitesimal element from its unstrained position x^μ.

The spacetime continuum is approximated by a deformable linear elastic medium that obeys Hooke's law. For a general anisotropic continuum in four dimensions [126, see pp. 50–53],

$$E^{\mu\nu\alpha\beta}\,\varepsilon_{\alpha\beta} = T^{\mu\nu} \tag{2.1}$$

*As used in most continuum mechanics textbooks (see for example [57, 144]).

where $\varepsilon_{\alpha\beta}$ is the strain tensor, $T^{\mu\nu}$ is the energy-momentum stress tensor, and $E^{\mu\nu\alpha\beta}$ is the elastic moduli tensor.

The spacetime continuum is further assumed to be isotropic and homogeneous. This assumption is in agreement with the conservation laws of energy-momentum and angular momentum as expressed by Noether's theorem [189, see pp. 23–30]. For an isotropic medium, the elastic moduli tensor simplifies to [126]:

$$E^{\mu\nu\alpha\beta} = \bar{\lambda}_0(g^{\mu\nu}g^{\alpha\beta}) + \bar{\mu}_0(g^{\mu\alpha}g^{\nu\beta} + g^{\mu\beta}g^{\nu\alpha}) \tag{2.2}$$

where $\bar{\lambda}_0$ and $\bar{\mu}_0$ are the Lamé elastic constants of the spacetime continuum. $\bar{\mu}_0$ is the shear modulus (the resistance of the continuum to *distortions*) and $\bar{\lambda}_0$ is expressed in terms of $\bar{\kappa}_0$, the bulk modulus (the resistance of the continuum to *dilatations*) according to

$$\bar{\lambda}_0 = \bar{\kappa}_0 - \bar{\mu}_0/2 \tag{2.3}$$

in a four-dimensional continuum.

The relation between κ, and μ and λ in N dimensions is given by [199, p. 769]

$$\kappa = \frac{2\mu + N\lambda}{N}\,. \tag{2.4}$$

Another elastic constant that is used in the literature is Poisson's ratio ν given by [199, p. 770]

$$\nu = \frac{\lambda}{2\mu + (N-1)\lambda}\,. \tag{2.5}$$

We do not use Poisson's ratio in this book, but this relation may be needed when converting equations from the literature.

A *dilatation*, given by the divergence of the displacements, corresponds to a change of volume of the spacetime continuum without a change of shape* while a *distortion*, given by the gradient of the displacements, corresponds to a change of shape (shear) of the spacetime continuum without a change in volume†. As we saw in §1.3, spacetime tensor fields can be decomposed in terms of dilatation and distortion

*As used in all continuum mechanics textbooks.

†As used for example in [77, 126, 216]. This is one of the terms where there are other definitions given by some authors in defect theory. For example, Volterra [360], in his study of elastic deformations of multiply-connected solids in 1907 called them distortions (also used by [297] in his extension of Volterra's work), but that terminology was subsequently changed to dislocations and disclinations.

components which allows us to also decompose relations involving these tensor fields into separate dilatation and distortion relations.

We remind the reader that in this book, we denote the *STCED* spacetime continuum constants $\bar{\kappa}_0, \bar{\lambda}_0, \bar{\mu}_0, \bar{\rho}_0$ with a diacritical mark over the symbols to differentiate them from similar symbols used in other fields of physics. This allows us to retain existing symbols such as μ_0 for the electromagnetic permeability of free space, compared to the Lamé elastic constant $\bar{\mu}_0$ used to denote the spacetime continuum shear modulus.

§2.2 Stress-strain relation of the spacetime continuum

The introduction of strains in the spacetime continuum as a result of the energy-momentum stress tensor allows us to use by analogy results from continuum mechanics, in particular the stress-strain relation, to provide a better understanding of strained spacetime. The stress-strain relation is a characteristic of a continuum, and for a linear elastic continuum obeying Hooke's law, the stress-strain relation is linear. One of the consequences of linearity is that the principle of superposition is applicable, as observed in physical laws [305].

By substituting (2.2) into (2.1), we obtain the stress-strain relation for an isotropic and homogeneous spacetime continuum

$$\boxed{2\bar{\mu}_0\varepsilon^{\mu\nu} + \bar{\lambda}_0 g^{\mu\nu}\varepsilon = T^{\mu\nu}} \tag{2.6}$$

where

$$\varepsilon = \varepsilon^{\alpha}{}_{\alpha} \tag{2.7}$$

is the trace of the strain tensor obtained by contraction. The volume dilatation ε is defined as the change in volume per original volume [320, see pp. 149–152] and is an invariant of the strain tensor.

It is interesting to note that the structure of (2.6) is similar to that of the field equations of general relativity, *viz.*

$$R^{\mu\nu} - \tfrac{1}{2}\, g^{\mu\nu} R = -\varkappa T^{\mu\nu} \tag{2.8}$$

where $\varkappa = 8\pi G/c^4$ and G is the gravitational constant. This strengthens our conjecture that the geometry of the spacetime continuum can be seen to be a representation of the deformations of the spacetime continuum resulting from the strains generated by the energy-momentum stress tensor. We will come back to the relation between *STCED* and general relativity in section §2.5 in this chapter.

Using (1.16) to (1.21) into the strain-stress relation of (2.6) and making use of (2.10) and (2.3), we obtain separated dilatation and distortion relations respectively:

$$\begin{aligned} &\text{dilatation} : t_s = 2(\bar{\mu}_0 + 2\bar{\lambda}_0)e_s = 4\bar{\kappa}_0 e_s = \bar{\kappa}_0 \varepsilon \\ &\text{distortion} : t^{\mu\nu} = 2\bar{\mu}_0 e^{\mu\nu}. \end{aligned} \tag{2.9}$$

The distortion-dilatation decomposition is evident in the dependence of the dilatation relation on the bulk modulus $\bar{\kappa}_0$ and of the distortion relation on the shear modulus $\bar{\mu}_0$. The dilatation relation of (2.9) corresponds to rest-mass energy as we will see in the next section §2.3, while the distortion relation is traceless and thus massless, and corresponds to shear transverse waves.

This decomposition of spacetime continuum deformations into a massive dilatation and a massless transverse wave distortion provides a mechanism for wave-particle duality. This could explain why dilatation-measuring apparatus measure the massive "particle" properties of the deformation, while distortion-measuring apparatus measure the massless transverse "wave" properties of the deformation. Wave-particle duality will be considered in more details in Chapter 12.

§2.3 Rest-mass energy relation

We now derive a relation for rest-mass energy density that clarifies the nature of mass in the spacetime continuum of *STCED*. As derived in (2.6), the stress-strain relation for an isotropic and homogeneous spacetime continuum can be written as:

$$2\bar{\mu}_0 \varepsilon^{\mu\nu} + \bar{\lambda}_0 g^{\mu\nu} \varepsilon = T^{\mu\nu}.$$

The contraction of (2.6) yields the relation

$$2(\bar{\mu}_0 + 2\bar{\lambda}_0)\varepsilon = T^{\alpha}{}_{\alpha} \equiv T. \tag{2.10}$$

The time-time component T^{00} of the energy-momentum stress tensor represents the total energy density given by [279, see pp. 37–41]

$$T^{00}(x^k) = \int d^3\mathbf{p}\, E_p\, f(x^k, \mathbf{p}) \tag{2.11}$$

where $E_p = (\rho^2 c^4 + p^2 c^2)^{1/2}$, ρ is the rest-mass energy density, c is the speed of light, $\mathbf{p}$ is the momentum 3-vector and $f(x^k, \mathbf{p})$ is the distribution function representing the number of particles in a small phase

space volume $d^3\mathbf{x}\, d^3\mathbf{p}$. The space-space components T^{ij} of the energy-momentum stress tensor represent the stresses within the medium given by

$$T^{ij}(x^k) = c^2 \int d^3\mathbf{p}\, \frac{p^i p^j}{E_p}\, f(x^k, \mathbf{p})\,. \tag{2.12}$$

They are the components of the net force acting across a unit area of a surface, across the x^i planes in the case where $i = j$. In the simple case of a particle, they are given by [92, see p. 117]

$$T^{ii} = \rho\, v^i v^i \tag{2.13}$$

where v^i are the spatial components of velocity. If the particles are subjected to forces, these stresses must be included in the energy-momentum stress tensor.

Explicitly separating the time-time and the space-space components, the trace of the energy-momentum stress tensor is written as

$$T^{\alpha}{}_{\alpha} = T^{0}{}_{0} + T^{i}{}_{i}\,. \tag{2.14}$$

Substituting from (2.11) and (2.12), using the Minkowski metric $\eta^{\mu\nu}$ of signature $(+---)$, we obtain:

$$T^{\alpha}{}_{\alpha}(x^k) = \int d^3\mathbf{p} \left(E_p - \frac{p^2c^2}{E_p}\right) f(x^k, \mathbf{p}) \tag{2.15}$$

which simplifies to

$$T^{\alpha}{}_{\alpha}(x^k) = \rho^2 c^4 \int d^3\mathbf{p}\, \frac{f(x^k, \mathbf{p})}{E_p}\,. \tag{2.16}$$

Using the relation [279, see p. 37]

$$\frac{1}{\overline{E}_{har}(x^k)} = \int d^3\mathbf{p}\, \frac{f(x^k, \mathbf{p})}{E_p} \tag{2.17}$$

in equation (2.16), we obtain the relation

$$T^{\alpha}{}_{\alpha}(x^k) = \frac{\rho^2 c^4}{\overline{E}_{har}(x^k)} \tag{2.18}$$

where $\overline{E}_{har}(x^k)$ is the Lorentz invariant harmonic mean of the energy of the particles at x^k.

In the harmonic mean of the energy of the particles $\overline{E}_{har}$, the momentum contribution $\mathbf{p}$ will tend to average out and be dominated by the mass term ρc^2, so that we can write

$$\overline{E}_{har}(x^k) \simeq \rho c^2 \,. \tag{2.19}$$

Substituting for $\overline{E}_{har}$ in (2.18), we obtain the relation

$$T^{\alpha}{}_{\alpha}(x^k) \simeq \rho c^2 \,. \tag{2.20}$$

The total rest-mass energy density of the system is obtained by integrating over all space:

$$T^{\alpha}{}_{\alpha} = \int d^3\mathbf{x}\; T^{\alpha}{}_{\alpha}(x^k) \,. \tag{2.21}$$

The expression for the trace derived from (2.14) depends on the composition of the sources of the gravitational field. Considering the energy-momentum stress tensor of the electromagnetic field, we can show that $T^{\alpha}{}_{\alpha} = 0$ as expected for massless photons, while

$$T^{00} = \frac{\epsilon_0}{2}\left(E^2 + c^2 B^2\right)$$

is the total energy density, where ϵ_0 is the electromagnetic permittivity of free space, and E and B have their usual significance (see section §5.3).

Hence $T^{\alpha}{}_{\alpha}$ corresponds to the invariant rest-mass energy density and we write

$$T^{\alpha}{}_{\alpha} = T = \rho c^2 \tag{2.22}$$

where ρ is the rest-mass density. Using (2.22) into (2.10), the relation between the invariant volume dilatation ε and the invariant rest-mass energy density becomes

$$2(\bar{\mu}_0 + 2\bar{\lambda}_0)\varepsilon = \rho c^2 \tag{2.23}$$

or, in terms of the bulk modulus $\bar{\kappa}_0$,

$$\boxed{\rho c^2 = 4\bar{\kappa}_0\, \varepsilon} \,. \tag{2.24}$$

This equation demonstrates that rest-mass energy density arises from the volume dilatation of the spacetime continuum. The rest-mass energy is equivalent to the energy required to dilate the volume of the

spacetime continuum. It is a measure of the energy stored in the spacetime continuum that is perceived as mass. The volume dilatation is an *invariant*, as is the rest-mass energy density.

This is an important result as it demonstrates that mass is not independent of the spacetime continuum, but rather mass is part of the spacetime continuum fabric itself. As we will see in Chapter 3, mass results from the dilatation of the spacetime continuum in the longitudinal propagation of energy-momentum in the spacetime continuum. Matter does not warp spacetime, but rather, matter *is* warped spacetime (*i.e.* dilated spacetime). The universe consists of the spacetime continuum and energy-momentum that propagates in it by deformation of its (*i.e.* *STC*) structure.

Another important consequence of this relation is that it provides a definition of mass. The definition of mass is still one of the open questions in physics, with most authors adopting an indirect definition of mass based on the ratio of force to acceleration [178, see Chapter 8]. However, mass is one of the fundamental dimensions of modern systems of units, and as such, should be defined directly, not indirectly. This is a reflection of the current lack of understanding of the nature of mass in modern physics. *STCED* provides a direct physical definition of mass: *mass is the invariant change in volume of spacetime in the longitudinal propagation of energy-momentum in the spacetime continuum.*

§2.4 Dilatation-distortion decomposition of the Ricci tensor

In this section, we apply the natural decomposition of spacetime continuum tensor fields, based on the continuum mechanical decomposition of tensors in terms of dilatations and distortions, to the Ricci tensor used in general relativity. From this, we will show that this results in a separation of the field equations of general relativity into a dilatation relation and a distortion relation. We will then evaluate these equations in the weak field approximation to show that the longitudinal dilatation mass relation leads to Poisson's equation for a newtonian gravitational potential, and that the transverse distortion wave relation leads to the linearized field equation of gravity in the Transverse Traceless gauge. Hence the results derived in *STCED* also apply to general relativity.

As shown in section §1.3, the stress tensor $T^{\mu\nu}$ of general relativity can be separated into a stress deviation tensor $t^{\mu\nu}$ and a scalar t_s according to (1.19), (1.20) and (1.21). The Ricci curvature tensor $R^{\mu\nu}$ can also be separated into a curvature deviation tensor $r^{\mu\nu}$ (corresponding

to a distortion) and a scalar r_s (corresponding to a dilatation) according to

$$R^{\mu\nu} = r^{\mu\nu} + r_s\, g^{\mu\nu} \tag{2.25}$$

where similarly

$$r^{\mu}{}_{\nu} = R^{\mu}{}_{\nu} - r_s\, \delta^{\mu}{}_{\nu} \tag{2.26}$$

$$r_s = \tfrac{1}{4}\, R^{\alpha}{}_{\alpha} = \tfrac{1}{4}\, R \tag{2.27}$$

where R is the contracted Ricci curvature tensor.

Using (1.19) to (1.21) and (2.25) to (2.27) into the field equations of general relativity [362, see p. 72],

$$R^{\mu\nu} - \tfrac{1}{2}\, g^{\mu\nu} R = -\varkappa T^{\mu\nu} \tag{2.28}$$

where again $\varkappa = 8\pi G/c^4$ and G is the gravitational constant, we obtain a separation of the field equations of general relativity into dilatation and distortion relations respectively:

$$\begin{aligned} &\text{dilatation} : r_s = -\varkappa\, t_s \\ &\text{distortion} : r^{\mu\nu} = \varkappa\, t^{\mu\nu}\,. \end{aligned} \tag{2.29}$$

The dilatation relation of (2.29) can also be expressed as

$$R = -\varkappa T. \tag{2.30}$$

The distortion-dilatation separation of tensor fields is thus also applicable to the field equations of general relativity, resulting in separated dilatation and distortion relations. This result follows from the geometry of the spacetime continuum used in general relativity being generated by the combination of all deformations present in the spacetime continuum as seen previously.

§2.4.1 *Weak field approximation*

We now evaluate these separated field equations (2.29) in the weak field approximation to show that these relations satisfy the massive longitudinal dilatation and massless transverse distortion results of *STCED*.

In the weak field approximation [258, see pp. 435–441], the metric tensor $g_{\mu\nu}$ is written as $g_{\mu\nu} = \eta_{\mu\nu} + h_{\mu\nu}$ where $\eta_{\mu\nu}$ is the flat spacetime diagonal metric with signature $(+---)$ and $|h_{\mu\nu}| \ll 1$. The connection coefficients are then given by

$$\Gamma^{\mu}{}_{\alpha\beta} = \tfrac{1}{2}\, \eta^{\mu\nu}(h_{\alpha\nu,\beta} + h_{\beta\nu,\alpha} - h_{\alpha\beta,\nu}) \tag{2.31}$$

or, after raising the indices,

$$\Gamma^{\mu}{}_{\alpha\beta} = \tfrac{1}{2}\,(h_{\alpha}{}^{\mu}{}_{,\beta} + h_{\beta}{}^{\mu}{}_{,\alpha} - h_{\alpha\beta}{}^{,\mu}). \tag{2.32}$$

The Ricci tensor is also linearized to give

$$R_{\mu\nu} = \Gamma^{\alpha}{}_{\mu\nu,\alpha} - \Gamma^{\alpha}{}_{\mu\alpha,\nu} \tag{2.33}$$

which becomes

$$R_{\mu\nu} = \tfrac{1}{2}\,(h_{\mu}{}^{\alpha}{}_{,\nu\alpha} + h_{\nu}{}^{\alpha}{}_{,\mu\alpha} - h_{\mu\nu,\alpha}{}^{\alpha} - h^{\alpha}{}_{\alpha,\mu\nu}). \tag{2.34}$$

The contracted Ricci tensor

$$R = g^{\mu\nu}R_{\mu\nu} \simeq \eta^{\mu\nu}R_{\mu\nu} \tag{2.35}$$

then becomes

$$R = \tfrac{1}{2}\,\eta^{\mu\nu}(h_{\mu}{}^{\alpha}{}_{,\nu\alpha} + h_{\nu}{}^{\alpha}{}_{,\mu\alpha} - h_{\mu\nu,\alpha}{}^{\alpha} - h^{\alpha}{}_{\alpha,\mu\nu}) \tag{2.36}$$

which, after raising the indices and re-arranging the dummy indices, simplifies to

$$R = h^{\alpha\beta}{}_{,\alpha\beta} - h^{\alpha}{}_{\alpha,\beta}{}^{\beta}. \tag{2.37}$$

§2.4.2 *Dilatation (mass) relation*

Making use of (2.37) and (2.27) into the dilatation relation (2.30), we obtain the *longitudinal dilatation mass relation*

$$h^{\alpha}{}_{\alpha,\beta}{}^{\beta} - h^{\alpha\beta}{}_{,\alpha\beta} = \varkappa T \tag{2.38}$$

and, substituting for $\varkappa$ from (2.28) and $T = \rho c^2$ from (2.22),

$$\nabla^2 h^{\alpha}{}_{\alpha} - \partial_{\alpha}\partial_{\beta}h^{\alpha\beta} = \frac{8\pi G}{c^2}\,\rho \tag{2.39}$$

where ρ is the rest-mass density. This equation is shown to lead to Poisson's equation for a newtonian gravitational potential in the next section.

The second term of (2.39) would typically be set equal to zero using a gauge condition analogous to the Lorenz condition [258, see p. 438]. However, the second term is a divergence term, and it should not be set equal to zero in the general case where sources may be present.

§2.4.3 *Static newtonian gravitational field*

We consider the metric perturbation [258, see pp. 412–416]

$$\begin{aligned} h_{00} &= -2\Phi/c^2 \\ h_{ii} &= 0, \quad \text{for } i = 1, 2, 3 \end{aligned} \tag{2.40}$$

where Φ is a static (*i.e.* time independent) newtonian gravitational field. Then the term

$$h^{\alpha\beta}{}_{,\alpha\beta} = h^{00}{}_{,00} = 0 \tag{2.41}$$

and (2.38) becomes

$$\nabla^2 h^0{}_0 = \varkappa T. \tag{2.42}$$

Using h_{00} from (2.40) and $\varkappa$ from (2.28), (2.42) becomes

$$\nabla^2 \Phi = \frac{4\pi G}{c^2}\, T. \tag{2.43}$$

Substituting for $T = \rho c^2$ from (2.22), we obtain

$$\nabla^2 \Phi = 4\pi G \rho \tag{2.44}$$

where ρ is the mass density. This equation is Poisson's equation for a newtonian gravitational potential.

§2.4.4 *Distortion (wave) relation*

Combining (2.34) and (2.37) with (2.26) and (2.27) into the distortion relation of (2.29), we obtain the *transverse distortion wave relation*

$$\begin{aligned} &\tfrac{1}{2}\left(h_{\mu\alpha,\nu}{}^{\alpha} + h_{\nu\alpha,\mu}{}^{\alpha} - h_{\mu\nu,\alpha}{}^{\alpha} - h^{\alpha}{}_{\alpha,\mu\nu}\right) - \\ &\qquad -\tfrac{1}{4}\,\eta_{\mu\nu}\left(h^{\alpha\beta}{}_{,\alpha\beta} - h^{\alpha}{}_{\alpha,\beta}{}^{\beta}\right) = \varkappa t_{\mu\nu} \end{aligned} \tag{2.45}$$

where $t_{\mu\nu}$ is obtained from (1.20) and (1.21). This equation can be shown to be equivalent to the equation derived by Misner *et al* [258, see their Eq.(18.5)] from which they derive their linearized field equation and transverse wave equation in the Transverse Traceless gauge [258, see pp. 946–950]. This shows that this equation of the linearized theory of gravity corresponds to a transverse wave equation.

This result highlights the importance of carefully selecting the gauge transformation used to simplify calculations. For example, the use of the Transverse Traceless gauge eliminates massive solutions which, as

shown above, are longitudinal in nature, while yielding only non-massive (transverse) solutions for which the trace equals zero.

We thus find that the dilatation-distortion decomposition of tensor fields also applies to general relativity. In addition, the results of *STCED* are found to be applicable to general relativity. As mentioned previously, this is not surprising as the postulates of *STCED* derive from general relativity, and vice versa in that the geometry of spacetime used in general relativity derives from the combination of the spacetime deformations of *STCED*.

§2.5 Relation between General Relativity and STCED

The previous section §2.4 shows that the results of *STCED* should be applicable to general relativity. This is a reasonable expectation, given that the postulates of *STCED* derive from general relativity. In this section, we show the relation between the general relativistic spacetime geometry and its generation from the combination of the spacetime deformations of *STCED*.

This is derived from the *STCED* stress-strain relation of (2.6), *viz.*

$$2\bar{\mu}_0\varepsilon^{\mu\nu} + \bar{\lambda}_0 g^{\mu\nu}\varepsilon = T^{\mu\nu}$$

and the Einstein field equations of general relativity of (2.8), *viz.*

$$R^{\mu\nu} - \tfrac{1}{2}\, g^{\mu\nu} R = -\varkappa T^{\mu\nu}\,.$$

As noted in §2.2, the structure of the *STCED* stress-strain relation (2.6) is similar to that of the Einstein field equations of general relativity (2.8).

Eq. (2.8) is a field equation in terms of the curvature of the spacetime continuum while (2.6) is a field equation in terms of the strains of the spacetime continuum which are themselves expressed in terms of displacements u^μ from the equilibrium position x^μ. Both field equations are thus describing the same phenomenon of spacetime warping from different perspectives.

However, the Ricci curvature tensor $R^{\mu\nu}$ is a function of the connection coefficients Γ and their derivatives which are in turn functions of the derivative of the metric tensor $g^{\mu\nu}$. On the other hand, the strain tensor $\varepsilon^{\mu\nu}$ is expressed as the difference between the deformed metric $\widetilde{g}^{\mu\nu}$ and the original metric $g^{\mu\nu}$

$$\varepsilon^{\mu\nu} = \tfrac{1}{2}(\widetilde{g}^{\mu\nu} - g^{\mu\nu}) \tag{2.46}$$

which is at most a function of the derivative of the metric tensor. The curvature description is understandably going to be more complicated

than the strain description as it needs to account for the combination of the simpler deformations causing the geometry of the spacetime continuum.

Eq. (2.8) is a complex relation that corresponds to a macroscopic description of the gravitational field equations in terms of the geometry of spacetime. Eq. (2.6) is a simpler relation which corresponds to a microscopic description of the deformations of the spacetime continuum due to energy-momentum. The geometry of spacetime used in (2.8) should thus be considered to be a linear composition (represented by a sum) of *STC* deformations, starting with the total energy-momentum generating the geometry of general relativity, $T^{\mu\nu}_{GR}$, being a composition of the energy-momentum of the individual deformations of *STCED*, $T^{\mu\nu}_{STCED}$:

$$T^{\mu\nu}_{GR} = \sum T^{\mu\nu}_{STCED} \,. \tag{2.47}$$

Substituting into (2.47) from (2.6) and (2.8), we obtain

$$-\frac{1}{\varkappa}\left[R^{\mu\nu} - \tfrac{1}{2}\, g^{\mu\nu} R\right] = \sum \left[2\bar{\mu}_0\, \varepsilon^{\mu\nu} + \bar{\lambda}_0\, g^{\mu\nu}\varepsilon\right] \,. \tag{2.48}$$

This explains the complexity of (2.8) relative to (2.6).

Contraction of (2.48) yields the relation

$$\frac{1}{\varkappa}\, R = \sum 2(\bar{\mu}_0 + 2\bar{\lambda}_0)\, \varepsilon \tag{2.49}$$

which, using (2.3) and (2.24), simplifies to

$$\frac{1}{\varkappa}\, R = \sum 4\, \bar{\kappa}_0\, \varepsilon = \sum \rho\, c^2 \tag{2.50}$$

i.e. the curvature of the spacetime continuum arises from the composition of the effect of individual deformations and is proportional to the rest-mass energy density present in the spacetime continuum. Substituting for $R/\varkappa$ from (2.50) into (2.48), and rearranging terms, we obtain

$$\frac{1}{\varkappa}\, R^{\mu\nu} = \sum \left[(\bar{\lambda}_0 + \bar{\mu}_0) g^{\mu\nu}\varepsilon - 2\bar{\mu}_0\, \varepsilon^{\mu\nu}\right] \,. \tag{2.51}$$

Eq. (2.50) and (2.51) give the relation between the microscopic description of the strains (*i.e.* deformations of the spacetime continuum) and the macroscopic description of the gravitational field in terms of the curvature of the spacetime continuum resulting from the combination of the many microscopic displacements of the spacetime continuum from equilibrium.

§2.5.1 *The cosmological constant*

The observant reader will notice that the Einstein field equations of general relativity of (2.8) does not include the cosmological constant term $+\Lambda g_{\mu\nu}$ where Λ is the cosmological constant. The cosmological constant term was initially introduced by Einstein [96] to deal with the cosmological solutions of his field equations. As the *STCED* stress-strain relation of (2.6) provides a local small- to intermediate-scale description of the fundamental processes of the spacetime continuum, it is not meant to be a cosmological relation, which is the domain of the macroscopic, large-scale description of the spacetime continuum provided by the General Theory of Relativity. Hence there is no purpose in using the cosmological constant in the comparison of the *STCED* stress-strain relation and the Einstein field equations of general relativity of the previous section §2.5. There is no value in introducing the cosmological constant in the Elastodynamics of the Spacetime Continuum.

It should be noted that the cosmological constant term $+\Lambda g_{\mu\nu}$ can be equivalently incorporated in the second term $-\frac{1}{2}\, g^{\mu\nu} R$ of the Einstein field equations by writing the cosmological constant as

$$\Lambda = -\tfrac{1}{2}\, \delta R \tag{2.52}$$

and incorporating it in the second term of the Einstein field equations as $-\frac{1}{2}\, g^{\mu\nu} R'$ where $R' = R + \delta R$. Given the previous considerations summarized in (2.50), we see that the introduction of the cosmological constant term $+\Lambda g_{\mu\nu}$ is equivalent to introducing additional rest-mass energy density in the spacetime continuum. The resurgent interest in the cosmological constant is due to this characteristic, which is seen as a possible solution to the question of dark matter and dark energy which is considered to be a major problem by modern cosmologists. We will come back to this question in Chapter 19 of this book.

§2.6 The question of relativistic mass

The concept of relativistic mass has been a part of special relativistic physics since it was first introduced by Einstein [94, 95] and explored by the early relativists (see for example [346, 347]). Other terminology is also used for relativistic mass, representing the users' perspective on the concept. For example, Aharoni [2] refers to it as the "relative mass", while Dixon [84] refers to it as "apparent mass". Oas [270] and Okun [274] provide good overviews on the development of the historical use of the concept of relativistic mass. Oas [271] has prepared a bibliography of published works where the concept is used and where it is ignored.

It is clear that there is no consensus in the physics community on the validity and use of the concept of relativistic mass. Some consider relativistic mass to represent an actual increase in the inertial mass of a body [287]. However, there have been objections raised against this interpretation (see Taylor and Wheeler [344], Okun [273–275], Oas [270]). The situation seems to arise from confusion on the meaning of the special relativistic dynamics equations. In this section, we revisit the question of relativistic mass to clarify the meaning of this concept within special relativity, in light of the Elastodynamics of the Spacetime Continuum (*STCED*) [238, 254].

§2.6.1 *Relativistic mass depends on the frame of reference*

In the following sections, we show that the inertial mass of a body is the rest-mass energy while the relativistic mass is in effect an effective mass m^*. The relativistic mass m^* is given by

$$m^* = \gamma m_0 \,, \tag{2.53}$$

where

$$\gamma = \frac{1}{(1-\beta^2)^{1/2}} \,, \tag{2.54}$$

$\beta = v/c$ and m_0 is the rest-mass or proper mass which is an invariant. Some authors [275] suggest that rest-mass should be denoted as m as this is the real measure of inertial mass. The relativistic mass of an object corresponds to the total energy of an object (invariant proper mass plus kinetic energy). The first point to note is that the relativistic mass is the same as the proper mass in the frame of reference at rest with the object, *i.e.* $m^* = m_0$ for $v = 0$. In any other frame of reference in motion with velocity v with respect to the object, the relativistic mass will depend on v according to (2.53).

For example, when the relativistic mass of a cosmic ray particle is measured[†] in an earth lab, it depends on the speed of the particle measured with respect to the earth lab. Similarly for a particle in a particle accelerator, where its speed is measured with respect to the earth lab. The relativistic mass of the cosmic ray particle measured from say a space station in orbit around the earth or a spaceship in transit in space would depend on the speed of the particle measured with respect to the space station or the spaceship respectively.

We thus see that relativistic mass is an effect similar to length contraction and time dilation in that it is dependent on the difference in

[†] what is measured is the energy of the particle, not its mass.

velocity v between the object's frame of reference and the frame of reference from which it is measured. Observers in different moving frames will measure different relativistic masses of an object as there is no absolute frame of reference with respect to which an object's speed can be measured.

§2.6.2 *Time dilation and space contraction*

To further understand this conclusion, we need to look into time dilation and length contraction in more detail. These special relativistic concepts are often misunderstood by physicists. Many consider these changes to be actual physical changes, taking the Lorentz-Fitzgerald contraction and the time dilation effect to be real.

For example, John Bell in [20] relates the problem of the thread tied between two spaceships and whether the thread will break at relativistic speeds due to length contraction. He insists that it will – he relates how "[a] distinguished experimental physicist refused to accept that the thread would break, and regarded my assertion, that indeed it would, as a personal misinterpretation of special relativity". Bell appealed to the CERN Theory Division for arbitration, and was dismayed that a clear consensus agreed that the thread would not break, as indeed is correct. As the number of special relativistic "paradoxes" attest, many physicists, scientists and engineers have similar misunderstandings, not clearly understanding the concepts.

This situation arises due to not realizing that v is the difference in velocity between an object's frame of reference and the frame of reference from which it is measured, not an absolute velocity, as discussed in the previous section §2.6.1. In a nutshell, time dilation and length contraction are apparent effects. In the frame of reference at rest with an object that is moving at relativistic speeds with respect to another frame of reference, there is no length contraction or time dilation.

The proper time in the frame of reference at rest with the object is the physical time, and the length of the object in the frame of reference at rest with the object is the physical length – there is no time dilation or length contraction. These are observed in other frames of reference moving with respect to that object and are only apparent dilations or contractions perceived in those frames only. Indeed, observers in frames of reference moving at different speeds with respect to the object of interest will see *different* time dilations and length contractions. These cannot all be correct – hence time dilation and length contraction are apparent, not real.

This can be demonstrated to be the case from physical considerations, and in so doing, we clarify further the nature of length contraction. Petkov [288] provides graphically a physical explanation of time dilation and length contraction, based on Minkowski's 1908 paper [257] where the latter first introduced the concept of a four-dimensional spacetime and the description of particles in that spacetime as worldlines. Worldlines of particles at rest are vertical straight lines in a *space*−*ct* diagram, while particles moving at a constant velocity v are oblique lines and accelerated particles are curved lines (see Fig. 2.3).

The basic physical reason for these effects can be seen from the special relativistic line element (using x to represent the direction of propagation and $c = 1$)

$$d\tau^2 = dt^2 - dx^2 \,. \tag{2.55}$$

One sees that for a particle at rest, the vertical straight line in a *space*−*ct* diagram is equivalent to

$$d\tau^2 = dt^2 \,, \tag{2.56}$$

which is the only case where the time t is equivalent to the proper time τ (in the object's frame of reference). In all other cases, in particular for the oblique line in the case of constant velocity v, (2.55) applies and there is a mixing of space x and time t, resulting in the perceived special relativistic effects observed in a frame of reference moving at speed v with respect to the object of interest.

Loedel diagrams [313], a variation on *space*−*ct* diagrams allowing to display the Lorentz transformation graphically, are used to demonstrate graphically length contraction, time dilation and other special relativistic effects in problems that involve two frames of reference. Figs. 2.1 and 2.2, adapted from Petkov's Figs. 4.18 [287, p. 86], and 4.20 [287, p. 91] respectively, and Sartori's Fig. 5.15 [313, p. 160], provide a graphical view of the physical explanation of time dilation and length contraction respectively.

From Fig. 2.1, we see that $\Delta t' > \Delta t$ as expected – the moving observer sees time interval $\Delta t'$ of the observed object to be dilated, while the observed object's time interval Δt is actually the physical proper time interval $\Delta\tau$. From Fig. 2.2, we see that space distance measurements, *i.e.* space intervals, $\Delta x' < \Delta x$ as expected – the moving observer sees space interval $\Delta x'$ of the observed object to be contracted, while the observed object's space interval Δx is actually the proper space interval.

This provides a physical explanation for length contraction as a manifestation of the reality of a particle's extended worldline, where the cross-section measured by an observer moving relative to it (*i.e.* at an oblique line in the *space*−*ct* diagram), creates the difference in perceived length between a body in its rest frame and a frame in movement, as seen in Fig. 2.2. It is important to understand that space itself is perceived to be contracted, not just objects in space. As seen in *STCED* [238], objects are not independent of spacetime, but are themselves deformations of spacetime, and are as such perceived to be contracted as space itself is. In actual practice, this phenomenon should be called *space contraction*, to avoid confusion, and demonstrate the complementary nature of time dilation and space contraction.

Thus we see that apparent time dilation and space contraction are perfectly valid physical results of Special Relativity, and there is nothing anomalous about them. Proper consideration of these phenomena eliminates the so-called paradoxes of Special Relativity as demonstrated by various authors, see for example [287, 313, 344]. We now explore the

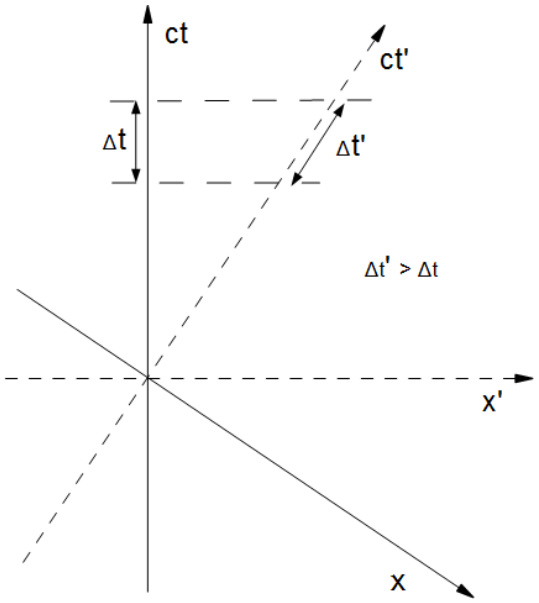

Figure 2.1: Physical explanation of time dilation in a Loedel *space*−*ct* diagram

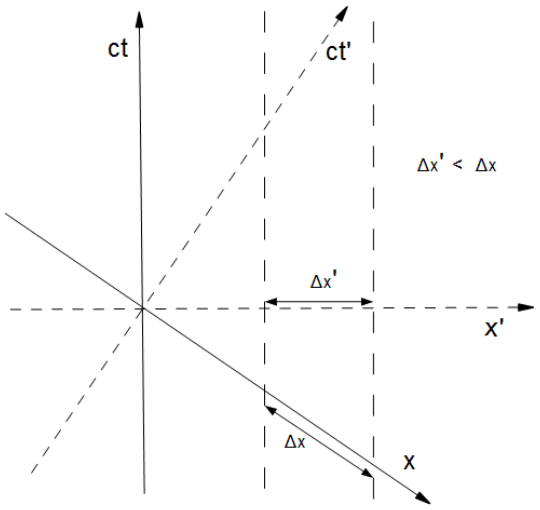

Figure 2.2: Physical explanation of length contraction in a Loedel *space*$-ct$ diagram

question of relativistic mass, which we first considered in section §2.6.1, in light of these considerations.

§2.6.3 *Relativistic mass as an effective mass*

In this section, we show that the inertial mass of a body is its proper mass while the relativistic mass m^* is in effect an effective mass or, as Dixon [84] refers to it, an apparent mass. An effective mass is often introduced in dynamic equations in various fields of physics. An effective mass is not an actual mass – it represents a quantity of energy that behaves in dynamic equations similar to a mass. Using the effective mass, we can write the energy E as the sum of the proper mass and the kinetic energy K of the body, which is typically written as

$$E = m^* c^2 = m_0\, c^2 + K \tag{2.57}$$

to give

$$K = (\gamma - 1)\, m_0\, c^2\,. \tag{2.58}$$

In general, the energy relation in special relativity is quadratic, given by

$$E^2 = m_0^2\, c^4 + p^2 c^2\,, \tag{2.59}$$

where p is the momentum. Making use of the effective mass (2.53) allows us to obtain a linear expression from (2.59), starting from

$$m^{*2}c^4 = \gamma^2 m_0^2\, c^4 = m_0^2\, c^4 + p^2c^2\,, \tag{2.60}$$

which becomes

$$pc = \sqrt{\gamma^2 - 1}\, m_0\, c^2 \tag{2.61}$$

or

$$pc = \beta\gamma m_0\, c^2 = \frac{v}{c}\,\gamma m_0\, c^2 = \frac{v}{c}\,E\,. \tag{2.62}$$

Then

$$p = m^* v\,. \tag{2.63}$$

As [287, p. 112] shows, the γ factor corresponds to the derivative of time with respect to proper time, *i.e.*

$$\frac{\mathrm{d}t}{\mathrm{d}\tau} = \frac{1}{(1-\beta^2)^{1/2}} = \gamma\,, \tag{2.64}$$

such that the velocity with respect to the proper time, u, is given by

$$u = \gamma v\,. \tag{2.65}$$

Hence using (2.65) in (2.63) yields the correct special relativistic relation

$$p = m_0\, u\,, \tag{2.66}$$

which again shows that m^* in (2.63) is an effective mass when dealing with dynamic equations in the local time t instead of the invariant proper time τ. It is easy to see that differentiating (2.66) with respect to proper time results in a force law that obeys Newton's law with the proper mass acting as the inertial mass.

Hence we find that relativistic mass results from dealing with mass in local time t in a frame of reference moving with respect to the object of interest, instead of the invariant proper time τ in the frame of reference at rest with the object, and, from that perspective, is an effect similar to space contraction and time dilation seen in section §2.6.2. We see that the rest-mass m_0 should really be referred to as the proper mass, to avoid any confusion about the invariant mass of a body.

Relativistic mass is not apparent as time dilation and space contraction are, but rather is a measure of energy that depends on the relative speed v between two frames of reference, and is not an intrinsic property of an object as there is no absolute frame of reference to measure

an object's speed against. The relativistic mass energy m^*c^2 is actually the total energy of an object (proper mass plus kinetic energy) measured with respect to a given frame of reference and is not a mass *per se* as mass is a relativistic invariant, *i.e.* a four-dimensional scalar, while energy is the fourth component of a four-vector.

§2.6.4 *Relativistic mass and STCED*

In *STCED*, the proper mass corresponds to the invariant longitudinal volume dilatation given by (2.24), *viz.*

$$\rho c^2 = 4\kappa_0\, \varepsilon$$

which is equivalent to the inertial mass. The constant κ_0 is the spacetime bulk modulus and ε is the spacetime volume dilatation. Clearly, the longitudinal volume dilatation does not increase with velocity as it is an invariant. The result (2.66) is as expected from *STCED*.

For a spacetime volume element, the apparent space contraction in the direction of motion will be cancelled out by the apparent time dilation, *i.e.* the γ factors will cancel out. Thus the volume dilatation ε and the proper mass density ρ of (2.24) remain unchanged from the perspective of all frames of reference.

The only quantity that is impacted by the observer's frame of reference is the kinetic energy K or alternatively the quantity pc. In the frame of reference at rest with the object (which we can call the proper frame of reference), the kinetic energy $K = 0$ as seen from (2.58), while $pc = 0$ as seen from (2.61). The relativistic mass of an object is an effective mass defined to correspond to the total energy of an object (invariant proper mass plus kinetic energy) as observed from the perspective of another frame of reference. It does not represent an increase in the proper mass of an object, which as we have seen in section §2.6.3, corresponds to the inertial mass of the object.

Hence we see that relativistic mass is dependent on the difference in velocity v between an object's proper frame of reference that is at rest with the object and the frame of reference from which it is observed. Furthermore, relativistic mass results from dealing with dynamic equations in local time t in a frame of reference moving with respect to the object of interest, instead of the invariant proper time τ in the frame of reference at rest with the object. The results obtained are in agreement with the Elastodynamics of the Spacetime Continuum.

§2.7 The question of acceleration in special relativity

In the previous section §2.6, we showed that time dilation and space contraction in inertial reference frames, that is unaccelerated reference frames moving at a constant velocity, are apparent effects perceived in a frame of reference moving with respect to an object of interest. The real physical time and length are in the frame of reference at rest with the object, and in that frame, there is no time dilation or space contraction as $v = 0$ (and acceleration $a = 0$). This is seen clearly in Fig. 2.1 where a time dilation is perceived in the frame of reference moving at speed v with respect to the object of interest ($\Delta t'$), while there is no dilation in the object's frame of reference (Δt).

This result would seem to be at odds with the often quoted experimental tests of special relativity confirming time dilation and length contraction. But if we consider, for example, Bailey *et al*'s muon experiment [11], we find that there is no contradiction with the experimental observations: a perceived time dilation is observed in the Earth's laboratory frame of reference while the muon, in its frame of reference has no time dilation – note that no measurements were carried out in the muon's frame of reference in the Bailey experiment.

Careful examination of experimental tests of special relativity also often reveals the presence of acceleration in the experiments, contrary to the conditions under which special relativity applies. The question of how to deal with acceleration in special relativity underlies many of the analytical and experimental conundrums encountered in the theory and is investigated in more details in this section.

§2.7.1 *Measuring the impact of acceleration in special relativity*

The theory of special relativity applies to unaccelerated (constant velocity) frames of reference, known as inertial frames of reference, in a four-dimensional Minkowski spacetime [257], of which the three-dimensional Euclidean space is a subspace. When the Lorentz-Fitzgerald contraction was first introduced, it was considered to be a real physical effect in Euclidean space to account for the null results of the Michelson-Morley experiment. Einstein derived length contraction and time dilation as effects originating in special relativity. These depend on the velocity of the frame of reference with respect to which an object is being observed, not the object's velocity which can only be relative to another frame of reference, as there is no absolute frame of reference against which to measure the object's velocity. Indeed, if time dilation and length con-

traction were real effects in special relativity, this would be equivalent to saying that there is an absolute frame of reference against which it is possible to measure an object's velocity, contrary to the theory.

Increasingly, special relativity has been applied to accelerated frames of reference for which the theory does not apply. Some physicists claim that acceleration does not matter in special relativity and that it has no impact on its results, but there are many indications that this is not the case. The Clock Hypothesis (or Postulate) is used to justify the use of accelerated frames in special relativity: "when a clock is accelerated, the effect of motion on the rate of the clock is no more than that associated with its instantaneous velocity – the acceleration adds nothing" [37, p. 9], and further postulates that if the Clock Hypothesis applies to a clock, "then the clock's proper time will be proportional to the Minkowski distance along its worldline" [37, p. 95] as required.

Two experimental confirmations of the Clock Hypothesis are usually given. The postulate is claimed to have been shown to be true for accelerations of $\sim 10^{16} g$ in a Mössbauer spectroscopy experiment by Kündig [209] and of $\sim 10^{18} g$ in Bailey *et al*'s muon experiment [11], which uses rotational motion of particles to generate the acceleration – one obtains the quoted acceleration for a particle velocity close to the speed of light. However, a close examination of these experiments shows that they don't quite provide the experimental confirmation they are purported to give.

Kholmetskii *et al* [192] reviewed and corrected the processing of Kündig's experimental data and obtained an appreciable difference of the relative energy shift $\Delta E/E$ between emission and absorption resonant lines from the predicted relativistic time dilation $\Delta E/E = -v^2/2c^2$ (to order c^{-2}), where v is the tangential velocity of the resonant radiation absorber. Writing the relative energy shift as $\Delta E/E = -k\, v^2/c^2$, they found that $k = 0.596 \pm 0.006$ instead of $k = 0.5$ as predicted by special relativity and Kündig's original reported result of $k = 0.5003 \pm 0.006$. They then performed a similar Mössbauer spectroscopy experiment [193] with two absorbers with a substantially different isomer shift to be able to correct the Mössbauer data for vibrations in the rotor system at various rotational frequencies. They obtained a value of $k = 0.68 \pm 0.03$, a value similar to $2/3$. Since then Kholmetskii and others [68, 194–197] have performed additional experimental and theoretical work to try to explain the difference, but the issue remains unresolved at this time, and is a clear indication that acceleration is not compatible with special relativity.

Bailey *et al* [11], in their experiment of the measurement of the

lifetime of positive and negative muons in a circular orbit, obtained lifetimes of high-speed muons which they then reduced to a mean proper lifetime at rest, assuming that special relativity holds in their accelerated muon experimental setup. This experiment was carried out at CERN's second Muon Storage Ring (MSR) [65, 235] which stores relativistic muons in a ring in a uniform magnetic field. The MSR was specifically designed to carry out muon $(g-2)$ precession experiments (g is the Landé g-factor) with muons of momentum $3.094\,\mathrm{GeV}/c$ corresponding to a γ-factor of 29.3 (effective relativistic mass [248]), so that the electrons emitted from muon decay in the lab frame were very nearly parallel to the muon momentum. The decay times of the emitted electrons were measured in shower counters inside the ring to a high precision, and the muon lifetimes in the laboratory frame were calculated by fitting the experimental decay electron time spectrum to a six-parameter exponential decay modulated by the muon spin precession frequency, using the maximum likelihood method – one of the six parameters is the muon relativistic lifetime.

It is important to note that the decay electrons would be ejected at the instantaneous velocity of the muon ($0.9994c$ from the $\gamma = 29.3$ factor) tangential to the muon's orbit. Thus the ejected electron moves at the constant velocity of ejection to the shower counter and acceleration does not play a role. Even though the muons are accelerated, the detected electrons are not, and the experiment is not a test of the Clock Hypothesis under acceleration as claimed. There is thus no way of knowing the impact of acceleration from the experimental results as acceleration is non-existent in the detection and measurement process.

It should also be noted that Hafele *et al* [145] in their time dilation "twin paradox" experiment applied a correction for centripetal acceleration to their experimental results. in addition to a gravitational time dilation correction, to obtain results in agreement with Lorentz time dilation. The effect of acceleration cannot be disregarded in that experiment. This will be considered in more details in section §2.7.3. We thus find that the experimental support of the Clock Hypothesis is questionable at best.

§2.7.2 *The case for the impact of acceleration in special relativity*

Having determined that there is little experimental support for the validity of the Clock Hypothesis in accelerated frames of reference in special relativity, we consider the case for the impact of acceleration in special

relativity. Einstein developed general relativity to deal with accelerated frames of reference – if acceleration can be used in special relativity, why bother to develop a more general theory of relativity? Inspection of an accelerated worldline in a Minkowski *space-ct* diagram shows that indeed there is no basis for the Clock Hypothesis, as seen in Fig. 2.3. The accelerated worldline suffers an increasing rate of time dilation, somewhat like gravitational time dilation where increasing height in the gravitational potential results in increasing time dilation.

This brings to mind Einstein's equivalence principle introduced in the analysis of accelerated frames of reference in general relativity. The simplest formulation of this principle states that on a local scale, the physical effects of a gravitational field are indistinguishable from the physical effects of an accelerated frame of reference [268] (*i.e.* an accelerated frame of reference is locally equivalent to a gravitational field). Hence, as displayed graphically for the accelerated worldline in the Minkowski *space-ct* diagram of Fig. 2.3, an accelerated frame of reference undergoes time dilation similar to gravitational time dilation [268]. Indeed, assuming that acceleration has no impact in special relativity

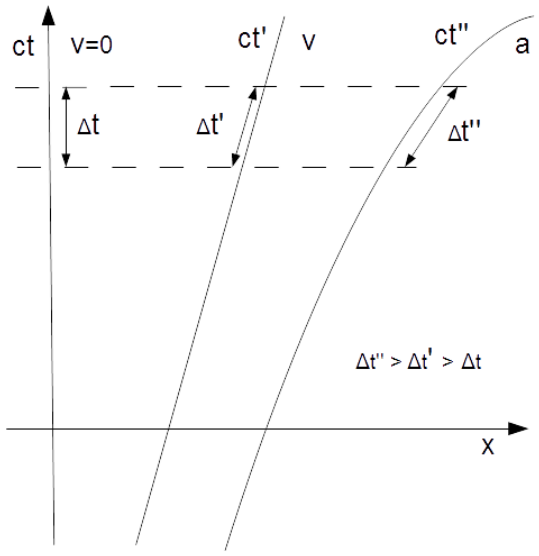

Figure 2.3: Physical explanation of an accelerated worldline in a Minkowski *space*$-$*ct* diagram

cannot be correct as it violates the equivalence principle of general relativity.

We explore the connection between gravitational time dilation and the time dilation in an accelerated frame of reference in greater details. Gravitational time dilation can be derived starting from the Schwarzschild metric with signature $(+---)$ [64, p. 40]

$$\begin{aligned} c^2 d\tau^2 = \left(1 - \frac{2GM}{rc^2}\right) c^2 dt^2 - \left(1 - \frac{2GM}{rc^2}\right)^{-1} dr^2 - \\ - r^2 \left(d\theta^2 + \sin^2\theta \, d\varphi^2\right) , \end{aligned} \tag{2.67}$$

where τ is the proper time, (r, θ, φ, t) are the spherical polar coordinates including time, G is the gravitational constant, M is the mass of the earth and c is the speed of light in vacuo. The gravitational time dilation is obtained from the dt^2 term to give

$$\Delta t = \left(1 - \frac{2GM}{rc^2}\right)^{-\frac{1}{2}} \Delta t_0 \, , \tag{2.68}$$

where Δt_0 is the undilated (proper) time interval and Δt is the dilated time interval in the earth's gravitational field. This can be rewritten as

$$\Delta t = \left(1 - \frac{2GMr}{r^2 c^2}\right)^{-\frac{1}{2}} \Delta t_0 \, , \tag{2.69}$$

where the term GM/r^2 is an acceleration a equal to g for $r = R$, the earth's radius, and finally

$$\Delta t = \left(1 - \frac{2ar}{c^2}\right)^{-\frac{1}{2}} \Delta t_0 \, . \tag{2.70}$$

By the equivalence principle, this is also the time dilation in an accelerated frame of reference. For small accelerations, using the first few terms of the Taylor expansion, this time dilation expression can be written as

$$\Delta t \simeq \left(1 + \frac{ar}{c^2}\right) \Delta t_0 \, . \tag{2.71}$$

The impact of acceleration on time dilation for small acceleration will usually be small due to the c^{-2} dependency.

We note in particular the expressions for centripetal acceleration $a = v^2/r$ in the case of circular motion

$$\Delta t = \left(1 - \frac{2v^2}{c^2}\right)^{-\frac{1}{2}} \Delta t_0 \, , \tag{2.72}$$

which becomes for small accelerations, again using the first few terms of the Taylor expansion,

$$\Delta t \simeq \left(1 + \frac{v^2}{c^2}\right) \Delta t_0 \,. \tag{2.73}$$

In this case, the impact can be significant, of the same order as the relativistic Lorentz time dilation. Hence there is no doubt that accelerated frames of reference also undergo time dilation compared to unaccelerated (inertial) frames of reference.

§2.7.3 *The consequences of acceleration in special relativity*

The presence of acceleration in a frame of reference provides a means of determining the motion of that frame of reference as acceleration can be easily detected compared to constant velocity which cannot. Whereas in an inertial frame of reference there is no way of determining one's velocity, this limitation disappears in accelerated frames of reference.

Physical time dilation due to acceleration is a reality, as is physical space contraction, which, from (2.67), is seen to have the inverse of the functional form of (2.70), to give the acceleration space contraction relation

$$\Delta x = \left(1 - \frac{2ar}{c^2}\right)^{\frac{1}{2}} \Delta x_0 \tag{2.74}$$

which for small accelerations, using the first few terms of the Taylor expansion, becomes

$$\Delta x \simeq \left(1 - \frac{ar}{c^2}\right) \Delta x_0 \,. \tag{2.75}$$

Till now, we have not discussed the so-called "twin paradox" of special relativity. This is not truly a paradox for there is no way to avoid acceleration in the problem and it is thus not a special relativity problem. Assume that by some miracle we have twins moving at constant velocity with respect to one another from departure to return with no acceleration and that they are able to compare their age. It is important to notice that in their inertial frames of reference, both proper times $d\tau$, the one in the frame of reference at rest with the earth, and the one in the frame of reference at rest with the spaceship, are equal to the physical time in both the frame of reference at rest with the earth and the frame of reference at rest with the spaceship. From the earth, it looks like the spaceship's time is dilated, and from the spaceship, it

looks like the earth's time is dilated. It doesn't matter as the time dilation in one location as seen from the other location is apparent as seen in [248]. When the spaceship comes back to earth, the twins would see that indeed they have the same age.

The problem can be recast in a simpler fashion. Suppose instead of the earth and a spaceship, we have two spaceships moving at constant relativistic speed with respect to one another from start to finish with no acceleration, and that the twins are able to compare their age at the start and the finish. One spaceship moves slowly because of engine problems, while the other moves at relativistic speeds. The resolution would be as described in the previous paragraph: the twins would see that indeed they have the same age at the finish.

The complication in this problem is that forces have to be applied to accelerate the spaceship, then decelerate it to turn around, accelerate it again and finally decelerate it when it comes back to the earth. The problem then needs to be treated using accelerated frames of reference for those periods on the spaceship. As we have seen in section §2.7.2, because of time dilation in accelerated frames of reference, the astronaut will age less than its earth-bound twin, but only during periods of acceleration. During periods of unaccelerated constant velocity travel, there will be no differential aging between the twins. However, the earth-bound twin is itself in an accelerated frame of reference the whole time, so its time will also be dilated. The details of who is older and younger will depend on the details of the acceleration periods, with the earth-bound twin's time dilation depending on (2.68) and (2.72), and the spaceship-bound twin's time dilation depending on (2.70).

Comparing how these findings line up with the results of Hafele's circumglobal experiment [145, 146], it is important to note that Hafele's experiment was done the whole time in a non-inertial accelerated frame of reference. Its results were corrected for gravitational time dilation and centripetal acceleration time dilation, the latter correction clearly showing that acceleration has an impact on special relativity. The centripetal acceleration time dilation correction used by Hafele *et al* [145] is similar to (2.72). One side effect of the experiment being conducted in gravitational and accelerated frames of reference is that it was possible to determine their motion, contrary to special relativity. The Lorentz time dilation would then become a real effect in this purported test of the "twin paradox". There was no symmetry in the relative motions that would have seen the plane stationary and the earth moving given that gravitational and centripetal accelerations clearly showed who was moving and at what velocity.

Hence we find that acceleration has an impact in special relativity and needs to be treated with general relativity. Paradoxes of special relativity such as the "twin paradox" need to be handled with care as there is no way to avoid acceleration in the problem and it is thus not a special relativity problem. Indeed because of time dilation in accelerated frames of reference, the differential aging of the twins will depend on the details of the acceleration periods of both twins. During periods of unaccelerated constant velocity travel, there will be no differential aging between the twins. Reviewing how these findings line up with the results of Hafele's circumglobal experiment [145, 146], we find no contradiction.

Chapter 3

Spacetime Wave Equations

§3.1 Kinematic relations

As we have seen previously in section §1.2, the strain $\varepsilon^{\mu\nu}$ can be expressed in terms of the displacement u^{μ} through the kinematic relation [320, see pp. 149–152]:

$$\varepsilon^{\mu\nu} = \tfrac{1}{2}\left(u^{\mu;\nu} + u^{\nu;\mu} + u^{\alpha;\mu}u_{\alpha}{}^{;\nu}\right) \tag{3.1}$$

where the semicolon (;) denotes covariant differentiation. For small displacements, this expression can be linearized to give the symmetric tensor

$$\varepsilon^{\mu\nu} = \tfrac{1}{2}\left(u^{\mu;\nu} + u^{\nu;\mu}\right) = u^{(\mu;\nu)} \tag{3.2}$$

where the parentheses around the indices of $u^{(\mu;\nu)}$ denote a symmetric combination of the indices. We use the small displacement approximation in this analysis.

An antisymmetric tensor $\omega^{\mu\nu}$ can also be defined from the displacement u^{μ}. This tensor is called the *rotation tensor* and is defined as [320]:

$$\omega^{\mu\nu} = \tfrac{1}{2}\left(u^{\mu;\nu} - u^{\nu;\mu}\right) = u^{[\mu;\nu]} \tag{3.3}$$

where the square brackets around the indices of $u^{[\mu;\nu]}$ denote an antisymmetric combination of the indices.

Where needed, displacements in expressions derived from (3.2) will be written as $u_{\parallel}$ while displacements in expressions derived from (3.3) will be written as $u_{\perp}$. Using different symbolic subscripts for these displacements provides a reminder that symmetric displacements are along the direction of motion (longitudinal), while antisymmetric displacements are perpendicular to the direction of motion (transverse).

In general, we have [320]

$$u^{\mu;\nu} = \varepsilon^{\mu\nu} + \omega^{\mu\nu} \tag{3.4}$$

where the tensor $u^{\mu;\nu}$ is a combination of symmetric and antisymmetric tensors. Lowering index ν and contracting, we get the volume dilatation of the spacetime continuum

$$u^{\mu}{}_{;\mu} = \varepsilon^{\mu}{}_{\mu} = u_{\parallel}{}^{\mu}{}_{;\mu} = \varepsilon \tag{3.5}$$

where the relation

$$\omega^{\mu}{}_{\mu} = u_{\perp}{}^{\mu}{}_{;\mu} = 0 \tag{3.6}$$

has been used.

§3.2 Dynamic equations

In this section, we consider the dynamics of the spacetime continuum, more specifically its elastodynamic equations given that the spacetime continuum is modelled as a linear elastic continuum obeying Hooke's law. In general, a volume (or body) force X^{ν} may be present in the spacetime continuum, representing the forces internal to the continuum.

§3.2.1 *Equilibrium condition*

Under equilibrium conditions, the dynamics of the spacetime continuum is described by the equation [126, see pp. 88–89],

$$T^{\mu\nu}{}_{;\mu} = -X^{\nu} \tag{3.7}$$

where X^{ν} is the volume force. As Wald [362, see p. 286] points out, in general relativity the local energy density of matter as measured by a given observer is well-defined, and the relation

$$T^{\mu\nu}{}_{;\mu} = 0 \tag{3.8}$$

can be taken as expressing local conservation of the energy-momentum of matter. However, it does not in general lead to a global conservation law. The value $X^{\nu} = 0$ is thus taken to represent the macroscopic local case, while (3.7) provides a more general relation.

At the microscopic level, energy is conserved within the limits of the Heisenberg Uncertainty Principle. The volume force may thus be very small, but not exactly zero. It again makes sense to retain the volume force in the equation, and use (3.7) in the general case, while (3.8) can be used at the macroscopic local level, obtained by setting the volume force X^{ν} equal to zero.

§3.2.2 *Dynamic equation*

In three-dimensional space, the dynamic equation is written as [126, see pp. 88–89]

$$T^{ij}{}_{,j} = -X^{i} + \bar{\rho}_0 \ddot{u}^{i} \tag{3.9}$$

where $\bar{\rho}_0$ corresponds to the spacetime continuum density, X^{i} is the volume force, the comma (,) represents differentiation and $\dot{u}$ denotes the

derivative with respect to time. Substituting for $\varepsilon^{\mu\nu} = \frac{1}{2}(u^{\mu;\nu} + u^{\nu;\mu})$ in (2.6), using (2.7) and $u^{\mu}{}_{;\mu} = \varepsilon^{\mu}{}_{\mu} = \varepsilon$ in this equation, we obtain

$$\bar{\mu}_0 \overrightarrow{\nabla}^2 u^i + (\bar{\mu}_0 + \bar{\lambda}_0)\varepsilon^{;i} = -X^i + \bar{\rho}_0 \ddot{u}^i \tag{3.10}$$

which, upon converting the time derivative to indicial notation and rearranging, is written as

$$\bar{\mu}_0 \overrightarrow{\nabla}^2 u^i - \bar{\rho}_0 c^2 u^i{}_{,00} + (\bar{\mu}_0 + \bar{\lambda}_0)\varepsilon^{;i} = -X^i \,. \tag{3.11}$$

We use the arrow above the nabla symbol to indicate the three-dimensional gradient whereas the four-dimensional gradient is written with no arrow. Using the relation [238]

$$c = \sqrt{\frac{\bar{\mu}_0}{\bar{\rho}_0}} \tag{3.12}$$

in the above, (3.11) becomes

$$\bar{\mu}_0(\overrightarrow{\nabla}^2 u^i - u^i{}_{,00}) + (\bar{\mu}_0 + \bar{\lambda}_0)\varepsilon^{;i} = -X^i \tag{3.13}$$

and, combining the space and time derivatives, we obtain

$$\bar{\mu}_0 \nabla^2 u^i + (\bar{\mu}_0 + \bar{\lambda}_0)\varepsilon^{;i} = -X^i \,. \tag{3.14}$$

This equation is the space portion of the *STCED displacement wave equation* (3.18)

$$\bar{\mu}_0 \nabla^2 u^\nu + (\bar{\mu}_0 + \bar{\lambda}_0)\varepsilon^{;\nu} = -X^\nu \,.$$

Hence the dynamics of the spacetime continuum is described by the dynamic equation (3.7), which includes the accelerations from the applied forces.

§3.3 Displacement wave equation

We derive the *STCED* displacement wave equation from the stress-strain relation (2.6) for the spacetime continuum. Substituting for $T^{\mu\nu}$ from (2.6), (3.7) becomes

$$2\bar{\mu}_0 \varepsilon^{\mu\nu}{}_{;\mu} + \bar{\lambda}_0 g^{\mu\nu}\varepsilon_{;\mu} = -X^\nu \tag{3.15}$$

and, using (3.2),

$$\bar{\mu}_0(u^{\mu;\nu}{}_{\mu} + u^{\nu;\mu}{}_{\mu}) + \bar{\lambda}_0 \varepsilon^{;\nu} = -X^\nu. \tag{3.16}$$

Interchanging the order of differentiation in the first term and using (3.5) to express ε in terms of u, this equation simplifies to

$$\bar{\mu}_0 u^{\nu;\mu}{}_{\mu} + (\bar{\mu}_0 + \bar{\lambda}_0) u^{\mu}{}_{;\mu}{}^{\nu} = -X^{\nu} \tag{3.17}$$

which can also be written as

$$\boxed{\bar{\mu}_0 \nabla^2 u^{\nu} + (\bar{\mu}_0 + \bar{\lambda}_0) \varepsilon^{;\nu} = -X^{\nu}}\,. \tag{3.18}$$

This is the *displacement wave equation* seen in the previous section §3.2.2.

In the case where there is no volume force ($X^{\nu} = 0$), we obtain the macroscopic displacement wave equation

$$\nabla^2 u^{\nu} = -\frac{\bar{\mu}_0 + \bar{\lambda}_0}{\bar{\mu}_0}\, \varepsilon^{;\nu}\,. \tag{3.19}$$

where ∇^2 is the four-dimensional operator and again the semi-colon (;) represents covariant differentiation. This equation has stationary solutions ($\partial_t u^{\nu} = 0$) for $-\infty < x, y, z < \infty$ [292, see p. 544]:

$$\begin{aligned} u^{\nu}(x,y,z) &= \frac{1}{4\pi}\, \frac{\bar{\mu}_0 + \bar{\lambda}_0}{\bar{\mu}_0} \\ &\times \iiint_{-\infty}^{+\infty} \frac{\varepsilon^{;\nu}(\xi,\eta,\zeta)\; d\xi d\eta d\zeta}{\sqrt{(x-\xi)^2 + (y-\eta)^2 + (z-\zeta)^2}}\,. \end{aligned} \tag{3.20}$$

The general time-dependent solutions for $-\infty < x, y, z < \infty$ are given by [292, see p. 412]:

$$\begin{aligned} u^{\nu}(x,y,z,t) &= \frac{1}{4\pi}\, \frac{\bar{\mu}_0 + \bar{\lambda}_0}{\bar{\mu}_0} \\ &\times \iiint_{r \le ct} \frac{1}{r}\; \varepsilon^{;\nu}(\xi,\eta,\zeta, t - r/c)\; d\xi d\eta d\zeta \\ &+ \frac{1}{4\pi c}\, \frac{\partial}{\partial t} \iint_{r=ct} \frac{f^{\nu}(\xi,\eta,\zeta)}{r}\; dS \\ &+ \frac{1}{4\pi c} \iint_{r=ct} \frac{g^{\nu}(\xi,\eta,\zeta)}{r}\; dS \end{aligned} \tag{3.21}$$

where

$$r = \sqrt{(\xi - x)^2 + (\eta - y)^2 + (\zeta - z)^2}$$

$$f^\nu(x, y, z) = u^\nu|_{t=0}$$

$$g^\nu(x, y, z) = \partial_t u^\nu|_{t=0}$$

and where the integration is performed over the surface of the sphere ($r = ct$) and the volume of the sphere ($r \leq ct$) with center at (x, y, z).

The R.H.S. of (3.19) is a source term, proportional to a current-like term $\varepsilon^{;\nu}$ which we call the *dilatation current* written as ξ^ν (not the same as coordinate ξ used in (3.20) and (3.21))

$$\boxed{\xi^\nu = \varepsilon^{;\nu} = \nabla\xi}\,. \tag{3.22}$$

Eq. (3.19) then becomes

$$\nabla^2 u^\nu = -\frac{\bar{\mu}_0 + \bar{\lambda}_0}{\bar{\mu}_0}\,\xi^\nu \tag{3.23}$$

and the general displacement wave equation (3.18) with a non-zero volume force becomes

$$\bar{\mu}_0 \nabla^2 u^\nu + (\bar{\mu}_0 + \bar{\lambda}_0)\,\xi^\nu = -X^\nu\,. \tag{3.24}$$

Eqs. (3.23) and (3.24) can be separated into longitudinal and transverse components. Separating u^ν into a longitudinal (irrotational) component $u^\nu_\parallel$ and a transverse (solenoidal) component $u^\nu_\perp$ using the Helmholtz theorem in four dimensions [378] according to

$$u^\nu = u^\nu_\parallel + u^\nu_\perp\,, \tag{3.25}$$

and similarly for the separation of the dilatation current ξ^ν into a longitudinal (irrotational) component $\xi^\nu_\parallel$ and a transverse (solenoidal) component $\xi^\nu_\perp$

$$\xi^\nu = \xi^\nu_\parallel + \xi^\nu_\perp\,, \tag{3.26}$$

and the volume force X^ν into a longitudinal (irrotational) component $X^\nu_\parallel$ and a transverse (solenoidal) component $X^\nu_\perp$

$$X^\nu = X^\nu_\parallel + X^\nu_\perp\,, \tag{3.27}$$

the displacement wave equation (3.24) with a volume force can be separated into a longitudinal displacement equation

$$\bar{\mu}_0 \nabla^2 u^\nu_\parallel = -(\bar{\mu}_0 + \bar{\lambda}_0)\,\xi^\nu_\parallel - X^\nu_\parallel \tag{3.28}$$

and a transverse displacement equation

$$\nabla^2 u^\nu_\perp = -\frac{\bar{\mu}_0 + \bar{\lambda}_0}{\bar{\mu}_0}\, \xi^\nu_\perp - \frac{1}{\bar{\mu}_0}\, X^\nu_\perp \tag{3.29}$$

which, in the absence of a current ($\xi^\nu_\perp = 0$), becomes

$$\nabla^2 u^\nu_\perp = -\frac{1}{\bar{\mu}_0}\, X^\nu_\perp \,. \tag{3.30}$$

These equations correspond to a wave and a particle displacement equation respectively, and hence displacement equations (3.23) and (3.24) include wave-particle duality in their formulation.

§3.4 Continuity equation

We derive a continuity equation for *STC* deformations. Taking the divergence of (3.4), we obtain

$$u^{\mu;\nu}{}_{\mu} = \varepsilon^{\mu\nu}{}_{;\mu} + \omega^{\mu\nu}{}_{;\mu}. \tag{3.31}$$

Interchanging the order of partial differentiation in the first term, and using (3.5) to express u in terms of ε, this equation simplifies to

$$\boxed{\varepsilon^{\mu\nu}{}_{;\mu} + \omega^{\mu\nu}{}_{;\mu} = \varepsilon^{;\nu} = \xi^\nu}\,. \tag{3.32}$$

Hence the divergence of the strain and rotation tensors equals the gradient of the massive volume dilatation, the dilatation current, which acts as a source term. This is the continuity equation for deformations of the spacetime continuum.

§3.5 Field wave equations

We now obtain a series of specialized field wave equations from the displacement wave equation.

§3.5.1 *Dilatational (longitudinal) wave equation*

Taking the divergence of (3.17) and interchanging the order of partial differentiation in the first term, we obtain

$$(2\bar{\mu}_0 + \bar{\lambda}_0) u^\mu{}_{;\mu}{}^\nu{}_\nu = -X^\nu{}_{;\nu}\,. \tag{3.33}$$

Using (3.5) to express u in terms of ε, this equation simplifies to

$$(2\bar{\mu}_0 + \bar{\lambda}_0) \varepsilon^{;\nu}{}_\nu = -X^\nu{}_{;\nu} \tag{3.34}$$

or

$$\boxed{(2\bar{\mu}_0 + \bar{\lambda}_0)\nabla^2\varepsilon = -X^{\nu}{}_{;\nu}}. \tag{3.35}$$

In the case where there is no volume force ($X^\nu = 0$), we obtain the macroscopic longitudinal wave equation

$$(2\bar{\mu}_0 + \bar{\lambda}_0)\nabla^2\varepsilon = 0. \tag{3.36}$$

The volume dilatation ε satisfies a wave equation known as the dilatational wave equation [320, see p. 260]. The solutions of the homogeneous equation are dilatational waves which are longitudinal waves, propagating along the direction of motion. Dilatations thus propagate in the spacetime continuum as longitudinal waves.

§3.5.2 *Rotational (transverse) wave equation*

Differentiating (3.17) with respect to x^α, we obtain

$$\bar{\mu}_0 u^{\nu;\mu}{}_{\mu}{}^{\alpha} + (\bar{\mu}_0 + \bar{\lambda}_0)u^{\mu}{}_{;\mu}{}^{\nu\alpha} = -X^{\nu;\alpha}. \tag{3.37}$$

Interchanging the dummy indices ν and α, and subtracting the resulting equation from (3.37), we obtain the relation

$$\bar{\mu}_0(u^{\nu;\mu}{}_{\mu}{}^{\alpha} - u^{\alpha;\mu}{}_{\mu}{}^{\nu}) = -(X^{\nu;\alpha} - X^{\alpha;\nu}). \tag{3.38}$$

Interchanging the order of partial differentiations and using the definition of the rotation tensor $\omega^{\nu\alpha}$ of (3.3), the following wave equation is obtained:

$$\boxed{\bar{\mu}_0\nabla^2\omega^{\mu\nu} = -X^{[\mu;\nu]}} \tag{3.39}$$

where $X^{[\mu;\nu]}$ is the antisymmetric component of the gradient of the volume force defined as

$$X^{[\mu;\nu]} = \tfrac{1}{2}(X^{\mu;\nu} - X^{\nu;\mu})\,. \tag{3.40}$$

In the case where there is no volume force ($X^\nu = 0$), we obtain the macroscopic transverse wave equation

$$\bar{\mu}_0\nabla^2\omega^{\mu\nu} = 0. \tag{3.41}$$

The rotation tensor $\omega^{\mu\nu}$ satisfies a wave equation known as the rotational wave equation [320, see p. 260]. The solutions of the homogeneous equation are rotational waves which are transverse waves, propagating perpendicular to the direction of motion. Massless waves thus propagate in the spacetime continuum as transverse waves.

§3.5.3 *Strain (symmetric) wave equation*

A corresponding symmetric wave equation can also be derived for the strain $\varepsilon^{\mu\nu}$. Starting from (3.37), interchanging the dummy indices ν and α, adding the resulting equation to (3.37), and interchanging the order of partial differentiation, the following wave equation is obtained:

$$\boxed{\bar{\mu}_0 \nabla^2 \varepsilon^{\mu\nu} + (\bar{\mu}_0 + \bar{\lambda}_0)\varepsilon^{;\mu\nu} = -X^{(\mu;\nu)}} \tag{3.42}$$

where $X^{(\mu;\nu)}$ is the symmetric component of the gradient of the volume force defined as

$$X^{(\mu;\nu)} = \tfrac{1}{2}(X^{\mu;\nu} + X^{\nu;\mu})\,. \tag{3.43}$$

In the case where there is no volume force ($X^{\nu} = 0$), we obtain the macroscopic symmetric wave equation

$$\nabla^2 \varepsilon^{\mu\nu} = -\frac{\bar{\mu}_0 + \bar{\lambda}_0}{\bar{\mu}_0}\, \varepsilon^{;\mu\nu}. \tag{3.44}$$

This strain wave equation is similar to the displacement wave equation (3.19).

§3.6 Spin analysis of the wave equations

We thus find that deformations propagate in the spacetime continuum by longitudinal and transverse wave displacements. As mentioned previously, this is in keeping with wave-particle duality, with the transverse mode corresponding to the wave aspects and the longitudinal mode corresponding to the particle aspects.

We consider the spin of the scalar, vector and tensor fields for the wave equations derived in this chapter [124, p, 31]. We note that as seen in Chapter 1, (1.16) to (1.18), the strain tensor $\varepsilon^{\mu\nu}$ can be separated into the traceless, and hence massless, part of $\varepsilon^{\mu\nu}$ of spin 2 given by [199, p. 753]

$$\boxed{\varepsilon^{\mu\nu}_{(2)} = e^{\mu\nu} = \varepsilon^{\mu\nu} - \tfrac{1}{4}\,\delta^{\mu\nu}\varepsilon} \tag{3.45}$$

and the trace, and hence massive, part of $\varepsilon^{\mu\nu}$ of spin 0 given by

$$\boxed{\varepsilon^{\mu\nu}_{(0)} = e_s \delta^{\mu\nu} = \tfrac{1}{4}\,\delta^{\mu\nu}\varepsilon}\,. \tag{3.46}$$

The rotation tensor $\omega^{\mu\nu}$ of (3.3) can be written as a rotation vector, also known as the spin vector ω^{μ} given by

$$\omega^{\mu} = \tfrac{1}{2}\,\epsilon^{\mu\alpha\beta}\,\omega_{\alpha\beta}\,. \tag{3.47}$$

The trace of the antisymmetric field $\omega^{\mu\nu}$ is zero, and hence massless. The field $\omega^{\mu\nu}$ is of spin 1, and since it is massless, it does not have a spin 0 component. This field will be studied in more details in Chapter 4 and will be seen to correspond to electromagnetism.

From (3.4), *viz.*

$$u^{\mu;\nu} = \varepsilon^{\mu\nu} + \omega^{\mu\nu}\,,$$

we can write $u^{\mu;\nu}$ as a combination of spin 0, 1 and 2 fields. From (3.45) and (3.46),

$$\begin{aligned} \varepsilon^{\mu\nu} &= e^{\mu\nu} + \tfrac{1}{4}\,\delta^{\mu\nu}\varepsilon \\ &= \varepsilon^{\mu\nu}_{(2)} + \varepsilon^{\mu\nu}_{(0)} \end{aligned} \tag{3.48}$$

and from (3.47),

$$\omega^{\mu\nu}_{(1)} = \tfrac{1}{2}\,\epsilon^{\mu\nu\alpha}\,\omega_\alpha\,. \tag{3.49}$$

Then

$$\boxed{u^{\mu;\nu} = \varepsilon^{\mu\nu}_{(0)} + \varepsilon^{\mu\nu}_{(2)} + \omega^{\mu\nu}_{(1)}}\,, \tag{3.50}$$

i.e. a combination of spin 0 (mass as deformation particle aspect), spin 1 (electromagnetism) and spin 2 (deformation wave aspect). Substituting from (3.45), (3.46) and (3.49), (3.50) becomes

$$u^{\mu;\nu} = \tfrac{1}{4}\,\delta^{\mu\nu}\varepsilon + e^{\mu\nu} + \tfrac{1}{2}\,\epsilon^{\mu\nu\alpha}\,\omega_\alpha\,. \tag{3.51}$$

Note that some authors also refer to $u^{\mu;\nu}$ as the *distortion* tensor $\beta^{\mu\nu}$ [77] (see the footnote on page 26 on the terminology used in this book). In this work, we will use $\beta^{\mu\nu}$ when referring specifically to the distortion tensor.

The wave equations derived in this chapter can be further characterized as follows.

§3.6.1 *Scalar field equation*

The dilatational wave equation (3.35) is a nonhomogeneous scalar field equation. The quanta of the scalar field are spin 0 (spinless) particles [124, 141]. The scalar field ε corresponds to the massive particle as per (2.24). Massive particles are longitudinal wave solutions of the dilatational (longitudinal) wave equation, propagating along the direction of motion.

§3.6.2 *Vector field equation*

The displacement wave equation (3.18) is a nonhomogeneous vector field equation. It is similar to the Proca equation for spin-1 particles (massive vector boson). As shown in (3.28) and (3.29), this equation corresponds to both a wave and a particle displacement equation respectively, and hence includes wave-particle duality in its formulation. The Proca equation is considered in more details in section §4.8 in Chapter 4.

§3.6.3 *Massless vector field equation*

The rotational wave equation (3.39) is a nonhomogeneous antisymmetric tensor field equation equivalent to a massless vector wave equation. The quanta of the vector field are equivalent to massless spin 1 transverse waves [141]. The massless transverse waves will be seen to be electromagnetic waves in Chapter 4. The solutions of the rotational (transverse) wave equation are transverse waves, propagating perpendicular to the direction of motion.

§3.6.4 *Symmetric tensor field equation*

The strain wave equation (3.42) is a nonhomogeneous symmetric tensor field equation. The quanta of this tensor field are equivalent to massless transverse waves of spin 2 and, as seen above, massive particles of spin 0 [141] (see section §3.6.1 above). This explains wave-particle duality, with the spin 2 transverse mode corresponding to the wave aspects and the spin 0 longitudinal mode corresponding to the particle aspects. The massless transverse waves of spin 2 are the gravitational waves of General Relativity with the corresponding graviton quanta.

Chapter 4

Electromagnetism in STCED

§4.1 Electromagnetic field strength

Since Einstein first published his General Theory of Relativity in 1915, the problem of the unification of gravitation and electromagnetism has been and remains the subject of continuing investigation (see for example [31, 58, 62, 166, 298, 324, 325, 363, 379] for recent attempts). Einstein himself spent a good part of his remaining years of research on the investigation of Unified Field Theory.

In this chapter, we derive electromagnetism from the Elastodynamics of the Spacetime Continuum. *STCED* is based on the application of a continuum mechanical approach to the spacetime continuum. Electromagnetism is found to come out naturally from the theory in a straightforward manner. While the search has been for a geometric unification, instead, the solution is found to lie in the physical properties of the spacetime continuum, in its displacements from equilibrium. This theory thus provides a unified description of the spacetime deformation processes underlying general relativistic gravitation and electromagnetism, in terms of spacetime continuum displacements resulting from the strains generated by the energy-momentum stress tensor.

In the Elastodynamics of the Spacetime Continuum, the antisymmetric rotation tensor $\omega^{\mu\nu}$ is given by (3.3), *viz.*

$$\omega^{\mu\nu} = \tfrac{1}{2}\left(u^{\mu;\nu} - u^{\nu;\mu}\right) \tag{4.1}$$

where u^μ is the displacement of an infinitesimal element of the spacetime continuum from its unstrained position x^μ. This tensor has the same structure as the electromagnetic field-strength tensor $F^{\mu\nu}$ defined as [176, see p. 550]:

$$F^{\mu\nu} = \partial^\mu A^\nu - \partial^\nu A^\mu \tag{4.2}$$

where A^μ is the electromagnetic potential four-vector $(\phi/c, \boldsymbol{A})$, ϕ is the scalar potential and $\boldsymbol{A}$ the vector potential.

Identifying the rotation tensor $\omega^{\mu\nu}$ with the electromagnetic field-strength tensor according to

$$\boxed{F^{\mu\nu} = \varphi_0 \omega^{\mu\nu}} \tag{4.3}$$

leads to the relation

$$\boxed{A^{\mu} = -\tfrac{1}{2}\,\varphi_0 u^{\mu}_{\perp}} \tag{4.4}$$

where the symbolic subscript $\perp$ of the displacement u^{μ} indicates that the relation holds for a transverse displacement (perpendicular to the direction of motion). The constant of proportionality φ_0 is referred to as the "*STC electromagnetic shearing potential constant*", and it has units of $[\mathrm{V}\cdot\mathrm{s}\cdot\mathrm{m}^{-2}]$ or equivalently [T].

Due to the difference in the definition of $\omega^{\mu\nu}$ and $F^{\mu\nu}$ with respect to their indices, a negative sign is introduced, and is attributed to (4.4). This relation provides a physical explanation of the electromagnetic potential: it arises from transverse (shearing) displacements of the spacetime continuum, in contrast to mass which arises from longitudinal (dilatational) displacements of the spacetime continuum. Sheared spacetime is manifested as electromagnetic potentials and fields.

§4.2 Maxwell's equations

Taking the divergence of the rotation tensor of (4.1), gives

$$\omega^{\mu\nu}{}_{;\mu} = \tfrac{1}{2}\,(u^{\mu;\nu}{}_{\mu} - u^{\nu;\mu}{}_{\mu}). \tag{4.5}$$

Recalling (3.17), *viz.*

$$\bar{\mu}_0 u^{\nu;\mu}{}_{\mu} + (\bar{\mu}_0 + \bar{\lambda}_0) u^{\mu}{}_{;\mu}{}^{\nu} = -X^{\nu}$$

where X^{ν} is the volume force and $\bar{\lambda}_0$ and $\bar{\mu}_0$ are the Lamé elastic constants of the spacetime continuum, substituting for $u^{\nu;\mu}{}_{\mu}$ from (3.17) into (4.5), interchanging the order of partial differentiation in $u^{\mu;\nu}{}_{\mu}$ in (4.5), and using the relation $u^{\mu}{}_{;\mu} = \varepsilon^{\mu}{}_{\mu} = \varepsilon$ from (3.5), we obtain

$$\omega^{\mu\nu}{}_{;\mu} = \frac{2\bar{\mu}_0 + \bar{\lambda}_0}{2\bar{\mu}_0}\,\varepsilon^{;\nu} + \frac{1}{2\bar{\mu}_0}\,X^{\nu}. \tag{4.6}$$

As seen previously in section §3.2, in the macroscopic local case, the volume force X^{ν} is set equal to zero to obtain the macroscopic relation

$$\omega^{\mu\nu}{}_{;\mu} = \frac{2\bar{\mu}_0 + \bar{\lambda}_0}{2\bar{\mu}_0}\,\varepsilon^{;\nu} \tag{4.7}$$

Using (4.3) in (4.7), we obtain

$$F^{\mu\nu}{}_{;\mu} = \varphi_0\,\frac{2\bar{\mu}_0 + \bar{\lambda}_0}{2\bar{\mu}_0}\,\varepsilon^{;\nu}\,. \tag{4.8}$$

§4.3 Current density four-vector

Comparing (4.8) with the covariant form of Maxwell's equations [59, see pp. 42–43]

$$F^{\mu\nu}{}_{;\mu} = \mu_0 j^\nu \tag{4.9}$$

where j^ν is the current density four-vector $(c\varrho, \boldsymbol{j})$, ϱ is the charge density scalar, and $\boldsymbol{j}$ is the current density vector, we obtain the following relation for the current density four-vector j^ν

$$\boxed{j^\nu = \frac{\varphi_0}{\mu_0}\,\frac{2\bar{\mu}_0 + \bar{\lambda}_0}{2\bar{\mu}_0}\,\varepsilon^{;\nu}} \tag{4.10}$$

or, in terms of the dilatation current ξ^ν,

$$j^\nu = \frac{\varphi_0}{\mu_0}\,\frac{2\bar{\mu}_0 + \bar{\lambda}_0}{2\bar{\mu}_0}\,\xi^\nu\,. \tag{4.11}$$

(Note the difference between μ_0 and $\bar{\mu}_0$ as discussed under "A note on spacetime continuum constants" in the Preface.) This relation provides a physical explanation of the current density four-vector: it arises from the 4-gradient of the volume dilatation of the spacetime continuum (the dilatation current). A corollary of this relation is that massless (transverse) waves cannot carry an electric charge.

Substituting for j^ν from (4.10) in the relation [14, see p. 94]

$$j^\nu j_\nu = \varrho^2 c^2, \tag{4.12}$$

we obtain the expression for the charge density

$$\boxed{\varrho = \frac{1}{2}\,\frac{\varphi_0}{\mu_0 c}\,\frac{2\bar{\mu}_0 + \bar{\lambda}_0}{2\bar{\mu}_0}\,\sqrt{\varepsilon^{;\nu}\varepsilon_{;\nu}}} \tag{4.13}$$

or, using the relation $c = 1/\sqrt{\epsilon_0\mu_0}$,

$$\varrho = \frac{1}{2}\,\varphi_0\epsilon_0 c\,\frac{2\bar{\mu}_0 + \bar{\lambda}_0}{2\bar{\mu}_0}\,\sqrt{\varepsilon^{;\nu}\varepsilon_{;\nu}}\,. \tag{4.14}$$

Up to now, our identification of the rotation tensor $\omega^{\mu\nu}$ of the Elastodynamics of the Spacetime Continuum with the electromagnetic field-strength tensor $F^{\mu\nu}$ has generated consistent results, with no contradictions.

§4.4 Lorenz condition

The Lorenz condition can be derived directly from the theory. Taking the divergence of (4.4), we obtain

$$A^{\mu}{}_{;\mu} = -\tfrac{1}{2}\,\varphi_0 u_{\perp}{}^{\mu}{}_{;\mu}. \tag{4.15}$$

From (3.6), (4.15) simplifies to

$$A^{\mu}{}_{;\mu} = 0. \tag{4.16}$$

The Lorenz condition is thus obtained directly from the theory. The reason for the value of zero is that transverse displacements are massless because such displacements arise from a change of shape (distortion) of the spacetime continuum, not a change of volume (dilatation).

§4.5 Four-vector potential

Substituting (4.4) into (4.5) and rearranging terms, we obtain the equation

$$\nabla^2 A^{\nu} - A^{\mu;\nu}{}_{\mu} = \varphi_0\,\omega^{\mu\nu}{}_{;\mu} \tag{4.17}$$

and, using (4.3) and (4.9), this equation becomes

$$\nabla^2 A^{\nu} - A^{\mu;\nu}{}_{\mu} = \mu_0\, j^{\nu}. \tag{4.18}$$

which is similar to the Proca equation to be considered in more details in section §4.8.

Interchanging the order of partial differentiation in the term $A^{\mu;\nu}{}_{\mu}$ and using the Lorenz condition of (4.16), we obtain the well-known wave equation for the four-vector potential [59, see pp. 42–43]

$$\nabla^2 A^{\nu} = \mu_0\, j^{\nu}. \tag{4.19}$$

The results we obtain are thus consistent with the macroscopic theory of electromagnetism, with no contradictions.

§4.6 Electromagnetism and the STC volume force

We now investigate the impact of the volume force X^{ν} on the equations of electromagnetism. Recalling (4.6), Maxwell's equation in terms of the rotation tensor is given by

$$\omega^{\mu\nu}{}_{;\mu} = \frac{2\bar{\mu}_0 + \bar{\lambda}_0}{2\bar{\mu}_0}\,\varepsilon^{;\nu} + \frac{1}{2\bar{\mu}_0}\,X^{\nu}. \tag{4.20}$$

Substituting for $\omega^{\mu\nu}$ from (4.3), this equation becomes

$$F^{\mu\nu}{}_{;\mu} = \varphi_0 \frac{2\bar{\mu}_0 + \bar{\lambda}_0}{2\bar{\mu}_0} \varepsilon^{;\nu} + \frac{\varphi_0}{2\bar{\mu}_0} X^\nu. \tag{4.21}$$

The additional X^ν term can be allocated in one of two ways:

1. either j^ν remains unchanged as given by (4.10) and the expression for $F^{\mu\nu}{}_{;\mu}$ has an additional term as developed in the first section below;
2. or $F^{\mu\nu}{}_{;\mu}$ remains unchanged as given by (4.9) and the expression for j^ν has an additional term as developed in the second section below.

Option 2 is shown in the following derivation to be the logically consistent approach.

§4.6.1 j^ν unchanged (contradiction)

Using (4.10) into (4.21), Maxwell's equation becomes (j^ν unchanged)

$$F^{\mu\nu}{}_{;\mu} = \mu_0 j^\nu + \frac{\varphi_0}{2\bar{\mu}_0} X^\nu. \tag{4.22}$$

Using (4.20) into (4.17) and making use of the Lorenz condition, the wave equation for the four-vector potential becomes

$$\nabla^2 A^\nu - \frac{\varphi_0}{2\bar{\mu}_0} X^\nu = \mu_0 j^\nu. \tag{4.23}$$

In this case, the equations for $F^{\mu\nu}{}_{;\mu}$ and A^ν both contain an additional term proportional to X^ν.

We show that this option is not logically consistent as follows. Using (4.10) into the continuity condition for the current density [59]

$$\partial_\nu j^\nu = 0 \tag{4.24}$$

yields the expression

$$\nabla^2 \varepsilon = 0. \tag{4.25}$$

This equation is valid in the macroscopic case where $X^\nu = 0$, but disagrees with the general case (non-zero X^ν) given by (3.35), *viz.*

$$(2\bar{\mu}_0 + \bar{\lambda}_0)\nabla^2 \varepsilon = -X^\nu{}_{;\nu}.$$

The analysis in this section leads to a contradiction and consequently is not valid.

§4.6.2 $F^{\mu\nu}{}_{;\mu}$ unchanged (logically consistent)

Proper treatment of the general case requires that the current density four-vector be proportional to the RHS of (4.21) as follows ($F^{\mu\nu}{}_{;\mu}$ unchanged):

$$\mu_0\, j^\nu = \varphi_0\, \frac{2\bar{\mu}_0 + \bar{\lambda}_0}{2\bar{\mu}_0}\, \varepsilon^{;\nu} + \frac{\varphi_0}{2\bar{\mu}_0}\, X^\nu. \tag{4.26}$$

This yields the following general form of the current density four-vector:

$$\boxed{j^\nu = \frac{1}{2}\, \frac{\varphi_0}{\mu_0\, \bar{\mu}_0} \left[(2\bar{\mu}_0 + \bar{\lambda}_0)\, \varepsilon^{;\nu} + X^\nu \right]}. \tag{4.27}$$

Using this expression in the continuity condition for the current density given by (4.24) yields (3.35) as required.

Using (4.27) into (4.21) yields the same covariant form of the Maxwell equations as in the macroscopic case:

$$F^{\mu\nu}{}_{;\mu} = \mu_0\, j^\nu \tag{4.28}$$

and the same four-vector potential equation

$$\nabla^2 A^\nu = \mu_0\, j^\nu \tag{4.29}$$

in the Lorenz gauge.

§4.7 Homogeneous Maxwell equation

The validity of this analysis can be further demonstrated from the homogeneous Maxwell equation [59]

$$\partial^\alpha F^{\beta\gamma} + \partial^\beta F^{\gamma\alpha} + \partial^\gamma F^{\alpha\beta} = 0. \tag{4.30}$$

Taking the divergence of this equation over α,

$$\partial_\alpha \partial^\alpha F^{\beta\gamma} + \partial_\alpha \partial^\beta F^{\gamma\alpha} + \partial_\alpha \partial^\gamma F^{\alpha\beta} = 0. \tag{4.31}$$

Interchanging the order of differentiation in the last two terms and making use of (4.28) and the antisymmetry of $F^{\mu\nu}$, we obtain

$$\nabla^2 F^{\beta\gamma} + \mu_0 (j^{\beta;\gamma} - j^{\gamma;\beta}) = 0. \tag{4.32}$$

Substituting for j^ν from (4.27),

$$\nabla^2 F^{\beta\gamma} = -\frac{\varphi_0}{2\bar{\mu}_0} \left[(2\bar{\mu}_0 + \bar{\lambda}_0)(\varepsilon^{;\beta\gamma} - \varepsilon^{;\gamma\beta}) + (X^{\beta;\gamma} - X^{\gamma;\beta}) \right]. \tag{4.33}$$

Equation (3.42), *viz.*

$$\bar{\mu}_0 \nabla^2 \varepsilon^{\mu\nu} + (\bar{\mu}_0 + \bar{\lambda}_0)\varepsilon^{;\mu\nu} = -X^{(\mu;\nu)}$$

shows that $\varepsilon^{;\mu\nu}$ is a symmetric tensor. Consequently the difference term $(\varepsilon^{;\beta\gamma} - \varepsilon^{;\gamma\beta})$ disappears and (4.33) becomes

$$\nabla^2 F^{\beta\gamma} = -\frac{\varphi_0}{2\bar{\mu}_0}\,(X^{\beta;\gamma} - X^{\gamma;\beta}). \tag{4.34}$$

Expressing $F^{\mu\nu}$ in terms of $\omega^{\mu\nu}$ using (4.3), the resulting equation is identical to (3.39), *viz.*

$$\bar{\mu}_0 \nabla^2 \omega^{\mu\nu} = -X^{[\mu;\nu]}$$

confirming the validity of this analysis of electromagnetism including the volume force.

Equations (4.27) to (4.29) are the self-consistent electromagnetic equations derived from the Elastodynamics of the Spacetime Continuum with the volume force. In conclusion, Maxwell's equations remain unchanged. The current density four-vector is the only quantity affected by the volume force, with the addition of a second term proportional to the volume force.

It is interesting to note that the current density obtained from the quantum mechanical Klein-Gordon equation with an electromagnetic field also consists of the sum of two terms [141, see p. 35]. We will return to this peculiarity in section §7.1.

§4.8 Proca-like equation

As discussed previously in section §3.6.2, the displacement wave equation (3.18) is similar to a Proca-like vector field equation. In the macroscopic case where the volume force X^ν is equal to zero, one obtains the classical four-vector potential wave equation (4.19).

However, in the case of a non-zero volume force as is expected at the quantum level, an additional term is present in (4.18). We show this by substituting the general form of the current density four-vector (4.26) into (4.18):

$$\nabla^2 A^\nu - A^{\mu;\nu}{}_{\mu} = \varphi_0\,\frac{2\bar{\mu}_0 + \bar{\lambda}_0}{2\bar{\mu}_0}\,\varepsilon^{;\nu} + \frac{\varphi_0}{2\bar{\mu}_0}\,X^\nu\,. \tag{4.35}$$

The first term on the R.H.S. is written as the classical current density four-vector

$$\mu_0\, j^{\nu}_{classical} = \varphi_0\,\frac{2\bar{\mu}_0 + \bar{\lambda}_0}{2\bar{\mu}_0}\,\varepsilon^{;\nu}\,. \tag{4.36}$$

Using (4.36) into (4.35) and rearranging, we obtain

$$\nabla^2 A^\nu - A^{\mu;\nu}{}_\mu - \frac{\varphi_0}{2\bar{\mu}_0} X^\nu = \mu_0 j^\nu_{classical} \tag{4.37}$$

which includes an additional term on the L.H.S. as found in the Proca equation.

In Chapter 7, we will derive a quantum mechanical volume force which will be seen to be of the form

$$X^\nu \propto -A^\nu \,. \tag{4.38}$$

Substituting for (4.38) into (4.37), the wave equation for the four-vector potential becomes

$$\nabla^2 A^\nu - A^{\mu;\nu}{}_\mu + K A^\nu = \mu_0 j^\nu_{classical} \tag{4.39}$$

where K is a constant. The second term on the L.H.S. of the equation can be set to zero using the Lorenz condition (4.16). The resulting equation is similar to the well-known Proca equation [176] and is investigated further in section §7.3.5.

Chapter 5

Energy in the Spacetime Continuum

§5.1 Strain energy density of the spacetime continuum

Energy in the spacetime continuum is present as strain energy density. This strain energy density is a scalar given by [126, see p. 51]

$$\mathcal{E} = \tfrac{1}{2}\, T^{\alpha\beta}\varepsilon_{\alpha\beta} \tag{5.1}$$

where $\varepsilon_{\alpha\beta}$ is the strain tensor and $T^{\alpha\beta}$ is the energy-momentum stress tensor. Introducing the strain and stress deviators from (1.16) and (1.19), this equation becomes

$$\mathcal{E} = \tfrac{1}{2}\left(t^{\alpha\beta} + t_s g^{\alpha\beta}\right)\left(e_{\alpha\beta} + e_s g_{\alpha\beta}\right). \tag{5.2}$$

Multiplying and using relations $e^{\alpha}{}_{\alpha} = 0$ and $t^{\alpha}{}_{\alpha} = 0$ from the definition of the strain and stress deviators, we obtain

$$\mathcal{E} = \tfrac{1}{2}\left(4t_s e_s + t^{\alpha\beta}e_{\alpha\beta}\right). \tag{5.3}$$

Using (2.9) to express the stresses in terms of the strains, this expression becomes

$$\boxed{\mathcal{E} = \tfrac{1}{2}\,\bar{\kappa}_0\,\varepsilon^2 + \bar{\mu}_0\, e^{\alpha\beta}e_{\alpha\beta}} \tag{5.4}$$

where the Lamé elastic constant of the spacetime continuum $\bar{\mu}_0$ is the shear modulus (the resistance of the continuum to *distortions*) and $\bar{\kappa}_0$ is the bulk modulus (the resistance of the continuum to *dilatations*). Alternatively, again using (2.9) to express the strains in terms of the stresses, this expression can be written as

$$\mathcal{E} = \frac{1}{2\bar{\kappa}_0}\, t_s^2 + \frac{1}{4\bar{\mu}_0}\, t^{\alpha\beta}t_{\alpha\beta}. \tag{5.5}$$

§5.2 Physical interpretation of the strain energy density

We observe in (5.4) and (5.5) that the strain energy density is separated into two terms: the first one expresses the dilatation energy density (the "mass" longitudinal term) while the second one expresses the distortion energy density (the "massless" transverse term):

$$\mathcal{E} = \mathcal{E}_{\parallel} + \mathcal{E}_{\perp} \tag{5.6}$$

where

$$\mathcal{E}_{\parallel} = \frac{1}{2}\,\bar{\kappa}_0 \varepsilon^2 \equiv \frac{1}{2\bar{\kappa}_0}\,t^2 \tag{5.7}$$

and

$$\mathcal{E}_{\perp} = \bar{\mu}_0 e^{\alpha\beta} e_{\alpha\beta} \equiv \frac{1}{4\bar{\mu}_0}\,t^{\alpha\beta} t_{\alpha\beta}. \tag{5.8}$$

Using (2.24) into (5.7), we obtain

$$\mathcal{E}_{\parallel} = \frac{1}{32\,\bar{\kappa}_0}\,\left[\rho c^2\right]^2 = \frac{1}{32\,\bar{\kappa}_0}\,\rho^2 c^4. \tag{5.9}$$

The rest-mass energy density divided by the bulk modulus $\bar{\kappa}_0$, and the transverse energy density divided by the shear modulus $\bar{\mu}_0$, have dimensions of energy density as expected.

Multiplying (5.5) by $32\,\bar{\kappa}_0$ and using (5.9), we obtain

$$32\,\bar{\kappa}_0\,\mathcal{E} = \rho^2 c^4 + 8\,\frac{\bar{\kappa}_0}{\bar{\mu}_0}\,t^{\alpha\beta} t_{\alpha\beta}. \tag{5.10}$$

Noting that $t^{\alpha\beta} t_{\alpha\beta}$ is quadratic in structure, we see that this equation is similar to the energy relation of Special Relativity [214, see p. 51] for energy density

$$\hat{E}^2 = \rho^2 c^4 + \hat{p}^{\,2} c^2 \tag{5.11}$$

where $\hat{E}$ is the total energy density and $\hat{p}$ the momentum density.

The quadratic structure of the energy relation of Special Relativity is thus found to be present in the Elastodynamics of the Spacetime Continuum. Eqs. (5.10) and (5.11) also imply that the kinetic energy pc is carried by the distortion part of the deformation, while the dilatation part carries only the rest-mass energy.

This observation is in agreement with photons which are massless ($\mathcal{E}_{\parallel} = 0$), as will be shown in the next section §5.3, but still carry kinetic energy in the transverse electromagnetic wave distortions ($\mathcal{E}_{\perp} = t^{\alpha\beta} t_{\alpha\beta}/4\bar{\mu}_0$).

As we will see in forthcoming chapters, the dilatation energy density $\mathcal{E}_{\parallel}$ is usually fairly straightforward to calculate as it is proportional to the square of the spacetime continuum volume dilatation ε, which is itself equal to the trace of the strain tensor

$$\varepsilon = \mathrm{Trace}(\varepsilon^{\mu\nu})\,. \tag{5.12}$$

However, the calculation of the distortion energy density $\mathcal{E}_{\perp}$ is usually a time-consuming exercise that results in complicated expressions.

§5.3 Electromagnetic strain energy density

The strain energy density of the electromagnetic energy-momentum stress tensor is now calculated. Starting from the symmetric electromagnetic stress tensor [59, see pp. 64–66]

$$\Theta^{\mu\nu} = \frac{1}{\mu_0}\left(F^{\mu}{}_{\alpha}F^{\alpha\nu} + \frac{1}{4}\,g^{\mu\nu}F^{\alpha\beta}F_{\alpha\beta}\right) \equiv \sigma^{\mu\nu}, \tag{5.13}$$

with $g^{\mu\nu} = \eta^{\mu\nu}$ of signature $(+---)$, and the field-strength tensor components [59, see p. 43]

$$F^{\mu\nu} = \begin{pmatrix} 0 & -E_x/c & -E_y/c & -E_z/c \\ E_x/c & 0 & B_z & -B_y \\ E_y/c & -B_z & 0 & B_x \\ E_z/c & B_y & -B_x & 0 \end{pmatrix} \tag{5.14}$$

and

$$F_{\mu\nu} = \begin{pmatrix} 0 & E_x/c & E_y/c & E_z/c \\ -E_x/c & 0 & B_z & -B_y \\ -E_y/c & -B_z & 0 & B_x \\ -E_z/c & B_y & -B_x & 0 \end{pmatrix}, \tag{5.15}$$

we obtain [59, see p. 66] [258, see p. 141],

$$\begin{aligned} \sigma^{00} &= \tfrac{1}{2}\left(\epsilon_0 E^2 + \tfrac{1}{\mu_0}B^2\right) = \tfrac{1}{2}\,\epsilon_0\left(E^2 + c^2B^2\right) \\ \sigma^{0j} &= \sigma^{j0} = \tfrac{1}{c\mu_0}\,(E\times B)^j = \epsilon_0 c\,(E\times B)^j = \tfrac{1}{c}\,S^j \\ \sigma^{jk} &= -\left(\epsilon_0 E^j E^k + \tfrac{1}{\mu_0}\,B^jB^k\right) + \tfrac{1}{2}\,\delta^{jk}\left(\epsilon_0 E^2 + \tfrac{1}{\mu_0}\,B^2\right) \\ &= -\epsilon_0\left[\left(E^jE^k + c^2B^jB^k\right) - \tfrac{1}{2}\,\delta^{jk}\left(E^2 + c^2B^2\right)\right] \end{aligned} \tag{5.16}$$

where S^j is the Poynting vector, and where we use the notation $\sigma^{\mu\nu} \equiv \Theta^{\mu\nu}$ as a generalization of the σ^{ij} Maxwell stress tensor notation. Hence the electromagnetic stress tensor is given by [59, see p. 66]:

$$\sigma^{\mu\nu} = \begin{pmatrix} \frac{1}{2}\,\epsilon_0\left(E^2 + c^2B^2\right) & S_x/c & S_y/c & S_z/c \\ S_x/c & -\sigma_{xx} & -\sigma_{xy} & -\sigma_{xz} \\ S_y/c & -\sigma_{yx} & -\sigma_{yy} & -\sigma_{yz} \\ S_z/c & -\sigma_{zx} & -\sigma_{zy} & -\sigma_{zz} \end{pmatrix}, \tag{5.17}$$

where σ^{ij} is the Maxwell stress tensor. Using the relation $\sigma_{\alpha\beta} = \eta_{\alpha\mu}\eta_{\beta\nu}\sigma^{\mu\nu}$ to lower the indices of $\sigma^{\mu\nu}$, we obtain

$$\sigma_{\mu\nu} = \begin{pmatrix} \frac{1}{2}\,\epsilon_0\left(E^2 + c^2B^2\right) & -S_x/c & -S_y/c & -S_z/c \\ -S_x/c & -\sigma_{xx} & -\sigma_{xy} & -\sigma_{xz} \\ -S_y/c & -\sigma_{yx} & -\sigma_{yy} & -\sigma_{yz} \\ -S_z/c & -\sigma_{zx} & -\sigma_{zy} & -\sigma_{zz} \end{pmatrix}. \tag{5.18}$$

§5.3.1 *Longitudinal (mass) term*

The longitudinal mass term is calculated from (5.7) and (1.21):

$$\mathcal{E}_{\|} = \frac{1}{2\bar{\kappa}_0}\, t_s^2 = \frac{1}{32\bar{\kappa}_0}\,(\sigma^{\alpha}{}_{\alpha})^2. \tag{5.19}$$

The term $\sigma^{\alpha}{}_{\alpha}$ is calculated from:

$$\begin{aligned} \sigma^{\alpha}{}_{\alpha} &= \eta_{\alpha\beta}\sigma^{\alpha\beta} \\ &= \eta_{\alpha 0}\sigma^{\alpha 0} + \eta_{\alpha 1}\sigma^{\alpha 1} + \eta_{\alpha 2}\sigma^{\alpha 2} + \eta_{\alpha 3}\sigma^{\alpha 3} \\ &= \eta_{00}\sigma^{00} + \eta_{11}\sigma^{11} + \eta_{22}\sigma^{22} + \eta_{33}\sigma^{33}. \end{aligned} \tag{5.20}$$

Substituting from (5.17) and the metric $\eta^{\mu\nu}$ of signature $(+---)$, we obtain:

$$\sigma^{\alpha}{}_{\alpha} = \frac{1}{2}\,\epsilon_0\left(E^2 + c^2B^2\right) + \sigma_{xx} + \sigma_{yy} + \sigma_{zz}. \tag{5.21}$$

Substituting from (5.16), this expands to:

$$\begin{aligned} \sigma^{\alpha}{}_{\alpha} = \tfrac{1}{2}\,\epsilon_0\left(E^2 + c^2B^2\right) + \epsilon_0\left({E_x}^2 + c^2{B_x}^2\right) + \\ + \epsilon_0\left({E_y}^2 + c^2{B_y}^2\right) + \epsilon_0\left({E_z}^2 + c^2{B_z}^2\right) - \\ - \tfrac{3}{2}\,\epsilon_0\left(E^2 + c^2B^2\right) \end{aligned} \tag{5.22}$$

and further,

$$\begin{aligned} \sigma^{\alpha}{}_{\alpha} = \tfrac{1}{2}\,\epsilon_0\left(E^2 + c^2B^2\right) + \epsilon_0\left(E^2 + c^2B^2\right) - \\ - \tfrac{3}{2}\,\epsilon_0\left(E^2 + c^2B^2\right). \end{aligned} \tag{5.23}$$

Hence

$$\sigma^{\alpha}{}_{\alpha} = 0 \tag{5.24}$$

and, substituting into (5.19),

$$\boxed{\mathcal{E}_{\|} = 0} \tag{5.25}$$

as expected [59, see pp. 64–66]. This derivation thus shows that the rest-mass energy density of the photon is zero, *i.e.* the photon is massless.

§5.3.2 *Transverse (massless) term*

The transverse term is calculated from (5.8), *viz.*

$$\mathcal{E}_{\perp} = \frac{1}{4\bar{\mu}_0}\, t^{\alpha\beta} t_{\alpha\beta}. \tag{5.26}$$

Given that $t_s = \frac{1}{4}\,\sigma^{\alpha}{}_{\alpha} = 0$, then $t^{\alpha\beta} = \sigma^{\alpha\beta}$ and the terms $\sigma^{\alpha\beta}\sigma_{\alpha\beta}$ are calculated from the components of the electromagnetic stress tensors of (5.17) and (5.18). Substituting for the diagonal elements and making use of the symmetry of the Poynting component terms and of the Maxwell stress tensor terms from (5.17) and (5.18), this expands to:

$$\begin{aligned}
\sigma^{\alpha\beta}\sigma_{\alpha\beta} = {} & \tfrac{1}{4}\,\epsilon_0^2 \left(E^2 + c^2B^2\right)^2 + \\
& + \epsilon_0^2 \left[\left(E_x E_x + c^2 B_x B_x\right) - \tfrac{1}{2}\,\left(E^2 + c^2B^2\right)\right]^2 + \\
& + \epsilon_0^2 \left[\left(E_y E_y + c^2 B_y B_y\right) - \tfrac{1}{2}\,\left(E^2 + c^2B^2\right)\right]^2 + \\
& + \epsilon_0^2 \left[\left(E_z E_z + c^2 B_z B_z\right) - \tfrac{1}{2}\,\left(E^2 + c^2B^2\right)\right]^2 - \\
& - 2\left(S_x/c\right)^2 - 2\left(S_y/c\right)^2 - 2\left(S_z/c\right)^2 + \\
& + 2\left(\sigma_{xy}\right)^2 + 2\left(\sigma_{yz}\right)^2 + 2\left(\sigma_{zx}\right)^2.
\end{aligned} \tag{5.27}$$

The EB terms expand to:

$$\begin{aligned}
\text{EB terms} = \epsilon_0^2 \Big[& \tfrac{1}{4}\,\left(E^2 + c^2B^2\right)^2 + \\
& + \left({E_x}^2 + c^2{B_x}^2\right)^2 - \left({E_x}^2 + c^2{B_x}^2\right)\left(E^2 + c^2B^2\right) + \\
& + \left({E_y}^2 + c^2{B_y}^2\right)^2 - \left({E_y}^2 + c^2{B_y}^2\right)\left(E^2 + c^2B^2\right) + \\
& + \left({E_z}^2 + c^2{B_z}^2\right)^2 - \left({E_z}^2 + c^2{B_z}^2\right)\left(E^2 + c^2B^2\right) + \\
& + \tfrac{3}{4}\,\left(E^2 + c^2B^2\right)^2 \Big].
\end{aligned} \tag{5.28}$$

Simplifying,

$$\begin{aligned}\text{EB terms} = \epsilon_0^2 \Big[&\left(E^2 + c^2B^2\right)^2 - \left({E_x}^2 + c^2{B_x}^2 + \right. \\ &+ {E_y}^2 + c^2{B_y}^2 + {E_z}^2 + c^2{B_z}^2\Big)\left(E^2 + c^2B^2\right) + \\ &+ \left({E_x}^2 + c^2{B_x}^2\right)^2 + \left({E_y}^2 + c^2{B_y}^2\right)^2 + \\ &+ \left({E_z}^2 + c^2{B_z}^2\right)^2 \Big]\end{aligned} \tag{5.29}$$

which gives

$$\begin{aligned}\text{EB terms} = \epsilon_0^2 \Big[&\left(E^2 + c^2B^2\right)^2 - \left(E^2 + c^2B^2\right)^2 + \\ &+ \left({E_x}^2 + c^2{B_x}^2\right)^2 + \left({E_y}^2 + c^2{B_y}^2\right)^2 + \\ &+ \left({E_z}^2 + c^2{B_z}^2\right)^2 \Big]\end{aligned} \tag{5.30}$$

and finally

$$\begin{aligned}\text{EB terms} = \epsilon_0^2 \Big[&\left({E_x}^4 + {E_y}^4 + {E_z}^4\right) + \\ &+ c^4\left({B_x}^4 + {B_y}^4 + {B_z}^4\right) + \\ &+ 2c^2\left({E_x}^2{B_x}^2 + {E_y}^2{B_y}^2 + {E_z}^2{B_z}^2\right)\Big].\end{aligned} \tag{5.31}$$

Including the EB terms in (5.27), substituting from (5.16), expanding the Poynting vector and rearranging, we obtain

$$\begin{aligned}\sigma^{\alpha\beta}\sigma_{\alpha\beta} = \epsilon_0^2 \Big[&\left({E_x}^4 + {E_y}^4 + {E_z}^4\right) + c^4\left({B_x}^4 + {B_y}^4 + {B_z}^4\right) + \\ &+ 2c^2\left({E_x}^2{B_x}^2 + {E_y}^2{B_y}^2 + {E_z}^2{B_z}^2\right)\Big] - \\ &- 2\epsilon_0^2c^2\Big[\left(E_yB_z - E_zB_y\right)^2 + \left(-E_xB_z + E_zB_x\right)^2 + \\ &+ \left(E_xB_y - E_yB_x\right)^2\Big] + 2\epsilon_0^2\Big[\left(E_xE_y + c^2B_xB_y\right)^2 + \\ &+ \left(E_yE_z + c^2B_yB_z\right)^2 + \left(E_zE_x + c^2B_zB_x\right)^2\Big].\end{aligned} \tag{5.32}$$

Expanding the quadratic expressions,

$$\begin{aligned}\sigma^{\alpha\beta}\sigma_{\alpha\beta} = \epsilon_0^2 \Big[& \left({E_x}^4 + {E_y}^4 + {E_z}^4\right) + \\ & + c^4\left({B_x}^4 + {B_y}^4 + {B_z}^4\right) + \\ & + 2c^2\left({E_x}^2{B_x}^2 + {E_y}^2{B_y}^2 + {E_z}^2{B_z}^2\right)\Big] - \\ & - 2\epsilon_0^2 c^2 \Big[{E_x}^2{B_y}^2 + {E_y}^2{B_z}^2 + {E_z}^2{B_x}^2 + \\ & + {B_x}^2{E_y}^2 + {B_y}^2{E_z}^2 + {B_z}^2{E_x}^2 - \\ & - 2\left(E_xE_yB_xB_y + E_yE_zB_yB_z + E_zE_xB_zB_x\right)\Big] + \\ & + 2\epsilon_0^2 \Big[\left({E_x}^2{E_y}^2 + {E_y}^2{E_z}^2 + {E_z}^2{E_x}^2\right) + \\ & + 2c^2\left(E_xE_yB_xB_y + E_yE_zB_yB_z + E_zE_xB_zB_x\right) + \\ & + c^4\left({B_x}^2{B_y}^2 + {B_y}^2{B_z}^2 + {B_z}^2{B_x}^2\right)\Big].\end{aligned} \tag{5.33}$$

Grouping the terms in powers of c together,

$$\begin{aligned}\frac{1}{\epsilon_0^2}\,\sigma^{\alpha\beta}\sigma_{\alpha\beta} = \Big[& \left({E_x}^4 + {E_y}^4 + {E_z}^4\right) + \\ & + 2\left({E_x}^2{E_y}^2 + {E_y}^2{E_z}^2 + {E_z}^2{E_x}^2\right)\Big] + \\ & + 2c^2\Big[\left({E_x}^2{B_x}^2 + {E_y}^2{B_y}^2 + {E_z}^2{B_z}^2\right) - \\ & - \left({E_x}^2{B_y}^2 + {E_y}^2{B_z}^2 + {E_z}^2{B_x}^2 + \right. \\ & + {B_x}^2{E_y}^2 + {B_y}^2{E_z}^2 + {B_z}^2{E_x}^2) + \\ & + 4\left(E_xE_yB_xB_y + E_yE_zB_yB_z + \right. \\ & \left. + E_zE_xB_zB_x\right)\Big] + c^4\Big[\left({B_x}^4 + {B_y}^4 + {B_z}^4\right) + \\ & + 2\left({B_x}^2{B_y}^2 + {B_y}^2{B_z}^2 + {B_z}^2{B_x}^2\right)\Big].\end{aligned} \tag{5.34}$$

Simplifying,

$$\begin{aligned}\frac{1}{\epsilon_0^2}\,\sigma^{\alpha\beta}\sigma_{\alpha\beta} = &\left({E_x}^2+{E_y}^2+{E_z}^2\right)^2+\\ &+2c^2\,\left({E_x}^2+{E_y}^2+{E_z}^2\right)\left({B_x}^2+{B_y}^2+{B_z}^2\right)-\\ &-2c^2\,\Big[2\big({E_x}^2{B_y}^2+{E_y}^2{B_z}^2+{E_z}^2{B_x}^2+\\ &+{B_x}^2{E_y}^2+{B_y}^2{E_z}^2+{B_z}^2{E_x}^2\big)-\\ &-4\left(E_xE_yB_xB_y+E_yE_zB_yB_z+E_zE_xB_zB_x\right)\Big]+\\ &+c^4\,\left({B_x}^2+{B_y}^2+{B_z}^2\right)^2\end{aligned} \tag{5.35}$$

which is further simplified to

$$\begin{aligned}\frac{1}{\epsilon_0^2}\,\sigma^{\alpha\beta}\sigma_{\alpha\beta} = &\left(E^4+2c^2E^2B^2+c^4B^4\right)-\\ &-4c^2\,\Big[\left(E_yB_z-B_yE_z\right)^2+\left(E_zB_x-B_zE_x\right)^2+\\ &+\left(E_xB_y-B_xE_y\right)^2\Big].\end{aligned} \tag{5.36}$$

Making use of the definition of the Poynting vector from (5.16), we obtain

$$\begin{aligned}\sigma^{\alpha\beta}\sigma_{\alpha\beta} = &\,\epsilon_0^2\,\left(E^2+c^2B^2\right)^2-\\ &-4\epsilon_0^2c^2\,\left[{(E\times B)_x}^2+{(E\times B)_y}^2+{(E\times B)_z}^2\right]\end{aligned} \tag{5.37}$$

and finally

$$\sigma^{\alpha\beta}\sigma_{\alpha\beta} = \epsilon_0^2\,\left(E^2+c^2B^2\right)^2-\frac{4}{c^2}\,\left({S_x}^2+{S_y}^2+{S_z}^2\right). \tag{5.38}$$

Substituting in (5.26), the transverse term becomes

$$\mathcal{E}_\perp = \frac{1}{4\bar{\mu}_0}\,\left[\epsilon_0^2\,\left(E^2+c^2B^2\right)^2-\frac{4}{c^2}\,S^2\right] \tag{5.39}$$

or

$$\boxed{\mathcal{E}_\perp = \frac{1}{\bar{\mu}_0}\,\left[{U_{em}}^2-\frac{1}{c^2}\,S^2\right]} \tag{5.40}$$

where $U_{em}=\frac{1}{2}\,\epsilon_0(E^2+c^2B^2)$ is the electromagnetic field energy density.

§5.4 Electromagnetic field strain energy density and the photon

$\boldsymbol{S}$ is the electromagnetic energy flux along the direction of propagation [59, see p. 62]. As noted by Feynman [122, see pp. 27-1–2], local conservation of the electromagnetic field energy can be written as

$$-\frac{\partial U_{em}}{\partial t} = \nabla \cdot \boldsymbol{S}, \tag{5.41}$$

where the term $\boldsymbol{E} \cdot \boldsymbol{j}$ representing the work done on the matter inside the volume is 0 in the absence of charges (due to the absence of mass). By analogy with the current density four-vector $j^\nu = (c\varrho, \boldsymbol{j})$, where ϱ is the charge density, and $\boldsymbol{j}$ is the current density vector, which obeys a similar conservation relation, we define the Poynting four-vector

$$\boxed{S^\nu = (cU_{em}, \boldsymbol{S})}, \tag{5.42}$$

where U_{em} is the electromagnetic field energy density, and $\boldsymbol{S}$ is the Poynting vector. Furthermore, as per (5.41), S^ν satisfies

$$\partial_\nu S^\nu = 0\,. \tag{5.43}$$

Using definition (5.42) in (5.40), that equation becomes

$$\mathcal{E}_\perp = \frac{1}{\bar{\mu}_0 c^2}\, S_\nu S^\nu\,. \tag{5.44}$$

The indefiniteness of the location of the field energy referred to by Feynman [122, see p. 27-6] is thus resolved: the electromagnetic field energy resides in the distortions (transverse displacements) of the spacetime continuum.

Hence the invariant electromagnetic strain energy density is given by

$$\boxed{\mathcal{E} = \frac{1}{\bar{\mu}_0 c^2}\, S_\nu S^\nu} \tag{5.45}$$

where we have used $\rho = 0$ as per (5.24). This confirms that S^ν as defined in (5.42) is a four-vector.

It is surprising that a longitudinal energy flow term is part of the transverse strain energy density *i.e.* $S^2/\bar{\mu}_0 c^2$ in (5.40). We note that this term arises from the time-space components of (5.17) and (5.18) and can be seen to correspond to the transverse displacements along the *time-space planes* which are folded along the direction of propagation

in 3-space as the Poynting vector. The electromagnetic field energy density term ${U_{em}}^2/\bar{\mu}_0$ and the electromagnetic field energy flux term $S^2/\bar{\mu}_0 c^2$ are thus combined into the transverse strain energy density. The negative sign arises from the signature $(+---)$ of the Minkowski metric tensor $\eta^{\mu\nu}$.

This longitudinal electromagnetic energy flux is massless as it is due to distortion, not dilatation, of the spacetime continuum. However, because this energy flux is along the direction of propagation (*i.e.* longitudinal), it gives rise to the particle aspect of the electromagnetic field, the photon. As shown in [219, see pp. 174-5] [155, see p. 58], in the quantum theory of electromagnetic radiation, an intensity operator derived from the Poynting vector has, as expectation value, photons in the direction of propagation.

This implies that the $(pc)^2$ term of the energy relation of Special Relativity needs to be separated into transverse and longitudinal massless terms as follows:

$$\hat{E}^2 = \underbrace{\rho^2 c^4}_{\mathcal{E}_\parallel} + \underbrace{\hat{p}_\parallel^2 c^2 + \hat{p}_\perp^2 c^2}_{massless\ \mathcal{E}_\perp} \tag{5.46}$$

where $\hat{p}_\parallel$ is the massless longitudinal momentum density. Eq. (5.40) shows that the electromagnetic field energy density term ${U_{em}}^2/\bar{\mu}_0$ is reduced by the electromagnetic field energy flux term $S^2/\bar{\mu}_0 c^2$ in the transverse strain energy density, due to photons propagating in the longitudinal direction. Hence we can write [155, see p. 58]

$$\int_V \frac{1}{\bar{\mu}_0 c^2}\, S^2 \mathrm{d}V = \sum_k n_k h \nu_k. \tag{5.47}$$

where h is Planck's constant and n_k is the number of photons of frequency ν_k. Thus the kinetic energy is carried by the distortion part of the deformation, while the dilatation part carries only the rest-mass energy, which in this case is 0.

As shown in (5.9), (5.10) and (5.11), the constant of proportionality to transform energy density squared ($\hat{E}^2$) into strain energy density ($\mathcal{E}$) is $1/(32\bar{\kappa}_0)$:

$$\mathcal{E}_\parallel = \frac{1}{32\bar{\kappa}_0}\, \left[\rho c^2\right]^2 \tag{5.48}$$

$$\mathcal{E} = \frac{1}{32\bar{\kappa}_0}\, \hat{E}^2 \tag{5.49}$$

$$\mathcal{E}_\perp = \frac{1}{32\bar{\kappa}_0}\, \left[\hat{p}_\parallel^2 c^2 + \hat{p}_\perp^2 c^2\right] = \frac{1}{4\bar{\mu}_0}\, t^{\alpha\beta} t_{\alpha\beta}. \tag{5.50}$$

Substituting (5.40) into (5.50), we obtain

$$\mathcal{E}_\perp = \frac{1}{32\bar{\kappa}_0}\left[\hat{p}_\parallel^2 c^2 + \hat{p}_\perp^2 c^2\right] = \frac{1}{\bar{\mu}_0}\left[{U_{em}}^2 - \frac{1}{c^2}\,S^2\right] \tag{5.51}$$

and

$$\hat{p}_\parallel^2 c^2 + \hat{p}_\perp^2 c^2 = \frac{32\bar{\kappa}_0}{\bar{\mu}_0}\left[{U_{em}}^2 - \frac{1}{c^2}\,S^2\right]. \tag{5.52}$$

This suggests that

$$\boxed{\bar{\mu}_0 = 32\bar{\kappa}_0}, \tag{5.53}$$

to obtain the relation

$$\hat{p}_\parallel^2 c^2 + \hat{p}_\perp^2 c^2 = {U_{em}}^2 - \frac{1}{c^2}\,S^2\,. \tag{5.54}$$

§5.5 Origin of inertial mass in the spacetime continuum

> *It must also be said that the origin of inertia is and remains* ***the*** *most obscure subject in the theory of particles and fields. A. Pais, 1982 [282, p. 288]*
>
> *... the notion of mass, although fundamental to physics, is still shrouded in mystery. M. Jammer, 2000 [180, p. ix]*

In this section, we revisit the nature of inertial mass as provided by the Elastodynamics of the Spacetime Continuum (*STCED*) [238, 254]. We combine the various elements to the solution of the origin of inertial mass sprinkled in this book in this section. This results in some repetition of previously presented results, but the bringing-together of these results under one umbrella section helps to understand the logical consistency of the origin of inertial mass in the spacetime continuum.

As we have seen previously, *STCED* is a natural extension of Einstein's General Theory of Relativity which blends continuum mechanical and general relativistic descriptions of the spacetime continuum. The introduction of strains $\varepsilon^{\mu\nu}$ in the spacetime continuum as a result of the energy-momentum stress tensor $T^{\mu\nu}$ allows us to use, by analogy, results from continuum mechanics, in particular the stress-strain relation, to provide a better understanding of the general relativistic spacetime.

§5.5.1 *Inertial mass in STCED*

In *STCED*, as shown in [238, 254], energy propagates in the spacetime continuum (*STC*) as wave-like deformations which can be decomposed into *dilatations* and *distortions*. *Dilatations* involve an invariant change

in volume of the spacetime continuum which is the source of the associated rest-mass energy density of the deformation. On the other hand, *distortions* correspond to a change of shape (shearing) of the spacetime continuum without a change in volume and are thus massless.

Thus deformations propagate in the spacetime continuum by longitudinal (*dilatation*) and transverse (*distortion*) wave displacements. This provides a natural explanation for wave-particle duality, with the massless transverse mode corresponding to the wave aspects of the deformations and the massive longitudinal mode corresponding to the particle aspects of the deformations.

The rest-mass energy density of the longitudinal mode is given by [238, see Eq. (32)]

$$\rho c^2 = 4\bar{\kappa}_0 \varepsilon \tag{5.55}$$

where ρ is the rest-mass density, c is the speed of light, $\bar{\kappa}_0$ is the bulk modulus of the *STC*, and $\varepsilon = \varepsilon^{\alpha}{}_{\alpha}$, the trace of the strain tensor $\varepsilon^{\mu\nu}$ obtained by contraction, is the volume dilatation defined as the change in volume per original volume [320, see pp. 149–152] and is an invariant of the strain tensor. Integrating over the 3-D space volume,

$$\int_{V_3} \rho c^2 \, \mathrm{d}V_3 = 4\bar{\kappa}_0 \int_{V_3} \varepsilon \, \mathrm{d}V_3 \,, \tag{5.56}$$

and using

$$m = \int_{V_3} \rho \, \mathrm{d}V_3 \tag{5.57}$$

in (5.56), where m is the rest mass (often denoted as m_0) of the deformation, we obtain

$$mc^2 = 4\bar{\kappa}_0 \, V_{\varepsilon s} \tag{5.58}$$

where

$$V_{\varepsilon s} = \int_{V_3} \varepsilon \, \mathrm{d}V_3 \tag{5.59}$$

is the space volume dilatation corresponding to rest-mass m, and spacetime continuum volume dilatation ε is the solution of the 4-D dilatational (longitudinal) wave equation [254, see Eq. (3.35)]

$$(2\bar{\mu}_0 + \bar{\lambda}_0) \, \nabla^2 \varepsilon = -\partial_\nu X^\nu \tag{5.60}$$

where ∇ and ∂ are the 4-D operators and X^ν is the spacetime continuum volume force.

This demonstrates that mass is not independent of the spacetime continuum, but rather mass is part of the spacetime continuum fabric

itself. Hence mass results from the dilatation of the spacetime continuum in the longitudinal propagation of energy-momentum in the spacetime continuum. Matter does not warp spacetime, but rather, matter *is* warped spacetime (*i.e.* dilated spacetime). The universe consists of the spacetime continuum and energy-momentum that propagates in it by deformation of its structure.

It is interesting to note that Pais, in his scientific biography of Einstein *'Subtle is the Lord...'*, mentions [282, p. 253]

> The trace of the energy momentum tensor does vanish for electromagnetic fields but not for matter.

which is correct, as shown in [239, 242], where the zero trace of the electromagnetic field energy-momentum stress tensor is reflected in the zero mass of the photon. The missing link in general relativity is the understanding that the trace of the energy-momentum stress tensor is related to the trace of the spacetime continuum strain tensor and is proportional to the mass of matter as given by (5.55) and (5.58).

There are basic questions of physics that can be resolved given this understanding of the origin of inertial mass. The following sections deal with many of these unresolved questions.

§5.5.2 *Definition of mass*

An important consequence of relations (5.55) and (5.58) is that they provide a definition of mass. The definition of mass is still one of the open questions in physics, with most authors adopting an indirect definition of mass based on the ratio of force to acceleration [178, see Ch. 8]. However, mass is one of the fundamental dimensions of modern systems of units, and as such, should be defined directly, not indirectly. This is a reflection of the current incomplete understanding of the nature of mass in physics. *STCED* provides a direct physical definition of mass: *mass is the invariant change in volume of spacetime in the longitudinal propagation of energy-momentum in the spacetime continuum.*

Note that the operational definition of mass ($m = F/a$) is still needed to measure the mass of objects and compare them. Jammer covers the various operational and philosophical definitions of mass that have been proposed [180, Ch. 1].

§5.5.3 *Point particles*

The fact that the mass of a particle corresponds to a finite spacetime volume dilatation $V_{\varepsilon s}$ shows that a singular "point" particle is not physically valid. All particles occupy a finite volume, even if that volume

can be very small. Problems arising from point particles are thus seen to result from the abstraction of representing some particles as point objects. Instead, particles need to be given a finite volume to give physically realistic results and avoid invalid results.

§5.5.4 *Equivalence of inertial and gravitational mass*

Einstein's general relativistic principle of equivalence of inertial and gravitational mass can be given added confirmation in *STCED*. As shown in [239, 243], the Ricci tensor can also be decomposed into dilatation and distortion components. The dilatation component can be shown to result in Poisson's equation for a newtonian gravitational potential [254, see Eq. (2.44)] where the gravitational mass density is identical to the rest-mass density identified in *STCED*. This confirms theoretically the equivalence of inertial mass and gravitational mass, as demonstrated experimentally within the accuracy currently achievable [102].

§5.5.5 *Mach's principle*

Mach's principle, a terminology first used by Einstein [282, p. 287], was not explicitly stated by Mach, and hence various takes on its statement exist. One of the better formulation holds that one can determine rotation and hence define inertial frames with respect to the fixed stars [365, see pp. 86–88]. By extension, inertia would then be due to an interaction with the average mass of the universe [365, see p. 17].

This principle played an important role in the initial development of general relativity by Einstein which is well documented by Pais [282, pp. 283–287]. It also had an impact on the initial work performed in cosmology by Einstein who was searching for a cosmological model that would be in accord with Mach's principle. Einstein's evolving perspective on Mach's work is best summarized by Pais [282, p. 287]:

> So strongly did Einstein believe at that time in the relativity of inertia that in 1918 he stated as being on equal footing three principles on which a satisfactory theory of gravitation should rest [Mach's principle was the third] ... In later years, Einstein's enthusiasm for Mach's principle waned and finally vanished.

Modifications of Einstein's Theory of General Relativity have been proposed in an attempt to incorporate Mach's principle into general relativity (see for example [33, 134]).

The book *Gravitation and Inertia* by Ciufolini and Wheeler [371], with its emphasis on geometrodynamics and its well-known sayings

"spacetime tells mass how to move and mass tells spacetime how to curve" and "inertia here arises from mass there", explores these ideas in detail. However, it is important to realize that this perspective is an interpretation of Einstein's field equations of general relativity (2.8). These equations are simply a relation between the geometry of the spacetime continuum and the energy-momentum present in its structure. *STCED* shows that mass is not outside of the spacetime continuum telling it how to curve (so to speak), but rather mass is part of the spacetime continuum fabric itself participating in the curvature of the spacetime continuum. The geometry of the spacetime continuum is generated by the combination of all spacetime continuum deformations which are composed of longitudinal massive dilatations and transverse massless distortions.

As shown in section §2.5, the geometry of spacetime used in (2.8) can thus be considered to be a linear composition (represented by a sum) of *STC* deformations, starting with the total energy-momentum generating the geometry of general relativity, $T^{\mu\nu}_{GR}$, being a composition of the energy-momentum of the individual deformations of *STCED*, $T^{\mu\nu}_{STCED}$ as given by (2.8), *viz.*

$$T^{\mu\nu}_{GR} = \sum T^{\mu\nu}_{STCED}\,.$$

As shown in section §2.5, from (2.6) and (2.8), we obtain the relations (2.50) and (2.51), *viz.*

$$\frac{1}{\varkappa}\,R = \sum 4\,\bar{\kappa}_0\,\varepsilon = \sum \rho\,c^2$$

i.e. the curvature of the spacetime continuum arises from the composition of the effect of individual deformations and is proportional to the rest-mass energy density present in the spacetime continuum, and

$$\frac{1}{\varkappa}\,R^{\mu\nu} = \sum \left[(\bar{\lambda}_0 + \bar{\mu}_0)g^{\mu\nu}\varepsilon - 2\bar{\mu}_0\,\varepsilon^{\mu\nu}\right]\,.$$

Eqs. (2.50) and (2.51) give the relation between the microscopic description of the strains (*i.e.* deformations of the spacetime continuum) and the macroscopic description of the gravitational field in terms of the curvature of the spacetime continuum resulting from the combination of the many microscopic displacements of the spacetime continuum from equilibrium. The source of the inertia is thus in the massive dilatation associated with each deformation, and Mach's principle (or conjecture as it is also known) is seen to be incorrect.

§5.5.6 *Electromagnetic mass*

The advent of Maxwell's theory of electromagnetism in the second half of the nineteenth century led to the possibility of inertia resulting from electromagnetism, first proposed in 1881 by J. J. Thomson [178, see Chapter 11]. The application of the concept of electromagnetic mass to the electron discovered by J. J. Thomson in 1897, by modelling it as a small charged sphere, led to promising results [122, see Chapter 28]. One can then calculate the energy in the electron's electric field and divide the result by c^2. Alternatively, the electromagnetic momentum of a moving electron can be calculated from Poynting's vector and the electromagnetic mass set equal to the factor multiplying the electron's velocity vector. Different methods give different results.

Using the classical electron radius

$$r_0 = \frac{e^2}{m_e c^2} \tag{5.61}$$

where e is the electronic charge and m_e the mass of the electron, then the electromagnetic mass of the electron can be written as

$$m_{em} = k_e \frac{e^2}{r_0 c^2} \tag{5.62}$$

where the factor k_e depends on the assumed charge distribution in the sphere and the method of calculation used. For a surface charge distribution, $k_e = 2/3$, while for a uniform volume distribution, $k_e = 4/5$. Numerous modifications were attempted to get $m_{em} = m_e$ [122, 178] with Poincaré introducing non-electrical forces known as "Poincaré stresses" to get the desired result. This is a classical treatment that does not take relativistic or quantum effects into consideration.

It should be noted that the simpler classical treatment of the electromagnetic mass of the electron based purely on the electric charge density of the electron is a calculation of the static mass of the electron. In *STCED*, the charge density ϱ can be calculated from the current density four-vector j^ν (see section §4.3)

$$j^\nu = \frac{\varphi_0}{\mu_0} \frac{2\bar{\mu}_0 + \bar{\lambda}_0}{2\bar{\mu}_0} \varepsilon^{;\nu} \tag{5.63}$$

where φ_0 is the *STC electromagnetic shearing potential constant*, which has units of $[\mathrm{V} \cdot \mathrm{s} \cdot \mathrm{m}^{-2}]$ or equivalently [T], μ_0 is the electromagnetic permeability of free space, and $\varepsilon^{;\nu}$ can be written as the dilatation

current $\xi^\nu = \varepsilon^{;\nu}$. Substituting for j^ν from (5.63) in the relation [14, see p. 94]

$$j^\nu j_\nu = \varrho^2 c^2, \tag{5.64}$$

we obtain the expression for the charge density

$$\varrho = \frac{1}{2}\,\frac{\varphi_0}{\mu_0 c}\,\frac{2\bar{\mu}_0 + \bar{\lambda}_0}{2\bar{\mu}_0}\,\sqrt{\varepsilon^{;\nu}\varepsilon_{;\nu}}\,. \tag{5.65}$$

Note the difference between the electromagnetic permeability of free space μ_0 and the Lamé elastic constant $\bar{\mu}_0$ used to denote the spacetime continuum shear modulus.

We see that the charge density derives from the norm of the gradient of the volume dilatation ε, *i.e.*

$$\begin{aligned} \|\varepsilon^{;\nu}\| &= \sqrt{\varepsilon^{;\nu}\varepsilon_{;\nu}} \\ &= \sqrt{\left(\frac{\partial\varepsilon}{\partial x}\right)^2 + \left(\frac{\partial\varepsilon}{\partial y}\right)^2 + \left(\frac{\partial\varepsilon}{\partial z}\right)^2 + \frac{1}{c^2}\left(\frac{\partial\varepsilon}{\partial t}\right)^2} \end{aligned} \tag{5.66}$$

in cartesian coordinates, and from the above, (5.65) becomes

$$\varrho = \frac{1}{2}\,\frac{\varphi_0}{\mu_0 c}\,\frac{2\bar{\mu}_0 + \bar{\lambda}_0}{2\bar{\mu}_0}\,\|\varepsilon^{;\nu}\|\,. \tag{5.67}$$

The charge density is a manifestation of the spacetime fabric itself, however it does not depend on the volume dilatation ε, only on its gradient, and it does not contribute to inertial mass as given by (5.55). The electromagnetic mass calculation is based on the energy in the electron's electric field and we now consider electromagnetic field energy in *STCED* to clarify its contribution, if any, to inertial mass. This also covers the calculation of electromagnetic mass from the Poynting vector.

§5.5.7 *Mass of electromagnetic field energy*

As shown in section §2.6.3, the correct special relativistic relation for momentum p is given by

$$p = m_0\, u\,, \tag{5.68}$$

where m_0 is the proper or rest mass, u is the velocity with respect to the proper time τ, given by $u = \gamma v$, where

$$\gamma = \frac{1}{(1-\beta^2)^{1/2}}\,, \tag{5.69}$$

$\beta = v/c$, and v is the velocity with respect to the local time t. When dealing with dynamic equations in the local time t instead of the invariant proper time τ, momentum p is given by

$$p = m^* v \,, \tag{5.70}$$

where the relativistic mass m^* is given by

$$m^* = \gamma m_0 \,. \tag{5.71}$$

Eq. (5.70), compared to (5.68), shows that relativistic mass m^* is an effective mass which results from dealing with dynamic equations in the local time t instead of the invariant proper time τ. The relativistic mass energy $m^* c^2$ corresponds to the total energy of an object (invariant proper mass plus kinetic energy) measured with respect to a given frame of reference [248]. As noted by Jammer [180, p. 41],

> Since [velocity v] depends on the choice of [reference frame] S relative to which it is being measured, [relativistic mass m^*] also depends on S and is consequently a relativistic quantity and not an intrinsic property of the particle.

Using the effective mass, we can write the energy E as the sum of the proper mass and the kinetic energy K of the body, which is typically written as

$$E = m^* c^2 = m_0 \, c^2 + K \,. \tag{5.72}$$

If the particles are subjected to forces, these stresses must be included in the energy-momentum stress tensor, and hence added to K. Thus we see that the inertial mass corresponds to the proper or rest mass of a body, while relativistic mass does not represent an actual increase in the inertial mass of a body, just its total energy (see Taylor and Wheeler [344], Okun [273–275], Oas [270, 271]).

Considering the energy-momentum stress tensor of the electromagnetic field, we can show that $T^{\alpha}{}_{\alpha} = 0$ as expected for massless photons, while

$$T^{00} = \frac{\epsilon_0}{2} \left(E^2 + c^2 B^2 \right) = U_{em} \tag{5.73}$$

is the total energy density, where U_{em} is the electromagnetic field energy density, ϵ_0 is the electromagnetic permittivity of free space, and E and B have their usual significance for the electric and magnetic fields (see [254, §5.3]). As $m_0 = 0$ for the electromagnetic field, the electromagnetic field energy then needs to be included in the K term in (5.72).

In general, the energy relation in special relativity is quadratic, given by

$$E^2 = m_0^2\, c^4 + p^2 c^2\,, \tag{5.74}$$

where p is the momentum. Making use of the effective mass (2.53) allows us to obtain (2.63) from (5.74) [242], starting from

$$m^{*2} c^4 = \gamma^2 m_0^2\, c^4 = m_0^2\, c^4 + p^2 c^2\,. \tag{5.75}$$

This section provides a description of the electromagnetic field energy using a quadratic energy relation which corresponds to the more complete classical treatment of the electromagnetic mass of the electron based on the Poynting vector of the electron in motion.

In *STCED*, energy is stored in the spacetime continuum as strain energy [242]. As seen in section §5.2, the strain energy density of the spacetime continuum is separated into two terms given by (5.6), *viz.*

$$\mathcal{E} = \mathcal{E}_{\parallel} + \mathcal{E}_{\perp}$$

The first one (5.7) expresses the dilatation energy density (the mass longitudinal term) while the second one (5.8) expresses the distortion energy density (the massless transverse term), *viz.*

$$\mathcal{E}_{\parallel} = \frac{1}{2}\,\bar{\kappa}_0 \varepsilon^2 \equiv \frac{1}{32\bar{\kappa}_0}\,\rho^2 c^4\,,$$

where ρ is the rest-mass density of the deformation, and

$$\mathcal{E}_{\perp} = \bar{\mu}_0\, e^{\alpha\beta} e_{\alpha\beta} = \frac{1}{4\bar{\mu}_0}\, t^{\alpha\beta} t_{\alpha\beta}\,,$$

with the strain distortion (1.17)

$$e^{\alpha\beta} = \varepsilon^{\alpha\beta} - e_s\, g^{\alpha\beta}$$

and the strain dilatation $e_s = \frac{1}{4}\,\varepsilon^{\alpha}{}_{\alpha}$. Similarly for the stress distortion $t^{\alpha\beta}$ and the stress dilatation t_s. Then the dilatation (massive) strain energy density of the deformation is given by the longitudinal strain energy density (5.7) and the distortion (massless) strain energy density of the deformation is given by the transverse strain energy density (5.8).

As shown in section §5.3 for the electromagnetic field, the longitudinal term is given by (5.25), *viz.*

$$\mathcal{E}_{\parallel} = 0$$

as expected [59, see pp. 64–66]. This result thus shows that the rest-mass energy density of the electromagnetic field, and hence of the photon is zero, *i.e.* the photon is massless. The transverse term is given by (5.39) and (5.40), *viz.*

$$\mathcal{E}_\perp = \frac{1}{4\bar{\mu}_0}\left[\epsilon_0^2\left(E^2 + c^2B^2\right)^2 - \frac{4}{c^2}S^2\right]$$

or

$$\mathcal{E}_\perp = \frac{1}{\bar{\mu}_0}\left[{U_{em}}^2 - \frac{1}{c^2}S^2\right]$$

where $U_{em} = \frac{1}{2}\epsilon_0(E^2 + c^2B^2)$ is the electromagnetic field energy density as before and S is the magnitude of the Poynting vector. Using the Poynting four-vector $S^\nu = (cU_{em}, \boldsymbol{S})$ defined in (5.42) where $\boldsymbol{S}$ is the Poynting vector, in the above equation, we obtain the transverse massless energy density of the electromagnetic field (5.44), *viz.*

$$\mathcal{E}_\perp = \frac{1}{\bar{\mu}_0 c^2}S_\nu S^\nu\,.$$

As we stated previously, the indefiniteness of the location of the field energy referred to by Feynman [122, see p. 27-6] is thus resolved: the electromagnetic field energy resides in the distortions (transverse displacements) of the spacetime continuum.

Hence the electromagnetic field is transverse and massless, and has no massive longitudinal component. The electromagnetic field has energy, but no rest mass, and hence no inertia. From *STCED*, we see that electromagnetism as the source of inertia is not valid.

Electromagnetic mass is thus seen to be an unsuccessful attempt to account for the inertial mass of a particle from its electromagnetic field energy. The electromagnetic field contributes to the particle's total energy, but not to its inertial mass which *STCED* shows originates in the particle's dilatation energy density (the mass longitudinal term) which is zero for the electromagnetic field.

§5.5.8 *Summary*

In this section, we have revisited the nature of inertial mass as provided by the Elastodynamics of the Spacetime Continuum (*STCED*) which provides a better understanding of general relativistic spacetime. Mass is shown to be the invariant change in volume of spacetime in the longitudinal propagation of energy-momentum in the spacetime continuum.

Hence mass is not independent of the spacetime continuum, but rather mass is part of the spacetime continuum fabric itself.

STCED provides a direct physical definition of mass. In addition, it answers many of the unresolved questions that pertain to the nature of mass:

- The mass of a particle corresponds to a finite spacetime volume dilatation $V_{\varepsilon s}$ and particles need to be given a finite volume (as opposed to "point particles") to give physically realistic results and avoid invalid results.
- It confirms theoretically the equivalence of inertial and gravitational mass.
- The source of inertia is in the massive dilatation associated with each deformation, and Mach's principle (or conjecture), which holds that inertia results from interaction with the average mass of the universe, is seen to be incorrect.
- The electromagnetic field is transverse and massless, and has no massive longitudinal component. It has energy, but no rest mass, and hence no inertia. The electromagnetic field contributes to the particle's total energy, but not to its inertial mass.

STCED thus provides a physical model of the nature of inertial mass, which also includes an explanation for wave-particle duality. This model leads to the clarification and resolution of unresolved and contentious questions pertaining to inertial mass and its nature.

Chapter 6

Spacetime Continuum Volume Force

§6.1 STC volume force

The volume (or body) force X^ν has been introduced in the equilibrium dynamic equation of the spacetime continuum in (3.7) of section §3.2.1 *viz.*

$$T^{\mu\nu}{}_{;\mu} = -X^\nu. \tag{6.1}$$

Comparison with the corresponding general relativistic expression showed that the volume force is equal to zero at the macroscopic local level. Indeed, as pointed out by Wald [362, see p. 286], in general relativity the local energy density of matter as measured by a given observer is well-defined, and the relation

$$T^{\mu\nu}{}_{;\mu} = 0 \tag{6.2}$$

can be taken as expressing local conservation of the energy-momentum of matter.

It was also pointed out in that section that at the microscopic level, energy is known to be conserved only within the limits of the Heisenberg Uncertainty Principle, suggesting that the volume force may be very small, but not exactly zero. This is analogous to quantum theory where Planck's constant h must be taken into consideration at the microscopic level while at the macroscopic level, the limit $h \to 0$ holds.

In this chapter, we investigate the volume force and its impact on the equations of the Elastodynamics of the Spacetime Continuum.

§6.2 Linear elastic volume force

First we consider a simple linear elastic volume force. Based on the results obtained, we will then consider a variation of that linear elastic volume force based on the Klein-Gordon quantum mechanical current density in the next chapter.

We investigate a volume force that consists of an elastic linear force in a direction opposite to the displacements. This is the well-known elastic "spring" force

$$X^\nu = \bar{k}_0 u^\nu \tag{6.3}$$

where $\bar{k}_0$ is the postulated elastic force constant of the spacetime continuum volume force. Eq. (6.3) is positive as the volume force X^ν is defined positive in the direction opposite to the displacement [126]. Introduction of this volume force into our previous analysis of the spacetime continuum wave equations in sections §3.3 and §3.5 yields the following relations.

§6.2.1 *Displacement wave equation*

Substituting (6.3) into (3.18), *viz.*

$$\bar{\mu}_0 \nabla^2 u^\nu + (\bar{\mu}_0 + \bar{\lambda}_0)\varepsilon^{;\nu} = -X^\nu, \tag{6.4}$$

the dynamic equation in terms of displacements becomes

$$\bar{\mu}_0 \nabla^2 u^\nu + (\bar{\mu}_0 + \bar{\lambda}_0)\varepsilon^{;\nu} = -\bar{k}_0 u^\nu. \tag{6.5}$$

This equation can be rewritten as

$$\nabla^2 u^\nu + \frac{\bar{k}_0}{\bar{\mu}_0}\, u^\nu = -\frac{\bar{\mu}_0 + \bar{\lambda}_0}{\bar{\mu}_0}\, \varepsilon^{;\nu}\,. \tag{6.6}$$

This displacement equation is similar to a nonhomogeneous Klein-Gordon equation for a vector field, with a source term.

Separating u^ν into a longitudinal (irrotational) component $u^\nu_\parallel$ and a transverse (solenoidal) component $u^\nu_\perp$ using the Helmholtz theorem in four dimensions [378] according to

$$u^\nu = u^\nu_\parallel + u^\nu_\perp\,, \tag{6.7}$$

and similarly separating the dilatation current $\xi^\nu = \varepsilon^{;\nu}$ into a longitudinal component $\xi^\nu_\parallel$ and a transverse component $\xi^\nu_\perp$

$$\xi^\nu = \xi^\nu_\parallel + \xi^\nu_\perp\,, \tag{6.8}$$

and substituting into (6.6), we obtain the separated equations

$$\begin{aligned} \nabla^2 u^\nu_\parallel + \frac{\bar{k}_0}{\bar{\mu}_0}\, u^\nu_\parallel &= -\frac{\bar{\mu}_0 + \bar{\lambda}_0}{\bar{\mu}_0}\, \xi^\nu_\parallel \\ \nabla^2 u^\nu_\perp + \frac{\bar{k}_0}{\bar{\mu}_0}\, u^\nu_\perp &= -\frac{\bar{\mu}_0 + \bar{\lambda}_0}{\bar{\mu}_0}\, \xi^\nu_\perp \end{aligned} \tag{6.9}$$

which becomes

$$\nabla^2 u^\nu_\perp + \frac{\bar{k}_0}{\bar{\mu}_0}\, u^\nu_\perp = 0 \tag{6.10}$$

given that $\xi^\nu_\perp = \varepsilon^{;\nu}_\perp = 0$. The wave equation for $u^\nu_\parallel$ describes the propagation of longitudinal displacements, while the wave equation for $u^\nu_\perp$ describes the propagation of transverse displacements.

§6.2.2 *Wave equations*

Additional wave equations as shown in section §3.5, can be derived from this volume force.

Dilatational (longitudinal) wave equation. Substituting (6.3) into (3.35), *viz.*

$$(2\bar{\mu}_0 + \bar{\lambda}_0)\nabla^2\varepsilon = -X^{\nu}{}_{;\nu}, \tag{6.11}$$

the longitudinal (dilatational) wave equation becomes

$$(2\bar{\mu}_0 + \bar{\lambda}_0)\nabla^2\varepsilon = -\bar{k}_0 u^{\nu}{}_{;\nu}. \tag{6.12}$$

Using $u^{\mu}{}_{;\mu} = \varepsilon$ from (3.5) and rearranging, this equation can be rewritten as

$$\nabla^2\varepsilon + \frac{\bar{k}_0}{2\bar{\mu}_0 + \bar{\lambda}_0}\,\varepsilon = 0\,. \tag{6.13}$$

This wave equation applies to the volume dilatation ε. This equation is similar to the homogeneous Klein-Gordon equation for a scalar field, a field whose quanta are spinless particles [141].

Rotational (transverse) wave equation. Substituting (6.3) into (3.39), *viz.*

$$\bar{\mu}_0\nabla^2\omega^{\mu\nu} = -X^{[\mu;\nu]}\,, \tag{6.14}$$

the transverse (rotational) wave equation becomes

$$\bar{\mu}_0\nabla^2\omega^{\mu\nu} = -\frac{\bar{k}_0}{2}(u^{\mu;\nu} - u^{\nu;\mu})\,. \tag{6.15}$$

Using the definition of $\omega^{\mu\nu}$ from (3.3) and rearranging, this equation can be rewritten as

$$\nabla^2\omega^{\mu\nu} + \frac{\bar{k}_0}{\bar{\mu}_0}\,\omega^{\mu\nu} = 0\,. \tag{6.16}$$

This antisymmetric equation is also similar to an homogeneous Klein-Gordon equation for an antisymmetric tensor field.

Strain (symmetric) wave equation. Substituting (6.3) into (3.42), *viz.*

$$\bar{\mu}_0\nabla^2\varepsilon^{\mu\nu} + (\bar{\mu}_0 + \bar{\lambda}_0)\varepsilon^{;\mu\nu} = -X^{(\mu;\nu)}, \tag{6.17}$$

the symmetric (strain) wave equation becomes

$$\bar{\mu}_0\nabla^2\varepsilon^{\mu\nu} + (\bar{\mu}_0 + \bar{\lambda}_0)\varepsilon^{;\mu\nu} = -\frac{\bar{k}_0}{2}(u^{\mu;\nu} + u^{\nu;\mu}). \tag{6.18}$$

Using the definition of $\varepsilon^{\mu\nu}$ from (3.2) and rearranging, this equation can be rewritten as

$$\nabla^2 \varepsilon^{\mu\nu} + \frac{\bar{k}_0}{\bar{\mu}_0}\, \varepsilon^{\mu\nu} = -\frac{\bar{\mu}_0 + \bar{\lambda}_0}{\bar{\mu}_0}\, \varepsilon^{;\mu\nu}\,. \tag{6.19}$$

This symmetric equation is also similar to a nonhomogeneous Klein-Gordon equation for a symmetric tensor field with a source term.

§6.2.3 *Electromagnetism*

We consider the impact of this volume force on the equations of electromagnetism derived previously. Substituting (6.3) into (4.20), *viz.*

$$\omega^{\mu\nu}{}_{;\mu} = \frac{2\bar{\mu}_0 + \bar{\lambda}_0}{2\bar{\mu}_0}\, \varepsilon^{;\nu} + \frac{1}{2\bar{\mu}_0}\, X^\nu, \tag{6.20}$$

Maxwell's equations in terms of the rotation tensor become

$$\omega^{\mu\nu}{}_{;\mu} = \frac{2\bar{\mu}_0 + \bar{\lambda}_0}{2\bar{\mu}_0}\, \varepsilon^{;\nu} + \frac{\bar{k}_0}{2\bar{\mu}_0}\, u^\nu. \tag{6.21}$$

Separating u^ν into its longitudinal (irrotational) component $u^\nu_\parallel$ and its transverse (solenoidal) component $u^\nu_\perp$ using the Helmholtz theorem in four dimensions [378] according to

$$u^\nu = u^\nu_\parallel + u^\nu_\perp, \tag{6.22}$$

substituting for $\omega^{\mu\nu}$ from $F^{\mu\nu} = \varphi_0 \omega^{\mu\nu}$ and for $u^\nu_\perp$ from $A^\mu = -\frac{1}{2}\,\varphi_0 u^\mu_\perp$, this equation becomes

$$F^{\mu\nu}{}_{;\mu} = \varphi_0 \frac{2\bar{\mu}_0 + \bar{\lambda}_0}{2\bar{\mu}_0}\, \varepsilon^{;\nu} + \frac{\varphi_0 \bar{k}_0}{2\bar{\mu}_0}\, u^\nu_\parallel - \frac{\bar{k}_0}{\bar{\mu}_0}\, A^\nu. \tag{6.23}$$

Proper treatment of this case requires that the current density four-vector be proportional to the RHS of (6.23) as follows:

$$\mu_0 j^\nu = \frac{\varphi_0}{2\bar{\mu}_0}\, \left[(2\bar{\mu}_0 + \bar{\lambda}_0)\, \varepsilon^{;\nu} + \bar{k}_0 u^\nu_\parallel\right] - \frac{\bar{k}_0}{\bar{\mu}_0}\, A^\nu. \tag{6.24}$$

This thus yields the following microscopic form of the current density four-vector:

$$j^\nu = \frac{\varphi_0}{2\bar{\mu}_0 \mu_0}\, \left[(2\bar{\mu}_0 + \bar{\lambda}_0)\varepsilon^{;\nu} + \bar{k}_0 u^\nu_\parallel\right] - \frac{\bar{k}_0}{\bar{\mu}_0 \mu_0}\, A^\nu. \tag{6.25}$$

We thus find that the second term is proportional to A^ν as is the second term of the current density obtained from the quantum mechanical Klein-Gordon equation with an electromagnetic field [141, see p. 35]. in addition, we find that j^ν includes a longitudinal component $\bar{k}_0 u^\nu_\parallel$ propagating along the direction of propagation.

§6.3 Discussion of linear elastic volume force results

This section has been useful in that consideration of a simple linear elastic volume force leads to equations which are of the Klein-Gordon type. The wave equations that are obtained for the scalar ε, the 4-vector u^ν, and the symmetric and antisymmetric tensors $\varepsilon^{\mu\nu}$ and $\omega^{\mu\nu}$ respectively, are all equations that are similar to homogeneous or non-homogeneous Klein-Gordon equations. The solutions of these equations are well understood [292, see pp. 414–433].

It should be noted that we cannot simply put

$$\frac{m^2c^2}{\hbar^2} = \frac{\bar{k}_0}{2\bar{\mu}_0 + \bar{\lambda}_0} \tag{6.26}$$

or

$$\frac{m^2c^2}{\hbar^2} = \frac{\bar{k}_0}{\bar{\mu}_0} \tag{6.27}$$

from the Klein-Gordon equation, as the expression to use depends on the wave equation considered. This ambiguity in the equivalency of the constant $m^2c^2/\hbar^2$ to *STCED* constants indicates that the postulated elastic linear volume force proposed in (6.3) is not quite correct, even if it is a step in the right direction. It has provided insight into the impact of the volume force on this analysis, but the volume force is not quite the simple linear elastic expression considered in (6.3).

In the next chapter, we will derive a volume force from the general current density four-vector expression (4.27) seen previously in section §4.6.2. We find that the volume force (6.3) and consequently the current density four-vector (6.25) need to be modified.

§6.4 Designer STC volume forces

The spacetime continuum volume force can thus be tailored to the spacetime continuum characteristics. This we refer to as *designer volume forces*, that is volume forces designed to meet the needs of the spacetime continuum under consideration. This approach is similar to that followed to design Lagrangians in quantum electrodynamics. As we will see in the upcoming chapters on spacetime continuum defects, the

characteristics of the spacetime continuum can vary depending on the nature and density of defects in its structure.

In the next Chapter 7, we derive a quantum mechanical volume force based on the similarity in the structure of the current density four-vector in *STCED* and that derived from the spin-0 Klein-Gordon equation. It is expected that other *STC* volume forces can be derived from similar identifications with other equations.

Eshelby [113] and deWit [78, 79] point out that a fictitious volume force can be used to simulate the field of a defect in the spacetime continuum. deWit [79] provides examples, including one for an isotropic continuum. This approach provides another method of obtaining spacetime continuum volume forces tailored to the characteristics of the spacetime continuum. This is considered further in section §8.4.

Chapter 7

Quantum Mechanical Volume Force

§7.1 Derivation of a quantum mechanical volume force

In this chapter, we derive a quantum mechanical volume force based on the similarity in the structure of the current density four-vector in *STCED* and the one from the spin-0 Klein-Gordon equation. Hence one identification of the volume force based on quantum mechanical considerations is possible by comparing (4.27), *viz.*

$$j^{\nu} = \frac{1}{2}\,\frac{\varphi_0}{\mu_0\,\bar{\mu}_0}\left[(2\bar{\mu}_0 + \bar{\lambda}_0)\varepsilon^{;\nu} + X^{\nu}\right], \tag{7.1}$$

with the quantum mechanical expression of the current density four-vector j^{ν} obtained from the Klein-Gordon equation for a spin-0 particle. The Klein-Gordon equation can also describe the interaction of a spin-0 particle with an electromagnetic field. The current density four-vector j^{ν} in that case is written as [141, see p. 35]

$$j^{\nu} = \frac{ie\hbar}{2m}(\psi^{*}\partial^{\nu}\psi - \psi\,\partial^{\nu}\psi^{*}) - \frac{e^2}{m}\,A^{\nu}(\psi\psi^{*}) \tag{7.2}$$

where the superscript $*$ denotes complex conjugation.

The first term of (7.2) includes the following derivative-like expression:

$$i(\psi^{*}\partial^{\nu}\psi - \psi\,\partial^{\nu}\psi^{*}). \tag{7.3}$$

It is generated by multiplying the Klein-Gordon equation for ψ by ψ^{*} and subtracting the complex conjugate [141]. The general form of the expression can be generated by writing

$$\psi \sim \exp(i\vartheta) \tag{7.4}$$

which is a qualitative representation of the wavefunction. One can then see that with (7.4), the expression

$$\partial^{\nu}(\psi\psi^{*}) \tag{7.5}$$

has the qualitative structure of (7.3) although it is not strictly equivalent. However, given that the steps followed to generate (7.3) are not

repeated in this derivation, strict equivalence is not expected. Replacing (7.3) with (7.5), (7.2) becomes

$$j^{\nu} = \frac{e\hbar}{2m}\,\partial^{\nu}(\psi\psi^{*}) - \frac{e^{2}}{m}\,A^{\nu}(\psi\psi^{*})\,. \tag{7.6}$$

We see that the first term of (7.6) is similar to the first term of (7.1) and setting them to be equal, we obtain

$$\frac{\varphi_0}{2\mu_0\,\bar{\mu}_0}\,(2\bar{\mu}_0 + \bar{\lambda}_0)\varepsilon^{;\nu} = \frac{e\hbar}{2m}\,\partial^{\nu}(\psi\psi^{*}). \tag{7.7}$$

Similarly, the second terms of (7.1) and (7.2) are also similar and setting them to be equal, we obtain

$$\frac{\varphi_0}{2\mu_0\,\bar{\mu}_0}\,X^{\nu} = -\frac{e^{2}}{m}\,A^{\nu}(\psi\psi^{*}). \tag{7.8}$$

The equalities (7.7) and (7.8) thus result from the comparison of (7.1) and (7.2).

The first identification that can be determined from (7.7) is

$$\varepsilon\,(x^{\mu}) = \upsilon_0\psi\psi^{*} \tag{7.9}$$

where the proportionality constant has been set to υ_0 which has units of $[m^3]$. While ε which is the change in volume per original volume as a function of position x^{μ}, which is stated explicitly in (7.9), is a dimensionless quantity, the Klein-Gordon wavefunction ψ has units of $\mathrm{L}^{-Nn/2}$ and the norm of the wavefunction $\psi\psi^{*}$ has units L^{-Nn} where N is the number of particles and n is the number of spatial dimensions. For one particle in three-dimensional space, the units of the proportionality constant υ_0 are thus $[m^3]$. This equation indicates that the Klein-Gordon quantum mechanical wavefunction describes longitudinal wave propagations in the spacetime continuum corresponding to the volume dilatation associated with the particle property of an object.

Making use of (7.9) in (7.7), the *STC* electromagnetic shearing potential constant φ_0 of (4.4) is then given by:

$$\varphi_0 = \frac{2\bar{\mu}_0}{2\bar{\mu}_0 + \bar{\lambda}_0}\,\frac{\mu_0}{\upsilon_0}\,\frac{e\hbar}{2m}\,. \tag{7.10}$$

The units of φ_0 are $[\mathrm{V}\cdot\mathrm{s}\cdot\mathrm{m}^{-2}]$ or [T] as required. Using (7.5) and (7.9) in (7.2), we obtain

$$j^{\nu} = \frac{e\hbar}{2m\upsilon_0}\,\varepsilon^{;\nu} - \frac{e^{2}}{m\upsilon_0}\,A^{\nu}\varepsilon\,(x^{\mu})\,. \tag{7.11}$$

The units of j^ν are $[\mathrm{C}\cdot\mathrm{s}^{-1}\cdot\mathrm{m}^{-2}]$ as required.

Using (4.4) *viz.*

$$A^\nu = -\tfrac{1}{2}\,\varphi_0 u_\perp^\nu \tag{7.12}$$

and (7.9) in (7.8), the quantum mechanical volume force is given by

$$X^\nu = \frac{\bar{\mu}_0\mu_0}{\upsilon_0}\,\frac{e^2}{m}\,\varepsilon\,(x^\mu)\;u_\perp^\nu. \tag{7.13}$$

Using the definition for the dimensionless fine structure constant $\alpha = \mu_0 c e^2/h$, (7.13) becomes

$$X^\nu = \frac{\bar{\mu}_0\alpha}{\upsilon_0}\,\frac{h}{mc}\,\varepsilon\,(x^\mu)\;u_\perp^\nu \tag{7.14}$$

or

$$X^\nu = \frac{\bar{\mu}_0\alpha}{\upsilon_0}\,\lambda_c\,\varepsilon\,(x^\mu)\;u_\perp^\nu \tag{7.15}$$

where $\lambda_c = h/mc$ is the electron's Compton wavelength.

Thus the *STCED* elastic force constant of (6.3) is given by

$$\bar{k}_0 = \frac{\bar{\mu}_0\mu_0}{\upsilon_0}\,\frac{e^2}{m} = \frac{\bar{\mu}_0\alpha}{\upsilon_0}\,\frac{h}{mc} = \frac{\bar{\mu}_0\alpha}{\upsilon_0}\,\lambda_c\,, \tag{7.16}$$

where we have included the constant υ_0 in $\bar{k}_0$. The volume force is proportional to $\varepsilon\,(x^\mu)\,u_\perp^\nu$ as opposed to just u^ν as in (6.3):

$$X^\nu = \bar{k}_0\,\varepsilon\,(x^\mu)\;u_\perp^\nu\,. \tag{7.17}$$

The units are $[\mathrm{N}\cdot\mathrm{m}^{-3}]$ as expected.

The volume force X^ν is proportional to the Planck constant as suspected previously. This explains why the volume force tends to zero in the macroscopic case. The volume force is also proportional to the *STC* volume dilatation $\varepsilon\,(x^\mu)$ in addition to the displacements $u_\perp^\nu$. This makes sense as all deformations, both distortions and dilatations, should be subject to the *STC* elastic spring force. This is similar to an elastic spring law as X^ν is defined positive in the direction opposite to the displacement [126]. The volume force also describes the interaction with an electromagnetic field given that (7.2) from which it is derived includes electromagnetic interactions.

§7.2 Displacements equation

Substituting (7.17) into (6.4), the dynamic equation in terms of displacements becomes

$$\bar{\mu}_0 \nabla^2 u^\nu + (\bar{\mu}_0 + \bar{\lambda}_0)\varepsilon^{;\nu} = -\bar{k}_0\, \varepsilon(x^\mu)\, u^\nu_\perp . \tag{7.18}$$

This equation can be rewritten as

$$\nabla^2 u^\nu + \frac{\bar{k}_0}{\bar{\mu}_0}\, \varepsilon\,(x^\mu)\; u^\nu_\perp = -\frac{\bar{\mu}_0 + \bar{\lambda}_0}{\bar{\mu}_0}\, \varepsilon^{;\nu}\,. \tag{7.19}$$

We note that $\varepsilon(x^\mu)$ is a scalar function of 4-position only, and plays a role similar to the potential $V(\boldsymbol{r}\,)$ in the Schrödinger equation. Indeed, $\varepsilon(x^\mu)$ represents the mass energy structure (similar to an energy potential) impacting the solutions of this equation.

Separating u^ν into its longitudinal (irrotational) component $u^\nu_\parallel$ and its transverse (solenoidal) component $u^\nu_\perp$ using the Helmholtz theorem in four dimensions [378] according to

$$u^\nu = u^\nu_\parallel + u^\nu_\perp\,, \tag{7.20}$$

and similarly separating the dilatation current $\xi^\nu = \varepsilon^{;\nu}$ into a longitudinal component $\xi^\nu_\parallel$ and a transverse component $\xi^\nu_\perp$

$$\xi^\nu = \xi^\nu_\parallel + \xi^\nu_\perp\,, \tag{7.21}$$

we obtain the separated equations

$$\begin{aligned} \nabla^2 u^\nu_\parallel &= -\frac{\bar{\mu}_0 + \bar{\lambda}_0}{\bar{\mu}_0}\, \xi^\nu_\parallel \\ \nabla^2 u^\nu_\perp + \frac{\bar{k}_0}{\bar{\mu}_0}\, u^\nu_\perp &= -\frac{\bar{\mu}_0 + \bar{\lambda}_0}{\bar{\mu}_0}\, \xi^\nu_\perp \end{aligned} \tag{7.22}$$

which becomes

$$\nabla^2 u^\nu_\perp + \frac{\bar{k}_0}{\bar{\mu}_0}\, u^\nu_\perp = 0 \tag{7.23}$$

given that $\xi^\nu_\perp = \varepsilon^{;\nu}_\perp = 0$. The wave equation for $u^\nu_\parallel$ describes the propagation of longitudinal displacements, while the wave equation for $u^\nu_\perp$ describes the propagation of transverse displacements.

§7.2.1 *Longitudinal displacements equation*

Substituting for $\varepsilon^{,\nu}$ from (7.11) in the first equation of (7.22), we obtain

$$\nabla^2 u_{\parallel}^{\nu} = -\frac{2k_L}{\hbar}\left(\frac{e^2}{m}\,\upsilon_0\, j^{\nu} + eA^{\nu}\varepsilon\left(x^{\mu}\right)\right) \tag{7.24}$$

where the dimensionless ratio

$$k_L = \frac{\bar{\mu}_0 + \bar{\lambda}_0}{\bar{\mu}_0} \tag{7.25}$$

has been introduced. Hence the source term on the RHS of this equation includes the mass resulting from the dilatation displacements, the current density four-vector, and the vector potential resulting from the distortion displacements. It provides a full description of the gravitational and electromagnetic interactions at the microscopic level.

§7.2.2 *Transverse displacements equation*

Substituting for $u_{\perp}^{\nu}$ from (4.4) in the second equation of (7.22), we obtain

$$\nabla^2 A^{\nu} + \frac{\bar{k}_0}{\bar{\mu}_0}\,\varepsilon\left(x^{\mu}\right)\, A^{\nu} = 0. \tag{7.26}$$

Substituting for $\bar{k}_0$ from (7.16), this equation becomes

$$\nabla^2 A^{\nu} + \frac{\mu_0}{\upsilon_0}\,\frac{e^2}{m}\,\varepsilon\left(x^{\mu}\right)\, A^{\nu} = 0 \tag{7.27}$$

or

$$\nabla^2 A^{\nu} + \frac{\alpha}{\upsilon_0}\,\frac{h}{mc}\,\varepsilon\left(x^{\mu}\right)\, A^{\nu} = 0\,. \tag{7.28}$$

This equation is similar to a Proca equation except that the coefficient of A^{ν} is not the familiar $m^2c^2/\hbar^2$. Given that transverse displacements are massless, the Proca equation coefficient is not expected given its usual interpretation that it represents the mass of the particle described by the equation. This is discussed in more details in section §7.3.5.

§7.3 Wave equations

We derive the additional wave equations as shown in section §3.5, from this volume force.

§7.3.1 *Longitudinal wave equation*

Substituting (7.17) into (6.11), the longitudinal (dilatational) wave equation becomes

$$(2\bar{\mu}_0 + \bar{\lambda}_0)\,\nabla^2\varepsilon = -\nabla_\nu \left[\bar{k}_0\,\varepsilon\,(x^\mu)\; u_\perp^\nu\right]. \tag{7.29}$$

Taking the divergence on the RHS, using $u_{\perp;\nu}^{\nu} = 0$ from (3.6) and rearranging, this equation can be rewritten as

$$\nabla^2\varepsilon = -\frac{\bar{k}_0}{2\bar{\mu}_0 + \bar{\lambda}_0}\, u_\perp^\nu \varepsilon_{;\nu}\,. \tag{7.30}$$

Substituting for $u_\perp^\nu$ from (4.4), for $\bar{k}_0$ from (7.16) and for $\varepsilon_{;\nu}$ from (7.11), we obtain

$$\nabla^2\varepsilon - 4\,\frac{e^2}{\hbar^2}\,A^\nu A_\nu\,\varepsilon = 4\,\frac{m\upsilon_0}{\hbar^2}\,A^\nu j_\nu. \tag{7.31}$$

Recognizing that

$$e^2\,A^\nu A_\nu = P^\nu P_\nu = -m^2c^2, \tag{7.32}$$

and substituting in (7.31), the equation becomes

$$\nabla^2\varepsilon + 4\,\frac{m^2c^2}{\hbar^2}\,\varepsilon = 4\,\frac{m\upsilon_0}{\hbar^2}\,A^\nu j_\nu\,. \tag{7.33}$$

This is the Klein-Gordon equation except for the factor of 4 multiplying the ε coefficient and the source term. The term on the RHS of this equation is an interaction term of the form $\boldsymbol{A}\cdot\boldsymbol{j}$.

As identified from (7.9) and confirmed by this equation, the Klein-Gordon quantum mechanical wavefunction describes longitudinal wave propagations in the spacetime continuum corresponding to the volume dilatation associated with the particle property of an object. The RHS of the equation indicates an interaction between the longitudinal current density j_ν and the transverse vector potential A^ν. This is interpreted in electromagnetism as energy in the static magnetic induction field to establish the steady current distribution [67, see p. 150]. It is also the form of the interaction term introduced in the vacuum Lagrangian for classical electrodynamics [262, see p. 428].

Although (7.33) with the $m^2c^2/\hbar^2$ coefficient is how the Klein-Gordon equation is typically written, (7.31) is a more physically accurate way of writing that equation, *i.e.*

$$\frac{\hbar^2}{4}\,\nabla^2\varepsilon - e^2\,A^\nu A_\nu\,\varepsilon = m\,\upsilon_0\,A^\nu j_\nu\,, \tag{7.34}$$

as the massive nature of the equation resides in its solutions $\varepsilon\,(x^\mu)$. The constant m needs to be interpreted in the same way as the constant e. The constant e in the Klein-Gordon equation is the elementary unit of electrical charge (notwithstanding the quark fractional charges), not the electrical charge of the particle represented by the equation. Similarly, the constant m in the Klein-Gordon equation needs to be interpreted as the elementary unit of mass (the electron's mass), not the mass of the particle represented by the equation. That is obtained from the solutions $\varepsilon\,(x^\mu)$ of the equation.

§7.3.2 *Transverse wave equation*

Using (7.17) into (6.14), the transverse (rotational) wave equation becomes

$$\bar{\mu}_0 \nabla^2 \omega^{\mu\nu} = -\frac{\bar{k}_0}{2}\left[(\varepsilon u_\perp^\mu)^{;\nu} - (\varepsilon u_\perp^\nu)^{;\mu}\right]. \tag{7.35}$$

Using (3.3) and rearranging, this equation can be rewritten as

$$\nabla^2 \omega^{\mu\nu} + \frac{\bar{k}_0}{\bar{\mu}_0}\,\varepsilon\,(x^\mu)\;\omega^{\mu\nu} = \frac{1}{2}\,\frac{\bar{k}_0}{\bar{\mu}_0}\,(\varepsilon^{;\mu} u_\perp^\nu - \varepsilon^{;\nu} u_\perp^\mu)\,. \tag{7.36}$$

Substituting for $\omega^{\mu\nu}$ using $F^{\mu\nu} = \varphi_0 \omega^{\mu\nu}$ from (4.3), for $u_\perp^\nu$ from (4.4), for $\bar{k}_0$ from (7.16) and for $\varepsilon^{;\nu}$ from (7.11), we obtain

$$\nabla^2 F^{\mu\nu} + \frac{\mu_0}{\upsilon_0}\,\frac{e^2}{m}\,\varepsilon\,(x^\mu)\;F^{\mu\nu} = \mu_0\,\frac{e}{\hbar}\;(A^\mu j^\nu - A^\nu j^\mu)\;. \tag{7.37}$$

This equation can also be written as

$$\nabla^2 F^{\mu\nu} + \frac{\alpha}{\upsilon_0}\,\lambda_c\,\varepsilon\,(x^\mu)\;F^{\mu\nu} = \mu_0\,\frac{e}{\hbar}\;(A^\mu j^\nu - A^\nu j^\mu)\,. \tag{7.38}$$

This is a new equation of the electromagnetic field strength $F^{\mu\nu}$. The term on the RHS of this equation is an interaction term of the form $\boldsymbol{A}\times\boldsymbol{j}$. In electromagnetism, this term is the volume density of the magnetic torque (magnetic torque density), and is interpreted as the "longitudinal tension" between two successive current elements (Helmholtz's longitudinal tension), observed experimentally by Ampère (hairpin experiment) [307].

§7.3.3 *Strain wave equation*

Substituting (7.17) into (6.17), the strain (symmetric) wave equation becomes

$$\bar{\mu}_0 \nabla^2 \varepsilon^{\mu\nu} + (\bar{\mu}_0 + \bar{\lambda}_0)\varepsilon^{;\mu\nu} = -\frac{\bar{k}_0}{2}[(\varepsilon u_\perp^\mu)^{;\nu} + (\varepsilon u_\perp^\nu)^{;\mu}] \tag{7.39}$$

which can be rewritten as

$$\begin{aligned}&\nabla^2\varepsilon^{\mu\nu}+\frac{\bar{\mu}_0+\bar{\lambda}_0}{\bar{\mu}_0}\,\varepsilon^{;\mu\nu}=\\&=\frac{1}{2}\,\frac{\bar{k}_0}{\bar{\mu}_0}\left[\varepsilon\left(u_\perp^{\mu;\nu}+u_\perp^{\nu;\mu}\right)+\left(\varepsilon^{;\mu}u_\perp^{\nu}+\varepsilon^{;\nu}u_\perp^{\mu}\right)\right].\end{aligned}\tag{7.40}$$

Substituting for $u_\perp^\nu$ from (4.4), for $\bar{k}_0$ from (7.16) and for $\varepsilon^{;\nu}$ from (7.11), we obtain

$$\begin{aligned}&\nabla^2\varepsilon^{\mu\nu}+k_L\,\varepsilon^{;\mu\nu}=k_T\,\frac{2m}{\hbar^2}\left(A^\mu j^\nu+A^\nu j^\mu\right)+\\&+k_T\,\frac{\varepsilon}{\upsilon_0}\left[\frac{e}{\hbar}\left(A^{\mu;\nu}+A^{\nu;\mu}\right)+\frac{2e^2}{\hbar^2}\left(A^\mu A^\nu+A^\nu A^\mu\right)\right]\end{aligned}\tag{7.41}$$

where the dimensionless ratio

$$k_T=\frac{2\bar{\mu}_0+\bar{\lambda}_0}{\bar{\mu}_0}\tag{7.42}$$

has been introduced and ratio k_L has been used from (7.25). The last term can be summed to $2A^\mu A^\nu$. This new equation for the symmetric strain tensor field includes on the RHS symmetric interaction terms between the current density four-vector and the vector potential resulting from the distortion displacements and between the vector potential and the mass resulting from the dilatation displacements.

§7.3.4 *Simplified wave equations*

Inspection of the wave equations derived previously shows that common factors are associated with A^ν and j^ν in all the equations. We thus introduce the reduced physical variables $A^{*\nu}$ and $j^{*\nu}$ defined according to

$$\begin{aligned}A^{*\nu}&=eA^\nu\\j^{*\nu}&=\frac{m}{e}\,j^\nu,\end{aligned}\tag{7.43}$$

and $\underline{A}^{*\nu}$ and $\underline{j}^{*\nu}$ defined according to

$$\begin{aligned}\underline{A}^{*\nu}&=\frac{2e}{\hbar}\,A^\nu\\\underline{j}^{*\nu}&=\frac{2m}{e\hbar}\,j^\nu.\end{aligned}\tag{7.44}$$

The various wave equations then simplify to the following.

Longitudinal displacements equation

$$\nabla^2 u_{\parallel}^{\nu} = -\frac{2k_L}{\hbar}\left(\upsilon_0\, j^{*\,\nu} + \varepsilon A^{*\,\nu}\right) \tag{7.45}$$

$$\nabla^2 u_{\parallel}^{\nu} = -k_L\left(\upsilon_0\, \underline{j}^{*\,\nu} + \varepsilon \underline{A}^{*\,\nu}\right) \tag{7.46}$$

Transverse displacements equation

$$\nabla^2 A^{*\,\nu} + \frac{\alpha}{\upsilon_0}\,\lambda_c\,\varepsilon A^{*\,\nu} = 0 \tag{7.47}$$

$$\nabla^2 \underline{A}^{*\,\nu} + \frac{\alpha}{\upsilon_0}\,\lambda_c\,\varepsilon \underline{A}^{*\,\nu} = 0 \tag{7.48}$$

Longitudinal wave equation

$$\frac{\hbar^2}{4}\,\nabla^2\varepsilon - A^{*\,\nu} A^{*}_{\nu}\,\varepsilon = \upsilon_0\, A^{*\,\nu} j^{*}_{\nu} \tag{7.49}$$

$$\nabla^2\varepsilon - \underline{A}^{*\,\nu}\,\underline{A}^{*}_{\nu}\,\varepsilon = \upsilon_0\,\underline{A}^{*\,\nu}\,\underline{j}^{*}_{\nu} \tag{7.50}$$

Transverse wave equation

$$\nabla^2 F^{\mu\nu} + \frac{\alpha}{\upsilon_0}\,\lambda_c\,\varepsilon\,(x^{\mu})\; F^{\mu\nu} = \mu_0\,\frac{e}{\hbar m}\,\left(A^{*\,\mu} j^{*\,\nu} - A^{*\,\nu} j^{*\,\mu}\right) \tag{7.51}$$

$$\nabla^2 F^{\mu\nu} + \frac{\alpha}{\upsilon_0}\,\lambda_c\,\varepsilon\,(x^{\mu})\; F^{\mu\nu} = \tfrac{1}{2}\,\mu_0\,\mu_B\,\left(\underline{A}^{*\,\mu}\,\underline{j}^{*\,\nu} - \underline{A}^{*\,\nu}\,\underline{j}^{*\,\mu}\right) \tag{7.52}$$

Strain wave equation

$$\begin{aligned}\nabla^2\varepsilon^{\mu\nu} + k_L\,\varepsilon^{;\mu\nu} &= k_T\,\frac{2}{\hbar^2}\left(A^{*\,\mu} j^{*\,\nu} + A^{*\,\nu} j^{*\,\mu}\right) + \\ &+ k_T\,\frac{\varepsilon}{\upsilon_0}\left[\frac{1}{\hbar}\left(A^{*\,\mu;\nu} + A^{*\,\nu;\mu}\right) + \frac{2}{\hbar^2}\left(A^{*\,\mu} A^{*\,\nu} + A^{*\,\nu} A^{*\,\mu}\right)\right]\end{aligned} \tag{7.53}$$

$$\begin{aligned}\nabla^2\varepsilon^{\mu\nu} + k_L\,\varepsilon^{;\mu\nu} &= \tfrac{1}{2}\,k_T\left(\underline{A}^{*\,\mu}\,\underline{j}^{*\,\nu} + \underline{A}^{*\,\nu}\,\underline{j}^{*\,\mu}\right) + \\ &+ \tfrac{1}{2}\,k_T\,\frac{\varepsilon}{\upsilon_0}\left[\left(\underline{A}^{*\,\mu;\nu} + \underline{A}^{*\,\nu;\mu}\right) + \left(\underline{A}^{*\,\mu}\,\underline{A}^{*\,\nu} + \underline{A}^{*\,\nu}\,\underline{A}^{*\,\mu}\right)\right]\end{aligned} \tag{7.54}$$

§7.3.5 *Proca wave equation*

As seen in section §4.8, a Proca-like equation (4.37) is obtained from the electromagnetic equations with a volume force X^ν given by

$$\nabla^2 A^\nu - A^{\mu;\nu}{}_{\mu} - \frac{\varphi_0}{2\bar{\mu}_0}\, X^\nu = \mu_0\, j^\nu_{classical}\,. \tag{7.55}$$

Using the volume force derived from (7.8) and (7.9), (7.55) becomes

$$\nabla^2 A^\nu - A^{\mu;\nu}{}_{\mu} + \frac{\mu_0 e^2}{m}\,\frac{\varepsilon(x^\mu)}{\upsilon_0}\, A^\nu = \mu_0\, j^\nu_{classical}\,. \tag{7.56}$$

Re-arranging the derivatives in the second term on the L.H.S. and using the Lorenz condition (4.16), we obtain

$$\nabla^2 A^\nu + \frac{\mu_0 e^2}{m}\,\frac{\varepsilon(x^\mu)}{\upsilon_0}\, A^\nu = \mu_0\, j^\nu_{classical} \tag{7.57}$$

which is similar to (7.27) obtained previously in section §7.2.2. This equation can be rewritten as

$$\nabla^2 A^\nu + \alpha\,\frac{h}{mc}\,\frac{\varepsilon(x^\mu)}{\upsilon_0}\, A^\nu = \mu_0\, j^\nu_{classical}\,. \tag{7.58}$$

This equation has the same structure as the Proca equation, although the coefficient of the second term on the L.H.S. is not the familiar $(mc/\hbar)^2$.

§7.4 Alternative derivation of the quantum mechanical volume force

In this section we consider an alternative derivation of the quantum mechanical volume force from the comparison of (7.1) *viz.*

$$j^\nu = \frac{1}{2}\,\frac{\varphi_0}{\mu_0\,\bar{\mu}_0}\left[(2\bar{\mu}_0 + \bar{\lambda}_0)\varepsilon^{;\nu} + X^\nu\right] \tag{7.59}$$

and (7.2) *viz.*

$$j^\nu = \frac{ie\hbar}{2m}(\psi^*\partial^\nu\psi - \psi\,\partial^\nu\psi^*) - \frac{e^2}{m}\,A^\nu(\psi\psi^*)\,. \tag{7.60}$$

Based on (7.4), we write ψ as

$$\psi = \mathcal{A}\exp(i\vartheta) \tag{7.61}$$

where $\mathcal{A}$ is the amplitude of the wavefunction. Then

$$\partial^\nu \psi = i\mathcal{A} \exp(i\vartheta)\, \partial^\nu \vartheta \tag{7.62}$$

and

$$i(\psi^* \partial^\nu \psi - \psi\, \partial^\nu \psi^*) = -2\, \mathcal{A}^* \mathcal{A}\, \partial^\nu \vartheta = -2\, |\mathcal{A}|^2\, \partial^\nu \vartheta \tag{7.63}$$

which can be seen to be a type of antisymmetrical derivative

$$\bar{\partial}^\nu (\psi \psi^*) = i(\psi^* \partial^\nu \psi - \psi\, \partial^\nu \psi^*)\,, \tag{7.64}$$

to generate a transverse quantity in line with (7.60) which is an equation for the transverse current $j^\nu = j^\nu_\perp$ in terms of the transverse vector potential $A^\nu \propto u^\nu_\perp$.

Substituting (7.61) and (7.63) into (7.60), we obtain

$$j^\nu = -\frac{e\hbar}{m}\, |\mathcal{A}|^2\, \partial^\nu \vartheta - \frac{e^2}{m}\, |\mathcal{A}|^2\, A^\nu \tag{7.65}$$

or

$$j^\nu = -\frac{e}{m}\, |\mathcal{A}|^2\, \left[\hbar\, \partial^\nu \vartheta + eA^\nu\right]\,. \tag{7.66}$$

Comparing (7.59) and (7.65), the first term of (7.59) is similar to the first term of (7.65) and setting them to be equal, we obtain

$$\frac{\varphi_0}{2\mu_0\, \bar{\mu}_0}\, (2\bar{\mu}_0 + \bar{\lambda}_0) \varepsilon^{;\nu} = -\frac{e\hbar}{m}\, |\mathcal{A}|^2\, \partial^\nu \vartheta\,. \tag{7.67}$$

Similarly, the second terms of (7.59) and (7.65) are also similar and setting them to be equal, we obtain

$$\frac{\varphi_0}{2\mu_0\, \bar{\mu}_0}\, X^\nu = -\frac{e^2}{m}\, |\mathcal{A}|^2\, A^\nu\,. \tag{7.68}$$

The equalities (7.67) and (7.68) result from the comparison of (7.59) and (7.60).

From (7.67) and (7.63), we see that

$$\varepsilon^{;\nu} = -2\, \upsilon_0 |\mathcal{A}|^2\, \partial^\nu \vartheta \tag{7.69}$$

and hence

$$\varepsilon\, (x^\mu) = \upsilon_0 |\mathcal{A}|^2 \tag{7.70}$$

where the proportionality constant υ_0 has been introduced as in §7.1. This leads to the STC electromagnetic shearing potential constant φ_0 as defined previously in (7.10):

$$\varphi_0 = \frac{2\bar{\mu}_0}{2\bar{\mu}_0 + \bar{\lambda}_0} \frac{\mu_0}{\upsilon_0} \frac{e\hbar}{2m} . \tag{7.71}$$

Setting $\varepsilon\,(x^\mu) = \upsilon_0 \psi\psi^* = \upsilon_0 |\mathcal{A}|^2$ as done in (7.9), results in the volume force X^ν (7.17) as used in section §7.1. Setting $\varepsilon^{;\nu}$ equal to (7.63) leads to relation (7.7) and the results of sections §7.1 to §7.3.

However, the approach followed in this section provides another way of allocating the variables. In the relations (7.67) and (7.68), the factor $|\mathcal{A}|^2$ is common to both, and represents the intensity of the unnormalized wavefunction. We see that the current density j^ν given by (7.66) consists of the ratio e/m multiplied by the intensity of the wavefunction and by the sum of two terms, the first representing the energy in the wave from (7.67) and the second the energy from the vector potential from (7.68).

From (7.68), we can determine the volume force, given by

$$X^\nu = -\frac{2\bar{\mu}_0\,\mu_0}{\varphi_0} \frac{e^2}{m} |\mathcal{A}|^2\, A^\nu . \tag{7.72}$$

Using (4.4), (7.72) can be rewritten as

$$X^\nu = \bar{\mu}_0\,\mu_0 \frac{e^2}{m} |\mathcal{A}|^2\, u_\perp^\nu . \tag{7.73}$$

Defining $\bar{k}_0$, the elastic force constant of the STC volume force, given by

$$\bar{k}_0 = \mu_0\,\bar{\mu}_0 \frac{e^2}{m} = \bar{\mu}_0 \alpha \frac{h}{mc} , \tag{7.74}$$

then the volume force is given by

$$X^\nu = \bar{k}_0\, |\mathcal{A}|^2\, u_\perp^\nu . \tag{7.75}$$

Setting $\varepsilon\,(x^\mu) = \upsilon_0 \psi\psi^* = \upsilon_0 |\mathcal{A}|^2$, we obtain (7.16) and (7.17) as previously:

$$\bar{k}_0' = \frac{\bar{\mu}_0 \mu_0}{\upsilon_0} \frac{e^2}{m} = \frac{\bar{\mu}_0 \alpha}{\upsilon_0} \frac{h}{mc} , \tag{7.76}$$

where we have included the constant υ_0 in $\bar{k}_0'$. Then the volume force is proportional to $\varepsilon\,(x^\mu)\, u_\perp^\nu$ as previously:

$$X^\nu = \bar{k}_0'\, \varepsilon\,(x^\mu)\; u_\perp^\nu . \tag{7.77}$$

Eq. (7.77) is equivalent to (7.75).

Using the volume force (7.72) in (7.59), the following expression is obtained for $\xi^\nu = \varepsilon^{;\nu}$:

$$\varepsilon^{;\nu} = \frac{2\bar{\mu}_0}{2\bar{\mu}_0 + \bar{\lambda}_0} \frac{\mu_0}{\varphi_0} \left[j^\nu + \frac{e^2}{m} |\mathcal{A}|^2 A^\nu \right] . \tag{7.78}$$

This equation is the same as the one used in sections §7.1 to §7.3 obtained by setting $\varepsilon(x^\mu) = \upsilon_0 \psi\psi^* = \upsilon_0 |\mathcal{A}|^2$. From (7.67), we can also write

$$\varepsilon^{;\nu} = -\frac{2\bar{\mu}_0}{2\bar{\mu}_0 + \bar{\lambda}_0} \frac{\mu_0}{\varphi_0} \frac{e\hbar}{m} |\mathcal{A}|^2 \partial^\nu \vartheta . \tag{7.79}$$

Equating (7.78) and (7.79), we obtain

$$j^\nu = -\frac{e}{m} |\mathcal{A}|^2 \left[\hbar \partial^\nu \vartheta + eA^\nu \right] \tag{7.80}$$

which is the same as (7.66), indicating that the equations are self-consistent.

Using

$$\vartheta = k_\mu x^\mu , \tag{7.81}$$

where k^μ is the 4-vector wavevector given by $(\omega/c, \mathbf{k})$, $\partial^\nu \vartheta$ is given by

$$\partial^\nu \vartheta = k^\nu \tag{7.82}$$

and (7.80) becomes

$$j^\nu = -\frac{e}{m} |\mathcal{A}|^2 \left[\hbar k^\nu + eA^\nu \right] . \tag{7.83}$$

The time component is given by

$$j^t = -\frac{e}{mc} |\mathcal{A}|^2 \left[\hbar \omega + e\phi \right] . \tag{7.84}$$

and the space component by

$$\mathbf{j} = -\frac{e}{m} |\mathcal{A}|^2 \left[\hbar \mathbf{k} + e\mathbf{A} \right] . \tag{7.85}$$

We obtain explicitly the sum of two terms, with the first giving the energy in the wave given by the Einstein quantum mechanical expression and the second giving the energy in the vector potential.

Substituting (7.82) into (7.79), the dilatation current becomes

$$\xi^\nu = \varepsilon^{;\nu} = -\frac{2\bar{\mu}_0}{2\bar{\mu}_0 + \bar{\lambda}_0} \frac{\mu_0}{\varphi_0} \frac{e\hbar}{m} |\mathcal{A}|^2 k^\nu = -2\, \upsilon_0 |\mathcal{A}|^2 k^\nu \tag{7.86}$$

or alternatively

$$\xi^{\nu} = \varepsilon^{;\nu} = -\frac{2\bar{\mu}_0}{2\bar{\mu}_0 + \bar{\lambda}_0} \frac{\mu_0}{\varphi_0 \upsilon_0} \frac{e\hbar}{m} \varepsilon\left(x^{\mu}\right) k^{\nu} = -2\,\varepsilon\left(x^{\mu}\right) k^{\nu}\,. \tag{7.87}$$

These results are supplemental to those of sections §7.1 to §7.3.

§7.5 Alternative volume forces

This chapter provides an example of a volume force derived by comparison with the Klein-Gordon current density for spin-0 particles with electromagnetic interaction. It has one unknown parameter υ_0, of units $[m^{-3}]$, which corresponds to the normalization factor for the Klein-Gordon wavefunction norm. It corresponds to an inverse volume and could be set to an appropriate constant such as

$$\upsilon_0 = \left(\frac{mc}{\hbar}\right)^3 \tag{7.88}$$

or

$$\upsilon_0 = (b_0)^{-3}\,, \tag{7.89}$$

where b_0 is defined in section §14.2. The actual value depends on the actual equivalent Klein-Gordon solutions under consideration.

This procedure of devising a volume force for a given situation provides one approach to dealing with quantum physics in *STCED*. This is an approach similar to how Lagrangians are determined in quantum electrodynamics. The results obtained in this chapter provide interesting insights into the physical nature of the quantum level. However, the Klein-Gordon equation has limitations as a relativistic quantum wave equation [141], and the quantum mechanical volume force derived from the equation should thus be considered to have limited application. In subsequent chapters, we consider a more general approach to analyzing quantum physics based on the analysis of defects in the spacetime continuum.

Chapter 8

Defects in the Spacetime Continuum

§8.1 Analysis of spacetime continuum defects

Given that the spacetime continuum behaves as a deformable medium, there is no reason not to expect dislocations, disclinations and other defects to be present in the spacetime continuum. Dislocations and disclinations of the spacetime continuum represent the fundamental displacement processes that occur in its structure. These fundamental displacement processes should correspond to basic quantum phenomena and provide a framework for the description of quantum physics in *STCED*.

In the following chapters, we use the word *defect* to mean specifically dislocations and disclinations, but without in general excluding other defects such as point defects. *Dislocations* are translational deformations, while *disclinations* are rotational deformations. Defects can be characterized using the Volterra [360] classification or using the theory of topological stability [201]. The two methods are not equivalent and the topological classification is usually used as a supplement to the Volterra classification.

Dislocations and disclinations can be analyzed as either discrete defect lines, continuous infinitesimal defect loops, or as continuous distributions of defect densities [80], which is more suited to the methods of differential geometry. This breakdown applies both to dislocations and disclinations. The theory of disclinations is an extension of dislocation theory, that includes both dislocations and disclinations. It reduces to dislocation theory in the absence of disclinations.

Using defect density distributions results in field equations using the methods of differential geometry. These are also amenable to gauge theories and the modern theoretical descriptions are mostly in terms of gauge theory and differential geometry, using continuous distributions of defect densities (see for example [199]). Defect theory is applied mostly to condensed matter physics, although the extension of differential geometry methods to cosmic strings is an ongoing effort.

We will cover the analysis of distributions of defect densities in a later separate chapter (Chapter 11). In the following chapters on dislocations and disclinations, we cover discrete line defects, and to some degree,

infinitesimal defect loops, both of which are not given much coverage in modern defect analysis. These we will find provide a description of basic quantum processes in the microscopic description of the spacetime continuum.

Our analysis of spacetime defects is done in the isotropic linear elastic continuum we have been considering till now. However, it should be noted that modern defect theory in condensed matter physics is an advanced discipline that is rich in results derived from more complex continuum models.

Volterra [360] first studied and classified the elastic deformations of multiply-connected solids in 1907. These he named distortions, which was later changed by Love [220] to dislocations. The growing importance of rotational dislocations prompted Frank [127] to rename those to disinclinations which he later shortened to disclinations, the term that is still used today [78]. Defect theory has been the subject of investigation since the first half of the twentieth century and is a well-developed discipline in continuum mechanics [159, 172, 203, 211, 263, 364]. The more recent formulation of defects in solids is based on gauge theory and differential geometry as discussed previously [93, 199].

The last quarter of the twentieth century has seen the investigation of spacetime topological defects in the context of string theory, particularly cosmic strings [224, 297], and cosmic expansion [309, 340]. Teleparallel spacetime with defects [224,356,357] has resulted in a differential geometry of defects, which can be folded into the Einstein-Cartan Theory (ECT) of gravitation, an extension of Einstein's theory of gravitation that includes torsion [309, 310]. Recently, the phenomenology of spacetime defects has been considered in the context of quantum gravity [167–169].

There are many papers that have been published on the subject of defects in the spacetime continuum. Unfortunately, like all areas under development, there are papers that have errors, while others have inconsistencies that are not fatal, but that lead to conclusions that are questionable if not incorrect. The specific papers will in most cases not be identified, although some may be mentioned where required. While not claiming to be infallible, the results presented in the following chapters on defects in the spacetime continuum and its application to quantum physics provide a self-consistent picture in agreement with the established references in this area of research.

§8.2 Defects in four-dimensional spacetime

The theory of defects in three-dimensional space is well developed, including non-linearity, finite displacements, fracture mechanics, *etc.* The theory of defects in four-dimensional spacetime is limited to an elastic homogeneous spacetime continuum, based on the properties indicated by the physical laws, as discussed in section §2.1.

The challenge we face lies in extending the three-dimensional elastic homogeneous space theory to four dimensions. For example, Puntigam *et al* [297], in extending the Volterra defect analysis from three to four dimensions, considered the problem topologically, deforming Minkowski spacetime by 4 dislocations and 6 disclinations into 10 differently structured Riemann-Cartan spacetimes. Instead of the process described by Volterra [360], the cut is three-dimensional (instead of two-dimensional as in the Volterra process). Although this is a mathematically valid procedure which may well bring to light new physical processes, this is not strictly equivalent to Volterra's analysis.

An equally valid approach is to apply Volterra's analysis to the four-dimensional spacetime continuum. Then the challenge is the application of the analysis to cases that involve the time ct dimension, such as for example a screw dislocation or an edge dislocation along the ct-axis. The problem then becomes one of analyzing the ct-axis consequences on a case-by-case basis as we will see in the following chapters.

As noted by Nabarro [265, see p. 588], Frank seems to have been the first to have raised the possibility of time-like dislocations, in which a clock taken around a circuit would lose or gain a definite interval of time.

§8.3 Defects and the incompatibility tensor

The spacetime continuum overall is isotropic and elastic, with defects in its structure. The approach followed in our analysis of spacetime continuum defects is to start from the elastic theory and add the defects to determine their impact. We thus consider an elastic isotropic homogeneous spacetime continuum as our starting point. The *distortion* tensor $\beta^{\mu\nu}$ is defined according to [77]

$$\beta^{\mu\nu} = u^{\mu;\nu} \tag{8.1}$$

which equals, as per (3.4),

$$\beta^{\mu\nu} = \varepsilon^{\mu\nu} + \omega^{\mu\nu} \tag{8.2}$$

where $\varepsilon^{\mu\nu}$ is the symmetric strain tensor and $\omega^{\mu\nu}$ is the antisymmetric rotation tensor.

The strain tensor is also subject to *compatibility conditions* which are both necessary and sufficient conditions to determine a single-valued displacement field u^{μ}. The compatibility conditions are valid in a simply-connected continuum* such that when it is deformed, it remains continuous, free of gaps. The compatibility conditions in three-dimensional space are written as

$$\nabla \times \nabla \times \varepsilon = \epsilon_{ijk}\, \epsilon_{lmn}\, \varepsilon_{il,jm} = 0 \tag{8.3}$$

where ϵ_{ijk} is the permutation symbol. There is no straightforward equivalent of the curl operator (or cross-product) in four dimensions, so care is required when converting (8.3) for the spacetime continuum.

The derivation in [153, see p. 262] shows that conversion of three-dimensional indices to four-dimensional indices is valid in this case, resulting in the following compatibility equations:

$$\varepsilon_{\mu\nu;\alpha\beta} + \varepsilon_{\alpha\beta;\mu\nu} - \varepsilon_{\mu\beta;\nu\alpha} - \varepsilon_{\alpha\nu;\beta\mu} = 0\,. \tag{8.4}$$

Provided that the permutation symbol in the four-dimensional spacetime continuum $\epsilon_{\alpha\beta\gamma}$ is defined as per the three-dimensional permutation symbol, *i.e.* equal to $+1$ for even permutations of $\alpha\beta\gamma$, -1 for odd permutations of $\alpha\beta\gamma$, 0 for other cases, we can write

$$\boxed{\mathbf{inc}\ \varepsilon^{\mu\nu} = \epsilon_{\alpha\gamma\mu}\, \epsilon_{\beta\delta\nu}\, \varepsilon^{\alpha\beta;\gamma\delta} = 0} \tag{8.5}$$

where **inc** is the *incompatibility operator*. There are 10 linearly independent conditions in four dimensions.

In defect theory, gaps are generated as a result of the defect deformations, and the continuum can become multiply-connected. In that case, the compatibility conditions may not be equal to zero, but rather equal to the *incompatibility tensor*, $i^{\mu\nu}$:

$$\boxed{\mathbf{inc}\ \varepsilon^{\mu\nu} = i^{\mu\nu}}\,. \tag{8.6}$$

This tensor is symmetric and satisfies the continuity condition

$$i^{\mu\nu}{}_{;\nu} = 0\,. \tag{8.7}$$

*In a simply-connected continuum, a closed curve within the continuum can be shrunk to a point.

The properties of the incompatibility tensor will be explored further in later sections.

For an elastic strain tensor, the incompatibility tensor $i^{\mu\nu} = 0$ as the spacetime continuum is then simply-connected. An elastic continuum with defects will include localized defects where the incompatibility tensor is not zero, in a continuum that obeys the compatibility conditions (8.5) in most locations. The strain tensor can then be broken down into [78]

$$\boxed{{}^*\varepsilon^{\mu\nu} = \varepsilon^{\mu\nu} + \not{\varepsilon}^{\mu\nu}} \tag{8.8}$$

where ${}^*\varepsilon^{\mu\nu}$ represents the total (effective) strain tensor including the defects, $\varepsilon^{\mu\nu}$ is the elastic strain tensor and $\not{\varepsilon}^{\mu\nu}$ is the defect strain tensor. Note that the defect tensors are also often referred to as plastic fields to denote non-elastic plastic deformations in the field theory of elastoplasticity.

Substituting (8.8) into (8.6), the incompatibility tensor is then given by

$$\boxed{i^{\mu\nu} = \mathbf{inc}\ {}^*\varepsilon^{\mu\nu} = \epsilon_{\alpha\gamma\mu}\,\epsilon_{\beta\delta\nu}\,\not{\varepsilon}^{\alpha\beta;\gamma\delta}} \tag{8.9}$$

where we have used

$$\mathbf{inc}\,\varepsilon^{\mu\nu} = 0 \tag{8.10}$$

for the elastic strain tensor $\varepsilon^{\mu\nu}$.

Similarly, the rotation tensor, distortion tensor and the bend-twist tensor to be defined in (10.10) can usually be separated into elastic and defect parts,

$${}^*\omega^{\mu\nu} = \omega^{\mu\nu} + \not{\omega}^{\mu\nu} \tag{8.11}$$

$${}^*\beta^{\mu\nu} = \beta^{\mu\nu} + \not{\beta}^{\mu\nu} \tag{8.12}$$

$${}^*\kappa^{\mu\nu} = \kappa^{\mu\nu} + \not{\kappa}^{\mu\nu}\,. \tag{8.13}$$

However, the displacement u^μ cannot be split into elastic and defect parts in all cases [80]. Similarly for the distortion tensor $\beta^{\mu\nu}$. In that case, the symmetric part of the distortion tensor can be split according to

$$\beta^{(\mu\nu)} = {}^*\varepsilon^{\mu\nu} = \varepsilon^{\mu\nu} + \not{\varepsilon}^{\mu\nu} \tag{8.14}$$

from (8.2) and (8.8).

§8.4 Defects and the volume force

As mentioned in §8.3, the strain tensor in the elastic homogeneous spacetime continuum considered in this book is elastic and the incompatibility tensor $i^{\mu\nu} = 0$. However, defects in the spacetime continuum introduce imperfections in the continuum that can result in the incompatibility tensor $i^{\mu\nu} \neq 0$. Eshelby [78, 113] showed that a defect described by a strain tensor $\not{\varepsilon}^{\mu\nu}$ can be represented by a fictitious volume force

$$\boxed{X^{\nu} = -E^{\mu\nu\alpha\beta}\not{\varepsilon}_{\alpha\beta;\mu}}\,. \tag{8.15}$$

This can be shown from (3.7), *viz.*

$$T^{\mu\nu}{}_{;\mu} = -X^{\nu}\,,$$

making use of (2.6) and (8.8) into the above equation, to obtain

$$2\bar{\mu}_0\varepsilon^{\mu\nu}{}_{;\mu} + 2\bar{\mu}_0\not{\varepsilon}^{\mu\nu}{}_{;\mu} + \bar{\lambda}_0\varepsilon^{;\nu} + \bar{\lambda}_0\not{\varepsilon}^{;\nu} = -X^{\nu}\,. \tag{8.16}$$

Since the elastic strain tensor $\varepsilon^{\mu\nu}$ has a volume force of zero, we obtain

$$\boxed{X^{\nu} = -\left(2\bar{\mu}_0\not{\varepsilon}^{\mu\nu}{}_{;\mu} + \bar{\lambda}_0\not{\varepsilon}^{;\nu}\right)}\,. \tag{8.17}$$

However, it should be noted that the volume force for a defect could still be zero if the situation is such that the incompatibility tensor is zero. In the absence of defects, $\not{\varepsilon}_{\mu\nu} = 0$, the incompatibility tensor is zero, and the volume force is also zero.

In Chapter 7, we derived a non-zero quantum mechanical volume force which indicates the presence of defects in the spacetime continuum at the quantum level.

§8.5 Defects dynamics

In section §3.3, we showed that the dynamics of the spacetime continuum is described by the dynamic equation (3.18), which includes the accelerations from the applied forces, *viz.*

$$\bar{\mu}_0\nabla^2 u^{\nu} + (\bar{\mu}_0 + \bar{\lambda}_0)\varepsilon^{;\nu} = -X^{\nu}\,.$$

In this analysis, we consider the simpler problem of defects in an isotropic continuum under equilibrium conditions with no volume force. As seen in §6.4, the field of a defect in the spacetime continuum can

always be simulated by a fictitious volume force if necessary. Then (3.18) becomes

$$\bar{\mu}_0 \nabla^2 u^\nu + (\bar{\mu}_0 + \bar{\lambda}_0)\varepsilon^{;\nu} = 0, \tag{8.18}$$

where ∇^2 is the four-dimensional operator and the semi-colon (;) represents covariant differentiation.

Separating u^ν into its longitudinal (irrotational) component $u^\nu_\parallel$ and its transverse (solenoidal) component $u^\nu_\perp$ using the Helmholtz theorem in four dimensions [378] according to

$$u^\nu = u^\nu_\parallel + u^\nu_\perp, \tag{8.19}$$

(8.18) can be separated into a screw dislocation displacement (transverse) equation

$$\bar{\mu}_0 \nabla^2 u^\nu_\perp = 0 \tag{8.20}$$

and an edge dislocation displacement (longitudinal) equation

$$\nabla^2 u^\nu_\parallel = -\frac{\bar{\mu}_0 + \bar{\lambda}_0}{\bar{\mu}_0}\, \varepsilon^{;\nu}. \tag{8.21}$$

The components of the energy-momentum stress tensor are given by [258]:

$$\begin{aligned} T^{00} &= H \\ T^{0j} &= s^j \\ T^{i0} &= g^i \\ T^{ij} &= \sigma^{ij} \end{aligned} \tag{8.22}$$

where H is the total energy density, s^j is the energy flux vector, g^i is the momentum density vector, and σ^{ij} is the Cauchy stress tensor which is the i^{th} component of force per unit area at x^j.

From the stress tensor $T^{\mu\nu}$, we can calculate the strain tensor $\varepsilon^{\mu\nu}$ and then calculate the strain energy density of the dislocations. As shown in §2.1, for a general anisotropic continuum in four dimensions, the spacetime continuum is approximated by a deformable linear elastic medium that obeys Hooke's law [126, see pp. 50–53]

$$E^{\mu\nu\alpha\beta}\varepsilon_{\alpha\beta} = T^{\mu\nu} \tag{8.23}$$

where $E^{\mu\nu\alpha\beta}$ is the elastic moduli tensor. For an isotropic and homogeneous medium, the elastic moduli tensor simplifies to [126]:

$$E^{\mu\nu\alpha\beta} = \bar{\lambda}_0 \left(g^{\mu\nu} g^{\alpha\beta}\right) + \bar{\mu}_0 \left(g^{\mu\alpha} g^{\nu\beta} + g^{\mu\beta} g^{\nu\alpha}\right). \tag{8.24}$$

For the metric tensor $g_{\mu\nu}$, we use the flat spacetime diagonal metric $\eta_{\mu\nu}$ with signature $(+---)$ as the spacetime continuum is locally flat at the microscopic level. Substituting for (8.24) into (8.23) and expanding, we obtain

$$\begin{aligned}
T^{00} &= (\bar{\lambda}_0 + 2\bar{\mu}_0)\,\varepsilon^{00} - \bar{\lambda}_0\,\varepsilon^{11} - \bar{\lambda}_0\,\varepsilon^{22} - \bar{\lambda}_0\,\varepsilon^{33} \\
T^{11} &= -\bar{\lambda}_0\,\varepsilon^{00} + (\bar{\lambda}_0 + 2\bar{\mu}_0)\,\varepsilon^{11} + \bar{\lambda}_0\,\varepsilon^{22} + \bar{\lambda}_0\,\varepsilon^{33} \\
T^{22} &= -\bar{\lambda}_0\,\varepsilon^{00} + \bar{\lambda}_0\,\varepsilon^{11} + (\bar{\lambda}_0 + 2\bar{\mu}_0)\,\varepsilon^{22} + \bar{\lambda}_0\,\varepsilon^{33} \\
T^{33} &= -\bar{\lambda}_0\,\varepsilon^{00} + \bar{\lambda}_0\,\varepsilon^{11} + \bar{\lambda}_0\,\varepsilon^{22} + (\bar{\lambda}_0 + 2\bar{\mu}_0)\,\varepsilon^{33} \\
T^{\mu\nu} &= 2\bar{\mu}_0\,\varepsilon^{\mu\nu}, \quad \mu \neq \nu.
\end{aligned} \tag{8.25}$$

In terms of the stress tensor, the inverse of (8.25) is given by

$$\begin{aligned}
\varepsilon^{00} &= \frac{1}{4\bar{\mu}_0(2\bar{\lambda}_0 + \bar{\mu}_0)}\Big[(3\bar{\lambda}_0 + 2\bar{\mu}_0)\,T^{00} + \\
&\quad + \bar{\lambda}_0\,(T^{11} + T^{22} + T^{33})\Big] \\
\varepsilon^{11} &= \frac{1}{4\bar{\mu}_0(2\bar{\lambda}_0 + \bar{\mu}_0)}\Big[(3\bar{\lambda}_0 + 2\bar{\mu}_0)\,T^{11} + \\
&\quad + \bar{\lambda}_0\,(T^{00} - T^{22} - T^{33})\Big] \\
\varepsilon^{22} &= \frac{1}{4\bar{\mu}_0(2\bar{\lambda}_0 + \bar{\mu}_0)}\Big[(3\bar{\lambda}_0 + 2\bar{\mu}_0)\,T^{22} + \\
&\quad + \bar{\lambda}_0\,(T^{00} - T^{11} - T^{33})\Big] \\
\varepsilon^{33} &= \frac{1}{4\bar{\mu}_0(2\bar{\lambda}_0 + \bar{\mu}_0)}\Big[(3\bar{\lambda}_0 + 2\bar{\mu}_0)\,T^{33} + \\
&\quad + \bar{\lambda}_0\,(T^{00} - T^{11} - T^{22})\Big] \\
\varepsilon^{\mu\nu} &= \frac{1}{2\bar{\mu}_0}\,T^{\mu\nu}, \quad \mu \neq \nu.
\end{aligned} \tag{8.26}$$

where $T^{ij} = \sigma^{ij}$. We calculate $\varepsilon = \varepsilon^{\alpha}{}_{\alpha}$ from the values of (8.26). Using $\eta_{\mu\nu}$, (2.3) and $T^{\alpha}{}_{\alpha} = \rho c^2$ from (2.22), we obtain (2.24) as required. This confirms the validity of the strain tensor in terms of the energy-momentum stress tensor as given by (8.26).

Eshelby [114–116] introduced an elastic field energy-momentum tensor for continuous media to deal with cases where defects (such as dislocations) lead to changes in configuration. The displacements u^ν are considered to correspond to a field defined at points x^μ of the spacetime continuum. This tensor was first derived by Morse and Feshback [261] for an isotropic elastic medium, using dyadics. The energy flux vector s_j and the field momentum density vector g_i are then given by [114, 261]:

$$\begin{aligned} s_j &= -\dot{u}_k\, \sigma_{kj} \\ g_i &= \bar{\rho}_0\, u_{k,i}\, \dot{u}_k \\ b_{ij} &= L\, \delta_{ij} - u_{k,i}\, \sigma_{kj} \end{aligned} \tag{8.27}$$

where $\bar{\rho}_0$ is the density of the medium, in this case the spacetime continuum, L is the Lagrangian equal to $K - W$ where W is the strain energy density and K is the kinetic energy density ($H = K + W$), and b_{ij} is known as the Eshelby stress tensor [229, see p. 27]. If the energy-momentum stress tensor is symmetric, then $g^i = s^i$. In this paper, we consider the case where there are no changes in configuration, and use the energy-momentum stress tensor given by (8.22) and (8.25).

Chapter 9

Dislocations in the Spacetime Continuum

§9.1 Analysis of spacetime continuum dislocations

In this chapter, we investigate dislocations in the spacetime continuum in the context of *STCED*. The approach followed till now by investigators has been to use Einstein-Cartan differential geometry, with dislocations (translational deformations) impacting curvature and disclinations (rotational deformations) impacting torsion. The dislocation itself is modelled via the line element ds^2 [297].

In this chapter, we investigate spacetime continuum dislocations using the underlying displacements u^ν and the energy-momentum stress tensor. We thus work from the RHS of the general relativistic equation (the stress tensor side) rather than the LHS (the geometric tensor side). It should be noted that the general relativistic equation used can be the standard Einstein equation or a suitably modified version, as in Einstein-Cartan or Teleparallel formulations.

In this section, we review the basic physical characteristics and dynamics of dislocations in the spacetime continuum. The energy-momentum stress tensor was considered in section §8.5. A detailed review of stationary and moving screw and edge dislocations follows in sections §9.2 and §9.3, along with their strain energy density as calculated from *STCED*. The Volterra and deWit treatment of discrete dislocation lines is then covered in sections §9.4 and §9.5, and we close with curved dislocations in sections §9.6. The relation of spacetime continuum defects to quantum physics is covered starting in Chapter 14.

A dislocation is characterized by its dislocation-displacement vector, known as the *Burgers vector*, b^μ in a four-dimensional continuum, defined positive in the direction of a vector ξ^μ tangent to the dislocation line in the spacetime continuum [159, see pp.17–24].

A *Burgers circuit* encloses the dislocation. A similar reference circuit can be drawn to enclose a region free of dislocation (see Fig. 9.1). The Burgers vector is the vector required to make the Burgers circuit equivalent to the reference circuit (see Fig. 9.2). It is a measure of the displacement between the initial and final points of the circuit due to the dislocation.

It is important to note that there are two conventions used to define the Burgers vector. In this chapter, we use the convention used by

Figure 9.1: A reference circuit in a region free of dislocation, S: start, F: finish

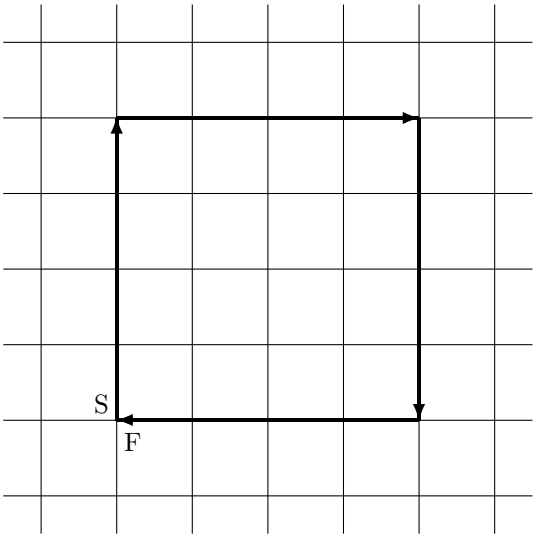

Hirth [159] referred to as the local Burgers vector. The local Burgers vector is equivalently given by the line integral

$$b^\mu = \oint_C \frac{\partial u^\mu}{\partial s} ds \tag{9.1}$$

taken in a right-handed sense relative to ξ^μ, where u^μ is the displacement vector.

A dislocation is thus characterized by a line direction ξ^μ and a Burgers vector b^μ. There are two types of dislocations: an *edge dislocation* for which $b^\mu \xi_\mu = 0$ and a *screw dislocation* which can be right-handed for which $b^\mu \xi_\mu = b$, or left-handed for which $b^\mu \xi_\mu = -b$, where b is the magnitude of the Burgers vector. Arbitrary mixed dislocations can be decomposed into a screw component, along vector ξ^μ, and an edge component, perpendicular to vector ξ^μ.

The edge dislocation was first proposed by Orowan [278], Polanyi [291] and Taylor [343] in 1934, while the screw dislocation was proposed by Burgers [40] in 1939. In this chapter, we extend the concept of dislocations to the elastodynamics of the spacetime continuum. Edge

Figure 9.2: A dislocation showing the Burgers vector b^μ, direction vector ξ^μ which points into the paper and the Burgers circuit, S: start, F: finish

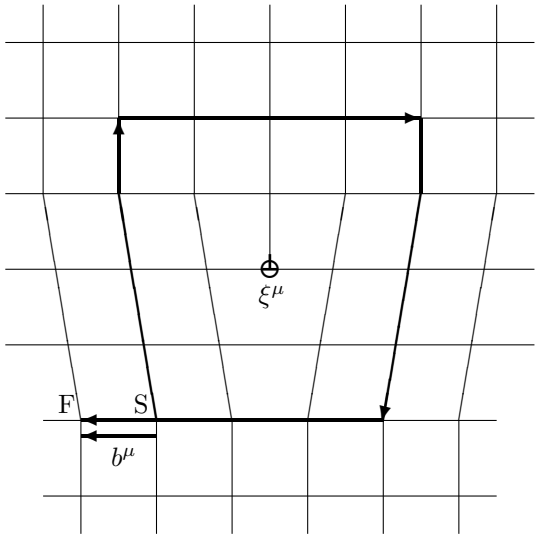

dislocations correspond to *dilatations* (longitudinal displacements) and hence have an associated rest-mass energy, while screw dislocations correspond to *distortions* (transverse displacements) and are massless [245].

§9.2 Screw dislocations

We first consider the simplest dislocation, the discrete screw dislocation, both in the stationary and the moving case.

§9.2.1 *Stationary screw dislocation*

We consider a stationary screw dislocation in the spacetime continuum, with cylindrical polar coordinates (r, θ, z), with the dislocation line along the z-axis (see Fig. 9.3). Then the Burgers vector is along the z-axis and is given by $b_r = b_\theta = 0$, $b_z = b$, the magnitude of the Burgers vector. The only non-zero component of the deformations is given by [159, see pp. 60–61] [203, see p. 51]

$$u_z = \frac{b}{2\pi}\,\theta = \frac{b}{2\pi}\,\tan^{-1}\frac{y}{x}. \tag{9.2}$$

Figure 9.3: A stationary screw dislocation in cartesian (x, y, z) and cylindrical polar (r, θ, z) coordinates.

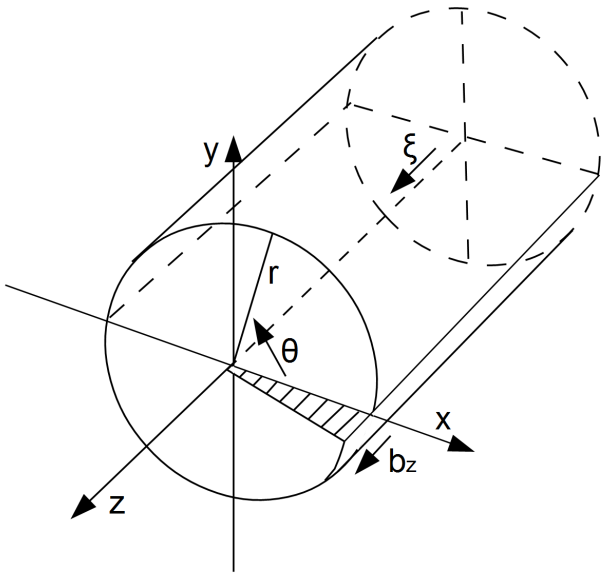

This solution satisfies (8.20), the screw dislocation displacement equation seen previously in section §8.5.

Similarly, the only non-zero components of the stress and strain tensors are given by

$$\begin{aligned} \sigma_{\theta z} &= \frac{b}{2\pi}\,\frac{\bar{\mu}_0}{r} \\ \varepsilon_{\theta z} &= \frac{b}{4\pi}\,\frac{1}{r} \end{aligned} \tag{9.3}$$

respectively.

The rotation tensor is calculated from (3.3), *viz.*

$$\omega^{\mu\nu} = \tfrac{1}{2}(u^{\mu;\nu} - u^{\nu;\mu})\,.$$

Substituting for the displacements from (9.2), we find that the only non-zero component of the rotation tensor is

$$\omega_{z\theta} = -\omega_{\theta z} = \frac{b}{4\pi}\,. \tag{9.4}$$

In terms of the rotation vector (see section §10.1), using (10.1) *viz.*

$$\omega^\alpha = \frac{1}{2}\,\epsilon^{\alpha\mu\nu}\,\omega_{\mu\nu}\,,$$

we obtain

$$\omega_r = -\frac{b}{4\pi}\,. \tag{9.5}$$

Using (14.3), the rotation vector can also be written as

$$\omega_r = -\frac{\hbar}{2}\,, \tag{9.6}$$

where, as we will see in section §14.2, $\hbar = b/2\pi$. For the stationary screw dislocation of (9.2), we thus obtain a constant, left-handed rotation vector. Note that if we consider a stationary screw dislocation with a negative Burgers vector $-b$ ($b > 0$),

$$u_z = -\frac{b}{2\pi}\,\theta = -\frac{b}{2\pi}\,\tan^{-1}\frac{y}{x}\,, \tag{9.7}$$

we obtain a constant, right-handed rotation vector

$$\omega_r = \frac{b}{4\pi}\,. \tag{9.8}$$

It should be noted that even though (9.6) is similar to $\hbar/2$, the units of $\hbar$ are [m] while those of $\hbar$ are [J·s], and are thus not the same quantities.

§9.2.2 *Moving screw dislocation*

We now consider the previous screw dislocation, moving along the x-axis, parallel to the dislocation, at a constant speed $v_x = v$. Equation (8.18) then simplifies to the wave equation for massless transverse shear waves for the displacements u_z along the z-axis, with speed $c_t = c$ given by (3.12), where c_t is the speed of the transverse waves corresponding to c the speed of light.

If coordinate system (x', y', z', t') is attached to the uniformly moving screw dislocation, then the transformation between the stationary

and the moving screw dislocation is given by [159]

$$\begin{aligned} x' &= \frac{x - vt}{(1 - v^2/c^2)^{1/2}} \\ y' &= y \\ z' &= z \\ t' &= \frac{t - vx/c^2}{(1 - v^2/c^2)^{1/2}}. \end{aligned} \tag{9.9}$$

which is the special relativistic transformation.

The only non-zero component of the deformation in cartesian coordinates is given by [159, see pp. 184–185]

$$u_z = \frac{b}{2\pi} \tan^{-1} \frac{\alpha y}{x - vt}, \tag{9.10}$$

where

$$\alpha = \sqrt{1 - \frac{v^2}{c^2}}. \tag{9.11}$$

The Lorentz gamma-factor is given by

$$\gamma = \frac{1}{\alpha} = \left(1 - \frac{v^2}{c^2}\right)^{-\frac{1}{2}}. \tag{9.12}$$

This solution also satisfies the screw dislocation displacement equation (8.20). It simplifies to the case of the stationary screw dislocation when the speed $v = 0$.

Using (9.9) into (9.10) to transform to the moving coordinate system (x', y', z', t'), we obtain

$$u_{z'} = \frac{b}{2\pi} \tan^{-1} \frac{y'}{x'}, \tag{9.13}$$

and the rotation vector is given by

$$\omega_{r'} = -\frac{b}{4\pi} \tag{9.14}$$

in the moving coordinate system (x', y', z', t'), the same as (9.5) in the stationary coordinate system.

The only non-zero components of the stress tensor in cartesian coordinates are given by [159]

$$\begin{aligned}\sigma_{xz} &= -\frac{b\bar{\mu}_0}{2\pi}\,\frac{\alpha y}{(x-vt)^2+\alpha^2y^2}\\ \sigma_{yz} &= \frac{b\bar{\mu}_0}{2\pi}\,\frac{\alpha(x-vt)}{(x-vt)^2+\alpha^2y^2}.\end{aligned} \tag{9.15}$$

The only non-zero components of the strain tensor in cartesian coordinates are derived from $\varepsilon^{\mu\nu} = \frac{1}{2}(u^{\mu;\nu} + u^{\nu;\mu})$ [238, see Eq.(41)]:

$$\begin{aligned}\varepsilon_{xz} &= -\frac{b}{4\pi}\,\frac{\alpha y}{(x-vt)^2+\alpha^2y^2}\\ \varepsilon_{yz} &= \frac{b}{4\pi}\,\frac{\alpha(x-vt)}{(x-vt)^2+\alpha^2y^2},\end{aligned} \tag{9.16}$$

in an isotropic continuum.

Non-zero components involving time are given by

$$\begin{aligned}\varepsilon_{tz} = \varepsilon_{zt} &= \frac{1}{2}\left(\frac{\partial u_z}{\partial(ct)} + \frac{\partial u_t}{\partial z}\right)\\ \varepsilon_{tz} &= \frac{b}{4\pi}\,\frac{v}{c}\,\frac{\alpha y}{(x-vt)^2+\alpha^2y^2}\end{aligned} \tag{9.17}$$

where $u_t = 0$ has been used. This assumes that the screw dislocation is fully formed and moving with velocity v as described. Using (8.25), the non-zero stress components involving time are given by

$$\sigma_{tz} = \sigma_{zt} = \frac{b\bar{\mu}_0}{2\pi}\,\frac{v}{c}\,\frac{\alpha y}{(x-vt)^2+\alpha^2y^2}. \tag{9.18}$$

Screw dislocations are thus found to be Lorentz invariant.

§9.2.3 *Screw dislocation strain energy density*

We consider the stationary screw dislocation in the spacetime continuum of section §9.2.1, with cylindrical polar coordinates (r, θ, z), with the dislocation line along the z-axis and the Burgers vector along the z-axis $b_z = b$.

Then the strain energy density of the screw dislocation is given by the transverse distortion energy density [238, see Eq. (74)]

$$\mathcal{E}_\perp = \bar{\mu}_0\, e^{\alpha\beta} e_{\alpha\beta} \tag{9.19}$$

where from [238, see Eq. (33)],

$$e^{\alpha\beta} = \varepsilon^{\alpha\beta} - e_s g^{\alpha\beta} \tag{9.20}$$

where $e_s = \frac{1}{4}\,\varepsilon^{\alpha}{}_{\alpha}$ is the dilatation which for a screw dislocation is equal to 0. The screw dislocation is thus massless and $\mathcal{E}_{\parallel} = 0$.

The non-zero components of the strain tensor are as defined in (9.3). Hence

$$\mathcal{E}_{\perp} = \bar{\mu}_0 \left({\varepsilon_{\theta z}}^2 + {\varepsilon_{z\theta}}^2 \right). \tag{9.21}$$

Substituting from (9.3),

$$\mathcal{E}_{\perp} = \frac{\bar{\mu}_0\, b^2}{8\pi^2}\, \frac{1}{r^2} = \mathcal{E}. \tag{9.22}$$

We now consider the more general case of the moving screw dislocation in the spacetime continuum of section §9.2.2, with cartesian coordinates (x, y, z). The non-zero components of the strain tensor are as defined in (9.16) and (9.17). Substituting in (9.19), the equation becomes [238, see Eqs.(114–115)]

$$\mathcal{E}_{\perp} = 2\bar{\mu}_0 \left(-{\varepsilon_{tz}}^2 + {\varepsilon_{xz}}^2 + {\varepsilon_{yz}}^2 \right). \tag{9.23}$$

Substituting from (9.16) and (9.17) into (9.23), the screw dislocation strain energy density becomes

$$\mathcal{E}_{\perp} = \frac{\bar{\mu}_0\, b^2}{8\pi^2}\, \frac{\alpha^2}{(x - vt)^2 + \alpha^2 y^2} = \mathcal{E}. \tag{9.24}$$

This equation simplifies to (9.22) in the case where $v = 0$, as expected. In addition, the energy density (which is quadratic in energy as per [238, see Eq.(76)]) is multiplied by the special relativistic α factor.

§9.2.4 *Screw dislocation current and charge density*

The current density four-vector is calculated from (4.10), *viz.*

$$j^{\nu} = \frac{\varphi_0}{\mu_0}\, \frac{2\bar{\mu}_0 + \bar{\lambda}_0}{2\bar{\mu}_0}\, \varepsilon^{;\nu} = \frac{\varphi_0}{2\mu_0\, \bar{\alpha}_0}\, \varepsilon^{;\nu}$$

and the charge density from (4.14), *viz.*

$$\varrho = \frac{1}{2}\, \varphi_0 \epsilon_0 c\, \frac{2\bar{\mu}_0 + \bar{\lambda}_0}{2\bar{\mu}_0}\, \sqrt{\varepsilon^{;\nu} \varepsilon_{;\nu}} = \frac{\varphi_0 \epsilon_0 c}{4\bar{\alpha}_0}\, \sqrt{\varepsilon^{;\nu} \varepsilon_{;\nu}}$$

where φ_0 is the spacetime continuum electromagnetic shearing potential constant and

$$\bar{\alpha}_0 = \frac{\bar{\mu}_0}{2\bar{\mu}_0 + \bar{\lambda}_0}\,.$$

For the screw dislocation,

$$j^\nu = 0 \tag{9.25}$$

$$\varrho = 0 \tag{9.26}$$

given that $\varepsilon = 0$.

§9.3 Edge dislocations

We next consider discrete edge dislocations, both in the stationary and the moving case.

§9.3.1 *Stationary edge dislocation*

We consider a stationary edge dislocation in the spacetime continuum in cartesian coordinates (x, y, z), with the dislocation line along the z-axis and the Burgers vector $b_x = b, b_y = b_z = 0$ (see Fig. 9.4). Then the non-zero components of the deformations are given in cartesian coordinates by [159, see p. 78]

$$\begin{aligned} u_x &= \frac{b}{2\pi}\left(\tan^{-1}\frac{y}{x} + \frac{\bar{\mu}_0 + \bar{\lambda}_0}{2\bar{\mu}_0 + \bar{\lambda}_0}\,\frac{xy}{x^2+y^2}\right) \\ u_y &= -\frac{b}{2\pi}\left(\frac{1}{2}\,\frac{\bar{\mu}_0}{2\bar{\mu}_0 + \bar{\lambda}_0}\,\ln(x^2+y^2) + \right. \\ &\quad \left. + \frac{1}{2}\,\frac{\bar{\mu}_0 + \bar{\lambda}_0}{2\bar{\mu}_0 + \bar{\lambda}_0}\,\frac{x^2-y^2}{x^2+y^2}\right). \end{aligned} \tag{9.27}$$

This solution results in a non-zero R.H.S. of the edge dislocation displacement equation (8.21) as required. Equation (8.21) can be evaluated to give a value of ε in agreement with the results of section §9.3.4 as shown in that section.

The rotation tensor is calculated from (3.3). Substituting for the displacements from (9.27), we find that the only non-zero component of the rotation tensor is

$$\omega_{xy} = -\omega_{yx} = \frac{b}{2\pi}\,\frac{x}{x^2+y^2}\,. \tag{9.28}$$

Figure 9.4: A stationary edge dislocation in cartesian (x, y, z) and cylindrical polar (r, θ, z) coordinates.

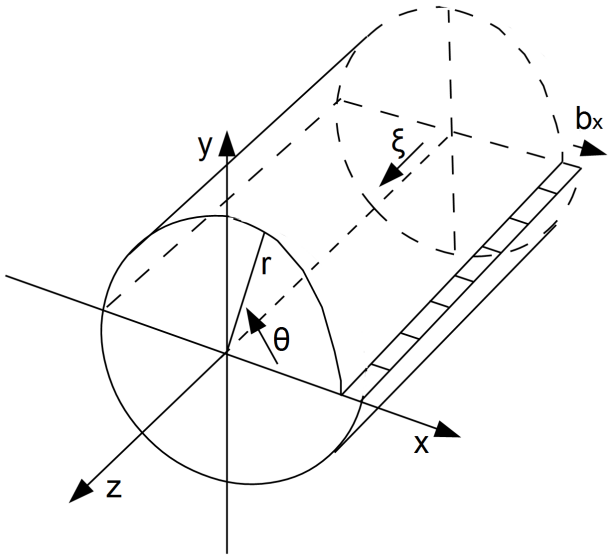

In terms of the rotation vector, using (10.1), we obtain

$$\omega_z = \frac{b}{\pi} \frac{x}{x^2 + y^2} \,. \tag{9.29}$$

In cylindrical polar coordinates, the rotation vector can also be written as

$$\omega_z = \frac{b}{\pi} \frac{\cos\theta}{r} \,. \tag{9.30}$$

For a stationary edge dislocation, we thus obtain a right-handed rotation vector that decreases as $1/r$ and varies sinusoidally with θ.

The cylindrical polar coordinate description of the edge dislocation is more complex than the cartesian coordinate description. We thus use cartesian coordinates in the following sections, transforming to polar coordinate expressions as warranted. The non-zero components of the

stress tensor in cartesian coordinates are given by [159, see p. 76]

$$\begin{aligned}
\sigma_{xx} &= -\frac{b\bar{\mu}_0}{\pi}\,\frac{\bar{\mu}_0+\bar{\lambda}_0}{2\bar{\mu}_0+\bar{\lambda}_0}\,\frac{y(3x^2+y^2)}{(x^2+y^2)^2}\\
\sigma_{yy} &= \frac{b\bar{\mu}_0}{\pi}\,\frac{\bar{\mu}_0+\bar{\lambda}_0}{2\bar{\mu}_0+\bar{\lambda}_0}\,\frac{y(x^2-y^2)}{(x^2+y^2)^2}\\
\sigma_{zz} &= \frac{1}{2}\,\frac{\bar{\lambda}_0}{\bar{\mu}_0+\bar{\lambda}_0}\,(\sigma_{xx}+\sigma_{yy})\\
&= -\frac{b\bar{\mu}_0}{\pi}\,\frac{\bar{\lambda}_0}{2\bar{\mu}_0+\bar{\lambda}_0}\,\frac{y}{x^2+y^2}\\
\sigma_{xy} &= \frac{b\bar{\mu}_0}{\pi}\,\frac{\bar{\mu}_0+\bar{\lambda}_0}{2\bar{\mu}_0+\bar{\lambda}_0}\,\frac{x(x^2-y^2)}{(x^2+y^2)^2}.
\end{aligned} \tag{9.31}$$

The non-zero components of the strain tensor in cartesian coordinates are derived from $\varepsilon^{\mu\nu} = \frac{1}{2}(u^{\mu;\nu} + u^{\nu;\mu})$ [238, see Eq.(41)]:

$$\begin{aligned}
\varepsilon_{xx} &= -\frac{b}{2\pi}\,\frac{y}{x^2+y^2}\left(1+\frac{\bar{\mu}_0+\bar{\lambda}_0}{2\bar{\mu}_0+\bar{\lambda}_0}\,\frac{x^2-y^2}{x^2+y^2}\right)\\
&= -\frac{by}{2\pi}\,\frac{(3\bar{\mu}_0+2\bar{\lambda}_0)x^2+\bar{\mu}_0y^2}{(2\bar{\mu}_0+\bar{\lambda}_0)\,(x^2+y^2)^2}\\
\varepsilon_{yy} &= -\frac{b}{2\pi}\,\frac{\bar{\mu}_0}{2\bar{\mu}_0+\bar{\lambda}_0}\,\frac{y}{x^2+y^2}\left(1-\frac{\bar{\mu}_0+\bar{\lambda}_0}{\bar{\mu}_0}\,\frac{2x^2}{x^2+y^2}\right)\\
&= \frac{by}{2\pi}\,\frac{(\bar{\mu}_0+2\bar{\lambda}_0)x^2-\bar{\mu}_0y^2}{(2\bar{\mu}_0+\bar{\lambda}_0)\,(x^2+y^2)^2}\\
\varepsilon_{xy} &= \frac{b}{2\pi}\,\frac{\bar{\mu}_0+\bar{\lambda}_0}{2\bar{\mu}_0+\bar{\lambda}_0}\,\frac{x(x^2-y^2)}{(x^2+y^2)^2}
\end{aligned} \tag{9.32}$$

in an isotropic continuum.

§9.3.2 *Moving edge dislocation*

We now consider the previous edge dislocation, moving along the x-axis, parallel to the z-axis, along the slip plane $x{-}z$, at a constant speed $v_x = v$. The solutions of (8.18) for the moving edge dislocation then include both longitudinal and transverse components. The only non-zero components of the deformations in cartesian coordinates are

given by [364, see pp. 39–40] [117, see pp. 218–219]

$$\begin{aligned} u_x &= \frac{bc^2}{\pi v^2}\left(\tan^{-1}\frac{\alpha_l y}{x-vt} - \alpha_2^2\,\tan^{-1}\frac{\alpha y}{x-vt}\right) \\ u_y &= \frac{bc^2}{2\pi v^2}\left(\alpha_l \ln\left[(x-vt)^2+\alpha_l^2 y^2\right] - \right. \\ &\quad \left. - \frac{\alpha_2^2}{\alpha}\,\ln\left[(x-vt)^2+\alpha^2 y^2\right]\right), \end{aligned} \tag{9.33}$$

where

$$\alpha_2 = \sqrt{1-\frac{v^2}{2c^2}}, \tag{9.34}$$

$$\alpha_l = \sqrt{1-\frac{v^2}{c_l^2}} \tag{9.35}$$

and c_l is the speed of longitudinal deformations given by

$$c_l = \sqrt{\frac{2\bar{\mu}_0+\bar{\lambda}_0}{\bar{\rho}_0}}. \tag{9.36}$$

Similarly to (9.12), we have

$$\begin{aligned} \gamma_2 &= \frac{1}{\alpha_2} = \left(1-\frac{v^2}{2c^2}\right)^{-\frac{1}{2}} \\ \gamma_l &= \frac{1}{\alpha_l} = \left(1-\frac{v^2}{c_l^2}\right)^{-\frac{1}{2}}. \end{aligned} \tag{9.37}$$

This solution again results in a non-zero R.H.S. of the edge dislocation displacement equation (8.21) as required, and (8.21) can be evaluated to give a value of ε as in section §9.3.4. This solution simplifies to the case of the stationary edge dislocation when the speed $v = 0$.

The rotation tensor is calculated from (3.3). Substituting for the displacements from (9.33), we find that the only non-zero space component of the rotation tensor is

$$\omega_{xy} = -\omega_{yx} = \frac{b}{2\pi}\,\frac{\alpha_2^2}{\alpha}\,\frac{x-vt}{(x-vt)^2+(\alpha y)^2}\,. \tag{9.38}$$

In terms of the rotation vector, using (10.1), we obtain

$$\omega_z = \frac{b}{\pi}\,\frac{\alpha_2^2}{\alpha}\,\frac{x-vt}{(x-vt)^2+(\alpha y)^2}\,. \tag{9.39}$$

From (9.11) and (9.34), using a Taylor expansion for α^{-1}, we have

$$\frac{\alpha_2^2}{\alpha} \simeq 1 - \frac{v^4}{4c^4} \to 1 \tag{9.40}$$

and hence

$$\omega_z \to \frac{b}{\pi} \frac{x - vt}{(x - vt)^2 + (\alpha y)^2} \,. \tag{9.41}$$

This expression is the same as that of the stationary edge dislocation of (9.29) in the case where $v \to 0$. For a moving edge dislocation, we thus find that the z-component of the rotation vector includes only the transverse terms of the dislocation, with the longitudinal terms cancelling out.

The non-zero time components of the rotation tensor are also obtained from (3.3) and (9.33):

$$\begin{aligned} \omega_{xt} &= \frac{1}{2} \left(\frac{1}{c} \frac{\partial u_x}{\partial t} - \frac{\partial u_t}{\partial x} \right) = -\omega_{tx} \\ &= \frac{b}{2\pi} \frac{c}{v} \left(\frac{\alpha_l y}{(x - vt)^2 + (\alpha_l y)^2} - \alpha_2^2 \frac{\alpha y}{(x - vt)^2 + (\alpha y)^2} \right) \\ \omega_{yt} &= -\frac{b}{2\pi} \frac{c}{v} \left(\frac{\alpha_l (x - vt)}{(x - vt)^2 + (\alpha_l y)^2} - \frac{\alpha_2^2}{\alpha^2} \frac{\alpha (x - vt)}{(x - vt)^2 + (\alpha y)^2} \right) . \end{aligned} \tag{9.42}$$

The corresponding space rotation vector components are then given by

$$\begin{aligned} \omega_x &= -\frac{b}{\pi} \frac{c}{v} \left(\frac{\alpha_l (x - vt)}{(x - vt)^2 + (\alpha_l y)^2} - \frac{\alpha_2^2}{\alpha} \frac{x - vt}{(x - vt)^2 + (\alpha y)^2} \right) \\ \omega_y &= -\frac{b}{\pi} \frac{c}{v} \left(\frac{\alpha_l y}{(x - vt)^2 + (\alpha_l y)^2} - \alpha_2^2 \frac{\alpha y}{(x - vt)^2 + (\alpha y)^2} \right) . \end{aligned} \tag{9.43}$$

The x- and the y-components of the rotation vector include both transverse and longitudinal terms of the dislocation.

Finally, the time component of the rotation vector is given by

$$\begin{aligned} \omega_t &= \epsilon_{txy} \, \omega^{xy} + \epsilon_{tyx} \, \omega^{yx} \\ &= \omega_{xy} - \omega_{yx} = 2\omega_{xy} \\ &= \frac{b}{\pi} \frac{\alpha_2^2}{\alpha} \frac{x - vt}{(x - vt)^2 + (\alpha y)^2} \,. \end{aligned} \tag{9.44}$$

The non-zero components of the stress tensor in cartesian coordinates are given by [159, see pp. 189–190] [364, see pp. 39–40]

$$\begin{aligned}
\sigma_{xx} &= \frac{bc^2 y}{\pi v^2}\left(\frac{\bar{\lambda}_0\alpha_l^3 - (2\bar{\mu}_0+\bar{\lambda}_0)\alpha_l}{(x-vt)^2+\alpha_l^2 y^2} + \frac{2\bar{\mu}_0\alpha_2^2\alpha}{(x-vt)^2+\alpha^2 y^2}\right)\\
\sigma_{yy} &= \frac{bc^2 y}{\pi v^2}\left(\frac{(2\bar{\mu}_0+\bar{\lambda}_0)\alpha_l^3 - \bar{\lambda}_0\alpha_l}{(x-vt)^2+\alpha_l^2 y^2} - \frac{2\bar{\mu}_0\alpha_2^2\alpha}{(x-vt)^2+\alpha^2 y^2}\right)\\
\sigma_{zz} &= \frac{1}{2}\,\frac{\bar{\lambda}_0}{\bar{\mu}_0+\bar{\lambda}_0}\,(\sigma_{xx}+\sigma_{yy})\\
&= \frac{\bar{\lambda}_0 b}{\pi}\,\frac{c^2}{c_l^2}\,\frac{-\alpha_l y}{(x-vt)^2+\alpha_l^2 y^2}\\
&= \frac{b}{\pi}\,\frac{\bar{\lambda}_0\bar{\mu}_0}{2\bar{\mu}_0+\bar{\lambda}_0}\,\frac{-\alpha_l y}{(x-vt)^2+\alpha_l^2 y^2}\\
\sigma_{xy} &= \frac{\bar{\mu}_0 bc^2}{\pi v^2}\left(\frac{2\alpha_l(x-vt)}{(x-vt)^2+\alpha_l^2 y^2} - \frac{\alpha_2^2(\alpha+1/\alpha)(x-vt)}{(x-vt)^2+\alpha^2 y^2}\right).
\end{aligned} \tag{9.45}$$

It is important to note that for a screw dislocation, the stress on the plane $x - vt = 0$ becomes infinite at $v = c$. This sets an upper limit on the speed of screw dislocations in the spacetime continuum, and provides an explanation for the speed of light limit. This upper limit also applies to edge dislocations, as the shear stress becomes infinite everywhere at $v = c$, even though the speed of longitudinal deformations c_l is greater than that of transverse deformations c [159, see p. 191] [364, see p. 40].

The non-zero components of the strain tensor in cartesian coordinates are derived from $\varepsilon^{\mu\nu} = \frac{1}{2}(u^{\mu;\nu} + u^{\nu;\mu})$ [238, see Eq.(41)]:

$$\begin{aligned}
\varepsilon_{xx} &= \frac{bc^2 y}{\pi v^2}\left(\frac{-\alpha_l}{(x-vt)^2+(\alpha_l y)^2} + \frac{\alpha_2^2\alpha}{(x-vt)^2+(\alpha y)^2}\right)\\
\varepsilon_{yy} &= \frac{bc^2 y}{\pi v^2}\left(\frac{\alpha_l^3}{(x-vt)^2+(\alpha_l y)^2} - \frac{\alpha_2^2\alpha}{(x-vt)^2+(\alpha y)^2}\right)\\
\varepsilon_{xy} &= \frac{bc^2}{2\pi v^2}\left(\frac{2\alpha_l(x-vt)}{(x-vt)^2+(\alpha_l y)^2} - \frac{\alpha_2^2(\alpha+1/\alpha)(x-vt)}{(x-vt)^2+(\alpha y)^2}\right)
\end{aligned} \tag{9.46}$$

in an isotropic continuum.

Non-zero components involving time are given by

$$\begin{aligned}
\varepsilon_{tx} &= \varepsilon_{xt} = \frac{1}{2}\left(\frac{\partial u_x}{\partial(ct)} + \frac{\partial u_t}{\partial x}\right)\\
\varepsilon_{ty} &= \varepsilon_{yt} = \frac{1}{2}\left(\frac{\partial u_y}{\partial(ct)} + \frac{\partial u_t}{\partial y}\right)\\
\varepsilon_{tx} &= \frac{b}{2\pi}\,\frac{c}{v}\left(\frac{\alpha_l y}{(x-vt)^2+\alpha_l^2 y^2} - \alpha_2^2\,\frac{\alpha y}{(x-vt)^2+\alpha^2 y^2}\right)\\
\varepsilon_{ty} &= -\frac{b}{2\pi}\,\frac{c}{v}\left(\frac{\alpha_l (x-vt)}{(x-vt)^2+\alpha_l^2 y^2} - \frac{\alpha_2^2}{\alpha^2}\,\frac{\alpha (x-vt)}{(x-vt)^2+\alpha^2 y^2}\right)
\end{aligned} \tag{9.47}$$

where $u_t = 0$ has been used. This assumes that the edge dislocation is fully formed and moving with velocity v as described. Using (8.25), the non-zero stress components involving time are given by

$$\begin{aligned}
\sigma_{tx} &= \frac{b\bar{\mu}_0}{\pi}\,\frac{c}{v}\left(\frac{\alpha_l y}{(x-vt)^2+\alpha_l^2 y^2} - \alpha_2^2\,\frac{\alpha y}{(x-vt)^2+\alpha^2 y^2}\right)\\
\sigma_{ty} &= -\frac{b\bar{\mu}_0}{\pi}\,\frac{c}{v}\left(\frac{\alpha_l (x-vt)}{(x-vt)^2+\alpha_l^2 y^2} - \frac{\alpha_2^2}{\alpha^2}\,\frac{\alpha (x-vt)}{(x-vt)^2+\alpha^2 y^2}\right).
\end{aligned} \tag{9.48}$$

§9.3.3 *Edge dislocation strain energy density*

As we have seen in section §9.2.3, the screw dislocation is massless as $\varepsilon = 0$ and hence $\mathcal{E}_\parallel = 0$ for the screw dislocation: it is a pure distortion, with no dilatation. In this section, we evaluate the strain energy density of the edge dislocation.

As seen in [238, see section 8.1], the strain energy density of the spacetime continuum is separated into two terms: the first one expresses the dilatation energy density (the mass longitudinal term) while the second one expresses the distortion energy density (the massless transverse term):

$$\mathcal{E} = \mathcal{E}_\parallel + \mathcal{E}_\perp \tag{9.49}$$

where

$$\mathcal{E}_\parallel = \frac{1}{2}\,\bar{\kappa}_0 \varepsilon^2 \equiv \frac{1}{32\bar{\kappa}_0}\,\left(\rho c^2\right)^2 \equiv \frac{1}{2\bar{\kappa}_0}\,t_s^2 \tag{9.50}$$

where ε is the volume dilatation and ρ is the mass energy density of the edge dislocation, and

$$\mathcal{E}_\perp = \bar{\mu}_0 e^{\alpha\beta} e_{\alpha\beta} \equiv \frac{1}{4\bar{\mu}_0}\,t^{\alpha\beta} t_{\alpha\beta} \tag{9.51}$$

where from [238, see Eq. (36)] the energy-momentum stress tensor $T^{\alpha\beta}$ is decomposed into a stress deviation tensor $t^{\alpha\beta}$ and a scalar t_s, according to

$$t^{\alpha\beta} = T^{\alpha\beta} - t_s g^{\alpha\beta} \tag{9.52}$$

where $t_s = \frac{1}{4} T^{\alpha}{}_{\alpha}$. Then the dilatation strain energy density of the edge dislocation is given by the (massive) longitudinal dilatation energy density (9.50) and the distortion (massless) strain energy density of the edge dislocation is given by the transverse distortion energy density (9.51).

§9.3.4 *Stationary edge dislocation strain energy density*

We first consider the case of the stationary edge dislocation of section §9.3.1. The volume dilatation ε for the stationary edge dislocation is given by

$$\varepsilon = \varepsilon^{\alpha}{}_{\alpha} = \varepsilon_{xx} + \varepsilon_{yy} \tag{9.53}$$

where the non-zero diagonal elements of the strain tensor are obtained from (9.32). Substituting for ε_{xx} and ε_{yy} from (9.32), we obtain

$$\varepsilon = -\frac{b}{\pi} \frac{\bar{\mu}_0}{2\bar{\mu}_0 + \bar{\lambda}_0} \frac{y}{x^2 + y^2}. \tag{9.54}$$

In cylindrical polar coordinates, (9.54) is expressed as

$$\varepsilon = -\frac{b}{\pi} \frac{\bar{\mu}_0}{2\bar{\mu}_0 + \bar{\lambda}_0} \frac{\sin\theta}{r}. \tag{9.55}$$

We can disregard the negative sign in (9.54) and (9.55) as it can be eliminated by using the $\mathbf{FS}/RH$ convention instead of the $\mathbf{SF}/RH$ convention for the Burgers vector [159, see p. 22]).

As mentioned in section §9.3.1, the volume dilatation ε can be calculated from the edge dislocation displacement (longitudinal) equation (8.21), *viz.*

$$\nabla^2 u_{\parallel}^{\nu} = -\frac{\bar{\mu}_0 + \bar{\lambda}_0}{\bar{\mu}_0} \varepsilon^{;\nu}.$$

For the x-component, this equation gives

$$\nabla^2 u_x = \frac{\partial^2 u_x}{\partial x^2} + \frac{\partial^2 u_x}{\partial y^2} = -\frac{\bar{\mu}_0 + \bar{\lambda}_0}{\bar{\mu}_0} \varepsilon_{,x}. \tag{9.56}$$

Substituting for u_x from (9.27), we obtain

$$\nabla^2 u_x = -\frac{2b}{\pi} \frac{\bar{\mu}_0 + \bar{\lambda}_0}{2\bar{\mu}_0 + \bar{\lambda}_0} \frac{xy}{(x^2 + y^2)^2} = -\frac{\bar{\mu}_0 + \bar{\lambda}_0}{\bar{\mu}_0} \varepsilon_{,x}. \tag{9.57}$$

Hence

$$\varepsilon_{,x} = \frac{2b}{\pi} \frac{\bar{\mu}_0}{2\bar{\mu}_0 + \bar{\lambda}_0} \frac{xy}{(x^2+y^2)^2} \tag{9.58}$$

and

$$\varepsilon = \frac{2b}{\pi} \frac{\bar{\mu}_0}{2\bar{\mu}_0 + \bar{\lambda}_0} \int \frac{xy}{(x^2+y^2)^2}\, dx. \tag{9.59}$$

Evaluating the integral [376], we obtain

$$\varepsilon = -\frac{b}{\pi} \frac{\bar{\mu}_0}{2\bar{\mu}_0 + \bar{\lambda}_0} \frac{y}{x^2+y^2} \tag{9.60}$$

in agreement with (9.54).

Similarly for the y-component, substituting for u_y from (9.27), the equation

$$\nabla^2 u_y = \frac{\partial^2 u_y}{\partial x^2} + \frac{\partial^2 u_y}{\partial y^2} = -\frac{\bar{\mu}_0 + \bar{\lambda}_0}{\bar{\mu}_0}\, \varepsilon_{,y} \tag{9.61}$$

gives

$$\varepsilon_{,y} = -\frac{b}{\pi} \frac{\bar{\mu}_0}{2\bar{\mu}_0 + \bar{\lambda}_0} \frac{x^2-y^2}{(x^2+y^2)^2}. \tag{9.62}$$

Evaluating the integral [376]

$$\varepsilon = -\frac{b}{\pi} \frac{\bar{\mu}_0}{2\bar{\mu}_0 + \bar{\lambda}_0} \int \frac{x^2-y^2}{(x^2+y^2)^2}\, dy, \tag{9.63}$$

we obtain

$$\varepsilon = -\frac{b}{\pi} \frac{\bar{\mu}_0}{2\bar{\mu}_0 + \bar{\lambda}_0} \frac{y}{x^2+y^2} \tag{9.64}$$

again in agreement with (9.54).

The mass energy density is calculated from (2.24)

$$\rho c^2 = 4\bar{\kappa}_0\, \varepsilon = 2(2\bar{\lambda}_0 + \bar{\mu}_0)\, \varepsilon \tag{9.65}$$

where (2.3) has been used. Substituting for ε from (9.54), the mass energy density of the stationary edge dislocation is given by

$$\rho c^2 = \frac{4b}{\pi} \frac{\bar{\kappa}_0 \bar{\mu}_0}{2\bar{\mu}_0 + \bar{\lambda}_0} \frac{y}{x^2+y^2}. \tag{9.66}$$

In cylindrical polar coordinates, (9.66) is expressed as

$$\rho c^2 = \frac{4b}{\pi} \frac{\bar{\kappa}_0 \bar{\mu}_0}{2\bar{\mu}_0 + \bar{\lambda}_0} \frac{\sin\theta}{r}. \tag{9.67}$$

Using (9.54) in (9.50), the stationary edge dislocation longitudinal dilatation strain energy density is then given by

$$\mathcal{E}_{\parallel} = \frac{b^2}{2\pi^2}\,\frac{\bar{\kappa}_0\,\bar{\mu}_0^2}{(2\bar{\mu}_0+\bar{\lambda}_0)^2}\,\frac{y^2}{(x^2+y^2)^2}. \tag{9.68}$$

In cylindrical polar coordinates, (9.68) is expressed as

$$\mathcal{E}_{\parallel} = \frac{b^2}{2\pi^2}\,\frac{\bar{\kappa}_0\,\bar{\mu}_0^2}{(2\bar{\mu}_0+\bar{\lambda}_0)^2}\,\frac{\sin^2\theta}{r^2}. \tag{9.69}$$

The distortion strain energy density is calculated from (9.51), *viz.*

$$\mathcal{E}_{\perp} = \bar{\mu}_0 e^{\alpha\beta} e_{\alpha\beta}\,.$$

As seen previously in (9.20),

$$e^{\alpha\beta} = \varepsilon^{\alpha\beta} - e_s g^{\alpha\beta} \tag{9.70}$$

where $e_s = \frac{1}{4}\,\varepsilon$ is the volume dilatation calculated in (9.54). Then

$$e^{\alpha\beta}e_{\alpha\beta} = \left(\varepsilon^{\alpha\beta} - \tfrac{1}{4}\,\varepsilon g^{\alpha\beta}\right)\left(\varepsilon_{\alpha\beta} - \tfrac{1}{4}\,\varepsilon g_{\alpha\beta}\right) \tag{9.71}$$

and the distortion strain energy density equation becomes

$$\begin{aligned}\mathcal{E}_{\perp} &= \bar{\mu}_0\left(\varepsilon^{\alpha\beta}\varepsilon_{\alpha\beta} - \tfrac{1}{4}\,\varepsilon g^{\alpha\beta}\varepsilon_{\alpha\beta} - \tfrac{1}{4}\,\varepsilon g_{\alpha\beta}\varepsilon^{\alpha\beta} + \tfrac{1}{16}\,\varepsilon^2 g^{\alpha\beta}g_{\alpha\beta}\right)\\ &= \bar{\mu}_0\left(\varepsilon^{\alpha\beta}\varepsilon_{\alpha\beta} - \tfrac{1}{4}\,\varepsilon^2 - \tfrac{1}{4}\,\varepsilon^2 + \tfrac{1}{4}\,\varepsilon^2\right)\end{aligned} \tag{9.72}$$

for $g^{\alpha\beta} = \eta^{\alpha\beta}$. Hence

$$\mathcal{E}_{\perp} = \bar{\mu}_0\left(\varepsilon^{\alpha\beta}\varepsilon_{\alpha\beta} - \tfrac{1}{4}\,\varepsilon^2\right)\,. \tag{9.73}$$

This expression is expanded using the non-zero elements of the strain tensor (9.32) to give

$$\mathcal{E}_{\perp} = \bar{\mu}_0\left({\varepsilon_{xx}}^2 + {\varepsilon_{yy}}^2 + 2{\varepsilon_{xy}}^2 - \tfrac{1}{4}\,\varepsilon^2\right) \tag{9.74}$$

where $2{\varepsilon_{xy}}^2 = {\varepsilon_{xy}}^2 + {\varepsilon_{yx}}^2$. Substituting from (9.32) and (9.54) in the above, simplifying the $\bar{\beta}_0^2$ terms (see (9.76) and following definition), followed by the other terms, completing the squares for r^2 and performing polynomial division, we obtain

$$\mathcal{E}_{\perp} = \frac{\bar{\mu}_0\,b^2}{4\pi^2}\,\frac{2\,\bar{\beta}_0^2\,x^2 + \bar{\alpha}_0^2\,y^2}{(x^2+y^2)^2} \tag{9.75}$$

where

$$\bar{\alpha}_0 = \frac{\bar{\mu}_0}{2\bar{\mu}_0 + \bar{\lambda}_0} \tag{9.76}$$

$$\bar{\beta}_0 = \frac{\bar{\mu}_0 + \bar{\lambda}_0}{2\bar{\mu}_0 + \bar{\lambda}_0}\,. \tag{9.77}$$

Substituting for $\bar{\alpha}_0^2$ and $\bar{\beta}_0^2$, (9.75) becomes

$$\mathcal{E}_\perp = \frac{b^2}{4\pi^2}\,\frac{\bar{\mu}_0}{(2\bar{\mu}_0 + \bar{\lambda}_0)^2}\,\frac{2(\bar{\mu}_0 + \bar{\lambda}_0)^2\,x^2 + \bar{\mu}_0^2\,y^2}{(x^2+y^2)^2}\,. \tag{9.78}$$

In cylindrical polar coordinates, (9.78) is expressed as

$$\mathcal{E}_\perp = \frac{b^2}{4\pi^2}\,\frac{\bar{\mu}_0}{(2\bar{\mu}_0 + \bar{\lambda}_0)^2}\,\frac{2(\bar{\mu}_0 + \bar{\lambda}_0)^2\,\cos^2\theta + \bar{\mu}_0^2\,\sin^2\theta}{r^2}\,. \tag{9.79}$$

This equation can also be written as

$$\mathcal{E}_\perp = \frac{\bar{\mu}_0\,b^2}{4\pi^2}\,\left(\bar{\alpha}_0^2\,\frac{\sin^2\theta}{r^2} + 2\bar{\beta}_0^2\,\frac{\cos^2\theta}{r^2}\right)\,. \tag{9.80}$$

§9.3.5 *Moving edge dislocation strain energy density*

We next consider the general case of the moving edge dislocation in the spacetime continuum of section §9.3.2, with cartesian coordinates (x, y, z). We first evaluate the volume dilatation ε for the moving edge dislocation. The volume dilatation is given by

$$\varepsilon = \varepsilon^\alpha{}_\alpha = \varepsilon_{xx} + \varepsilon_{yy} \tag{9.81}$$

where the non-zero diagonal elements of the strain tensor are obtained from (9.46). Substituting for ε_{xx} and ε_{yy} from (9.46) in (9.81), we notice that the transverse terms cancel out, and we are left with the following longitudinal term:

$$\varepsilon = \frac{bc^2 y}{\pi v^2}\,\frac{\alpha_l^3 - \alpha_l}{(x - vt)^2 + \alpha_l^2 y^2} \tag{9.82}$$

This equation can be further reduced to

$$\varepsilon = \frac{bc^2}{\pi v^2}\,\frac{v^2}{{c_l}^2}\,\frac{\alpha_l y}{(x - vt)^2 + \alpha_l^2 y^2} \tag{9.83}$$

and finally, using $c^2/{c_l}^2 = \bar{\mu}_0/(2\bar{\mu}_0 + \bar{\lambda}_0)$ (see (3.12) and (9.36)),

$$\varepsilon(x_i, t) = \frac{b}{2\pi} \frac{2\bar{\mu}_0}{2\bar{\mu}_0 + \bar{\lambda}_0} \frac{\alpha_l y}{(x - vt)^2 + \alpha_l^2 y^2}. \tag{9.84}$$

As we have seen previously, the mass energy density is calculated from (9.65)

$$\rho c^2 = 4\bar{\kappa}_0 \, \varepsilon = 2(2\bar{\lambda}_0 + \bar{\mu}_0) \, \varepsilon. \tag{9.85}$$

Substituting for ε from (9.84), the mass energy density of an edge dislocation is given by

$$\rho(x_i, t) \, c^2 = \frac{b}{2\pi} \frac{8\bar{\kappa}_0\bar{\mu}_0}{2\bar{\mu}_0 + \bar{\lambda}_0} \frac{\alpha_l y}{(x - vt)^2 + \alpha_l^2 y^2}. \tag{9.86}$$

Using (9.84) in (9.50), the edge dislocation longitudinal dilatation strain energy density is then given by

$$\mathcal{E}_{\parallel} = \frac{1}{2} \bar{\kappa}_0 \left(\frac{b}{2\pi} \frac{2\bar{\mu}_0}{2\bar{\mu}_0 + \bar{\lambda}_0} \frac{\alpha_l y}{(x - vt)^2 + \alpha_l^2 y^2} \right)^2. \tag{9.87}$$

The distortion strain energy density is calculated from (9.73) as derived from (9.51). The expression is expanded using the non-zero elements of the strain tensor (9.46) and (9.47) to obtain [238, see Eqs.(114–115)])

$$\mathcal{E}_{\perp} = \bar{\mu}_0 \left({\varepsilon_{xx}}^2 + {\varepsilon_{yy}}^2 - 2{\varepsilon_{tx}}^2 - 2{\varepsilon_{ty}}^2 + 2{\varepsilon_{xy}}^2 - \tfrac{1}{4}\varepsilon^2 \right) \tag{9.88}$$

Substituting from (9.46), (9.47) and (9.82) in the above and simplifying, we obtain

$$\begin{aligned} \mathcal{E}_{\perp} = {} & \frac{\bar{\mu}_0 \, b^2}{\pi^2} \frac{c^4}{v^4} \\ & \left[\frac{\alpha_2^4}{2\alpha^2} \frac{\left((1+\alpha^2)^2 - v^2/c^2\right) \, (x - vt)^2 + 2\alpha^4(1+\alpha_2^2) \, y^2}{r^{*4}} - \right. \\ & - 2 \, \alpha_l \, \alpha_2^2 \, \alpha \, \frac{\left(1 + \alpha_2^2/\alpha^2\right) (x - vt)^2 + \left(\alpha_2^2 + \alpha_l^2\right) \, y^2}{r^{*2} \, r_l^{*2}} + \\ & \left. + \alpha_l^2 \, \frac{(1+\alpha_2^2) \, (x - vt)^2 + \left(\alpha_2^2 + \alpha_l^4 - \frac{1}{4} \, v^4/c_l^4\right) \, y^2}{r_l^{*4}} \right] \end{aligned} \tag{9.89}$$

where

$$r^{*2} = (x - vt)^2 + \alpha^2 y^2 \tag{9.90}$$

$$r_l^{*2} = (x - vt)^2 + \alpha_l^2 y^2 \,. \tag{9.91}$$

We consider the above equations for the moving edge dislocation in the limit as $v \to 0$. Then the terms

$$\frac{\alpha y}{(x - vt)^2 + \alpha^2 y^2} \to \frac{\sin\theta}{r} \tag{9.92}$$

and

$$\frac{x - vt}{(x - vt)^2 + \alpha^2 y^2} \to \frac{\cos\theta}{r} \tag{9.93}$$

in cylindrical polar coordinates. Similarly for the same terms with α_l instead of α.

The volume dilatation obtained from (9.84) is then given in cylindrical polar coordinates (r, θ, z) by

$$\varepsilon \to \frac{b}{2\pi} \frac{2\bar{\mu}_0}{2\bar{\mu}_0 + \bar{\lambda}_0} \frac{\sin\theta}{r}. \tag{9.94}$$

The mass energy density is obtained from (9.86) to give

$$\rho c^2 \to \frac{b}{2\pi} \frac{8\bar{\kappa}_0 \bar{\mu}_0}{2\bar{\mu}_0 + \bar{\lambda}_0} \frac{\sin\theta}{r}. \tag{9.95}$$

From (9.87), the edge dislocation dilatation strain energy density is then given by

$$\mathcal{E}_{\|} \to \frac{b^2}{2\pi^2} \frac{\bar{\kappa}_0 \, \bar{\mu}_0^2}{(2\bar{\mu}_0 + \bar{\lambda}_0)^2} \frac{\sin^2\theta}{r^2}. \tag{9.96}$$

These equations are in agreement with (9.55), (9.67) and (9.69) respectively.

The edge dislocation distortion strain energy density in the limit as $v \to 0$ is obtained by using (9.92) and (9.93) in (9.46), (9.47) and (9.82) to compute (9.88). For example, ε_{xx} becomes

$$\varepsilon_{xx} = \frac{b\, c^2}{\pi v^2} \left(-1 + \alpha_2^2\right) \frac{\sin\theta}{r} \,. \tag{9.97}$$

Using these limiting values in (9.46) and (9.47), and $c^2/{c_l}^2 = \bar{\mu}_0/(2\bar{\mu}_0 + \bar{\lambda}_0)$ (see (3.12) and (9.36)) in the expression for ε in (9.94), equation

(9.88) then becomes:

$$\mathcal{E}_\perp \to \frac{\bar{\mu}_0\, b^2}{\pi^2}\,\frac{c^4}{v^4}\left[-\frac{1}{4}\,\frac{v^4}{{c_l}^4}\,\frac{\sin^2\theta}{r^2}+\left(-1+\alpha_2^2\right)^2\frac{\sin^2\theta}{r^2}+\right.$$
$$+\left(\alpha_l^2-\alpha_2^2\right)^2\frac{\sin^2\theta}{r^2}+\left(2\alpha_l-\alpha_2^2\left(\alpha+\frac{1}{\alpha}\right)\right)^2\frac{\cos^2\theta}{r^2}- \tag{9.98}$$
$$\left.-\frac{v^2}{c^2}\,\left(1-\,\alpha_2^2\right)^2\frac{\sin^2\theta}{r^2}-\,\frac{v^2}{c^2}\,\left(-\alpha_l+\,\frac{\alpha_2^2}{\alpha}\right)^2\,\frac{\cos^2\theta}{r^2}\right].$$

Using the definitions of α^2, α_2^2 and α_l^2 from (9.11), (9.34) and (9.35) respectively, using the first term of the Taylor expansion for α and α_l as $v \to 0$, and neglecting the terms multiplied by $-v^2/c^2$ in (9.98) as they are of order v^6/c^6, (9.98) becomes

$$\mathcal{E}_\perp \to \frac{\bar{\mu}_0\, b^2}{\pi^2}\,\frac{c^4}{v^4}\left[\left(-\frac{1}{4}\,\frac{v^4}{{c_l}^4}+\frac{v^4}{4c^4}+\left(-\frac{v^2}{c_l^2}+\frac{v^2}{2c^2}\right)^2\right)\,\frac{\sin^2\theta}{r^2}+\right.$$
$$\left.+\,4\left(1-\frac{v^2}{2c_l^2}-1+\frac{v^2}{2c^2}\right)^2\,\frac{\cos^2\theta}{r^2}\right]. \tag{9.99}$$

Squaring and simplifying, we obtain

$$\mathcal{E}_\perp \to \frac{\bar{\mu}_0\, b^2}{\pi^2}\,\frac{c^4}{v^4}\left[\left(\frac{3}{4}\,\frac{v^4}{{c_l}^4}-\frac{v^4}{c_l^2c^2}+\frac{v^4}{2c^4}\right)\,\frac{\sin^2\theta}{r^2}+\right.$$
$$\left.+\left(\frac{v^4}{{c_l}^4}-2\,\frac{v^4}{c_l^2c^2}+\frac{v^4}{c^4}\right)\frac{\cos^2\theta}{r^2}\right] \tag{9.100}$$

and further

$$\mathcal{E}_\perp \to \frac{\bar{\mu}_0\, b^2}{2\pi^2}\left[\left(1-2\,\frac{c^2}{c_l^2}+\frac{3}{2}\,\frac{c^4}{{c_l}^4}\right)\,\frac{\sin^2\theta}{r^2}+\right.$$
$$\left.+\,2\left(1-2\,\frac{c^2}{c_l^2}+\frac{c^4}{{c_l}^4}\right)\frac{\cos^2\theta}{r^2}\right]. \tag{9.101}$$

Using ${c^2}/{{c_l}^2} = \bar{\mu}_0/(2\bar{\mu}_0+\bar{\lambda}_0)$ (see (3.12) and (9.36)), (9.101) becomes

$$\mathcal{E}_\perp \to \frac{\bar{\mu}_0\, b^2}{2\pi^2}\left[\left(1-2\,\bar{\alpha}_0+\frac{3}{2}\,\bar{\alpha}_0^2\right)\,\frac{\sin^2\theta}{r^2}+\right.$$
$$\left.+\,2\left(1-2\bar{\alpha}_0+\bar{\alpha}_0^2\right)\frac{\cos^2\theta}{r^2}\right] \tag{9.102}$$

where

$$\left(1 - 2\bar{\alpha}_0 + \bar{\alpha}_0^2\right) = \left(1 - \bar{\alpha}_0\right)^2 = \bar{\beta}_0^2 \tag{9.103}$$

and $\bar{\alpha}_0$ and $\bar{\beta}_0$ are as defined in (9.76). This equation represents the impact of the time terms included in the calculation of $\mathcal{E}_\perp$ and the limit operation $v \to 0$ used in (9.89). Adding the terms of the $\sin^2\theta/r^2$ coefficient by setting $c \simeq c_l$ in (9.100), we obtain the same term as in (9.80). Hence, comparing this expression with (9.80) for the stationary dislocation, we find that it has the same structure, with some additional details resulting from the time limit operation.

§9.3.6 *Edge dislocation current and charge density*

The current density four-vector is calculated from (4.10), *viz.*

$$j^\nu = \frac{\varphi_0}{\mu_0}\,\frac{2\bar{\mu}_0 + \bar{\lambda}_0}{2\bar{\mu}_0}\,\varepsilon^{;\nu} = \frac{\varphi_0}{2\mu_0\bar{\alpha}_0}\,\varepsilon^{;\nu}$$

and the charge density from (4.14), *viz.*

$$\varrho = \frac{1}{2}\,\varphi_0\epsilon_0 c\,\frac{2\bar{\mu}_0 + \bar{\lambda}_0}{2\bar{\mu}_0}\,\sqrt{\varepsilon^{;\nu}\varepsilon_{;\nu}} = \frac{\varphi_0\epsilon_0 c}{4\bar{\alpha}_0}\,\sqrt{\varepsilon^{;\nu}\varepsilon_{;\nu}}$$

where φ_0 is the spacetime continuum electromagnetic shearing potential constant.

We first consider the stationary edge dislocation. Using the expression for ε from (9.64), the non-zero components of the current density are given by

$$\begin{aligned} j_x &= \frac{\varphi_0 b}{\pi\mu_0}\,\frac{xy}{r^4} = \frac{\varphi_0 b}{2\pi\mu_0}\,\frac{\sin 2\theta}{r^2} \\ j_y &= -\frac{\varphi_0 b}{\pi\mu_0}\,\frac{x^2 - y^2}{r^4} = -\frac{\varphi_0 b}{\pi\mu_0}\,\frac{\cos 2\theta}{r^2} \end{aligned} \tag{9.104}$$

where $r^2 = x^2 + y^2$. The charge density is given by

$$\varrho = \pm\frac{1}{4\pi}\,\varphi_0\epsilon_0 c\,\frac{b}{r^2}\,. \tag{9.105}$$

The sign depends on the problem under consideration.

The charge is given by integrating ϱ over the volume V:

$$Q = \int_V \varrho\, dV = \int_V \varrho\, r^2 dr \sin\varphi\, d\varphi\, d\theta \tag{9.106}$$

in spherical polar coordinates. This becomes

$$Q = \pm\frac{1}{4\pi}\,\varphi_0\epsilon_0 c\,b\int_0^R dr\int_0^\pi \sin\varphi\,d\varphi\int_0^{2\pi} d\theta \tag{9.107}$$

where R is the "radius" of the deformation. Evaluating the integrals, we get

$$Q = \pm\varphi_0\epsilon_0 c\,bR \tag{9.108}$$

where the units are [C] as expected. Using $b = nb_0$ (see (14.2)),

$$Q = \pm\, n\varphi_0\epsilon_0 c\,b_0 R = \pm\, n\,\frac{\varphi_0 b_0}{\mu_0 c}\,R \tag{9.109}$$

where n is the number of elementary Burgers displacement b_0.

We next consider the moving edge dislocation. Using the expression for ε from (9.84), the non-zero components of the current density are given by

$$\begin{aligned} j_x &= -\frac{\varphi_0 b}{\pi\mu_0}\,\alpha_l\,\frac{(x-vt)y}{\left[(x-vt)^2+(\alpha_l y)^2\right]^2} \\ j_y &= \frac{\varphi_0 b}{2\pi\mu_0}\,\alpha_l\,\frac{(x-vt)^2-(\alpha_l y)^2}{\left[(x-vt)^2+(\alpha_l y)^2\right]^2} \\ j_{ct} &= \frac{\varphi_0 b}{\pi\mu_0}\,\alpha_l\,\frac{v}{c}\,\frac{(x-vt)y}{\left[(x-vt)^2+(\alpha_l y)^2\right]^2}\,. \end{aligned} \tag{9.110}$$

The charge density is given by

$$\begin{aligned} \varrho = \pm\frac{1}{4\pi}\,\varphi_0\epsilon_0 c\,\alpha_l\,&\frac{b}{(x-vt)^2+(\alpha_l y)^2} \\ &\left[1+2(1+\bar\alpha_0)\,\frac{v^2}{c^2}\,\frac{(x-vt)^2y^2}{\left[(x-vt)^2+(\alpha_l y)^2\right]^2}\right]^{\frac{1}{2}} \end{aligned} \tag{9.111}$$

and for $v/c \ll 1$

$$\begin{aligned} \varrho \simeq \pm\frac{1}{4\pi}\,\varphi_0\epsilon_0 c\,\alpha_l\,&\frac{b}{(x-vt)^2+(\alpha_l y)^2} \\ &\left[1+(1+\bar\alpha_0)\,\frac{v^2}{c^2}\,\frac{(x-vt)^2y^2}{\left[(x-vt)^2+(\alpha_l y)^2\right]^2}\right]. \end{aligned} \tag{9.112}$$

which tends to

$$\varrho \to \pm\frac{1}{4\pi}\,\varphi_0\epsilon_0 c\,\alpha_l\,\frac{b}{(x-vt)^2+(\alpha_l y)^2} \tag{9.113}$$

and the results of the stationary edge dislocation as $v \to 0$. The sign again depends on the problem under consideration.

§9.4 Volterra discrete dislocation line

In this section, we consider a discrete straight dislocation line running along the z-axis, composed of both screw and edge dislocations first proposed by Volterra [360]. The dislocations include a screw dislocation with displacement b_z and edge dislocations with displacements b_x and b_y. We will review the Volterra analysis in greater details in §10.2.

The displacements are given by

$$\begin{aligned} u_x &= \frac{1}{2\pi}\left(b_x\theta - b_y \ln r\right) \\ u_y &= \frac{1}{2\pi}\left(b_y\theta + b_x \ln r\right) \\ u_z &= \frac{1}{2\pi} b_z\theta \end{aligned} \tag{9.114}$$

where

$$r^2 = x^2 + y^2 \tag{9.115}$$

$$\theta = \arctan\left(\frac{y}{x}\right) . \tag{9.116}$$

The components of the strain tensor in cartesian coordinates are derived from $\varepsilon^{\mu\nu} = \frac{1}{2}(u^{\mu;\nu} + u^{\nu;\mu})$:

$$\begin{aligned} \varepsilon_{xx} &= -\frac{b_x}{2\pi}\frac{y}{r^2} - \frac{b_y}{2\pi}\frac{x}{r^2} \\ \varepsilon_{yy} &= \frac{b_x}{2\pi}\frac{y}{r^2} + \frac{b_y}{2\pi}\frac{x}{r^2} \\ \varepsilon_{zz} &= 0 \\ \varepsilon_{xy} &= \frac{b_x}{\pi}\frac{x}{r^2} - \frac{b_y}{\pi}\frac{y}{r^2} \\ \varepsilon_{yz} &= \frac{b_z}{2\pi}\frac{x}{r^2} \\ \varepsilon_{xz} &= -\frac{b_z}{2\pi}\frac{y}{r^2} . \end{aligned} \tag{9.117}$$

The volume dilatation ε for the discrete dislocation line is then given by

$$\varepsilon = \varepsilon^{\alpha}{}_{\alpha} = \varepsilon_{xx} + \varepsilon_{yy} + \varepsilon_{zz} \,. \tag{9.118}$$

Substituting for ε_{xx}, ε_{yy} and ε_{zz} from (9.117), we obtain

$$\varepsilon = 0 \,. \tag{9.119}$$

Hence the mass energy density is zero

$$\rho c^2 = 0 \tag{9.120}$$

and the longitudinal dilatation strain energy density is also zero

$$\mathcal{E}_{\parallel} = 0 \,. \tag{9.121}$$

This indicates a problem with the Volterra displacements (9.114) as the volume dilatation of an edge dislocation is not equal to zero.

The distortion strain energy density is calculated from (9.147)

$$\mathcal{E}_{\perp} = \bar{\mu}_0 \left(\varepsilon^{\alpha\beta} \varepsilon_{\alpha\beta} - \tfrac{1}{4} \varepsilon^2 \right) , \tag{9.122}$$

using the non-zero elements of the strain tensor (9.117) to give

$$\mathcal{E}_{\perp} = \bar{\mu}_0 \left({\varepsilon_{xx}}^2 + {\varepsilon_{yy}}^2 + 2{\varepsilon_{xy}}^2 + 2{\varepsilon_{yz}}^2 + 2{\varepsilon_{xz}}^2 \right) . \tag{9.123}$$

Substituting from (9.117) in the above, we obtain

$$\mathcal{E}_{\perp} = \frac{\bar{\mu}_0}{4\pi^2} \left(\frac{b_z^2}{r^2} + 2\,\frac{\left(b_x^2 + b_y^2\right)}{r^2} + 2\,\frac{\left(b_x x - b_y y\right)^2}{r^4} \right) . \tag{9.124}$$

The components of the stress tensor in cartesian coordinates are given by:

$$\begin{aligned}
\sigma_{xx} &= -\frac{\bar{\mu}_0 b_x}{\pi}\,\frac{y}{r^2} - \frac{\bar{\mu}_0 b_y}{\pi}\,\frac{x}{r^2} \\
\sigma_{yy} &= \frac{\bar{\mu}_0 b_x}{\pi}\,\frac{y}{r^2} + \frac{\bar{\mu}_0 b_y}{\pi}\,\frac{x}{r^2} \\
\sigma_{zz} &= 0 \\
\sigma_{xy} &= \frac{2\bar{\mu}_0 b_x}{\pi}\,\frac{x}{r^2} - \frac{2\bar{\mu}_0 b_y}{\pi}\,\frac{y}{r^2} \\
\sigma_{yz} &= \frac{\bar{\mu}_0 b_z}{\pi}\,\frac{x}{r^2} \\
\sigma_{xz} &= -\frac{\bar{\mu}_0 b_z}{\pi}\,\frac{y}{r^2} \,.
\end{aligned} \tag{9.125}$$

The volume force calculated from [80]

$$X^\nu = -\sigma^{\mu\nu}{}_{;\mu}\,, \tag{9.126}$$

gives

$$\begin{aligned} X_x &= \frac{\bar{\mu}_0 b_x}{\pi}\,\frac{2xy}{r^4} + \frac{\bar{\mu}_0 b_y}{\pi}\,\frac{x^2-y^2}{r^4} \\ X_y &= -\frac{\bar{\mu}_0 b_y}{\pi}\,\frac{2xy}{r^4} + \frac{\bar{\mu}_0 b_x}{\pi}\,\frac{x^2-y^2}{r^4} \\ X_z &= 0 \end{aligned} \tag{9.127}$$

and the fields are not in equilibrium. As pointed out by deWit [80], this is another problem with the Volterra displacements in that there is a net volume force present. Another example, for the stationary screw (9.3) and edge (9.31) dislocations considered previously, it is straightforward to show that there is no net volume force present ($X^\nu = 0$).

§9.5 deWit discrete dislocation line

In this section, we consider a discrete straight dislocation line running along the z-axis, composed of both screw and edge dislocations as derived by deWit [80] to correct the Volterra displacements so that no net volume force is present

Displacements are often difficult to derive, and minimal simplified expressions are often used. For example, the Volterra dislocation expressions that we analyzed in the previous section §9.4 are a case in point. deWit corrects the Volterra expressions to ensure no net volume force is present and mentions that the displacements (9.130) below are as he derived them, "except for some trivial constants". In our work, correct displacement expressions are needed as they are the basis of the physical characteristics of the deformations, including their strain energy density.

The cartesian (x, y, z) and cylindrical polar (r, θ, z) coordinates used by deWit [80] in his analysis are as per Fig. 9.5. deWit defined his analysis in terms of coordinates (x_1, x_2, x_3) which correspond and are equivalent to our use of (x, y, z). Specific screw and edge dislocation defects are oriented along these axes: the screw dislocation along the z-axis with Burgers vector b_z represented in Fig. 9.3, the edge dislocation along the z-axis with Burgers vector b_x represented in Fig. 9.4, and a different edge dislocation along the z-axis with Burgers vector b_y represented in Fig. 9.6 which we call the gap dislocation. In all cases,

Figure 9.5: Cartesian (x, y, z) and cylindrical polar (r, θ, z) coordinates used by deWit [80] in his analysis. The cut line corresponds to the displacement discontinuity of the dislocation.

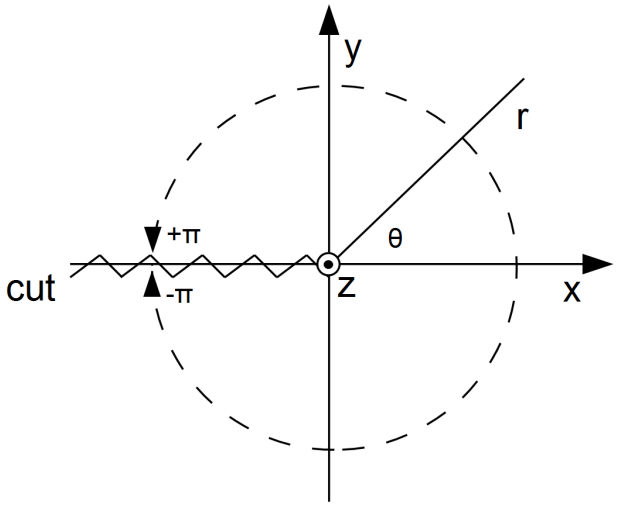

the dislocation line ξ is along the z-axis, but the Burgers vectors are oriented along different axes.

The cut along the negative x-axis represents the discontinuity in the displacement given by (10.4) and extends in the $x - z$ plane. It should be noted that the dislocation illustrations should be on the negative x-axis in accordance with Fig. 9.5 – they have been drawn on the positive x-axis for clarity of illustration only. It is also important to note that there are two types of edge dislocations: the edge dislocation proper which can be called the ledge dislocation and the gap dislocation. It will usually be clear from the context whether we are referring to edge dislocations in general or to the edge dislocation proper – this will be stated explicitly in cases where it is not clear.

Defining the constants $\bar{\alpha}_0$ and $\bar{\beta}_0$

$$\bar{\alpha}_0 = \frac{\bar{\mu}_0}{2\bar{\mu}_0 + \bar{\lambda}_0} \tag{9.128}$$

$$\bar{\beta}_0 = \frac{\bar{\mu}_0 + \bar{\lambda}_0}{2\bar{\mu}_0 + \bar{\lambda}_0}\,, \tag{9.129}$$

Figure 9.6: A stationary gap dislocation in cartesian (x, y, z) and cylindrical polar (r, θ, z) coordinates.

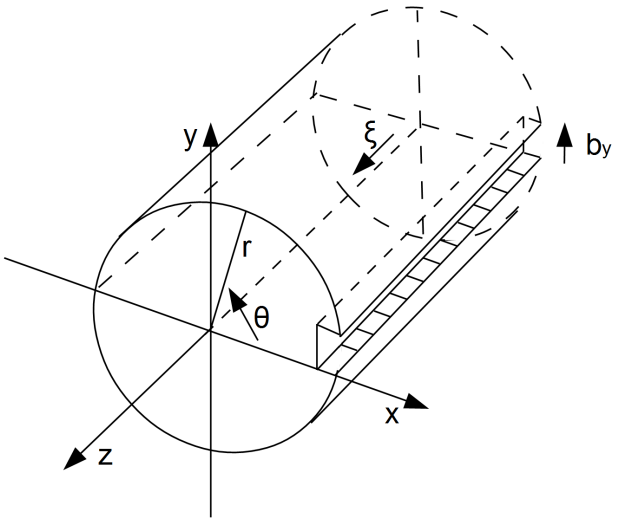

the deWit displacements are given by [80]

$$
\begin{aligned}
u_x &= \frac{b_x^{(e)}}{2\pi}\left(\theta + \bar{\beta}_0\,\frac{xy}{r^2}\right) + \frac{b_y^{(g)}}{2\pi}\left(\bar{\alpha}_0\,\ln r + \bar{\beta}_0\,\frac{y^2}{r^2}\right) \\
u_y &= -\frac{b_x^{(e)}}{2\pi}\left(\bar{\alpha}_0\,\ln r + \bar{\beta}_0\,\frac{x^2}{r^2}\right) + \frac{b_y^{(g)}}{2\pi}\left(\theta - \bar{\beta}_0\,\frac{xy}{r^2}\right) \\
u_z &= \frac{b_z^{(s)}}{2\pi}\,\theta
\end{aligned}
\tag{9.130}
$$

where we have specifically appended superscripts to the Burgers vectors for clarity: $b_x^{(e)}$ for the edge dislocation proper, $b_y^{(g)}$ for the gap dislocation, and $b_z^{(s)}$ for the screw dislocation. In general, we will not append these superscripts except where required for clarity. We can obtain specific expressions for screw dislocations by putting $b_x = 0$ and $b_y = 0$, for edge dislocations by putting $b_y = 0$ and $b_z = 0$, and for gap dislocations by putting $b_x = 0$ and $b_z = 0$, and similarly for the other expressions below.

The components of the strain tensor in cartesian coordinates are derived from $\varepsilon^{\mu\nu} = \frac{1}{2}(u^{\mu;\nu} + u^{\nu;\mu})$:

$$\begin{aligned}
\varepsilon_{xx} &= -\frac{b_x}{2\pi}\left(\bar{\alpha}_0\,\frac{y}{r^2} + \bar{\beta}_0\,\frac{2x^2y}{r^4}\right) + \frac{b_y}{2\pi}\left(\bar{\alpha}_0\,\frac{x}{r^2} - \bar{\beta}_0\,\frac{2xy^2}{r^4}\right)\\
\varepsilon_{yy} &= -\frac{b_x}{2\pi}\left(\bar{\alpha}_0\,\frac{y}{r^2} - \bar{\beta}_0\,\frac{2x^2y}{r^4}\right) + \frac{b_y}{2\pi}\left(\bar{\alpha}_0\,\frac{x}{r^2} + \bar{\beta}_0\,\frac{2xy^2}{r^4}\right)\\
\varepsilon_{zz} &= 0\\
\varepsilon_{xy} &= \frac{b_x}{2\pi}\,\bar{\beta}_0\,\left(\frac{x}{r^2} - \frac{2xy^2}{r^4}\right) - \frac{b_y}{2\pi}\,\bar{\beta}_0\,\left(\frac{y}{r^2} - \frac{2x^2y}{r^4}\right)\\
\varepsilon_{yz} &= \frac{b_z}{4\pi}\,\frac{x}{r^2}\\
\varepsilon_{xz} &= -\frac{b_z}{4\pi}\,\frac{y}{r^2}\,.
\end{aligned} \tag{9.131}$$

The volume dilatation ε for the discrete dislocation line is then given by

$$\varepsilon = \varepsilon^{\alpha}{}_{\alpha} = \varepsilon_{xx} + \varepsilon_{yy} + \varepsilon_{zz}\,. \tag{9.132}$$

Substituting for ε_{xx}, ε_{yy} and ε_{zz} from (9.131), we obtain

$$\varepsilon = -\frac{1}{\pi}\,\frac{\bar{\mu}_0}{2\bar{\mu}_0 + \bar{\lambda}_0}\,\frac{b_x y - b_y x}{r^2}\,. \tag{9.133}$$

The mass energy density is calculated from (2.24), *viz.*

$$\rho c^2 = 4\bar{\kappa}_0\,\varepsilon = 2(2\bar{\lambda}_0 + \bar{\mu}_0)\,\varepsilon\,.$$

Substituting for ε from (9.133), using the positive value of ε as per section §9.3.4, the mass energy density of the discrete dislocation line is given by

$$\rho c^2 = \frac{4}{\pi}\,\frac{\bar{\kappa}_0\bar{\mu}_0}{2\bar{\mu}_0 + \bar{\lambda}_0}\,\frac{b_x y - b_y x}{r^2}\,. \tag{9.134}$$

The components of the stress tensor in cartesian coordinates are

given by [80]:

$$\begin{aligned}
\sigma_{xx} &= -\frac{\bar{\mu}_0 b_x}{\pi}\,\bar{\beta}_0\,\left(\frac{y}{r^2}+\frac{2x^2y}{r^4}\right)+\frac{\bar{\mu}_0 b_y}{\pi}\,\bar{\beta}_0\,\left(\frac{x}{r^2}-\frac{2xy^2}{r^4}\right)\\
\sigma_{yy} &= -\frac{\bar{\mu}_0 b_x}{\pi}\,\bar{\beta}_0\,\left(\frac{y}{r^2}-\frac{2x^2y}{r^4}\right)+\frac{\bar{\mu}_0 b_y}{\pi}\,\bar{\beta}_0\,\left(\frac{x}{r^2}+\frac{2xy^2}{r^4}\right)\\
\sigma_{zz} &= -\frac{1}{\pi}\,\frac{\bar{\mu}_0\bar{\lambda}_0}{2\bar{\mu}_0+\bar{\lambda}_0}\,\left(\frac{b_x y-b_y x}{r^2}\right)\\
\sigma_{xy} &= \frac{\bar{\mu}_0 b_x}{\pi}\,\bar{\beta}_0\,\left(\frac{x}{r^2}-\frac{2xy^2}{r^4}\right)-\frac{\bar{\mu}_0 b_y}{\pi}\,\bar{\beta}_0\,\left(\frac{y}{r^2}-\frac{2x^2y}{r^4}\right)\\
\sigma_{yz} &= \frac{\bar{\mu}_0 b_z}{2\pi}\,\frac{x}{r^2}\\
\sigma_{xz} &= -\frac{\bar{\mu}_0 b_z}{2\pi}\,\frac{y}{r^2}\,.
\end{aligned} \tag{9.135}$$

As shown in [80], the volume force is zero,

$$X^\nu = -\sigma^{\mu\nu}{}_{;\mu} = 0\,, \tag{9.136}$$

and the fields are in equilibrium.

We now consider the rotation tensor defined by (3.3), *viz.*

$$\omega^{\mu\nu} = \tfrac{1}{2}(u^{\mu;\nu}-u^{\nu;\mu})\,.$$

Given that $u^{\mu;\nu}=u^{\nu;\mu}$, the diagonal elements of the rotation tensor are zero. Only the off-diagonal elements are non-zero. Substituting for the displacements from (9.131), we obtain

$$\begin{aligned}
\omega_{xy} &= -\omega_{yx} = \frac{1}{2\pi}\,\frac{b_x x+b_y y}{r^2}\\
\omega_{yz} &= -\omega_{zy} = -\frac{b_z}{4\pi}\,\frac{x}{r^2}\\
\omega_{xz} &= -\omega_{zx} = \frac{b_z}{4\pi}\,\frac{y}{r^2}\,.
\end{aligned} \tag{9.137}$$

In terms of the rotation vector, using (10.1) *viz.*

$$\omega^\alpha = \frac{1}{2}\,\epsilon^{\alpha\mu\nu}\,\omega_{\mu\nu}\,,$$

we obtain

$$\begin{aligned}\omega_x &= -\frac{b_z}{4\pi}\,\frac{x}{r^2}\\ \omega_y &= -\frac{b_z}{4\pi}\,\frac{y}{r^2}\\ \omega_z &= \frac{1}{2\pi}\,\frac{b_x x + b_y y}{r^2}\,.\end{aligned} \tag{9.138}$$

The x and y components of the rotation vector are the components of b_z along those axes respectively, attenuated by a factor $1/r$ (*i.e.* $x/r = \cos\theta$ and $y/r = \sin\theta$), while the z component of the rotation vector is the moment of the components of b_x and b_y along the x and y axes also attenuated by a factor $1/r$.

§9.5.1 *deWit dislocation line strain energy density*

The strain energy density of the discrete dislocation line is calculated as follows. Using (9.133) in (9.50), the discrete dislocation line longitudinal dilatation strain energy density is then given by

$$\mathcal{E}_{\parallel} = \frac{1}{2\pi^2}\,\frac{\bar\kappa_0\,\bar\mu_0^2}{(2\bar\mu_0+\bar\lambda_0)^2}\,\frac{(b_x y - b_y x)^2}{r^4}\,. \tag{9.139}$$

Expanding the quadratic term, we obtain

$$\mathcal{E}_{\parallel} = \mathcal{E}_{\parallel}^{E} + \mathcal{E}_{\parallel}^{G} + \mathcal{E}_{\parallel\ int}^{E-G} \tag{9.140}$$

where the edge dislocation longitudinal dilatation strain energy density $\mathcal{E}_{\parallel}^{E}$, the gap dislocation longitudinal dilatation strain energy density $\mathcal{E}_{\parallel}^{G}$, and the edge-gap interaction longitudinal dilatation strain energy density $\mathcal{E}_{\parallel\ int}^{E-G}$ are given by

$$\mathcal{E}_{\parallel}^{E} = \frac{1}{2\pi^2}\bar\kappa_0\bar\alpha_0^2\,\frac{b_x^{(e)\,2}y^2}{r^4} \tag{9.141}$$

$$\mathcal{E}_{\parallel}^{G} = \frac{1}{2\pi^2}\bar\kappa_0\bar\alpha_0^2\,\frac{b_y^{(g)\,2}x^2}{r^4} \tag{9.142}$$

$$\mathcal{E}_{\parallel\ int}^{E-G} = -\frac{1}{\pi^2}\bar\kappa_0\bar\alpha_0^2\,\frac{b_x^{(e)}b_y^{(g)}xy}{r^4}\,. \tag{9.143}$$

The distortion strain energy density is calculated from (9.51), *viz.*

$$\mathcal{E}_{\perp} = \bar\mu_0 e^{\alpha\beta}e_{\alpha\beta}\,.$$

As seen previously in (9.20),

$$e^{\alpha\beta} = \varepsilon^{\alpha\beta} - e_s g^{\alpha\beta} \tag{9.144}$$

where $e_s = \frac{1}{4}\,\varepsilon$ is the volume dilatation calculated in (9.54). Then

$$e^{\alpha\beta} e_{\alpha\beta} = \left(\varepsilon^{\alpha\beta} - \tfrac{1}{4}\,\varepsilon g^{\alpha\beta}\right)\left(\varepsilon_{\alpha\beta} - \tfrac{1}{4}\,\varepsilon g_{\alpha\beta}\right) \tag{9.145}$$

and the distortion strain energy density equation becomes

$$\begin{aligned}\mathcal{E}_\perp &= \bar{\mu}_0\left(\varepsilon^{\alpha\beta}\varepsilon_{\alpha\beta} - \tfrac{1}{4}\,\varepsilon g^{\alpha\beta}\varepsilon_{\alpha\beta} - \tfrac{1}{4}\,\varepsilon g_{\alpha\beta}\varepsilon^{\alpha\beta} + \tfrac{1}{16}\,\varepsilon^2 g^{\alpha\beta} g_{\alpha\beta}\right)\\ &= \bar{\mu}_0\left(\varepsilon^{\alpha\beta}\varepsilon_{\alpha\beta} - \tfrac{1}{4}\,\varepsilon^2 - \tfrac{1}{4}\,\varepsilon^2 + \tfrac{1}{4}\,\varepsilon^2\right)\end{aligned} \tag{9.146}$$

for $g^{\alpha\beta} = \eta^{\alpha\beta}$. Hence

$$\mathcal{E}_\perp = \bar{\mu}_0\left(\varepsilon^{\alpha\beta}\varepsilon_{\alpha\beta} - \tfrac{1}{4}\,\varepsilon^2\right)\,. \tag{9.147}$$

This expression is expanded using the non-zero elements of the strain tensor (9.131) to give

$$\mathcal{E}_\perp = \bar{\mu}_0\left({\varepsilon_{xx}}^2 + {\varepsilon_{yy}}^2 + 2{\varepsilon_{xy}}^2 + 2{\varepsilon_{yz}}^2 + 2{\varepsilon_{xz}}^2 - \tfrac{1}{4}\,\varepsilon^2\right)\,. \tag{9.148}$$

Substituting from (9.131) and (9.133) in the above and simplifying, we obtain

$$\begin{aligned}\mathcal{E}_\perp = \frac{\bar{\mu}_0}{8\pi^2}\,\frac{b_z^2}{r^2} + \frac{\bar{\mu}_0}{4\pi^2}\,\bar{\alpha}_0^2\,\frac{(b_x y - b_y x)^2}{r^4} +\\ + \frac{\bar{\mu}_0}{2\pi^2}\,\bar{\beta}_0^2\,\frac{(b_x x + b_y y)^2}{r^4} - \frac{3}{2\pi^2}\,\frac{\bar{\mu}_0\bar{\lambda}_0}{2\bar{\mu}_0 + \bar{\lambda}_0}\,\frac{b_x b_y xy}{r^4}\,.\end{aligned} \tag{9.149}$$

Setting $b_z = 0$ and $b_y = 0$ in the above, we obtain the distortion strain energy density expression (9.75) for the stationary edge dislocation.

Expanding the quadratic terms, we obtain

$$\mathcal{E}_\perp = \mathcal{E}_\perp^S + \mathcal{E}_\perp^E + \mathcal{E}_\perp^G + \mathcal{E}_{\perp\ int}^{E-G} \tag{9.150}$$

where the screw dislocation distortion strain energy density $\mathcal{E}_\perp^S$, the edge dislocation distortion strain energy density $\mathcal{E}_\perp^E$, the gap dislocation distortion strain energy density $\mathcal{E}_\perp^G$, and the edge-gap interaction

distortion strain energy density $\mathcal{E}_{\perp\ int}^{E-G}$ are given by

$$\mathcal{E}_{\perp}^{S} = \frac{\bar{\mu}_0}{8\pi^2}\,\frac{b_z^{(s)\,2}}{r^2} \tag{9.151}$$

$$\mathcal{E}_{\perp}^{E} = \frac{\bar{\mu}_0}{4\pi^2}\,\frac{b_x^{(e)\,2}\left(\bar{\alpha}_0^2 y^2 + 2\bar{\beta}_0^2 x^2\right)}{r^4} \tag{9.152}$$

$$\mathcal{E}_{\perp}^{G} = \frac{\bar{\mu}_0}{4\pi^2}\,\frac{b_y^{(g)\,2}\left(\bar{\alpha}_0^2 x^2 + 2\bar{\beta}_0^2 y^2\right)}{r^4} \tag{9.153}$$

$$\mathcal{E}_{\perp\ int}^{E-G} = -\frac{\bar{\mu}_0}{2\pi^2}\left(\bar{\alpha}_0^2 - 2\bar{\beta}_0^2 + 3\bar{\gamma}_0\right)\,\frac{b_x^{(e)} b_y^{(g)} xy}{r^4} \tag{9.154}$$

where

$$\bar{\gamma}_0 = \frac{\bar{\lambda}_0}{2\bar{\mu}_0 + \bar{\lambda}_0}\,. \tag{9.155}$$

We can also separate (9.149) into different components as follows. Substituting from (9.138) and (9.139), (9.149) becomes

$$\begin{aligned}\mathcal{E}_{\perp} = \frac{\bar{\mu}_0}{8\pi^2}\,\frac{b_z^2}{r^2} + \frac{1}{2}\,\frac{\bar{\mu}_0}{\bar{\kappa}_0}\,\mathcal{E}_{\parallel} + 2\bar{\mu}_0\left(\frac{\bar{\mu}_0 + \bar{\lambda}_0}{2\bar{\mu}_0 + \bar{\lambda}_0}\right)^2 \omega_z^2 - \\ - \frac{3}{2\pi^2}\,\frac{\bar{\mu}_0\bar{\lambda}_0}{2\bar{\mu}_0 + \bar{\lambda}_0}\,\frac{b_x b_y xy}{r^4}\,.\end{aligned} \tag{9.156}$$

The first term is the screw dislocation strain energy density of (9.22), the second term is proportional to the edge dislocation distortion strain energy density arising from the longitudinal strain energy density of (9.139), the third term is the edge dislocation distortion strain energy density arising from the rotation vector of (9.138) and the last term is part of the edge-gap dislocation interaction strain energy density term. It is interesting to note that there are no interaction terms (cross-terms) between screw and edge dislocations for a dislocation line although there are interaction terms between edge dislocations (edge and gap dislocations). However, as we will see in section §18.6, a dislocation line does exhibit self-energy processes.

§9.5.2 *deWit dislocation line current and charge density*

The current density four-vector is calculated from (4.10), *viz.*

$$j^{\nu} = \frac{\varphi_0}{\mu_0}\,\frac{2\bar{\mu}_0 + \bar{\lambda}_0}{2\bar{\mu}_0}\,\varepsilon^{;\nu} = \frac{\varphi_0}{2\mu_0\bar{\alpha}_0}\,\varepsilon^{;\nu}$$

and the charge density from (4.14), *viz.*

$$\varrho = \frac{1}{2}\,\varphi_0\epsilon_0 c\,\frac{2\bar{\mu}_0 + \bar{\lambda}_0}{2\bar{\mu}_0}\,\sqrt{\varepsilon^{;\nu}\varepsilon_{;\nu}} = \frac{\varphi_0\epsilon_0 c}{4\bar{\alpha}_0}\,\sqrt{\varepsilon^{;\nu}\varepsilon_{;\nu}}$$

where φ_0 is the spacetime continuum electromagnetic shearing potential constant.

Using the expression for ε from (9.133), the non-zero components of the current density are given by

$$\begin{aligned} j_x &= \frac{\varphi_0}{2\pi\mu_0}\,\frac{b_y r^2 + 2x\,(b_x y - b_y x)}{r^4} \\ j_y &= -\frac{\varphi_0}{2\pi\mu_0}\,\frac{b_x r^2 - 2y\,(b_x y - b_y x)}{r^4} \end{aligned} \tag{9.157}$$

where $r^2 = x^2 + y^2$. These can be separated in terms of edge proper and gap dislocations as follows:

$$\begin{aligned} j_x &= \frac{\varphi_0}{2\pi\mu_0}\,\frac{2xy\,b_x^{(e)} - \left(x^2 - y^2\right) b_y^{(g)}}{r^4} \\ j_y &= -\frac{\varphi_0}{2\pi\mu_0}\,\frac{\left(x^2 - y^2\right) b_x^{(e)} + 2xy\,b_y^{(g)}}{r^4} \end{aligned} \tag{9.158}$$

which, as per (9.104), can be further simplified to

$$\begin{aligned} j_x &= \frac{\varphi_0}{2\pi\mu_0}\,\frac{b_x^{(e)}\sin 2\theta - b_y^{(g)}\cos 2\theta}{r^2} \\ j_y &= -\frac{\varphi_0}{2\pi\mu_0}\,\frac{b_x^{(e)}\cos 2\theta + b_y^{(g)}\sin 2\theta}{r^2}\,, \end{aligned} \tag{9.159}$$

which simplifies to (9.104) in the case where $b_y^{(g)} = 0$ when we are dealing with an edge proper dislocation. The charge density is given by

$$\varrho = \pm\frac{1}{4\pi}\,\varphi_0\epsilon_0 c\,\frac{1}{r^2}\,\sqrt{b_x^{(e)\,2} + b_y^{(g)\,2}}\,. \tag{9.160}$$

The sign depends on the problem under consideration.

§9.6 Curved dislocations

In this section, we consider the equations for generally curved dislocations (also known as infinitesimal dislocation loops) generated by infinitesimal elements of a dislocation. These allow us to handle complex dislocations that are encountered in the spacetime continuum.

§9.6.1 *The Burgers displacement equation*

The Burgers displacement equation for an infinitesimal element of a dislocation $d\mathbf{l} = \boldsymbol{\xi} dl$ in vector notation is given by [159, see p. 102]

$$\begin{aligned}\mathbf{u}(\mathbf{r}) = \frac{\mathbf{b}}{4\pi}\int_A \frac{\hat{\mathbf{R}}\cdot d\mathbf{A}}{R^2} - \frac{1}{4\pi}\oint_C \frac{\mathbf{b}\times d\mathbf{l}'}{R} + \\ + \frac{1}{4\pi}\,\frac{\bar{\mu}_0+\bar{\lambda}_0}{2\bar{\mu}_0+\bar{\lambda}_0}\,\nabla\left[\oint_C \frac{(\mathbf{b}\times\mathbf{R})\cdot d\mathbf{l}'}{R}\right]\end{aligned} \tag{9.161}$$

where $\mathbf{u}$ is the displacement vector, $\mathbf{r}$ is the vector to the displaced point, $\mathbf{r}'$ is the vector to the dislocation infinitesimal element $d\mathbf{l}'$, $\mathbf{R} = \mathbf{r}' - \mathbf{r}$, $\mathbf{b}$ is the Burgers vector, and closed loop C bounds the area A.

In tensor notation, (9.161) is given by

$$\begin{aligned}u_\mu(r^\nu) = -\frac{1}{8\pi}\int_A b_\mu\,\frac{\partial}{\partial x'^\alpha}\left(\nabla'^2 R\right)dA^\alpha - \\ -\frac{1}{8\pi}\oint_C b^\beta\,\epsilon_{\mu\beta\gamma}\,\nabla'^2 R\,dx'^\gamma - \\ -\frac{1}{4\pi}\,\frac{\bar{\mu}_0+\bar{\lambda}_0}{2\bar{\mu}_0+\bar{\lambda}_0}\oint_C b_\beta\,\epsilon^{\beta\alpha\gamma}\,\frac{\partial^2 R}{\partial x'^\mu\,\partial x'^\alpha}\,dx'_\gamma\end{aligned} \tag{9.162}$$

where $\epsilon^{\alpha\beta\gamma}$ is the permutation symbol, equal to 1 for cyclic permutations, -1 for anti-cyclic permutations, and 0 for permutations involving repeated indices. As noted by Hirth [159, see p. 103], the first term of this equation gives a discontinuity $\Delta\mathbf{u} = \mathbf{b}$ over the surface A, while the two other terms are continuous except at the dislocation line. This equation is used to calculate the displacement produced at a point $\mathbf{r}$ by an arbitrary curved dislocation by integration over the dislocation line.

§9.6.2 *The Peach and Koehler stress equation*

The Peach and Koehler stress equation for an infinitesimal element of a dislocation is derived by differentiation of (9.162) and substitution of the result in (8.25) [159, see p. 103–106]. In this equation, the dislocation is defined continuous except at the dislocation core, removing the discontinuity over the surface A and allowing to express the stresses in

terms of line integrals alone.

$$\begin{aligned}\sigma_{\mu\nu} = &-\frac{\bar{\mu}_0}{8\pi}\oint_C b^\alpha\,\epsilon_{\beta\alpha\mu}\,\frac{\partial}{\partial x'^\beta}\left(\nabla'^2 R\right)dx'_\nu - \\ &-\frac{\bar{\mu}_0}{8\pi}\oint_C b^\alpha\,\epsilon_{\beta\alpha\nu}\,\frac{\partial}{\partial x'^\beta}\left(\nabla'^2 R\right)\,dx'_\mu - \\ &-\frac{\bar{\mu}_0}{4\pi}\,\frac{\bar{\mu}_0+\bar{\lambda}_0}{2\bar{\mu}_0+\bar{\lambda}_0}\oint_C b_\alpha\,\epsilon^{\beta\alpha\gamma}\times \\ &\times\left(\frac{\partial^3 R}{\partial x'^\beta\,\partial x'^\mu\partial x'^\nu}-\delta_{\mu\nu}\,\frac{\partial}{\partial x'^\beta}\left(\nabla'^2 R\right)\right)\,dx'_\gamma.\end{aligned} \tag{9.163}$$

This equation is used to calculate the stress field of an arbitrary curved dislocation by line integration.

Chapter 10

Disclinations in the Spacetime Continuum

§10.1 Analysis of spacetime continuum disclinations

In this chapter, we investigate disclinations in the spacetime continuum in the context of *STCED*. As discussed in section §9.1, the theory of disclinations is derived by introducing disclinations in the theory of dislocations, as the theory of disclinations is actually a combined theory of dislocations and disclinations. The term *dispiration* is also used to indicate a defect that is a combination of both a translation and a rotation.

A *disclination* is a deformation characterized by a discrete rotation Ω which is represented by the *Frank vector* Ω^μ in a four-dimensional continuum. The rotation is about an axis L in the spacetime continuum. This corresponds to a closure failure of the rotation of a closed circuit around the disclination line L.

Three types of disclinations can be distinguished (see Fig. 10.1): i) a *wedge disclination*, in which the Frank vector Ω^μ is parallel to the axis L and to the cut; ii) a *splay disclination*, in which the Frank vector Ω^μ is perpendicular to the axis L and parallel to the cut; and iii) a *twist disclination*, in which the Frank vector Ω^μ is perpendicular to the axis L and to the cut. Note that some authors consider the splay disclination to be a special case of the twist disclination.

The Frank vector is the fundamental invariant of a disclination. It is for disclinations what the Burgers vector is for dislocations. In a continuous isotropic continuum, the Burgers and Frank vectors can be arbitrarily small. This allows us to characterize disclinations similarly to how dislocations are characterized using a Burgers circuit integral (see section §9.1). As seen in section §3.1, the local rotation tensor is defined using (3.3), *viz.*

$$\omega^{\mu\nu} = \tfrac{1}{2}(u^{\mu;\nu} - u^{\nu;\mu})\,.$$

A rotation vector ω^α can be associated with the rotation tensor $\omega^{\mu\nu}$ according to

$$\omega^\alpha = \tfrac{1}{2}\,\epsilon^{\alpha\mu\nu}\,\omega_{\mu\nu} \tag{10.1}$$

Figure 10.1: Three types of disclinations: wedge (top), splay (middle), twist (bottom) [200].

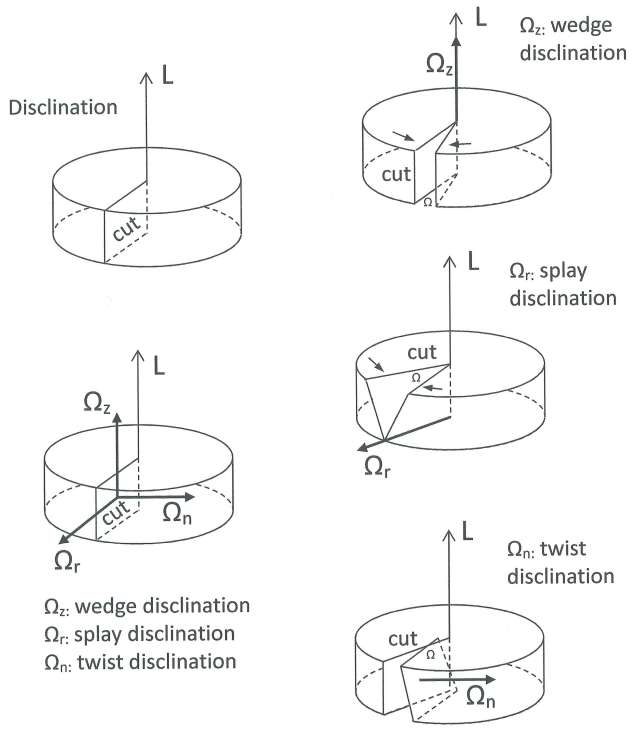

where the permutation symbol $\epsilon_{\alpha\mu\nu}$ is as defined in §8.3, equal to $+1$ for even permutations of $\alpha\mu\nu$, -1 for odd permutations of $\alpha\mu\nu$, 0 for other cases. Then the Frank vector is given by the line integral

$$\Omega^\mu = \oint_C d\omega^\mu \tag{10.2}$$

where the contour C encloses the disclination line L. Note that the Frank vector can also be associated with a rotation tensor

$$\Omega^\mu = \tfrac{1}{2}\,\epsilon^{\mu\alpha\beta}\,\Omega_{\alpha\beta}\,. \tag{10.3}$$

In section §9.1, we saw that the Burgers vector is a measure of the displacement between the initial and final points of a Burgers circuit due to a dislocation. This displacement represents a discontinuity in the spacetime continuum resulting from the dislocation. For a defect that includes dislocations and disclinations, this discontinuity is characterized by Weingarten's theorem [77, 78, 200]: following an irreducible circuit in a multiply-connected continuum satisfying the elastic compatibility conditions, the discontinuity in the rotation and displacement can only consist of a constant vector (the Burgers vector) and a fixed rotation (the Frank vector), given by [78]

$$[u^\mu] = b^\mu + \epsilon^{\mu\alpha\beta}\,\Omega_\alpha x_\beta \tag{10.4}$$

$$[\omega^\alpha] = \Omega^\alpha \tag{10.5}$$

where the [ ] notation represents a discontinuous change. Frank vectors satisfy a Kirchhoff relation at disclination nodes, as do Burgers vectors at dislocation nodes.

Disclinations, as rotational deformations, are associated with spaces with torsion $S^\lambda{}_{\mu\nu}$ defined by

$$S^\lambda{}_{\mu\nu} = \tfrac{1}{2}\left(\Gamma^\lambda{}_{\mu\nu} - \Gamma^\lambda{}_{\nu\mu}\right)\,, \tag{10.6}$$

which is the antisymmetric component of the connection $\Gamma^\lambda{}_{\mu\nu}$ and which transforms like a proper tensor.

The contortion tensor $K^\lambda{}_{\mu\nu}$ is built from the torsion tensor as follows:

$$K^\lambda{}_{\mu\nu} = \tfrac{1}{2}\left(S^\lambda_{\cdot\mu\nu} - S_{\mu\cdot\nu}^{\ \ \lambda} - S_{\nu\cdot\mu}^{\ \ \lambda}\right) \tag{10.7}$$

It can more explicitly be defined in terms of the associated torsion tensor $S_{\mu\nu\lambda} = S_{\mu\nu}{}^\alpha g_{\alpha\lambda}$ as

$$K_{\mu\nu\lambda} = S_{\mu\nu\lambda} - S_{\nu\lambda\mu} + S_{\lambda\mu\nu}\,. \tag{10.8}$$

The contortion can also be defined in terms of the connection as follows:

$$K^\lambda{}_{\mu\nu} = \Gamma^\lambda{}_{\mu\nu} - \left\{ {}^{\ \lambda}_{\mu\ \nu} \right\} \tag{10.9}$$

where $\left\{ {}^{\ \lambda}_{\mu\ \nu} \right\}$ is the Christoffel symbol. Note that in a space with torsion, the gamma connection coefficient is not symmetric over the indices $\mu\nu$, while the Christoffel symbol is, hence explaining relation (10.9).

Another field arising from torsion is the *bend-twist* field [78, 199], also known as *torsion-flexure* in civil engineering or *curvature-twist*, is defined as the gradient of the rotation vector:

$$\kappa^{\mu\nu} = \omega^{\mu;\nu} \tag{10.10}$$

where the diagonal elements describe a twisting and the off-diagonal elements describe a bending.

§10.2 Volterra dislocations and disclinations

Volterra [360] in his analysis of 1907 considered 6 types of defects: 3 dislocations and 3 disclinations. The dislocations included the screw dislocation with displacement b_z and two edge dislocations with displacements b_x and b_y. The disclinations included the wedge disclination normal to the d_{xy} surface, and two twist disclinations normal to the d_{yz} and d_{zx} surfaces. He was the first to derive the displacements for the dislocations and disclinations about the z-axis as follows [265, see p. 58]:

$$\begin{aligned}
2\pi u_x &= (b_x - d_{zx}z + d_{xy}y)\arctan\left(\frac{y}{x}\right) + \\
&\quad + \tfrac{1}{2}\,(-b_y - d_{yz}z - \bar{\alpha}_0\, d_{xy}x)\ln(x^2+y^2) \\
2\pi u_y &= (b_y - d_{xy}x + d_{yz}z)\arctan\left(\frac{y}{x}\right) + \\
&\quad + \tfrac{1}{2}\,(b_x - d_{zx}z - \bar{\alpha}_0\, d_{xy}y)\ln(x^2+y^2) \\
2\pi u_z &= (b_z - d_{yz}y + d_{zx}x)\arctan\left(\frac{y}{x}\right) + \\
&\quad + \tfrac{1}{2}\,(d_{yz}x + d_{zx}y)\ln(x^2+y^2)
\end{aligned} \tag{10.11}$$

where as before

$$\bar{\alpha}_0 = \frac{\bar{\mu}_0}{2\bar{\mu}_0 + \bar{\lambda}_0}\,, \tag{10.12}$$

the b_i's are dislocation constants specifying the relative displacement of the dislocation and the d_{ij}'s are disclination constants specifying their relative rotation. These maintain the equilibrium without volume forces except at the core of the defect along the z-axis.

We write (10.11) using the Frank vector as follows:

$$\begin{aligned}
2\pi u_x &= (b_x - \Omega_y z + \Omega_z y)\arctan\left(\frac{y}{x}\right) + \\
&\quad + \tfrac{1}{2}\,(-b_y - \Omega_x z - \bar{\alpha}_0\,\Omega_z x)\ln(x^2+y^2) \\
2\pi u_y &= (b_y - \Omega_z x + \Omega_x z)\arctan\left(\frac{y}{x}\right) + \\
&\quad + \tfrac{1}{2}\,(b_x - \Omega_y z - \bar{\alpha}_0\,\Omega_z y)\ln(x^2+y^2) \\
2\pi u_z &= (b_z - \Omega_x y + \Omega_y x)\arctan\left(\frac{y}{x}\right) + \\
&\quad + \tfrac{1}{2}\,(\Omega_x x + \Omega_y y)\ln(x^2+y^2)
\end{aligned} \tag{10.13}$$

where (b_x, b_y, b_z) is the dislocation Burgers vector and $(\Omega_x, \Omega_y, \Omega_z)$ is the disclination Frank vector, and where Ω_z is the component for the wedge disclination of the core of the defect along the z-axis. Note that one has

$$\begin{aligned}
r^2 &= x^2 + y^2 \\
\theta &= \arctan\left(\frac{y}{x}\right)
\end{aligned} \tag{10.14}$$

in cylindrical polar coordinates (r, θ, z).

The rotation tensor and rotation vector are calculated as in section §9.2 from the displacements (10.13). The rotation tensor is then given by

$$\begin{aligned}
\omega_{xy} &= \frac{\Omega_z}{2\pi}\,\arctan\left(\frac{y}{x}\right) = \frac{\Omega_z}{2\pi}\,\theta \\
\omega_{yz} &= \frac{\Omega_x}{2\pi}\,\arctan\left(\frac{y}{x}\right) - \frac{\Omega_y}{4\pi}\,\left[1 + \ln\left(x^2+y^2\right)\right] - \frac{b_z}{4\pi} \\
&= \frac{\Omega_x}{2\pi}\,\theta - \frac{\Omega_y}{4\pi}\,(1 + 2\ln r) - \frac{b_z}{4\pi} \\
\omega_{xz} &= -\frac{\Omega_y}{2\pi}\,\arctan\left(\frac{y}{x}\right) - \frac{\Omega_x}{4\pi}\,\left[1 + \ln\left(x^2+y^2\right)\right] + \frac{b_z}{4\pi} \\
&= -\frac{\Omega_y}{2\pi}\,\theta - \frac{\Omega_x}{4\pi}\,(1 + 2\ln r) + \frac{b_z}{4\pi}
\end{aligned} \tag{10.15}$$

and the rotation vector by

$$\begin{aligned}
\omega_x &= \frac{\Omega_x}{2\pi}\,\arctan\left(\frac{y}{x}\right) - \frac{\Omega_y}{4\pi}\,\left[1+\ln\left(x^2+y^2\right)\right] - \frac{b_z}{4\pi} \\
&= \frac{\Omega_x}{2\pi}\,\theta - \frac{\Omega_y}{4\pi}\,(1+2\ln r) - \frac{b_z}{4\pi} \\
\omega_y &= \frac{\Omega_y}{2\pi}\,\arctan\left(\frac{y}{x}\right) + \frac{\Omega_x}{4\pi}\,\left[1+\ln\left(x^2+y^2\right)\right] - \frac{b_z}{4\pi} \\
&= \frac{\Omega_y}{2\pi}\,\theta + \frac{\Omega_x}{4\pi}\,(1+2\ln r) - \frac{b_z}{4\pi} \\
\omega_z &= \frac{\Omega_z}{2\pi}\,\arctan\left(\frac{y}{x}\right) = \frac{\Omega_z}{2\pi}\,\theta\,.
\end{aligned} \tag{10.16}$$

The bend-twist tensor is given by

$$\kappa^{\mu\nu} = \omega^{\mu;\nu}\,. \tag{10.17}$$

The components of the bend-twist tensor in cartesian coordinates are then given by

$$\begin{aligned}
\kappa_{xx} &= -\frac{\Omega_x}{2\pi}\,\frac{y}{r^2} - \frac{\Omega_y}{2\pi}\,\frac{x}{r^2} \\
\kappa_{xy} &= \frac{\Omega_x}{2\pi}\,\frac{x}{r^2} - \frac{\Omega_y}{2\pi}\,\frac{y}{r^2} \\
\kappa_{xz} &= 0 \\
\kappa_{yx} &= -\frac{\Omega_y}{2\pi}\,\frac{y}{r^2} + \frac{\Omega_x}{2\pi}\,\frac{x}{r^2} \\
\kappa_{yy} &= \frac{\Omega_y}{2\pi}\,\frac{x}{r^2} + \frac{\Omega_x}{2\pi}\,\frac{y}{r^2} \\
\kappa_{yz} &= 0 \\
\kappa_{zx} &= -\frac{\Omega_z}{2\pi}\,\frac{y}{r^2} \\
\kappa_{zy} &= \frac{\Omega_z}{2\pi}\,\frac{x}{r^2} \\
\kappa_{zz} &= 0\,.
\end{aligned} \tag{10.18}$$

The trace of the bend-twist tensor is zero:

$$\text{Trace}(\kappa^{\mu\nu}) = \kappa^{\alpha}{}_{\alpha} = 0\,. \tag{10.19}$$

The components of the strain tensor in cartesian coordinates are derived from $\varepsilon^{\mu\nu} = \frac{1}{2}(u^{\mu;\nu} + u^{\nu;\mu})$:

$$
\begin{aligned}
\varepsilon_{xx} &= -\frac{1}{2\pi}\,(b_x - \Omega_y z + \Omega_z y)\,\frac{y}{x^2+y^2} - \\
&\quad - \frac{1}{2\pi}\,(b_y + \Omega_x z + \bar{\alpha}_0\,\Omega_z x)\,\frac{x}{x^2+y^2} - \frac{\bar{\alpha}_0}{4\pi}\,\Omega_z \ln(x^2+y^2) \\
\varepsilon_{yy} &= \frac{1}{2\pi}\,(b_y - \Omega_z x + \Omega_x z)\,\frac{x}{x^2+y^2} + \\
&\quad + \frac{1}{2\pi}\,(b_x - \Omega_y z - \bar{\alpha}_0\,\Omega_z y)\,\frac{y}{x^2+y^2} - \frac{\bar{\alpha}_0}{4\pi}\Omega_z \ln(x^2+y^2) \\
\varepsilon_{zz} &= 0 \\
\varepsilon_{xy} &= \frac{1}{2\pi}\,(2b_x - 2\Omega_y z + (1-\bar{\alpha}_0)\,\Omega_z y)\,\frac{x}{x^2+y^2} - \\
&\quad - \frac{1}{2\pi}\,(2b_y + 2\Omega_x z - (1-\bar{\alpha}_0)\,\Omega_z x)\,\frac{y}{x^2+y^2} \\
\varepsilon_{yz} &= \frac{1}{2\pi}\,(b_z - \Omega_x y + \Omega_y x)\,\frac{x}{x^2+y^2} + \\
&\quad + \frac{1}{2\pi}\,(\Omega_x x + \Omega_y y)\,\frac{y}{x^2+y^2} \\
\varepsilon_{xz} &= -\frac{1}{2\pi}\,(b_z - \Omega_x y + \Omega_y x)\,\frac{y}{x^2+y^2} + \\
&\quad + \frac{1}{2\pi}\,(\Omega_x x + \Omega_y y)\,\frac{x}{x^2+y^2}
\end{aligned}
\tag{10.20}
$$

in an isotropic continuum. The volume dilatation ε for the Volterra dislocations and disclinations is then given by

$$
\varepsilon = \varepsilon^{\alpha}{}_{\alpha} = \varepsilon_{xx} + \varepsilon_{yy} + \varepsilon_{zz}\,. \tag{10.21}
$$

Substituting for ε_{xx}, ε_{yy} and ε_{zz} from (10.20) into (10.21),

$$
\begin{aligned}
\varepsilon = &-\frac{1}{2\pi}\,(1+\bar{\alpha}_0)\,\Omega_z x\,\frac{x}{x^2+y^2} - \frac{1}{2\pi}\,(1+\bar{\alpha}_0)\,\Omega_z y\,\frac{y}{x^2+y^2} - \\
&- \frac{\bar{\alpha}_0}{2\pi}\,\Omega_z \ln\left(x^2+y^2\right)
\end{aligned}
\tag{10.22}
$$

and using (10.12), we obtain

$$\varepsilon = -\frac{\Omega_z}{2\pi}\left[1 + \frac{\bar{\mu}_0}{2\bar{\mu}_0 + \bar{\lambda}_0}\left[1 + \ln\left(x^2 + y^2\right)\right]\right]. \tag{10.23}$$

The components of the stress tensor in cartesian coordinates are obtained by substituting (10.20) into (8.25):

$$\begin{aligned}
\sigma_{xx} &= 2\bar{\mu}_0\varepsilon_{xx} + \bar{\lambda}_0\varepsilon \\
&= -\frac{\bar{\mu}_0}{\pi}\left(b_x - \Omega_y z + \Omega_z y\right)\frac{y}{x^2+y^2} - \\
&- \frac{\bar{\mu}_0}{\pi}\left(b_y + \Omega_x z + \bar{\alpha}_0\,\Omega_z x\right)\frac{x}{x^2+y^2} - \\
&- \frac{\bar{\mu}_0\bar{\alpha}_0}{2\pi}\Omega_z \ln(x^2+y^2) \\
&- \frac{\Omega_z\bar{\lambda}_0}{2\pi}\left[1 + \bar{\alpha}_0\left[1 + \ln\left(x^2+y^2\right)\right]\right] \\
\sigma_{yy} &= 2\bar{\mu}_0\varepsilon_{yy} + \bar{\lambda}_0\varepsilon \\
&= \frac{\bar{\mu}_0}{\pi}\left(b_y - \Omega_z x + \Omega_x z\right)\frac{x}{x^2+y^2} + \\
&+ \frac{\bar{\mu}_0}{\pi}\left(b_x - \Omega_y z - \bar{\alpha}_0\,\Omega_z y\right)\frac{y}{x^2+y^2} - \\
&- \frac{\bar{\mu}_0\bar{\alpha}_0}{2\pi}\,\Omega_z \ln(x^2+y^2) \\
&- \frac{\Omega_z\bar{\lambda}_0}{2\pi}\left[1 + \bar{\alpha}_0\left[1 + \ln\left(x^2+y^2\right)\right]\right] \\
\sigma_{zz} &= \bar{\lambda}_0\varepsilon = -\frac{\Omega_z\bar{\lambda}_0}{2\pi}\left[1 + \bar{\alpha}_0\left[1 + \ln\left(x^2+y^2\right)\right]\right] \\
\sigma_{xy} &= \frac{\bar{\mu}_0}{\pi}\left(2b_x - 2\Omega_y z + (1-\bar{\alpha}_0)\,\Omega_z y\right)\frac{x}{x^2+y^2} - \\
&- \frac{\bar{\mu}_0}{\pi}\left(2b_y + 2\Omega_x z - (1-\bar{\alpha}_0)\,\Omega_z x\right)\frac{y}{x^2+y^2}
\end{aligned} \tag{10.24}$$

$$\sigma_{yz} = \frac{\bar{\mu}_0}{\pi}\,(b_z - \Omega_x y + \Omega_y x)\,\frac{x}{x^2+y^2} + \\ + \frac{\bar{\mu}_0}{\pi}\,(\Omega_x x + \Omega_y y)\,\frac{y}{x^2+y^2}$$

$$\sigma_{xz} = -\frac{\bar{\mu}_0}{\pi}\,(b_z - \Omega_x y + \Omega_y x)\,\frac{y}{x^2+y^2} + \\ + \frac{\bar{\mu}_0}{\pi}\,(\Omega_x x + \Omega_y y)\,\frac{x}{x^2+y^2}\,.$$

The σ_{xx} and σ_{yy} components simplify as follows:

$$\begin{aligned}
\sigma_{xx} &= -\frac{\bar{\mu}_0}{\pi}\,(b_x - \Omega_y z + \Omega_z y)\,\frac{y}{x^2+y^2} - \\
&\quad - \frac{\bar{\mu}_0}{\pi}\,(b_y + \Omega_x z + \bar{\alpha}_0\,\Omega_z x)\,\frac{x}{x^2+y^2} - \\
&\quad - \frac{\Omega_z}{2\pi}\,\left[\bar{\lambda}_0(1+\bar{\alpha}_0) + \bar{\alpha}_0(\bar{\mu}_0+\bar{\lambda}_0)\,\ln\left(x^2+y^2\right)\right] \\
\sigma_{yy} &= \frac{\bar{\mu}_0}{\pi}\,(b_y - \Omega_z x + \Omega_x z)\,\frac{x}{x^2+y^2} + \\
&\quad + \frac{\bar{\mu}_0}{\pi}\,(b_x - \Omega_y z - \bar{\alpha}_0\,\Omega_z y)\,\frac{y}{x^2+y^2} - \\
&\quad - \frac{\Omega_z}{2\pi}\,\left[\bar{\lambda}_0(1+\bar{\alpha}_0) + \bar{\alpha}_0(\bar{\mu}_0+\bar{\lambda}_0)\,\ln\left(x^2+y^2\right)\right]\,.
\end{aligned} \tag{10.25}$$

The mass energy density is calculated from (2.24), *viz.*

$$\rho c^2 = 4\bar{\kappa}_0\,\varepsilon = 2(2\bar{\lambda}_0 + \bar{\mu}_0)\,\varepsilon\,.$$

Substituting for ε from (10.23), using the positive value of ε as per section §9.3.4, the mass energy density of the Volterra dislocations and disclinations is given by

$$\rho c^2 = \frac{2\bar{\kappa}_0\Omega_z}{\pi}\,\left[1 + \frac{\bar{\mu}_0}{2\bar{\mu}_0+\bar{\lambda}_0}\,\left[1+\ln\left(x^2+y^2\right)\right]\right]\,. \tag{10.26}$$

We calculate the strain energy density of the Volterra dislocations and disclinations as follows. Using (10.23) in (9.50), the longitudinal dilatation strain energy density is then given by

$$\mathcal{E}_{\|} = \frac{\bar{\kappa}_0\Omega_z^2}{8\pi^2}\,\left[1 + \frac{\bar{\mu}_0}{2\bar{\mu}_0+\bar{\lambda}_0}\,\left[1+\ln\left(x^2+y^2\right)\right]\right]^2\,. \tag{10.27}$$

The distortion strain energy density is calculated from (9.51), *viz.*

$$\mathcal{E}_\perp = \bar{\mu}_0 e^{\alpha\beta} e_{\alpha\beta} \, .$$

As seen previously, using (9.20), *viz.*

$$e^{\alpha\beta} = \varepsilon^{\alpha\beta} - e_s g^{\alpha\beta}$$

where $e_s = \frac{1}{4}\,\varepsilon$, (9.51) simplifies to

$$\mathcal{E}_\perp = \bar{\mu}_0 \left(\varepsilon^{\alpha\beta} \varepsilon_{\alpha\beta} - \tfrac{1}{4}\,\varepsilon^2 \right) \, . \tag{10.28}$$

This expression is expanded using the non-zero elements of the strain tensor (10.20) to give

$$\mathcal{E}_\perp = \bar{\mu}_0 \left({\varepsilon_{xx}}^2 + {\varepsilon_{yy}}^2 + 2{\varepsilon_{xy}}^2 + 2{\varepsilon_{yz}}^2 + 2{\varepsilon_{xz}}^2 - \tfrac{1}{4}\,\varepsilon^2 \right) \, . \tag{10.29}$$

Substituting from (10.20) and (10.23) in the above, we obtain

$$\begin{aligned} \mathcal{E}_\perp = \frac{\bar{\mu}_0}{4\pi^2} \Bigg(& c_1 \, \frac{x^2}{r^4} + c_2 \, \frac{y^2}{r^4} + c_3 \, \frac{xy}{r^4} + c_4 \, \frac{x}{r^2} \, \ln r^2 + \\ & + c_5 \, \frac{y}{r^2} \, \ln r^2 + c_6 \, \ln^2 r^2 - 4\pi^2 \varepsilon^2 \Bigg) \end{aligned} \tag{10.30}$$

where the coefficients c_i are complicated functions of the following variables:

$$\begin{aligned} c_1 &= f_1(x, y, z, b_x, b_y, b_z, \Omega_x, \Omega_y, \Omega_z) \\ c_2 &= f_2(x, y, z, b_x, b_y, \Omega_x, \Omega_y, \Omega_z) \\ c_3 &= f_3(x, y, z, b_x, b_y, \Omega_x, \Omega_y, \Omega_z) \\ c_4 &= \bar{\alpha}_0 \, (1 + \bar{\alpha}_0) \, \Omega_z^2 \, x \\ c_5 &= \bar{\alpha}_0 \, (1 + \bar{\alpha}_0) \, \Omega_z^2 \, y \\ c_6 &= \tfrac{1}{2} \, \bar{\alpha}_0^2 \, \Omega_z^2 \\ \text{last term} &= -\tfrac{1}{4} \, \Omega_z^2 \left[1 + \bar{\alpha}_0 \left(1 + \ln r^2 \right) \right]^2 \, . \end{aligned} \tag{10.31}$$

Note that we have explicitly written out the simpler coefficients. Specific cases of the distortion strain energy densities are calculated for combinations of the dislocation Burgers vector (b_x, b_y, b_z) and the disclination Frank vector $(\Omega_x, \Omega_y, \Omega_z)$ in other sections of this book.

The volume force for Volterra dislocations and disclinations can be calculated from

$$X^\nu = -T^{\mu\nu}{}_{;\mu} \tag{10.32}$$

using the stress tensor (10.25). Alternatively, we can make use of (2.6) into the above equation to calculate the volume force from the strain tensor using (8.16), viz.

$$2\bar{\mu}_0 \varepsilon^{\mu\nu}{}_{;\mu} + 2\bar{\mu}_0 \not{\varepsilon}^{\mu\nu}{}_{;\mu} + \bar{\lambda}_0 \varepsilon^{;\nu} + \bar{\lambda}_0 \not{\varepsilon}^{;\nu} = -X^\nu \,.$$

The full strain tensor of (10.20) can be used in (8.16) as the elastic portion of the strain tensor does not contribute to the volume force, only the defect portion. The volume force is then given by

$$\begin{aligned}
X_x &= -\frac{\bar{\mu}_0\,\Omega_z}{\pi}\left(1 - \frac{3\bar{\mu}_0}{2\bar{\mu}_0+\bar{\lambda}_0} - \frac{\bar{\lambda}_0}{(2\bar{\mu}_0+\bar{\lambda}_0)^2}\right)\frac{x}{x^2+y^2} - \\
&\quad - \frac{\bar{\mu}_0}{\pi}\,(-b_x + \Omega_y z + \bar{\alpha}_0\,\Omega_z y)\,\frac{2xy}{(x^2+y^2)^2} - \\
&\quad - \frac{\bar{\mu}_0}{\pi}\,(-b_y - \Omega_x z + \Omega_z x)\,\frac{x^2-y^2}{(x^2+y^2)^2} \\
X_y &= -\frac{\bar{\mu}_0\,\Omega_z}{\pi}\left(1 - \frac{3\bar{\mu}_0}{2\bar{\mu}_0+\bar{\lambda}_0} - \frac{\bar{\lambda}_0}{(2\bar{\mu}_0+\bar{\lambda}_0)^2}\right)\frac{y}{x^2+y^2} - \\
&\quad - \frac{\bar{\mu}_0}{\pi}\,(b_y + \Omega_x z + \bar{\alpha}_0\,\Omega_z x)\,\frac{2xy}{(x^2+y^2)^2} - \\
&\quad - \frac{\bar{\mu}_0}{\pi}\,(-b_x + \Omega_y z - \Omega_z y)\,\frac{x^2-y^2}{(x^2+y^2)^2} \\
X_z &= 0\,.
\end{aligned} \tag{10.33}$$

The volume force along the z-axis is zero, but there is a net volume force along the x-axis and the y-axis.

The Volterra displacements (10.13) can represent dislocations by setting the disclination Frank vector $(\Omega_x, \Omega_y, \Omega_z)$ to zero. Stationary screw dislocations are represented by setting $b_x = b_y = 0$. We then obtain the results of section §9.2. Stationary edge dislocations are represented by setting $b_z = 0$. The results are similar to those of section §9.3, except that only b_x is not equal to 0 in section §9.3, while both b_x and b_y are not equal to 0 in Volterra's displacements (10.13). Volterra dislocations were considered in greater details in §9.4.

Similarly, (10.13) can represent disclinations by setting the dislocation Burgers vector (b_x, b_y, b_z) to zero. Stationary wedge disclinations

are represented by setting $\Omega_x = \Omega_y = 0$ with only Ω_z not equal to zero. We then obtain the results for wedge disclinations of section §10.3. Stationary twist disclinations are represented by setting $\Omega_z = 0$. We then obtain the results for twist disclinations of section §10.4.

§10.3 Volterra wedge disclinations

Stationary wedge disclinations are represented by setting the dislocation Burgers vector (b_x, b_y, b_z) to zero and the disclination Frank vector components $\Omega_x = \Omega_y = 0$ with only Ω_z not equal to zero in (10.13) to obtain

$$\begin{aligned} u_x &= \frac{\Omega_z}{2\pi}\left[y \arctan\left(\frac{y}{x}\right) - \frac{\bar{\alpha}_0}{2}\, x \ln(x^2+y^2)\right] \\ u_y &= -\frac{\Omega_z}{2\pi}\left[x \arctan\left(\frac{y}{x}\right) + \frac{\bar{\alpha}_0}{2}\, y \ln(x^2+y^2)\right] \\ u_z &= 0 \end{aligned} \tag{10.34}$$

which can also be written as

$$\begin{aligned} u_x &= \frac{\Omega_z}{2\pi}\left[y\,\theta - \bar{\alpha}_0\, x \ln r\right] \\ u_y &= -\frac{\Omega_z}{2\pi}\left[x\,\theta + \bar{\alpha}_0\, y \ln r\right] \\ u_z &= 0 \end{aligned} \tag{10.35}$$

where again

$$\begin{aligned} r^2 &= x^2 + y^2 \\ \theta &= \arctan\left(\frac{y}{x}\right) \end{aligned} \tag{10.36}$$

in cylindrical polar coordinates (r, θ, z).

The rotation tensor and rotation vector are calculated as in section §9.2 from the displacements (10.34). The rotation tensor is then given by

$$\begin{aligned} \omega_{xy} &= \frac{\Omega_z}{2\pi} \arctan\left(\frac{y}{x}\right) = \frac{\Omega_z}{2\pi}\,\theta \\ \omega_{yz} &= 0 \\ \omega_{xz} &= 0 \end{aligned} \tag{10.37}$$

and the rotation vector by

$$\begin{aligned}\omega_x &= 0\\ \omega_y &= 0\\ \omega_z &= \frac{\Omega_z}{2\pi}\,\arctan\left(\frac{y}{x}\right) = \frac{\Omega_z}{2\pi}\,\theta\,.\end{aligned} \tag{10.38}$$

The rotation vector has only one component along the z-axis.

The bend-twist tensor is given by

$$\kappa^{\mu\nu} = \omega^{\mu;\nu}\,. \tag{10.39}$$

The components of the bend-twist tensor in cartesian coordinates are then given by

$$\begin{aligned}&\kappa_{xx} = 0\,, && \kappa_{xy} = 0\,, && \kappa_{xz} = 0\,,\\ &\kappa_{yx} = 0\,, && \kappa_{yy} = 0\,, && \kappa_{yz} = 0\,,\\ &\kappa_{zx} = -\frac{\Omega_z}{2\pi}\,\frac{y}{r^2}\,, && \kappa_{zy} = \frac{\Omega_z}{2\pi}\,\frac{x}{r^2}\,, && \kappa_{zz} = 0\,.\end{aligned} \tag{10.40}$$

The diagonal elements are zero, indicating no twist, while the zx and zy off-diagonal elements are non-zero, indicating bending along that direction.

The components of the strain tensor in cartesian coordinates are derived from $\varepsilon^{\mu\nu} = \frac{1}{2}(u^{\mu;\nu} + u^{\nu;\mu})$:

$$\begin{aligned}\varepsilon_{xx} &= -\frac{\Omega_z}{2\pi}\left[\frac{y^2}{x^2+y^2} + \bar{\alpha}_0\,\frac{x^2}{x^2+y^2} + \frac{\bar{\alpha}_0}{2}\,\ln(x^2+y^2)\right]\\ \varepsilon_{yy} &= -\frac{\Omega_z}{2\pi}\left[\frac{x^2}{x^2+y^2} + \bar{\alpha}_0\,\frac{y^2}{x^2+y^2} + \frac{\bar{\alpha}_0}{2}\,\ln(x^2+y^2)\right]\\ \varepsilon_{zz} &= 0\\ \varepsilon_{xy} &= \frac{\Omega_z}{2\pi}\,(1-\bar{\alpha}_0)\,\frac{xy}{x^2+y^2}\\ \varepsilon_{yz} &= 0\\ \varepsilon_{xz} &= 0\end{aligned} \tag{10.41}$$

which can be written as

$$\begin{aligned}
\varepsilon_{xx} &= -\frac{\Omega_z}{2\pi}\left[\frac{y^2}{r^2} + \bar{\alpha}_0\,\frac{x^2}{r^2} + \bar{\alpha}_0 \ln r\right] \\
\varepsilon_{yy} &= -\frac{\Omega_z}{2\pi}\left[\frac{x^2}{r^2} + \bar{\alpha}_0\,\frac{y^2}{r^2} + \bar{\alpha}_0 \ln r\right] \\
\varepsilon_{zz} &= 0 \\
\varepsilon_{xy} &= \frac{\Omega_z}{2\pi}\,(1-\bar{\alpha}_0)\,\frac{xy}{r^2} \\
\varepsilon_{yz} &= 0 \\
\varepsilon_{xz} &= 0\,.
\end{aligned} \tag{10.42}$$

The volume dilatation ε for the wedge disclination is then given by

$$\varepsilon = \varepsilon^{\alpha}{}_{\alpha} = \varepsilon_{xx} + \varepsilon_{yy} + \varepsilon_{zz}\,. \tag{10.43}$$

Substituting for ε_{xx}, ε_{yy} and ε_{zz} from (10.41) into (10.43),

$$\begin{aligned}
\varepsilon &= -\frac{\Omega_z}{2\pi}\,\left[1 + \bar{\alpha}_0 + \bar{\alpha}_0 \ln\left(x^2+y^2\right)\right] \\
\varepsilon &= -\frac{\Omega_z}{2\pi}\,\left[1 + \bar{\alpha}_0 + 2\bar{\alpha}_0 \ln\ r\right]
\end{aligned} \tag{10.44}$$

and using (10.12), we obtain

$$\varepsilon = -\frac{\Omega_z}{2\pi}\,\left[1 + \frac{\bar{\mu}_0}{2\bar{\mu}_0 + \bar{\lambda}_0}\,\left[1 + \ln\left(x^2+y^2\right)\right]\right]\,. \tag{10.45}$$

The components of the stress tensor in cartesian coordinates are

obtained from (10.24):

$$
\begin{aligned}
\sigma_{xx} &= -\frac{\bar{\mu}_0\Omega_z}{\pi}\,\frac{\bar{\alpha}_0 x^2+y^2}{x^2+y^2} - \\
&\quad -\frac{\Omega_z}{2\pi}\,\left[\bar{\lambda}_0(1+\bar{\alpha}_0)+(\bar{\mu}_0+\bar{\lambda}_0)\bar{\alpha}_0\ln\left(x^2+y^2\right)\right] \\
\sigma_{yy} &= -\frac{\bar{\mu}_0\Omega_z}{\pi}\,\frac{x^2+\bar{\alpha}_0 y^2}{x^2+y^2} - \\
&\quad -\frac{\Omega_z}{2\pi}\,\left[\bar{\lambda}_0(1+\bar{\alpha}_0)+(\bar{\mu}_0+\bar{\lambda}_0)\bar{\alpha}_0\ln\left(x^2+y^2\right)\right] \\
\sigma_{zz} &= -\frac{\bar{\lambda}_0\Omega_z}{2\pi}\,\left[1+\bar{\alpha}_0+\bar{\alpha}_0\ln\left(x^2+y^2\right)\right] \\
\sigma_{xy} &= \frac{\bar{\mu}_0\Omega_z}{\pi}\,(1-\bar{\alpha}_0)\,\frac{xy}{x^2+y^2} \\
\sigma_{yz} &= 0 \\
\sigma_{xz} &= 0
\end{aligned}
\tag{10.46}
$$

which can also be written as

$$
\begin{aligned}
\sigma_{xx} &= -\frac{\bar{\mu}_0\Omega_z}{\pi}\,\frac{\bar{\alpha}_0 x^2+y^2}{r^2} - \\
&\quad -\frac{\Omega_z}{2\pi}\,\left[\bar{\lambda}_0(1+\bar{\alpha}_0)+2(\bar{\mu}_0+\bar{\lambda}_0)\bar{\alpha}_0\ln r\right] \\
\sigma_{yy} &= -\frac{\bar{\mu}_0\Omega_z}{\pi}\,\frac{x^2+\bar{\alpha}_0 y^2}{r^2} - \\
&\quad -\frac{\Omega_z}{2\pi}\,\left[\bar{\lambda}_0(1+\bar{\alpha}_0)+2(\bar{\mu}_0+\bar{\lambda}_0)\bar{\alpha}_0\ln r\right] \\
\sigma_{zz} &= -\frac{\bar{\lambda}_0\Omega_z}{2\pi}\,\left[1+\bar{\alpha}_0+2\bar{\alpha}_0\ln r\right] \\
\sigma_{xy} &= \frac{\bar{\mu}_0\Omega_z}{\pi}\,(1-\bar{\alpha}_0)\,\frac{xy}{r^2} \\
\sigma_{yz} &= 0 \\
\sigma_{xz} &= 0\,.
\end{aligned}
\tag{10.47}
$$

The mass energy density is calculated from (2.24), *viz.*

$$\rho c^2 = 4\bar{\kappa}_0\,\varepsilon = 2(2\bar{\lambda}_0 + \bar{\mu}_0)\,\varepsilon\,.$$

Substituting for ε from (10.45), using the positive value of ε as per section §9.3.4, the mass energy density of the wedge disclination is given by

$$\rho c^2 = \frac{2\bar{\kappa}_0\Omega_z}{\pi}\,\left[1 + \frac{\bar{\mu}_0}{2\bar{\mu}_0 + \bar{\lambda}_0}\,\left[1 + \ln\left(x^2 + y^2\right)\right]\right]\,. \tag{10.48}$$

We calculate the strain energy density of the wedge disclination as follows. Using (10.45) in (9.50), the longitudinal dilatation strain energy density is then given by

$$\mathcal{E}_{\parallel} = \frac{\bar{\kappa}_0\Omega_z^2}{8\pi^2}\,\left[1 + \frac{\bar{\mu}_0}{2\bar{\mu}_0 + \bar{\lambda}_0}\,\left[1 + \ln\left(x^2 + y^2\right)\right]\right]^2\,. \tag{10.49}$$

The distortion strain energy density is calculated from (9.51), *viz.*

$$\mathcal{E}_{\perp} = \bar{\mu}_0 e^{\alpha\beta} e_{\alpha\beta}\,.$$

As seen previously, using (9.20), *viz.*

$$e^{\alpha\beta} = \varepsilon^{\alpha\beta} - e_s g^{\alpha\beta}$$

where $e_s = \frac{1}{4}\,\varepsilon$, (9.51) simplifies to

$$\mathcal{E}_{\perp} = \bar{\mu}_0\left(\varepsilon^{\alpha\beta}\varepsilon_{\alpha\beta} - \tfrac{1}{4}\,\varepsilon^2\right)\,. \tag{10.50}$$

This expression is expanded using the non-zero elements of the strain tensor (10.42) to give

$$\mathcal{E}_{\perp} = \bar{\mu}_0\left({\varepsilon_{xx}}^2 + {\varepsilon_{yy}}^2 + 2{\varepsilon_{xy}}^2 - \tfrac{1}{4}\,\varepsilon^2\right)\,. \tag{10.51}$$

Substituting from (10.42) and (10.45) in the above, we obtain

$$\mathcal{E}_{\perp} = \frac{\bar{\mu}_0\Omega_z^2}{4\pi^2}\left[\frac{3}{4}\left(1 - \frac{2}{3}\,\bar{\alpha}_0 + \bar{\alpha}_0^2\right) + \bar{\alpha}_0\left[1 + \bar{\alpha}_0(1 + \ln r)\ln r\right]\right] \tag{10.52}$$

where

$$\bar{\alpha}_0 = \frac{\bar{\mu}_0}{2\bar{\mu}_0 + \bar{\lambda}_0}\,. \tag{10.53}$$

The volume force for wedge disclinations can be calculated from

$$X^{\nu} = -{T^{\mu\nu}}_{;\mu} \tag{10.54}$$

using the stress tensor (10.47). The volume force is then given by

$$
\begin{aligned}
X_x &= -\frac{\bar{\mu}_0\,\Omega_z}{\pi}\,\frac{x}{x^2+y^2}\left(\frac{\bar{\mu}_0+\bar{\lambda}_0}{2\bar{\mu}_0+\bar{\lambda}_0}-\frac{2(1-\bar{\alpha}_0)x^2}{x^2+y^2}\right)\\
X_y &= \frac{\bar{\mu}_0\,\Omega_z}{\pi}\,\frac{y}{x^2+y^2}\left(\frac{\bar{\mu}_0+\bar{\lambda}_0}{2\bar{\mu}_0+\bar{\lambda}_0}-\frac{2(1-\bar{\alpha}_0)y^2}{x^2+y^2}\right)\\
X_z &= 0\,.
\end{aligned}
\tag{10.55}
$$

The volume force along the z-axis is zero, but there is a net volume force along the x-axis and the y-axis.

§10.4 Volterra twist disclinations

Stationary twist disclinations are represented by setting the dislocation Burgers vector (b_x, b_y, b_z) to zero and the disclination Frank vector component $\Omega_z = 0$ in (10.13). Both Ω_x and Ω_y are not equal to zero. Note that we do not differentiate between twist and splay disclinations in this section as twist disclination expressions include both twist disclinations proper and splay disclinations. Note that when we need to differentiate between splay and twist disclinations, we will use the terminology "twist disclination proper" to refer to the twist disclination. With these substitutions, we obtain

$$
\begin{aligned}
u_x &= -\frac{\Omega_y}{2\pi}\,z\arctan\left(\frac{y}{x}\right)-\frac{\Omega_x}{4\pi}\,z\ln(x^2+y^2)\\
u_y &= \frac{\Omega_x}{2\pi}\,z\arctan\left(\frac{y}{x}\right)-\frac{\Omega_y}{4\pi}\,z\ln(x^2+y^2)\\
u_z &= \left(-\frac{\Omega_x}{2\pi}\,y+\frac{\Omega_y}{2\pi}\,x\right)\arctan\left(\frac{y}{x}\right)+\\
&\quad+\left(\frac{\Omega_x}{4\pi}\,x+\frac{\Omega_y}{4\pi}\,y\right)\ln(x^2+y^2)
\end{aligned}
\tag{10.56}
$$

which can be written as

$$
\begin{aligned}
u_x &= -\frac{\Omega_y}{2\pi}\,z\,\theta-\frac{\Omega_x}{2\pi}\,z\ln r\\
u_y &= \frac{\Omega_x}{2\pi}\,z\,\theta-\frac{\Omega_y}{2\pi}\,z\ln r\\
u_z &= \left(-\frac{\Omega_x}{2\pi}\,y+\frac{\Omega_y}{2\pi}\,x\right)\theta+\left(\frac{\Omega_x}{2\pi}\,x+\frac{\Omega_y}{2\pi}\,y\right)\ln r
\end{aligned}
\tag{10.57}
$$

in cylindrical polar coordinates (r, θ, z).

The rotation tensor and rotation vector are calculated as in section §9.2 from the displacements (10.56). The rotation tensor is then given by

$$\begin{aligned}
\omega_{xy} &= 0 \\
\omega_{yz} &= \frac{\Omega_x}{2\pi} \arctan\left(\frac{y}{x}\right) - \frac{\Omega_y}{4\pi} \left[1 + \ln\left(x^2 + y^2\right)\right] \\
&= \frac{\Omega_x}{2\pi}\,\theta - \frac{\Omega_y}{4\pi}\,(1 + 2\ln r) \\
\omega_{xz} &= -\frac{\Omega_y}{2\pi} \arctan\left(\frac{y}{x}\right) - \frac{\Omega_x}{4\pi} \left[1 + \ln\left(x^2 + y^2\right)\right] \\
&= -\frac{\Omega_y}{2\pi}\,\theta - \frac{\Omega_x}{4\pi}\,(1 + 2\ln r)\,.
\end{aligned} \tag{10.58}$$

and the rotation vector by

$$\begin{aligned}
\omega_x &= \frac{\Omega_x}{2\pi} \arctan\left(\frac{y}{x}\right) - \frac{\Omega_y}{4\pi} \left[1 + \ln\left(x^2 + y^2\right)\right] \\
&= \frac{\Omega_x}{2\pi}\,\theta - \frac{\Omega_y}{4\pi}\,(1 + 2\ln r) \\
\omega_y &= \frac{\Omega_y}{2\pi} \arctan\left(\frac{y}{x}\right) + \frac{\Omega_x}{4\pi} \left[1 + \ln\left(x^2 + y^2\right)\right] \\
&= \frac{\Omega_y}{2\pi}\,\theta + \frac{\Omega_x}{4\pi}\,(1 + 2\ln r) \\
\omega_z &= 0\,.
\end{aligned} \tag{10.59}$$

The rotation vector has x and y components, but no z component, which is associated with the wedge disclination.

The bend-twist tensor is given by

$$\kappa^{\mu\nu} = \omega^{\mu;\nu}\,. \tag{10.60}$$

The components of the bend-twist tensor in cartesian coordinates are

then given by

$$\begin{aligned}
\kappa_{xx} &= -\frac{\Omega_x}{2\pi}\,\frac{y}{r^2} - \frac{\Omega_y}{2\pi}\,\frac{x}{r^2}\,, \\
\kappa_{xy} &= \frac{\Omega_x}{2\pi}\,\frac{x}{r^2} - \frac{\Omega_y}{2\pi}\,\frac{y}{r^2}\,, \qquad \kappa_{xz} = 0\,, \\
\kappa_{yx} &= -\frac{\Omega_y}{2\pi}\,\frac{y}{r^2} + \frac{\Omega_x}{2\pi}\,\frac{x}{r^2}\,, \\
\kappa_{yy} &= \frac{\Omega_y}{2\pi}\,\frac{x}{r^2} + \frac{\Omega_x}{2\pi}\,\frac{y}{r^2}\,, \qquad \kappa_{yz} = 0\,, \\
\kappa_{zx} &= 0\,, \qquad\qquad\qquad\qquad \kappa_{zy} = 0\,, \quad \kappa_{zz} = 0\,.
\end{aligned} \tag{10.61}$$

The trace of the bend-twist tensor is zero as required:

$$\text{Trace}(\kappa^{\mu\nu}) = \kappa^{\alpha}{}_{\alpha} = 0\,, \tag{10.62}$$

The components of the strain tensor in cartesian coordinates are derived from $\varepsilon^{\mu\nu} = \frac{1}{2}(u^{\mu;\nu} + u^{\nu;\mu})$:

$$\begin{aligned}
\varepsilon_{xx} &= \frac{\Omega_y}{2\pi}\,z\,\frac{y}{x^2+y^2} - \frac{\Omega_x}{2\pi}\,z\,\frac{x}{x^2+y^2} \\
\varepsilon_{yy} &= \frac{\Omega_x}{2\pi}\,z\,\frac{x}{x^2+y^2} - \frac{\Omega_y}{2\pi}\,z\,\frac{y}{x^2+y^2} \\
\varepsilon_{zz} &= 0 \\
\varepsilon_{xy} &= -\frac{\Omega_y}{\pi}\,z\,\frac{x}{x^2+y^2} - \frac{\Omega_x}{\pi}\,z\,\frac{y}{x^2+y^2} \\
\varepsilon_{yz} &= \left(-\frac{\Omega_x}{2\pi}\,y + \frac{\Omega_y}{2\pi}\,x\right)\,\frac{x}{x^2+y^2} + \\
&\quad + \left(\frac{\Omega_x}{2\pi}\,x + \frac{\Omega_y}{2\pi}\,y\right)\,\frac{y}{x^2+y^2} \\
\varepsilon_{xz} &= \left(\frac{\Omega_x}{2\pi}\,y - \frac{\Omega_y}{2\pi}\,x\right)\,\frac{y}{x^2+y^2} + \\
&\quad + \left(\frac{\Omega_x}{2\pi}\,x + \frac{\Omega_y}{2\pi}\,y\right)\,\frac{x}{x^2+y^2}\,.
\end{aligned} \tag{10.63}$$

The volume dilatation ε for the twist disclinations is then given by

$$\varepsilon = \varepsilon^{\alpha}{}_{\alpha} = \varepsilon_{xx} + \varepsilon_{yy} + \varepsilon_{zz}\,. \tag{10.64}$$

Substituting for ε_{xx}, ε_{yy} and ε_{zz} from (10.63) into (10.64),

$$\varepsilon = 0\,. \tag{10.65}$$

Hence the Volterra twist disclination does not have a volume dilatation like a wedge disclination, but is rather a pure distortion. As we will see later, this means that there is no rest-mass energy density associated with the Volterra twist disclination. We will revisit this result for the deWit twist disclination.

The components of the stress tensor in cartesian coordinates are obtained from (10.24) as follows:

$$\begin{aligned}
\sigma_{xx} &= \frac{\bar{\mu}_0\Omega_y}{\pi}\, z\, \frac{y}{x^2+y^2} - \frac{\bar{\mu}_0\Omega_x}{\pi}\, z\, \frac{x}{x^2+y^2} \\
\sigma_{yy} &= \frac{\bar{\mu}_0\Omega_x}{\pi}\, z\, \frac{x}{x^2+y^2} - \frac{\bar{\mu}_0\Omega_y}{\pi}\, z\, \frac{y}{x^2+y^2} \\
\sigma_{zz} &= 0 \\
\sigma_{xy} &= -\frac{2\bar{\mu}_0\Omega_y}{\pi}\, z\, \frac{x}{x^2+y^2} - \frac{2\bar{\mu}_0\Omega_x}{\pi}\, z\, \frac{y}{x^2+y^2} \\
\sigma_{yz} &= \left(-\frac{\bar{\mu}_0\Omega_x}{\pi}\, y + \frac{\bar{\mu}_0\Omega_y}{\pi}\, x\right) \frac{x}{x^2+y^2} + \\
&\quad + \left(\frac{\bar{\mu}_0\Omega_x}{\pi}\, x + \frac{\bar{\mu}_0\Omega_y}{\pi}\, y\right) \frac{y}{x^2+y^2} = \frac{\bar{\mu}_0\Omega_y}{\pi} \\
\sigma_{xz} &= \left(\frac{\bar{\mu}_0\Omega_x}{\pi}\, y - \frac{\bar{\mu}_0\Omega_y}{\pi}\, x\right) \frac{y}{x^2+y^2} + \\
&\quad + \left(\frac{\bar{\mu}_0\Omega_x}{\pi}\, x + \frac{\bar{\mu}_0\Omega_y}{\pi}\, y\right) \frac{x}{x^2+y^2} = \frac{\bar{\mu}_0\Omega_x}{\pi}\,.
\end{aligned} \tag{10.66}$$

The mass energy density is calculated from (2.24), *viz.*

$$\rho c^2 = 4\bar{\kappa}_0\, \varepsilon = 2(2\bar{\lambda}_0 + \bar{\mu}_0)\, \varepsilon\,.$$

Substituting for ε from (10.65), the mass energy density of the twist disclinations is 0 as discussed previously:

$$\rho c^2 = 0\,. \tag{10.67}$$

Similarly, when we calculate the strain energy density of the twist disclinations using (10.65) in (9.50), the longitudinal dilatation strain energy

density is also 0 (*i.e.* it is massless):

$$\mathcal{E}_{\|} = 0\,. \tag{10.68}$$

The distortion strain energy density is calculated from (9.51), *viz.*

$$\mathcal{E}_{\perp} = \bar{\mu}_0 e^{\alpha\beta} e_{\alpha\beta}\,.$$

As seen previously, using (9.20), *viz.*

$$e^{\alpha\beta} = \varepsilon^{\alpha\beta} - e_s g^{\alpha\beta}$$

where $e_s = \frac{1}{4}\,\varepsilon$, (9.51) simplifies to

$$\mathcal{E}_{\perp} = \bar{\mu}_0 \left(\varepsilon^{\alpha\beta}\varepsilon_{\alpha\beta} - \tfrac{1}{4}\,\varepsilon^2\right)\,. \tag{10.69}$$

This expression is expanded using the non-zero elements of the strain tensor (10.63) to give

$$\mathcal{E}_{\perp} = \bar{\mu}_0 \left({\varepsilon_{xx}}^2 + {\varepsilon_{yy}}^2 + 2{\varepsilon_{xy}}^2 + 2{\varepsilon_{yz}}^2 + 2{\varepsilon_{xz}}^2 - \tfrac{1}{4}\,\varepsilon^2\right)\,. \tag{10.70}$$

Substituting from (10.63) and (10.65) in the above, we obtain

$$\begin{aligned} \mathcal{E}_{\perp} &= \frac{\bar{\mu}_0}{2\pi^2}\left(\Omega_x^2 + \Omega_y^2\right)\left(1 + \frac{z^2}{r^2}\right) + \\ &\quad + \frac{\bar{\mu}_0}{2\pi^2}\,\left(\Omega_x y + \Omega_y x\right)^2\,\frac{z^2}{r^4} \end{aligned} \tag{10.71}$$

which can be also expressed as

$$\begin{aligned} \mathcal{E}_{\perp} &= \frac{\bar{\mu}_0}{2\pi^2}\left(\Omega_x^2 + \Omega_y^2\right) + \\ &\quad + \frac{\bar{\mu}_0}{2\pi^2}\,\frac{z^2}{r^2}\left[\Omega_x^2 + \Omega_y^2 + \frac{\left(\Omega_x y + \Omega_y x\right)^2}{r^2}\right]\,. \end{aligned} \tag{10.72}$$

The volume force for twist disclinations can be calculated from

$$X^{\nu} = -{\sigma^{\mu\nu}}_{;\mu} \tag{10.73}$$

using the stress tensor (10.66). The volume force is then given by

$$\begin{aligned} X_x &= \frac{\bar{\mu}_0\Omega_x}{\pi}\,z\,\frac{x^2 - y^2}{(x^2+y^2)^2} - \frac{\bar{\mu}_0\Omega_y}{\pi}\,z\,\frac{2xy}{(x^2+y^2)^2} \\ X_y &= -\frac{\bar{\mu}_0\Omega_x}{\pi}\,z\,\frac{2xy}{(x^2+y^2)^2} - \frac{\bar{\mu}_0\Omega_y}{\pi}\,z\,\frac{x^2 - y^2}{(x^2+y^2)^2} \\ X_z &= 0\,. \end{aligned} \tag{10.74}$$

The volume force along the z-axis is zero, but there is a net volume force along the x-axis and the y-axis.

§10.5 deWit discrete disclination lines

As we have seen in the previous sections on dislocations, deWit [80] points out that the Volterra dislocation and disclination displacements (10.11) are not in equilibrium, and that a volume force X^ν is present in the continuum. He proposed corrected disclination line displacements that are in equilibrium, for which no volume force is present ($X^\nu = 0$). These are given by [80]

$$
\begin{aligned}
u_x &= -\frac{\Omega_x}{2\pi}\, z \left(\frac{\bar{\mu}_0}{2\bar{\mu}_0 + \bar{\lambda}_0}\, \ln r + \frac{\bar{\mu}_0 + \bar{\lambda}_0}{2\bar{\mu}_0 + \bar{\lambda}_0}\, \frac{y^2}{r^2} \right) + \\
&\quad + \frac{\Omega_y}{2\pi}\, z \left(\theta + \frac{\bar{\mu}_0 + \bar{\lambda}_0}{2\bar{\mu}_0 + \bar{\lambda}_0}\, \frac{xy}{r^2} \right) - \\
&\quad - \frac{\Omega_z}{2\pi} \left(y\,\theta - \frac{\bar{\mu}_0}{2\bar{\mu}_0 + \bar{\lambda}_0}\, x\,(\ln r - 1) \right) \\
u_y &= -\frac{\Omega_x}{2\pi}\, z \left(\theta - \frac{\bar{\mu}_0 + \bar{\lambda}_0}{2\bar{\mu}_0 + \bar{\lambda}_0}\, \frac{xy}{r^2} \right) - \\
&\quad - \frac{\Omega_y}{2\pi}\, z \left(\frac{\bar{\mu}_0}{2\bar{\mu}_0 + \bar{\lambda}_0}\, \ln r + \frac{\bar{\mu}_0 + \bar{\lambda}_0}{2\bar{\mu}_0 + \bar{\lambda}_0}\, \frac{x^2}{r^2} \right) + \\
&\quad + \frac{\Omega_z}{2\pi} \left(x\,\theta + \frac{\bar{\mu}_0}{2\bar{\mu}_0 + \bar{\lambda}_0}\, y\,(\ln r - 1) \right) \\
u_z &= \frac{\Omega_x}{2\pi} \left(y\,\theta - \frac{\bar{\mu}_0}{2\bar{\mu}_0 + \bar{\lambda}_0}\, x\,(\ln r - 1) \right) - \\
&\quad - \frac{\Omega_y}{2\pi} \left(x\,\theta + \frac{\bar{\mu}_0}{2\bar{\mu}_0 + \bar{\lambda}_0}\, y\,(\ln r - 1) \right)
\end{aligned}
\tag{10.75}
$$

where $r^2 = x^2 + y^2$ and $\theta = \arctan(y/x)$ in cylindrical polar coordinates (r, θ, z). These displacements do not include the dislocation Burgers vector b^μ as it has been set to zero. Those were covered in section §9.4. Only disclination displacements are included in the above, modified by DeWit to obtain a zero volume force. We note in particular added terms proportional to x^2/r^2, y^2/r^2 and xy/r^2 which are present in (10.33). As pointed out in [80], the asymptotic dependence of the displacements is $r \ln r$.

The cartesian (x, y, z) and cylindrical polar (r, θ, z) coordinates used by deWit [80] in his analysis for disclinations are as used for dislocations per Fig. 9.5. The cut in the $x - z$ plane is still along the negative x-axis and represents the discontinuity resulting from the rotational

displacememnt as given by (10.4) and the following equation. As done for dislocations, deWit uses subscripts $(\Omega_1, \Omega_2, \Omega_3)$ for the Frank vector axes of the three types of disclinations. These are equivalent to our use of $(\Omega_x, \Omega_y, \Omega_z)$ which correspond to the three axes $(\Omega_r, \Omega_n, \Omega_z)$ used in Fig. 10.1 for the splay, twist and wedge disclinations respectively. Ω_x is thus the axis of rotation about which the rotation is applied for the splay disclination, Ω_y is the axis of rotation about which the rotation is applied for the twist disclination proper, and Ω_z is the axis of rotation about which the rotation is applied for the wedge disclination.

We simplify (10.75) with the use of the parameters $\bar{\alpha}_0$ and $\bar{\beta}_0$:

$$\begin{aligned}
u_x &= -\frac{\Omega_x^{(s)}}{2\pi}\, z \left[\bar{\alpha}_0 \ln r + \bar{\beta}_0 \,\frac{y^2}{r^2}\right] + \\
&\quad + \frac{\Omega_y^{(t)}}{2\pi}\, z \left[\theta + \bar{\beta}_0 \,\frac{xy}{r^2}\right] - \\
&\quad - \frac{\Omega_z^{(w)}}{2\pi}\, [y\,\theta - \bar{\alpha}_0\, x\,(\ln r - 1)] \\
u_y &= -\frac{\Omega_x^{(s)}}{2\pi}\, z \left[\theta - \bar{\beta}_0 \,\frac{xy}{r^2}\right] - \frac{\Omega_y^{(t)}}{2\pi}\, z \left[\bar{\alpha}_0 \ln r + \bar{\beta}_0 \,\frac{x^2}{r^2}\right] + \\
&\quad + \frac{\Omega_z^{(w)}}{2\pi}\, [x\,\theta + \bar{\alpha}_0\, y\,(\ln r - 1)] \\
u_z &= \frac{\Omega_x^{(s)}}{2\pi}\, [y\,\theta - \bar{\alpha}_0\, x\,(\ln r - 1)] - \frac{\Omega_y^{(t)}}{2\pi}\, [x\,\theta + \bar{\alpha}_0\, y\,(\ln r - 1)]
\end{aligned} \tag{10.76}$$

where

$$\bar{\alpha}_0 = \frac{\bar{\mu}_0}{2\bar{\mu}_0 + \bar{\lambda}_0} \tag{10.77}$$

$$\bar{\beta}_0 = \frac{\bar{\mu}_0 + \bar{\lambda}_0}{2\bar{\mu}_0 + \bar{\lambda}_0} \tag{10.78}$$

and where we have specifically appended superscripts to the Frank vectors for clarity: $\Omega_x^{(s)}$ for the splay disclination, $\Omega_y^{(t)}$ for the twist disclination proper, and $\Omega_z^{(w)}$ for the wedge disclination. As for dislocations, in general, we will not append these superscripts except where required for clarity. We can obtain specific expressions for wedge disclinations by putting $\Omega_x = 0$ and $\Omega_y = 0$, for splay disclinations by putting $\Omega_y = 0$

and $\Omega_z = 0$, and for twist disclinations proper by putting $\Omega_x = 0$ and $\Omega_z = 0$, and similarly for the other expressions below.

The displacements vector above is the total effective displacement including both elastic and defect components. The total effective strain tensor is separated into elastic and defect components as per (8.8), viz.

$$^{*}\varepsilon^{\mu\nu} = \varepsilon^{\mu\nu} + \not{\varepsilon}^{\mu\nu} \, .$$

The elastic strain components are calculated from $\varepsilon_{ij} = \frac{1}{2}(u_{i,j} + u_{j,i})$:

$$\begin{aligned}
\varepsilon_{xx} &= -\frac{\Omega_x}{2\pi} z \left(\bar{\alpha}_0 \frac{x}{r^2} - 2\bar{\beta}_0 \frac{xy^2}{r^4} \right) - \\
&\quad - \frac{\Omega_y}{2\pi} z \left(\bar{\alpha}_0 \frac{y}{r^2} + 2\bar{\beta}_0 \frac{x^2 y}{r^4} \right) + \frac{\Omega_z}{2\pi} \left(\bar{\alpha}_0 \ln r + \bar{\beta}_0 \frac{y^2}{r^2} \right) \\
\varepsilon_{yy} &= -\frac{\Omega_x}{2\pi} z \left(\bar{\alpha}_0 \frac{x}{r^2} + 2\bar{\beta}_0 \frac{xy^2}{r^4} \right) - \\
&\quad - \frac{\Omega_y}{2\pi} z \left(\bar{\alpha}_0 \frac{y}{r^2} - 2\bar{\beta}_0 \frac{x^2 y}{r^4} \right) + \frac{\Omega_z}{2\pi} \left(\bar{\alpha}_0 \ln r + \bar{\beta}_0 \frac{x^2}{r^2} \right) \\
\varepsilon_{zz} &= 0 \\
\varepsilon_{xy} &= \frac{\Omega_x}{2\pi} z \bar{\beta}_0 \left(\frac{y}{r^2} - 2 \frac{x^2 y}{r^4} \right) + \\
&\quad + \frac{\Omega_y}{2\pi} z \bar{\beta}_0 \left(\frac{x}{r^2} - 2 \frac{xy^2}{r^4} \right) - \frac{\Omega_z}{2\pi} \bar{\beta}_0 \frac{xy}{r^2} \\
\varepsilon_{yz} &= \frac{\Omega_x}{2\pi} \bar{\beta}_0 \frac{xy}{r^2} - \frac{\Omega_y}{2\pi} \left(\bar{\alpha}_0 \ln r + \bar{\beta}_0 \frac{x^2}{r^2} \right) \\
\varepsilon_{zx} &= -\frac{\Omega_x}{2\pi} \left(\bar{\alpha}_0 \ln r + \bar{\beta}_0 \frac{y^2}{r^2} \right) + \frac{\Omega_y}{2\pi} \bar{\beta}_0 \frac{xy}{r^2} \, .
\end{aligned} \tag{10.79}$$

while the non-zero defect strain components are given by [80]

$$\begin{aligned}
\not{\varepsilon}_{xy} &= \tfrac{1}{2} \, \Omega_y \, z H(-x) \delta(y) \\
\not{\varepsilon}_{yy} &= (\Omega_z x - \Omega_x z) \, H(-x) \delta(y) \\
\not{\varepsilon}_{yz} &= -\tfrac{1}{2} \, \Omega_y x H(-x) \delta(y)
\end{aligned} \tag{10.80}$$

where $H(x)$ is the Heavyside function defined as 0 for $x < 0$ and 1 for $x > 0$, used to describe the discontinuity defined by [80] along the $-x - z$ half-plane by restricting the range $\theta = (-\pi, +\pi)$ as per Fig. 9.5.

Again, the volume dilatation ε is given by

$$\varepsilon = \varepsilon^{\alpha}{}_{\alpha} = \varepsilon_{xx} + \varepsilon_{yy} + \varepsilon_{zz}\,. \tag{10.81}$$

Substituting for ε_{xx}, ε_{yy} and ε_{zz} from (10.79) into (10.81), we obtain

$$\begin{aligned}\varepsilon = &-\frac{1}{\pi}\,\frac{\bar{\mu}_0}{2\bar{\mu}_0+\bar{\lambda}_0}\,(\Omega_x x+\Omega_y y)\;\frac{z}{r^2}+\\ &+\frac{\Omega_z}{\pi}\left(\frac{\bar{\mu}_0}{2\bar{\mu}_0+\bar{\lambda}_0}\,\ln r+\frac{1}{2}\,\frac{\bar{\mu}_0+\bar{\lambda}_0}{2\bar{\mu}_0+\bar{\lambda}_0}\right).\end{aligned} \tag{10.82}$$

The components of the stress tensor in cartesian coordinates are given by

$$\begin{aligned}
\sigma_{xx} &= -\frac{\bar{\mu}_0\bar{\beta}_0}{\pi}\left[\Omega_x\,z\left(\frac{x}{r^2}-2\,\frac{xy^2}{r^4}\right)+\Omega_y\,z\left(\frac{y}{r^2}+2\,\frac{x^2y}{r^4}\right)-\right.\\
&\quad\left.-\,\Omega_z\left(\ln r+\frac{y^2}{r^2}+\frac{\bar{\lambda}_0}{2\bar{\mu}_0}\right)\right]\\
\sigma_{yy} &= -\frac{\bar{\mu}_0\bar{\beta}_0}{\pi}\left[\Omega_x\,z\left(\frac{x}{r^2}+2\,\frac{xy^2}{r^4}\right)+\Omega_y\,z\left(\frac{y}{r^2}-2\,\frac{x^2y}{r^4}\right)-\right.\\
&\quad\left.-\Omega_z\left(\ln r+\frac{x^2}{r^2}+\frac{\bar{\lambda}_0}{2\bar{\mu}_0}\right)\right]\\
\sigma_{zz} &= -\frac{\bar{\lambda}_0}{\pi}\left[\bar{\alpha}_0\,(\Omega_x x+\Omega_y y)\;\frac{z}{r^2}-\Omega_z\left(\bar{\alpha}_0\ln r+\frac{1}{2}\,\bar{\beta}_0\right)\right]\\
\sigma_{xy} &= \frac{\bar{\mu}_0\bar{\beta}_0}{\pi}\left[\Omega_x\,z\left(\frac{y}{r^2}-2\,\frac{x^2y}{r^4}\right)+\right.\\
&\quad\left.+\Omega_y\,z\left(\frac{x}{r^2}-2\,\frac{xy^2}{r^4}\right)-\Omega_z\,\frac{xy}{r^2}\right]\\
\sigma_{yz} &= \frac{\bar{\mu}_0\Omega_x}{\pi}\,\bar{\beta}_0\,\frac{xy}{r^2}-\;\frac{\bar{\mu}_0\Omega_y}{\pi}\left(\bar{\alpha}_0\ln r+\bar{\beta}_0\,\frac{x^2}{r^2}\right)\\
\sigma_{zx} &= -\frac{\bar{\mu}_0\Omega_x}{\pi}\left(\bar{\alpha}_0\ln r+\bar{\beta}_0\,\frac{y^2}{r^2}\right)+\;\frac{\bar{\mu}_0\Omega_y}{\pi}\,\bar{\beta}_0\,\frac{xy}{r^2}\,.
\end{aligned} \tag{10.83}$$

Calculating the volume force from

$$X^{\nu} = -\sigma^{\mu\nu}{}_{;\mu}\,,$$

we find that this stress tensor results in no volume force in the continuum ($X^{\nu}=0$) as required.

The components of the rotation vector in cartesian coordinates are given by

$$\begin{aligned}\omega_x &= \frac{\Omega_x}{2\pi}\,\theta \\ \omega_y &= \frac{\Omega_y}{2\pi}\,\theta \\ \omega_z &= \frac{\Omega_z}{2\pi}\,\theta + \frac{\Omega_x}{2\pi}\,\frac{yz}{r^2} - \frac{\Omega_y}{2\pi}\,\frac{xz}{r^2}\,.\end{aligned} \tag{10.84}$$

while the components of the defect rotation vector (see (8.11)) in cartesian coordinates are given by [80]

$$\begin{aligned}\phi_x &= -\frac{1}{2}\,\Omega_y x H(-x)\delta(y) \\ \phi_y &= 0 \\ \phi_z &= -\frac{1}{2}\,\Omega_y z H(-x)\delta(y)\,.\end{aligned} \tag{10.85}$$

where as before, $H(x)$ is the Heavyside function defined as 0 for $x < 0$ and 1 for $x > 0$, used to describe the discontinuity defined by [80] along the $-x - z$ half-plane by restricting the range $\theta = (-\pi, +\pi)$ as per Fig. 9.5.

The bend-twist tensor can be separated into elastic and defect components according to

$${}^{*}\kappa^{\mu\nu} = {}^{*}\omega^{\mu;\nu} = \kappa^{\mu\nu} + \not{\kappa}^{\mu\nu} \tag{10.86}$$

where ${}^{*}\kappa^{\mu\nu}$ is the total effective bend-twist tensor, $\kappa^{\mu\nu}$ is the elastic bend-twist tensor and $\not{\kappa}^{\mu\nu}$ is the defect bend-twist tensor.

The components of the elastic bend-twist tensor in cartesian coordinates are given by

$$\begin{aligned}\kappa_{xx} &= -\frac{\Omega_x}{2\pi}\,\frac{y}{r^2} \\ \kappa_{yx} &= \frac{\Omega_x}{2\pi}\,\frac{x}{r^2} \\ \kappa_{zx} &= 0\end{aligned} \tag{10.87}$$

$$\kappa_{xy} = -\frac{\Omega_y}{2\pi}\,\frac{y}{r^2}$$

$$\kappa_{yy} = \frac{\Omega_y}{2\pi}\,\frac{x}{r^2}$$

$$\kappa_{zy} = 0$$

$$\kappa_{xz} = -\frac{\Omega_x}{\pi}\,\frac{xyz}{r^4} - \frac{\Omega_y}{2\pi}\,z\left[\frac{1}{r^2} - 2\,\frac{x^2}{r^4}\right] - \frac{\Omega_z}{2\pi}\,\frac{y}{r^2}$$

$$\kappa_{yz} = -\frac{\Omega_x}{2\pi}\,z\left[\frac{1}{r^2} - 2\,\frac{y^2}{r^4}\right] + \frac{\Omega_y}{\pi}\,\frac{xyz}{r^4} + \frac{\Omega_z}{2\pi}\,\frac{x}{r^2}$$

$$\kappa_{zz} = \frac{\Omega_x}{2\pi}\,\frac{y}{r^2} - \frac{\Omega_y}{2\pi}\,\frac{x}{r^2}\,.$$

while the components of the defect bend-twist tensor in cartesian coordinates are given by [80]

$$\begin{aligned}
\not{\kappa}_{xx} &= -\tfrac{1}{2}\,\Omega_y\,H(-x)\delta(y)\\
\not{\kappa}_{yx} &= -\tfrac{1}{2}\,\Omega_y x H(-x)\delta'(y) + \Omega_x H(-x)\delta(y)\\
\not{\kappa}_{yy} &= \Omega_y\,H(-x)\delta(y)\\
\not{\kappa}_{xz} &= \tfrac{1}{2}\,\Omega_y\,z\delta(x)\delta(y)\\
\not{\kappa}_{yz} &= -\tfrac{1}{2}\,\Omega_y z H(-x)\delta'(y) + \Omega_z H(-x)\delta(y)\\
\not{\kappa}_{zz} &= -\tfrac{1}{2}\,\Omega_y\,H(-x)\delta(y)\\
\not{\kappa}_{zx} &= \not{\kappa}_{xy} = \not{\kappa}_{zy} = 0
\end{aligned} \tag{10.88}$$

where again as before, $H(x)$ is the Heavyside function defined as 0 for $x < 0$ and 1 for $x > 0$, used to describe the discontinuity defined by [80] along the $-x-z$ half-plane by restricting the range $\theta = (-\pi, +\pi)$ as per Fig. 9.5. We find that as expected, the trace of the elastic bend-twist tensor is zero

$$\text{Trace}(\kappa^{\mu\nu}) = \kappa^{\alpha}{}_{\alpha} = 0\,, \tag{10.89}$$

as is the trace of the defect bend-twist tensor

$$\text{Trace}(\not{\kappa}^{\mu\nu}) = \not{\kappa}^{\alpha}{}_{\alpha} = 0\,, \tag{10.90}$$

indicating that there is no net twist present in the continuum.

The mass energy density is calculated from (2.24), *viz.*

$$\rho c^2 = 4\bar{\kappa}_0\,\varepsilon = 2(2\bar{\lambda}_0 + \bar{\mu}_0)\,\varepsilon\,.$$

Substituting for ε from (10.82), using the positive value of ε as per section §9.3.4, the mass energy density of the disclination line is given by

$$\rho c^2 = \frac{4\bar{\kappa}_0}{\pi}\,\bar{\alpha}_0\,(\Omega_x x + \Omega_y y)\;\frac{z}{r^2} - \frac{4\bar{\kappa}_0\Omega_z}{\pi}\left(\bar{\alpha}_0 \ln r + \frac{1}{2}\,\bar{\beta}_0\right). \qquad (10.91)$$

We will encounter other combinations of positive and negative rest-mass energy density terms in other cases.

We calculate the strain energy density of the disclination line as follows. Using (10.82) in (9.50), the longitudinal dilatation strain energy density is then given by

$$\mathcal{E}_{\parallel} = \frac{\bar{\kappa}_0}{2\pi^2}\left[-\bar{\alpha}_0\,(\Omega_x x + \Omega_y y)\;\frac{z}{r^2} + \Omega_z\left(\bar{\alpha}_0 \ln r + \frac{1}{2}\,\bar{\beta}_0\right)\right]^2. \qquad (10.92)$$

The distortion strain energy density is calculated from (9.51), *viz.*

$$\mathcal{E}_{\perp} = \bar{\mu}_0 e^{\alpha\beta} e_{\alpha\beta}\,.$$

As seen previously, using (9.20), *viz.*

$$e^{\alpha\beta} = \varepsilon^{\alpha\beta} - e_s g^{\alpha\beta}$$

where $e_s = \frac{1}{4}\,\varepsilon$, (9.51) simplifies to

$$\mathcal{E}_{\perp} = \bar{\mu}_0\left(\varepsilon^{\alpha\beta}\varepsilon_{\alpha\beta} - \tfrac{1}{4}\,\varepsilon^2\right). \qquad (10.93)$$

This expression is expanded using the non-zero elements of the strain tensor (10.79) to give

$$\mathcal{E}_{\perp} = \bar{\mu}_0\left({\varepsilon_{xx}}^2 + {\varepsilon_{yy}}^2 + 2{\varepsilon_{xy}}^2 - \tfrac{1}{4}\,\varepsilon^2\right). \qquad (10.94)$$

Substituting from (10.79) and (10.82) in the above, we note that $\mathcal{E}_{\perp}$ can be separated into the following terms:

$$\mathcal{E}_{\perp} = \mathcal{E}_{\perp}^{W} + \mathcal{E}_{\perp}^{T} + \Omega_x\Omega_z\text{terms} + \Omega_y\Omega_z\text{terms} \qquad (10.95)$$

where $\mathcal{E}_{\perp}^{W}$ is the wedge disclination distortion strain energy density given by (10.113) and $\mathcal{E}_{\perp}^{T}$ is the twist disclination distortion strain energy density given by (10.132). The $\Omega_x\Omega_z$ and $\Omega_y\Omega_z$ cross-terms represent the energy interaction terms for the wedge and twist disclinations:

$$\mathcal{E}_{\perp\ int}^{W-T} = \Omega_x\Omega_z\text{terms} + \Omega_y\Omega_z\text{terms}\,. \qquad (10.96)$$

Computing the $\Omega_x\Omega_z$ terms and the $\Omega_y\Omega_z$ terms, we obtain the wedge-twist disclination interaction strain energy density

$$\begin{aligned}\mathcal{E}^{W-T}_{\perp\ int} = &-\frac{\bar{\mu}_0\Omega_x\Omega_z}{2\pi^2}\,\frac{xz}{r^2}\left[2\bar{\alpha}_0^2\ln r + \bar{\alpha}_0\bar{\beta}_0 + \bar{\beta}_0^2\,\frac{y^2}{r^2}\left(1-\frac{2y^2}{r^2}\right)\right]\\ &-\frac{\bar{\mu}_0\Omega_y\Omega_z}{2\pi^2}\,\frac{yz}{r^2}\left[2\bar{\alpha}_0^2\ln r + \bar{\alpha}_0\bar{\beta}_0 + \bar{\beta}_0^2\,\frac{x^2}{r^2}\left(1-\frac{2x^2}{r^2}\right)\right].\end{aligned} \tag{10.97}$$

Hence

$$\mathcal{E}_\perp = \mathcal{E}^W_\perp + \mathcal{E}^T_\perp + \mathcal{E}^{W-T}_{\perp\ int}\,. \tag{10.98}$$

It is important to note that the interaction does not involve longitudinal terms, only distortion terms. In section §17.2, we consider the interaction terms of dislocations and disclinations arising from the general displacements derived from the general combined deWit dislocation displacements (9.130) and disclination displacements (10.76).

§10.6 deWit wedge disclinations

The deWit wedge disclinations are represented by setting the disclination Frank vector components $\Omega_x = \Omega_y = 0$ with only Ω_z not equal to zero in (10.75) to obtain

$$\begin{aligned}u_x &= -\frac{\Omega_z}{2\pi}\,(y\,\theta - \bar{\alpha}_0\,x\,(\ln r - 1))\\ u_y &= \frac{\Omega_z}{2\pi}\,(x\,\theta + \bar{\alpha}_0\,y\,(\ln r - 1))\\ u_z &= 0\end{aligned} \tag{10.99}$$

where $r^2 = x^2 + y^2$ and $\theta = \arctan(y/x)$ in cylindrical polar coordinates (r, θ, z).

The elastic strain components are calculated from $\varepsilon_{ij} = \frac{1}{2}(u_{i,j} + u_{j,i})$:

$$\begin{aligned}\varepsilon_{xx} &= \frac{\Omega_z}{2\pi}\left(\bar{\alpha}_0\ln r + \bar{\beta}_0\,\frac{y^2}{r^2}\right)\\ \varepsilon_{yy} &= \frac{\Omega_z}{2\pi}\left(\bar{\alpha}_0\,\ln r + \bar{\beta}_0\,\frac{x^2}{r^2}\right)\\ \varepsilon_{zz} &= 0\end{aligned} \tag{10.100}$$

$$\varepsilon_{xy} = -\frac{\Omega_z}{2\pi}\bar{\beta}_0 \frac{xy}{r^2}$$

$$\varepsilon_{yz} = 0$$

$$\varepsilon_{zx} = 0\,.$$

Again, the volume dilatation ε is given by

$$\varepsilon = \varepsilon^{\alpha}{}_{\alpha} = \varepsilon_{xx} + \varepsilon_{yy} + \varepsilon_{zz}\,. \tag{10.101}$$

Substituting for ε_{xx}, ε_{yy} and ε_{zz} from (10.100) into (10.101), we obtain

$$\varepsilon = \frac{\Omega_z}{\pi}\left(\frac{\bar{\mu}_0}{2\bar{\mu}_0 + \bar{\lambda}_0}\,\ln r + \frac{1}{2}\,\frac{\bar{\mu}_0 + \bar{\lambda}_0}{2\bar{\mu}_0 + \bar{\lambda}_0}\right). \tag{10.102}$$

The components of the stress tensor in cartesian coordinates are given by

$$\begin{aligned}
\sigma_{xx} &= \frac{\bar{\mu}_0\bar{\beta}_0\Omega_z}{\pi}\left(\ln r + \frac{y^2}{r^2} + \frac{\bar{\lambda}_0}{2\bar{\mu}_0}\right)\\
\sigma_{yy} &= \frac{\bar{\mu}_0\bar{\beta}_0\Omega_z}{\pi}\left(\ln r + \frac{x^2}{r^2} + \frac{\bar{\lambda}_0}{2\bar{\mu}_0}\right)\\
\sigma_{zz} &= \frac{\bar{\lambda}_0\Omega_z}{\pi}\left(\bar{\alpha}_0 \ln r + \frac{1}{2}\,\bar{\beta}_0\right)\\
\sigma_{xy} &= -\frac{\bar{\mu}_0\bar{\beta}_0\Omega_z}{\pi}\;\frac{xy}{r^2}\\
\sigma_{yz} &= 0\\
\sigma_{zx} &= 0\,.
\end{aligned} \tag{10.103}$$

Calculating the volume force from

$$X^{\nu} = -\sigma^{\mu\nu}{}_{;\mu}\,,$$

we find that this stress tensor results in no volume force in the continuum ($X^{\nu} = 0$) as required.

The components of the rotation vector in cartesian coordinates are given by

$$\begin{aligned}
\omega_x &= 0\\
\omega_y &= 0\\
\omega_z &= \frac{\Omega_z}{2\pi}\,.
\end{aligned} \tag{10.104}$$

The components of the elastic bend-twist tensor in cartesian coordinates are given by

$$\begin{aligned}
&\kappa_{xx} = 0\,, \quad \kappa_{xy} = 0\,, \quad \kappa_{xz} = -\frac{\Omega_z}{2\pi}\,\frac{y}{r^2}\,,\\
&\kappa_{yx} = 0\,, \quad \kappa_{yy} = 0\,, \quad \kappa_{yz} = \frac{\Omega_z}{2\pi}\,\frac{x}{r^2}\,,\\
&\kappa_{zx} = 0\,, \quad \kappa_{zy} = 0\,, \quad \kappa_{zz} = 0\,.
\end{aligned} \tag{10.105}$$

We find that as expected, the trace of the elastic bend-twist tensor is zero

$$\text{Trace}(\kappa^{\mu\nu}) = \kappa^{\alpha}{}_{\alpha} = 0\,, \tag{10.106}$$

indicating that there is no net twist present in the continuum.

The mass energy density is calculated from (2.24), *viz.*

$$\rho c^2 = 4\bar{\kappa}_0\,\varepsilon = 2(2\bar{\lambda}_0 + \bar{\mu}_0)\,\varepsilon\,.$$

Substituting for ε from (10.102), using the positive value of ε as per section §9.3.4, the mass energy density of the wedge disclination is given by

$$\rho c^2 = \frac{4\bar{\kappa}_0\Omega_z}{\pi}\,\left(\frac{\bar{\mu}_0}{2\bar{\mu}_0 + \bar{\lambda}_0}\,\ln r + \frac{1}{2}\,\frac{\bar{\mu}_0 + \bar{\lambda}_0}{2\bar{\mu}_0 + \bar{\lambda}_0}\right)\,. \tag{10.107}$$

We calculate the strain energy density of the wedge disclination as follows. Using (10.102) in (9.50), the longitudinal dilatation strain energy density is then given by

$$\mathcal{E}_{\parallel} = \frac{\bar{\kappa}_0\Omega_z^2}{2\pi^2}\,\left(\frac{\bar{\mu}_0}{2\bar{\mu}_0 + \bar{\lambda}_0}\,\ln r + \frac{1}{2}\,\frac{\bar{\mu}_0 + \bar{\lambda}_0}{2\bar{\mu}_0 + \bar{\lambda}_0}\right)^2 \tag{10.108}$$

or

$$\mathcal{E}_{\parallel} = \frac{\bar{\kappa}_0\Omega_z^2}{2\pi^2}\,\left(\bar{\alpha}_0\ln r + \frac{1}{2}\,\bar{\beta}_0\right)^2\,. \tag{10.109}$$

The distortion strain energy density is calculated from (9.51), *viz.*

$$\mathcal{E}_{\perp} = \bar{\mu}_0 e^{\alpha\beta} e_{\alpha\beta}\,.$$

As seen previously, using (9.20), *viz.*

$$e^{\alpha\beta} = \varepsilon^{\alpha\beta} - e_s g^{\alpha\beta}$$

where $e_s = \frac{1}{4}\,\varepsilon$, (9.51) simplifies to

$$\mathcal{E}_\perp = \bar{\mu}_0 \left(\varepsilon^{\alpha\beta}\varepsilon_{\alpha\beta} - \tfrac{1}{4}\,\varepsilon^2\right) . \tag{10.110}$$

This expression is expanded using the non-zero elements of the strain tensor (10.100) to give

$$\mathcal{E}_\perp = \bar{\mu}_0 \left({\varepsilon_{xx}}^2 + {\varepsilon_{yy}}^2 + 2{\varepsilon_{xy}}^2 - \tfrac{1}{4}\,\varepsilon^2\right) . \tag{10.111}$$

Substituting from (10.100) and (10.102) in the above and simplifying, we obtain

$$\mathcal{E}_\perp = \frac{\bar{\mu}_0\Omega_z^2}{4\pi^2}\left(\bar{\alpha}_0^2 \ln^2 r + 3\bar{\alpha}_0\bar{\beta}_0 \ln r + \frac{3}{4}\,\bar{\beta}_0^2\right) \tag{10.112}$$

which can be further simplified to

$$\mathcal{E}_\perp = \frac{\bar{\mu}_0\Omega_z^2}{4\pi^2}\left[\left(\bar{\alpha}_0 \ln r + \frac{3}{2}\,\bar{\beta}_0\right)^2 - \left(\frac{3}{2}\,\bar{\beta}_0\right)^2\right] . \tag{10.113}$$

§10.6.1 *deWit wedge disclination current and charge density*

The current density four-vector is calculated from (4.10), *viz.*

$$j^\nu = \frac{\varphi_0}{\mu_0}\,\frac{2\bar{\mu}_0 + \bar{\lambda}_0}{2\bar{\mu}_0}\,\varepsilon^{;\nu} = \frac{\varphi_0}{2\mu_0\bar{\alpha}_0}\,\varepsilon^{;\nu}$$

and the charge density from (4.14), *viz.*

$$\varrho = \frac{1}{2}\,\varphi_0\epsilon_0 c\,\frac{2\bar{\mu}_0 + \bar{\lambda}_0}{2\bar{\mu}_0}\,\sqrt{\varepsilon^{;\nu}\varepsilon_{;\nu}} = \frac{\varphi_0\epsilon_0 c}{4\bar{\alpha}_0}\,\sqrt{\varepsilon^{;\nu}\varepsilon_{;\nu}}$$

where φ_0 is the spacetime continuum electromagnetic shearing potential constant.

Using the expression for ε from (10.102), the non-zero components of the current density are given by

$$\begin{aligned} j_x &= \frac{\varphi_0\Omega_z}{2\pi\mu_0}\,\frac{x}{r^2} = \frac{\varphi_0\Omega_z}{2\pi\mu_0}\,\frac{\cos\theta}{r} \\ j_y &= -\frac{\varphi_0\Omega_z}{2\pi\mu_0}\,\frac{y}{r^2} = \frac{\varphi_0\Omega_z}{2\pi\mu_0}\,\frac{\sin\theta}{r} \end{aligned} \tag{10.114}$$

where $r^2 = x^2 + y^2$. The charge density is given by

$$\varrho = \pm\frac{1}{4\pi}\,\varphi_0\epsilon_0 c\,\frac{\Omega_z}{r^2} . \tag{10.115}$$

The sign depends on the problem under consideration.

The charge is given by integrating ϱ over the volume V:

$$Q = \int_V \varrho \, dV = \int_V \varrho \, r dr \, d\theta \, dz \tag{10.116}$$

in cylindrical polar coordinates. This becomes

$$Q = \pm \frac{1}{4\pi} \, \varphi_0 \epsilon_0 c \, \Omega_z \int_{b_0}^{R} \frac{1}{r} \, dr \int_0^{2\pi} d\theta \int_0^{\ell} dz \tag{10.117}$$

where b_0 is the radius of the core of the disclination and R is the "radius" of the cylindrical deformation. Evaluating the integrals, we get

$$Q = \pm \frac{1}{2} \, \varphi_0 \, \epsilon_0 \, c \, \ell \, \Omega_z \ln \left(\frac{R}{b_0} \right) \tag{10.118}$$

where Ω_z is a rotation along the z-axis, perpendicular to the x-y plane. If a vector perpendicular to the x-y plane can be associated with Ω_z, then its units will be [m] along the z-axis, and the units of Q will be [C] as expected. If Ω_z is purely a rotation, then the units of Q will be $[\mathrm{C} \cdot \mathrm{m}^{-1}]$.

§10.7 deWit twist disclinations

The deWit twist disclinations are represented by setting the disclination Frank vector component $\Omega_z = 0$ in (10.75). Both Ω_x and Ω_y are not equal to zero. Note that again we do not differentiate between twist and splay disclinations in this section as twist disclination expressions include both twist disclinations proper and splay disclinations. Note that when we need to differentiate between splay and twist disclinations, we will use the terminology "twist disclination proper" to refer to the twist disclination. With these substitutions, we obtain

$$\begin{aligned}
u_x &= -\frac{\Omega_x}{2\pi} \, z \left(\bar{\alpha}_0 \ln r + \bar{\beta}_0 \, \frac{y^2}{r^2} \right) + \frac{\Omega_y}{2\pi} \, z \left(\theta + \bar{\beta}_0 \, \frac{xy}{r^2} \right) \\
u_y &= -\frac{\Omega_x}{2\pi} \, z \left(\theta - \bar{\beta}_0 \, \frac{xy}{r^2} \right) - \frac{\Omega_y}{2\pi} \, z \left(\bar{\alpha}_0 \ln r + \bar{\beta}_0 \, \frac{x^2}{r^2} \right) \\
u_z &= \frac{\Omega_x}{2\pi} \left(y \, \theta - \bar{\alpha}_0 \, x \left(\ln r - 1 \right) \right) - \frac{\Omega_y}{2\pi} \left(x \, \theta + \bar{\alpha}_0 \, y \left(\ln r - 1 \right) \right)
\end{aligned} \tag{10.119}$$

where $r^2 = x^2 + y^2$ and $\theta = \arctan(y/x)$ in cylindrical polar coordinates (r, θ, z).

The elastic strain components are calculated from $\varepsilon_{ij} = \frac{1}{2}(u_{i,j}+u_{j,i})$:

$$\begin{aligned}
\varepsilon_{xx} &= -\frac{\Omega_x}{2\pi}\, z \left(\bar{\alpha}_0 \,\frac{x}{r^2} - 2\bar{\beta}_0 \,\frac{xy^2}{r^4}\right) - \\
&\quad - \frac{\Omega_y}{2\pi}\, z \left(\bar{\alpha}_0 \,\frac{y}{r^2} + 2\bar{\beta}_0 \,\frac{x^2 y}{r^4}\right) \\
\varepsilon_{yy} &= -\frac{\Omega_x}{2\pi}\, z \left(\bar{\alpha}_0 \,\frac{x}{r^2} + 2\bar{\beta}_0 \,\frac{xy^2}{r^4}\right) - \\
&\quad - \frac{\Omega_y}{2\pi}\, z \left(\bar{\alpha}_0 \,\frac{y}{r^2} - 2\bar{\beta}_0 \,\frac{x^2 y}{r^4}\right) \\
\varepsilon_{zz} &= 0 \\
\varepsilon_{xy} &= \frac{\Omega_x}{2\pi}\, z\, \bar{\beta}_0 \left(\frac{y}{r^2} - 2\,\frac{x^2 y}{r^4}\right) + \\
&\quad + \frac{\Omega_y}{2\pi}\, z\, \bar{\beta}_0 \left(\frac{x}{r^2} - 2\,\frac{xy^2}{r^4}\right) \\
\varepsilon_{yz} &= \frac{\Omega_x}{2\pi}\, \bar{\beta}_0 \,\frac{xy}{r^2} - \frac{\Omega_y}{2\pi} \left(\bar{\alpha}_0 \ln r + \bar{\beta}_0 \,\frac{x^2}{r^2}\right) \\
\varepsilon_{zx} &= -\frac{\Omega_x}{2\pi} \left(\bar{\alpha}_0 \ln r + \bar{\beta}_0 \,\frac{y^2}{r^2}\right) + \frac{\Omega_y}{2\pi}\, \bar{\beta}_0 \,\frac{xy}{r^2}\,.
\end{aligned} \tag{10.120}$$

Again, the volume dilatation ε is given by

$$\varepsilon = \varepsilon^{\alpha}{}_{\alpha} = \varepsilon_{xx} + \varepsilon_{yy} + \varepsilon_{zz}\,. \tag{10.121}$$

Substituting for ε_{xx}, ε_{yy} and ε_{zz} from (10.120) into (10.121), we obtain

$$\varepsilon = -\frac{1}{\pi}\, \frac{\bar{\mu}_0}{2\bar{\mu}_0 + \bar{\lambda}_0}\, (\Omega_x x + \Omega_y y)\, \frac{z}{r^2} \tag{10.122}$$

or

$$\varepsilon = -\frac{\bar{\alpha}_0}{\pi}\, (\Omega_x x + \Omega_y y)\, \frac{z}{r^2}\,. \tag{10.123}$$

The components of the stress tensor in cartesian coordinates are

given by

$$\begin{aligned}
\sigma_{xx} &= -\frac{\bar{\mu}_0\bar{\beta}_0}{\pi}\left[\Omega_x\, z\left(\frac{x}{r^2}-2\,\frac{xy^2}{r^4}\right)+\Omega_y\, z\left(\frac{y}{r^2}+2\,\frac{x^2y}{r^4}\right)\right]\\
\sigma_{yy} &= -\frac{\bar{\mu}_0\bar{\beta}_0}{\pi}\left[\Omega_x\, z\left(\frac{x}{r^2}+2\,\frac{xy^2}{r^4}\right)+\Omega_y\, z\left(\frac{y}{r^2}-2\,\frac{x^2y}{r^4}\right)\right]\\
\sigma_{zz} &= -\frac{\bar{\lambda}_0}{\pi}\left[\bar{\alpha}_0\,(\Omega_x x+\Omega_y y)\;\frac{z}{r^2}\right]\\
\sigma_{xy} &= \frac{\bar{\mu}_0\bar{\beta}_0}{\pi}\left[\Omega_x\, z\left(\frac{y}{r^2}-2\,\frac{x^2y}{r^4}\right)+\Omega_y\, z\left(\frac{x}{r^2}-2\,\frac{xy^2}{r^4}\right)\right]\\
\sigma_{yz} &= \frac{\bar{\mu}_0\Omega_x}{\pi}\,\bar{\beta}_0\,\frac{xy}{r^2}-\;\frac{\bar{\mu}_0\Omega_y}{\pi}\left(\bar{\alpha}_0\ln r+\bar{\beta}_0\,\frac{x^2}{r^2}\right)\\
\sigma_{zx} &= -\frac{\bar{\mu}_0\Omega_x}{\pi}\left(\bar{\alpha}_0\ln r+\bar{\beta}_0\,\frac{y^2}{r^2}\right)+\;\frac{\bar{\mu}_0\Omega_y}{\pi}\,\bar{\beta}_0\,\frac{xy}{r^2}\,.
\end{aligned}\tag{10.124}$$

Calculating the volume force from

$$X^\nu = -\sigma^{\mu\nu}{}_{;\mu}\,,$$

we find that this stress tensor results in no volume force in the continuum ($X^\nu = 0$) as required.

The components of the rotation vector in cartesian coordinates are given by

$$\begin{aligned}
\omega_x &= \frac{\Omega_x}{2\pi}\,\theta\\
\omega_y &= \frac{\Omega_y}{2\pi}\,\theta\\
\omega_z &= \frac{\Omega_x}{2\pi}\,\frac{yz}{r^2}-\frac{\Omega_y}{2\pi}\,\frac{xz}{r^2}\,.
\end{aligned}\tag{10.125}$$

The components of the elastic bend-twist tensor in cartesian coordinates are given by

$$\begin{aligned}
\kappa_{xx} &= -\frac{\Omega_x}{2\pi}\,\frac{y}{r^2}\\
\kappa_{yx} &= \frac{\Omega_x}{2\pi}\,\frac{x}{r^2}\\
\kappa_{zx} &= 0
\end{aligned}\tag{10.126}$$

$$\kappa_{xy} = -\frac{\Omega_y}{2\pi}\,\frac{y}{r^2}$$

$$\kappa_{yy} = \frac{\Omega_y}{2\pi}\,\frac{x}{r^2}$$

$$\kappa_{zy} = 0$$

$$\kappa_{xz} = -\frac{\Omega_x}{\pi}\,\frac{xyz}{r^4} - \frac{\Omega_y}{2\pi}\,z\left(\frac{1}{r^2} - 2\,\frac{x^2}{r^4}\right)$$

$$\kappa_{yz} = -\frac{\Omega_x}{2\pi}\,z\left(\frac{1}{r^2} - 2\,\frac{y^2}{r^4}\right) + \frac{\Omega_y}{\pi}\,\frac{xyz}{r^4}$$

$$\kappa_{zz} = \frac{\Omega_x}{2\pi}\,\frac{y}{r^2} - \frac{\Omega_y}{2\pi}\,\frac{x}{r^2}\,.$$

We find that as expected, the trace of the elastic bend-twist tensor is zero

$$\text{Trace}(\kappa^{\mu\nu}) = \kappa^{\alpha}{}_{\alpha} = 0\,, \tag{10.127}$$

indicating that there is no net twist present in the continuum.

The mass energy density is calculated from (2.24), *viz.*

$$\rho c^2 = 4\bar{\kappa}_0\,\varepsilon = 2(2\bar{\lambda}_0 + \bar{\mu}_0)\,\varepsilon\,.$$

Substituting for ε from (10.122), using the positive value of ε as per section §9.3.4, the mass energy density of the twist disclination is given by

$$\rho c^2 = \frac{4\bar{\kappa}_0}{\pi}\,\frac{\bar{\mu}_0}{2\bar{\mu}_0 + \bar{\lambda}_0}\,(\Omega_x x + \Omega_y y)\,\frac{z}{r^2}\,. \tag{10.128}$$

We calculate the strain energy density of the twist disclination as follows. Using (10.122) in (9.50), the longitudinal dilatation strain energy density is then given by

$$\mathcal{E}_{\parallel} = \frac{\bar{\kappa}_0}{2\pi^2}\left(\frac{\bar{\mu}_0}{2\bar{\mu}_0 + \bar{\lambda}_0}\,(\Omega_x x + \Omega_y y)\,\frac{z}{r^2}\right)^2\,. \tag{10.129}$$

The distortion strain energy density is calculated from (9.51), *viz.*

$$\mathcal{E}_{\perp} = \bar{\mu}_0 e^{\alpha\beta} e_{\alpha\beta}\,.$$

As seen previously, using (9.20), *viz.*

$$e^{\alpha\beta} = \varepsilon^{\alpha\beta} - e_s g^{\alpha\beta}$$

where $e_s = \frac{1}{4}\,\varepsilon$, (9.51) simplifies to

$$\mathcal{E}_\perp = \bar{\mu}_0 \left(\varepsilon^{\alpha\beta}\varepsilon_{\alpha\beta} - \tfrac{1}{4}\,\varepsilon^2\right) . \tag{10.130}$$

This expression is expanded using the non-zero elements of the strain tensor (10.120) to give

$$\mathcal{E}_\perp = \bar{\mu}_0 \left({\varepsilon_{xx}}^2 + {\varepsilon_{yy}}^2 + 2{\varepsilon_{xy}}^2 + 2{\varepsilon_{yz}}^2 + 2{\varepsilon_{zx}}^2 - \tfrac{1}{4}\,\varepsilon^2\right) . \tag{10.131}$$

Substituting from (10.120) and (10.122) in the above, we obtain

$$\begin{aligned}
\mathcal{E}_\perp = {} & \frac{\bar{\mu}_0\Omega_x^2}{2\pi^2}\left[\bar{\alpha}_0^2 \ln^2 r + \frac{\bar{\beta}_0^2}{r^2} + 2\bar{\alpha}_0\bar{\beta}_0\,\frac{y^2}{r^2}\,\ln r + \right. \\
& \left. + \left[\left(\bar{\alpha}_0^2 - \tfrac{1}{2}\,\bar{\beta}_0^2\right)x^2 + \bar{\beta}_0^2 y^2\right]\frac{z^2}{r^4}\right] + \\
& + \frac{\bar{\mu}_0\Omega_y^2}{2\pi^2}\left[\bar{\alpha}_0^2 \ln^2 r + \frac{\bar{\beta}_0^2}{r^2} + 2\bar{\alpha}_0\bar{\beta}_0\,\frac{x^2}{r^2}\,\ln r + \right. \\
& \left. + \left[\bar{\beta}_0^2 x^2 + \left(\bar{\alpha}_0^2 - \tfrac{1}{2}\,\bar{\beta}_0^2\right)y^2\right]\frac{z^2}{r^4}\right] - \\
& - \frac{\bar{\mu}_0\Omega_x\Omega_y}{\pi^2}\left[\bar{\beta}_0\left(\bar{\alpha}_0 \ln r + \tfrac{1}{2}\,\bar{\beta}_0\right) + \left(\bar{\beta}_0^2 - \tfrac{1}{2}\,\bar{\alpha}_0^2\right)\frac{z^2}{r^2}\right] .
\end{aligned} \tag{10.132}$$

In the case where $\Omega_x = \Omega_y = \Omega$, this equation simplifies to

$$\mathcal{E}_\perp = \frac{\bar{\mu}_0\Omega^2}{2\pi^2}\left[2\bar{\alpha}_0^2 \ln^2 r - \bar{\beta}_0^2 + \left(3\bar{\alpha}_0^2 - \bar{\beta}_0^2\right)\frac{z^2}{r^2}\right] . \tag{10.133}$$

§10.7.1 *deWit twist dislocation current and charge density*

The current density four-vector is calculated from (4.10), *viz.*

$$j^\nu = \frac{\varphi_0}{\mu_0}\,\frac{2\bar{\mu}_0 + \bar{\lambda}_0}{2\bar{\mu}_0}\,\varepsilon^{;\nu} = \frac{\varphi_0}{2\mu_0\bar{\alpha}_0}\,\varepsilon^{;\nu}$$

and the charge density from (4.14), *viz.*

$$\varrho = \frac{1}{2}\,\varphi_0\epsilon_0 c\,\frac{2\bar{\mu}_0 + \bar{\lambda}_0}{2\bar{\mu}_0}\,\sqrt{\varepsilon^{;\nu}\varepsilon_{;\nu}} = \frac{\varphi_0\epsilon_0 c}{4\bar{\alpha}_0}\,\sqrt{\varepsilon^{;\nu}\varepsilon_{;\nu}}$$

where φ_0 is the spacetime continuum electromagnetic shearing potential constant.

Using the expression for ε from (10.123), the non-zero components of the current density are given by

$$\begin{aligned} j_x &= -\frac{\varphi_0}{2\pi\mu_0}\,\frac{\Omega_x z r^2 - 2xz\,(\Omega_x x + \Omega_y y)}{r^4} \\ j_y &= -\frac{\varphi_0}{2\pi\mu_0}\,\frac{\Omega_y z r^2 - 2yz\,(\Omega_x x + \Omega_y y)}{r^4} \\ j_z &= -\frac{\varphi_0}{2\pi\mu_0}\,\frac{\Omega_x x + \Omega_y y}{r^2} \end{aligned} \tag{10.134}$$

where $r^2 = x^2 + y^2$. The charge density is given by

$$\varrho = \pm\frac{1}{4\pi}\,\varphi_0\epsilon_0 c\,\frac{1}{r^2}\,\sqrt{\left(\Omega_x^2 + \Omega_y^2\right) z^2 + \left(\Omega_x x + \Omega_y y\right)^2}\,. \tag{10.135}$$

The sign depends on the problem under consideration.

It is interesting to note that the charge density for the previous dislocations and disclinations considered (edge dislocation (9.105), deWit dislocation line (9.160), wedge disclination (10.115)) all have the same functional dependence:

$$\varrho = \pm\frac{1}{4\pi}\,\varphi_0\epsilon_0 c\,\frac{f(b^\nu, \Omega^\nu)}{r^2}\,, \tag{10.136}$$

while the charge density for the twist disclination (10.135) also includes coordinates x^ν in $f(b^\nu, \Omega^\nu, x^\nu)$.

Chapter 11

Field Theory of Defects

§11.1 Analysis of distributions of defect densities

In this chapter, we deal with distributions of defect densities, namely dislocation densities and disclination densities. We first consider the treatment of defect densities based on the tensor methods of defects analysis [79, 80, 199].

We then provide an overview of the gauge theory and Cartan differential geometry treatment introduced in the 1980s, also referred to as the field theory of defects. The treatment is based on Kleinert [199] who is a key reference on this topic (as applied to condensed matter). This theory is popular for the investigation of defects in condensed matter physics and in string theory due to the mathematical elegance and popularity of gauge theories and Cartan differential geometry.

However, it should be noted that, as Kröner [206] (quoted in [201]) has pointed out, "[a]lthough the field theory of defects has found many applications, the early hope that it could become the basis of a general theory of plasticity has not been fulfilled".

§11.2 Dislocation and disclination densities

Dislocation and disclination densities are functions of position and are denoted as $\alpha^{\mu\nu}(x^\xi)$ and $\theta^{\mu\nu}(x^\xi)$ respectively. More specifically, they are defined by [79, 80, 199]

$$\begin{aligned} \alpha^{\mu\nu}(x^\xi) &= \epsilon^{\mu\sigma\tau} u^\nu{}_{;\sigma\tau}(x^\xi) \\ \theta^{\mu\nu}(x^\xi) &= \epsilon^{\mu\sigma\tau} \omega^\nu{}_{;\sigma\tau}(x^\xi) \end{aligned} \tag{11.1}$$

respectively, where u^ν is the displacement vector and ω^ν is the rotation vector. For a defect line along L, (11.1) becomes

$$\begin{aligned} \alpha^{\mu\nu}(x^\xi) &= \delta^\mu(L)\,(b^\nu - \Omega^{\nu\tau} x_\tau) \\ \theta^{\mu\nu}(x^\xi) &= \delta^\mu(L)\,\Omega^\nu \end{aligned} \tag{11.2}$$

respectively, where b^ν is the Burgers vector and Ω^ν is the Frank vector defined as per (10.3), and the defect line L has a core discontinuity in

the displacement and rotation fields, represented by the delta function $\delta(L)$ (see also (10.4) and subsequent equation). If the disclination axis is passing through x^0_τ, then the top equation (11.2) is given by

$$\alpha^{\mu\nu}(x^\xi) = \delta^\mu(L)\left(b^\nu - \epsilon^{\sigma\tau\nu}\Omega_\sigma(x_\tau - x^0_\tau)\right) . \tag{11.3}$$

Lazar [215] has proposed an approach to avoid the core discontinuity for a straight twist disclination in the field theory of elastoplasticity.

For dislocation density tensor $\alpha^{\mu\nu}$, the diagonal elements correspond to screw components, while off-diagonal components correspond to edge components. For disclination density tensor $\theta^{\mu\nu}$, the diagonal elements correspond to wedge components, while off-diagonal components correspond to twist components [78]. These defect density tensors satisfy the conservation laws [199]

$$\begin{aligned} \alpha^{\mu\nu}{}_{;\mu} &= -\epsilon^{\nu\sigma\tau}\theta_{\sigma\tau} \\ \theta^{\mu\nu}{}_{;\mu} &= 0 . \end{aligned} \tag{11.4}$$

In the following sections of this chapter, we will see how these defect density tensors impact the geometric properties of the spacetime continuum.

§11.3 Defect densities in continua

The dislocation and disclination density tensors $\alpha^{\mu\nu}$ and $\theta^{\mu\nu}$ can be written in terms of the defect strain and defect bend-twist tensors as [80]

$$\begin{aligned} \alpha^{\mu\nu} &= -\epsilon^{\mu\sigma\tau}\left(\not{\varepsilon}_\tau{}^\nu{}_{;\sigma} + \epsilon_\tau{}^{\nu\lambda}\not{\kappa}_{\sigma\lambda}\right) \\ \theta^{\mu\nu} &= -\epsilon^{\mu\sigma\tau}\not{\kappa}_\tau{}^\nu{}_{;\sigma} . \end{aligned} \tag{11.5}$$

The incompatibility tensor is given by [112, p. 124] [80]

$$i^{\mu\nu} = \tfrac{1}{2}\left(\epsilon^{\mu\sigma\tau}\alpha_\tau{}^\nu{}_{;\sigma} + \epsilon^{\nu\sigma\tau}\alpha_\tau{}^\mu{}_{;\sigma}\right) \tag{11.6}$$

where $i^{\mu\nu}$ is symmetric over the indices $(\mu\nu)$.

The contortion $K^{\mu\nu}$ and bend-twist $\kappa^{\mu\nu}$ tensors are expressed in terms of the dislocation density tensor $\alpha^{\mu\nu}$ and the disclination density tensor $\theta^{\mu\nu}$ as follows [79]:

$$K^{\nu\mu} = -\alpha^{\mu\nu} + \tfrac{1}{2}\,\delta^{\mu\nu}\alpha^\lambda{}_\lambda \tag{11.7}$$

$$\theta^{\mu\nu} - \tfrac{1}{2}\,\delta^{\mu\nu}\theta^\lambda{}_\lambda = -\epsilon^{\mu\alpha\beta}\left(\not{\kappa}^\nu{}_{\beta;\alpha} - \not{\kappa}_{\alpha\beta}{}^{;\nu}\right) . \tag{11.8}$$

where $\not{\kappa}^{\mu\nu}$ is the defect bend-twist tensor. The inverse relation is given by

$$\alpha^{\mu\nu} = -K^{\nu\mu} + \delta^{\mu\nu} K^{\lambda}{}_{\lambda} \,. \tag{11.9}$$

§11.4 Differential geometry of defects

As pointed out by Kleinert, "[a] crystal filled with dislocations and disclinations turns out to have the same geometric properties as an affine space with torsion and curvature, respectively" [199, p. 1333]. We follow the development of Kleinert [199, see Part IV, Chapter 2] in this section.

To properly deal with rotational deformations in the spacetime continuum, we need to add torsion to the differential geometry of general relativity which deals only with curvature. As we saw previously in section §11.1, this means that certain tensors are introduced, which are zero in the absence of torsion, in particular the *torsion tensor* $S_{\mu\nu}{}^{\lambda}$ defined by

$$S_{\mu\nu}{}^{\lambda} = \tfrac{1}{2} \left(\Gamma_{\mu\nu}{}^{\lambda} - \Gamma_{\nu\mu}{}^{\lambda} \right) \,, \tag{11.10}$$

which is the antisymmetric part of the connection $\Gamma_{\mu\nu}{}^{\lambda}$ and which transforms like a proper tensor.

The connection can then be decomposed into a Christoffel part and the contortion tensor. Defining the modified connection $\Gamma_{\mu\nu\lambda}$ according to

$$\Gamma_{\mu\nu\lambda} = \Gamma_{\mu\nu}{}^{\tau} g_{\tau\lambda} \,, \tag{11.11}$$

the modified connection is written as

$$\Gamma_{\mu\nu\lambda} = \{\mu\nu, \lambda\} + K_{\mu\nu\lambda} \tag{11.12}$$

where $\{\mu\nu, \lambda\}$ is the Christoffel symbol of the first kind and $K_{\mu\nu\lambda}$ is the *contortion tensor* defined as

$$K_{\mu\nu\lambda} = S_{\mu\nu\lambda} - S_{\nu\lambda\mu} + S_{\lambda\mu\nu} \tag{11.13}$$

and $S_{\mu\nu\lambda} = S_{\mu\nu}{}^{\tau} g_{\tau\lambda}$. $K_{\mu\nu\lambda}$ is antisymmetric in the last two indices.

The *curvature tensor* $R_{\mu\nu\sigma\tau}$ is still given by

$$R_{\mu\nu\sigma\tau} = \partial_{\mu} \Gamma_{\nu\sigma}{}^{\tau} - \partial_{\nu} \Gamma_{\mu\sigma}{}^{\tau} + \Gamma_{\mu\sigma}{}^{\kappa} \Gamma_{\nu\kappa}{}^{\tau} - \Gamma_{\nu\sigma}{}^{\kappa} \Gamma_{\mu\kappa}{}^{\tau} \,. \tag{11.14}$$

However, it is important to note that the connection is given by (11.12), using (11.11), and includes the contortion tensor in addition to the Christoffel symbol. The curvature tensor of general relativity uses only the Christoffel symbol, without the contortion tensor, and is known

as the *Riemann curvature tensor*. Spaces with curvature and torsion are known as *Riemann-Cartan* spaces, while spaces with no torsion are known as *Riemann* spaces [199].

We consider the metric tensor of (1.7) for small displacements in Minkowski spacetime:

$$g_{\mu\nu} = \eta_{\mu\nu} + \partial_\mu u_\nu + \partial_\nu u_\mu \,. \tag{11.15}$$

Then the connection, torsion tensor and curvature tensor are given by [199, p. 1359]

$$\begin{aligned} \Gamma_{\mu\nu\lambda} &= \partial_\mu \partial_\nu u_\lambda \\ S_{\mu\nu\lambda} &= \tfrac{1}{2} \left(\partial_\mu \partial_\nu - \partial_\nu \partial_\mu \right) u_\lambda \\ R_{\mu\nu\kappa\lambda} &= \left(\partial_\mu \partial_\nu - \partial_\nu \partial_\mu \right) \partial_\kappa u_\lambda \end{aligned} \tag{11.16}$$

respectively. The Einstein tensor is given by [199, p. 1360]

$$G^{\mu\nu} = \tfrac{1}{4}\, e_\gamma{}^{\nu\kappa\lambda} e^{\mu\gamma\sigma\tau} R_{\kappa\lambda\sigma\tau} \tag{11.17}$$

where the Levi-Civita pseudo-tensor $e^{\mu\nu\sigma\tau}$ is the covariant version of the Levi-Civita pseudo-tensor $\epsilon^{\mu\nu\sigma\tau}$ given by

$$e_{\mu\nu\sigma\tau} = \sqrt{-g}\, \varepsilon_{\mu\nu\sigma\tau} \tag{11.18}$$

and $\sqrt{-g}$ is the positive determinant of $-g_{\mu\nu}$. Note also that

$$e^{\mu\nu\sigma\tau} = \frac{1}{\sqrt{-g}}\, \epsilon^{\mu\nu\sigma\tau} \,. \tag{11.19}$$

We note that the curvature tensor is that of *Riemann-Cartan* spaces.

The dislocation density tensor is related to the torsion tensor according to

$$\alpha_{\mu\nu} = \epsilon_\mu{}^{\kappa\lambda} \Gamma_{\kappa\lambda\nu} = \epsilon_\mu{}^{\kappa\lambda} S_{\kappa\lambda\nu} \tag{11.20}$$

and from (11.12), to the contortion tensor according to

$$\alpha_{\mu\nu} = \epsilon_\mu{}^{\kappa\lambda} K_{\kappa\lambda\nu} \,. \tag{11.21}$$

Nye's contortion tensor of rank two is obtained from the contortion tensor using

$$K_{\mu\nu} = \tfrac{1}{2}\, K_{\mu\kappa\lambda} \epsilon^{\kappa\lambda}{}_\nu \tag{11.22}$$

and substituting into (11.21), we obtain

$$\alpha^{\mu\nu} = -K^{\nu\mu} + \delta^{\mu\nu} K^\lambda{}_\lambda \tag{11.23}$$

as before (see (11.9)). Nye's contortion tensor can also be written in terms of the displacement and rotation fields as

$$K_{\mu\nu} = \partial_\mu \omega_\nu - \epsilon_\nu{}^{\sigma\tau} \partial_\sigma u_{\tau\mu} \,. \tag{11.24}$$

The disclination density tensor is related to the Einstein tensor of (11.17)

$$\theta_{\mu\nu} = G_{\mu\nu} \tag{11.25}$$

while the incompatibility tensor, also known as the defect density tensor (dislocations and disclinations), is related to the Einstein tensor formed from the Riemannian curvature tensor (no torsion), which we denote with a flat diacritical mark, as follows

$$i_{\mu\nu} = \bar{G}_{\mu\nu} \,. \tag{11.26}$$

§11.5 Implications for STCED and GTR

This chapter provides a brief introduction to the field theory of defects. As mentioned in section §8.1, using defect density distributions results in field equations using the methods of differential geometry which are amenable to gauge theories. The modern theoretical descriptions, used mostly in condensed matter physics, are mostly in terms of gauge theory and differential geometry, using continuous distributions of defect densities (see for example [199]). At this time, *STCED* does not use distributions of defect densities, although its future use is not precluded, and this chapter has been presented for completeness to allow readers to position research papers in the theoretical framework of defect theory.

It is of particular interest to note that the introduction of small displacements in Minkowski spacetime results in the introduction of the infinitesimal strain tensor in the metric, as seen in (11.15). Of particular interest also is that the dislocation density tensor is related to the torsion tensor while the disclination density tensor is related to the Einstein tensor. Finally, the incompatibility tensor, also known as the defect density tensor that includes both dislocations and disclinations, is related to the Einstein tensor formed from the Riemannian curvature tensor as evidenced in (11.26). This leads us again to the differential geometry of the General Theory of Relativity and shows the close relationship between *STCED* and GTR.

Chapter 12

Wave-Particle Duality in STCED

§12.1 Wave-particle duality in electromagnetism

In this chapter, we concentrate on the built-in wave-particle duality that is present in *STCED*. We first consider the simpler case of electromagnetism, in particular the photon wavefunction, and then generalize the result to *STCED* in general.

In electromagnetism, as shown in §5.3.1, the volume dilatation is given by $\varepsilon = 0$. Hence, the photon is massless and there is no longitudinal mode of propagation. Electromagnetic waves are massless transverse distortion waves.

Photons correspond to an energy flow along the direction of propagation in 3-space resulting from the Poynting vector. This longitudinal electromagnetic energy flux is massless as it is due to distortion, not dilatation, of the spacetime continuum. However, because this energy flux is along the direction of propagation, it gives rise to the particle aspect of the electromagnetic field, the photon, even though the photon is not a particle.

We should note that the modern understanding of photons is that they are massless excitations of the quantized electromagnetic field, not particles *per se*. Thus in this case, the kinetic energy in the longitudinal direction is carried by the distortion part of the deformation, while the dilatation part, which carries the rest-mass energy, is not present as the mass is 0. This result is thus in agreement with orthodox quantum electrodynamics.

This situation provides us with an opportunity to investigate the transverse mode of propagation, independently of the longitudinal mode. In general, the transverse propagation of electromagnetic waves is given by sinusoidal waves ψ and the intensity of the waves, corresponding to the energy density, is given by $|\psi|^2$. This is equivalent to the modulus squared of the wavefunction used in quantum mechanics as a probability density. A full analysis requires that we investigate further the quantum mechanics of the photon, and in particular, the photon wavefunction.

§12.2 Photon wavefunction

The photon wavefunction is a first quantization description of the electromagnetic field [41, 56]. Historically, this development was not done, as second quantization of the electromagnetic field was first developed. As a result, photon wave mechanics is not fully accepted in the scientific community, mainly because of the differences between particle and photon dynamics. As opposed to a particle, the photon has zero rest-mass and propagates at the speed of light. In addition, the position operator cannot be defined for a photon, only the momentum operator (known as the *photon localization problem*).

Bialynicki-Birula [41–45], Sipe [328], and more recently Mohr [259], Raymer and Smith [301–303] and others have derived and promoted the use of the photon wavefunction. Bialynicki-Birula defines the photon wavefunction as "a complex vector-function of space coordinates r and time t that adequately describes the quantum state of a single photon" [41]. He sees three advantages to introducing a photon wavefunction [44]: it provides 1) a unified description of both massive and massless particles both in first quantization and second quantization; 2) an easier description of photon dynamics without having to resort to second quantization; 3) new methods of describing photons.

As pointed out in [56] and references therein, the photon wave equation is now used to study the propagation of photons in media, the quantum properties of electromagnetic waves in structured media, and the scattering of electromagnetic waves in both isotropic and anisotropic inhomogeneous media. Raymer and Smith [302, 303] have extended the use of the photon wavefunction to the analysis of multi-photon states and coherence theory. To the above list, in this book, we add an additional benefit of the photon wavefunction: the clarification of the physical interpretation of the quantum mechanical wavefunction [244].

The photon wavefunction is derived from the description of the electromagnetic field based on the complex form of the Maxwell equations first used by Riemann, Silberstein and Bateman [41] (the Riemann–Silberstein vector). As summarized by Bialynicki-Birula [45], "[t]he Riemann–Silberstein vector on the one hand contains full information about the state of the classical electromagnetic field and on the other hand it may serve as the photon wave function in the quantum theory". The Maxwell equations are then written as [41]

$$\begin{aligned} i\,\partial_t \mathbf{F}(\mathbf{r},t) &= c\,\nabla \times \mathbf{F}(\mathbf{r},t) \\ \nabla \cdot \mathbf{F}(\mathbf{r},t) &= 0 \end{aligned} \tag{12.1}$$

where

$$\mathbf{F}(\mathbf{r},t) = \left(\frac{\mathbf{D}(\mathbf{r},t)}{\sqrt{2\epsilon_0}} + i\,\frac{\mathbf{B}(\mathbf{r},t)}{\sqrt{2\mu_0 R}} \right) \tag{12.2}$$

and where $\mathbf{D}(\mathbf{r},t)$ and $\mathbf{B}(\mathbf{r},t)$ have their usual significance.

Then the dynamical quantities like the energy density and the Poynting vector are given by [41]

$$\begin{aligned} E &= \int \mathbf{F}^* \cdot \mathbf{F}\ \mathrm{d}^3 r \\ \mathbf{S} &= \frac{1}{2ic} \int \mathbf{F}^* \times \mathbf{F}\ \mathrm{d}^3 r \end{aligned} \tag{12.3}$$

where $\mathbf{F}^*$ denotes the complex conjugate. The sign selected in (12.2) reflects positive helicity (projection of the spin on the direction of momentum) corresponding to left-handed circular polarization. Photons of negative helicity corresponding to right-handed circular polarization are represented by changing the sign from i to $-i$ in (12.2). Hence (12.2) can be written as

$$\mathbf{F}_{\pm}(\mathbf{r},t) = \left(\frac{\mathbf{D}(\mathbf{r},t)}{\sqrt{2\epsilon_0}} \pm i\,\frac{\mathbf{B}(\mathbf{r},t)}{\sqrt{2\mu_0}} \right) \tag{12.4}$$

to represent both photon polarization states.

A photon of arbitrary polarization is thus represented by a combination of left- and right-handed circular polarization states. The photon wavefunction is then given by the six-component vector

$$\Psi(\mathbf{r},t) = \begin{pmatrix} \mathbf{F}_+(\mathbf{r},t) \\ \mathbf{F}_-(\mathbf{r},t) \end{pmatrix}. \tag{12.5}$$

The corresponding photon wave equation is discussed in [44].

§12.3 Physical interpretation of the photon wavefunction

From (12.5) and (12.4), we calculate the modulus squared of the photon wavefunction to obtain [56]

$$|\Psi(\mathbf{r},t)|^2 = \left(\frac{\epsilon_0 |\mathbf{E}|^2}{2} + \frac{|\mathbf{B}|^2}{2\mu_0} \right). \tag{12.6}$$

The modulus squared of the photon wavefunction $\Psi(\mathbf{r},t)$ gives the electromagnetic energy density at a given position and time. This is the physical interpretation of the quantum mechanical $|\Psi(\mathbf{r},t)|^2$ for electromagnetic transverse waves in the absence of longitudinal waves.

Bialynicki-Birula proposes to convert $|\Psi(\mathbf{r},t)|^2$ to a probability density as required by the accepted quantum mechanical probabilistic interpretation [44]. This he achieves by dividing the modulus squared of the photon wavefunction by the expectation value of the energy $<E>$ [44, see his equation (44)]. In this way, it is made to describe in probabilistic terms the energy distribution in space associated with a photon.

Thus the probabilistic formulation of quantum theory is preserved, while the physical interpretation of $|\Psi|^2$ is shown to correspond to an energy density. Raymer and Smith [303] state that "[a] strong argument in favour of the energy-density wave function form of PWM [Photon Wave Mechanics] is that it bears strong connections to other, well-established theories—both quantum and classical—such as photodetection theory, classical and quantum optical coherence theory, and the biphoton amplitude, which is used in most discussions of spontaneous parametric down conversion".

Hence, we have to conclude that the appropriate physical interpretation of $|\Psi|^2$ is that it represents a physical energy density, not a probability density. However, the energy density can be converted to a probability density once it is normalized with the system energy (as done by Bialynicki-Birula for the photon wavefunction). In this way, *STCED* does not replace the probabilistic formulation of quantum theory, it just helps to understand the physics of quantum theory. The two formulations are equivalent, which explains the success of the probabilistic formulation of quantum theory. In actual practice, the quantum mechanical probability formulation can be used as is, as it gives the same results as the physical energy density formulation of *STCED*. However, the physical intensity waves of *STCED* help us understand the physics of the quantum mechanical wavefunction and the physics of wave-particle duality.

It is important to note that the energy density physical interpretation of $|\Psi|^2$ applies just as much to systems as to single particles, as for the probability density interpretation.

§12.4 Wave-particle duality in STCED

In *STCED*, the displacement u^ν of a deformation from its undeformed state can be decomposed into a longitudinal (dilatation) component $u^\nu_\parallel$ and a transverse (distortion) component $u^\nu_\perp$. The volume dilatation ε is given by the relation [238, see (44)]

$$\varepsilon = u^\mu{}_{;\mu} \equiv u_\parallel{}^\mu{}_{;\mu}. \tag{12.7}$$

The longitudinal displacement wave equation and the transverse displacement wave equation of a deformation are given respectively by (see §7.2)

$$\begin{aligned} \nabla^2 u_{\parallel}^{\nu} &= -\frac{\bar{\mu}_0 + \bar{\lambda}_0}{\bar{\mu}_0}\, \varepsilon^{,\nu} \\ \nabla^2 u_{\perp}^{\nu} + \frac{\bar{k}_0}{\bar{\mu}_0}\, \varepsilon\,(x^{\mu})\; u_{\perp}^{\nu} &= 0 \end{aligned} \tag{12.8}$$

where ∇^2 is the four-dimensional operator, $\bar{\lambda}_0$ and $\bar{\mu}_0$ are the Lamé elastic constants of the spacetime continuum and $\bar{k}_0$ is the elastic force constant of the spacetime continuum. The constant $\bar{\mu}_0$ is the shear modulus (the resistance of the continuum to *distortions*) and $\bar{\lambda}_0$ is expressed in terms of $\bar{\kappa}_0$, the bulk modulus (as in section §2.1) according to

$$\bar{\lambda}_0 = \bar{\kappa}_0 - \bar{\mu}_0/2 \tag{12.9}$$

in a four-dimensional continuum. The wave equation for $u_{\parallel}^{\nu}$ describes the propagation of longitudinal displacements, while the wave equation for $u_{\perp}^{\nu}$ describes the propagation of transverse displacements in the spacetime continuum. The *STCED* deformation wave displacements solution is similar to Louis de Broglie's "double solution" [75, 76].

§12.4.1 *Wave propagation in* STCED

The electromagnetic case, as seen in section §12.1, provides a physical interpretation of the wavefunction for transverse wave displacements. This interpretation should apply in general to any wavefunction Ψ. In *STCED*, in the general case, every deformation can be decomposed into a combination of a transverse mode corresponding to the wave aspect of the deformation, and a longitudinal mode corresponding to the particle aspect of the deformation [239]. Thus the physical interpretation of section §12.3 applies to the general *STCED* transverse wave displacements, not only to the electromagnetic ones.

Hence, $|\Psi|^2$ represents the physical intensity (energy density) of the transverse (*distortion*) wave, rather than the probability density of quantum theory. It corresponds to the transverse field energy of the deformation. It is not the same as the particle, which corresponds to the longitudinal (*dilatation*) wave displacement and is localized within the deformation via the massive volume dilatation, as discussed in the next section §12.4.2. However, $|\Psi|^2$ can be normalized with the system energy and converted into a probability density, thus allowing the use of the existing probabilistic formulation of quantum theory. Additionally,

the physical intensity waves of *STCED* help us understand the physics of wave-particle duality and resolve the paradoxes of quantum theory.

§12.4.2 *Particle propagation in* STCED

Particles propagate in the spacetime continuum as longitudinal wave displacements. Mass is proportional to the volume dilatation ε of the longitudinal mode of the deformation as per (2.24). This longitudinal mode displacement satisfies a wave equation for ε, different from the transverse mode displacement wave equation for Ψ. This longitudinal dilatation wave equation for ε is given by [238, see (204)]

$$\nabla^2 \varepsilon = -\frac{\bar{k}_0}{2\bar{\mu}_0 + \bar{\lambda}_0}\, u^{\nu}_{\perp} \varepsilon_{;\nu}\,. \tag{12.10}$$

It is important to note that the inhomogeneous term on the R.H.S. includes a dot product coupling between the transverse displacement $u^{\nu}_{\perp}$ and the gradient of the volume dilatation $\varepsilon_{;\nu}$ for the solution of the longitudinal dilatation wave equation for ε. This explains the behavior of electrons in the double slit interference experiment.

The transverse distortion wave equation for $\omega^{\mu\nu}$ [238, see (210)]

$$\nabla^2 \omega^{\mu\nu} + \frac{\bar{k}_0}{\bar{\mu}_0}\, \varepsilon\left(x^{\mu}\right) \omega^{\mu\nu} = \frac{1}{2}\, \frac{\bar{k}_0}{\bar{\mu}_0}\, (\varepsilon^{;\mu} u^{\nu}_{\perp} - \varepsilon^{;\nu} u^{\mu}_{\perp}) \tag{12.11}$$

shows a R.H.S. cross product coupling between the transverse displacement $u^{\nu}_{\perp}$ and the gradient of the volume dilatation $\varepsilon^{;\mu}$ for the solution of the transverse distortion wave equation for $\omega^{\mu\nu}$. The transverse distortion wave $\omega^{\mu\nu}$ corresponds to a multi-component wavefunction Ψ.

A deformation propagating in the spacetime continuum consists of a combination of a transverse and a longitudinal wave. The transverse wave is the source of the interference pattern in double slit experiments, which impacts the location of the associated longitudinal wave of the individual particle in generating the interference pattern. The longitudinal dilatation wave behaves as a particle and goes through one of the slits, even as it follows the interference pattern dictated by the transverse distortion wave, as observed experimentally [150, see in particular Figure 4] and as seen in the coupling between $\varepsilon_{;\nu}$ and $u^{\nu}_{\perp}$ in (12.10) and (12.11) above.

These results are in agreement with the results of the Jánossy-Naray, Clauser, and Dagenais and Mandel experiments on the self-interference of photons and the neutron interferometry experiments performed by Bonse and Rauch [322, see pp. 73-81]. The transverse distortion wave

generates the interference pattern, while the longitudinal wave's dilatation (particle) follows a specific action, with its final location guided by the transverse wave's interference pattern.

The longitudinal wave is similar to the de Broglie "singularity-wave function" [75]. However, in *STCED* the particle is not a singularity of the wave, but is instead characterized by its mass which arises from the volume dilatation propagating as part of the longitudinal wave. There is no need for the collapse of the wavefunction Ψ, as the particle resides in the longitudinal wave, not the transverse one. A measurement of a particle's position is a measurement of the longitudinal wave, not the transverse wave.

Chapter 13

Wavefunctions, Operators and Measurements

§13.1 The mathematics of wavefunctions

In this chapter, we will review the mathematics and physics of quantum theory to be in a better position to analyze the theory and clarify its physical nature within *STCED* in the following chapters. One will often hear physicists say that quantum mechanics is difficult to understand as it is not intuitive. However, as the saying goes, "ce qui se conçoit bien s'énonce clairement", *i.e.* "that which is well understood is clearly explained".

To understand quantum mechanics, one must understand the mathematics that underlie the theory. We will not start by jumping in the middle of the mathematics as is done in most textbooks, as this just confuses the situation. Instead, we will start with the basic mathematical concepts and see how they pertain to the mathematics of quantum theory to be better able to understand the physics, and interpretation, of quantum physics. We will eventually get into the more arcane aspects of the theory, but first, we have to start at the beginning.

A point P_3 in three dimensions is specified by numbers along three mutually independent axes, such as the cartesian coordinates (x, y, z), that span (cover) the three-dimensional space. The cartesian axes are characterized by three vectors $\vec{i}, \vec{j}, \vec{k}$ that are usually normalized to 1 to provide three unit vectors $\hat{i}, \hat{j}, \hat{k}$. Their mutual independence is shown by their (dot) products being equal to zero: $\hat{i} \cdot \hat{j} = 0$, $\hat{j} \cdot \hat{k} = 0$ and $\hat{k} \cdot \hat{i} = 0$ which shows that the unit vectors are orthogonal (orthonormal to be exact).

The coordinates of the point can then be written as

$$P_3 = x\hat{i} + y\hat{j} + z\hat{k}\,. \tag{13.1}$$

This is known as a vector space. Mathematicians have other conditions that they impose on the vector space, but these are the basic concepts. The three-dimensional vector space can be extended to an n-dimensional vector space using

$$P_n = \sum_{m=1}^{n} x_m \hat{i}_m \tag{13.2}$$

where $\hat{i}_m$ are the n unit vectors spanning the n-dimensional vector space and the x_m are the coordinate values along the axes spanning the vector space that describes the point P_n. This is very basic mathematics, but it is highly relevant to understanding the mathematical theory of quantum mechanics.

At the end of the nineteenth century, mathematicians, including David Hilbert, noticed that orthogonal sets of basis functions $g_m(x)$ could also be obtained in connection with Sturm-Liouville problems (related to certain types of differential equations) that had the same properties as vector spaces, including [205]

– product of basis functions

$$(g_m, g_n) = \int_a^b g_m(x) g_n(x) dx \,; \tag{13.3}$$

– norm ("length") of a basis function

$$\|g_m\|^2 = \int_a^b g_m^2(x) dx \,; \tag{13.4}$$

– orthogonality of the set of, in this case orthonormal, basis functions where their norm is equal to one

$$(g_m, g_n) = \delta_{mn} \,; \tag{13.5}$$

– representation of an arbitrary function $f(x)$ in terms of the basis functions $g_m(x)$

$$\begin{aligned} f(x) &= \sum_m c_m g_m(x) \quad \text{where} \\ (f, g_m) &= c_m \|g_m\|^2 . \end{aligned} \tag{13.6}$$

This is known as a function space.

In particular, quantum mechanics uses a function space known as a Hilbert space, where the (inner) product is defined as

$$\langle f, g \rangle = \int_{-\infty}^{\infty} f(x) g(x) dx \,. \tag{13.7}$$

More specifically, a complex Hilbert space is used in quantum theory, meaning that the functions are complex functions, not just real functions. It is important to note that the complex Hilbert space is a *mathematical* space spanned (covered) by a set of orthogonal basis functions.

Any function in that mathematical space can be expressed as a combination of the set of orthogonal basis functions as (13.6), where the coefficients c_m are themselves complex functions of the coordinates.

This is, in a nutshell, the mathematical basis of quantum theory, as laid out by mathematician von Neumann in the 1930s [361]. In quantum mechanics, the Hilbert space is known as the state space, and the set of basis functions are known as state vectors. General system states (wavefunctions) are combinations of the state vectors similar to (13.6) in the *mathematical* state space. The coefficients of (13.6) are expressed as probability amplitudes.

Some may consider this to be an oversimplification of the mathematical theory, but at this time, this is sufficient for our purpose as we are pushing back the foliage to have a better view at the physics and interpretation of the theory. We have not looked at other aspects of quantum mechanics such as operators as these are embellishments of the theory that are not required for our current discussion of the quantum physics fundamentals. We will look at those in due time.

Everything we have looked at till now makes sense and is a very reasonable approach to the analysis of quantum physics. Quantum physics needs to be based on probabilistic analysis as we, at our level, are not currently in a position to analyze the quantum physics at that level to the same degree that we can at the macroscopic level, although this does not preclude being able to do so in the future as our physical theories improve further.

This mathematical theory provides an elegant mean of carrying calculations on quantum physical systems, as is evidenced by the calculational success of quantum theory. However, problems are encountered in the interpretation of the theory which is taken too literally. The basic source of the problem is that the mathematical Hilbert space is taken to be a physical space, and the wavefunction written as for example (13.6) is taken to represent a physical system state that is a combination of state vectors that exists in an evanescent state until it is measured (*i.e.* observed). At that point, the wavefunction "collapses" into one of the states that is measured. This is an interpretation of the mathematics that is not required and that really belongs into metaphysics. Interpretations based on giving physical reality to the Hilbert mathematical space are philosophical musings at best.

The justification for this interpretation is usually ascribed to the indeterminacy of the quantum world resulting from, among other reasons, the Heisenberg Uncertainty Principle and, since the 1960s, to Bell's theorem [19]. As shown in [237] and section §13.3, the Heisenberg Un-

certainty Principle arises because of the dependency of momentum on wave number that exists at the quantum level. Quantum mechanical conjugate variables are Fourier transform pairs of variables. It is important to differentiate between the measurement limitations that arise from the properties of Fourier transform pairs, and any inherent limitations that may or may not exist for those same variables independently of the measurement process. Quantum theory currently assumes that the inherent limitations are the same as the measurement limitations. As shown in [237] and section §13.3, quantum measurement limitations affect our perception of the quantum environment only, and are not inherent limitations of the quantum level. Bell's theorem will be considered in greater detail in section §13.4.

Independently of this analysis, when systems are "prepared", they end up being in definite physical states, not evanescent states. These states obey the *STCED* wave equations, which can include entangled states as we will see in section §18.9. When a component of an entangled state is measured, one does not see superluminal communication between the entangled states, but rather one measures the states that the system was initially prepared in, and the probability analysis needs to be based on mathematical probability theory and Bayesian analysis, *i.e.* conditional probabilities, as clearly demonstrated by Jaynes [182–184]. What changes instantaneously is our state of knowledge of the system, not the system itself. Certainly, there is evidence of nonlocality of field theories at the quantum level, as covered further for *STCED* in section §18.8, but there is a large degree of separation between the nonlocality concept and the wavefunction "collapse" concept. This will be considered in greater detail in sections §13.5 and §13.6.

The latter leads to concepts such as Schrödinger's cat where, given a proper experimental setup, an unobserved cat is in a half-alive or half-dead physical state depending on whether a random event has happened or not. When an observer checks on the cat, the wavefunction "collapses" and the cat is found either dead or alive. This is empty philosophy, taken to its *reductio ad absurdum* limit. If the random event occurs, the cat will die, and we will eventually find out from the smell – no need for an observer to "collapse" the wavefunction! Or is it the smell acting as surrogate observer that "collapses" the wavefunction?

We see questions asked such as whether there is a sound generated if a tree crashes in a forest with no observer to hear the sound. Of course, a physical analysis of the problem shows that sound energy is still emitted in the audible range, whether there is an observer present to hear it or not. This example is an evident one, but there is much confusion that

arises from this concept that is flowing in the undercurrents of modern physics research. For example, a search for "wavefunction collapse" (and "wave function collapse") in the arXiv archive paper titles results in more than 120 papers. This is a modern equivalent of the middle ages question on the number of angels that can dance on the head of a pin. The need for an observer to force the wavefunction to "collapse" is a modern version of anthropocentrism, *i.e.* human-centric philosophy.

§13.2 Wavefunctions and operators

Now that we have a better perspective on the mathematical formalism of quantum mechanics and its interpretation difficulties, we will consider the physical underpinnings of quantum theory to better understand quantum physics and its interpretation.

In the previous section §13.1, we have used the probabilistic interpretation of the wavefunction to discuss its physical reality. As we have seen in section §12.3 on the physical interpretation of the photon wavefunction, the probabilistic use of the wavefunction is valid provided that it is normalized as discussed in that section. The modulus squared of the photon wavefunction $\Psi(\mathbf{r}, t)$ given by (12.6) corresponds to the electromagnetic energy density at a given position and time. It is converted to a probability density by dividing the modulus squared of the photon wavefunction by the system energy [44].

These results were derived using the wavefunction of the simpler and better understood electromagnetic field photon. As we saw in §12.4.1, in the general *STCED* case, $|\Psi|^2$ represents the physical intensity (energy density) of the transverse (*distortion*) wave, corresponding to the transverse field energy of the deformation. $|\Psi|^2$ can be normalized with the system energy and converted into a probability density, thus allowing the use of the existing probabilistic formulation of quantum theory. This we now cover in greater detail.

In particular, wavefunctions are the solution of quantum mechanical wave equations. They are thus wave solutions, which we call wavefunctions, also known as kets $|\psi\rangle$ in the Dirac formalism. As the modulus squared of the wavefunction $|\psi|^2$ corresponds to the energy density of the wavefunction as mentioned previously, this means that the integral over the volume V is the system energy. It is calculated from

$$E = \int_{-\infty}^{\infty} |\psi|^2 \, dV = \int_{-\infty}^{\infty} \psi^* \psi \, dV \,, \tag{13.8}$$

where ψ^* denotes complex conjugation. In quantum mechanics, this is

also written as $\langle\psi|\psi\rangle$ using Dirac notation, and is used as normalization factor which, in addition to ensuring that the wavefunctions are orthonormal, also unwittingly converts $|\psi|^2$ from an energy density to a probability density.

As seen in section §13.1 and in this section, quantum mechanics is couched in its own formalism and terminology, although it is using standard mathematical theory. A good part of this is due to its historical development where a formalism different from the mathematical one, and a terminology that reflected a certain physical picture of what was perceived as the explanation of the new theory were adopted.

The formalism and terminology has gradually become more formalized and less physical in its understanding of the theory. One only needs to look at textbooks, such as [296, 300] from the 1960s with its emphasis on wave packets and wave mechanics and [12] from the late 1990s with its formal presentation of the theory and absence of wave packets or wave mechanics concepts. The axiomatization of quantum mechanics has resulted in a theory steeped in its own mathematical formalism disconnected from physical reality, reinforced by the mysterious aura projected by the current interpretation of the theory.

The calculation of observables using operators is a case in point. For example, [12, see p. 43] states

> To each *dynamical variable* (physical concept) there corresponds a *linear operator* (mathematical object), and the possible values of the dynamical variable are the eigenvalues of the operator. [emphasis in original]

and later states that operators correspond to observables. This is calculated from $\text{Obs} = \langle\psi|\text{Op}|\psi\rangle$ using Dirac notation. Mathematically, this is derived from the expectation value of variable X which is given by

$$\langle X\rangle = \frac{\int_{-\infty}^{\infty} \psi^*\, X\, \psi\, dV}{\int_{-\infty}^{\infty} \psi^*\psi\, dV} \tag{13.9}$$

where $\langle X\rangle$ can be measured experimentally.

The momentum and energy operators, $-i\hbar\,\vec{\nabla}$ and $i\hbar\,\partial/\partial t$ respectively, give rise to questions on their nature and is best understood as a result of the relationship between momentum $\vec{p}$ and wave vector $\vec{k}$ at the quantum level [237]. Starting with the wavefunction of a free particle in one dimension

$$\psi(x,t) = A\exp i(k_x x - \omega t + \varphi) \tag{13.10}$$

where A is the amplitude and φ is a phase factor, and taking the partial derivative with respect to x, we have

$$\frac{\partial}{\partial x}\,\psi(x,t) = ik_x A \exp i(k_x x - \omega t + \varphi) = i\frac{p_x}{\hbar}\,\psi(x,t)\,, \tag{13.11}$$

and hence the operator for p_x operating on the wavefunction is given by

$$\mathrm{Op}(p_x) = -i\hbar\,\frac{\partial}{\partial x}\,. \tag{13.12}$$

Similarly, by partial differentiation of (13.10) with respect to t, we obtain the operator for E operating on the wavefunction given by

$$\mathrm{Op}(E) = i\hbar\,\frac{\partial}{\partial t}\,. \tag{13.13}$$

Mathematically, observables are nothing more than the expectation value of a variable (that is called an operator) of a function named ψ the wavefunction. The requirement that the operator be hermitian, *etc* comes from the mathematics. Hence this aspect of quantum theory is couched in terminology and interpretation that is not required by the mathematical theory or the physical nature of the process.

§13.3 The Heisenberg Uncertainty Principle and the Nyquist-Shannon Sampling Theorem

The Heisenberg Uncertainty Principle is a cornerstone of quantum mechanics. As noted by Hughes [171, see pp. 265-266], the interpretation of the Principle varies

- from expressing a limitation on measurement as originally derived by Heisenberg [154] (Heisenberg's microscope),
- to being the variance of a measurement carried out on an ensemble of particles [294] [226],
- to being inherent to a microsystem [73], meaning essentially that there is an indeterminism to the natural world which is a basic characteristic of the quantum level.

Greenstein retains only the first and last alternatives [140, see p. 51].

However, the Heisenberg Uncertainty Principle can be derived from considerations which clearly demonstate that these interpretations of the principle are not required by its mathematical formulation. This derivation, based on the application of Fourier methods, is given in various mathematical and engineering textbooks, for example [54, see p. 141].

§13.3.1 *Consistent derivation of the Heisenberg Uncertainty Principle*

In the Fourier transform literature, the Heisenberg Uncertainty Principle is derived from a general theorem of Fourier theory called the Uncertainty Theorem [54]. This theorem states that the effective width of a function times the effective width of its transform cannot be less than a minimum value given by

$$W(f) \cdot W(\tilde{f}) \geq 1/2 \tag{13.14}$$

where f is the function of interest and $\tilde{f}$ is its Fourier transform. $W(f)$ is the effective width of function f, defined by

$$|W(f)|^2 = \frac{\int_{-\infty}^{\infty} |f(u)|^2 [u - M(f)]^2 du}{\int_{-\infty}^{\infty} |f(u)|^2 du} \tag{13.15}$$

and $M(f)$ is the mean ordinate defined by

$$M(f) = \frac{\int_{-\infty}^{\infty} |f(u)|^2 u du}{\int_{-\infty}^{\infty} |f(u)|^2 du}. \tag{13.16}$$

There are several points that must be noted with respect to this derivation: Eq.(13.14) applies to a Fourier transform pair of variables. Taking the simple case of time t and frequency ν to illustrate the point: If we consider the function f to be the function that describes a time function t, then the width of the function, $W(f)$, can be denoted as $W(f) = \Delta t$. The Fourier transform of function t is the frequency function ν and the width of this function can be denoted as $W(\tilde{t}) = W(\nu) = \Delta\nu$. Substituting in (13.14), the Uncertainty Theorem then yields

$$\Delta t \cdot \Delta\nu \geq 1/2. \tag{13.17}$$

However, if one wishes to use the circular frequency $\omega = 2\pi\nu$ instead, (13.17) becomes

$$\Delta t \cdot \Delta\omega \geq \pi. \tag{13.18}$$

It is thus necessary to take special care to clearly identify the Fourier transform variable used as it impacts the R.H.S. of the resulting Uncertainty relation (see for example [367] and [142, pp. 21-22]).

Equations (13.17) and (13.18) above correspond to the following definitions of the Fourier transform respectively [367]:

Equation (13.17):

$$f(t) = \int_{-\infty}^{\infty} \tilde{f}(\nu) \exp(2\pi i \nu t) d\nu \tag{13.19}$$

$$\tilde{f}(\nu) = \int_{-\infty}^{\infty} f(t) \exp(-2\pi i \nu t) dt \tag{13.20}$$

Equation (13.18):

$$f(t) = \frac{1}{2\pi} \int_{-\infty}^{\infty} \tilde{f}(\omega) \exp(i\omega t) d\omega \tag{13.21}$$

$$\tilde{f}(\omega) = \int_{-\infty}^{\infty} f(t) \exp(-i\omega t) dt. \tag{13.22}$$

Sometimes the factor $1/2\pi$ is distributed between the two integrals (the Fourier and the Inverse Fourier Transform Integrals) as $1/\sqrt{2\pi}$. In Physics, (13.21) and (13.22) are preferred, as this eliminates the cumbersome factor of 2π in the exponential (see for example [382, p. 12]), but care must then be taken to ensure the resulting factor of $1/2\pi$ in (13.21) is propagated forward in derivations using that definition.

Using the relation $E = h\nu$, where h is Planck's constant, in (13.17) above, or the relation $E = \hbar\omega$, where $\hbar = h/2\pi$, in (13.18) above, one obtains the same statement of the Heisenberg Uncertainty Principle namely

$$\Delta E \cdot \Delta t \geq h/2 \tag{13.23}$$

in both cases.

Similarly for the position x, if we consider the function f to be the function that describes the position x of a particle, then the width of the function, $W(f)$, can be denoted as $W(f) = \Delta x$. The Fourier transform of function x is the function $\tilde{x} = \lambda^{-1}$ and the width of this function can be denoted as $W(\tilde{x}) = W(\lambda^{-1}) = \Delta(\lambda^{-1})$ which we write as $\Delta\lambda^{-1}$ for brevity. You will note that we have not used the wavenumber function k, as this is usually defined as $k = 2\pi/\lambda$ (see for example [368] and references). Substituting in (13.14), we obtain the relation

$$\Delta x \cdot \Delta\lambda^{-1} \geq 1/2. \tag{13.24}$$

In terms of the wavenumber k, (13.24) becomes

$$\Delta x \cdot \Delta k \geq \pi. \tag{13.25}$$

Given that the momentum of a quantum particle is given by $p = h/\lambda$ or by $p = \hbar k$, both (13.24) and (13.25) can be expressed as

$$\Delta x \cdot \Delta p \geq h/2. \tag{13.26}$$

Equations (13.23) and (13.26) are both different statements of the Heisenberg Uncertainty Principle.

The R.H.S. of these equations is different from the usual statement of the Heisenberg Uncertainty Principle where the value $\hbar/2$ is used instead of the value $h/2$ obtained in this analysis. The application of (13.17) to circular variables (i.e. using ω in (13.17) instead of (13.18)) would result in the (incorrect) expression

$$\Delta t \cdot \Delta \omega \geq 1/2 \tag{13.27}$$

and the more commonly encountered (incorrect) expression

$$\Delta E \cdot \Delta t \geq \hbar/2. \tag{13.28}$$

However, Heisenberg's original derivation [154] had the R.H.S. of (13.26) approximately equal to h, and Greenstein's re-derivation [140, see p. 47] of Heisenberg's principle results in the value $h/2$. Kennard's formal derivation [191] using standard deviations established the value of $\hbar/2$ used today. This would thus seem to be the reason for the use of the value $\hbar/2$ in the formulation of the Heisenberg Uncertainty Principle.

Recently, Schürmann et al [317] have shown that in the case of a single slit diffraction experiment, the standard deviation of the momentum typically does not exist. They derive the conditions under which the standard deviation of the momentum is finite, and show that the R.H.S. of the resulting inequality satisfies (13.26). It thus seems that (13.26) is the more general formulation of the Heisenberg Uncertainty Principle, while the expression with the value $\hbar/2$ derived using standard deviations is a more specific case.

Whether one uses $\hbar/2$ or $h/2$ has little impact on the Heisenberg Uncertainty Principle as the R.H.S. is used to provide an order of magnitude estimate of the effect considered. However, the difference becomes evident when we apply our results to the Brillouin zone formulation of the solid state in Condensed Matter Physics (as will be seen in Section 13.3.4) since this now impacts calculations resulting from models that can be compared with experimental values.

§13.3.2 *Interpretation of the Heisenberg Uncertainty Principle*

This derivation demonstrates that the Heisenberg Uncertainty Principle arises because x and p form a Fourier transform pair of variables. It is a characteristic of Quantum Mechanics that conjugate variables are Fourier transform pairs of variables. Thus the Heisenberg Uncertainty Principle arises because the momentum p of a quantum particle is proportional to the de Broglie wave number k of the particle. If momentum was not proportional to wave number, the Heisenberg Uncertainty Principle would not exist for those variables.

This argument elucidates why the Heisenberg Uncertainty Principle exists. Can it shed light on the meaning of the Heisenberg Uncertainty Principle in relation to the basic nature of the quantum level? First, we note that the Uncertainty Principle, according to Fourier transform theory, relates the effective width of Fourier transform pairs of functions or variables. It is not a measurement theorem *per se*. It does not describe what happens when Fourier transform variables are measured, only that their effective widths must satisfy the Uncertainty Principle.

Indeed, as pointed out by Omnès [276, see p. 57],"it is quite legitimate to write down an eigenstate of energy at a well-defined time". Omnès ascribes this seeming violation of the Heisenberg Uncertainty Principle to the fact that time is not an observable obtained from an operator like momentum, but rather a parameter. Greenstein [140, see p. 65] makes the same argument. However, time t multiplied by the speed of light c is a component of the 4-vector x^μ and energy E divided by c is a component of the energy-momentum 4-vector P^μ. The time component of these 4-vectors should not be treated differently than the space component. The operator versus parameter argument is weak.

What Omnès' example shows is that the impact of the effective widths Δt and ΔE of the Heisenberg Uncertainty Principle depends on the observation of the time function t and of the energy function E that is performed. A time interval Δt can be associated with the time function t during which is measured the energy eigenstate function E which itself has a certain width ΔE, with both widths (Δ) satisfying (13.23). This example demonstrates that the Heisenberg Uncertainty Principle is not a measurement theorem as often used. Rather, it is a relationship between the effective widths of Fourier transform pairs of variables that can have an impact on the observation of those variables.

A more stringent scenario for the impact of the energy-time Heisenberg Uncertainty Principle is one where the time and energy functions

are small quantities. For example, we consider the impact of Δt on the observation of τ_n, the lifetime of an atom in energy eigenstate n, and the impact of ΔE on the transition energy E_{mn}, for a transition between states n and m during spectral line emission. The conditions to be able to observe τ_n and E_{mn} are:

$$\tau_n \geq \Delta t \tag{13.29}$$

$$E_{mn} \geq \Delta E. \tag{13.30}$$

Using (13.23) in (13.29),

$$\tau_n \geq \Delta t \geq h/(2\Delta E). \tag{13.31}$$

Hence

$$\Delta E \geq \frac{h}{2}\frac{1}{\tau_n}. \tag{13.32}$$

As state n increases, the lifetime τ_n decreases. Eq.(13.32) is thus more constrained in the limit of large n. Using the following hydrogenic asymptotic expression for τ_n from Millette et al [236]

$$\tau_n \sim \frac{n^5}{\ln(n)} \tag{13.33}$$

into (13.32), (13.30) becomes

$$E_{mn} \geq \Delta E \gtrsim \frac{h}{2}\, k\, \frac{\ln(n)}{n^5} \tag{13.34}$$

where $1/k$ is the constant of proportionality of (13.33) given by

$$k = \frac{2^6}{3}\sqrt{\frac{\pi}{3}}\, Z^2\alpha^3 cR_H \tag{13.35}$$

where Z is the nuclear charge of the hydrogenic ion, α is the fine-structure constant, and R_H is the hydrogen Rydberg constant. Eliminating the middle term, (13.34) becomes

$$E_{mn} \gtrsim \frac{h}{2}\, k\, \frac{\ln(n)}{n^5}. \tag{13.36}$$

Applying L'Hôpital's rule, the R.H.S. of the above equation is of order

$$\text{R.H.S.} \sim O\left(\frac{1}{n^5}\right) \text{ as } n \to \infty \tag{13.37}$$

while the L.H.S. is of order [26, see p. 9]

$$\text{L.H.S.} \sim O\left(\frac{1}{n^2}\right) \text{ as } n \to \infty. \tag{13.38}$$

Given that (13.37) tends to zero faster than (13.38), (13.36) is satisfied. Both τ_n, the lifetime of the atom in energy eigenstate n, and the transition energy E_{mn} for the transition between states n and m satisfy the conditions for observation of the spectral line emission. Thus for the time interval Δt, given by (13.29), associated with the time function τ_n for the transition energy function E_{mn} which itself has a certain width ΔE, given by (13.30), both Δ's satisfy (13.23) as expected, given the observation of spectral line emission.

§13.3.3 *Quantum measurements and the Nyquist-Shannon Sampling Theorem*

At the quantum level, one must interact to some degree with a quantum system to perform a measurement. When describing the action of measurements of Fourier transform variables, one can consider two limiting measurement cases: 1) truncation of the variable time series as a result of a fully interacting measurement or 2) sampling of the variable time series at intervals which we consider to be regular in this analysis, in the case of minimally interacting measurements. As we will see, the action of sampling allows for measurements that otherwise would not be possible in the case of a single minimal interaction.

It should be noted that the intermediate case of a partial measurement interaction resulting for example in a transfer of energy or momentum to a particle can be considered as the truncation of the original time series and the initiation of a new time series after the interaction. The advantage of decomposing measurement actions in this fashion is that their impact on Fourier transform variables can be described by the Nyquist-Shannon Sampling Theorem of Fourier transform theory. This theorem is a measurement theorem for Fourier transform variables based on sampling and truncation operations.

The Nyquist-Shannon Sampling Theorem is fundamental to the field of information theory, and is well known in digital signal processing and remote sensing [277]. In its most basic form, the theorem states that the rate of sampling of a signal (or variable) f_s must be greater than or equal to the Nyquist sampling rate f_S to avoid loss of information in the sampled signal, where the Nyquist sampling rate is equal to twice

that of the highest frequency component, f_{max}, present in the signal:

$$f_s \geq f_S = 2f_{max}. \tag{13.39}$$

If the sampling rate is less than that of (13.39), aliasing occurs, which results in a loss of information.

In general, natural signals are not infinite in duration and, during measurement, sampling is also accompanied by truncation of the signal. There is thus loss of information during a typical measurement process. The Nyquist-Shannon Sampling theorem elucidates the relationship between the process of sampling and truncating a variable and the effect this action has on its Fourier transform [35, see p. 83]. In effect, it explains what happens to the information content of a variable when its conjugate is measured.

Sampling a variable x at a rate δx will result in the measurement of its conjugate variable $\tilde{x}$ being limited to its maximum Nyquist range value $\tilde{x}_N$ as given by the Nyquist-Shannon Sampling theorem:

$$\tilde{x} \leq \tilde{x}_N \tag{13.40}$$

where

$$\tilde{x}_N = 1/(2\delta x). \tag{13.41}$$

Combining these two equations, we get the relation

$$\tilde{x} \cdot \delta x \leq 1/2, \quad \text{for}\, \tilde{x} \leq \tilde{x}_N. \tag{13.42}$$

Conversely, truncating a variable x at a maximum value x_N ($x \leq x_N$) will result in its conjugate variable $\tilde{x}$ being sampled at a rate $\delta\tilde{x}$ given by the Nyquist-Shannon Sampling theorem $\delta\tilde{x} = 1/(2x_N)$ resulting in the relation

$$\delta\tilde{x} \cdot x \leq 1/2, \quad \text{for}\, x \leq x_N. \tag{13.43}$$

The impact of the Nyquist-Shannon Sampling theorem is now considered for a particle's position x and momentum p. Applying the theorem to the case where a particle's trajectory is truncated to x_N, we can write from (13.43), for $x \leq x_N$,

$$x \cdot \delta\lambda^{-1} \leq 1/2, \quad \text{for}\, x \leq x_N \tag{13.44}$$

or

$$x \cdot \delta k \leq \pi, \quad \text{for}\, x \leq x_N \tag{13.45}$$

which becomes

$$x \cdot \delta p \leq h/2, \quad \text{for}\, x \leq x_N \tag{13.46}$$

where δp is the p-domain sampling rate and the x values can be measured up to x_N (corresponding to the equality in the equations above).

Conversely, applying the theorem to the case where a particle's trajectory is sampled at a rate δx, one can also write from (13.42), for $\tilde{x} \leq \tilde{x}_N$, where $\tilde{x}$ stands for either of λ^{-1}, k, or p,

$$\delta x \cdot \lambda^{-1} \leq 1/2, \quad \text{for } \lambda^{-1} \leq \lambda_N^{-1} \tag{13.47}$$

or

$$\delta x \cdot k \leq \pi, \quad \text{for } k \leq k_N \tag{13.48}$$

which becomes

$$\delta x \cdot p \leq h/2, \quad \text{for } p \leq p_N \tag{13.49}$$

where δx is the x-domain sampling rate and k_N is the wave number range that can be measured. For the case where the equality holds, we have $k_N = \pi/\delta x$ where k_N is the Nyquist wave number, the maximum wave number that can be measured with a δx sampling interval.

Sampling in one domain leads to truncation in the other. Sampling (δx) and truncation (x_N) in one domain leads to truncation (k_N) and sampling (δk) respectively in the other. As x and k form a Fourier transform pair in quantum mechanics, the Nyquist-Shannon Sampling theorem must also apply to this pair of conjugate variables. Similar relations can be derived for the E and ν pair of conjugate variables.

§13.3.4 *Implications of the Nyquist-Shannon Sampling Theorem at the quantum level*

Equations (13.45) and (13.48) lead to the following measurement behaviors at the quantum level:

Lower-bound limit: If the position of a particle is measured over an interval x_N, its wave number cannot be resolved with a resolution better than sampling rate δk as given by (13.45) with $x = x_N$. If the momentum of a particle is measured over an interval k_N, its position cannot be resolved with a resolution better than sampling rate δx as given by (13.48) with $k = k_N$.

Upper-bound limit: If the position of a particle is sampled at a rate δx, wave numbers up to k_N can be resolved, while wave numbers larger than k_N cannot be resolved as given by (13.48). If the momentum of a particle is sampled at a rate δk, lengths up to x_N can be resolved, while lengths longer than x_N cannot be resolved as given by (13.45).

The lower-bound limit is similar to how the Heisenberg Uncertainty Principle is usually expressed when it is used as a measurement principle, although it is not strictly equivalent. The Nyquist-Shannon Sampling Theorem provides the proper formulation and limitations of this type of measurement.

The upper-bound limit suggests a different type of quantum measurement: regular sampling of a particle's position or momentum. In this case, one can obtain as accurate a measurement of the Fourier transform variable as desired, up to the Nyquist-Shannon Sampling limit of $h/2$ (i.e. in the interval $[0, h/2]$).

An example of this phenomenon occurs in the solid state in Condensed Matter Physics where the translational symmetry of atoms in a solid resulting from the regular lattice spacing, is equivalent to an effective sampling of the atoms of the solid and gives rise to the Brillouin zone for which the valid values of k are governed by (13.48). Setting $\delta x = a$, the lattice spacing, and extending by symmetry the k values to include the symmetric negative values, one obtains [149, see p. 34], [55, see p. 100], [382, see p. 21]:

$$-\pi/a \leq k \leq \pi/a \tag{13.50}$$

or alternatively

$$k \leq |\pi/a|. \tag{13.51}$$

This is called the reduced zone scheme and π/a is called the Brillouin zone boundary [198, see p. 307]. The Brillouin zones of the solid state in Condensed Matter Physics are thus a manifestation of the Nyquist-Shannon Sampling theorem at the quantum level.

In essence, this is a theory of measurement for variables that are Fourier transform pairs. The resolution of our measurements is governed by limitations that arise from the Nyquist-Shannon Sampling theorem. Equations (13.45) and (13.48) are recognized as measurement relationships for quantum-mechanical conjugate variables. Currently, Quantum Mechanics only considers the Uncertainty Theorem but not the Sampling Theorem. The two theorems are applicable to Quantum Mechanics and have different interpretations: the Uncertainty Theorem defines a relationship between the widths of conjugate variables, while the Sampling Theorem establishes sampling and truncation measurement relationships for conjugate variables.

The value δx is a sampled measurement and as a result can resolve values of p up to its Nyquist value p_N given by the Nyquist-Shannon

Sampling theorem, (13.49). This is a surprising result as the momentum can be resolved up to its Nyquist value, in apparent contradiction to the Heisenberg Uncertainty Principle. Yet this result is known to be correct as demonstrated by the Brillouin zones formulation of the solid state in Condensed Matter Physics. Physically this result can be understood from the sampling measurement operation which builds up the momentum information during the sampling process, up to the Nyquist limit p_N. It must be remembered that the Nyquist limit depends on the sampling rate δx as per the Nyquist-Shannon Sampling theorem, (13.49). The Nyquist value must also satisfy (13.39) to avoid loss of information in the sampling process, due to aliasing.

This improved understanding of the Heisenberg Uncertainty Principle and its sampling counterpart allows us to clarify its interpretation. This is based on our understanding of the behavior of the Uncertainty Theorem and the Nyquist-Shannon Sampling Theorem in other applications such as, for example, Digital Signal Processing.

§13.3.5 *Measurement limitations and inherent limitations*

It is important to differentiate between the measurement limitations that arise from the properties of Fourier transform pairs previously considered, and any inherent limitations that may or may not exist for those same variables independently of the measurement process. Quantum theory currently assumes that the inherent limitations are the same as the measurement limitations. This assumption needs to be re-examined based on the improved understanding obtained from the effect of the Uncertainty and Sampling Theorems in other applications.

The properties of Fourier transform pairs considered in the previous sections do not mean that the underlying quantities we are measuring are inherently limited by our measurement limitations. On the contrary, we know from experience in other applications that our measurement limitations do not represent an inherent limitation on the measured quantities in Fourier Transform theory: for example, in Digital Signal Processing, a signal is continuous even though our measurement of the signal results in discrete and aliased values of limited resolution subject to the Nyquist-Shannon Sampling Theorem (analog and digital representation of the signal). The effective width of the signal and its transform are related by the Uncertainty theorem. Even though the time and frequency evolution of a signal that we measure is limited by our measurement limitations, the time domain and frequency domain signals are both continuous, independently of how we measure them.

The measurement limitations apply equally to the macroscopic level and to the quantum level as they are derived from the properties of Fourier transform pairs of variables which are the same at all scales. However, at the quantum level, contrary to our macroscopic environment, we cannot perceive the underlying quantities other than by instrumented measurements. Hence during a measurement process, the quantum level is limited by our measurement limitations. However, assuming that these measurement limitations represent inherent limitations and form a basic characteristic of the quantum level is an assumption that is not justified based on the preceding considerations. Indeed, the Nyquist-Shannon Sampling Theorem of Fourier Transform theory shows that the range of values of variables below the Heisenberg Uncertainty Principle value of $h/2$ is accessible under sampling measurement conditions, as demonstrated by the Brillouin zones formulation of the solid state in Condensed Matter Physics.

§13.3.6 *Overlap of the Heisenberg Uncertainty Principle and the Nyquist-Shannon Sampling Theorem*

Brillouin zone analysis in the solid state in Condensed Matter Physics demonstrates that one can arbitrarily measure k from 0 up to its Nyquist limit, as long as the variable x is sampled at a constant rate (rather than performing a single x measurement). The Nyquist-Shannon Sampling Theorem can thus be considered to cover the range that the Heisenberg Uncertainty Principle excludes.

However, one should recognize that the coverage results from two disparate theorems, and one should be careful not to try to tie the two Theorems at their value of overlap π. The reason is that one expression involves the widths of conjugate variables as determined by (13.14) to (13.16), while the other involves sampling a variable and truncating its conjugate, or vice versa as determined by (13.45) and (13.48). The equations are not continuous at the point of overlap π. Indeed, any relation obtained would apply only at the overlap π and would have no applicability or physical validity on either side of the overlap.

§13.3.7 *Summary*

In this section, we have shown that a consistent application of Fourier Transform theory to the derivation of the Heisenberg Uncertainty Principle requires that the R.H.S. of the Heisenberg inequality be $h/2$, not $\hbar/2$. This is confirmed when extending the analysis to the Brillouin zones formulation of the solid state in Condensed Matter Physics.

We have noted that the Heisenberg Uncertainty Principle, obtained from the Uncertainty Theorem of Fourier Transform theory, arises because of the dependency of momentum on wave number that exists at the quantum level. Quantum mechanical conjugate variables are Fourier Transform pairs of variables.

We have shown from Fourier Transform theory that the Nyquist-Shannon Sampling Theorem affects the nature of-measurements of quantum mechanical conjugate variables. We have shown that Brillouin zones in the solid state in Condensed Matter Physics are a manifestation of the Nyquist-Shannon Sampling Theorem at the quantum level.

We have noted that both the Sampling Theorem and the Uncertainty Theorem are required to fully describe quantum mechanical conjugate variables. The Nyquist-Shannon Sampling Theorem complements the Heisenberg Uncertainty Principle. The overlap of these Theorems at the $h/2$ equality value is a mathematical artifact and has no physical significance.

We have noted that the Uncertainty Theorem and the Nyquist-Shannon Sampling Theorem apply to Fourier Transform pairs of variables independently of the level at which the theorems are applied (macroscopic or microscopic). Conjugate variable measurement limitations due to these Theorems affect how we perceive quantum level events as these can only be perceived by instrumented measurements at that level. However, based on our analysis, quantum measurement limitations affect our perception of the quantum environment only, and are not inherent limitations of the quantum level, as demonstrated by the Brillouin zones formulation of the solid state in Condensed Matter Physics.

The application of the Nyquist-Shannon Sampling Theorem to the quantum level offers the possibility of investigating new experimental conditions beyond the Brillouin zone example from the solid state in Condensed Matter Physics considered in this section, allowing a unique vista into a range of variable values previously considered unreachable due to the Heisenberg Uncertainty Principle. Regular sampling of position allows us to determine momentum below its Nyquist limit, and similarly the regular sampling of momentum will allow us to determine position below its Nyquist limit.

§13.4 The EPR paradox and Bell's inequality

Bell's inequality [19,135,137,142] sets constraints for the existence of local hidden variable theories in quantum mechanics. Bohr, of the Copen-

hagen probabilistic school, and Einstein, of the objective reality school, who both contributed to the foundation of quantum mechanics, did not agree on its interpretation – their views and correspondence on the topic are well documented in many books [163, 232, 332, 372].

In 1935, Einstein, Podolsky and Rosen published a paper [100] that aimed to show that quantum mechanics was not a complete description of physical reality. Bohr provided a response to the challenge [29], but the EPR paper remained an argument for hidden variables in quantum mechanics. In 1964, Bell [19] published an inequality that imposed constraints for local hidden variable theories to be valid in quantum mechanics. The experiments performed by Aspect *et al* [6] with entangled photons confirmed that Bell's inequality was violated within experimental errors, taken to mean that local hidden variable theories are not valid in quantum mechanics. Only non-local hidden variable theories are possible, based on these results.

In this section, we investigate the applicability of Bell's inequality, based on the assumptions used in its derivation.

§13.4.1 *Bell's inequality*

Bell's derivation [19] considers a pair of spin one-half particles of spin $\sigma_{\mathbf{1}}$ and $\sigma_{\mathbf{2}}$ respectively, formed in the singlet state, and moving freely in opposite directions. Then $\sigma_{\mathbf{1}} \cdot \mathbf{a}$ is the measurement of the component of $\sigma_{\mathbf{1}}$ along some vector $\mathbf{a}$, and similarly for $\sigma_{\mathbf{2}} \cdot \mathbf{b}$ along some vector $\mathbf{b}$. Bell then considers the possibility of a more complete description using hidden variable parameters λ.

He writes down the following equation for the expectation value of the product of the two components $\sigma_{\mathbf{1}} \cdot \mathbf{a}$ and $\sigma_{\mathbf{2}} \cdot \mathbf{b}$ with parameters λ:

$$P(\mathbf{a}, \mathbf{b}) = \int d\lambda \, \rho(\lambda) \, A(\mathbf{a}, \lambda) \, B(\mathbf{b}, \lambda) \tag{13.52}$$

where

$$A(\mathbf{a}, \lambda) = \pm 1 \text{ and } B(\mathbf{b}, \lambda) = \pm 1 \tag{13.53}$$

and $\rho(\lambda)$ is the probability distribution of parameter λ. This should equal the quantum mechanical expectation value

$$\langle \sigma_{\mathbf{1}} \cdot \mathbf{a} \, \sigma_{\mathbf{2}} \cdot \mathbf{b} \rangle = -\mathbf{a} \cdot \mathbf{b} \, . \tag{13.54}$$

Bell says that it does not matter whether λ is "a single variable or a set, or even a set of functions, and whether the variables are discrete or continuous" [19]. He uses a single continuous parameter described by

a probability distribution. In a later paragraph, he states that (13.52) represents all kinds of possibilities, such as any number of hidden variables, two sets of hidden variables dependent on A and B, or even as initial values of the variables λ at a given time if one wants to assign "dynamical significance and laws of motion" [19] to it. However, it is doubtful that the probability distribution $\rho(\lambda)$ can be used to represent all possible theories of hidden variables.

Indeed, the basic limitation of (13.52) with its use of a probability distribution $\rho(\lambda)$ is that it imposes a quantum mechanical calculation representation on the analysis. Other quantum level dynamic theories, which we will refer to as hidden variable dynamic theories, could obey totally different dynamic principles, in which case, (13.52) would not be applicable. Eq. (13.52) is only applicable to a specific class of hidden variable theories that can be represented by that equation, which Jaynes [182] refers to as Bell theories. In the following sections, we consider examples of quantum dynamical processes that cannot be represented by (13.52) or by the probability distribution $\rho(\lambda)$ used in (13.52).

§13.4.2 *Measurement limitations and inherent limitations*

It is important to note that Bohr's responses to Einstein's *gedanken* experiments were based on measurements arguments, which acted as a barrier to any further analysis beyond that consideration. As pointed out by Jaynes [183], Einstein and Bohr "were both right in the essentials, but just thinking on different levels. Einstein's thinking [was] always on the ontological level traditional in physics; trying to describe the realities of Nature. Bohr's thinking [was] always on the epistemological level, describing not reality but only our information about reality".

As discussed in [237] and in previous section §13.3.5, the Heisenberg Uncertainty Principle arises because x and p form a Fourier transform pair of variables at the quantum level due to the momentum p of a quantum particle being proportional to the de Broglie wave number k of the particle. It is a characteristic of quantum mechanics that conjugate variables are Fourier transform pairs of variables.

As we have noted, and it deserves to be repeated, it is thus important to differentiate between the measurement limitations that arise from the properties of Fourier transform pairs, and any inherent limitations that may or may not exist at the quantum level for those same variables, independently of the measurement process. Conjugate variable measurement limitations affect how we perceive quantum level events as those can only be perceived by instrumented measurements at that

level. However, as shown in [237] and in previous section §13.3.5, conjugate variable measurement limitations affect *only* our perception of the quantum environment, and are *not* inherent limitations of the quantum level as seen in the following.

The properties of Fourier transform pairs are the same at all scales, from the microscopic to the macroscopic. We know from experience in other applications that our measurement limitations do not represent an inherent limitation on the measured quantities in Fourier Transform theory as for example in Digital Signal Processing, where a signal is continuous even though our measurement of the signal results in discrete and aliased values of limited resolution subject to the Nyquist-Shannon Sampling Theorem. Even though the time and frequency evolution of a signal that we measure is limited by our measurement limitations, the time domain and frequency domain signals are both continuous and fully defined, independently of how we measure them.

Furthermore, the Nyquist-Shannon Sampling Theorem of Fourier transform theory allows access to the range of values of variables below the Heisenberg Uncertainty Principle limit under sampling measurement conditions, as demonstrated by the Brillouin zones formulation of the solid state in Condensed Matter Physics [237] [382, see p. 21] [55, see p. 100]. This shows that local hidden variables are possible at the quantum level, independently of the measurement process. The dynamical process in this case is masked by the properties of the Fourier transform.

§13.4.3 *Bohmian mechanics and STCED wave-particle duality*

In this section we take a second look at wave-particle duality in *STCED*, in particular with respect to Bohmian mechanics and hidden variables theory. The Elastodynamics of the Spacetime Continuum (*STCED*) [238] has similarities to Bohmian mechanics in that the solutions of the *STCED* wave equations are similar to Louis de Broglie's "double solution" [75, 76]. Bohmian mechanics also known as de Broglie-Bohm theory [90, 136, 160] is a theory of quantum physics developed by David Bohm in 1952 [28], based on Louis de Broglie's original work on the *pilot wave*, that provides a causal interpretation of quantum mechanics. It is empirically equivalent to orthodox quantum mechanics, but is free of the conceptual difficulties and the metaphysical aspects that plague the interpretation of quantum theory.

Interestingly, Bell was aware of and a proponent of Bohmian mechanics when he derived his inequality [21]:

> Bohm showed explicitly how parameters could indeed be introduced, into nonrelativistic wave mechanics, with the help of which the indeterministic description could be transformed into a deterministic one. More importantly, in my opinion, the subjectivity of the orthodox version, the necessary reference to the 'observer,' could be eliminated... I will try to present the essential idea... so compactly, so lucidly, that even some of those who know they will dislike it may go on reading, rather than set the matter aside for another day.

In Bohmian mechanics, a system of particles is described by a combination of the wavefunction from Schrodinger's equation and a guiding equation that specifies the location of the particles. "Thus, in Bohmian mechanics the configuration of a system of particles evolves via a deterministic motion choreographed by the wave function" [136] such as in the two-slit experiment. We will see a similar behaviour in the *STCED* wave equations below. Bohmian mechanics is equivalent to a non-local hidden variables theory.

In the Elastodynamics of the Spacetime Continuum, as discussed in [244] and shown in Chapter 12, energy propagates in the spacetime continuum by longitudinal (*dilatation*) and transverse (*distortion*) wave displacements. This provides a natural explanation for wave-particle duality, with the transverse mode corresponding to the wave aspects of the deformations and the longitudinal mode corresponding to the particle aspects of the deformations.

The displacement u^ν of a deformation from its undeformed state can be decomposed into a longitudinal component $u^\nu_\parallel$ and a transverse component $u^\nu_\perp$. The volume dilatation ε is given by the relation $\varepsilon = u_\parallel{}^\mu{}_{;\mu}$ [238]. The wave equation for $u^\nu_\parallel$ describes the propagation of longitudinal displacements, while the wave equation for $u^\nu_\perp$ describes the propagation of transverse displacements in the spacetime continuum. The u^ν displacement wave equations can be expressed as a longitudinal wave equation for the dilatation ε and a transverse wave equation for the rotation tensor $\omega^{\mu\nu}$ [238].

Particles propagate in the spacetime continuum as longitudinal wave displacements. Mass is proportional to the volume dilatation ε of the longitudinal mode of the deformation [238, see (32)]. This longitudinal mode displacement satisfies a wave equation for ε, different from the transverse mode displacement wave equation for $\omega^{\mu\nu}$. This longitudinal dilatation wave equation for ε is given by [238, see (204)]

$$\nabla^2\varepsilon = -\frac{\bar{k}_0}{2\bar{\mu}_0 + \bar{\lambda}_0}\, u^\nu_\perp \varepsilon_{;\nu} \tag{13.55}$$

where $\bar{\mu}_0$ and $\bar{\lambda}_0$ are the Lamé constants and $\bar{k}_0$ the elastic volume force constant of the spacetime continuum. It is important to note that the inhomogeneous term on the R.H.S. includes a dot product coupling between the transverse displacement and the volume dilatation for the solution of the longitudinal dilatation wave equation for ε.

The transverse distortion wave equation for $\omega^{\mu\nu}$ [238, see (210)]

$$\nabla^2\omega^{\mu\nu} + \frac{\bar{k}_0}{\bar{\mu}_0}\,\varepsilon\left(x^\mu\right)\,\omega^{\mu\nu} = \frac{1}{2}\,\frac{\bar{k}_0}{\bar{\mu}_0}\left(\varepsilon^{,\mu}u_\perp^\nu - \varepsilon^{,\nu}u_\perp^\mu\right) \tag{13.56}$$

also includes a R.H.S. coupling, in this case a cross product, between the transverse displacement and the volume dilatation for the solution of the transverse distortion wave equation for $\omega^{\mu\nu}$. The transverse distortion wave $\omega^{\mu\nu}$ corresponds to a multi-component wavefunction Ψ.

A deformation propagating in the spacetime continuum consists of a combination of longitudinal and transverse waves. The coupling between $\varepsilon^{,\mu}$ and $u_\perp^\nu$ on the R.H.S. of both wave equations explains the behavior of electrons in the double slit interference experiment. It shows that even though the transverse wave is the source of the interference pattern in double slit experiments, the longitudinal dilatation wave, which behaves as a particle, follows the interference pattern dictated by the transverse distortion wave as observed experimentally.

The longitudinal dilatation wave behaves as a particle and goes through one of the slits, even as it follows the interference pattern dictated by the transverse distortion wave, as observed experimentally [150, see in particular Figure 4] and as seen in the coupling between $\varepsilon^{,\mu}$ and $u_\perp^\nu$ in (13.55) and (13.56) above. This behaviour is the same as that in Bohmian mechanics seen above. These results are in agreement with the results of the Jánossy-Naray, Clauser, and Dagenais and Mandel experiments on the self-interference of photons and the neutron interferometry experiments performed by Bonse and Rauch [322, see pp. 73-81].

As mentioned previously, the solutions of the *STCED* wave equations are similar to Louis de Broglie's "double solution". The longitudinal wave is similar to the de Broglie "singularity-wave function" [75]. In *STCED* however, the particle is not a singularity of the wave, but is instead characterized by its mass which arises from the volume dilatation propagating as part of the longitudinal wave. There is no need for the collapse of the wavefunction Ψ, as the particle resides in the longitudinal wave, not the transverse one. A measurement of a particle's position is a measurement of the longitudinal wave, not the transverse wave.

In addition, $|\Psi|^2$ represents the physical energy density of the transverse (*distortion*) wave. It corresponds to the transverse field energy of the deformation. It is not the same as the particle, which corresponds to the longitudinal (*dilatation*) wave displacement and is localized within the deformation via the massive volume dilatation. However, $|\Psi|^2$ can be normalized with the system energy and converted into a probability density, thus allowing the use of the existing probabilistic formulation of quantum theory.

The dynamical process, although it has some similarities to Bohmian mechanics, is also different from it as it is centered on longitudinal (particle) and transverse (wavefunction) wave equations derived from the properties of the spacetime continuum of general relativity. It is thus deterministic and causal as is general relativity.

§13.4.4 *Physical influence versus logical inference*

We have considered two examples of quantum dynamical processes where the starting equation (13.52) and the probability distribution $\rho(\lambda)$ used in (13.52) do not apply to the situation. We now examine in greater details the probabilistic formulation of Bell's inequality derivation of section §13.4.1 to better understand its limitations.

Physicist E. T. Jaynes was one of the pioneers of the usage of probability theory as an extension of deductive logic. His textbook "Probability Theory: The Logic of Science" [184] published posthumously is an invaluable resource for scientists looking to understand the scientific use of probability theory as opposed to the conventional mathematical measure theory. As he states in [182],

> Many circumstances seem mysterious or paradoxical to one who thinks that probabilities are real physical properties existing in Nature. But when we adopt the "Bayesian Inference" viewpoint of Harold Jeffreys [185,186], paradoxes often become simple platitudes and we have a more powerful tool for useful calculations.

Jaynes clarifies this approach to probability theory and contrasts it to frequencies as follows [182]:

> In our system, a probability is a theoretical construct, on the epistemological level, which we assign in order to represent a state of knowledge, or that we calculate from other probabilities according to the rules of probability theory. A frequency is a property of the real world, on the ontological level, that we measure or estimate.

The probability distributions used for inference do not describe a property of the world, only a certain state of information about the world,

which provides us with the means to use prior information for analysis as powerfully demonstrated in numerous applications in [182–184].

The Einstein–Podolsky–Rosen (EPR) paradox and Bell inequality in quantum theory is one of the examples examined by Jaynes in [182]. In quantum mechanics, the belief that probabilities are real physical properties leads to quandaries such as the EPR paradox which lead some to conclude that there is no real world and that physical influences travel faster than the speed of light, or worse ("a spooky kind of action at a distance" as Einstein called it). As Jaynes points out, it is important to note that the EPR article did not question the existence of the correlations, which were expected, but rather the need for a physical causation instead of what he calls "instantaneous psychokinesis", based on experimenter decisions, to control distant events.

Jaynes' analysis of the derivation of Bell's inequality uses the following notation for conditional probabilities which corresponds to Bell's notation as follows:

$$P(AB \,|\, ab) = P(\mathbf{a}, \mathbf{b}) \tag{13.57}$$

$$P(A \,|\, a\lambda) = A(\mathbf{a}, \lambda)\,, \tag{13.58}$$

such that Bell's equation (13.52) above becomes

$$P(AB \,|\, ab) = \int d\lambda\, \rho(\lambda)\, P(A \,|\, a\lambda)\, P(B \,|\, b\lambda)\,. \tag{13.59}$$

However, as Jaynes notes, the fundamentally correct relation for $P(AB \,|\, ab)$ according to probability theory should be

$$P(AB \,|\, ab) = \int d\lambda\, P(AB \,|\, ab\lambda)\, P(\lambda \,|\, ab)\,. \tag{13.60}$$

Assuming that knowledge of the experimenters' choices gives no information about λ, then one can write

$$P(\lambda \,|\, ab) = \rho(\lambda)\,. \tag{13.61}$$

The fundamentally correct factorization of the other probability factor of (13.60), $P(AB \,|\, ab\lambda)$, is given by [182]

$$P(AB \,|\, ab\lambda) = P(A \,|\, ab\lambda)\, P(B \,|\, Aab\lambda)\,. \tag{13.62}$$

However, as Jaynes notes, one could argue as Bell did that EPR demands that A should not influence events at B for space-like intervals.

This requirement then leads to the factorization used by Bell to represent the EPR problem

$$P(AB \,|\, ab\lambda) = P(A \,|\, a\lambda)\, P(B \,|\, b\lambda)\,. \tag{13.63}$$

Nonetheless, the factorization (13.63) disagrees with the formalism of quantum mechanics in that the result of the measurement at A must be known before the correlation affects the measurement at B, *i.e.* $P(B \,|\, Aab)$. Hence it is not surprising that Bell's inequality is not satisfied in systems that obey quantum mechanics.

Two additional hidden assumptions are identified by Jaynes in Bell's derivation, in addition to those mentioned above:

1. Bell assumes that a conditional probability $P(X \,|\, Y)$ represents a physical causal influence of Y on X. However, consistency requires that conditional probabilities express logical inferences not physical influences.
2. The class of Bell hidden variable theories mentioned in section §13.4.1 does not include all local hidden variable theories. As mentioned in that section, hidden variable theories don't need to satisfy the form of (13.52) (or alternatively (13.59)), to reproduce quantum mechanical results, as evidenced in Bohmian mechanics.

Bell's inequality thus applies to the class of hidden variable theories that satisfy his relation (13.52), *i.e.* Bell hidden variable theories, but not necessarily to other hidden variable dynamic theories.

The superluminal communication implication stems from the first hidden assumption above which shows that what is thought to travel faster than the speed of light is actually a logical inference, not a physical causal influence. As summarized by Jaynes [182],

> The measurement at A at time t does not change the real physical situation at B; but it changes our state of knowledge about that situation, and therefore it changes the predictions we are able to make about B at some time t'. Since this is a matter of logic rather than physical causation, there is no action at a distance and no difficulty with relativity.

There is simply no superluminal communication, as required by special relativity. Assuming otherwise would be similar to Pauli assuming that the established law of conservation of energy mysteriously fails in weak interactions instead of successfully postulating a new particle (the neutrino).

§13.4.5 *Quantum confusion*

In this section, we have investigated the applicability of Bell's inequality, based on the assumptions used in its derivation. We have considered two examples of hidden variable dynamic theories that do not satisfy Bell's initial equation (13.52) used to derive his inequality, and consequently for which Bell's inequality is not applicable: one based on the Nyquist-Shannon Sampling Theorem of Fourier transform theory and the other based on the wave-particle solutions of the *STCED* wave equations which are similar to Louis de Broglie's "double solution". We highlight two hidden assumptions identified by Jaynes [182] that limit the applicability of Bell's inequality, as derived, to Bell hidden variable theories and that show that there are no superluminal physical influences, only logical inferences.

We close with a quote from Jaynes [184, see p. 328] that captures well the difficulty we are facing:

> What is done in quantum theory today... when no cause is apparent one simply postulates that no cause exists – ergo, the laws of physics are indeterministic and can be expressed only in probability form.

Thus we encounter paradoxes such as seemingly superluminal physical influences that contradict special relativity, and "spooky action at a distance" is considered as an explanation rather than working to understand the physical root cause of the problem. This section shows that, in this case, the root cause is due to improper assumptions, specifically the first hidden assumption identified by Jaynes highlighted in section §13.4.4 above, that is assuming that a conditional probability represents a physical influence instead of the physically correct logical inference. In summary,

> He who confuses reality with his knowledge of reality generates needless artificial mysteries. [182]

§13.5 Quantum entanglement

Quantum entanglement is a quantum mechanical property of a composite quantum system consisting of two or more subsystems (such as particles), describing a situation where a quantum subsystem is linked to another via a specific process leading to correlations between observable physical properties of the subsystems. The two-particle *spin-singlet* state

$$|\,\psi^{-}\rangle = \frac{1}{\sqrt{2}}\Big(\,|\uparrow_1\downarrow_2\rangle - |\downarrow_1\uparrow_2\rangle\Big) \tag{13.64}$$

is an example of state entanglement in bipartite systems [177, p. 19].

Schrödinger first introduced the term *entangled state* to describe the non-separable pure states of quantum systems [315], [177, p. 17]. Consider for example the emission of two photons of opposite polarization from a given process, such as the stimulated emission of polarization-entangled photons (see for example [151,210]). The emitted photons are then conceived of as "entangled" pure states. The system is described by the wavefunction [151]

$$|\,\psi\rangle = \frac{1}{\sqrt{2}}\Big(\,|\,\circlearrowright_1\,\rangle\,|\,\circlearrowleft_2\,\rangle + |\,\circlearrowleft_1\,\rangle\,|\,\circlearrowright_2\,\rangle\,\Big) \tag{13.65}$$

where $\circlearrowright_i$ and $\circlearrowleft_i$ represent the right-hand and left-hand circularly polarized photons for $i = 1$ or 2. This wavefunction represents what we know of the entangled system, or alternatively represents our lack of knowledge of the specific properties of each photon that is emitted. All we know is that if one emitted photon is right-hand circularly polarized, then the other will be left-hand circularly polarized, and vice versa. Eq. (13.65) is a statement of this situation.

The predominant interpretation (the orthodox viewpoint [213]) is that the wavefunction (13.65) represents a physical description of the emitted photons in an unresolved evanescent state, and that once a measurement is performed on one of them, the wavefunction collapses, the measured photon's actual properties are then known and an instantaneous propagation of that information is perceived by the other photon so that it can assume the complementary properties required by the process – "spooky action at a distance" (SAAD) as Einstein called it, a process that some physicists like to think of as quantum magic, an approach that speaks more of metaphysics than physics. The reasons for the acceptance of this description will be considered in greater detail in Section §13.6.

Over the past decades, experiments have been devised to extend the range of quantum entanglements, to the point where classical scales have been achieved. This includes both the size of entangled objects (*e.g.* [5, 22, 86, 217, 266]) and the distances over which entanglement has been maintained (*e.g.* [156, 380]).

These are particularly stunning results as, according to the orthodox interpretation, any interaction of one of the entangled components with its environment will collapse the entanglement. The probability of preventing such interactions and preserving entanglements over classical sizes and distances is exceedingly small. As noted by Jaeger [177, p. 20] "Indeed, *pure* such states of two-particle systems are exceptional rather

than typical in the world; typically, a system very soon interacts with a number of other systems, so that, even if it were prepared in a pure state, it is typically described by a mixed state".

The probability that a photon can travel a distance x without interaction is given by [349] [162, Section 3.3.1] [163, p 304]

$$P_{no-int}(x) = \exp(-n_p\,\sigma\,x) \tag{13.66}$$

where n_p is the particle number density and σ is the total photon interaction cross-section including absorption and scattering. For propagation of photons in the atmosphere, $n_p \sim 2.5 \times 10^{25}\,\mathrm{m}^{-3}$ [71] and $\sigma \sim 180\,\mathrm{barn/molecule} \equiv 1.8 \times 10^{-26}\,\mathrm{m}^2/\mathrm{molecule}$ [289]. Using these values in (13.66), the no-interaction probability becomes

$$P_{no-int}(x) = e^{-0.45\,x} \tag{13.67}$$

where x is in meters. We see that for classical distances x, the probability $P_{no-int}(x)$ increasingly becomes very small. For example,

$$\begin{aligned} P_{no-int}(1\,\mathrm{m}) &= 0.64 \\ P_{no-int}(10\,\mathrm{m}) &= 0.011 \\ P_{no-int}(100\,\mathrm{m}) &= 2.9 \times 10^{-20} \\ P_{no-int}(1\,\mathrm{km}) &= 3.6 \times 10^{-196}\,. \end{aligned} \tag{13.68}$$

For the value of 143 km of [156, 380] the probability that a photon can travel such a distance without interaction is astronomically small.

Hence the probability of preserving entanglements over classical sizes and distances and preventing the entanglement from collapsing due to physical interactions is exceedingly small. The question has to be raised: in light of these successful classical-scale experiments, are we currently misunderstanding the quantum entanglement process such that instead of a fragile entanglement situation as the above considerations indicate, we can derive a quantum entanglement process that leads to a physically robust entanglement situation that persists to classical scales as observed?

§13.5.1 *Quantum entanglement questions*

Questions have been raised concerning entanglement and its extension to the classical (or macro) domain [38]. There is no doubt that some

processes generate particle or photon pairs that have a definite relationship (correlation) between them (which are referred to as being entangled) and these relationships are confirmed experimentally. At stake here is the interpretation of the quantum entanglement process, and the impact of the understanding of this process on the development and technological applications of this quantum mechanical process – a misinterpretation can lead to considerations that are not physically realistic.

Questions have also been raised on the limited applicability of Bell's inequality [182,247,381], based on the assumptions used in its derivation as seen in previous section §13.4. Bell [18] uses a single continuous parameter λ described by a probability distribution $\rho(\lambda)$: the basic limitation of this approach is that it imposes a quantum mechanical calculation approach on the analysis. Bell's derivation is only applicable to a specific class of hidden variable theories that can be represented by his starting equation and assumptions, which Jaynes [182] refers to as Bell theories. Some hidden variable theories don't need to satisfy Bell's starting equation to reproduce quantum mechanical results, as evidenced by Bohmian mechanics [90]. Bell's inequality is thus found to apply to a limited set of circumstances and situations, not to every quantum system. Selleri [322] provides a comprehensive review of the proofs of Bell's inequality.

Actual experimental demonstration of entanglement is a challenge. Entanglement experiments detect both entangled components within the same time window (see Section §13.6.3), so there is no way to confirm the presence or absence of SAAD – it is assumed to be present purely based on the predominant interpretation discussed in Section §13.5. Zhao [381] has proposed various experiments to clarify the physical properties of entanglement, including one to determine if the collapse of the entangled wavefunction due to the measurement of one component causes the transformation of the other component due to SAAD as is supposed in the orthodox interpretation. No reports of these experiments having been performed have surfaced – their execution should be given a high priority to help us better understand the phenomenon of entanglement.

§13.5.2 *Literal or physical interpretation?*

To be able to answer the question posed at the end of the previous Section §13.5 on a physically robust entanglement process, we need to have a better understanding of the physical description of quantum me-

chanics and of its transition to the classical domain. The orthodox view in the standard formalism of quantum mechanics is effected (done) via entanglement, wavefunction collapse and decoherence [187]. This is a literal interpretation of the Hilbert space mathematical theory of quantum mechanics developed by von Neumann and Dirac [83, 361]. However, as noted by Home and Whitaker [163, see p. 309], "[t]o conclude, there are aspects of classical reality pertaining to the macrophysical world that cannot be made consistent with quantum theory in any limit, at least using the standard formalism and decoherence models."

This thus leads us to consider other approaches to understand this problem. There are other interpretations of quantum mechanics which satisfy its principles – the book by Home [162] provides an excellent exposition of the conceptual foundations of quantum physics. As is well-known [335], the various formulations of quantum mechanics provide the same results (Schrödinger wave equation, Heisenberg matrix formulation, Dirac standard formalism, Feynman path integral, Bohm quantum potential among others) – the differences between them lie in the insights that these different formulations can provide. To understand the process under discussion, what is required is a physical interpretation based on a formulation of quantum mechanics that gives precedence to the physical rather than the mathematical aspects of the theory, and of its transition to the classical domain.

A physical theory of quantum mechanics which offers a logical transition into classical physics was first developed before it was displaced by the preferred standard formalism. This initial theory was instrumental in the development of quantum mechanics. Here we briefly recap this approach.

In classical mechanics [218], the phase space description of a system is given in terms of generalized coordinates $q = \{q_i\,;\, i = 1, 2, \cdots, N\}$ and canonical momenta $p = \{p_i\,;\, i = 1, 2, \cdots, N\}$ and its time evolution is described in terms of its Hamiltonian $H(q, p)$ using Hamilton's equations

$$\dot{q}_i = \frac{\partial H}{\partial p_i}\,, \quad \dot{p}_i = -\frac{\partial H}{\partial q_i}\,. \tag{13.69}$$

The Lagrangian of the system determines its dynamics in configuration space in terms of the coordinates $\{q_i\}$ through the Euler-Lagrange equations

$$\frac{\partial L}{\partial q_i} - \frac{d}{dt}\left(\frac{\partial L}{\partial \dot{q}_i}\right) = 0\,,\; i = 1, 2, \cdots, N\,. \tag{13.70}$$

If a statistical description of the system is desired, the state of the

system is described in terms of a probability function $P(q,p)$ defined on the phase space, and its time evolution is given by

$$\frac{dP}{dt} = \{P, H\} + \frac{\partial P}{\partial t}\,, \tag{13.71}$$

where the Poisson bracket $\{P, H\}$ is given by

$$\{P, H\} = \sum_i \left(\frac{\partial P}{\partial q_i}\,\frac{\partial H}{\partial p_i} - \frac{\partial H}{\partial q_i}\,\frac{\partial P}{\partial p_i} \right) . \tag{13.72}$$

The quantum mechanical description of the system derived from the foregoing considerations sees the dynamical variables (q,p) now interpreted as operators $(\hat{q},\hat{p})$ acting on complex wavefunctions $\psi(q)$ generating observables and satisfying the commutation relation

$$[\hat{q}_i, \hat{p}_j] = i\hbar\,\delta_{ij}\,, \tag{13.73}$$

where $\hbar$ is Planck's reduced constant. This transition from a classical to a quantum mechanical description, known as *canonical quantization*, is effected (done) by the replacement of classical variables by quantum operators according to

$$q_i \to \hat{q}_i\,, \quad p_i \to \hat{p}_i \tag{13.74}$$

and (classical) Poisson brackets by (quantum) commutators according to

$$\{A, B\} \to \frac{1}{i\hbar}\,[\hat{A}, \hat{B}]\,. \tag{13.75}$$

The close relation between the classical and quantum dynamical equations is evident in the similarity between the classical equation of motion (13.71) and the quantum equation of motion as derived by Heisenberg,

$$\frac{d}{dt}\langle A\rangle = \frac{1}{i\hbar}\,\left\langle [\hat{A}, \hat{H}] \right\rangle + \left\langle \frac{\partial A}{\partial t} \right\rangle . \tag{13.76}$$

This result is a manifestation of Ehrenfest's theorem [12, see pp. 389–394] which holds that quantum mechanical expectation values $\langle A\rangle$ obey the classical equations of motion. This similarity points to the relation between the classical probability functions defined on the (q,p) phase space and the quantum mechanical expectation values obtained from the $(\hat{q},\hat{p})$ operators acting on the complex wavefunctions $\psi(q)$ representing our knowledge of the system, which in the end obey the classical equations of motion.

This approach provides a physical interpretation that can be used to better understand the classical scaling of quantum entanglement. One of the characteristics of the above considerations is the physical reality of the underlying quantum mechanical system as it evolves into a classical system. In the following section, we consider the nature of quantum states as this has an impact on the robustness of entangled states.

§13.5.3 *The nature of quantum states*

Jaeger [177, pp. 19–22] clearly communicates the importance of understanding the difference between separable (product) and non-separable (entangled) states. Over the past quarter century, the definition of entanglement has been extended, from information theory, to include mixed states that are separable when given as combination of products of subsystem states. Separable subsystem states are entirely uncorrelated (not entangled), while the entangled mixed states are the inseparable states – however, "[t]he problem of determining whether or not a given state of a composite system is entangled is known as the *separability problem*." [177, p. 21]. These entangled mixed states tend to somewhat muddle the entanglement water.

When considering separable (product) states, as noted by Jaeger [177, p. 21], "...the outcomes of local measurements on any separable state can be simulated by a local hidden-variables theory, that is, the behavior of systems described by such states can be accounted for using common-cause explanations". In other words, *separable* states can have definite physical properties when they are prepared.

It is important to note that Bell's inequality is violated only by entangled (non-separable) states. As noted by Jaeger [177, p. 22], "[t]he quantum states in which correlations between [components] A and B can violate a Bell-type inequality are called *Bell correlated*, or *EPR correlated*. If a bipartite *pure* state is entangled, then it is Bell correlated with certainty, as was first pointed out by Sandu Popescu and Daniel Rohrlich [293] and by Nicolas Gisin in the early 1990s [133]. However, no simple logical relation between entanglement and Bell correlation holds for the mixed entangled states".

Home [162, pp. 203–209] also makes the point. He concludes "an arbitrary mixture of factorable or product state vectors always satisfies Bell's inequality" as first shown by [50, 165], while " [f]or any given nonfactorable state vector of correlated quantum systems it is always possible to choose observables so that Bell's inequality is violated by quantum mechanical predictions." [162, pp. 205, 208] which was first

demonstrated by [133] as seen previously.

Hence we have two different types of quantum states depending on whether they are product (separable) or entangled (non-separable) states. Separable states are consistent with local realism – they can be physical and local, while entangled states are not consistent with local realism, based on Bell's inequality. It is surprising to obtain two diametrically opposed types of behaviours of quantum states. The normal reaction would be that there should be one consistent behaviour across all states, that the entangled states' behaviour trumps the separable states' behaviour, and hence quantum states are not consistent with local realism. However, this approach imposes conditions on product (separable) states that are simply not applicable to them.

In addition, as seen in Section §13.5.1, questions have been raised about Bell's inequality, and this difference in behaviour between separable and entangled states may indicate that there is a problem with our understanding of Bell's inequality and of entanglement in general. We explore this question in greater details in the next section, and in doing so, show that we can in fact derive a robust entanglement process as observed in the classical scaling of quantum entanglement.

§13.6 A robust entanglement process

The considerations of section §13.5.2 reinforce the underlying physical building blocks of quantum mechanics: the superposition principle, Heisenberg's uncertainty principle and wave-particle duality. These are crucial to physically understand the entanglement process and demonstrate why it is a robust process. While the superposition property results from the linear wave equations used in the theory and Heisenberg's uncertainty principle results from the fact that quantum mechanical canonically conjugate dynamical variables are Fourier transform pairs of variables [237], wave-particle duality is a purely quantum mechanical property and is undoubtedly the most important of these. The truly quantum mechanical processes such as the double-slit interference pattern, potential barrier tunneling, and in particular the entanglement process as we will see in this section, depend on the quantum mechanical phenomenon of wave-particle duality. It is critical to analyze quantum phenomena in terms of wave-particle duality to fully understand them.

§13.6.1 *Non-existence of hidden-variables?*

Home [162] does an extensive review of all proofs of the non-existence of hidden-variable theories in quantum mechanics and concludes "[h]aving

established that contrary to folklore, no a priori compelling argument excludes the possibility of contextual hidden variable theories, the entire enterprise of developing a more complete description of quantum phenomena beyond the ambit of the standard interpretation becomes logically legitimate", and provides a reference to an example: "A pedagogically instructive model example of how a contextual hidden variable model can reproduce the standard quantum mechanical results is discussed by [164], who show in detail how such a model can provide an objectively real treatment of decaying, oscillating, and regenerating kaons" [162, p. 37].

A contextual hidden variable model is one "in which the value obtained by a measurement is a function of the premeasurement value as well as the measurement context." [162, pp. 195–196]. Furthermore, "Given that a contextual hidden variable theory can provide an objectively real description of individual microphysical events, such a model is often referred to as a realistic interpretation of quantum mechanics." [162, p. 37].

In addition, the basic deficiency of hidden-variable non-existence proofs is that they are derived within the context of quantum mechanics. By its very nature, quantum mechanics is a probabilistic theory – so it is not surprising that such "proofs" find that deterministic results cannot be derived from quantum mechanics. The reader is referred to [247] for an example of this approach in the assumptions used by Bell in the derivation of his inequality, which leads to the conclusion that "it is not surprising that Bell's inequality is not satisfied in systems that obey quantum mechanics".

It is important to note that the label "hidden-variable theories" is attached indiscriminately to more complete theories of quantum mechanics. However, as in the case of Bohmian mechanics, a deterministic quantum physics theory does not need to include hidden variables. The proper path to such a theory is to start outside of quantum mechanics, derive a deterministic microscopic theory, and show that quantum mechanics can be derived from it – see [244] for an example of this approach.

Home [162] continues "[t]here are strong physical grounds for suspecting that the standard framework (formalism and interpretation) of quantum mechanics is fundamentally inadequate, though its empirical success to date is unquestionably impressive" [162, p. 37]. Home identifies the following aspects of quantum mechanics that are not well understood in the standard framework: the quantum measurement paradox, the classic limit of quantum mechanics, nonlocality of quantum mechan-

ics arising from entanglement, and wave-particle duality [162, pp. 37-38]. These are the very factors at play in the robustness of the entanglement process as discussed in this paper.

§13.6.2 *Wave-particle q-objects*

Entanglement experiments compare the behaviour of classical particles with quantum mechanical results that are unknowingly assumed to represent the particle aspect of the wave-particle quantum object (which for brevity we refer to as a "q-object"). It is important to realize that a q-object does not behave as a classical object due to its explicit wave-particle nature. For the wave aspect of a macroscopic object, its de Broglie wavelength is extremely small and its effect is negligible – however, in the quantum mechanical domain the impact of the wave-particle nature of the q-object becomes significant as observed in quantum physics. It is interesting to note that the impact of wave-particle duality has been observed at mesoscopic scales as reported in [5]. Thus a q-object is an object where the effect of wave-particle duality cannot be neglected.

In entanglement experiments, the quantum mechanical results obtained are from the *wave* aspect of the wave-particle q-object, just like the interference pattern in double-slit experiments. Hence, the results obtained in Bell experiments [6] and other entanglement experiments devised since then are the quantum mechanical results of the wave aspect of the wave-particle q-objects which are different from the particle results, again as seen in double-slit experiments (classical double-particle pattern versus quantum mechanical wave interference pattern). Similarly in Hardy experiments [148], the non-zero probability $P(A_1, B_1)$ [143] obtained in contradistinction to the local realist probability of zero is due to the *wave* aspect of the wave-particle q-object.

Wave-particle duality is still somewhat of a mystery in quantum mechanics. It is still understood mostly in terms of Bohr's principle of wave-particle complementarity which holds that the wave aspect and the particle aspect of an object are complementary aspects of a quantum object [162, see Chapter 5]. However, wave-particle duality arises naturally in the theory of Spacetime Continuum Elastodynamics (*STCED*) [238, 254] and is covered in greater detail in Chapter 12 and in [244]. This model provides a natural explanation for wave-particle duality, where an object, represented as a spacetime deformation, is composed of transverse and longitudinal modes, with the transverse

mode corresponding to the wave aspects of the deformation and the longitudinal mode corresponding to the particle aspects of the deformation.

A wave-particle q-object is thus a hybrid object consisting of both wave and particle aspects which manifest themselves differently in experiments, depending on the type of measurement. We examine the experiments of Aspect *et al.* [7, 8, 139] using single-photon states covered in Home [162, Section 5.4] to demonstrate how they can be fully understood in terms of *STCED* wave-particle duality.

In the "light pulses on a beam splitter" experiment (Home's Fig. 5.2), for a pulsed photodiode light pulse, the wave aspect is expected to apply from the *STCED* wave-particle model – indeed, as Home comments "[t]he striking feature is that even under this apparently quantum condition, light pulses arriving at the beam splitter continued to behave as classical waves, and the inequality $[P_C \geq P_T P_R]$ was never observed to be violated" [162, p. 288], where P_T is the probability that a single count is transmitted, P_R is the probability that a single count is reflected, and P_C is the probability of a coincidence for that single count.

For a source of single photon pulses from an excited atom transition, using the same experimental setup, the particle aspect is expected to apply from the *STCED* wave-particle model – indeed, "a clear-cut violation of the inequality $[P_C \geq P_T P_R]$" was observed. "This confirmed single particle behavior of the single-photon states." [162, p. 288].

The experiment was then modified as per Home's Fig. 5.3 by removing the detectors on either side of the beam splitter and recombining the two beams using mirrors and a second beam splitter. Using the source of single photon pulses from an excited atom transition as previously, this time the wave aspect is expected to apply from the *STCED* wave-particle model as it is being treated as a wave (recombining the two beams) – indeed, the experiment "showed interference effects dependent on the difference in path lengths along two possible routes of single-photon pulses." [162, p. 288].

This provides experimental confirmation of the *STCED* wave-particle model where the wave-particle q-object consists of both wave and particle aspects which manifest themselves differently depending on the type of measurement. The behaviour is physical and logical. In addition, nothing precludes the wave-particle q-object from having the full physical properties encoded in the q-object. The results obtained in the case of non-rotated detectors are in agreement with local results that would be obtained classically, because there are no specific quantum effects coming out of the quantum mechanical calculations in this case.

This indicates that the entangled q-objects are emitted with deterministic physical properties. The wave aspect gives rise to the non-local behaviour (within causality requirements due to the particle aspect of the q-object) as would be expected from the quantum mechanical calculations, while the particle aspect exhibits local causal behaviour [244]. This explains why the entanglement process is robust: the wave-particle q-objects of entangled states have definite physical, not evanescent, characteristics at emission time.

§13.6.3 *Physical approach*

This leads us to consider a physical approach which posits that the photons (for example), as wave-particle q-objects, are emitted with specific properties, but that due to our lack of knowledge of their detailed characteristics, can only be probabilistically characterized with the wavefunction ψ as a combination of the possible states and their probabilities (the realistic viewpoint [213]). Once a measurement is performed on one of the photons, its properties are resolved, thereby increasing our knowledge of the system, and allowing us to specify the properties of the other photon – a simple physical understanding of the process [247]. Such a process can easily scale to classical objects and distances, and is undeniably very robust as the q-objects' properties are determined at emission time, not evanescent depending either on an experimenter's whim or thought process, or on not having an interaction that would destroy the entanglement on its way to measurement resolution. The classical-scale experiments considered previously are then seen to be a confirmation of this approach.

The wavefunction is thus seen to be a probabilistic description of our (limited) *knowledge* of a quantum mechanical system, not a complete physical description of the system, with this probability being proportional to the *intensity* of the wavefunction as seen in [244]. This explains the laws of quantum probability [120,123]. We note the same behaviour for electromagnetic radiation, where the intensity is proportional to the energy density of the field, which can be converted to a probability by normalization, as seen in [244].

As a result of the measurement process, the original wavefunction description is superceded (the so-called collapse of the wavefunction) and is replaced by a more accurate wavefunction description of the quantum mechanical system that takes into account the results of the measurement process. As [160] puts it, "When a detector clicks the wavefunction does not 'collapse' from all over space to a point, it is simply that only

part of it is now relevant.". It is important to note that this measurement process is effected (done) by the interaction of the quantum mechanical system with an outside agency, whether it is a measurement apparatus or an interaction with another quantum mechanical system.

This is a simple logical description of the physical process that does not require metaphysical "spooky action at a distance" explanations and, by the principle of Occam's razor, is a superior explanation of the entanglement process. It should be noted that the imaginary actors "Bob" and "Alice" which are used in the explanation of entanglement and SAAD, even though the explanation is presented as a sequential series of events, are both aware of the same experimental information within the same time window, as mentioned in Section §13.5.1, and hence fully satisfy Jaynes' analysis of entanglement experiments as discussed in [182, 247].

As Home points out, "[c]ontrary to a widely held misconception, we stress that no experiment probing quantum locality has yet tested quantum correlations measured across spacelike separation unambiguously." [162, p. 233]. In photon polarization correlation experiments [6], "[t]he claim of spacelike separation is usually based on ensuring that a photon on one side reaching a photomultiplier detector is spacelike separated from its partner passing the polarization analyzer on the other side." However, a typical photomultiplier detector requires about 30 ns for a current pulse to be generated following the arrival of a photon, which provides a different spacelike separation than that obtained from the resolution time of a photomultiplier which is usually of order 1 ns [162, p. 233].

It should be noted that the model proposed in this paper is independent of these so-called "loopholes". They are mentioned to indicate the difficulty of performing such experiments which raises cautionary notes on the concomitant dangers of wishful thinking and unrecognized assumptions, limitations and interpretation of the results.

§13.6.4 *Evidence for SAAD?*

So why introduce a mysterious agent, "spooky action at a distance", when none is required? As we asked in Section §13.5, what prompts the acceptance of this description as part of the orthodox interpretation? The reason is that SADD is believed to be supported by the experimental evidence. However, the aforementioned considerations and the analysis of Jaynes [182, 183, 247] show that the experimental evidence can be explained without resorting to metaphysics, that the problem

results from the assumption that a conditional probability represents a physical influence instead of the physically-correct logical inference that it is.

As Home and Whitaker write [163, p. 238],

> In one out of four cases, Alice is lucky with her measurement, and Bob's particle immediately becomes an identical replica of Alice's original. Then it might seem as if information has traveled instantly from Alice to Bob. Yet this strange feature cannot be used to send *usable information instantaneously*, because Bob has *no* way of knowing that his particle is already an identical replica. Only when he ***learns*** the result of Alice's Bell-state measurement, which is transmitted to him via classical means, can he exploit the information in the teleported quantum state.

where the emphasis is in the original text and we have in addition highlighted the word "learns".

In other words, what is believed to be "spooky action at a distance" is actually the experimenters' knowledge of the system suddenly increasing as a result of the measurement process, and the experimenters being in a position to logically infer the properties of the distant component, which is confirmed in the measurement performed on the distant component. In actual practice, in entanglement experiments, both measurements are done in the same time window (see Sections §13.5.1 and §13.6.3).

There is also a certain intellectual inertia at play. As Bell [21] commented, "Why is the pilot wave picture [Bohm's] ignored in text books? Should it not be taught, not as the only way, but as an antidote to the prevailing complacency? To show that vagueness, subjectivity, and indeterminism, are not forced on us by experimental facts, but by deliberate theoretical choice?" All very good questions.

§13.7 Quantum information causality

The emerging concept of *information causality* [131, 284, 306] is an attempt to preserve causality based on the underlying premise that it is information that is the core element in the analysis of the entanglement process. The approach followed is to impose this concept as a principle of nature to avoid the special relativistic causality problems raised by SAAD. This concept unwittingly reflects Jaynes' analysis of entanglement experiments in that it focuses on information – however, Jaynes' analysis [182,183] already accomplishes this without having to introduce an additional constraint in the guise of a new causality principle, and in so doing, also eliminates the need for SAAD.

§13.8 Weak quantum measurements

Weak quantum measurements [130, 336, 339, 358, 359] is another emerging concept in quantum mechanics that has an impact on the understanding of the entanglement process. What is interesting with this approach is that it is possible to make minimal-interacting measurements, which leaves the collapse of the wavefunction in the literal interpretation of the mathematical standard formalism of quantum mechanics in a quandary: how can any measurement be done without collapsing the wavefunction?

The accepted explanation [339] is that the quantum state is not collapsed into eigenvectors, but instead, by a weak coupling of the measurement device and the system, is biased by a small angle such that the measurement device shows a superposition of several eigenvalues. The current status is summarized as follows: "weak measurement theory presents a plethora of strange quantum phenomena, not yet completely understood." [339]. There is no doubt that even a weak interaction measurement will have an impact on the system, and this approach, certainly experimentally valid, puts the wavefunction collapse of the literal interpretation of quantum mechanics into question.

The proposal of weakly interacting measurements was also introduced in [237] and in section §13.3 in the context of the application of the Nyquist-Shannon Sampling Theorem to quantum measurements. The author showed that Brillouin zones in the solid state in Condensed Matter Physics are a manifestation of the Nyquist-Shannon Sampling Theorem at the quantum level, where the translational symmetry of atoms in a solid resulting from the regular lattice spacing, is equivalent to an effective sampling of the atoms of the solid giving rise to the Brillouin zones. This raised the possibility of investigating new experimental conditions leading to new measurements previously considered unreachable, a possibility that is also considered possible in the literature on weak quantum measurements.

§13.9 Physically realistic quantum mechanics

In this chapter, we have reviewed the physical difficulties present in quantum mechanics. One finds that, invariably, the problems arise because it is assumed that the mathematical theory represents a physical reality that is simply not the case. And we have not covered the more esoteric ideas such as the Everett multiple universe, multiverse, *etc* interpretations of the mathematical theory that give even more credence to the physicality of the mathematics, which are just larger cohorts of

angels dancing on a pinhead. The paradoxes are seen to result from assigning physical reality to the probabilities of quantum mechanics rather than the logical inferences that they are.

As it should by now be evident to the reader, at this time quantum mechanics can only deal with probabilities associated with quantum physical processes until a dynamic theory is developed that explains the probabilistic results that are obtained. This book proposes such a theory – consequently, we had to take this detour in the basic methodology of quantum mechanics to highlight its nature and problems. The current orthodox interpretation of quantum mechanics does not deter from the success of the theory when results are compared to the probabilistic predictions of quantum theory. The problem resides with the interpretation of those probabilities which has resulted in the stultification of further progress in quantum physics. We need to bring physics back into quantum mechanics to get a physically realistic theory of quantum physics.

In particular, we have reviewed the nature of quantum entanglement, a key quantum mechanical concept, and have considered the difference between separable (product) and non-separable (entangled) states. Mixtures of product (separable) states always satisfy Bell's inequality *i.e.* separable states can have definite physical properties when they are prepared. Bell's inequality fails only for entangled (non-separable) states. Hence separable states are consistent with local realism – they can be physical and local, while entangled states are not consistent with local realism, based on their violation of Bell's inequality.

These considerations reinforce the importance of the underlying physical building blocks of quantum mechanics: the superposition principle, Heisenberg's uncertainty principle and wave-particle duality which is the most important of these. The truly quantum mechanical processes such as the double-slit interference pattern, potential barrier tunneling, and in particular the entanglement process as we have seen in this chapter, depend on the quantum mechanical phenomenon of wave-particle duality.

It is thus critical to analyze quantum phenomena in terms of wave-particle duality to fully understand them. We have noted that in entanglement experiments, the quantum mechanical results obtained are from the *wave* aspect of the wave-particle quantum object (which for brevity we refer to as a "q-object"), just like the interference pattern in double-slit experiments. The wave aspect then gives rise to the non-local behaviour (within causality requirements due to the particle aspect of the q-object) as would be expected from the quantum mechanical cal-

culations, while the particle aspect exhibits local causal behaviour.

As demonstrated in Section §13.6, the resolution of the robustness of the entanglement process in classical scale quantum entanglement experiments is achieved within the wave-particle q-object explanation of the process in which entangled state q-objects have definite physical characteristics at emission time. Strong evidence has been provided to support this proposal.

It should be noted that quantum cryptography and quantum computing are then seen to depend on the *wave* aspect of the wave-particle q-object. This fundamental understanding should help accelerate the progress of these new development programs.

The design of experiments to provide experimental evidence requires that experimentalists shift the paradigm used to test quantum theories. Currently experiments are designed to try to prove the applicability of quantum mechanics to entangled states by verifying various inequalities such as Bell's. The experiments suggested by Zhao [381] try to clarify the physical properties of quantum entanglement and includes experimental tests of the locality of the measurements of Bell states, experimental tests of the constituents of Bell states, and experimental tests of determinism in quantum measurements. In addition, even though the entanglement experiments currently performed agree with the model proposed in this book, specific experiments need to be performed to test the model under conditions that emphasize that quantum entanglement behaviour results from the *wave* aspect of the wave-particle q-objects.

Chapter 14

STCED Framework for Quantum Physics

In this chapter, we cover the relation of spacetime continuum defects to quantum physics. The framework of quantum physics, based on dislocations and disclinations in the spacetime continuum is covered in the sections of this chapter. This covers the basic characteristics of quantum physics, including quantization, bosons and fermions and quantum electrodynamics. Subsequent chapters cover various aspects of quantum physics as covered by *STCED*.

In Chapter 15, screw dislocations in quantum physics are considered in section §15.1 and edge dislocations are covered in section §15.2. Wedge disclinations are considered in section §15.3 and twist disclinations in section §15.4. The association of these defects to fundamental quantum particles are covered in Chapter 16. Chapter 17 covers defect interactions in quantum physics.

Chapter 18 provides physical explanations of QED phenomena provided by defects in the spacetime continuum. We conclude with a summary of the framework used for the development of a physical description of physical processes at the quantum level, based on dislocations and disclinations in the spacetime continuum within the theory of the Elastodynamics of the Spacetime Continuum (*STCED*).

There is no doubt that the task we have set for ourselves is a tall order. The theories of quantum mechanics and quantum electrodynamics have been very successful at reproducing the results of quantum experimental measurements. In addition, electroweak and quantum chromodynamics theories have been derived from those. Reproducing these results within a new physical framework is a significant challenge. The possibility of providing a physical description of quantum physics is the driving force behind this effort which, if we are successful, can take us to the next level in our description of the subquantum level. In the following chapters, we will show that the characteristics of the proposed physical framework match those derived from quantum mechanics and can lay the foundation for quantum physical calculations.

§14.1 Framework for quantum physics

In a solid, dislocations represent the fundamental displacement processes that occur in its atomic structure. A solid viewed in electron

microscopy or other microscopic imaging techniques is a tangle of screw and edge dislocations [172, see p. 35 and accompanying pages]. Similarly, dislocations in the spacetime continuum are taken to represent the fundamental displacement processes that occur in its structure.

In a similar fashion, disclinations represent the fundamental rotational processes that occur in the spacetime continuum structure. These fundamental displacement and rotational processes should thus correspond to basic quantum phenomena and provide a framework for the description of quantum physics in *STCED*.

We find that dislocations and disclinations have fundamental properties that reflect those of particles at the quantum level. Dislocations, as translational processes, are found to correspond to bosons, while disclinations, as rotational processes, are found to correspond to fermions, based on their characteristics and symmetry transformations. In addition, the fundamental properties of defects in the spacetime continuum are found to include self-energy and interactions mediated by the strain energy density of the dislocations and disclinations.

§14.2 Quantization

The Burgers vector as defined by expression (9.1) has similarities to the Bohr-Sommerfeld quantization rule

$$\oint_C p\, dq = nh \tag{14.1}$$

where q is the position canonical coordinate, p is the momentum canonical coordinate and h is Planck's constant. This leads us to consider the following quantization rule for the spacetime continuum: at the quantum level, we assume that the spacetime continuum has a granularity characterized by a length b_0 corresponding to the smallest elementary Burgers dislocation-displacement vector possible in the spacetime continuum.

The idea that the existence of a shortest length in nature would lead to a natural cut-off to generate finite integrals in QED has been raised before [147]. The smallest elementary Burgers dislocation-displacement vector introduced here provides a lower bound as shown in calculations in forthcoming chapters. Then the magnitude of a Burgers vector can be expressed as a multiple of the elementary Burgers vector:

$$b = nb_0\,. \tag{14.2}$$

We find that b is usually divided by 2π in dislocation equations, and hence we define

$$\text{ƀ} = \frac{b}{2\pi}\,, \tag{14.3}$$

and similarly for the elementary Burgers dislocation-displacement vector b_0,

$$\text{ƀ}_0 = \frac{b_0}{2\pi}\,. \tag{14.4}$$

Similarly, the disclination Frank vector Ω is usually divided by 2π in disclination equations, and hence we define the symbol

$$\mathfrak{Q} = \frac{\Omega}{2\pi}\,. \tag{14.5}$$

The question of quantization in *STCED* is a thorny issue, as it implies a certain discreteness to the spacetime continuum. As we see in various chapters in this book, indications are that this discreteness would be lattice-like, possibly leading to the consideration of additional smaller spacetime continuum structures, similar to what is observed in the solid state in Condensed Matter Physics. It may be possible that there is no need to introduce discreteness in *STCED*, but at this time there are arguments that militate in favour of that requirement.

§14.3 Symmetry considerations

It has become *de rigueur* in physics books to specify the applicable symmetry principles such as U(1), SO(3), SU(2), SU(3) upfront to assist in the symmetry characterization of the subject matter. While it is useful to understand the symmetry representation of our theories, it does not provide a complete physical description of the theory. As noted by Georgi [132, p. 155] [375, p. 77],

> A symmetry principle should not be an end in itself. Sometimes the physics of a problem is so complicated that symmetry arguments are the only practical means of extracting information about the system. Then, by all means use them. But, do not stop looking for an explicit dynamical scheme that makes more detailed calculation possible. Symmetry is a tool that should be used to determine the underlying dynamics, which must in turn explain the success (or failure) of the symmetry arguments. Group theory is a useful technique, but it is no substitute for physics.

Hence we will include symmetry considerations in this book as an adjunct to our physical theories where justified.

As symmetry principles are associated with specific conservation laws, we list the main ones in the table below.

Symmetry principle	Invariance	Conservation law
Time translation	Time invariance	Mass-energy
Space translation	Translation symm.	Linear momentum
SO(3)*	Rotation invariance	Angular momentum
U(1)†	Gauge invariance	Electric charge
SU(2)‡	Gauge invariance	Isospin
SU(3)§	Gauge invariance	Color charge

*Group of special orthogonal transformations of three (real) variables.

†Group of unitary transformations of one complex variable.

‡Group of special unitary transformations of two complex variables.

§Group of special unitary transformations of three complex variables.

Table 14.1: Symmetry principles and conservations laws.

We have already used the conservation of energy-momentum and angular momentum to deduce that the spacetime continuum is isotropic and homogeneous as seen in section §2.1.

§14.4 Bosons and fermions

Elementary quantum particles are classified into bosons and fermions based on integral and half-integral multiples of $\hbar$ respectively. Bosons obey Bose-Einstein statistics while fermions obey Fermi-Dirac statistics and the Pauli Exclusion Principle. These determine the number of non-interacting indistinguishable particles that can occupy a given quantum state: there can only be one fermion per quantum state while there is no such restriction on bosons.

This is explained in quantum mechanics using the combined wave-function of two indistinguishable particles when they are interchanged:

$$\begin{aligned} &\text{Bosons}: \quad \Psi(1,2) = \Psi(2,1) \\ &\text{Fermions}: \quad \Psi(1,2) = -\Psi(2,1)\,. \end{aligned} \tag{14.6}$$

Bosons commute and as seen from (14.6) above, only the symmetric part contributes, while fermions anticommute and only the antisymmetric

part contributes. There have been attempts at a formal explanation of this phenomemon, the spin-statistics theorem, with Pauli's being one of the first [283]. Jabs [175] provides an overview of these and also offers his own attempt at an explanation.

However, as Feynman comments candidly in [123, see p. 4-3],

> We apologize for the fact that we cannot give you an elementary explanation. An explanation has been worked out by Pauli from complicated arguments of quantum field theory and relativity. He has shown that the two must necessarily go together, but we have not been able to find a way of reproducing his arguments on an elementary level. It appears to be one of the few places in physics where there is a rule which can be stated very simply, but for which no one has found a simple and easy explanation. The explanation is deep down in relativistic quantum mechanics. This probably means that we do not have a complete understanding of the fundamental principle involved. For the moment, you will just have to take it as one of the rules of the world.

The question of a simple and easy explanation is still outstanding. Eq. (14.6) is still the easily understood explanation, even though it is based on the exchange properties of particles, rather than on how the statistics of the particles are related to their spin properties. At this point in time, it is an empirical description of the phenomenon.

Ideally, the simple and easy explanation should be a *physical* explanation to provide a complete understanding of the fundamental principles involved. *STCED* provides such an explanation, based on dislocations and disclinations in the spacetime continuum. Part of the current problem is that there is no understandable physical picture of the quantum level. *STCED* provides such a picture.

The first point to note is that based on their properties, bosons obey the superposition principle in a quantum state. The location of quantum particles is given by the deformation displacement u^μ. Dislocations are translational displacements that commute, satisfy the superposition principle and behave as bosons. As we saw in section §3.6, particles with spin 0, 1 and 2 are described by (3.50) and (3.51) which are equations in terms of $u^{\mu;\nu}$.

Disclinations, on the other hand, are rotational displacements that do not commute and that do not obey the superposition principle. You cannot have two rotational displacements in a given quantum state. Hence their number is restricted to one per quantum state. They behave as fermions. Spinors represent spin one-half fermions. Dirac spinor fields represent electrons. Weyl spinors, derived from Dirac's four complex

components spinor fields, are a pair of fields that have two complex components. Interestingly enough, "[u]sing just one element of the pair, one gets a theory of massless spin-one-half particles that is asymmetric under mirror reflection and ... found ... to describe the neutrino and its weak interactions" [375, p. 63].

"From the point of view of representation theory, Weyl spinors are the fundamental representations that occur when one studies the representations of rotations in four-dimensional space-time... spin-one-half particles are representation of the group SU(2) of transformations on two complex variables." [375, p. 63]. To clarify this statement, each rotation in three dimensions (an element of SO(3)) corresponds to two distinct elements of SU(2). Consequently, the SU(2) transformation properties of a particle are known as the particle's spin.

Hence, the unavoidable conclusion is that bosons are dislocations in the spacetime continuum, while fermions are disclinations in the spacetime continuum.

§14.5 Quantum electrodynamics

In *STCED*, the role played by virtual particles in quantum electrodynamics (QED) is replaced by the interaction of the strain energy density of the dislocations and disclinations. QED is a perturbative theory, and the virtual particles are introduced as an interpretation of the perturbative expansion represented by Feynman diagrams.

Although the existence of virtual particles in QED is generally accepted, there are physicists who still question this interpretation of QED perturbation expansions. Weingard [366] "argues that if certain elements of the orthodox interpretation of states in QM are applicable to QED, then it must be concluded that virtual particles cannot exist. This follows from the fact that the transition amplitudes correspond to superpositions in which virtual particle type and number are not sharp. Weingard argues further that analysis of the role of measurement in resolving the superposition strengthens this conclusion. He then demonstrates in detail how in the path integral formulation of field theory no creation and annihilation operators need appear, yet virtual particles are still present. This analysis shows that the question of the existence of virtual particles is really the question of how to interpret the propagators which appear in the perturbation expansion of vacuum expectation values (scattering amplitudes)." [36]

The basic Feynman diagrams can be seen to represent screw dislocations as photons, edge dislocations as bosons, twist and wedge discli-

nations as fermions, and their interactions. Virtual particles would require the presence of virtual dislocations and virtual disclinations in the spacetime continuum, which clearly does not make sense. Instead, the exchange of virtual particles in interactions can be seen to be a perturbation expansion representation of the forces resulting from the overlap of the defects' strain energy density, with suitably modified diagrams. The perturbative expansions are thus replaced by finite analytical expressions.

This theory is not perturbative as in QED, but rather calculated from analytical expressions. The analytical equations can become very complicated, and in some cases, perturbative techniques are used to simplify the calculations, but the availability of analytical expressions permits a better understanding of the fundamental processes involved.

Chapter 15

Properties of Defects in STCED

In this chapter, we collect and summarize the properties of the screw dislocation, the edge dislocation, the wedge disclination and the twist disclination to help in the identification of these spacetime defects in quantum physics.

§15.1 Properties of screw dislocations

Screw dislocations are covered in section §9.2 and in section §9.5 on deWit's dislocation line for the case where $b_x = b_y = 0$. Using the parity operator $\mathbb{P}$ defined according to [87, see section 3.3]

$$f(\mathbf{x}, t) \to g(\mathbf{x}, t) = \mathbb{P} f(\mathbf{x}, t) = f(-\mathbf{x}, t)\,, \tag{15.1}$$

on (9.2) or (9.130) for $b_x = b_y = 0$, we obtain

$$\mathbb{P}(u_z) = \mathbb{P}\left(\frac{b_z}{2\pi}\,\tan^{-1}\frac{y}{x}\right) = \frac{-b_z}{2\pi}\,\tan^{-1}\left(\frac{-y}{-x}\right) = -u_z\,. \tag{15.2}$$

Hence the screw dislocation has odd parity under *parity reversal* as expected [87, see p. 71].

The rotation vector for the screw dislocation is given by (9.5)

$$\omega_r = -\frac{b_z}{4\pi}\,. \tag{15.3}$$

As seen in section §3.6, the trace of the antisymmetric field $\omega^{\mu\nu}$ is zero, and hence massless. The field $\omega^{\mu\nu}$ is of spin 1, and since it is massless, it does not have a spin 0 component. From section §9.2.3, the rest-mass density of the screw dislocation is indeed $\rho = 0$, and from section §9.2.4, so is its charge density $\varrho = 0$ and its current density $j^\nu = 0$. Screw dislocations are the easiest defect to analyze.

Screw dislocations in the spacetime continuum are massless, transverse deformations, and are hence identified specifically with photons. Consider the displacement of a stationary screw dislocation as derived in section §9.2.1:

$$u_z = \frac{b}{2\pi}\,\theta = \mathfrak{b}\,\theta\,. \tag{15.4}$$

Figure 15.1: A wavelength of a screw dislocation.

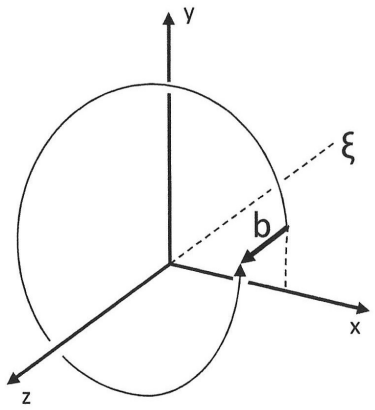

Taking the derivative with respect to time, we obtain

$$\dot{u}_z = v_z = \frac{b}{2\pi}\,\dot{\theta} = \frac{b}{2\pi}\,\omega\,. \tag{15.5}$$

The speed of the transverse displacement is c, the speed of light. Substituting for $\omega = 2\pi\nu$, (15.5) becomes

$$c = b\,\nu\,. \tag{15.6}$$

Hence

$$b = \lambda\,, \tag{15.7}$$

the wavelength of the screw dislocation. This result is illustrated in Fig. 15.1. It is important to note that this relation applies only to screw dislocations.

The strain energy density of the screw dislocation is given by the transverse distortion energy density derived in section §9.2.3. For a stationary screw dislocation, substituting (14.3) into (9.22),

$$\mathcal{E}_\perp = \frac{\bar{\mu}_0\,\mathfrak{b}^2}{2}\,\frac{1}{r^2}\,. \tag{15.8}$$

As we have seen previously in section §9.2.3, the longitudinal strain energy density is given by $\mathcal{E}_\parallel = 0$.

§15.2 Properties of edge dislocations

Edge dislocations are covered in section §9.3 and in section §9.5 on deWit's dislocation line for the case where $b_z = 0$. Using the parity operator $\mathbb{P}$ as per (15.1) on (9.130) for $b_z = 0$, we obtain

$$\begin{aligned}
\mathbb{P}(u_x) &= \mathbb{P}\left(\frac{b_x}{2\pi}\left(\theta + \bar{\beta}_0\,\frac{xy}{r^2}\right) + \frac{b_y}{2\pi}\left(\bar{\alpha}_0\,\ln r + \bar{\beta}_0\,\frac{y^2}{r^2}\right)\right) \\
&= -\frac{b_x}{2\pi}\left(\theta + \bar{\beta}_0\,\frac{xy}{r^2}\right) - \frac{b_y}{2\pi}\left(\bar{\alpha}_0\,\ln r + \bar{\beta}_0\,\frac{y^2}{r^2}\right) = -u_x \\
\mathbb{P}(u_y) &= \mathbb{P}\left(-\frac{b_x}{2\pi}\left(\bar{\alpha}_0\,\ln r + \bar{\beta}_0\,\frac{x^2}{r^2}\right) + \frac{b_y}{2\pi}\left(\theta - \bar{\beta}_0\,\frac{xy}{r^2}\right)\right) \\
&= \frac{b_x}{2\pi}\left(\bar{\alpha}_0\,\ln r + \bar{\beta}_0\,\frac{x^2}{r^2}\right) - \frac{b_y}{2\pi}\left(\theta - \bar{\beta}_0\,\frac{xy}{r^2}\right) = -u_y \\
u_z &= 0
\end{aligned} \tag{15.9}$$

where $\bar{\alpha}_0$ and $\bar{\beta}_0$ are as per (9.128) and both r and θ are unchanged by the substitution of (15.1). Hence the edge dislocation has odd parity under *parity reversal*.

The rotation vector for the edge dislocation is given by (9.138)

$$\omega_z = \frac{1}{2\pi}\,\frac{b_x x + b_y y}{r^2}\,. \tag{15.10}$$

From section §9.5, the mass energy density of the discrete dislocation line is given by (9.134)

$$\rho c^2 = \frac{4}{\pi}\,\frac{\bar{\kappa}_0\bar{\mu}_0}{2\bar{\mu}_0 + \bar{\lambda}_0}\,\frac{b_x y - b_y x}{r^2}\,, \tag{15.11}$$

and from section §9.5.2, the non-zero components of the current density are given by (9.157)

$$\begin{aligned}
j_x &= \frac{\varphi_0}{2\pi\mu_0}\,\frac{b_y r^2 + 2x\,(b_x y - b_y x)}{r^4} \\
j_y &= -\frac{\varphi_0}{2\pi\mu_0}\,\frac{b_x r^2 - 2y\,(b_x y - b_y x)}{r^4}
\end{aligned} \tag{15.12}$$

and the charge density by (9.160)

$$\varrho = \pm\frac{1}{4\pi}\,\varphi_0\epsilon_0 c\,\frac{1}{r^2}\,\sqrt{b_x^2 + b_y^2}\,. \tag{15.13}$$

.

The strain energy density of the edge dislocation is derived in section §9.3.3. The dilatation (massive) strain energy density of the edge dislocation is given by the longitudinal strain energy density $\mathcal{E}_{\parallel}$ (9.50) and the distortion (massless) strain energy density of the edge dislocation is given by the transverse strain energy density $\mathcal{E}_{\perp}$ (9.51).

The discrete dislocation line longitudinal dilatation strain energy density is given by (9.139)

$$\mathcal{E}_{\parallel} = \frac{1}{2\pi^2} \, \frac{\bar{\kappa}_0 \, \bar{\mu}_0^2}{(2\bar{\mu}_0 + \bar{\lambda}_0)^2} \, \frac{(b_x y - b_y x)^2}{r^4} \, . \tag{15.14}$$

The discrete dislocation line distortion strain energy density, which includes the screw dislocation, is given by (9.149)

$$\begin{aligned} \mathcal{E}_{\perp} = & \frac{\bar{\mu}_0}{8\pi^2} \, \frac{b_z^2}{r^2} + \frac{\bar{\mu}_0}{4\pi^2} \, \bar{\alpha}_0^2 \, \frac{(b_x y - b_y x)^2}{r^4} + \\ & + \frac{\bar{\mu}_0}{2\pi^2} \, \bar{\beta}_0^2 \, \frac{(b_x x + b_y y)^2}{r^4} - \frac{3}{2\pi^2} \, \frac{\bar{\mu}_0 \bar{\lambda}_0}{2\bar{\mu}_0 + \bar{\lambda}_0} \, \frac{b_x b_y x y}{r^4} \, . \end{aligned} \tag{15.15}$$

As done in §9.5.1, substituting from (9.138) and (9.139), (15.15) becomes

$$\begin{aligned} \mathcal{E}_{\perp} = & \frac{\bar{\mu}_0}{8\pi^2} \, \frac{b_z^2}{r^2} + \frac{1}{2} \, \frac{\bar{\mu}_0}{\bar{\kappa}_0} \, \mathcal{E}_{\parallel} + 2\bar{\mu}_0 \left(\frac{\bar{\mu}_0 + \bar{\lambda}_0}{2\bar{\mu}_0 + \bar{\lambda}_0} \right)^2 \omega_z^2 - \\ & - \frac{3}{2\pi^2} \, \frac{\bar{\mu}_0 \bar{\lambda}_0}{2\bar{\mu}_0 + \bar{\lambda}_0} \, \frac{b_x b_y x y}{r^4} \, . \end{aligned} \tag{15.16}$$

The first term is the screw dislocation strain energy density of (9.22), the second term is proportional to the edge dislocation distortion strain energy density arising from the longitudinal strain energy density of (9.139), the third term is the edge dislocation distortion strain energy density arising from the rotation vector of (9.138) and the last term is a moment distortion strain energy density term. It is interesting to note that there are no interaction terms (cross-terms) between screw and edge dislocations for a dislocation line.

§15.3 Properties of wedge disclinations

Wedge disclinations are covered in section §10.6 on deWit's disclination line for the case where $\Omega_x = \Omega_y = 0$. Using the parity operator $\mathbb{P}$ as

per (15.1) on the non-zero components of (10.99), we obtain

$$\begin{aligned}
\mathbb{P}(u_x) &= \mathbb{P}\left(-\frac{\Omega_z}{2\pi}\,(y\,\theta - \bar{\alpha}_0\,x\,(\ln r - 1))\right) \\
&= -\frac{\Omega_z}{2\pi}\,(y\,\theta - \bar{\alpha}_0\,x\,(\ln r - 1)) = u_x \\
\mathbb{P}(u_y) &= \mathbb{P}\left(\frac{\Omega_z}{2\pi}\,(x\,\theta + \bar{\alpha}_0\,y\,(\ln r - 1))\right) \\
&= \frac{\Omega_z}{2\pi}\,(x\,\theta + \bar{\alpha}_0\,y\,(\ln r - 1)) = u_y
\end{aligned} \tag{15.17}$$

where $\bar{\alpha}_0$ and $\bar{\beta}_0$ are as per (9.128) and both r and θ are unchanged by the substitution of (15.1). Hence the wedge disclination has even parity under *parity reversal* as expected from an axial vector.

The rotation vector for the wedge disclination is given by (10.104)

$$\omega_z = \frac{\Omega_z}{2\pi}\,. \tag{15.18}$$

From section §10.6, the mass energy density of the wedge disclination is given by (10.107)

$$\rho c^2 = \frac{4\bar{\kappa}_0\Omega_z}{\pi}\,\left(\frac{\bar{\mu}_0}{2\bar{\mu}_0 + \bar{\lambda}_0}\,\ln r + \frac{1}{2}\,\frac{\bar{\mu}_0 + \bar{\lambda}_0}{2\bar{\mu}_0 + \bar{\lambda}_0}\right)\,, \tag{15.19}$$

and from section §10.6.1, the non-zero components of the current density are given by (10.114)

$$\begin{aligned}
j_x &= \frac{\varphi_0\Omega_z}{2\pi\mu_0}\,\frac{x}{r^2} = \frac{\varphi_0\Omega_z}{2\pi\mu_0}\,\frac{\cos\theta}{r} \\
j_y &= -\frac{\varphi_0\Omega_z}{2\pi\mu_0}\,\frac{y}{r^2} = \frac{\varphi_0\Omega_z}{2\pi\mu_0}\,\frac{\sin\theta}{r}
\end{aligned} \tag{15.20}$$

and the charge density by (10.115)

$$\varrho = \pm\frac{1}{4\pi}\,\varphi_0\epsilon_0 c\,\frac{\Omega_z}{r^2}\,. \tag{15.21}$$

The strain energy density of the wedge disclination is derived in section §10.6. The dilatation (massive) strain energy density of the wedge disclination is given by the longitudinal strain energy density $\mathcal{E}_{\|}$ and the distortion (massless) strain energy density of the wedge disclination is

given by the transverse strain energy density $\mathcal{E}_\perp$. The wedge disclination longitudinal dilatation strain energy density is given by (10.109)

$$\mathcal{E}_\parallel = \frac{\bar{\kappa}_0 \Omega_z^2}{2\pi^2} \left(\bar{\alpha}_0 \ln r + \frac{1}{2}\, \bar{\beta}_0 \right)^2 \tag{15.22}$$

and the wedge disclination distortion strain energy density is given by (10.113)

$$\mathcal{E}_\perp = \frac{\bar{\mu}_0 \Omega_z^2}{4\pi^2} \left[\left(\bar{\alpha}_0 \ln r + \frac{3}{2}\, \bar{\beta}_0 \right)^2 - \left(\frac{3}{2}\, \bar{\beta}_0 \right)^2 \right] . \tag{15.23}$$

§15.4 Properties of twist disclinations

Twist disclinations are covered in section §10.7 on deWit's disclination line for the case where $\Omega_z = 0$. Using the parity operator $\mathbb{P}$ as per (15.1) on (10.119), we obtain

$$\begin{aligned}
&\mathbb{P}(u_x) = u_x \\
&\quad = -\frac{\Omega_x}{2\pi}\, z \left(\bar{\alpha}_0 \ln r + \bar{\beta}_0\, \frac{y^2}{r^2} \right) + \frac{\Omega_y}{2\pi}\, z \left(\theta + \bar{\beta}_0\, \frac{xy}{r^2} \right) \\
&\mathbb{P}(u_y) = u_y \\
&\quad = -\frac{\Omega_x}{2\pi}\, z \left(\theta - \bar{\beta}_0\, \frac{xy}{r^2} \right) - \frac{\Omega_y}{2\pi}\, z \left(\bar{\alpha}_0 \ln r + \bar{\beta}_0\, \frac{x^2}{r^2} \right) \\
&\mathbb{P}(u_z) = u_z \\
&\quad = \frac{\Omega_x}{2\pi} \left(y\, \theta - \bar{\alpha}_0\, x \left(\ln r - 1 \right) \right) - \frac{\Omega_y}{2\pi} \left(x\, \theta + \bar{\alpha}_0\, y \left(\ln r - 1 \right) \right)
\end{aligned} \tag{15.24}$$

where $\bar{\alpha}_0$ and $\bar{\beta}_0$ are as per (9.128) and both r and θ are unchanged by the substitution of (15.1). Hence the twist disclination has even parity under *parity reversal* as expected for an axial vector.

The rotation vector for the twist disclination is given by (10.125)

$$\begin{aligned}
\omega_x &= \frac{\Omega_x}{2\pi}\, \theta \\
\omega_y &= \frac{\Omega_y}{2\pi}\, \theta \\
\omega_z &= \frac{\Omega_x}{2\pi}\, \frac{yz}{r^2} - \frac{\Omega_y}{2\pi}\, \frac{xz}{r^2} .
\end{aligned} \tag{15.25}$$

From section §10.7, the mass energy density of the wedge disclination is given by (10.128)

$$\rho c^2 = \frac{4\bar{\kappa}_0}{\pi} \frac{\bar{\mu}_0}{2\bar{\mu}_0 + \bar{\lambda}_0} \left(\Omega_x x + \Omega_y y\right) \frac{z}{r^2}\,, \tag{15.26}$$

and from section §10.7.1, the non-zero components of the current density are given by (10.134)

$$\begin{aligned} j_x &= -\frac{\varphi_0}{2\pi\mu_0} \frac{\Omega_x z r^2 - 2xz\left(\Omega_x x + \Omega_y y\right)}{r^4} \\ j_y &= -\frac{\varphi_0}{2\pi\mu_0} \frac{\Omega_y z r^2 - 2yz\left(\Omega_x x + \Omega_y y\right)}{r^4} \\ j_z &= -\frac{\varphi_0}{2\pi\mu_0} \frac{\Omega_x x + \Omega_y y}{r^2} \end{aligned} \tag{15.27}$$

and the charge density by (10.135)

$$\varrho = \pm\frac{1}{4\pi} \varphi_0 \epsilon_0 c \frac{1}{r^2} \sqrt{\left(\Omega_x^2 + \Omega_y^2\right) z^2 + \left(\Omega_x x + \Omega_y y\right)^2}\,. \tag{15.28}$$

The strain energy density of the twist disclination is derived in section §10.7. The dilatation (massive) strain energy density of the twist disclination is given by the longitudinal strain energy density $\mathcal{E}_{\|}$ and the distortion (massless) strain energy density of the twist disclination is given by the transverse strain energy density $\mathcal{E}_{\perp}$. The twist disclination longitudinal dilatation strain energy density is given by (10.129)

$$\mathcal{E}_{\|} = \frac{\bar{\kappa}_0}{2\pi^2} \left(\frac{\bar{\mu}_0}{2\bar{\mu}_0 + \bar{\lambda}_0} \left(\Omega_x x + \Omega_y y\right) \frac{z}{r^2}\right)^2 \tag{15.29}$$

and the twist disclination distortion strain energy density is given by

(10.132)

$$\begin{aligned}
\mathcal{E}_{\perp} = \frac{\bar{\mu}_0 \Omega_x^2}{2\pi^2} \Bigg[& \bar{\alpha}_0^2 \ln^2 r + \frac{\bar{\beta}_0^2}{r^2} + 2\bar{\alpha}_0 \bar{\beta}_0 \, \frac{y^2}{r^2} \, \ln r + \\
& + \left[\left(\bar{\alpha}_0^2 - \tfrac{1}{2} \, \bar{\beta}_0^2 \right) x^2 + \bar{\beta}_0^2 y^2 \right] \frac{z^2}{r^4} \Bigg] + \\
& + \frac{\bar{\mu}_0 \Omega_y^2}{2\pi^2} \Bigg[\bar{\alpha}_0^2 \ln^2 r + \frac{\bar{\beta}_0^2}{r^2} + 2\bar{\alpha}_0 \bar{\beta}_0 \, \frac{x^2}{r^2} \, \ln r + \\
& + \left[\bar{\beta}_0^2 x^2 + \left(\bar{\alpha}_0^2 - \tfrac{1}{2} \, \bar{\beta}_0^2 \right) y^2 \right] \frac{z^2}{r^4} \Bigg] - \\
& - \frac{\bar{\mu}_0 \Omega_x \Omega_y}{\pi^2} \left[\bar{\beta}_0 \left(\bar{\alpha}_0 \ln r + \tfrac{1}{2} \, \bar{\beta}_0 \right) + \left(\bar{\beta}_0^2 - \tfrac{1}{2} \, \bar{\alpha}_0^2 \right) \frac{z^2}{r^2} \right] .
\end{aligned} \tag{15.30}$$

In the next chapter, we consider the strain energy of these defects as it applies to quantum physics.

Chapter 16

Defect Strain Energy in STCED

Strain energy is the fundamental defining energy characteristic of defects and their interactions in the spacetime continuum. In this chapter, we calculate the total strain energy W for the spacetime continuum defects, namely the screw dislocation, the edge dislocation, the wedge disclination and the twist disclination. These include both longitudinal dilatation strain energy $W_{\parallel}$ and transverse distortion strain energy $W_{\perp}$, except for the screw dislocation, where $\mathcal{E}_{\parallel} = 0$. The interaction of defects is mediated by their strain energy, and will be considered in the next chapter.

In general, the longitudinal dilatation strain energy $W_{\parallel}$ is easier to calculate than the transverse distortion strain energy $W_{\perp}$. The simplest case is the calculation of the screw dislocation strain energy. We consider stationary defects, that is defects that have no explicit time dependence. In the general case of moving dislocations, the derivation of the screw dislocation transverse strain energy and the edge dislocation transverse and longitudinal strain energies is much more difficult. In this chapter, we provide an overview discussion of the topic, and directions of possible exploration of the problem.

§16.1 Screw dislocation transverse strain energy

The total strain energy is calculated by integrating the strain energy density over the volume of the screw dislocation.

§16.1.1 *Stationary screw dislocation*

The total strain energy of the stationary screw dislocation is given by

$$W_{\perp}^{S} = \int_{V} \mathcal{E}_{\perp}^{S} \, \mathrm{d}V \tag{16.1}$$

where the volume element $\mathrm{d}V$ in cylindrical polar coordinates is given by $r\mathrm{d}r\,\mathrm{d}\theta\,\mathrm{d}z$. Substituting for $\mathcal{E}_{\perp}^{S}$ from (15.8), (16.1) becomes

$$W_{\perp}^{S} = \int_{V} \frac{\bar{\mu}_0\, \mathbb{b}^2}{2r^2} \, r\mathrm{d}r\,\mathrm{d}\theta\,\mathrm{d}z. \tag{16.2}$$

From (14.2), $\mathfrak{b}$ can be taken out of the integral to give

$$W_\perp^S = \frac{\bar{\mu}_0\,\mathfrak{b}^2}{2}\int_{b_0}^{\Lambda}\frac{1}{r}\mathrm{d}r\int_\theta \mathrm{d}\theta\int_z \mathrm{d}z \tag{16.3}$$

where Λ is a cut-off parameter corresponding to the radial extent of the dislocation, limited by the average distance to its nearest neighbours. The strain energy per wavelength is then given by

$$\frac{W_\perp^S}{\lambda} = \frac{\bar{\mu}_0\,\mathfrak{b}^2}{2}\ln\frac{\Lambda}{b_0}\int_0^{2\pi}\mathrm{d}\theta \tag{16.4}$$

and finally

$$\frac{W_\perp^S}{\lambda} = \frac{\bar{\mu}_0\,b^2}{4\pi}\ln\frac{\Lambda}{b_0}. \tag{16.5}$$

The implications of the total strain energy of the screw dislocation are discussed further in comparison to Quantum Electrodynamics (QED) in section §18.3.1.

§16.1.2 *Moving screw dislocation*

The transverse strain energy of a moving screw dislocation, which also corresponds to its total strain energy, is given by

$$W_\perp^S = \int_V \mathcal{E}_\perp^S\,\mathrm{d}V \tag{16.6}$$

where the strain energy density $\mathcal{E}_\perp^S$ is given by (9.24), *viz.*

$$\mathcal{E}_\perp^S = \frac{1}{2}\,\mathfrak{b}^2\,\bar{\mu}_0\,\frac{\alpha^2}{(x-vt)^2+\alpha^2y^2} \tag{16.7}$$

and V is the volume of the screw dislocation. The volume element $\mathrm{d}V$ in cartesian coordinates is given by $\mathrm{d}x\,\mathrm{d}y\,\mathrm{d}z\,\mathrm{d}(ct)$.

Substituting for $\mathcal{E}_\perp^S$, (16.6) becomes

$$W_\perp^S = \int_V \frac{1}{2}\,\mathfrak{b}^2\,\bar{\mu}_0\,\frac{\alpha^2}{(x-vt)^2+\alpha^2y^2}\,\mathrm{d}x\,\mathrm{d}y\,\mathrm{d}z\,\mathrm{d}(ct). \tag{16.8}$$

As before, $\mathfrak{b}$ is taken out of the integral from (14.2), and the integral over z is handled by considering the strain energy per unit length of the dislocation:

$$\frac{W_\perp^S}{\ell} = \frac{\mathfrak{b}^2\,\bar{\mu}_0}{2}\int_{ct}\int_y\int_x\limits_{b_0^2\le x^2+y^2\le\Lambda^2}\frac{\alpha^2}{(x-vt)^2+\alpha^2y^2}\,\mathrm{d}x\,\mathrm{d}y\,\mathrm{d}(ct) \tag{16.9}$$

where ℓ is the length of the dislocation and as before, Λ is a cut-off parameter corresponding to the radial extent of the dislocation, limited by the average distance to its nearest neighbours.

Evaluating the integral over x [376],

$$\begin{aligned}\frac{W_{\perp}^{S}}{\ell} = \frac{\hbar^2\,\bar{\mu}_0}{2}\,\alpha^2 \int_{ct}\int_{y} \mathrm{d}y\,\mathrm{d}(ct) \\ \left[\frac{1}{\alpha y}\,\arctan\left(\frac{x-vt}{\alpha y}\right)\right]_{\sqrt{y^2-b_0^2}}^{\sqrt{\Lambda^2-y^2}}\end{aligned} \tag{16.10}$$

where the limits corresponding to the maximum cut-off parameter Λ and minimum cut-off parameter b_0 are stated explicitly. Applying the limits of the integration, we obtain

$$\begin{aligned}\frac{W_{\perp}^{S}}{\ell} = \frac{\hbar^2\,\bar{\mu}_0}{2}\,\alpha^2 \int_{ct}\int_{y} \mathrm{d}y\,\mathrm{d}(ct) \\ \left\{\frac{1}{\alpha y}\,\arctan\left(\frac{\sqrt{\Lambda^2-y^2}-vt}{\alpha y}\right) - \right. \\ \left. -\frac{1}{\alpha y}\,\arctan\left(\frac{\sqrt{y^2-b_0^2}-vt}{\alpha y}\right)\right\}.\end{aligned} \tag{16.11}$$

This integration over y is not elementary and likely does not lead to a closed analytical form. If we consider the following simpler integral, the solution is given by

$$\begin{aligned}\int_{y}\frac{1}{\alpha y}\,\arctan\left(\frac{x-vt}{\alpha y}\right)\,\mathrm{d}y = \\ -\frac{i}{2}\left[\mathrm{Li}_2\left(-i\,\frac{x-vt}{\alpha y}\right) - \mathrm{Li}_2\left(i\,\frac{x-vt}{\alpha y}\right)\right]\end{aligned} \tag{16.12}$$

where $\mathrm{Li}_n(x)$ is the polylogarithm function. As pointed out in [377], "[t]he polylogarithm arises in Feynman diagram integrals (and, in particular, in the computation of quantum electrodynamics corrections to the electrons gyromagnetic ratio), and the special cases $n = 2$ and $n = 3$ are called the dilogarithm and the trilogarithm, respectively." This is a further indication that the interaction of strain energies are the physical source of quantum interaction phenomena described by Feynman diagrams as is discussed further in section §18.1.

§16.2 Edge dislocation longitudinal strain energy

The total longitudinal strain energy of the edge dislocation is calculated by integrating the edge dislocation dilatation strain energy density over the volume of the edge dislocation.

§16.2.1 *Stationary edge dislocation*

The longitudinal strain energy of the stationary edge dislocation is given by

$$W_{\parallel}^{E} = \int_{V} \mathcal{E}_{\parallel}^{E} \, \mathrm{d}V. \tag{16.13}$$

Substituting for $\mathcal{E}_{\parallel}$ from (9.69), this equation becomes

$$W_{\parallel}^{E} = \int_{V} \frac{b^2}{2\pi^2} \, \frac{\bar{\kappa}_0 \, \bar{\mu}_0^2}{(2\bar{\mu}_0 + \bar{\lambda}_0)^2} \, \frac{\sin^2\theta}{r^2} \, \mathrm{d}V. \tag{16.14}$$

Similarly to the previous derivation of section §16.1.1, this integral gives

$$\frac{W_{\parallel}^{E}}{\ell} = \frac{1}{2\pi} \, b^2 \, \bar{\kappa}_0 \, \left(\frac{\bar{\mu}_0}{2\bar{\mu}_0 + \bar{\lambda}_0} \right)^2 \, \ln \frac{\Lambda}{b_0}. \tag{16.15}$$

The total strain energy of the stationary screw and edge dislocations have similar functional forms, with the difference residing in the proportionality constants. This is due to the simpler nature of the stationary dislocations and their cylindrical polar symmetry. This similarity is not present for the general case of moving dislocations as evidenced in equations (9.24), (9.87) and (9.89).

§16.2.2 *Moving edge dislocation*

The longitudinal strain energy of a moving edge dislocation is given by

$$W_{\parallel}^{E} = \int_{V} \mathcal{E}_{\parallel}^{E} \, \mathrm{d}V \tag{16.16}$$

where the strain energy density $\mathcal{E}_{\parallel}^{E}$ is given by (9.87), *viz.*

$$\mathcal{E}_{\parallel}^{E} = \frac{1}{2} \, \bar{\kappa}_0 \, \mathfrak{b}^2 \left(\frac{2\bar{\mu}_0}{2\bar{\mu}_0 + \bar{\lambda}_0} \, \frac{\alpha_l y}{(x - vt)^2 + \alpha_l^2 y^2} \right)^2 \tag{16.17}$$

and V is the volume of the edge dislocation. The volume element $\mathrm{d}V$ in cartesian coordinates is given by $\mathrm{d}x \, \mathrm{d}y \, \mathrm{d}z \, \mathrm{d}(ct)$.

Substituting for $\mathcal{E}_{\parallel}^{E}$, (16.16) becomes

$$W_{\parallel}^{E} = \int_{V} \frac{1}{2}\,\bar{\kappa}_0\,\mathfrak{b}^2 \left(\frac{2\bar{\mu}_0}{2\bar{\mu}_0+\bar{\lambda}_0}\,\frac{\alpha_l y}{(x-vt)^2+\alpha_l^2 y^2}\right)^2 \times \\ \times \mathrm{d}x\,\mathrm{d}y\,\mathrm{d}z\,\mathrm{d}(ct). \tag{16.18}$$

As before, $\mathfrak{b}$ is taken out of the integral from (14.2), and the integral over z is handled by considering the strain energy per unit length of the dislocation:

$$\frac{W_{\parallel}^{E}}{\ell} = 2\,\bar{\kappa}_0\,\mathfrak{b}^2\,\frac{\bar{\mu}_0^2}{(2\bar{\mu}_0+\bar{\lambda}_0)^2} \\ \int_{ct}\int_{y}\int_{x}\limits_{b_0^2\le x^2+y^2\le\Lambda^2} \frac{(\alpha_l y)^2}{\left((x-vt)^2+\alpha_l^2 y^2\right)^2}\,\mathrm{d}x\,\mathrm{d}y\,\mathrm{d}(ct) \tag{16.19}$$

where ℓ is the length of the dislocation and as before, Λ is a cut-off parameter corresponding to the radial extent of the dislocation, limited by the average distance to its nearest neighbours.

The integrand has a functional form similar to that of (16.9), and a similar solution behaviour is expected. Evaluating the integral over x [376],

$$\frac{W_{\parallel}^{E}}{\ell} = 2\,\bar{\kappa}_0\,\mathfrak{b}^2\,\frac{\bar{\mu}_0^2}{(2\bar{\mu}_0+\bar{\lambda}_0)^2}\int_{ct}\int_{y}\mathrm{d}y\,\mathrm{d}(ct) \\ \left[\frac{1}{2}\,\frac{x-vt}{(x-vt)^2+(\alpha_l y)^2}+\right. \\ \left.+\frac{1}{2\alpha_l y}\,\arctan\left(\frac{x-vt}{\alpha_l y}\right)\right]_{\sqrt{y^2-b_0^2}}^{\sqrt{\Lambda^2-y^2}} \tag{16.20}$$

where the limits corresponding to the maximum cut-off parameter Λ and minimum cut-off parameter b_0 are stated explicitly. Applying the

limits of the integration, we obtain

$$\begin{aligned}\frac{W_{\parallel}^{E}}{\ell} = 2\,\bar{\kappa}_0\,\mathfrak{b}^2\,\frac{\bar{\mu}_0^2}{(2\bar{\mu}_0+\bar{\lambda}_0)^2}\int_{ct}\int_{y}\mathrm{d}y\,\mathrm{d}(ct)\\ \left[\frac{1}{2}\,\frac{\sqrt{\Lambda^2-y^2}-vt}{(\sqrt{\Lambda^2-y^2}-vt)^2+(\alpha_l y)^2}-\right.\\ -\frac{1}{2}\,\frac{\sqrt{y^2-b_0^2}-vt}{(\sqrt{y^2-b_0^2}-vt)^2+(\alpha_l y)^2}+\\ +\frac{1}{2\alpha_l y}\,\arctan\left(\frac{\sqrt{\Lambda^2-y^2}-vt}{\alpha_l y}\right)-\\ \left.-\frac{1}{2\alpha_l y}\,\arctan\left(\frac{\sqrt{y^2-b_0^2}-vt}{\alpha_l y}\right)\right].\end{aligned} \tag{16.21}$$

The integration over y is again found to be intractable. It includes that of (16.11) in its formulation, and likely does not lead to a closed analytical form. In the $\arctan\Lambda$ integral of (16.11) and (16.21), we can make the approximation $\sqrt{\Lambda^2-y^2}\simeq\Lambda$ and evaluate this term as seen in (16.12):

$$\begin{aligned}\int_{y}\frac{1}{\alpha_l y}\,\arctan\left(\frac{\Lambda-vt}{\alpha_l y}\right)\mathrm{d}y =\\ -\frac{i}{2}\left[\mathrm{Li}_2\left(-i\,\frac{\Lambda-vt}{\alpha_l y}\right)-\mathrm{Li}_2\left(i\,\frac{\Lambda-vt}{\alpha_l y}\right)\right]\end{aligned} \tag{16.22}$$

where $\mathrm{Li}_n(x)$ is the polylogarithm function as seen previously.

§16.2.3 *deWit dislocation line*

The longitudinal strain energy of the deWit dislocation line is obtained from

$$W_{\parallel}^{E}=\int_{V}\mathcal{E}_{\parallel}^{E}\,\mathrm{d}V. \tag{16.23}$$

Substituting for $\mathcal{E}_{\parallel}^{E}$ from (9.139), this equation becomes

$$W_{\parallel}^{E}=\int_{V}\frac{1}{2\pi^2}\,\frac{\bar{\kappa}_0\,\bar{\mu}_0^2}{(2\bar{\mu}_0+\bar{\lambda}_0)^2}\,\frac{(b_x y-b_y x)^2}{r^4}\,\mathrm{d}V \tag{16.24}$$

where V is the volume of the deWit line dislocation, with $\mathrm{d}V$ given by $\mathrm{d}x\,\mathrm{d}y\,\mathrm{d}z$ in cartesian coordinates. As before, $\mathfrak{b}$ can be taken out of the

integral from (14.2), and the integral over z is handled by considering the strain energy per unit length of the dislocation:

$$\frac{W_{\parallel}^{E}}{\ell} = \frac{2\bar{\kappa}_0\bar{\mu}_0^2}{(2\bar{\mu}_0+\bar{\lambda}_0)^2} \int_y \int_x \frac{\left(\text{ƀ}_x y - \text{ƀ}_y x\right)^2}{r^4}\,\mathrm{d}x\,\mathrm{d}y \qquad (16.25)$$
$$b_0^2 \le x^2+y^2 \le \Lambda^2$$

where ℓ is the length of the dislocation and as before, Λ is a cut-off parameter corresponding to the radial extent of the dislocation, limited by the average distance to its nearest neighbours.

In cylindrical polar coordinates, (16.25) is written as

$$\frac{W_{\parallel}^{E}}{\ell} = \frac{2\bar{\kappa}_0\bar{\mu}_0^2}{(2\bar{\mu}_0+\bar{\lambda}_0)^2} \int_0^{2\pi} \int_{b_0}^{\Lambda} \frac{\left(\text{ƀ}_x \sin\theta - \text{ƀ}_y \cos\theta\right)^2}{r^2}\, r\mathrm{d}r\,\mathrm{d}\theta\,. \qquad (16.26)$$

Evaluating the integral over r, (16.26) becomes

$$\begin{aligned}\frac{W_{\parallel}^{E}}{\ell} &= \frac{2\bar{\kappa}_0\bar{\mu}_0^2}{(2\bar{\mu}_0+\bar{\lambda}_0)^2}\,\ln\frac{\Lambda}{b_0} \\ &\int_0^{2\pi} \left(\text{ƀ}_x^2 \sin^2\theta - 2\text{ƀ}_x\text{ƀ}_y \sin\theta\cos\theta + \text{ƀ}_y^2\cos^2\theta\right)\,\mathrm{d}\theta\,.\end{aligned} \qquad (16.27)$$

Evaluating the integral over θ [376], we obtain

$$\frac{W_{\parallel}^{E}}{\ell} = \frac{2\bar{\kappa}_0\bar{\mu}_0^2}{(2\bar{\mu}_0+\bar{\lambda}_0)^2}\,\ln\frac{\Lambda}{b_0}\left(\text{ƀ}_x^2\pi + \text{ƀ}_y^2\pi\right) \qquad (16.28)$$

which is rewritten as

$$\frac{W_{\parallel}^{E}}{\ell} = \frac{1}{2\pi}\,\frac{\bar{\kappa}_0\bar{\mu}_0^2}{(2\bar{\mu}_0+\bar{\lambda}_0)^2}\,\left(b_x^2+b_y^2\right)\,\ln\frac{\Lambda}{b_0}\,. \qquad (16.29)$$

This equation reduces to (16.15) for the stationary edge dislocation of section §16.2.1.

§16.3 Edge dislocation transverse strain energy

The total transverse strain energy of the edge dislocation is calculated by integrating the edge dislocation distortion strain energy density over the volume of the edge dislocation. As mentioned previously, the distortion strain energy is in general more complicated to calculate than the simpler dilatation strain energy.

§16.3.1 *Stationary edge dislocation*

The transverse distortion strain energy of a stationary edge dislocation is given by

$$W_{\perp}^{E} = \int_{V} \mathcal{E}_{\perp}^{E} \, \mathrm{d}V \tag{16.30}$$

where the volume element $\mathrm{d}V$ in cylindrical polar coordinates is given by $r\mathrm{d}r\,\mathrm{d}\theta\,\mathrm{d}z$. Substituting for $\mathcal{E}_{\perp}^{E}$ from (9.79) and taking $\mathfrak{b}$ out of the integral, (16.30) becomes

$$\begin{aligned} W_{\perp}^{E} = {} & \frac{\mathfrak{b}^2 \bar{\mu}_0}{(2\bar{\mu}_0 + \bar{\lambda}_0)^2} \\ & \int_z \int_\theta \int_{b_0}^{\Lambda} \frac{2(\bar{\mu}_0 + \bar{\lambda}_0)^2 \, \cos^2\theta + \bar{\mu}_0^2 \, \sin^2\theta}{r^2} \, r\mathrm{d}r \, \mathrm{d}\theta \, \mathrm{d}z \end{aligned} \tag{16.31}$$

where again Λ is a cut-off parameter corresponding to the radial extent of the dislocation, limited by the average distance to its nearest neighbours. This equation can also be written as

$$W_{\perp}^{E} = \mathfrak{b}^2 \bar{\mu}_0 \int_z \int_\theta \int_{b_0}^{\Lambda} \left(\bar{\alpha}_0^2 \, \frac{\sin^2\theta}{r^2} + 2\bar{\beta}_0^2 \, \frac{\cos^2\theta}{r^2} \right) r\mathrm{d}r \, \mathrm{d}\theta \, \mathrm{d}z \tag{16.32}$$

where

$$\bar{\alpha}_0 = \frac{\bar{\mu}_0}{2\bar{\mu}_0 + \bar{\lambda}_0} \tag{16.33}$$

$$\bar{\beta}_0 = \frac{\bar{\mu}_0 + \bar{\lambda}_0}{2\bar{\mu}_0 + \bar{\lambda}_0} \, . \tag{16.34}$$

Evaluating the integral over r, (16.32) becomes

$$W_{\perp}^{E} = \mathfrak{b}^2 \bar{\mu}_0 \, \ln\frac{\Lambda}{b_0} \int_z \int_0^{2\pi} \left(\bar{\alpha}_0^2 \, \sin^2\theta + 2\bar{\beta}_0^2 \, \cos^2\theta \right) \mathrm{d}\theta \, \mathrm{d}z \, . \tag{16.35}$$

Evaluating the integral over θ [376], we obtain

$$\begin{aligned} W_{\perp}^{E} = {} & \mathfrak{b}^2 \bar{\mu}_0 \, \ln\frac{\Lambda}{b_0} \int_z \left[\frac{\bar{\alpha}_0^2}{2} \, (\theta - \sin\theta\cos\theta) + \right. \\ & \left. + \bar{\beta}_0^2 \, (\theta + \sin\theta\cos\theta) \right]_0^{2\pi} \mathrm{d}z \, . \end{aligned} \tag{16.36}$$

Applying the limits of integration, (16.36) becomes

$$W_{\perp}^{E} = \mathfrak{b}^2 \bar{\mu}_0 \, \ln \frac{\Lambda}{b_0} \int_0^{\ell} \left(\pi \bar{\alpha}_0^2 + 2\pi \bar{\beta}_0^2 \right) \, \mathrm{d}z \,, \tag{16.37}$$

and evaluating the integral over z, we obtain the stationary edge dislocation transverse strain energy per unit length

$$\frac{W_{\perp}^{E}}{\ell} = \frac{1}{4\pi} \, b^2 \bar{\mu}_0 \left(\bar{\alpha}_0^2 + 2\bar{\beta}_0^2 \right) \ln \frac{\Lambda}{b_0} \tag{16.38}$$

where ℓ is the length of the edge dislocation. We find that the stationary edge dislocation transverse strain energy per unit length is similar to the stationary screw dislocation transverse strain energy per unit length

$$\frac{W_{\perp}^{S}}{\ell} = \frac{1}{4\pi} \, b^2 \bar{\mu}_0 \, \ln \frac{\Lambda}{b_0} \tag{16.39}$$

except for the proportionality constant.

§16.3.2 *Moving edge dislocation*

The transverse strain energy of a moving edge dislocation is given by

$$W_{\perp}^{E} = \int_V \mathcal{E}_{\perp}^{E} \, \mathrm{d}V \tag{16.40}$$

where the strain energy density $\mathcal{E}_{\perp}^{E}$ is given by (9.89) and V is the volume of the edge dislocation. The volume element $\mathrm{d}V$ in cartesian coordinates is given by $\mathrm{d}x \, \mathrm{d}y \, \mathrm{d}z \, \mathrm{d}(ct)$.

Substituting for $\mathcal{E}_{\perp}^{E}$ from (9.89), taking $\mathfrak{b}$ out of the integral from (14.2), and handling the integral over z by considering the strain energy per unit length of the dislocation, (16.40) becomes

$$\begin{aligned}
\frac{W_{\perp}^{E}}{\ell} &= 4\bar{\mu}_0 \, \mathfrak{b}^2 \, \frac{c^4}{v^4} \int_{ct} \int_y \int_x \underset{b^2 \le x^2 + y^2 \le \Lambda^2}{} \mathrm{d}x \, \mathrm{d}y \, \mathrm{d}(ct) \\
&\left[\frac{\alpha_2^4}{2\alpha^2} \, \frac{\left((1+\alpha^2)^2 - v^2/c^2 \right) \, (x - vt)^2 + 2\alpha^4 (1 + \alpha_2^2) \, y^2}{r^{*4}} - \right. \\
&- 2 \, \alpha_l \, \alpha_2^2 \, \alpha \, \frac{\left(1 + \alpha_2^2/\alpha^2 \right) (x - vt)^2 + \left(\alpha_2^2 + \alpha_l^2 \right) \, y^2}{r^{*2} \, r_l^{*2}} + \\
&\left. + \alpha_l^2 \, \frac{(1 + \alpha_2^2) \, (x - vt)^2 + \left(\alpha_2^2 + \alpha_l^4 - \frac{1}{4} \, v^4/c_l^4 \right) \, y^2}{r_l^{*4}} \right]
\end{aligned} \tag{16.41}$$

where

$$r^{*2} = (x - vt)^2 + \alpha^2 y^2 \tag{16.42}$$

$$r_l^{*2} = (x - vt)^2 + \alpha_l^2 y^2 \,, \tag{16.43}$$

ℓ is the length of the dislocation and as before, Λ is a cut-off parameter corresponding to the radial extent of the dislocation, limited by the average distance to its nearest neighbours.

Again, the integrand has functional forms similar to that of (16.9) and (16.19). A similar, but more complex, solution behaviour is expected, due to the additional complexity of (16.41).

We consider the moving edge dislocation in the limit as $v \to 0$. Subsituting for (9.102) in (16.30) and using (14.3), we obtain

$$\begin{aligned} W_\perp^E \to 2\bar{b}^2\bar{\mu}_0 \int_z \int_\theta \int_{b_0}^{\Lambda} r \mathrm{d}r \, \mathrm{d}\theta \, \mathrm{d}z \\ \left\{ \left(1 + \frac{2\bar{\mu}_0}{2\bar{\mu}_0 + \bar{\lambda}_0} + \frac{5}{4} \frac{\bar{\mu}_0^2}{(2\bar{\mu}_0 + \bar{\lambda}_0)^2} \right) \frac{\sin^2\theta}{r^2} + \right. \\ \left. + \frac{1}{2} \left(1 - \frac{2\bar{\mu}_0}{2\bar{\mu}_0 + \bar{\lambda}_0} + \frac{\bar{\mu}_0^2}{(2\bar{\mu}_0 + \bar{\lambda}_0)^2} \right) \frac{\cos^2\theta}{r^2} \right\} \end{aligned} \tag{16.44}$$

where again Λ is a cut-off parameter corresponding to the radial extent of the dislocation, limited by the average distance to its nearest neighbours.

Evaluating the integral over r,

$$\begin{aligned} W_\perp^E \to 2\bar{b}^2\bar{\mu}_0 \ln\frac{\Lambda}{b_0} \int_z \int_0^{2\pi} \mathrm{d}\theta \, \mathrm{d}z \\ \left\{ \left(1 + \frac{2\bar{\mu}_0}{2\bar{\mu}_0 + \bar{\lambda}_0} + \frac{5}{4} \frac{\bar{\mu}_0^2}{(2\bar{\mu}_0 + \bar{\lambda}_0)^2} \right) \sin^2\theta + \right. \\ \left. + \frac{1}{2} \left(1 - \frac{2\bar{\mu}_0}{2\bar{\mu}_0 + \bar{\lambda}_0} + \frac{\bar{\mu}_0^2}{(2\bar{\mu}_0 + \bar{\lambda}_0)^2} \right) \cos^2\theta \right\}. \end{aligned} \tag{16.45}$$

Evaluating the integral over θ [376] and applying the limits of the inte-

gration, we obtain

$$W_\perp^E \to 2\bar{b}^2\bar{\mu}_0 \ln\frac{\Lambda}{b_0}\int_0^\ell \mathrm{d}z \left\{\left(1+\frac{2\bar{\mu}_0}{2\bar{\mu}_0+\bar{\lambda}_0}+\frac{5}{4}\,\frac{\bar{\mu}_0^2}{(2\bar{\mu}_0+\bar{\lambda}_0)^2}\right)(\pi)+ +\frac{1}{2}\left(1-\frac{2\bar{\mu}_0}{2\bar{\mu}_0+\bar{\lambda}_0}+\frac{\bar{\mu}_0^2}{(2\bar{\mu}_0+\bar{\lambda}_0)^2}\right)(\pi)\right\} \tag{16.46}$$

and evaluating the integral over z, we obtain the moving edge dislocation transverse strain energy per unit length in the limit as $v \to 0$

$$\frac{W_\perp^E}{\ell} \to \frac{3}{4\pi}\,b^2\bar{\mu}_0\left(1+\frac{2}{3}\,\frac{\bar{\mu}_0}{2\bar{\mu}_0+\bar{\lambda}_0}+ +\frac{7}{6}\,\frac{\bar{\mu}_0^2}{(2\bar{\mu}_0+\bar{\lambda}_0)^2}\right)\ln\frac{\Lambda}{b_0} \tag{16.47}$$

where ℓ is the length of the edge dislocation.

§16.3.3 *deWit dislocation line*

The transverse strain energy of the deWit dislocation line is obtained from

$$W_\perp^E = \int_V \mathcal{E}_\perp^E\,\mathrm{d}V. \tag{16.48}$$

Substituting for $\mathcal{E}_\perp^E$ from (9.149), this equation becomes

$$W_\perp^E = \int_V \left[\frac{\bar{\mu}_0}{8\pi^2}\,\frac{b_z^2}{r^2}+\frac{\bar{\mu}_0}{4\pi^2}\,\bar{\alpha}_0^2\,\frac{(b_x y-b_y x)^2}{r^4}+ +\frac{\bar{\mu}_0}{2\pi^2}\,\bar{\beta}_0^2\,\frac{(b_x x+b_y y)^2}{r^4}-\frac{3}{2\pi^2}\,\frac{\bar{\mu}_0\bar{\lambda}_0}{2\bar{\mu}_0+\bar{\lambda}_0}\,\frac{b_x b_y xy}{r^4}\right]\mathrm{d}V \tag{16.49}$$

where V is the volume of the deWit line dislocation, with $\mathrm{d}V$ given by $\mathrm{d}x\,\mathrm{d}y\,\mathrm{d}z$ in cartesian coordinates. The first term in the integral is the screw dislocation transverse strain energy density which is as expected, given that the dislocation line includes both screw and edge dislocations. As before, $\bar{b}$ can be taken out of the integral from (14.2), and the integral over z is handled by considering the strain energy per unit length of the

dislocation:

$$\frac{W_{\perp}^{E}}{\ell} = \frac{\bar{\mu}_0}{4\pi^2} \int_{y}\int_{x}_{b_0^2 \le x^2+y^2 \le \Lambda^2} \left[\frac{1}{2}\,\frac{b_z^2}{r^2} + \bar{\alpha}_0^2\,\frac{(b_x y - b_y x)^2}{r^4} + \right. \\ \left. + 2\bar{\beta}_0^2\,\frac{(b_x x + b_y y)^2}{r^4} - 6\,\frac{\bar{\mu}_0\bar{\lambda}_0}{2\bar{\mu}_0+\bar{\lambda}_0}\,\frac{b_x b_y xy}{r^4}\right] \mathrm{d}x\,\mathrm{d}y \tag{16.50}$$

where ℓ is the length of the dislocation and as before, Λ is a cut-off parameter corresponding to the radial extent of the dislocation, limited by the average distance to its nearest neighbours.

In cylindrical polar coordinates, (16.50) is written as

$$\frac{W_{\perp}^{E}}{\ell} = \frac{\bar{\mu}_0}{4\pi^2} \int_0^{2\pi}\int_{b_0}^{\Lambda} \left[\frac{1}{2}\,\frac{b_z^2}{r^2} + \bar{\alpha}_0^2\,\frac{(b_x \sin\theta - b_y\cos\theta)^2}{r^2} + \right. \\ + 2\bar{\beta}_0^2\,\frac{(b_x\cos\theta + b_y\sin\theta)^2}{r^2} - \\ \left. - 6\,\frac{\bar{\mu}_0\bar{\lambda}_0}{2\bar{\mu}_0+\bar{\lambda}_0}\,\frac{b_x b_y \cos\theta\sin\theta}{r^2}\right] r\,\mathrm{d}r\,\mathrm{d}\theta\,. \tag{16.51}$$

Evaluating the integral over r, (16.51) becomes

$$\frac{W_{\perp}^{E}}{\ell} = \frac{\bar{\mu}_0}{4\pi^2}\,\ln\frac{\Lambda}{b_0} \int_0^{2\pi} \left[\frac{1}{2}\,b_z^2 + \bar{\alpha}_0^2\,(b_x\sin\theta - b_y\cos\theta)^2 + \right. \\ + 2\bar{\beta}_0^2\,(b_x\cos\theta + b_y\sin\theta)^2 - \\ \left. - 6\,\frac{\bar{\mu}_0\bar{\lambda}_0}{2\bar{\mu}_0+\bar{\lambda}_0}\,b_x b_y\cos\theta\sin\theta\right] \mathrm{d}\theta\,. \tag{16.52}$$

Evaluating the integral over θ [376], we obtain

$$\frac{W_{\perp}^{E}}{\ell} = \frac{\bar{\mu}_0}{4\pi^2}\,\ln\frac{\Lambda}{b_0} \left[\pi b_z^2 + \bar{\alpha}_0^2\,(\pi b_x^2 + \pi b_y^2) + \right. \\ \left. + 2\bar{\beta}_0^2\,(\pi b_x^2 + \pi b_y^2) - 0\right] \tag{16.53}$$

where we have preserved the structure of four terms of the distortion strain energy density of (9.156) corresponding to the screw dislocation strain energy of (16.5), the edge dislocation distortion strain energy arising from the longitudinal strain energy density of (9.139), the edge dislocation distortion strain energy arising from the rotation vector of

(9.138) and a moment distortion strain energy term which is zero. This expression is simplified to give

$$\frac{W^E_\perp}{\ell} = \frac{\bar{\mu}_0}{4\pi}\,\left[b_z^2 + \left(\bar{\alpha}_0^2 + 2\bar{\beta}_0^2\right)\left(b_x^2 + b_y^2\right)\right]\,\ln\frac{\Lambda}{b_0}\,. \tag{16.54}$$

This equation reduces to the sum of (16.5) for the stationary screw dislocation of section §16.1.1 and (16.15) for the stationary edge dislocation of section §16.3.1.

§16.4 Wedge disclination longitudinal strain energy

The longitudinal strain energy of the deWit wedge disclination is obtained from

$$W^W_\parallel = \int_V \mathcal{E}^W_\parallel \,\mathrm{d}V. \tag{16.55}$$

Substituting for $\mathcal{E}^W_\parallel$ from (10.109), this equation becomes

$$W^W_\parallel = \int_V 2\bar{\kappa}_0\Omega_z^2\left(\bar{\alpha}_0\ln r + \frac{1}{2}\,\bar{\beta}_0\right)^2\,\mathrm{d}V \tag{16.56}$$

where V is the volume of the wedge disclination, with $\mathrm{d}V$ given by $r\mathrm{d}r\,\mathrm{d}\theta\,\mathrm{d}z$ in cylindrical polar coordinates. As before, we take Ω out of the integral from (14.5), and the integral over z is handled by considering the strain energy per unit length of the disclination:

$$\frac{W^W_\parallel}{\ell} = 2\bar{\kappa}_0\Omega_z^2\int_0^{2\pi}\int_{b_c}^{\Lambda}\left(\bar{\alpha}_0\ln r + \frac{1}{2}\,\bar{\beta}_0\right)^2 r\mathrm{d}r\,\mathrm{d}\theta \tag{16.57}$$

where ℓ is the length of the disclination, b_c is the size of the core of the disclination, of order b_0, the smallest spacetime dislocation Burgers vector, and Λ is a cut-off parameter corresponding to the radial extent of the disclination, limited by the average distance to its nearest neighbours.

Evaluating the integral over θ, (16.57) becomes

$$\frac{W^W_\parallel}{\ell} = \frac{1}{\pi}\,\bar{\kappa}_0\,\Omega_z^2\int_{b_c}^{\Lambda}\left[\bar{\alpha}_0^2\ln^2 r + \bar{\alpha}_0\bar{\beta}_0\ln r + \frac{1}{4}\,\bar{\beta}_0^2\right] r\mathrm{d}r\,. \tag{16.58}$$

Evaluating the integral over r [376], we obtain

$$\begin{aligned}\frac{W^W_\parallel}{\ell} = \frac{1}{4\pi}\,\bar{\kappa}_0\,\Omega_z^2\Bigg[&\bar{\alpha}_0^2\,r^2\left(2\left(\ln r - 1\right)\ln r + 1\right) + \\ &+ \bar{\alpha}_0\bar{\beta}_0 r^2\left(2\ln r - 1\right) + \bar{\beta}_0^2\,\frac{r^2}{2}\Bigg]_{b_c}^{\Lambda}\,.\end{aligned} \tag{16.59}$$

Applying the limits of integration and rearranging, (16.59) becomes

$$\begin{aligned}\frac{W_{\parallel}^{W}}{\ell} = \frac{1}{4\pi}\,\bar{\kappa}_0\,\Omega_z^2\Big[\bar{\alpha}_0^2\,\left(2\Lambda^2\ln^2\Lambda - 2b_c^2\ln^2 b_c\right) - \\ - \left(\bar{\alpha}_0^2 - \bar{\alpha}_0\bar{\beta}_0\right)\left(2\Lambda^2\ln\Lambda - 2b_c^2\ln b_c\right) + \\ + \left(\bar{\alpha}_0^2 - \bar{\alpha}_0\bar{\beta}_0 + \tfrac{1}{2}\,\bar{\beta}_0^2\right)\left(\Lambda^2 - b_c^2\right)\Big]\,.\end{aligned} \tag{16.60}$$

Using the relations $\bar{\alpha}_0^2 - \bar{\alpha}_0\bar{\beta}_0 = -\bar{\alpha}_0\bar{\gamma}_0$ and $\bar{\alpha}_0^2 - \bar{\alpha}_0\bar{\beta}_0 + \frac{1}{2}\,\bar{\beta}_0^2 = \frac{1}{2}(\bar{\alpha}_0^2 + \bar{\gamma}_0^2)$ where

$$\bar{\gamma}_0 = \frac{\bar{\lambda}_0}{2\bar{\mu}_0 + \bar{\lambda}_0}\,, \tag{16.61}$$

(16.60) is rewritten as

$$\begin{aligned}\frac{W_{\parallel}^{W}}{\ell} = \frac{1}{4\pi}\,\bar{\kappa}_0\,\Omega_z^2\Big[\bar{\alpha}_0^2\,\left(2\Lambda^2\ln^2\Lambda - 2b_c^2\ln^2 b_c\right) + \\ + \bar{\alpha}_0\bar{\gamma}_0\left(2\Lambda^2\ln\Lambda - 2b_c^2\ln b_c\right) + \\ + \tfrac{1}{2}(\bar{\alpha}_0^2 + \bar{\gamma}_0^2)\left(\Lambda^2 - b_c^2\right)\Big]\,.\end{aligned} \tag{16.62}$$

In most cases $\Lambda \gg b_c$, and (16.62) reduces to

$$\frac{W_{\parallel}^{W}}{\ell} \simeq \frac{1}{2\pi}\,\bar{\kappa}_0\,\Omega_z^2\Lambda^2\Big[\bar{\alpha}_0^2\,\ln^2\Lambda + \,\bar{\alpha}_0\bar{\gamma}_0\ln\Lambda + \,\tfrac{1}{4}(\bar{\alpha}_0^2 + \bar{\gamma}_0^2)\Big] \tag{16.63}$$

which, using the definitions of $\bar{\alpha}_0$, $\bar{\beta}_0$ and $\bar{\gamma}_0$, can be rewritten as

$$\begin{aligned}\frac{W_{\parallel}^{W}}{\ell} \simeq \frac{1}{2\pi}\,\frac{\bar{\kappa}_0\bar{\mu}_0^2}{(2\bar{\mu}_0 + \bar{\lambda}_0)^2}\,\Omega_z^2\,\Lambda^2 \\ \left[\ln^2\Lambda + \frac{\bar{\lambda}_0}{\bar{\mu}_0}\,\ln\Lambda + \,\frac{1}{4}\left(1 + \frac{\bar{\lambda}_0^2}{\bar{\mu}_0^2}\right)\right]\,.\end{aligned} \tag{16.64}$$

The proportionality constant of this equation is similar to that of the longitudinal strain energy (16.15) for the stationary edge dislocation although the functional form is different for a disclination compared to a dislocation.

§16.5 Wedge disclination transverse strain energy

The transverse strain energy of the deWit wedge disclination is obtained from

$$W_{\perp}^{W} = \int_{V} \mathcal{E}_{\perp}^{W} \, \mathrm{d}V. \tag{16.65}$$

Substituting for $\mathcal{E}_{\perp}^{W}$ from (10.112), this equation becomes

$$W_{\perp}^{W} = \int_{V} \frac{\bar{\mu}_0 \Omega_z^2}{4\pi^2} \left(\bar{\alpha}_0^2 \ln^2 r + 3\bar{\alpha}_0 \bar{\beta}_0 \ln r + \frac{3}{4} \bar{\beta}_0^2 \right) \mathrm{d}V \tag{16.66}$$

where V is the volume of the wedge disclination, with $\mathrm{d}V$ given by $r\mathrm{d}r\,\mathrm{d}\theta\,\mathrm{d}z$ in cylindrical polar coordinates. As before, we take Ω out of the integral from (14.5), and the integral over z is handled by considering the strain energy per unit length of the disclination:

$$\frac{W_{\perp}^{W}}{\ell} = \frac{\bar{\mu}_0 \Omega_z^2}{4\pi^2} \int_0^{2\pi} \int_{b_c}^{\Lambda} \left(\bar{\alpha}_0^2 \ln^2 r + 3\bar{\alpha}_0 \bar{\beta}_0 \ln r + \frac{3}{4} \bar{\beta}_0^2 \right) r \mathrm{d}r \, \mathrm{d}\theta \tag{16.67}$$

where ℓ is the length of the disclination, b_c is the size of the core of the disclination, of order b_0, the smallest spacetime dislocation Burgers vector, and Λ is a cut-off parameter corresponding to the radial extent of the disclination, limited by the average distance to its nearest neighbours.

Evaluating the integral over θ, (16.67) becomes

$$\frac{W_{\perp}^{W}}{\ell} = \frac{\bar{\mu}_0 \Omega_z^2}{2\pi} \int_{b_c}^{\Lambda} \left(\bar{\alpha}_0^2 \ln^2 r + 3\bar{\alpha}_0 \bar{\beta}_0 \ln r + \frac{3}{4} \bar{\beta}_0^2 \right) r \mathrm{d}r \,. \tag{16.68}$$

This integral is similar to (16.58), but with coefficients that differ and impact the final expression. Evaluating the integral over r [376], we obtain

$$\begin{aligned} \frac{W_{\perp}^{W}}{\ell} = \frac{\bar{\mu}_0 \Omega_z^2}{8\pi} \Big[& \bar{\alpha}_0^2 r^2 \left(2 \left(\ln r - 1 \right) \ln r + 1 \right) + \\ & + 3\bar{\alpha}_0 \bar{\beta}_0 r^2 \left(2 \ln r - 1 \right) + 3\bar{\beta}_0^2 \frac{r^2}{2} \Big]_{b_c}^{\Lambda} . \end{aligned} \tag{16.69}$$

Applying the limits of integration and rearranging, (16.69) becomes

$$\begin{aligned}\frac{W_{\perp}^{W}}{\ell} = \frac{\bar{\mu}_0 \Omega_z^2}{4\pi}\Big[&\bar{\alpha}_0^2\,\left(\Lambda^2 \ln^2\Lambda - b_c^2 \ln^2 b_c\right) - \\ &- \left(\bar{\alpha}_0^2 - 3\bar{\alpha}_0\bar{\beta}_0\right)\left(\Lambda^2 \ln\Lambda - b_c^2 \ln b_c\right) + \\ &+ \frac{1}{2}\left(\bar{\alpha}_0^2 - 3\bar{\alpha}_0\bar{\beta}_0 + \frac{3}{2}\,\bar{\beta}_0^2\right)\left(\Lambda^2 - b_c^2\right)\Big].\end{aligned} \tag{16.70}$$

In most cases $\Lambda \gg b_c$, and (16.70) reduces to

$$\begin{aligned}\frac{W_{\perp}^{W}}{\ell} \simeq \frac{\bar{\mu}_0 \Omega_z^2}{4\pi}\Big[&\bar{\alpha}_0^2\,\Lambda^2 \ln^2\Lambda - \left(\bar{\alpha}_0^2 - 3\bar{\alpha}_0\bar{\beta}_0\right)\Lambda^2 \ln\Lambda + \\ &+ \frac{1}{2}\left(\bar{\alpha}_0^2 - 3\bar{\alpha}_0\bar{\beta}_0 + \frac{3}{2}\,\bar{\beta}_0^2\right)\Lambda^2\Big]\end{aligned} \tag{16.71}$$

which is rearranged as

$$\begin{aligned}\frac{W_{\perp}^{W}}{\ell} \simeq &\frac{\bar{\mu}_0}{4\pi}\,\bar{\alpha}_0^2\,\Omega_z^2\,\Lambda^2 \\ &\left[\ln^2\Lambda - \left(1 - 3\,\frac{\bar{\beta}_0}{\bar{\alpha}_0}\right)\ln\Lambda + \frac{1}{2}\left(1 - 3\,\frac{\bar{\beta}_0}{\bar{\alpha}_0} + \frac{3}{2}\,\frac{\bar{\beta}_0^2}{\bar{\alpha}_0^2}\right)\right]\end{aligned} \tag{16.72}$$

and finally, using the definitions of $\bar{\alpha}_0$ and $\bar{\beta}_0$, can be rewritten as

$$\begin{aligned}\frac{W_{\perp}^{W}}{\ell} \simeq \frac{\bar{\mu}_0}{4\pi}\,&\left(\frac{\bar{\mu}_0}{2\bar{\mu}_0 + \bar{\lambda}_0}\right)^2 \Omega_z^2\,\Lambda^2\Bigg[\ln^2\Lambda - \left(1 - 3\,\frac{\bar{\mu}_0 + \bar{\lambda}_0}{\bar{\mu}_0}\right)\times \\ &\times\,\ln\Lambda + \frac{1}{2}\left(1 - 3\,\frac{\bar{\mu}_0 + \bar{\lambda}_0}{\bar{\mu}_0} + \frac{3}{2}\,\left(\frac{\bar{\mu}_0 + \bar{\lambda}_0}{\bar{\mu}_0}\right)^2\right)\Bigg].\end{aligned} \tag{16.73}$$

The proportionality constant of this equation is similar to that of the transverse strain energy (16.38) for the stationary edge dislocation although the functional form is different for a disclination compared to a dislocation.

§16.6 Twist disclination longitudinal strain energy

The longitudinal strain energy of the deWit twist disclination is obtained from

$$W_{\parallel}^{T} = \int_V \mathcal{E}_{\parallel}^{T}\,\mathrm{d}V. \tag{16.74}$$

Substituting for $\mathcal{E}_{\parallel}^{T}$ from (10.129), this equation becomes

$$W_{\parallel}^{T} = \int_{V} \frac{\bar{\kappa}_0}{2\pi^2} \left(\frac{\bar{\mu}_0}{2\bar{\mu}_0 + \bar{\lambda}_0} \left(\Omega_x x + \Omega_y y \right) \frac{z}{r^2} \right)^2 \mathrm{d}V \tag{16.75}$$

where V is the volume of the wedge disclination, with $\mathrm{d}V$ given by $r\mathrm{d}r\,\mathrm{d}\theta\,\mathrm{d}z$ in cylindrical polar coordinates. As before, we take Ω out of the integral from (14.5), and (16.75) becomes

$$\begin{aligned} W_{\parallel}^{T} = & \frac{\bar{\kappa}_0}{2\pi^2} \left(\frac{\bar{\mu}_0}{2\bar{\mu}_0 + \bar{\lambda}_0} \right)^2 \\ & \int_0^{\ell} \int_0^{2\pi} \int_{b_c}^{\Lambda} \left(\Omega_x x + \Omega_y y \right)^2 \frac{z^2}{r^4} \, r\mathrm{d}r\,\mathrm{d}\theta\,\mathrm{d}z \end{aligned} \tag{16.76}$$

where ℓ is the length of the disclination, b_c is the size of the core of the disclination, of order b_0, the smallest spacetime dislocation Burgers vector, and Λ is a cut-off parameter corresponding to the radial extent of the disclination, limited by the average distance to its nearest neighbours.

Evaluating the integral over r, (16.76) becomes

$$\begin{aligned} W_{\parallel}^{T} = & \frac{\bar{\kappa}_0}{2\pi^2} \left(\frac{\bar{\mu}_0}{2\bar{\mu}_0 + \bar{\lambda}_0} \right)^2 \ln \frac{\Lambda}{b_c} \\ & \int_0^{\ell} \int_0^{2\pi} \left(\Omega_x \cos\theta + \Omega_y \sin\theta \right)^2 z^2 \, \mathrm{d}\theta\,\mathrm{d}z \end{aligned} \tag{16.77}$$

where we have used the relations $\cos\theta = x/r$ and $\sin\theta = y/r$. Evaluating the integral over θ [376], we obtain

$$\begin{aligned} W_{\parallel}^{T} = & \frac{\bar{\kappa}_0}{2\pi^2} \left(\frac{\bar{\mu}_0}{2\bar{\mu}_0 + \bar{\lambda}_0} \right)^2 \ln \frac{\Lambda}{b_c} \int_0^{\ell} \left[\frac{\Omega_x^2}{2} \left(\theta + \sin\theta\cos\theta \right) - \right. \\ & \left. - \Omega_x \Omega_y \cos^2\theta + \frac{\Omega_y^2}{2} \left(\theta - \sin\theta\cos\theta \right) \right]_0^{2\pi} z^2 \, \mathrm{d}z \, . \end{aligned} \tag{16.78}$$

Applying the limits of integration and rearranging, (16.78) becomes

$$W_{\parallel}^{T} = \frac{\bar{\kappa}_0}{2\pi} \left(\frac{\bar{\mu}_0}{2\bar{\mu}_0 + \bar{\lambda}_0} \right)^2 \ln \frac{\Lambda}{b_c} \left(\Omega_x^2 + \Omega_y^2 \right) \int_0^{\ell} z^2 \, \mathrm{d}z \, . \tag{16.79}$$

Evaluating the integral over z, (16.79) becomes

$$W_{\parallel}^{T} = \frac{\bar{\kappa}_0}{6\pi} \left(\frac{\bar{\mu}_0}{2\bar{\mu}_0 + \bar{\lambda}_0} \right)^2 \left(\Omega_x^2 + \Omega_y^2 \right) \ell^3 \ln \frac{\Lambda}{b_c} \, . \tag{16.80}$$

One interesting aspect of this equation is that the twist disclination longitudinal strain energy $W_{\parallel}^{T}$ is proportional to the cube of the length of the disclination (ℓ^3), and we can't dispose of it by considering the strain energy per unit length of the disclination as this would still be proportional to ℓ^2. We can say that the twist disclination longitudinal strain energy $W_{\parallel}^{T}$ is thus proportional to the space volume of the disclination. This is a dependence that we will consider in greater detail later.

It is interesting to note that $W_{\parallel}^{T}$ has the familiar dependence $\ln \Lambda/b_c$ of dislocations, different from the functional dependence obtained for wedge disclinations in §16.4 and §16.5. The form of this equation is similar to that of the longitudinal strain energy (16.15) for the stationary edge dislocation except for the factor $\ell^3/3$.

§16.7 Twist disclination transverse strain energy

The transverse strain energy of the deWit twist disclination is obtained from

$$W_{\perp}^{T} = \int_{V} \mathcal{E}_{\perp}^{T} \, \mathrm{d}V. \tag{16.81}$$

Substituting for $\mathcal{E}_{\perp}^{T}$ from (10.132), this equation becomes

$$\begin{aligned} W_{\perp}^{T} = \int_{V} \Bigg\{ & \frac{\bar{\mu}_0 \Omega_x^2}{2\pi^2} \Bigg[\bar{\alpha}_0^2 \ln^2 r + \frac{\bar{\beta}_0^2}{r^2} + 2\bar{\alpha}_0 \bar{\beta}_0 \, \frac{y^2}{r^2} \, \ln r + \\ & + \left[\left(\bar{\alpha}_0^2 - \tfrac{1}{2} \, \bar{\beta}_0^2 \right) x^2 + \bar{\beta}_0^2 y^2 \right] \frac{z^2}{r^4} \Bigg] + \\ & + \frac{\bar{\mu}_0 \Omega_y^2}{2\pi^2} \Bigg[\bar{\alpha}_0^2 \ln^2 r + \frac{\bar{\beta}_0^2}{r^2} + 2\bar{\alpha}_0 \bar{\beta}_0 \, \frac{x^2}{r^2} \, \ln r + \\ & + \left[\bar{\beta}_0^2 x^2 + \left(\bar{\alpha}_0^2 - \tfrac{1}{2} \, \bar{\beta}_0^2 \right) y^2 \right] \frac{z^2}{r^4} \Bigg] - \\ & - \frac{\bar{\mu}_0 \Omega_x \Omega_y}{\pi^2} \left[\bar{\beta}_0 \left(\bar{\alpha}_0 \ln r + \tfrac{1}{2} \, \bar{\beta}_0 \right) + \left(\bar{\beta}_0^2 - \tfrac{1}{2} \, \bar{\alpha}_0^2 \right) \frac{z^2}{r^2} \right] \Bigg\} \, \mathrm{d}V \end{aligned} \tag{16.82}$$

where V is the volume of the twist disclination, with $\mathrm{d}V$ given by $r \mathrm{d}r \, \mathrm{d}\theta \, \mathrm{d}z$ in cylindrical polar coordinates. As before, we take Ω out of the integral from (14.5). As in the case of the twist disclination longitudinal strain energy, the integral over z cannot be handled by considering the strain energy per unit length of the disclination as (16.82) also depends on z^2, again indicating an ℓ^3 dependence in the twist disclination transverse strain energy, in addition to the ℓ dependence.

The volume integral then becomes

$$
\begin{aligned}
W_{\perp}^{T} = \int_0^{\ell}\int_0^{2\pi}\int_{b_c}^{\Lambda} \Bigg\{ & \frac{\bar{\mu}_0\Omega_x^2}{2\pi^2}\Bigg[\bar{\alpha}_0^2\ln^2 r + \frac{\bar{\beta}_0^2}{r^2} + \\
& + 2\bar{\alpha}_0\bar{\beta}_0\,\frac{y^2}{r^2}\,\ln r + \left[\left(\bar{\alpha}_0^2 - \tfrac{1}{2}\,\bar{\beta}_0^2\right)x^2 + \bar{\beta}_0^2 y^2\right]\frac{z^2}{r^4}\Bigg] + \\
& + \frac{\bar{\mu}_0\Omega_y^2}{2\pi^2}\Bigg[\bar{\alpha}_0^2\ln^2 r + \frac{\bar{\beta}_0^2}{r^2} + 2\bar{\alpha}_0\bar{\beta}_0\,\frac{x^2}{r^2}\,\ln r + \\
& + \left[\bar{\beta}_0^2 x^2 + \left(\bar{\alpha}_0^2 - \tfrac{1}{2}\,\bar{\beta}_0^2\right)y^2\right]\frac{z^2}{r^4}\Bigg] - \\
& - \frac{\bar{\mu}_0\Omega_x\Omega_y}{\pi^2}\left[\bar{\beta}_0\left(\bar{\alpha}_0\ln r + \tfrac{1}{2}\,\bar{\beta}_0\right) + \left(\bar{\beta}_0^2 - \tfrac{1}{2}\,\bar{\alpha}_0^2\right)\frac{z^2}{r^2}\right]\Bigg\}\, r\mathrm{d}r\,\mathrm{d}\theta\,\mathrm{d}z
\end{aligned}
\tag{16.83}
$$

where ℓ is the length of the disclination, b_c is the size of the core of the disclination, of order b_0, the smallest spacetime dislocation Burgers vector, and Λ is a cut-off parameter corresponding to the radial extent of the disclination, limited by the average distance to its nearest neighbours.

Evaluating the integral over θ [376] using the relations $\cos^2\theta = x^2/r^2$ and $\sin^2\theta = y^2/r^2$ and re-arranging, (16.83) becomes

$$
\begin{aligned}
W_{\perp}^{T} = \frac{\bar{\mu}_0}{\pi}\int_0^{\ell}\int_{b_c}^{\Lambda} \Bigg\{ & \left(\Omega_x^2 + \Omega_y^2\right)\Bigg[\bar{\alpha}_0^2\ln^2 r + \frac{\bar{\beta}_0^2}{r^2} + \\
& + \bar{\alpha}_0\bar{\beta}_0\,\ln r + \tfrac{1}{2}\left[\left(\bar{\alpha}_0^2 - \tfrac{1}{2}\,\bar{\beta}_0^2\right) + \bar{\beta}_0^2\right]\frac{z^2}{r^2}\Bigg] - \\
& - 2\,\Omega_x\Omega_y\left[\bar{\beta}_0\left(\bar{\alpha}_0\ln r + \tfrac{1}{2}\,\bar{\beta}_0\right) + \left(\bar{\beta}_0^2 - \tfrac{1}{2}\,\bar{\alpha}_0^2\right)\frac{z^2}{r^2}\right]\Bigg\}\, r\mathrm{d}r\,\mathrm{d}z\,.
\end{aligned}
\tag{16.84}
$$

Evaluating the integral over z and simplifying, (16.84) becomes

$$
\begin{aligned}
W_{\perp}^{T} = \frac{\bar{\mu}_0}{\pi}\int_{b_c}^{\Lambda} \Bigg\{ & \left(\Omega_x^2 + \Omega_y^2\right)\Bigg[\ell\left(\bar{\alpha}_0^2\, r\ln^2 r + \bar{\alpha}_0\bar{\beta}_0\, r\ln r + \right. \\
& \left. + \bar{\beta}_0^2\,\frac{1}{r}\right) + \frac{1}{2}\,\frac{\ell^3}{3}\,\left(\bar{\alpha}_0^2 + \tfrac{1}{2}\,\bar{\beta}_0^2\right)\,\frac{1}{r}\Bigg] - \\
& - 2\,\Omega_x\Omega_y\left[\ell\left(\bar{\alpha}_0\bar{\beta}_0\, r\ln r + \tfrac{1}{2}\,\bar{\beta}_0^2\, r\right) + \frac{\ell^3}{3}\,\left(\bar{\beta}_0^2 - \tfrac{1}{2}\,\bar{\alpha}_0^2\right)\frac{1}{r}\right]\Bigg\}\,\mathrm{d}r\,.
\end{aligned}
\tag{16.85}
$$

Evaluating the integral over r [376], we obtain

$$\begin{aligned} W_{\perp}^{T} = \frac{\bar{\mu}_0}{2\pi}\,\frac{\ell^3}{3}\,\Big[& \left(\Omega_x^2+\Omega_y^2\right)\left(\bar{\alpha}_0^2+\tfrac{1}{2}\,\bar{\beta}_0^2\right)+ \\ & +2\,\Omega_x\Omega_y\left(\bar{\alpha}_0^2-2\bar{\beta}_0^2\right)\Big]\,\ln r\,\Big|_{b_c}^{\Lambda}+ \\ & +\frac{\bar{\mu}_0}{2\pi}\,\ell\,\Big[\left(\Omega_x^2+\Omega_y^2\right)\Big(\bar{\alpha}_0^2\,r^2\ln^2 r-\bar{\alpha}_0\left(\bar{\alpha}_0-\bar{\beta}_0\right)\,r^2\ln r+ \\ & +\frac{1}{2}\,\bar{\alpha}_0\left(\bar{\alpha}_0-\bar{\beta}_0\right)\,r^2+2\bar{\beta}_0^2\ln r\Big)- \\ & -2\,\Omega_x\Omega_y\left(\bar{\alpha}_0\bar{\beta}_0\,r^2\ln r-\tfrac{1}{2}\,\bar{\beta}_0\,\left(\bar{\alpha}_0-\bar{\beta}_0\right)r^2\right)\Big]\,\Big|_{b_c}^{\Lambda}. \end{aligned} \tag{16.86}$$

Using $\bar{\alpha}_0-\bar{\beta}_0=-\bar{\gamma}_0$ where $\bar{\gamma}_0$ is defined in (9.155), applying the limits of integration and rearranging, (16.86) becomes

$$\begin{aligned} W_{\perp}^{T} = \frac{\bar{\mu}_0}{2\pi}\,\frac{\ell^3}{3}\,\Big[& \left(\Omega_x^2+\Omega_y^2\right)\left(\bar{\alpha}_0^2+\tfrac{1}{2}\,\bar{\beta}_0^2\right)+ \\ & +2\,\Omega_x\Omega_y\left(\bar{\alpha}_0^2-2\bar{\beta}_0^2\right)\Big]\,\ln\frac{\Lambda}{b_c}+ \\ & +\frac{\bar{\mu}_0}{2\pi}\,\ell\,\Big[\left(\Omega_x^2+\Omega_y^2\right)\Big(\bar{\alpha}_0^2\,\left(\Lambda^2\ln^2\Lambda-b_c^2\ln^2 b_c\right)+ \\ & +\bar{\alpha}_0\bar{\gamma}_0\,\left(\Lambda^2\ln\Lambda-b_c^2\ln b_c\right)-\frac{1}{2}\bar{\alpha}_0\bar{\gamma}_0\left(\Lambda^2-b_c^2\right)+ \\ & +2\,\bar{\beta}_0^2\,\ln\frac{\Lambda}{b_c}\Big)-\,2\,\Omega_x\Omega_y\Big(\bar{\alpha}_0\bar{\beta}_0\left(\Lambda^2\ln\Lambda-b_c^2\ln b_c\right)+ \\ & +\frac{1}{2}\bar{\beta}_0\bar{\gamma}_0\left(\Lambda^2-b_c^2\right)\Big)\Big]. \end{aligned} \tag{16.87}$$

In most cases $\Lambda \gg b_c$, and (16.87) reduces to

$$\begin{aligned} W_{\perp}^{T} \simeq \frac{\bar{\mu}_0}{2\pi}\,\frac{\ell^3}{3}\,\Big[& \left(\Omega_x^2+\Omega_y^2\right)\left(\bar{\alpha}_0^2+\tfrac{1}{2}\,\bar{\beta}_0^2\right)+ \\ & +\,2\,\Omega_x\Omega_y\left(\bar{\alpha}_0^2-2\bar{\beta}_0^2\right)\Big]\,\ln\frac{\Lambda}{b_c}+ \end{aligned} \tag{16.88}$$

$$+\frac{\bar{\mu}_0}{2\pi}\,\ell\,\Lambda^2\,\Bigg[\,\big(\Omega_x^2+\Omega_y^2\big)\,\Big(\bar{\alpha}_0^2\,\ln^2\Lambda+\,\bar{\alpha}_0\bar{\gamma}_0\,\ln\Lambda-$$
$$-\,\frac{1}{2}\bar{\alpha}_0\bar{\gamma}_0\Big)-2\,\Omega_x\Omega_y\Big(\bar{\alpha}_0\bar{\beta}_0\ln\Lambda+\frac{1}{2}\bar{\beta}_0\bar{\gamma}_0\Big)\Bigg]$$

which can be rearranged as

$$\begin{aligned}W_\perp^T\simeq\frac{\bar{\mu}_0}{2\pi}\,\bar{\alpha}_0^2\,\frac{\ell^3}{3}\,\Bigg[\,\big(\Omega_x^2+\Omega_y^2\big)\,\Big(1+\frac{1}{2}\,\frac{\bar{\beta}_0^2}{\bar{\alpha}_0^2}\Big)+\\+2\,\Omega_x\Omega_y\,\Big(1-2\,\frac{\bar{\beta}_0^2}{\bar{\alpha}_0^2}\Big)\Bigg]\,\ln\frac{\Lambda}{b_c}+\\+\frac{\bar{\mu}_0}{2\pi}\,\bar{\alpha}_0^2\,\ell\,\Lambda^2\,\Bigg[\,\big(\Omega_x^2+\Omega_y^2\big)\,\Big(\ln^2\Lambda+\,\frac{\bar{\gamma}_0}{\bar{\alpha}_0}\,\ln\Lambda-\\-\,\frac{1}{2}\,\frac{\bar{\gamma}_0}{\bar{\alpha}_0}\Big)-2\,\Omega_x\Omega_y\Big(\frac{\bar{\beta}_0}{\bar{\alpha}_0}\ln\Lambda+\frac{1}{2}\,\frac{\bar{\beta}_0\bar{\gamma}_0}{\bar{\alpha}_0^2}\Big)\Bigg]\end{aligned}\tag{16.89}$$

and from the definitions of $\bar{\alpha}_0$, $\bar{\beta}_0$ and $\bar{\gamma}_0$, finally

$$\begin{aligned}W_\perp^T\simeq\frac{\bar{\mu}_0}{2\pi}\,\bar{\alpha}_0^2\,\frac{\ell^3}{3}\,\Bigg[\,\big(\Omega_x^2+\Omega_y^2\big)\,\Big(1+\frac{1}{2}\,\frac{(\bar{\mu}_0+\bar{\lambda}_0)^2}{\bar{\mu}_0^2}\Big)+\\+2\,\Omega_x\Omega_y\,\Big(1-2\,\frac{(\bar{\mu}_0+\bar{\lambda}_0)^2}{\bar{\mu}_0^2}\Big)\Bigg]\,\ln\frac{\Lambda}{b_c}+\\+\frac{\bar{\mu}_0}{2\pi}\,\bar{\alpha}_0^2\,\ell\,\Lambda^2\,\Bigg[\,\big(\Omega_x^2+\Omega_y^2\big)\,\Big(\ln^2\Lambda+\,\frac{\bar{\lambda}_0}{\bar{\mu}_0}\,\ln\Lambda-\\-\,\frac{1}{2}\,\frac{\bar{\lambda}_0}{\bar{\mu}_0}\Big)-2\,\Omega_x\Omega_y\Big(\frac{\bar{\mu}_0+\bar{\lambda}_0}{\bar{\mu}_0}\ln\Lambda+\frac{1}{2}\,\frac{(\bar{\mu}_0+\bar{\lambda}_0)\bar{\lambda}_0}{\bar{\mu}_0^2}\Big)\Bigg]\end{aligned}\tag{16.90}$$

We see that the twist disclination transverse strain energy $W_\perp^T$ has a portion which is proportional to the length of the disclination, and one which is proportional to the space volume of the disclination. This transverse strain energy for the twist disclination shows the most functional diversity of all defects considered in this chapter.

The quantum physics implications of the longitudinal and transverse strain energy for the screw and edge dislocations and for the wedge and twist disclination are considered in Chapter 18.

Chapter 17

Defect Interactions in STCED

§17.1 Defect interactions in STCED

In Chapter 14, we saw how *STCED* provides a framework for quantum physics based on defects in the spacetime continuum. In particular, dislocations and disclinations were identified with bosons and fermions respectively in section §14.4. We have discussed the quantum and energy characteristics of stationary dislocations and disclinations and the association of these defects to fundamental quantum particles in Chapter 15, and their strain energy in the stationary and moving case in Chapter 16.

In this chapter, we consider the interactions of defects in *STCED*, and how they relate to quantum physics. We have briefly considered this topic in section §14.5. In *STCED*, the interaction of dislocations and disclinations is mediated through the interaction of their strain energy density.

We find that this interaction of the strain energy density results from the overlap of the strain energy densities of defects, a process akin to the wavefunction overlap of quantum mechanics, which is physically explained by this process in *STCED*. One source of this overlap interaction comes from displacement defect interactions of different types of defects, characterized by their Burgers and Frank vectors as derived in the next section §17.2. Another source results from the overlap of the strain energy densities of multiple defects, including of the same type as shown in section §17.4.

We will then explore in greater details how Feynman diagrams are relevant to *STCED* quantum physics. As discussed in section §14.5, the role played by virtual particles in quantum electrodynamics (QED) will be shown to be replaced by the interaction of the strain energy density of the dislocations and disclinations in *STCED*.

§17.2 Displacement defect interactions

As mentioned in section §10.5, we consider the interaction terms of dislocations and disclinations arising from the general displacements derived from the general combined deWit dislocation displacements (9.130) and disclination displacements (10.76).

As seen in section §10.2 for the combined Volterra dislocation and disclination displacements, the combined deWit dislocation and disclination displacements are obtained by adding the dislocation displacements (9.130) and disclination displacements (10.76) to obtain

$$\begin{aligned}
u_x &= \frac{b_x}{2\pi}\left(\theta + \bar{\beta}_0\,\frac{xy}{r^2}\right) + \frac{b_y}{2\pi}\left(\bar{\alpha}_0\,\ln r + \bar{\beta}_0\,\frac{y^2}{r^2}\right) - \\
&\quad - \frac{\Omega_x}{2\pi}\,z\left(\bar{\alpha}_0 \ln r + \bar{\beta}_0\,\frac{y^2}{r^2}\right) + \frac{\Omega_y}{2\pi}\,z\left(\theta + \bar{\beta}_0\,\frac{xy}{r^2}\right) - \\
&\quad - \frac{\Omega_z}{2\pi}\,(y\,\theta - \bar{\alpha}_0\,x\,(\ln r - 1)) \\
u_y &= -\frac{b_x}{2\pi}\left(\bar{\alpha}_0\,\ln r + \bar{\beta}_0\,\frac{x^2}{r^2}\right) + \frac{b_y}{2\pi}\left(\theta - \bar{\beta}_0\,\frac{xy}{r^2}\right) - \\
&\quad - \frac{\Omega_x}{2\pi}\,z\left(\theta - \bar{\beta}_0\,\frac{xy}{r^2}\right) - \frac{\Omega_y}{2\pi}\,z\left(\bar{\alpha}_0 \ln r + \bar{\beta}_0\,\frac{x^2}{r^2}\right) + \\
&\quad + \frac{\Omega_z}{2\pi}\,(x\,\theta + \bar{\alpha}_0\,y\,(\ln r - 1)) \\
u_z &= \frac{b_z}{2\pi}\,\theta + \frac{\Omega_x}{2\pi}\,(y\,\theta - \bar{\alpha}_0\,x\,(\ln r - 1)) - \\
&\quad - \frac{\Omega_y}{2\pi}\,(x\,\theta + \bar{\alpha}_0\,y\,(\ln r - 1))
\end{aligned} \tag{17.1}$$

where

$$\bar{\alpha}_0 = \frac{\bar{\mu}_0}{2\bar{\mu}_0 + \bar{\lambda}_0} \tag{17.2}$$

$$\bar{\beta}_0 = \frac{\bar{\mu}_0 + \bar{\lambda}_0}{2\bar{\mu}_0 + \bar{\lambda}_0}\,. \tag{17.3}$$

The components of the strain tensor in cartesian coordinates are derived from $\varepsilon^{\mu\nu} = \frac{1}{2}(u^{\mu;\nu} + u^{\nu;\mu})$. As this is a linear operation, the combined components of the strain tensor are obtained by adding the dislocation strain tensor components (9.131) and the disclination strain tensor components (10.79):

$$\begin{aligned}
\varepsilon_{xx} &= -\frac{b_x}{2\pi}\left(\bar{\alpha}_0\,\frac{y}{r^2} + \bar{\beta}_0\,\frac{2x^2y}{r^4}\right) + \frac{b_y}{2\pi}\left(\bar{\alpha}_0\,\frac{x}{r^2} - \bar{\beta}_0\,\frac{2xy^2}{r^4}\right) - \\
&\quad - \frac{\Omega_x}{2\pi}\,z\left(\bar{\alpha}_0\,\frac{x}{r^2} - 2\bar{\beta}_0\,\frac{xy^2}{r^4}\right) -
\end{aligned} \tag{17.4}$$

$$
\begin{aligned}
&- \frac{\Omega_y}{2\pi}\, z \left(\bar{\alpha}_0 \, \frac{y}{r^2} + 2\bar{\beta}_0 \, \frac{x^2 y}{r^4} \right) + \frac{\Omega_z}{2\pi} \left(\bar{\alpha}_0 \ln r + \bar{\beta}_0 \, \frac{y^2}{r^2} \right) \\
\varepsilon_{yy} &= -\frac{b_x}{2\pi} \left(\bar{\alpha}_0 \, \frac{y}{r^2} - \bar{\beta}_0 \, \frac{2x^2 y}{r^4} \right) + \frac{b_y}{2\pi} \left(\bar{\alpha}_0 \, \frac{x}{r^2} + \bar{\beta}_0 \, \frac{2xy^2}{r^4} \right) - \\
&- \frac{\Omega_x}{2\pi}\, z \left(\bar{\alpha}_0 \, \frac{x}{r^2} + 2\bar{\beta}_0 \, \frac{xy^2}{r^4} \right) - \\
&- \frac{\Omega_y}{2\pi}\, z \left(\bar{\alpha}_0 \, \frac{y}{r^2} - 2\bar{\beta}_0 \, \frac{x^2 y}{r^4} \right) + \frac{\Omega_z}{2\pi} \left(\bar{\alpha}_0 \, \ln r + \bar{\beta}_0 \, \frac{x^2}{r^2} \right) \\
\varepsilon_{zz} &= 0 \\
\varepsilon_{xy} &= \frac{b_x}{2\pi} \, \bar{\beta}_0 \left(\frac{x}{r^2} - \frac{2xy^2}{r^4} \right) - \frac{b_y}{2\pi} \, \bar{\beta}_0 \left(\frac{y}{r^2} - \frac{2x^2 y}{r^4} \right) + \\
&+ \frac{\Omega_x}{2\pi}\, z\, \bar{\beta}_0 \left(\frac{y}{r^2} - \frac{2x^2 y}{r^4} \right) + \\
&+ \frac{\Omega_y}{2\pi}\, z\, \bar{\beta}_0 \left(\frac{x}{r^2} - \frac{2xy^2}{r^4} \right) - \frac{\Omega_z}{2\pi} \bar{\beta}_0 \, \frac{xy}{r^2} \\
\varepsilon_{yz} &= \frac{b_z}{4\pi} \, \frac{x}{r^2} + \frac{\Omega_x}{2\pi} \, \bar{\beta}_0 \, \frac{xy}{r^2} - \frac{\Omega_y}{2\pi} \left(\bar{\alpha}_0 \ln r + \bar{\beta}_0 \, \frac{x^2}{r^2} \right) \\
\varepsilon_{zx} &= -\frac{b_z}{4\pi} \, \frac{y}{r^2} - \frac{\Omega_x}{2\pi} \left(\bar{\alpha}_0 \ln r + \bar{\beta}_0 \, \frac{y^2}{r^2} \right) + \frac{\Omega_y}{2\pi} \, \bar{\beta}_0 \, \frac{xy}{r^2} \, .
\end{aligned}
$$

The volume dilatation ε for the discrete dislocation line is then given by

$$
\varepsilon = \varepsilon^{\alpha}{}_{\alpha} = \varepsilon_{xx} + \varepsilon_{yy} + \varepsilon_{zz} \, . \tag{17.5}
$$

Substituting for ε_{xx}, ε_{yy} and ε_{zz} from (17.4), we obtain

$$
\begin{aligned}
\varepsilon = &- \frac{1}{\pi} \, \frac{\bar{\mu}_0}{2\bar{\mu}_0 + \bar{\lambda}_0} \, \frac{b_x y - b_y x}{r^2} - \\
&- \frac{1}{\pi} \, \frac{\bar{\mu}_0}{2\bar{\mu}_0 + \bar{\lambda}_0} \, (\Omega_x x + \Omega_y y) \, \frac{z}{r^2} + \\
&+ \frac{\Omega_z}{\pi} \left(\frac{\bar{\mu}_0}{2\bar{\mu}_0 + \bar{\lambda}_0} \, \ln r + \frac{1}{2} \, \frac{\bar{\mu}_0 + \bar{\lambda}_0}{2\bar{\mu}_0 + \bar{\lambda}_0} \right) .
\end{aligned} \tag{17.6}
$$

The mass energy density is calculated from (2.24), *viz.*

$$
\rho c^2 = 4\bar{\kappa}_0 \, \varepsilon = 2(2\bar{\lambda}_0 + \bar{\mu}_0) \, \varepsilon \, .
$$

Substituting for ε from (17.6), using the absolute value of ε as per section §9.3.4, the mass energy density of the discrete dislocation line is given by

$$\begin{aligned}\rho c^2 = \Bigg| & \frac{4}{\pi}\,\frac{\bar{\kappa}_0\bar{\mu}_0}{2\bar{\mu}_0+\bar{\lambda}_0}\,\frac{b_x y - b_y x}{r^2} - \\ & + \frac{4}{\pi}\,\frac{\bar{\kappa}_0\bar{\mu}_0}{2\bar{\mu}_0+\bar{\lambda}_0}\,(\Omega_x x + \Omega_y y)\,\frac{z}{r^2} + \\ & - \frac{4\bar{\kappa}_0\Omega_z}{\pi}\left(\frac{\bar{\mu}_0}{2\bar{\mu}_0+\bar{\lambda}_0}\,\ln r + \frac{1}{2}\,\frac{\bar{\mu}_0+\bar{\lambda}_0}{2\bar{\mu}_0+\bar{\lambda}_0}\right)\Bigg|\end{aligned} \tag{17.7}$$

and using $\bar{\alpha}_0$ and $\bar{\beta}_0$,

$$\begin{aligned}\rho c^2 = \Bigg| & \frac{4}{\pi}\,\bar{\kappa}_0\bar{\alpha}_0\,\frac{b_x y - b_y x}{r^2} - \\ & + \frac{4}{\pi}\,\bar{\kappa}_0\bar{\alpha}_0\,(\Omega_x x + \Omega_y y)\,\frac{z}{r^2} + \\ & - \frac{4\bar{\kappa}_0\Omega_z}{\pi}\left(\bar{\alpha}_0\ln r + \frac{1}{2}\,\bar{\beta}_0\right)\Bigg|.\end{aligned} \tag{17.8}$$

The rest-mass density is thus the sum of the rest-mass density of edge dislocations, wedge and twist disclinations. Screw dislocations are not present as they are massless. The negative terms indicate a decrease in total rest-mass energy due to bound states.

§17.2.1 *Dislocation-dislocation interactions*

The strain energy density of the discrete dislocation line is calculated using (9.133) in (9.50) as seen previously in §9.5. The discrete dislocation line longitudinal dilatation strain energy density is then given by (9.139),

$$\mathcal{E}_{\parallel} = \frac{1}{2\pi^2}\,\frac{\bar{\kappa}_0\,\bar{\mu}_0^2}{(2\bar{\mu}_0+\bar{\lambda}_0)^2}\,\frac{(b_x y - b_y x)^2}{r^4}. \tag{17.9}$$

There is no longitudinal interaction strain energy density between edge dislocations and screw dislocations, as the latter are massless.

Comparing this result with (9.68) corresponding to an edge dislocation with the Burgers vector along the $x-axis$ as per Fig. 9.4, the result is the same as the $b_x y$ term of (17.9). Similarly, we see that the $b_y x$ term of (17.9) corresponds to an edge dislocation with the Burgers vector along the $y-axis$. Considering (17.9), we note that in the case

of two edge dislocations with Burgers vectors b_x and b_y respectively, the longitudinal overlap interaction strain energy density between the edge dislocations along b_x and b_y respectively would be given by

$$\mathcal{E}^{E-E}_{\parallel\ int} = -4\bar{\kappa}_0\bar{\alpha}_0^2\,\frac{\text{ƀ}_x x \text{ƀ}_y y}{r^4} \tag{17.10}$$

where $\text{ƀ} = b/2\pi$. The negative sign represents a reduction in the overall interaction energy of the two edge dislocations.

As seen previously in §9.5, the distortion strain energy density is calculated from (9.51), *viz.*

$$\mathcal{E}_\perp = \bar{\mu}_0 e^{\alpha\beta} e_{\alpha\beta}\,,$$

and using (9.20), *viz.*

$$e^{\alpha\beta} = \varepsilon^{\alpha\beta} - e_s g^{\alpha\beta}$$

where $e_s = \frac{1}{4}\,\varepsilon$, (9.51) simplifies to

$$\mathcal{E}_\perp = \bar{\mu}_0 \left(\varepsilon^{\alpha\beta}\varepsilon_{\alpha\beta} - \tfrac{1}{4}\,\varepsilon^2\right)\,. \tag{17.11}$$

This expression is expanded using the non-zero elements of the strain tensor (9.131) to give

$$\mathcal{E}_\perp = \bar{\mu}_0 \left({\varepsilon_{xx}}^2 + {\varepsilon_{yy}}^2 + 2{\varepsilon_{xy}}^2 + 2{\varepsilon_{yz}}^2 + 2{\varepsilon_{xz}}^2 - \tfrac{1}{4}\,\varepsilon^2\right)\,. \tag{17.12}$$

Substituting from (9.131) and (9.133) in the above and simplifying, we obtain (9.149):

$$\begin{aligned}\mathcal{E}_\perp = {}& \frac{\bar{\mu}_0}{8\pi^2}\,\frac{b_z^2}{r^2} + \frac{\bar{\mu}_0}{4\pi^2}\,\bar{\alpha}_0^2\,\frac{(b_x y - b_y x)^2}{r^4} + \\ & + \frac{\bar{\mu}_0}{2\pi^2}\,\bar{\beta}_0^2\,\frac{(b_x x + b_y y)^2}{r^4} - \frac{3}{2\pi^2}\,\frac{\bar{\mu}_0\bar{\lambda}_0}{2\bar{\mu}_0 + \bar{\lambda}_0}\,\frac{b_x b_y xy}{r^4}\,.\end{aligned} \tag{17.13}$$

As seen previously in §9.5, setting $b_z = 0$ and $b_y = 0$ in the above, we obtain the distortion strain energy density expression (9.75) for the stationary edge dislocation.

Substituting from (9.138) and (9.139), (17.13) becomes

$$\begin{aligned}\mathcal{E}_\perp = {}& \frac{\bar{\mu}_0}{8\pi^2}\,\frac{b_z^2}{r^2} + \frac{1}{2}\,\frac{\bar{\mu}_0}{\bar{\kappa}_0}\,\mathcal{E}_\parallel + 2\bar{\mu}_0\left(\frac{\bar{\mu}_0 + \bar{\lambda}_0}{2\bar{\mu}_0 + \bar{\lambda}_0}\right)^2 \omega_z^2 - \\ & - \frac{3}{2\pi^2}\,\frac{\bar{\mu}_0\bar{\lambda}_0}{2\bar{\mu}_0 + \bar{\lambda}_0}\,\frac{b_x b_y xy}{r^4}\,.\end{aligned} \tag{17.14}$$

The first term is the screw dislocation strain energy density of (9.22), the second term is proportional to the edge dislocation distortion strain energy density arising from the longitudinal strain energy density of (9.139), the third term is the edge dislocation distortion strain energy density arising from the rotation vector of (9.138) and the last term is a moment distortion strain energy density term. It is interesting to note that there are no interaction terms (cross-terms) between screw and edge dislocations for a dislocation line. However, as we will see in section §18.6, a dislocation line does exhibit self-energy processes.

§17.2.2 *Disclination-disclination interactions*

The strain energy density of the discrete disclination line is calculated using (10.82) in (9.50) as seen previously in §10.5. The discrete disclination longitudinal dilatation strain energy density is then given by

$$\mathcal{E}_{\parallel} = \frac{\bar{\kappa}_0}{2\pi^2}\left[\Omega_z\left(\bar{\alpha}_0 \ln r + \frac{1}{2}\,\bar{\beta}_0\right) - \bar{\alpha}_0\left(\Omega_x x + \Omega_y y\right)\,\frac{z}{r^2}\right]^2 . \qquad (17.15)$$

This can be written as

$$\mathcal{E}_{\parallel} = \mathcal{E}_{\parallel}^{W} + \mathcal{E}_{\parallel}^{T} + \mathcal{E}_{\parallel\ int}^{W-T} \qquad (17.16)$$

where $\mathcal{E}_{\parallel}^{W}$ is given by (10.109), $\mathcal{E}_{\parallel}^{T}$ is given by (10.129) and

$$\mathcal{E}_{\parallel\ int}^{W-T} = -\frac{\bar{\kappa}_0}{\pi^2}\,\bar{\alpha}_0\left(\Omega_x x + \Omega_y y\right)\,\frac{\Omega_z z}{r^2}\,\left(\bar{\alpha}_0 \ln r + \frac{1}{2}\,\bar{\beta}_0\right) \qquad (17.17)$$

is the interaction longitudinal strain energy density between the wedge and twist disclinations. The negative sign indicates an attractive force.

The distortion strain energy density is calculated from (9.51), *viz.*

$$\mathcal{E}_{\perp} = \bar{\mu}_0 e^{\alpha\beta} e_{\alpha\beta}\,.$$

As seen previously, using (9.20), *viz.*

$$e^{\alpha\beta} = \varepsilon^{\alpha\beta} - e_s g^{\alpha\beta}$$

where $e_s = \frac{1}{4}\,\varepsilon$, (9.51) simplifies to

$$\mathcal{E}_{\perp} = \bar{\mu}_0\left(\varepsilon^{\alpha\beta}\varepsilon_{\alpha\beta} - \tfrac{1}{4}\,\varepsilon^2\right)\,. \qquad (17.18)$$

This expression is expanded using the non-zero elements of the strain tensor (10.79) to give

$$\mathcal{E}_{\perp} = \bar{\mu}_0\left({\varepsilon_{xx}}^2 + {\varepsilon_{yy}}^2 + 2{\varepsilon_{xy}}^2 - \tfrac{1}{4}\,\varepsilon^2\right)\,. \qquad (17.19)$$

Substituting from (10.79) and (10.82) in the above, we note that $\mathcal{E}_\perp$ can be separated in the following terms:

$$\mathcal{E}_\perp = \mathcal{E}_\perp^W + \mathcal{E}_\perp^T + \mathcal{E}_{\perp\ int}^{W-T} \tag{17.20}$$

where $\mathcal{E}_\perp^W$ is the wedge disclination distortion strain energy density given by (10.113), $\mathcal{E}_\perp^T$ is the twist disclination distortion strain energy density given by (10.132) and $\mathcal{E}_{\perp\ int}^{W-T}$ is the wedge-twist disclination interaction distortion strain energy density between the wedge and twist disclinations given by (10.97):

$$\begin{aligned}\mathcal{E}_{\perp\ int}^{W-T} = &-\frac{\bar{\mu}_0\Omega_x\Omega_z}{2\pi^2}\,\frac{xz}{r^2}\left[2\bar{\alpha}_0^2\ln r + \bar{\alpha}_0\bar{\beta}_0 + \bar{\beta}_0^2\,\frac{y^2}{r^2}\left(1-\frac{2y^2}{r^2}\right)\right]\\ &-\frac{\bar{\mu}_0\Omega_y\Omega_z}{2\pi^2}\,\frac{yz}{r^2}\left[2\bar{\alpha}_0^2\ln r + \bar{\alpha}_0\bar{\beta}_0 + \bar{\beta}_0^2\,\frac{x^2}{r^2}\left(1-\frac{2x^2}{r^2}\right)\right].\end{aligned} \tag{17.21}$$

It is important to note that the interactions involve separate longitudinal and distortion expressions.

§17.2.3 *Dislocation-disclination interactions*

In this section, we consider the interaction terms of dislocations and disclinations arising from the general displacements derived from the general combined deWit dislocation displacements (9.130) and disclination displacements (10.76) given by (17.1).

We calculate the dislocation-disclination interaction strain energy density by first calculating the longitudinal dilatation strain energy density ($\mathcal{E}_\parallel$) of the general dislocation-disclination using (10.82) in (9.50) as seen previously in §10.5, from the general strain tensor (17.4). Using the non-zero elements of the strain tensor (17.4) in the dilatation (17.5), we use

$$\mathcal{E}_\parallel = \tfrac{1}{2}\,\bar{\kappa}_0\left(\varepsilon_{xx}{}^2 + \varepsilon_{yy}{}^2 + 2\varepsilon_{xx}\varepsilon_{yy}\right). \tag{17.22}$$

We also calculate the distortion strain energy density ($\mathcal{E}_\perp$) as done previously from (9.51), *viz.*

$$\mathcal{E}_\perp = \bar{\mu}_0 e^{\alpha\beta}e_{\alpha\beta}\,.$$

As seen previously, using (9.20), *viz.*

$$e^{\alpha\beta} = \varepsilon^{\alpha\beta} - e_s g^{\alpha\beta}$$

where $e_s = \frac{1}{4}\,\varepsilon$, (9.51) simplifies to

$$\mathcal{E}_\perp = \bar{\mu}_0\left(\varepsilon^{\alpha\beta}\varepsilon_{\alpha\beta} - \tfrac{1}{4}\,\varepsilon^2\right). \tag{17.23}$$

This expression is expanded using the non-zero elements of the strain tensor (17.4) to give

$$\mathcal{E}_{\perp} = \bar{\mu}_0 \left({\varepsilon_{xx}}^2 + {\varepsilon_{yy}}^2 + 2{\varepsilon_{xy}}^2 + 2{\varepsilon_{yz}}^2 + 2{\varepsilon_{yz}}^2 - \tfrac{1}{4}\,\varepsilon^2 \right) . \tag{17.24}$$

Some of the terms resulting from the computation have already been calculated for dislocations only and for disclinations only, including the dislocation-dislocation interaction terms and the disclination-disclination interaction terms as seen in the previous sections §17.2.1 and §17.2.2 respectively. In calculating the dislocation-disclination interaction terms from the general strain tensor (17.4), we will group together the terms combining Burgers and Frank vector components.

We first provide a complete high-level overview of the strain energy density terms that will be obtained from the above computation. We include the terms that have already been calculated with a reference to the equation numbers for the results.

The strain energy density $\mathcal{E}$ is first separated into the dislocation strain energy density $\mathcal{E}^{D_t}$ where D_t represents the dislocation (a translation), the disclination strain energy density $\mathcal{E}^{D_r}$ where D_r represents the disclination (a rotation), and the dislocation-disclination interaction strain energy density $\mathcal{E}_{int}^{D_t - D_r}$, according to

$$\mathcal{E} = \mathcal{E}^{D_t} + \mathcal{E}^{D_r} + \mathcal{E}_{int}^{D_t - D_r} . \tag{17.25}$$

Dislocations (D_t) consist of screw (S) and edge (E) dislocations, and disclinations (D_r) consist of wedge (W) and twist (T) disclinations. This is summarized as follows:

$$D_t = \{S, E\} \tag{17.26}$$

$$D_r = \{W, T\} . \tag{17.27}$$

The strain energy density $\mathcal{E}$ is further separated into a longitudinal dilatation strain energy density ($\mathcal{E}_{\parallel}$) and a distortion strain energy density ($\mathcal{E}_{\perp}$) as seen above. This applies to both dislocations and disclinations, and hence we can write (17.25) as

$$\mathcal{E} = \mathcal{E}_{\parallel}^{D_t} + \mathcal{E}_{\perp}^{D_t} + \mathcal{E}_{\parallel}^{D_r} + \mathcal{E}_{\perp}^{D_r} + \mathcal{E}_{int}^{D_t - D_r} . \tag{17.28}$$

The interaction term $\mathcal{E}_{int}^{D_t - D_r}$ can also be separated along similar lines, and the details are covered further in this section. We now consider the individual terms of (17.25).

The dislocation strain energy density $\mathcal{E}^{D_t}$ can be further separated into the following terms:

$$\mathcal{E}^{D_t} = \underbrace{\underbrace{\underbrace{\mathcal{E}^S_{\parallel}}_{=0}}_{(9.68)} + \underbrace{\mathcal{E}^E_{\parallel}}_{(9.139)}}_{(9.156)} + \underbrace{\underbrace{\mathcal{E}^S_{\perp}}_{(9.22)} + \underbrace{\mathcal{E}^E_{\perp}}_{(9.78)}}_{(9.156)} \tag{17.29}$$

where $\mathcal{E}^S_{\parallel}$ is the screw dislocation dilatation strain energy density, which is equal to 0, $\mathcal{E}^E_{\parallel}$ is the edge dislocation dilatation strain energy density, $\mathcal{E}^S_{\perp}$ is the screw dislocation distortion strain energy density, and $\mathcal{E}^E_{\perp}$ is the edge dislocation distortion strain energy density. It is important to note that there is no interaction strain energy density arising from the dislocation displacements, due to their translation nature, although there is an interaction strain energy density that arises from the overlap of dislocations of the same type as we will see in later sections.

The disclination strain energy density $\mathcal{E}^{D_r}$ can be further separated into the following terms:

$$\mathcal{E}^{D_r} = \underbrace{\underbrace{\underbrace{\mathcal{E}^W_{\parallel}}_{(10.108)} + \underbrace{\mathcal{E}^T_{\parallel}}_{(10.129)}}_{(10.92)} + \underbrace{\mathcal{E}^{W-T}_{\parallel\ int}}_{(17.17)} + \underbrace{\underbrace{\underbrace{\mathcal{E}^W_{\perp}}_{(10.113)} + \underbrace{\mathcal{E}^T_{\perp}}_{(10.133)}}_{(10.98)} + \underbrace{\mathcal{E}^{W-T}_{\perp\ int}}_{(17.21)}}_{(10.98)} \tag{17.30}$$

where $\mathcal{E}^W_{\parallel}$ is the wedge disclination dilatation strain energy density, $\mathcal{E}^T_{\parallel}$ is the twist disclination dilatation strain energy density, $\mathcal{E}^{W-T}_{\parallel\ int}$ is the wedge-twist interaction dilatation strain energy density, $\mathcal{E}^W_{\perp}$ is the wedge disclination distortion strain energy density, $\mathcal{E}^T_{\perp}$ is the twist disclination distortion strain energy density, and $\mathcal{E}^{W-T}_{\perp\ int}$ is the wedge-twist interaction distortion strain energy density. It is important to note that in this case there is interaction strain energy density arising from the disclination displacements, due to their rotational nature.

The dislocation-disclination interaction strain energy density $\mathcal{E}^{D_t-D_r}_{int}$ will be calculated in this section, and can be further separated into the following terms:

$$\mathcal{E}^{D_t-D_r}_{int} = \underbrace{\underbrace{\underbrace{\mathcal{E}^{E-W}_{\parallel\ int}}_{b_{x,y}\Omega_z} + \underbrace{\mathcal{E}^{E-T}_{\parallel\ int}}_{b_{x,y}\Omega_{x,y}}}_{\mathcal{E}^{D_t-D_r}_{\parallel\ int}} + \underbrace{\underbrace{\underbrace{\mathcal{E}^{S-T}_{\perp\ int}}_{b_z\Omega_{x,y}} + \underbrace{\mathcal{E}^{E-W}_{\perp\ int}}_{b_{x,y}\Omega_z}}_{\mathcal{E}^{D_t-D_r}_{\perp\ int}} + \underbrace{\mathcal{E}^{E-T}_{\perp\ int}}_{b_{x,y}\Omega_{x,y}}}_{\mathcal{E}^{D_t-D_r}_{\perp\ int}}}_{\mathcal{E}^{D_t-D_r}_{\perp\ int}} \tag{17.31}$$

where $\mathcal{E}^{E-W}_{\parallel\ int}$ is the edge-wedge interaction dilatation strain energy density ($b_{x,y}\Omega_z$ terms), $\mathcal{E}^{E-T}_{\parallel\ int}$ is the edge-twist interaction dilatation strain

energy density ($b_{x,y}\Omega_{x,y}$ terms), $\mathcal{E}^{S-T}_{\perp\ int}$ is the screw-twist interaction distortion strain energy density ($b_z\Omega_{x,y}$ terms), $\mathcal{E}^{E-W}_{\perp\ int}$ is the edge-wedge interaction distortion strain energy density ($b_{x,y}\Omega_z$ terms), and $\mathcal{E}^{E-T}_{\perp\ int}$ is the edge-twist interaction distortion strain energy density ($b_{x,y}\Omega_{x,y}$ terms).

We calculate the individual dislocation-disclination interaction terms of (17.31) by substituting for the strain tensor (17.4) and the dilatation (17.6) in (17.22) and (17.24) to calculate the combination of Burgers and Frank vector components indicated in (17.31) for each term.

The edge-wedge interaction dilatation strain energy density $\mathcal{E}^{E-W}_{\parallel\ int}$ is calculated from the $b_{x,y}\Omega_z$ terms to obtain

$$\begin{aligned}\mathcal{E}^{E-W}_{\parallel\ int} = &-\frac{\bar{\kappa}_0 b_x \Omega_z}{4\pi^2}\,\frac{y}{r^2}\left[3\bar{\alpha}_0\left(2\bar{\alpha}_0\ln r+\bar{\beta}_0\right)+\,\bar{\beta}_0^2\,\frac{x^2(x^2-y^2)}{r^4}\right]\\ &+\,\frac{\bar{\kappa}_0 b_y \Omega_z}{4\pi^2}\,\frac{x}{r^2}\left[3\bar{\alpha}_0\left(2\bar{\alpha}_0\ln r+\bar{\beta}_0\right)-\,\bar{\beta}_0^2\,\frac{y^2(x^2-y^2)}{r^4}\right]\end{aligned} \tag{17.32}$$

which can be simplified to

$$\begin{aligned}\mathcal{E}^{E-W}_{\parallel\ int} = &-\frac{\bar{\kappa}_0 \Omega_z}{4\pi^2}\left[3\bar{\alpha}_0\,\frac{b_x y-b_y x}{r^2}\left(2\bar{\alpha}_0\ln r+\bar{\beta}_0\right)+\right.\\ &\left.+\,\bar{\beta}_0^2\left(b_x x-b_y y\right)\frac{xy(x^2-y^2)}{r^6}\right].\end{aligned} \tag{17.33}$$

The edge-twist interaction dilatation strain energy density $\mathcal{E}^{E-T}_{\parallel\ int}$ is calculated from the $b_{x,y}\Omega_{x,y}$ terms to obtain

$$\begin{aligned}\mathcal{E}^{E-T}_{\parallel\ int} = &\,\frac{\bar{\kappa}_0 b_x \Omega_x}{2\pi^2}\,z\left(3\bar{\alpha}_0^2\,\frac{xy}{r^4}+4\bar{\beta}_0^2\,\frac{x^3y^3}{r^8}\right)-\\ &-\frac{\bar{\kappa}_0 b_y \Omega_y}{2\pi^2}\,z\left(3\bar{\alpha}_0^2\,\frac{xy}{r^4}+4\bar{\beta}_0^2\,\frac{x^3y^3}{r^8}\right)+\\ &+\frac{\bar{\kappa}_0 b_x \Omega_y}{2\pi^2}\,z\left(3\bar{\alpha}_0^2\,\frac{y^2}{r^4}-4\bar{\beta}_0^2\,\frac{x^4y^2}{r^8}\right)-\\ &-\frac{\bar{\kappa}_0 b_y \Omega_x}{2\pi^2}\,z\left(3\bar{\alpha}_0^2\,\frac{x^2}{r^4}-4\bar{\beta}_0^2\,\frac{x^2y^4}{r^8}\right)\end{aligned} \tag{17.34}$$

which can be simplified to

$$\begin{aligned}\mathcal{E}^{E-T}_{\parallel\ int} = &\frac{\bar\kappa_0}{2\pi^2}\,(b_x\Omega_x - b_y\Omega_y)\,\frac{xyz}{r^4}\,\left(3\bar\alpha_0^2 + 4\bar\beta_0^2\,\frac{x^2y^2}{r^4}\right) + \\ &+ \frac{\bar\kappa_0 b_x\Omega_y}{2\pi^2}\,\frac{y^2z}{r^4}\,\left(3\bar\alpha_0^2 - 4\bar\beta_0^2\,\frac{x^4}{r^4}\right) - \\ &- \frac{\bar\kappa_0 b_y\Omega_x}{2\pi^2}\,\frac{x^2z}{r^4}\,\left(3\bar\alpha_0^2 - 4\bar\beta_0^2\,\frac{y^4}{r^4}\right).\end{aligned} \tag{17.35}$$

The screw-twist interaction distortion strain energy density $\mathcal{E}^{S-T}_{\perp\ int}$ is calculated from the $b_z\Omega_{x,y}$ terms to obtain

$$\begin{aligned}\mathcal{E}^{S-T}_{\perp\ int} = &\frac{\bar\mu_0 b_z\Omega_x}{2\pi^2}\,\frac{y}{r^2}\,\left(\bar\alpha_0\,\ln r + \bar\beta_0\right) - \\ &- \frac{\bar\mu_0 b_z\Omega_y}{2\pi^2}\,\frac{x}{r^2}\,\left(\bar\alpha_0\,\ln r + \bar\beta_0\right)\end{aligned} \tag{17.36}$$

which can be simplified to

$$\mathcal{E}^{S-T}_{\perp\ int} = \frac{\bar\mu_0 b_z}{2\pi^2}\,\frac{\Omega_x y - \Omega_y x}{r^2}\,\left(\bar\alpha_0\,\ln r + \bar\beta_0\right). \tag{17.37}$$

The edge-wedge interaction distortion strain energy density $\mathcal{E}^{E-W}_{\perp\ int}$ is calculated from the $b_{x,y}\Omega_z$ terms to obtain

$$\begin{aligned}\mathcal{E}^{E-W}_{\perp\ int} = &-\frac{\bar\mu_0 b_x\Omega_z}{2\pi^2}\,\frac{y}{r^2}\,\left[\bar\alpha_0\left(\bar\alpha_0\ln r + \tfrac{1}{2}\,\bar\beta_0\right) + 2\bar\beta_0^2\,\frac{x^2y^2}{r^4}\right] + \\ &+ \frac{\bar\mu_0 b_y\Omega_z}{2\pi^2}\,\frac{x}{r^2}\,\left[\bar\alpha_0\left(\bar\alpha_0\ln r + \tfrac{1}{2}\,\bar\beta_0\right) + 2\bar\beta_0^2\,\frac{x^2y^2}{r^4}\right]\end{aligned} \tag{17.38}$$

which can be simplified to

$$\mathcal{E}^{E-W}_{\perp\ int} = -\frac{\bar\mu_0\Omega_z}{2\pi^2}\,\frac{b_x y - b_y x}{r^2}\,\left[\bar\alpha_0\left(\bar\alpha_0\ln r + \tfrac{1}{2}\bar\beta_0\right) + 2\bar\beta_0^2\,\frac{x^2y^2}{r^4}\right]. \tag{17.39}$$

The edge-twist interaction distortion strain energy density $\mathcal{E}^{E-T}_{\perp\ int}$ is

calculated from the $b_{x,y}\Omega_{x,y}$ terms to obtain

$$\begin{aligned}\mathcal{E}^{E-T}_{\perp\ int} = &\frac{\bar{\mu}_0 b_x \Omega_x}{\pi^2}\ \left(\bar{\alpha}_0^2 - \bar{\beta}_0^2\right)\ \frac{xyz}{r^4} - \\ &- \frac{\bar{\mu}_0 b_y \Omega_y}{\pi^2}\ \left(\bar{\alpha}_0^2 - \bar{\beta}_0^2\right)\ \frac{xyz}{r^4} + \\ &+ \frac{\bar{\mu}_0 b_x \Omega_y}{\pi^2}\ \left(\bar{\beta}_0^2 x^2 + \bar{\alpha}_0^2 y^2\right)\ \frac{z}{r^4} - \\ &- \frac{\bar{\mu}_0 b_y \Omega_x}{\pi^2}\ \left(\bar{\alpha}_0^2 x^2 + \bar{\beta}_0^2 y^2\right)\ \frac{z}{r^4}\end{aligned} \tag{17.40}$$

which can be simplified to

$$\begin{aligned}\mathcal{E}^{E-T}_{\perp\ int} = &-\frac{\bar{\mu}_0 \bar{\gamma}_0}{\pi^2}\left(b_x \Omega_x - b_y \Omega_y\right)\ \frac{xyz}{r^4} + \\ &+ \frac{\bar{\mu}_0 \bar{\alpha}_0^2}{\pi^2}\ \left(b_x \Omega_y y^2 - b_y \Omega_x x^2\right)\ \frac{z}{r^4} + \\ &+ \frac{\bar{\mu}_0 \bar{\beta}_0^2}{\pi^2}\ \left(b_x \Omega_y x^2 - b_y \Omega_x y^2\right)\ \frac{z}{r^4}\end{aligned} \tag{17.41}$$

where

$$\bar{\gamma}_0 = \frac{\bar{\lambda}_0}{2\bar{\mu}_0 + \bar{\lambda}_0}\,. \tag{17.42}$$

These elements form the basis of the calculation of defect displacement interactions in quantum physics in the following sections.

§17.3 Displacement defect interaction strain energy

In this section, we consider the interaction of defects as mediated by their strain energy. We consider the longitudinal dilatation strain energy $W_\parallel$ and the transverse distortion strain energy $W_\perp$ for the dislocation-dislocation, disclination-disclination and dislocation-disclination displacement defect interactions considered in section §17.2.

§17.3.1 *Dislocation-dislocation interactions*

There is no longitudinal interaction strain energy density between edge dislocations and screw dislocations, as the latter are massless. As we saw in (17.14) for the transverse interaction strain energy density, there are no displacement interaction terms (cross-terms) either between screw and edge dislocations for a general dislocation line. Hence there is no

displacement interaction strain energy for dislocation-dislocation interactions. However, as we will see in section §18.6, a dislocation line does exhibit self-energy processes.

§17.3.2 *Disclination-disclination interactions*

Wedge disclination - twist disclination interaction. The longitudinal strain energy for the interaction between the wedge and twist disclinations is calculated from

$$W_{\parallel\ int}^{W-T} = \int_V \mathcal{E}_{\parallel\ int}^{W-T}\,\mathrm{d}V. \tag{17.43}$$

Substituting for $\mathcal{E}_{\parallel\ int}^{W-T}$ from (17.17), this equation becomes

$$W_{\parallel\ int}^{W-T} = -\int_V \frac{\bar{\kappa}_0}{\pi^2}\,\bar{\alpha}_0\,(\Omega_x x + \Omega_y y)\,\frac{\Omega_z z}{r^2}\,\left(\bar{\alpha}_0 \ln r + \frac{1}{2}\,\bar{\beta}_0\right)\,\mathrm{d}V \tag{17.44}$$

where V is the volume of the interacting disclinations, with $\mathrm{d}V$ given by $r\mathrm{d}r\,\mathrm{d}\theta\,\mathrm{d}z$ in cylindrical polar coordinates. As before, we take Ω out of the integral from (14.5), and write (17.44) as

$$\begin{aligned} W_{\parallel\ int}^{W-T} = \frac{\bar{\kappa}_0}{\pi^2}\,\bar{\alpha}_0\Omega_z \int_0^{\ell}\int_0^{2\pi}\int_{b_c}^{\Lambda} (\Omega_x x + \Omega_y y) \\ \frac{z}{r^2}\,\left(\bar{\alpha}_0 \ln r + \frac{1}{2}\,\bar{\beta}_0\right)\,r\mathrm{d}r\,\mathrm{d}\theta\,\mathrm{d}z \end{aligned} \tag{17.45}$$

where ℓ is the length of the disclination, b_c is the size of the core of the disclination, of order b_0, the smallest spacetime dislocation Burgers vector, and Λ is a cut-off parameter corresponding to the radial extent of the disclination, limited by the average distance to its nearest neighbours.

Evaluating the integral over z, (17.45) becomes

$$\begin{aligned} W_{\parallel\ int}^{W-T} = \frac{\bar{\kappa}_0}{2\pi^2}\,\bar{\alpha}_0\Omega_z\ell^2 \int_0^{2\pi}\int_{b_c}^{\Lambda} (\Omega_x \cos\theta + \Omega_y \sin\theta) \\ \left(\bar{\alpha}_0 \ln r + \frac{1}{2}\,\bar{\beta}_0\right)\,\mathrm{d}r\,\mathrm{d}\theta \end{aligned} \tag{17.46}$$

where we have used the relations $\cos\theta = x/r$ and $\sin\theta = y/r$. Again, the integral over z cannot be handled by considering the strain energy

per unit length of the disclination due to the ℓ^2 (area) dependence. Evaluating the integral over θ [376], we obtain

$$W^{W-T}_{\parallel\ int} = \frac{\bar{\kappa}_0}{2\pi^2}\,\bar{\alpha}_0\Omega_z\ell^2\int_{b_c}^{\Lambda}\Bigg[(\Omega_x\sin\theta-\Omega_y\cos\theta)\left(\bar{\alpha}_0\ln r+\frac{1}{2}\,\bar{\beta}_0\right)\Bigg]_0^{2\pi} z^2\,\mathrm{d}z\,. \tag{17.47}$$

Applying the limits of integration, (17.47) becomes

$$W^{W-T}_{\parallel\ int} = 0\,. \tag{17.48}$$

Hence there is no longitudinal interaction between wedge and twist disclinations. Considering Fig. 10.1, we see that the Frank vectors are perpendicular for those disclinations, and hence the result is to be expected.

The transverse strain energy for the interaction between the wedge and twist disclinations is calculated from

$$W^{W-T}_{\perp\ int} = \int_V \mathcal{E}^{W-T}_{\perp\ int}\,\mathrm{d}V. \tag{17.49}$$

Substituting for $\mathcal{E}^{W-T}_{\perp\ int}$ from (17.21), this equation becomes

$$\begin{aligned} W^{W-T}_{\perp\ int} = -\frac{\bar{\mu}_0\Omega_z}{2\pi^2}\int_V\Bigg\{&\frac{\Omega_x xz}{r^2}\Bigg[2\bar{\alpha}_0^2\ln r+\bar{\alpha}_0\bar{\beta}_0+\\ &+\bar{\beta}_0^2\left(\frac{y^2}{r^2}-\frac{2y^4}{r^4}\right)\Bigg]+\frac{\Omega_y yz}{r^2}\Bigg[2\bar{\alpha}_0^2\ln r+\\ &+\bar{\alpha}_0\bar{\beta}_0+\bar{\beta}_0^2\left(\frac{x^2}{r^2}-\frac{2x^4}{r^4}\right)\Bigg]\Bigg\}\,\mathrm{d}V \end{aligned} \tag{17.50}$$

where V is the volume of the interacting disclinations, with $\mathrm{d}V$ given by $r\mathrm{d}r\,\mathrm{d}\theta\,\mathrm{d}z$ in cylindrical polar coordinates. As before, we take Ω out of the integral from (14.5), and write (17.50) as

$$\begin{aligned} W^{W-T}_{\perp\ int} = -\frac{\bar{\mu}_0\Omega_z}{2\pi^2}\int_0^{\ell}\int_0^{2\pi}\int_{b_c}^{\Lambda}\Bigg\{&\frac{\Omega_x xz}{r^2}\Bigg[2\bar{\alpha}_0^2\ln r+\bar{\alpha}_0\bar{\beta}_0+\\ &+\bar{\beta}_0^2\left(\frac{y^2}{r^2}-\frac{2y^4}{r^4}\right)\Bigg]+\frac{\Omega_y yz}{r^2}\Bigg[2\bar{\alpha}_0^2\ln r+\\ &+\bar{\alpha}_0\bar{\beta}_0+\bar{\beta}_0^2\left(\frac{x^2}{r^2}-\frac{2x^4}{r^4}\right)\Bigg]\Bigg\}\,r\mathrm{d}r\,\mathrm{d}\theta\,\mathrm{d}z \end{aligned} \tag{17.51}$$

where ℓ is the length of the disclination, b_c is the size of the core of the disclination, of order b_0, the smallest spacetime dislocation Burgers vector, and Λ is a cut-off parameter corresponding to the radial extent of the disclination, limited by the average distance to its nearest neighbours.

Evaluating the integral over z, (17.51) becomes

$$\begin{aligned} W^{W-T}_{\perp\ int} = -\frac{\bar{\mu}_0 \Omega_z}{4\pi^2}\, \ell^2 \int_0^{2\pi} \int_{b_c}^{\Lambda} \Big\{ \Omega_x \cos\theta \Big[2\bar{\alpha}_0^2 \ln r + \bar{\alpha}_0 \bar{\beta}_0 + \\ + \bar{\beta}_0^2 \left(\sin^2\theta - 2\sin^4\theta \right) \Big] + \Omega_y \sin\theta \Big[2\bar{\alpha}_0^2 \ln r + \\ + \bar{\alpha}_0 \bar{\beta}_0 + \bar{\beta}_0^2 \left(\cos^2\theta - 2\cos^4\theta \right) \Big] \Big\} \, \mathrm{d}r \, \mathrm{d}\theta \end{aligned} \tag{17.52}$$

where we have used the relations $\cos\theta = x/r$ and $\sin\theta = y/r$. Again, the integral over z cannot be handled by considering the strain energy per unit length of the disclination due to the ℓ^2 (area) dependence. Evaluating the integral over θ [376], we obtain

$$\begin{aligned} W^{W-T}_{\perp\ int} = -\frac{\bar{\mu}_0 \Omega_z}{4\pi^2}\, \ell^2 \int_{b_c}^{\Lambda} \Big\{ \Omega_x \Big[2\bar{\alpha}_0^2 \ln r \sin\theta + \bar{\alpha}_0 \bar{\beta}_0 \sin\theta + \\ + \bar{\beta}_0^2 \left(\frac{1}{3}\, \sin^3\theta - \frac{2}{5}\, \sin^5\theta \right) \Big] - \Omega_y \Big[2\bar{\alpha}_0^2 \ln r \cos\theta + \\ + \bar{\alpha}_0 \bar{\beta}_0 \cos\theta + \bar{\beta}_0^2 \left(\frac{1}{3}\, \cos^3\theta - \frac{2}{5}\, \cos^5\theta \right) \Big] \Big\} \Big|_0^{2\pi} \end{aligned} \tag{17.53}$$

Applying the limits of integration, (17.53) becomes

$$W^{W-T}_{\perp\ int} = 0\,. \tag{17.54}$$

Hence we find that there is no transverse interaction between wedge and twist disclinations, in agreement with the perpendicularity of the dislocation Frank vectors as seen in Fig. 10.1. As in the case of dislocation-dislocation interactions, there is no displacement interaction strain energy for disclination-disclination interactions.

§17.3.3 *Dislocation-disclination interactions*

In this section, we consider the interaction terms of dislocations and disclinations.

Edge dislocation - wedge disclination interaction. The longitudinal strain energy for the interaction between the edge dislocation and the wedge disclination is calculated from

$$W_{\parallel\ int}^{E-W} = \int_V \mathcal{E}_{\parallel\ int}^{E-W}\,\mathrm{d}V. \tag{17.55}$$

Substituting for $\mathcal{E}_{\parallel\ int}^{E-W}$ from (17.33), this equation becomes

$$\begin{aligned} W_{\parallel\ int}^{E-W} = -\int_V \frac{\bar{\kappa}_0\Omega_z}{4\pi^2}\Bigg[3\bar{\alpha}_0\,\frac{b_x y - b_y x}{r^2}\left(2\bar{\alpha}_0\ln r + \bar{\beta}_0\right) + \\ + \bar{\beta}_0^2\left(b_x x - b_y y\right)\frac{xy(x^2-y^2)}{r^6}\Bigg]\,\mathrm{d}V \end{aligned} \tag{17.56}$$

where V is the volume of the interacting defects, with $\mathrm{d}V$ given by $r\mathrm{d}r\,\mathrm{d}\theta\,\mathrm{d}z$ in cylindrical polar coordinates. As before, we take Ω out of the integral from (14.5), and the integral over z is handled by considering the strain energy per unit length of the interaction:

$$\begin{aligned} \frac{W_{\parallel\ int}^{E-W}}{\ell} = -\frac{\bar{\kappa}_0\Omega_z}{4\pi^2}\int_0^{2\pi}\int_{b_c}^{\Lambda}\Bigg[3\bar{\alpha}_0\,\frac{b_x y - b_y x}{r^2}\left(2\bar{\alpha}_0\ln r + \bar{\beta}_0\right) + \\ +\ \bar{\beta}_0^2\left(b_x x - b_y y\right)\frac{xy(x^2-y^2)}{r^6}\Bigg]\,r\mathrm{d}r\,\mathrm{d}\theta \end{aligned} \tag{17.57}$$

where ℓ is the length of the disclination, b_c is the size of the core of the disclination, of order b_0, the smallest spacetime dislocation Burgers vector, and Λ is a cut-off parameter corresponding to the radial extent of the disclination, limited by the average distance to its nearest neighbours.

Using the relations $\cos\theta = x/r$ and $\sin\theta = y/r$, (17.57) can be written as

$$\begin{aligned} \frac{W_{\parallel\ int}^{E-W}}{\ell} = -\frac{\bar{\kappa}_0\Omega_z}{4\pi^2}\int_0^{2\pi}\int_{b_c}^{\Lambda}\Bigg[3\bar{\alpha}_0\left(b_x\sin\theta - b_y\cos\theta\right) \\ \left(2\bar{\alpha}_0\ln r + \bar{\beta}_0\right) + \bar{\beta}_0^2\left(b_x\cos\theta - b_y\sin\theta\right) \\ \cos\theta\sin\theta\left(\cos^2\theta - \sin^2\theta\right)\Bigg]\,\mathrm{d}r\,\mathrm{d}\theta\,. \end{aligned} \tag{17.58}$$

Evaluating the integral over θ [376], we obtain

$$\begin{aligned}\frac{W^{E-W}_{\parallel\ int}}{\ell} = -\frac{\bar{\kappa}_0\Omega_z}{4\pi^2}\int_{b_c}^{\Lambda}\Big[&3\bar{\alpha}_0\left(-b_x\cos\theta - b_y\sin\theta\right)\left(2\bar{\alpha}_0\ln r + \bar{\beta}_0\right)\\ &+\bar{\beta}_0^2\, b_x\left(-\frac{1}{5}\,\cos^5\theta - \frac{1}{30}\,\cos^3\theta\,\left(3\cos 2\theta - 7\right)\right) -\\ &-\bar{\beta}_0^2\, b_y\left(\frac{1}{30}\,\sin^3\theta\,\left(3\cos 2\theta + 7\right) - \frac{1}{5}\,\sin^5\theta\right)\Big]_0^{2\pi}\mathrm{d}r\,.\end{aligned} \tag{17.59}$$

Applying the limits of integration, (17.59) becomes

$$\frac{W^{E-W}_{\parallel\ int}}{\ell} = 0\,. \tag{17.60}$$

Hence we find that there is no longitudinal interaction between the edge dislocation and the wedge disclination. We note that the Burgers and Frank vectors are perpendicular.

The transverse strain energy for the interaction between the edge dislocation and the wedge disclination is calculated from

$$W^{E-W}_{\perp\ int} = \int_V \mathcal{E}^{E-W}_{\perp\ int}\,\mathrm{d}V. \tag{17.61}$$

Substituting for $\mathcal{E}^{E-W}_{\perp\ int}$ from (17.39), this equation becomes

$$\begin{aligned}W^{E-W}_{\perp\ int} = -\int_V &\frac{\bar{\mu}_0\Omega_z}{2\pi^2}\,\frac{b_x y - b_y x}{r^2}\\ &\left[\bar{\alpha}_0\left(\bar{\alpha}_0\ln r + \tfrac{1}{2}\,\bar{\beta}_0\right) + 2\bar{\beta}_0^2\,\frac{x^2y^2}{r^4}\right]\mathrm{d}V\end{aligned} \tag{17.62}$$

where V is the volume of the interacting defects, with $\mathrm{d}V$ given by $r\mathrm{d}r\,\mathrm{d}\theta\,\mathrm{d}z$ in cylindrical polar coordinates. As before, we take Ω out of the integral from (14.5), and the integral over z is handled by considering the strain energy per unit length of the disclination:

$$\begin{aligned}\frac{W^{E-W}_{\perp\ int}}{\ell} = -\frac{\bar{\mu}_0\Omega_z}{2\pi^2}\int_0^{2\pi}\int_{b_c}^{\Lambda} &\frac{b_x y - b_y x}{r^2}\\ &\left[\bar{\alpha}_0\left(\bar{\alpha}_0\ln r + \tfrac{1}{2}\,\bar{\beta}_0\right) + 2\bar{\beta}_0^2\,\frac{x^2y^2}{r^4}\right] r\mathrm{d}r\,\mathrm{d}\theta\end{aligned} \tag{17.63}$$

where ℓ is the length of the disclination, b_c is the size of the core of the disclination, of order b_0, the smallest spacetime dislocation Burgers

vector, and Λ is a cut-off parameter corresponding to the radial extent of the disclination, limited by the average distance to its nearest neighbours.

Using the relations $\cos\theta = x/r$ and $\sin\theta = y/r$, (17.63) can be written as

$$\frac{W^{E-W}_{\perp\ int}}{\ell} = -\frac{\bar{\mu}_0\Omega_z}{2\pi^2}\int_0^{2\pi}\int_{b_c}^{\Lambda}(b_x\sin\theta - b_y\cos\theta) \left[\bar{\alpha}_0\left(\bar{\alpha}_0\ln r + \tfrac{1}{2}\,\bar{\beta}_0\right) + 2\bar{\beta}_0^2\cos^2\theta\sin^2\theta\right]\mathrm{d}r\,\mathrm{d}\theta\,. \tag{17.64}$$

Evaluating the integral over θ [376], we obtain

$$\frac{W^{E-W}_{\perp\ int}}{\ell} = \frac{\bar{\mu}_0\Omega_z}{2\pi^2}\int_{b_c}^{\Lambda}\Bigg[\bar{\alpha}_0\left(\bar{\alpha}_0\ln r + \tfrac{1}{2}\,\bar{\beta}_0\right)(b_x\cos\theta + b_y\sin\theta) + + 2\bar{\beta}_0^2\,b_x\,\frac{1}{30}\,\cos^3\theta\,(3\cos 2\theta - 7) - - 2\bar{\beta}_0^2\,b_y\,\frac{1}{30}\,\sin^3\theta\,(3\cos 2\theta + 7)\Bigg]_0^{2\pi}\mathrm{d}r\,. \tag{17.65}$$

Applying the limits of integration, (17.65) becomes

$$\frac{W^{E-W}_{\perp\ int}}{\ell} = 0\,. \tag{17.66}$$

Hence we find that there is no transverse interaction between the edge dislocation and the wedge disclination and there is no displacement interaction strain energy for edge dislocation-wedge disclination interactions.

Edge dislocation - twist disclination interaction. The longitudinal strain energy for the interaction between the edge dislocation and the twist disclination is calculated from

$$W^{E-T}_{\parallel\ int} = \int_V \mathcal{E}^{E-T}_{\parallel\ int}\,\mathrm{d}V. \tag{17.67}$$

Substituting for $\mathcal{E}^{E-T}_{\parallel\ int}$ from (17.35), this equation becomes

$$W^{E-T}_{\parallel\ int} = \int_V \Bigg[\frac{\bar{\kappa}_0}{2\pi^2}\,(b_x\Omega_x - b_y\Omega_y)\,\frac{xyz}{r^4}\left(3\bar{\alpha}_0^2 + 4\bar{\beta}_0^2\,\frac{x^2y^2}{r^4}\right) + + \frac{\bar{\kappa}_0 b_x\Omega_y}{2\pi^2}\,\frac{y^2z}{r^4}\left(3\bar{\alpha}_0^2 - 4\bar{\beta}_0^2\,\frac{x^4}{r^4}\right) - - \frac{\bar{\kappa}_0 b_y\Omega_x}{2\pi^2}\,\frac{x^2z}{r^4}\left(3\bar{\alpha}_0^2 - 4\bar{\beta}_0^2\,\frac{y^4}{r^4}\right)\Bigg]\mathrm{d}V \tag{17.68}$$

where V is the volume of the wedge disclination, with $\mathrm{d}V$ given by $r\mathrm{d}r\,\mathrm{d}\theta\,\mathrm{d}z$ in cylindrical polar coordinates. As before, we take Ω out of the integral from (14.5), and write (17.68) as

$$\begin{aligned} W^{E-T}_{\parallel\ int} = \frac{\bar{\kappa}_0}{2\pi^2}\int_0^{\ell}\int_0^{2\pi}\int_{b_c}^{\Lambda}\Bigg[& b_x\Omega_x\,\frac{xyz}{r^4}\,\left(3\bar{\alpha}_0^2+4\bar{\beta}_0^2\,\frac{x^2y^2}{r^4}\right)- \\ & -b_y\Omega_y\,\frac{xyz}{r^4}\,\left(3\bar{\alpha}_0^2+4\bar{\beta}_0^2\,\frac{x^2y^2}{r^4}\right)+ \\ & +b_x\Omega_y\,\frac{y^2z}{r^4}\,\left(3\bar{\alpha}_0^2-4\bar{\beta}_0^2\,\frac{x^4}{r^4}\right)- \\ & -b_y\Omega_x\,\frac{x^2z}{r^4}\,\left(3\bar{\alpha}_0^2-4\bar{\beta}_0^2\,\frac{y^4}{r^4}\right)\Bigg]\,r\mathrm{d}r\,\mathrm{d}\theta\,\mathrm{d}z \end{aligned} \tag{17.69}$$

where ℓ is the length of the disclination, b_c is the size of the core of the disclination, of order b_0, the smallest spacetime dislocation Burgers vector, and Λ is a cut-off parameter corresponding to the radial extent of the disclination, limited by the average distance to its nearest neighbours.

Evaluating the integral over z, (17.69) becomes

$$\begin{aligned} W^{E-T}_{\parallel\ int} = \frac{\bar{\kappa}_0}{4\pi^2}\,\ell^2\int_0^{2\pi}\int_{b_c}^{\Lambda} & \\ \Bigg[& \frac{b_x\Omega_x}{r}\,\cos\theta\sin\theta\,\left(3\bar{\alpha}_0^2+4\bar{\beta}_0^2\,\cos^2\theta\sin^2\theta\right)- \\ & -\frac{b_y\Omega_y}{r}\,\cos\theta\sin\theta\,\left(3\bar{\alpha}_0^2+4\bar{\beta}_0^2\,\cos^2\theta\sin^2\theta\right)+ \\ & +\frac{b_x\Omega_y}{r}\,\sin^2\theta\,\left(3\bar{\alpha}_0^2-4\bar{\beta}_0^2\,\cos^4\theta\right)- \\ & -\frac{b_y\Omega_x}{r}\,\cos^2\theta\,\left(3\bar{\alpha}_0^2-4\bar{\beta}_0^2\,\sin^4\theta\right)\Bigg]\,\mathrm{d}r\,\mathrm{d}\theta \end{aligned} \tag{17.70}$$

where we have used the relations $\cos\theta = x/r$ and $\sin\theta = y/r$. Again, the integral over z cannot be handled by considering the strain energy per unit length of the disclination due to the ℓ^2 (area) dependence.

Evaluating the integral over θ [376], we obtain

$$
\begin{aligned}
W^{E-T}_{\parallel\ int} = \frac{\bar{\kappa}_0}{4\pi^2}\,\ell^2 \int_{b_c}^{\Lambda} \Bigg[& -\frac{b_x\Omega_x}{r}\,3\bar{\alpha}_0^2\,\left(\frac{1}{2}\,\cos^2\theta\right) + \\
& + \frac{b_x\Omega_x}{r}\,4\bar{\beta}_0^2\,\left(\frac{1}{192}\,(\cos 6\theta - 9\cos 2\theta)\right) + \\
& + \frac{b_y\Omega_y}{r}\,\left(3\bar{\alpha}_0^2\,\frac{1}{2}\,\cos^2\theta - 4\bar{\beta}_0^2\,\frac{1}{192}\,(\cos 6\theta - 9\cos 2\theta)\right) + \\
& + \frac{b_x\Omega_y}{r}\,3\bar{\alpha}_0^2\,\left(\frac{1}{2}\,(\theta - \sin\theta\cos\theta)\right) - \\
& - \frac{b_x\Omega_y}{r}\,4\bar{\beta}_0^2\left(\frac{\theta}{16} + \frac{1}{64}\,\sin 2\theta - \frac{1}{64}\,\sin 4\theta - \frac{1}{192}\,\sin 6\theta\right) - \\
& - \frac{b_y\Omega_x}{r}\,3\bar{\alpha}_0^2\,\left(\frac{1}{2}\,(\theta + \sin\theta\cos\theta)\right) + \\
& + \frac{b_y\Omega_x}{r}\,4\bar{\beta}_0^2\left(\frac{\theta}{16} - \frac{1}{64}\sin 2\theta - \frac{1}{64}\sin 4\theta + \frac{1}{192}\sin 6\theta\right)\Bigg]_0^{2\pi} \mathrm{d}r\,.
\end{aligned}
\tag{17.71}
$$

Applying the limits of integration, (17.71) becomes

$$
\begin{aligned}
W^{E-T}_{\parallel\ int} = \frac{\bar{\kappa}_0}{4\pi^2}\,\ell^2 \int_{b_c}^{\Lambda} \Bigg[& \frac{b_x\Omega_y}{r}\,\left(3\pi\bar{\alpha}_0^2 - \frac{\pi}{2}\,\bar{\beta}_0^2\right) - \\
& - \frac{b_y\Omega_x}{r}\,\left(3\pi\bar{\alpha}_0^2 - \frac{\pi}{2}\,\bar{\beta}_0^2\right)\Bigg]\,\mathrm{d}r\,.
\end{aligned}
\tag{17.72}
$$

Integrating over r, we obtain

$$
W^{E-T}_{\parallel\ int} = \frac{\bar{\kappa}_0}{4\pi}\,\ell^2\,\left(3\bar{\alpha}_0^2 - \tfrac{1}{2}\,\bar{\beta}_0^2\right)\,(b_x\Omega_y - b_y\Omega_x)\,\ln\frac{\Lambda}{b_c}\,. \tag{17.73}
$$

Hence we find that there is a longitudinal interaction between the edge dislocation and the twist disclination which depends on the area of the defect. Only $b_{x,y}$ and $\Omega_{x,y}$ cross-terms interact. The displacement interaction strain energy for edge dislocation-twist disclination interactions is of the form $\mathbf{b}\times\mathbf{\Omega}$.

The transverse strain energy for the interaction between the edge dislocation and the twist disclination is calculated from

$$
W^{E-T}_{\perp\ int} = \int_V \mathcal{E}^{E-T}_{\perp\ int}\,\mathrm{d}V. \tag{17.74}
$$

Substituting for $\mathcal{E}^{E-T}_{\perp\ int}$ from (17.41), this equation becomes

$$\begin{aligned} W^{E-T}_{\perp\ int} = &- \int_V \frac{\bar{\mu}_0 \bar{\gamma}_0}{\pi^2} \left(b_x \Omega_x - b_y \Omega_y\right) \frac{xyz}{r^4} + \\ &+ \frac{\bar{\mu}_0 \bar{\alpha}_0^2}{\pi^2} \left(b_x \Omega_y y^2 - b_y \Omega_x x^2\right) \frac{z}{r^4} + \\ &+ \frac{\bar{\mu}_0 \bar{\beta}_0^2}{\pi^2} \left(b_x \Omega_y x^2 - b_y \Omega_x y^2\right) \frac{z}{r^4} \, \mathrm{d}V \end{aligned} \tag{17.75}$$

where as per (17.42)

$$\bar{\gamma}_0 = \frac{\bar{\lambda}_0}{2\bar{\mu}_0 + \bar{\lambda}_0}$$

and where V is the volume of the wedge disclination, with $\mathrm{d}V$ given by $r \mathrm{d}r \, \mathrm{d}\theta \, \mathrm{d}z$ in cylindrical polar coordinates. As before, we take Ω out of the integral from (14.5), and write (17.75) as

$$\begin{aligned} W^{E-T}_{\perp\ int} = \frac{\bar{\mu}_0}{\pi^2} \int_0^{\ell} \int_0^{2\pi} \int_{b_c}^{\Lambda} \Big[&- \bar{\gamma}_0 \left(b_x \Omega_x - b_y \Omega_y\right) \frac{xyz}{r^4} + \\ &+ \bar{\alpha}_0^2 \left(b_x \Omega_y y^2 - b_y \Omega_x x^2\right) \frac{z}{r^4} + \\ &+ \bar{\beta}_0^2 \left(b_x \Omega_y x^2 - b_y \Omega_x y^2\right) \frac{z}{r^4} \Big] r \mathrm{d}r \, \mathrm{d}\theta \, \mathrm{d}z \end{aligned} \tag{17.76}$$

where ℓ is the length of the disclination, b_c is the size of the core of the disclination, of order b_0, the smallest spacetime dislocation Burgers vector, and Λ is a cut-off parameter corresponding to the radial extent of the disclination, limited by the average distance to its nearest neighbours.

Evaluating the integral over z, (17.76) becomes

$$\begin{aligned} W^{E-T}_{\perp\ int} = \frac{\bar{\mu}_0}{2\pi^2} \, \ell^2 \int_0^{2\pi} \int_{b_c}^{\Lambda} \Big[&- \bar{\gamma}_0 \frac{b_x \Omega_x - b_y \Omega_y}{r} \cos\theta \sin\theta + \\ &+ \bar{\alpha}_0^2 \left(\frac{b_x \Omega_y}{r} \sin^2\theta - \frac{b_y \Omega_x}{r} \cos^2\theta \right) + \\ &+ \bar{\beta}_0^2 \left(\frac{b_x \Omega_y}{r} \cos^2\theta - \frac{b_y \Omega_x}{r} \sin^2\theta \right) \Big] \mathrm{d}r \, \mathrm{d}\theta \end{aligned} \tag{17.77}$$

where we have used the relations $\cos\theta = x/r$ and $\sin\theta = y/r$. Again, the integral over z cannot be handled by considering the strain energy per unit length of the disclination due to the ℓ^2 (area) dependence.

Evaluating the integral over θ [376], we obtain

$$W^{E-T}_{\perp\ int} = \frac{\bar{\mu}_0}{2\pi^2}\,\ell^2 \int_{b_c}^{\Lambda} \left[\bar{\gamma}_0 \frac{b_x\Omega_x - b_y\Omega_y}{r} \left(\frac{1}{2}\,\cos^2\theta \right) + \right.$$
$$+ \frac{\bar{\alpha}_0^2}{2} \left(\frac{b_x\Omega_y}{r}\,(\theta - \sin\theta\cos\theta) - \frac{b_y\Omega_x}{r}\,(\theta + \sin\theta\cos\theta) \right) + \tag{17.78}$$
$$\left. + \frac{\bar{\beta}_0^2}{2} \left(\frac{b_x\Omega_y}{r}\,(\theta + \sin\theta\cos\theta) - \frac{b_y\Omega_x}{r}\,(\theta - \sin\theta\cos\theta) \right) \right]_0^{2\pi} \mathrm{d}r\,.$$

Applying the limits of integration, (17.78) becomes

$$W^{E-T}_{\perp\ int} = \frac{\bar{\mu}_0}{2\pi^2}\,\ell^2 \int_{b_c}^{\Lambda} \left[\pi\bar{\alpha}_0^2 \left(\frac{b_x\Omega_y}{r} - \frac{b_y\Omega_x}{r} \right) + \right.$$
$$\left. + \pi\bar{\beta}_0^2 \left(\frac{b_x\Omega_y}{r} - \frac{b_y\Omega_x}{r} \right) \right] \mathrm{d}r\,. \tag{17.79}$$

Integrating over r, we obtain

$$W^{E-T}_{\perp\ int} = \frac{\bar{\mu}_0}{2\pi}\,\ell^2 \left(\bar{\alpha}_0^2 + \bar{\beta}_0^2 \right) (b_x\Omega_y - b_y\Omega_x)\,\ln\frac{\Lambda}{b_c}\,. \tag{17.80}$$

Hence we find that there is also a transverse interaction between the edge dislocation and the twist disclination which depends on the area of the defect. Again only $b_{x,y}$ and $\Omega_{x,y}$ cross-terms interact. The difference between the longitudinal and the transverse interaction lies in the proportionality constants. In both cases, the displacement interaction strain energy for edge dislocation-twist disclination interactions is of the form $\mathbf{b} \times \mathbf{\Omega}$.

Screw dislocation - twist disclination interaction. We recall that there is no longitudinal interaction between the screw dislocation and the twist disclination as the screw dislocation does not have a longitudinal component.

The transverse strain energy for the interaction between the screw dislocation and the twist disclination is calculated from

$$W^{S-T}_{\perp\ int} = \int_V \mathcal{E}^{S-T}_{\perp\ int}\,\mathrm{d}V. \tag{17.81}$$

Substituting for $\mathcal{E}^{S-T}_{\perp\ int}$ from (17.37), this equation becomes

$$W^{S-T}_{\perp\ int} = \int_V \frac{\bar{\mu}_0 b_z}{2\pi^2}\,\frac{\Omega_x y - \Omega_y x}{r^2}\,\left(\bar{\alpha}_0\,\ln r + \bar{\beta}_0 \right)\,\mathrm{d}V \tag{17.82}$$

where V is the volume of the wedge disclination, with $\mathrm{d}V$ given by $r\mathrm{d}r\,\mathrm{d}\theta\,\mathrm{d}z$ in cylindrical polar coordinates. As before, we take Ω out of the integral from (14.5), and the integral over z is handled by considering the strain energy per unit length of the disclination:

$$\frac{W^{S-T}_{\perp\ int}}{\ell} = \frac{\bar{\mu}_0 b_z}{2\pi^2}\int_0^{2\pi}\int_{b_c}^{\Lambda}\frac{\Omega_x y - \Omega_y x}{r^2}\left(\bar{\alpha}_0\,\ln r + \bar{\beta}_0\right) r\mathrm{d}r\,\mathrm{d}\theta \tag{17.83}$$

where ℓ is the length of the disclination, b_c is the size of the core of the disclination, of order b_0, the smallest spacetime dislocation Burgers vector, and Λ is a cut-off parameter corresponding to the radial extent of the disclination, limited by the average distance to its nearest neighbours.

Using the relations $\cos\theta = x/r$ and $\sin\theta = y/r$, (17.83) can be written as

$$\begin{aligned}\frac{W^{S-T}_{\perp\ int}}{\ell} = \frac{\bar{\mu}_0 b_z}{2\pi^2}\int_0^{2\pi}\int_{b_c}^{\Lambda}&\left(\Omega_x\sin\theta - \Omega_y\cos\theta\right)\\ &\left(\bar{\alpha}_0\,\ln r + \bar{\beta}_0\right)\mathrm{d}r\,\mathrm{d}\theta\,.\end{aligned} \tag{17.84}$$

Evaluating the integral over θ [376], we obtain

$$\begin{aligned}\frac{W^{S-T}_{\perp\ int}}{\ell} = \frac{\bar{\mu}_0 b_z}{2\pi^2}\int_{b_c}^{\Lambda}&\left(-\Omega_x\cos\theta - \Omega_y\sin\theta\right)\\ &\left(\bar{\alpha}_0\,\ln r + \bar{\beta}_0\right)\Big|_0^{2\pi}\mathrm{d}r\,.\end{aligned} \tag{17.85}$$

Applying the limits of integration, (17.85) becomes

$$\frac{W^{S-T}_{\perp\ int}}{\ell} = 0\,. \tag{17.86}$$

Hence we find that there is no transverse interaction between the screw dislocation and the twist disclination and there is no displacement interaction strain energy for screw dislocation-twist disclination interactions. Again we note the perpendicularity of the Burgers and Frank vectors.

§17.4 Overlap interaction of multiple defects

In this section, we consider the interactions of dislocations of multiple defects, including of the same type, which are seen to result from the force resulting from the overlap of their strain energy density in the

spacetime continuum [159, see p. 112]. As we have seen in §17.2.1, there is no longitudinal interaction strain energy density between edge dislocations and screw dislocations in a mixed dislocation, as the latter are massless. In addition, as shown in that section, there are no interaction terms (cross-terms) between screw and edge dislocations for a dislocation line which is a mixed dislocation. This is due to the perpendicularity of the two types of dislocations. However, multiple dislocations separated by a distance R can undergo defect interactions due to the overlap of their strain energy densities, both dislocation and disclination interactions.

These interactions can be calculated using various methods. Till now, we have concentrated on the calculation of the strain energy of the overlap based on the defect displacements. Another approach [364, see Chapter 3] that can be used is to calculate the force between the defects from the stress tensor, and obtain the strain energy of the overlap based on the work W performed by the application of the force F over a given distance d, from the well-known relation

$$W = \mathbf{F} \cdot \mathbf{d} \,. \tag{17.87}$$

Conversely, the force can be calculated from the negative of the derivative of the strain energy W with position. For example, for a dislocation line parallel to the z-axis positive along the z-axis, the force on the dislocation line can be written as

$$\mathbf{F} = -\left(\frac{\partial W}{\partial x}, \frac{\partial W}{\partial y} \right) . \tag{17.88}$$

This allows us to calculate the overlap interaction strain energy.

We consider the total strain energy W for two neighbouring defects. This can be written in terms of the strain energy density $\mathcal{E}$ for the two neighbouring defects as an integral over the volume

$$W = \int_V \mathcal{E} \, \mathrm{d}V \,. \tag{17.89}$$

$\mathcal{E}$ can be expressed in terms of the stress density σ using the stress tensor portion of (9.49) to (9.51). Following Weertman [364, see p. 62], as the stress density equations are linear (see section §8.5), we separate the stress density σ into a sum of two terms

$$W = \int_V (\sigma_1 + \sigma_2)^2 \, \mathrm{d}V \tag{17.90}$$

where we have not included the proportionality factor and where σ_2 is the stress density of the defect (dislocation or disclination) of interest in an otherwise strain-free continuum, and σ_1, known as the *internal stresses*, is the stress density of the rest of the continuum including the neighbouring defect(s), but excluding the defect of σ_2. Then $\sigma_1 + \sigma_2$ represents the stress density of a continuum including a defect of interest and internal stresses.

The total strain energy W can then be written as

$$W = \int_V \sigma_1^2 \, \mathrm{d}V + \int_V \sigma_2^2 \, \mathrm{d}V + 2 \int_V \sigma_1 \sigma_2 \, \mathrm{d}V \,. \tag{17.91}$$

The first two terms are position independent. Only the third term is position dependent, and leads to a force on the defect as per (17.88) and contributes to the interaction strain energy W_{12} :

$$W_{12} = 2 \int_V \sigma_1 \sigma_2 \, \mathrm{d}V \,. \tag{17.92}$$

§17.4.1 *Overlap interaction strain energy*

From (1.19) to (1.21) the energy-momentum stress tensor $T^{\alpha\beta}$ is decomposed into a stress deviation tensor $t^{\alpha\beta}$ and a scalar t_s, according to

$$T^{\alpha\beta} = t^{\alpha\beta} + t_s g^{\alpha\beta} \tag{17.93}$$

where $t_s = \frac{1}{4} T^{\alpha}{}_{\alpha}$. Separating $T^{\alpha\beta}$ into the sum of two terms as per (17.90), we have

$$T^{\alpha\beta} = {}_1T^{\alpha\beta} + {}_2T^{\alpha\beta} \,, \tag{17.94}$$

and using (17.93), we obtain

$$T^{\alpha\beta} = {}_1t^{\alpha\beta} + {}_1t_s g^{\alpha\beta} + {}_2t^{\alpha\beta} + {}_2t_s g^{\alpha\beta} \,. \tag{17.95}$$

Hence we can write

$$\begin{aligned} t^{\alpha\beta} &= {}_1t^{\alpha\beta} + {}_2t^{\alpha\beta} \\ t_s &= {}_1t_s + {}_2t_s \,. \end{aligned} \tag{17.96}$$

Going back to (17.89) and using (9.49) to (9.51), we have

$$W = \int_V \left(\mathcal{E}_{\parallel} + \mathcal{E}_{\perp} \right) \mathrm{d}V \tag{17.97}$$

where

$$\mathcal{E}_{\parallel} = \frac{1}{32\bar{\kappa}_0} \left(\rho c^2 \right)^2 \equiv \frac{1}{2\bar{\kappa}_0} \, t_s^2 \tag{17.98}$$

where ρ is the mass energy density of the edge dislocation, and

$$\mathcal{E}_\perp = \frac{1}{4\bar{\mu}_0}\, t^{\alpha\beta} t_{\alpha\beta}\,. \tag{17.99}$$

Substituting (17.98) and (17.99) into (17.97), we obtain

$$W = \int_V \left(\frac{1}{2\bar{\kappa}_0}\, t_s^2 + \frac{1}{4\bar{\mu}_0}\, t^{\alpha\beta} t_{\alpha\beta} \right) \mathrm{d}V \tag{17.100}$$

and using (17.96), (17.100) becomes

$$\begin{aligned} W = \int_V \Bigg[& \frac{1}{2\bar{\kappa}_0} \left({}_1t_s + {}_2t_s \right)^2 + \\ & + \frac{1}{4\bar{\mu}_0} \left({}_1t^{\alpha\beta} + {}_2t^{\alpha\beta} \right) \left({}_1t_{\alpha\beta} + {}_2t_{\alpha\beta} \right) \Bigg] \mathrm{d}V\,. \end{aligned} \tag{17.101}$$

Expanding and re-arranging, we obtain

$$\begin{aligned} W = \int_V \Bigg[& \frac{1}{2\bar{\kappa}_0}\, {}_1t_s^2 + \frac{1}{4\bar{\mu}_0}\, {}_1t^{\alpha\beta}\, {}_1t_{\alpha\beta} + \\ & + \frac{1}{2\bar{\kappa}_0}\, {}_2t_s^2 + \frac{1}{4\bar{\mu}_0}\, {}_2t^{\alpha\beta}\, {}_2t_{\alpha\beta} + \\ & + \frac{1}{\bar{\kappa}_0}\, {}_1t_s\, {}_2t_s + \frac{1}{4\bar{\mu}_0} \left({}_1t^{\alpha\beta}\, {}_2t_{\alpha\beta} + {}_2t^{\alpha\beta}\, {}_1t_{\alpha\beta} \right) \Bigg] \mathrm{d}V \end{aligned} \tag{17.102}$$

which can be written as

$$\begin{aligned} W = & \int_V \left[\mathcal{E}_\parallel + \mathcal{E}_\perp \right]_1 \mathrm{d}V + \int_V \left[\mathcal{E}_\parallel + \mathcal{E}_\perp \right]_2 \mathrm{d}V + \\ & + \int_V \left[\mathcal{E}_\parallel + \mathcal{E}_\perp \right]_{12} \mathrm{d}V \end{aligned} \tag{17.103}$$

which is equivalent to

$$W = W_1 + W_2 + W_{12}\,. \tag{17.104}$$

Hence the overlap interaction strain energy is given by the third term from (17.102):

$$W_{12} = \int_V \left[\frac{1}{\bar{\kappa}_0}\, {}_1t_s\, {}_2t_s + \frac{1}{4\bar{\mu}_0} \left({}_1t^{\alpha\beta}\, {}_2t_{\alpha\beta} + {}_2t^{\alpha\beta}\, {}_1t_{\alpha\beta} \right) \right] \mathrm{d}V\,. \tag{17.105}$$

Substituting from (17.93) (see (1.20) and (1.21)) into (17.105), we obtain

$$W_{12} = \frac{1}{16\bar{\kappa}_0}\int_V {}_1T^{\alpha}{}_{\alpha}\ {}_2T^{\alpha}{}_{\alpha}\,\mathrm{d}V + \\ + \frac{1}{4\bar{\mu}_0}\int_V \Bigg[\left({}_1T^{\alpha\beta} - \frac{1}{4}\ {}_1T^{\alpha}{}_{\alpha}g^{\alpha\beta}\right)\left({}_2T_{\alpha\beta} - \frac{1}{4}\ {}_2T^{\alpha}{}_{\alpha}g_{\alpha\beta}\right) + \\ + \left({}_2T^{\alpha\beta} - \frac{1}{4}\ {}_2T^{\alpha}{}_{\alpha}g^{\alpha\beta}\right)\left({}_1T_{\alpha\beta} - \frac{1}{4}\ {}_1T^{\alpha}{}_{\alpha}g_{\alpha\beta}\right)\Bigg]\,\mathrm{d}V\,. \tag{17.106}$$

Expanding the second integral, we obtain

$$\begin{aligned} W_{12} = {} & \frac{1}{16\bar{\kappa}_0}\int_V {}_1T^{\alpha}{}_{\alpha}\ {}_2T^{\alpha}{}_{\alpha}\,\mathrm{d}V + \\ & + \frac{1}{4\bar{\mu}_0}\int_V \Bigg[\ {}_1T^{\alpha\beta}\ {}_2T_{\alpha\beta} - \frac{1}{4}\ {}_1T^{\alpha\beta}\ {}_2T^{\alpha}{}_{\alpha}\,g_{\alpha\beta} - \\ & - \frac{1}{4}\ {}_1T^{\alpha}{}_{\alpha}\,g^{\alpha\beta}\ {}_2T_{\alpha\beta} + \frac{1}{16}\ {}_1T^{\alpha}{}_{\alpha}\ {}_2T^{\alpha}{}_{\alpha}\,g^{\alpha\beta}g_{\alpha\beta} + \\ & + {}_2T^{\alpha\beta}\ {}_1T_{\alpha\beta} - \frac{1}{4}\ {}_2T^{\alpha\beta}\ {}_1T^{\alpha}{}_{\alpha}\,g_{\alpha\beta} - \\ & - \frac{1}{4}\ {}_2T^{\alpha}{}_{\alpha}\,g^{\alpha\beta}\ {}_1T_{\alpha\beta} + \frac{1}{16}\ {}_2T^{\alpha}{}_{\alpha}\ {}_1T^{\alpha}{}_{\alpha}\,g^{\alpha\beta}g_{\alpha\beta}\Bigg]\,\mathrm{d}V\,. \end{aligned} \tag{17.107}$$

Using $g^{\alpha\beta}g_{\alpha\beta} = \eta^{\alpha\beta}\eta_{\alpha\beta} = 4$, expanding and simplifying the second integral, we obtain

$$W_{12} = \frac{1}{16\bar{\kappa}_0}\int_V {}_1T^{\alpha}{}_{\alpha}\ {}_2T^{\alpha}{}_{\alpha}\,\mathrm{d}V + \\ + \frac{1}{4\bar{\mu}_0}\int_V \left[\ {}_1T^{\alpha\beta}\ {}_2T_{\alpha\beta} + \ {}_2T^{\alpha\beta}\ {}_1T_{\alpha\beta} - \frac{1}{2}\ {}_1T^{\alpha}{}_{\alpha}\ {}_2T^{\alpha}{}_{\alpha}\right]\,\mathrm{d}V \tag{17.108}$$

where ${}_1T^{\alpha}{}_{\alpha} = \rho_1 c^2$ and ${}_2T^{\alpha}{}_{\alpha} = \rho_2 c^2$.

Hence the overlap interaction strain energy can be written as

$$W_{12} = W_{12}^{mass} + W_{12}^{field} \tag{17.109}$$

where W_{12}^{mass} is a pure mass longitudinal term given by

$$W_{12}^{mass} = \frac{1}{16\bar{\kappa}_0}\int_V {}_1T^{\alpha}{}_{\alpha}\ {}_2T^{\alpha}{}_{\alpha}\,\mathrm{d}V \tag{17.110}$$

and W_{12}^{field} is a pure massless transverse field term given by

$$W_{12}^{field} = \frac{1}{4\bar{\mu}_0}\int_V \Big[\ {}_1T^{\alpha\beta}\ {}_2T_{\alpha\beta} + \ {}_2T^{\alpha\beta}\ {}_1T_{\alpha\beta} - \\ - \frac{1}{2}\ {}_1T^{\alpha}{}_{\alpha}\ {}_2T^{\alpha}{}_{\alpha}\Big]\,\mathrm{d}V \tag{17.111}$$

Alternatively, (17.108) can be written as

$$W_{12} = \frac{1}{4\bar{\mu}_0}\int_V \Big[\ {}_1T^{\alpha\beta}\ {}_2T_{\alpha\beta} + \ {}_2T^{\alpha\beta}\ {}_1T_{\alpha\beta} - \\ - \frac{\bar{\lambda}_0}{\bar{\mu}_0 + 2\bar{\lambda}_0}\ {}_1T^{\alpha}{}_{\alpha}\ {}_2T^{\alpha}{}_{\alpha}\Big]\,\mathrm{d}V\,. \tag{17.112}$$

It is important to note that the overlap interaction strain energy is usually expressed as energy per unit length of the defect W_{12}/ℓ.

§17.4.2 *Parallel dislocation interactions*

From Hirth [159, see pp. 117-118], the energy of interaction per unit length between parallel dislocations (including screw and edge dislocation components) is given by

$$\begin{aligned}\frac{W_{12}}{\ell} &= -\frac{\bar{\mu}_0}{2\pi}\,(\mathbf{b_1}\cdot\boldsymbol{\xi})\,(\mathbf{b_2}\cdot\boldsymbol{\xi})\,\ln\frac{R}{R_\Lambda} - \\ &-\frac{\bar{\mu}_0}{\pi}\,\frac{\bar{\mu}_0+\bar{\lambda}_0}{2\bar{\mu}_0+\bar{\lambda}_0}\,(\mathbf{b_1}\times\boldsymbol{\xi})\cdot(\mathbf{b_2}\times\boldsymbol{\xi})\,\ln\frac{R}{R_\Lambda} - \\ &-\frac{\bar{\mu}_0}{\pi}\,\frac{\bar{\mu}_0+\bar{\lambda}_0}{2\bar{\mu}_0+\bar{\lambda}_0}\,\frac{[(\mathbf{b_1}\times\boldsymbol{\xi})\cdot\mathbf{R}]\,[(\mathbf{b_2}\times\boldsymbol{\xi})\cdot\mathbf{R}]}{R^2}\end{aligned} \tag{17.113}$$

where ξ is parallel to the z axis, $(\mathbf{b_i}\cdot\boldsymbol{\xi})$ are the screw components, $(\mathbf{b_i}\times\boldsymbol{\xi})$ are the edge components, R is the separation between the dislocations, and R_Λ is the distance from which the dislocations are brought together, resulting in the decrease in energy of the "system".

The components of the interaction force per unit length between the parallel dislocations are obtained by differentiation:

$$\begin{aligned}\frac{F_R}{\ell} &= -\frac{\partial(W_{12}/\ell)}{\partial R} \\ \frac{F_\theta}{\ell} &= -\frac{1}{R}\,\frac{\partial(W_{12}/\ell)}{\partial\theta}.\end{aligned} \tag{17.114}$$

Substituting from (17.113), (17.114) becomes

$$\begin{aligned}
\frac{F_R}{\ell} &= \frac{\bar{\mu}_0}{2\pi R}\left(\mathbf{b_1}\cdot\boldsymbol{\xi}\right)\left(\mathbf{b_2}\cdot\boldsymbol{\xi}\right)+\\
&\quad+\frac{\bar{\mu}_0}{\pi R}\,\frac{\bar{\mu}_0+\bar{\lambda}_0}{2\bar{\mu}_0+\bar{\lambda}_0}\left(\mathbf{b_1}\times\boldsymbol{\xi}\right)\cdot\left(\mathbf{b_2}\times\boldsymbol{\xi}\right)\\
\frac{F_\theta}{\ell} &= \frac{\bar{\mu}_0}{\pi R^3}\,\frac{\bar{\mu}_0+\bar{\lambda}_0}{2\bar{\mu}_0+\bar{\lambda}_0}\left[\left(\mathbf{b_1}\cdot\mathbf{R}\right)\left[\left(\mathbf{b_2}\times\mathbf{R}\right)\cdot\boldsymbol{\xi}\right]+\right.\\
&\quad\left.+\left(\mathbf{b_2}\cdot\mathbf{R}\right)\left[\left(\mathbf{b_1}\times\mathbf{R}\right)\cdot\boldsymbol{\xi}\right]\right].
\end{aligned}\tag{17.115}$$

§17.4.3 *Curved dislocation interactions*

In this section, we extend the investigation of curved dislocations initiated in section §9.5, to the interaction energy and interaction force between curved dislocations [159, see pp. 106-110]. The derivation considers the interaction between two dislocation loops, but has much more extensive applications, being extendable to the interaction energy between two arbitrarily positioned segments of dislocation lines.

If a dislocation loop 1 is brought in the vicinity of another dislocation loop 2, the stresses originating from loop 2 do work $-W_{12}$ on loop 1 where W_{12} is the interaction energy between the two dislocation loops. The work done on loop 1 represents a decrease in the strain energy of the total system. In that case, if W_{12} is negative, the energy of the system decreases and an attractive force exists between the loops [159, see p. 106].

The interaction energy between the two dislocation loops is given by [159, see p. 108]

$$\begin{aligned}
W_{12} &= -\frac{\bar{\mu}_0}{2\pi}\oint_{C_1}\oint_{C_2}\frac{\left(\mathbf{b_1}\times\mathbf{b_2}\right)\cdot\left(d\mathbf{l_1}\times d\mathbf{l_2}\right)}{R}+\\
&+\frac{\bar{\mu}_0}{4\pi}\oint_{C_1}\oint_{C_2}\frac{\left(\mathbf{b_1}\cdot d\mathbf{l_1}\right)\left(\mathbf{b_2}\cdot d\mathbf{l_2}\right)}{R}+\\
&+\frac{\bar{\mu}_0}{2\pi}\,\frac{\bar{\mu}_0+\bar{\lambda}_0}{2\bar{\mu}_0+\bar{\lambda}_0}\oint_{C_1}\oint_{C_2}\frac{\left(\mathbf{b_1}\times d\mathbf{l_1}\right)\cdot\mathbf{T}\cdot\left(\mathbf{b_2}\times d\mathbf{l_2}\right)}{R}
\end{aligned}\tag{17.116}$$

where $\mathbf{T}$ is given by

$$T_{ij}=\frac{\partial^2 R}{\partial x_i\partial x_j}.\tag{17.117}$$

The force produced by an external stress acting on a dislocation loop

is given by [159, see p. 109]

$$d\mathbf{F} = (\mathbf{b} \cdot \boldsymbol{\sigma}) \times d\mathbf{l} \tag{17.118}$$

where $\boldsymbol{\sigma}$ is the stress tensor in the medium, $\mathbf{b}$ is the Burgers vector, and $d\mathbf{l}$ is the dislocation element. This equation can be used with the Peach and Koehler stress equation (9.163) to determine the interaction force between dislocation segments.

As each element $d\mathbf{l}$ of a dislocation loop is acted upon by the forces caused by the stress of the other elements of the dislocation loop, the work done against these corresponds to the self-energy of the dislocation loop. The self-energy of a dislocation loop can be calculated from (17.116) to give [159, see p. 110]

$$\begin{aligned} W_{self} = & \frac{\bar{\mu}_0}{8\pi} \oint_{C_1=C} \oint_{C_2=C} \frac{(\mathbf{b} \cdot d\mathbf{l_1})\,(\mathbf{b} \cdot d\mathbf{l_2})}{R} + \\ & + \frac{\bar{\mu}_0}{4\pi} \frac{\bar{\mu}_0 + \bar{\lambda}_0}{2\bar{\mu}_0 + \bar{\lambda}_0} \oint_{C_1=C} \oint_{C_2=C} \frac{(\mathbf{b} \times d\mathbf{l_1}) \cdot \mathbf{T} \cdot (\mathbf{b} \times d\mathbf{l_2})}{R} \end{aligned} \tag{17.119}$$

where $\mathbf{T}$ is as defined in (17.117).

More complicated expressions can be obtained for interactions between two non-parallel straight dislocations [159, see pp. 121-123] and between a straight segment of a dislocation and a differential element of another dislocation [159, see pp. 124-131]. This latter derivation can be used for more arbitrary dislocation interactions.

Chapter 18

Quantum Physics in STCED

In this chapter, we synthesize the analysis of defects in the spacetime continuum considered in the previous ten chapters to model quantum physics within the framework of *STCED*. As we will see in the forthcoming sections, this model provides a physical explanation of quantum phenomena, quantum electrodynamics, and other quantum dynamic interactions that currently remain unexplained in quantum physics.

§18.1 Quantum particles from defects and their interactions

As seen previously in section §14.4, dislocations are translational displacements that commute, satisfy the superposition principle and behave as bosons. Disclinations, on the other hand, are rotational displacements that do not commute, do not obey the superposition principle and behave as fermions.

§18.1.1 *Dislocations (bosons)*

Dislocations, due to their translational nature, are defects that are easier to analyze than disclinations.

Screw dislocation. The screw dislocation was analyzed in sections §9.2 and §15.1. It is the first defect that we identified with the photon due to its being massless and of spin-1. Consequently, its longitudinal strain energy is zero

$$W_{\parallel}^{S} = 0. \tag{18.1}$$

Its transverse strain energy is given by (16.5)

$$W_{\perp}^{S} = \frac{\bar{\mu}_0}{4\pi}\, b^2\, \ell\, \ln \frac{\Lambda}{b_c} \tag{18.2}$$

where $\ell = \lambda$, the photon's wavelength, b_c is the size of the core of the dislocation, of order b_0, the smallest spacetime dislocation Burgers vector, and Λ is a cut-off parameter corresponding to the radial extent of the dislocation, limited by the average distance to its nearest neighbours.

Edge dislocation. The edge dislocation was analyzed in §9.3, §9.5 and §15.2. The longitudinal strain energy of the edge dislocation is

given by (16.29)

$$W_{\parallel}^{E} = \frac{\bar{\kappa}_0}{2\pi}\,\bar{\alpha}_0^2\,\left(b_x^2 + b_y^2\right)\,\ell\,\ln\frac{\Lambda}{b_c} \tag{18.3}$$

where b_x is the Burgers vector for the edge dislocation proper and b_y is the Burgers vector for the gap dislocation (see §9.5). The transverse strain energy is given by (16.54)

$$W_{\perp}^{E} = \frac{\bar{\mu}_0}{4\pi}\,\left(\bar{\alpha}_0^2 + 2\bar{\beta}_0^2\right)\left(b_x^2 + b_y^2\right)\,\ell\,\ln\frac{\Lambda}{b_c}\,. \tag{18.4}$$

The total longitudinal (massive) dislocation strain energy $W_{\parallel}^{Dt}$ is given by (18.3), as the screw dislocation longitudinal strain enrgy is zero, while the total transverse (massless) dislocation strain energy is given by the sum of the screw (along the z axis) and edge (in the $x-y$ plane) dislocation transverse strain energies

$$W_{\perp}^{Dt} = \frac{\bar{\mu}_0}{4\pi}\,\left[b_z^2 + \left(\bar{\alpha}_0^2 + 2\bar{\beta}_0^2\right)\left(b_x^2 + b_y^2\right)\right]\,\ell\,\ln\frac{\Lambda}{b_c}\,, \tag{18.5}$$

which can be rewritten as a sum of physical terms

$$W_{\perp}^{Dt} = \frac{\bar{\mu}_0}{4\pi}\left[b_z^2 + \bar{\alpha}_0^2\,(b_x^2 + b_y^2) + 2\bar{\beta}_0^2\,(b_x^2 + b_y^2)\right]\,\ell\,\ln\frac{\Lambda}{b_c} \tag{18.6}$$

where the first term of the distortion strain energy corresponds to the screw dislocation strain energy of (16.5), the second term to the edge dislocation distortion strain energy arising from the longitudinal strain energy density of (9.139) and the last term to the edge dislocation distortion strain energy arising from the rotation vector of (9.138). We note that the strain energy of dislocations is proportional to the length ℓ of the dislocations and has a functional dependence of $\ln\Lambda/b_c$.

The total strain energy of dislocations

$$W^{Dt} = W_{\parallel}^{Dt} + W_{\perp}^{Dt} \tag{18.7}$$

provides the total energy of massive bosons, with $W_{\parallel}^{Dt}$ corresponding to the longitudinal particle aspect of the bosons and $W_{\perp}^{Dt}$ corresponding to the wave aspect of the bosons. As seen in Chapter 12, the latter is associated with the wavefunction of the boson. The spin characteristics of these was considered in §3.6, where they were seen to correspond to spin-0 and spin-2 solutions.

§18.1.2 *Disclinations (fermions)*

Disclinations are defects that are more difficult to analyze than dislocations, due to their rotational nature. This mirrors the case of fermions, which are more difficult to analyze than bosons.

Wedge disclination. The wedge disclination was analyzed in §10.6 and §15.3. The longitudinal strain energy of the wedge disclination is given by (16.62)

$$\begin{aligned} W_{\parallel}^{W} = \frac{\bar{\kappa}_0}{4\pi}\,\Omega_z^2\,\ell\,\Big[\bar{\alpha}_0^2\,\left(2\Lambda^2\ln^2\Lambda - 2b_c^2\ln^2 b_c\right) + \\ + \bar{\alpha}_0\bar{\gamma}_0\left(2\Lambda^2\ln\Lambda - 2b_c^2\ln b_c\right) + \\ + \tfrac{1}{2}(\bar{\alpha}_0^2+\bar{\gamma}_0^2)\left(\Lambda^2 - b_c^2\right)\Big]. \end{aligned} \tag{18.8}$$

In most cases $\Lambda \gg b_c$, and (18.8) reduces to

$$W_{\parallel}^{W} \simeq \frac{\bar{\kappa}_0}{2\pi}\,\Omega_z^2\,\ell\,\Lambda^2\Big[\bar{\alpha}_0^2\,\ln^2\Lambda + \,\bar{\alpha}_0\bar{\gamma}_0\ln\Lambda + \,\tfrac{1}{4}(\bar{\alpha}_0^2+\bar{\gamma}_0^2)\Big] \tag{18.9}$$

which can be rearranged as

$$W_{\parallel}^{W} \simeq \frac{\bar{\kappa}_0}{2\pi}\,\bar{\alpha}_0^2\,\Omega_z^2\,\ell\,\Lambda^2\left[\ln^2\Lambda + \frac{\bar{\gamma}_0}{\bar{\alpha}_0}\,\ln\Lambda + \,\frac{1}{4}\left(1+\frac{\bar{\gamma}_0^2}{\bar{\alpha}_0^2}\right)\right]. \tag{18.10}$$

The transverse strain energy of the wedge disclination is given by (16.70)

$$\begin{aligned} W_{\perp}^{W} = \frac{\bar{\mu}_0}{4\pi}\,\Omega_z^2\,\ell\,\Big[\bar{\alpha}_0^2\,\left(\Lambda^2\ln^2\Lambda - b_c^2\ln^2 b_c\right) - \\ - \left(\bar{\alpha}_0^2 - 3\bar{\alpha}_0\bar{\beta}_0\right)\left(\Lambda^2\ln\Lambda - b_c^2\ln b_c\right) + \\ + \frac{1}{2}\left(\bar{\alpha}_0^2 - 3\bar{\alpha}_0\bar{\beta}_0 + \frac{3}{2}\,\bar{\beta}_0^2\right)\left(\Lambda^2 - b_c^2\right)\Big]. \end{aligned} \tag{18.11}$$

In most cases $\Lambda \gg b_c$, and (18.11) reduces to

$$\begin{aligned} W_{\perp}^{W} \simeq \frac{\bar{\mu}_0}{4\pi}\,\Omega_z^2\,\ell\,\Big[\bar{\alpha}_0^2\,\Lambda^2\ln^2\Lambda - \left(\bar{\alpha}_0^2 - 3\bar{\alpha}_0\bar{\beta}_0\right)\Lambda^2\ln\Lambda + \\ + \frac{1}{2}\left(\bar{\alpha}_0^2 - 3\bar{\alpha}_0\bar{\beta}_0 + \frac{3}{2}\,\bar{\beta}_0^2\right)\Lambda^2\Big] \end{aligned} \tag{18.12}$$

which is rearranged as

$$W_{\perp}^{W} \simeq \frac{\bar{\mu}_0}{4\pi}\,\bar{\alpha}_0^2\,\Omega_z^2\,\ell\,\Lambda^2 \left[\ln^2\Lambda - \left(1-3\,\frac{\bar{\beta}_0}{\bar{\alpha}_0}\right)\ln\Lambda + \frac{1}{2}\left(1-3\,\frac{\bar{\beta}_0}{\bar{\alpha}_0}+\frac{3}{2}\,\frac{\bar{\beta}_0^2}{\bar{\alpha}_0^2}\right)\right]. \tag{18.13}$$

We first note that both the longitudinal strain energy $W_{\parallel}^{W}$ and the transverse strain energy $W_{\perp}^{W}$ are both proportional to the length ℓ of the disclination, and to Λ^2 in the limit $\Lambda \gg b_c$. The parameter Λ is equivalent to the extent of the wedge disclination, and we find that as it becomes more extended, its strain energy is increasing parabolically. This behaviour is similar to that of quarks (confinement) which are fermions. In addition, as $\Lambda \to b_c$, the strain energy decreases and tends to 0, again in agreement with the behaviour of quarks (asymptotic freedom).

We thus identify wedge disclinations with quarks. The total strain energy of wedge disclinations

$$W^{W} = W_{\parallel}^{W} + W_{\perp}^{W} \tag{18.14}$$

provides the total energy of the massive quarks, with $W_{\parallel}^{W}$ corresponding to the longitudinal particle aspect of the quarks and $W_{\perp}^{W}$ corresponding to the wave aspect of the quarks. We note that the current classification of quarks include both ground and excited states – the current analysis needs to be extended to excited higher energy states.

We note also that the rest-mass energy density $\rho^{W}c^2$ of the wedge disclination is proportional to $\ln r$ which also increases with increasing r, while the rest-mass energy density $\rho^{E}c^2$ of the edge dislocation and $\rho^{T}c^2$ of the twist disclination are both proportional to $1/r^2$ which decreases with increasing r as expected of bosons and leptons.

Twist disclination. The twist disclination was analyzed in §10.7 and §15.4. Note that as mentioned in that section, we do not differentiate between twist and splay disclinations in this subsection as twist disclination expressions include both splay disclinations and twist disclinations proper.

The longitudinal strain energy of the twist disclination is given by (16.80)

$$W_{\parallel}^{T} = \frac{\bar{\kappa}_0}{6\pi}\,\bar{\alpha}_0^2\,\left(\Omega_x^2+\Omega_y^2\right)\ell^3\ln\frac{\Lambda}{b_c} \tag{18.15}$$

where Ω_x is the Frank vector for the splay disclination and Ω_y is the Frank vector for the twist disclination proper (see §10.5). The transverse strain energy of the twist disclination is given by (16.87)

$$\begin{aligned} W_\perp^T = \frac{\bar\mu_0}{2\pi}\,\frac{\ell^3}{3}\,\Big[& \left(\Omega_x^2+\Omega_y^2\right)\left(\bar\alpha_0^2+\tfrac{1}{2}\,\bar\beta_0^2\right)+ \\ & +2\,\Omega_x\Omega_y\left(\bar\alpha_0^2-2\bar\beta_0^2\right)\Big]\,\ln\frac{\Lambda}{b_c}+ \\ & +\frac{\bar\mu_0}{2\pi}\,\ell\,\Big[\left(\Omega_x^2+\Omega_y^2\right)\Big(\bar\alpha_0^2\,\left(\Lambda^2\ln^2\Lambda-b_c^2\ln^2 b_c\right)+ \\ & +\bar\alpha_0\bar\gamma_0\,\left(\Lambda^2\ln\Lambda-b_c^2\ln b_c\right)-\frac{1}{2}\bar\alpha_0\bar\gamma_0\left(\Lambda^2-b_c^2\right)+ \\ & +2\,\bar\beta_0^2\,\ln\frac{\Lambda}{b_c}\Big)-\,2\,\Omega_x\Omega_y\Big(\bar\alpha_0\bar\beta_0\left(\Lambda^2\ln\Lambda-b_c^2\ln b_c\right)+ \\ & +\frac{1}{2}\bar\beta_0\bar\gamma_0\left(\Lambda^2-b_c^2\right)\Big)\Big]. \end{aligned} \tag{18.16}$$

In most cases $\Lambda \gg b_c$, and (18.16) reduces to

$$\begin{aligned} W_\perp^T \simeq \frac{\bar\mu_0}{2\pi}\,\frac{\ell^3}{3}\,\Big[& \left(\Omega_x^2+\Omega_y^2\right)\left(\bar\alpha_0^2+\tfrac{1}{2}\,\bar\beta_0^2\right)+ \\ & +2\,\Omega_x\Omega_y\left(\bar\alpha_0^2-2\bar\beta_0^2\right)\Big]\,\ln\frac{\Lambda}{b_c}+ \\ & +\frac{\bar\mu_0}{2\pi}\,\ell\,\Lambda^2\,\Big[\left(\Omega_x^2+\Omega_y^2\right)\Big(\bar\alpha_0^2\,\ln^2\Lambda+\,\bar\alpha_0\bar\gamma_0\,\ln\Lambda- \\ & -\frac{1}{2}\bar\alpha_0\bar\gamma_0\Big)-2\,\Omega_x\Omega_y\Big(\bar\alpha_0\bar\beta_0\ln\Lambda+\frac{1}{2}\bar\beta_0\bar\gamma_0\Big)\Big] \end{aligned} \tag{18.17}$$

which can be rearranged to give

$$\begin{aligned} W_\perp^T \simeq \frac{\bar\mu_0}{2\pi}\,\bar\alpha_0^2\,\frac{\ell^3}{3}\,\Big[& \left(\Omega_x^2+\Omega_y^2\right)\left(1+\frac{1}{2}\,\frac{\bar\beta_0^2}{\bar\alpha_0^2}\right)+ \\ & +2\,\Omega_x\Omega_y\left(1-2\,\frac{\bar\beta_0^2}{\bar\alpha_0^2}\right)\Big]\,\ln\frac{\Lambda}{b_c}+ \\ & +\frac{\bar\mu_0}{2\pi}\,\bar\alpha_0^2\,\ell\,\Lambda^2\,\Big[\left(\Omega_x^2+\Omega_y^2\right)\Big(\ln^2\Lambda+\,\frac{\bar\gamma_0}{\bar\alpha_0}\,\ln\Lambda- \\ & -\frac{1}{2}\,\frac{\bar\gamma_0}{\bar\alpha_0}\Big)-2\,\Omega_x\Omega_y\Big(\frac{\bar\beta_0}{\bar\alpha_0}\ln\Lambda+\frac{1}{2}\,\frac{\bar\beta_0\bar\gamma_0}{\bar\alpha_0^2}\Big)\Big]. \end{aligned} \tag{18.18}$$

As noted previously, $W_{\parallel}^{T}$ depends on the space volume ℓ^3 of the disclination and has a functional dependence of $\ln \Lambda/b_c$ as do the dislocations. The strain energy $W_{\perp}^{T}$ depends on the space volume ℓ^3 of the disclination with a functional dependence of $\ln \Lambda/b_c$, but it also includes terms that have a dependence on the length ℓ of the disclination with a functional dependence similar to that of the wedge disclination including Λ^2 in the limit $\Lambda \gg b_c$. The difference in the case of the twist disclination is that its transverse strain energy $W_{\perp}^{T}$ combines ℓ^3 terms with the functional dependence $\ln \Lambda/b_c$ of dislocations, associated with the electromagnetic interaction and ℓ terms with the functional dependence $\Lambda^2 \ln^2 \Lambda$ of wedge disclinations, associated with the strong interaction. This, as we will see in later sections, seems to be the peculiar nature of the weak interaction, and uniquely positions twist disclinations to represent leptons and neutrinos as participants in the weak interaction.

This leads us to thus separate the longitudinal strain energy of the twist disclination as

$$W_{\parallel}^{T} = W_{\parallel}^{\ell^3} + W_{\parallel}^{\ell} = W_{\parallel}^{\ell^3} \tag{18.19}$$

given that $W_{\parallel}^{\ell} = 0$, and the transverse strain energy of the twist disclination as

$$W_{\perp}^{T} = W_{\perp}^{\ell^3} + W_{\perp}^{\ell} \,. \tag{18.20}$$

We consider both ℓ^3 twist disclination and ℓ twist disclination terms in the next subsections.

ℓ^3 twist disclination. The longitudinal strain energy of the ℓ^3 twist disclination is thus given by the ℓ^3 terms of (18.15)

$$W_{\parallel}^{\ell^3} = \frac{\bar{\kappa}_0}{6\pi}\, \bar{\alpha}_0^2 \, \left(\Omega_x^2 + \Omega_y^2\right) \ell^3 \ln \frac{\Lambda}{b_c} \,. \tag{18.21}$$

The transverse strain energy of the ℓ^3 twist disclination is given by the ℓ^3 terms of (18.16)

$$\begin{aligned} W_{\perp}^{\ell^3} = \frac{\bar{\mu}_0}{2\pi}\, \frac{\ell^3}{3} \Big[& \left(\Omega_x^2 + \Omega_y^2\right) \left(\bar{\alpha}_0^2 + \tfrac{1}{2}\, \bar{\beta}_0^2\right) + \\ & + 2\, \Omega_x \Omega_y \left(\bar{\alpha}_0^2 - 2\bar{\beta}_0^2\right) \Big] \, \ln \frac{\Lambda}{b_c} \,. \end{aligned} \tag{18.22}$$

In most cases $\Lambda \gg b_c$, and (18.22) is left unchanged due to its functional dependence on $\ln \Lambda/b_c$.

The total strain energy of the ℓ^3 twist disclination terms is given by

$$W^{\ell^3} = W_{\parallel}^{\ell^3} + W_{\perp}^{\ell^3} \,. \tag{18.23}$$

It is interesting to note that $W_{\parallel}^{\ell^3}$ of (18.21) and $W_{\perp}^{\ell^3}$ of (18.22) are proportional to $\ln \Lambda/b_c$, as are the screw dislocation (photon) and edge dislocation (bosons). This, and the results of the next subsection, leads us to identify the ℓ^3 twist disclination terms with the charged leptons (electron, muon, tau) fermions, where the heavier muon and tau are expected to be excited states of the electron.

ℓ ***twist disclination.*** The longitudinal strain energy of the ℓ twist disclination terms in this case is zero as mentioned previously

$$W_{\parallel}^{\ell} = 0 \,. \tag{18.24}$$

The transverse strain energy of the ℓ twist disclination is thus also given by the ℓ terms of (18.16):

$$\begin{aligned} W_{\perp}^{\ell} = \frac{\bar{\mu}_0}{2\pi}\,\ell \Bigg[\left(\Omega_x^2 + \Omega_y^2\right) \Bigg(\bar{\alpha}_0^2 \, \left(\Lambda^2 \ln^2 \Lambda - b_c^2 \ln^2 b_c\right) + \\ + \bar{\alpha}_0 \bar{\gamma}_0 \, \left(\Lambda^2 \ln \Lambda - b_c^2 \ln b_c\right) - \frac{1}{2} \bar{\alpha}_0 \bar{\gamma}_0 \left(\Lambda^2 - b_c^2\right) + \\ + 2\,\bar{\beta}_0^2 \, \ln \frac{\Lambda}{b_c} \Bigg) - \, 2\,\Omega_x \Omega_y \Big(\bar{\alpha}_0 \bar{\beta}_0 \left(\Lambda^2 \ln \Lambda - b_c^2 \ln b_c\right) + \\ + \frac{1}{2} \bar{\beta}_0 \bar{\gamma}_0 \left(\Lambda^2 - b_c^2\right) \Big) \Bigg] . \end{aligned} \tag{18.25}$$

In most cases $\Lambda \gg b_c$, and (18.25) reduces to

$$\begin{aligned} W_{\perp}^{\ell} = \frac{\bar{\mu}_0}{2\pi}\,\ell\,\Lambda^2 \Bigg[\left(\Omega_x^2 + \Omega_y^2\right) \Big(\bar{\alpha}_0^2 \, \ln^2 \Lambda + \, \bar{\alpha}_0 \bar{\gamma}_0 \, \ln \Lambda - \\ - \frac{1}{2} \bar{\alpha}_0 \bar{\gamma}_0 \Big) - 2\,\Omega_x \Omega_y \Big(\bar{\alpha}_0 \bar{\beta}_0 \ln \Lambda + \frac{1}{2} \bar{\beta}_0 \bar{\gamma}_0 \Big) \Bigg] \end{aligned} \tag{18.26}$$

which can be rearranged to give

$$\begin{aligned} W_{\perp}^{\ell} = \frac{\bar{\mu}_0}{2\pi}\,\bar{\alpha}_0^2\,\ell\,\Lambda^2 \Bigg[\left(\Omega_x^2 + \Omega_y^2\right) \Big(\ln^2 \Lambda + \, \frac{\bar{\gamma}_0}{\bar{\alpha}_0} \, \ln \Lambda - \\ - \frac{1}{2} \, \frac{\bar{\gamma}_0}{\bar{\alpha}_0} \Big) - 2\,\Omega_x \Omega_y \Big(\frac{\bar{\beta}_0}{\bar{\alpha}_0} \ln \Lambda + \frac{1}{2} \, \frac{\bar{\beta}_0 \bar{\gamma}_0}{\bar{\alpha}_0^2} \Big) \Bigg] . \end{aligned} \tag{18.27}$$

The total strain energy of the ℓ twist disclination is given by

$$W^{\ell} = W^{\ell}_{\parallel} + W^{\ell}_{\perp} = W^{\ell}_{\perp} \tag{18.28}$$

given that the ℓ twist disclination does not have a longitudinal (massive) component. Since the ℓ twist disclination is a massless fermion, this leads us to identify the ℓ twist disclination with the neutrino.

There is another aspect to the strain energy $W^{T}_{\perp}$ given by (18.16) that is important to note. As we have discussed, the ℓ^3 twist disclination terms and the $\ln \Lambda/b_c$ functional dependence as observed for the screw dislocation (photon) and edge dislocation (bosons) has led us to identify the ℓ^3 portion with the charged leptons (electron, muon, tau) fermions, where the heavier muon and tau are expected to be excited states of the electron. These are coupled with transverse ℓ twist disclination terms which are massless and which have a functional dependence similar to that of the wedge disclination, which has led us to identify the ℓ portion with the weakly interacting neutrino. If the muon and tau leptons are excited states of the electron derivable from (18.16), this would imply that the neutrino portion would also be specific to the muon and tau lepton excited states, thus leading to muon and tau neutrinos.

We will perform numerical calculations in a later section which will show that the dominance of the ℓ and ℓ^3 twist disclination terms depend on the extent ℓ of the disclination, with the ℓ "weak interaction" terms dominating for small values of ℓ and the ℓ^3 "electromagnetic interaction" terms dominating for larger values of ℓ. The ℓ twist disclination terms would correspond to weak interaction terms while the ℓ^3 twist disclination terms would correspond to electromagnetic interaction terms. The twist disclination represents the unification of both interactions under a single "electroweak interaction".

This analysis also shows why leptons (twist disclinations) are participants in the weak interaction but not the strong interaction, while quarks (wedge disclinations) are participants in the strong interaction but not the weak interaction.

It should be noted that even though the mass of the neutrino is currently estimated to be on the order of 10's of eV, this estimate is based on assuming neutrino oscillation between the currently known three lepton generations, to explain the anomalous solar neutrino problem. This is a weak explanation for that problem, which more than likely indicates that we do not yet fully understand solar astrophysics. One can only hope that a fourth generation of leptons will not be discovered! Until the anomaly is fully understood, we can consider the twist disclination

physical model where the mass of the neutrino is zero to be at least a first approximation of the neutrino STC defect model.

Twist disclination numerical sample calculation. In this section, we give a numerical sample calculation that shows the lepton-neutrino connection for the twist disclination. We start by isolating the common strain energy elements that don't need to be calculated in the example. Starting from the longitudinal strain energy of the twist disclination (18.15) and making use of (5.53), (18.15) can be simplified to

$$W_{\parallel}^{T} = \frac{\bar{\mu}_0}{2\pi}\,\bar{\alpha}_0^2\,2\Omega^2\left[32\,\frac{\ell^3}{3}\,\ln\frac{\Lambda}{b_c}\right] \tag{18.29}$$

where the non-descript Ω is used instead of Ω_x and Ω_y. Defining K as

$$K = \frac{\bar{\mu}_0}{2\pi}\,\bar{\alpha}_0^2\,2\Omega^2\,, \tag{18.30}$$

then (18.29) is written as

$$\frac{W_{\parallel}^{T}}{K} = 32\,\frac{\ell^3}{3}\,\ln\frac{\Lambda}{b_c}\,. \tag{18.31}$$

Similarly for the transverse strain energy of the twist disclination, starting from (18.18), the equation can be simplified to

$$\begin{aligned} W_{\perp}^{T} \simeq \frac{\bar{\mu}_0}{2\pi}\,\bar{\alpha}_0^2\,2\Omega^2\Bigg\{\Bigg[\frac{\ell^3}{3}\,\left(1+\frac{1}{2}\,\frac{\bar{\beta}_0^2}{\bar{\alpha}_0^2}+1-2\,\frac{\bar{\beta}_0^2}{\bar{\alpha}_0^2}\right)\,\ln\frac{\Lambda}{b_c}\Bigg]+ \\ +\Bigg[\ell\,\Lambda^2\Big(\ln^2\Lambda+\frac{\bar{\gamma}_0}{\bar{\alpha}_0}\,\ln\Lambda-\frac{1}{2}\,\frac{\bar{\gamma}_0}{\bar{\alpha}_0}- \\ -\frac{\bar{\beta}_0}{\bar{\alpha}_0}\ln\Lambda-\frac{1}{2}\,\frac{\bar{\beta}_0\bar{\gamma}_0}{\bar{\alpha}_0^2}\Big)\Bigg]\Bigg\}\,. \end{aligned} \tag{18.32}$$

Using the definition of K from (18.30), this equation becomes

$$\begin{aligned} \frac{W_{\perp}^{T}}{K} \simeq \frac{\ell^3}{3}\,\left(2-\frac{3}{2}\,\frac{\bar{\beta}_0^2}{\bar{\alpha}_0^2}\right)\ln\frac{\Lambda}{b_c}+ \\ +\ell\,\Lambda^2\left(\ln^2\Lambda+\frac{\bar{\gamma}_0-\bar{\beta}_0}{\bar{\alpha}_0}\,\ln\Lambda-\frac{1}{2}\,\frac{\bar{\gamma}_0}{\bar{\alpha}_0}\,\left(1+\bar{\beta}_0\right)\right)\,. \end{aligned} \tag{18.33}$$

Using the numerical values of the constants $\bar{\alpha}_0$, $\bar{\beta}_0$ and $\bar{\gamma}_0$ from (19.14) and (19.35) to be determined in the next chapter, (18.33) becomes

$$\begin{aligned} \frac{W_{\perp}^{T}}{K} \simeq \frac{\ell^3}{3}\,(1.565)\,\ln\frac{\Lambda}{b_c}+ \\ +\ell\,\Lambda^2\left(\ln^2\Lambda-\ln\Lambda-0.62\right)\,. \end{aligned} \tag{18.34}$$

For this numerical sample calculation, we use $b_c \sim 10^{-35}\,\mathrm{m}$ of the order of the spacetime Burgers dislocation constant, and the extent of the disclination $\Lambda \sim 10^{-18}\,\mathrm{m}$ of the order of the range of the weak force. Then

$$\frac{W_{\parallel}^{T}}{K} = \frac{32}{3}\,(39.1)\,\ell^3 = 417\,\ell^3\,. \tag{18.35}$$

and

$$\begin{aligned}\frac{W_{\perp}^{T}}{K} &\simeq 0.522\,(39.1)\,\ell^3 + \\ &\quad + \Lambda^2\,(1714 + 41.4 - 0.62)\;\ell\end{aligned} \tag{18.36}$$

which becomes

$$\frac{W_{\perp}^{T}}{K} \simeq 20.4\,\ell^3 + 1755\,\Lambda^2\,\ell \tag{18.37}$$

and finally

$$\frac{W_{\perp}^{T}}{K} \simeq 20.4\,\ell^3 + 1.76 \times 10^{-33}\,\ell\,. \tag{18.38}$$

We consider various values of ℓ to analyze its effect on the strain energy. For $\ell = 10^{-21}\,\mathrm{m}$,

$$\frac{W_{\parallel}^{T}}{K} = 4.2 \times 10^{-61} \quad (\ell^3 \text{ term}) \tag{18.39}$$

$$\frac{W_{\perp}^{T}}{K} = 2.0 \times 10^{-62} + 1.8 \times 10^{-54} \quad (\ell^3 \text{ term} + \ell \text{ term})\,. \tag{18.40}$$

For $\ell = 10^{-18}\,\mathrm{m}$,

$$\frac{W_{\parallel}^{T}}{K} = 4.2 \times 10^{-52} \quad (\ell^3 \text{ term}) \tag{18.41}$$

$$\frac{W_{\perp}^{T}}{K} = 2.0 \times 10^{-53} + 1.8 \times 10^{-51} \quad (\ell^3 \text{ term} + \ell \text{ term})\,. \tag{18.42}$$

For $\ell = 10^{-15}\,\mathrm{m}$,

$$\frac{W_{\parallel}^{T}}{K} = 4.2 \times 10^{-43} \quad (\ell^3 \text{ term}) \tag{18.43}$$

$$\frac{W_{\perp}^{T}}{K} = 2.0 \times 10^{-44} + 1.8 \times 10^{-48} \quad (\ell^3 \text{ term} + \ell \text{ term})\,. \tag{18.44}$$

For $\ell = 10^{-12}\,\mathrm{m}$,

$$\frac{W_{\parallel}^{T}}{K} = 4.2 \times 10^{-34} \quad (\ell^3 \text{ term}) \tag{18.45}$$

$$\frac{W_{\perp}^{T}}{K} = 2.0 \times 10^{-35} + 1.8 \times 10^{-45} \quad (\ell^3 \text{ term} + \ell \text{ term})\,. \tag{18.46}$$

In the sum of $W_{\perp}^{T}/K$ above, the first term ℓ^3 represents the electromagnetic interaction, while the second term ℓ represents the weak interaction. Thus we find that at low values of ℓ, the weak force predominates up to about $10^{-18}\,\mathrm{m}$, which is the generally accepted range of the weak force. At larger values of ℓ, the electromagnetic force predominates. The value of ℓ at which the two interactions in the transverse strain energy are equal is given by

$$20.4\,\ell^3 = 1.76 \times 10^{-33}\,\ell\,, \tag{18.47}$$

from which we obtain

$$\ell = 0.9 \times 10^{-17}\,\mathrm{m} \sim 10^{-17}\,\mathrm{m}\,. \tag{18.48}$$

At that value of ℓ, the strain energies are given by

$$\frac{W_{\parallel}^{T}}{K} = 3.0 \times 10^{-49} \tag{18.49}$$

$$\frac{W_{\perp}^{T}}{K} = 3.1 \times 10^{-50}\,. \tag{18.50}$$

The longitudinal (massive) strain energy predominates over the transverse strain energy by a factor of 10.

Alternatively, including the longitudinal ℓ^3 strain energy in the calculation, the value of ℓ at which the two interactions in the total strain energy are equal is given by

$$417\,\ell^3 + 20.4\,\ell^3 = 1.76 \times 10^{-33}\,\ell\,, \tag{18.51}$$

from which we obtain

$$\ell = 2.0 \times 10^{-18}\,\mathrm{m}\,. \tag{18.52}$$

At that value of ℓ, the strain energies are given by

$$\frac{W_{\parallel}^{T}}{K} = 3.3 \times 10^{-51} \tag{18.53}$$

$$\frac{W_{\perp}^{T}}{K} = 3.7 \times 10^{-51}\,. \tag{18.54}$$

The longitudinal (massive) strain energy and the transverse strain energy are then of the same order of magnitude.

§18.1.3 *Quantum particles and their associated spacetime defects*

Table 18.1 below provides a summary of the identification of quantum particles and their associated spacetime defects.

STC defect	Type of particle	Particles
Screw dislocation	Massless boson	Photon
Edge dislocation	Massive boson	Spin-0 particle
		Spin-1 Proca eqn
		Spin-2 graviton
Wedge disclination	Massive fermion	Quarks
ℓ^3 twist disclination	Massive fermion	Leptons
ℓ twist disclination	Massless fermion	Neutrino

Table 18.1: Identification of quantum particles and their associated defects.

§18.2 Feynman diagrams and defect interactions

As mentioned in section §14.5 and developed further in this chapter, the basic Feynman diagrams can be seen to represent screw dislocations as photons, edge dislocations as bosons, twist and wedge disclinations as fermions, and their interactions. More specifically, the external legs of Feynman diagrams that are on mass-shell representing real particles correspond to dislocations and disclinations, while the virtual off mass-shell particles are replaced by the interaction of the strain energy densities.

The exchange of virtual particles in QED interactions can be taken as the perturbation expansion representation of the forces resulting from the overlap of the strain energy density of the dislocations and disclinations. The Feynman diagram propagators are replaced by the defect strain energy density interaction expressions.

The properties of Burgers vectors and dislocations [159, see pp. 25-26] have rules similar to those of Feynman diagrams, but not equivalent as virtual particles are replaced by defect strain energy density interactions. A Burgers vector is invariant along a dislocation line. Two

Burgers circuits are equivalent if one can be deformed into the other without crossing dislocation lines. The resultant Burgers vector within equivalent Burgers circuits is the same.

Dislocation nodes are points where multiple dislocations meet. If all the dislocation vectors ξ_i are taken to be positive away from a node, then

$$\sum_{i=1}^{N} \boldsymbol{\xi}_i = 0 \tag{18.55}$$

for the N dislocations meeting at the node. Burgers vectors are conserved at dislocation nodes. Frank vectors also satisfy a Kirchhoff relation at disclination nodes, as do Burgers vectors at dislocation nodes.

§18.3 Interpretation of defect strain energy interactions

As seen in section §14.5, the role played by virtual particles in quantum electrodynamics (QED) is replaced by the interaction of the strain energy density of the dislocations and disclinations. QED is a perturbative theory, and the virtual particles are introduced as an interpretation of the perturbative expansion represented by Feynman diagrams.

Although the existence of virtual particles in QED is generally accepted, there are physicists who still question this interpretation of QED perturbation expansions. As noted previously in section §9.5, Weingard [366] "argues that if certain elements of the orthodox interpretation of states in QM are applicable to QED, then it must be concluded that virtual particles cannot exist. This follows from the fact that the transition amplitudes correspond to superpositions in which virtual particle type and number are not sharp. Weingard argues further that analysis of the role of measurement in resolving the superposition strengthens this conclusion. He then demonstrates in detail how in the path integral formulation of field theory no creation and annihilation operators need appear, yet virtual particles are still present. This analysis shows that the question of the existence of virtual particles is really the question of how to interpret the propagators which appear in the perturbation expansion of vacuum expectation values (scattering amplitudes)." [36]

The basic Feynman diagrams can be seen to represent screw dislocations as photons, edge dislocations as bosons, twist and wedge disclinations as fermions, and their interactions. Virtual particles would require the presence of virtual dislocations and virtual disclinations in the spacetime continuum, which clearly does not make sense. Instead, the exchange of virtual particles in interactions can be seen to be a perturbation expansion representation of the forces resulting from the

interaction of the defects' strain energy density, with suitably modified diagrams. The perturbative expansions are thus replaced by finite analytical expressions.

The analysis presented in the following sections is not perturbative as in QED, but rather calculated from analytical expressions. The analytical equations can become very complicated, and in some cases, perturbative techniques are used to simplify the calculations, but the availability of analytical expressions permit a better understanding of the fundamental quantum processes involved.

In quantum electrodynamics, these correspond to particle-particle and particle-photon interactions, which are taken to be mediated by virtual particles. This is in keeping with the QED picture, but as shown above, particle-particle and particle-photon interactions physically result from the overlap of their strain energy density which results in an interaction force. Again, this improved understanding of the physical nature of dislocation interactions demonstrates that the interactions do not need to be represented by virtual particle exchange as discussed in section §14.5.

This theory provides a straightforward physical explanation of particle-particle and particle-photon interactions that is not based on perturbation theory, but rather on a direct evaluation of the interactions.

§18.3.1 *Photons and screw dislocation interactions*

Screw dislocations interact via the force resulting from the overlap of the strain energy density of the dislocations and disclinations in the spacetime continuum [159, see p. 112].

As seen in section §15.1, screw dislocations in the spacetime continuum are identified with the massless, transverse deformations corresponding to photons. As pointed out in [222], it has been known since the 1960s that photons can interact with each other in atomic media much like massive particles do. A review of collective effects in photon-photon interactions is given in [227].

In QED, photon-photon interactions are known as photon-photon scattering, which is thought to be mediated by virtual particles. This reflects the perturbative calculation used to evaluate the scattering, but as shown in this work, photon-photon interactions physically result from the overlap of their strain energy density. This improved understanding of the physical nature of photon-photon interactions demonstrates that the interaction does not need to be represented by virtual particle exchanges, in that the nature of the physical processes involved is now

understood, and can be calculated directly.

From (17.113), the energy of interaction per unit length between parallel screw dislocations (photons) is given by

$$\frac{W_{12}^{S-S}}{\ell} = -\frac{\bar{\mu}_0}{2\pi}\,(\mathbf{b_1}\cdot\boldsymbol{\xi})\,(\mathbf{b_2}\cdot\boldsymbol{\xi})\,\ln\frac{R}{R_\Lambda} \tag{18.56}$$

where ξ is parallel to the z axis, $(\mathbf{b_i}\cdot\boldsymbol{\xi})$ are the screw components, R is the separation between the dislocations, and R_Λ is the distance from which the dislocations are brought together, resulting in the reduction in the energy of the 2-photon "system".

From (17.115), the components of the interaction force per unit length between the parallel screw dislocations are given by:

$$\begin{aligned}\frac{F_R^{S-S}}{\ell} &= \frac{\bar{\mu}_0}{2\pi R}\,(\mathbf{b_1}\cdot\boldsymbol{\xi})\,(\mathbf{b_2}\cdot\boldsymbol{\xi})\\ \frac{F_\theta^{S-S}}{\ell} &= 0.\end{aligned} \tag{18.57}$$

The interaction force is radial in nature, independent of the angle θ, as expected.

§18.3.2 *Photon-neutrino interactions*

It is surprising to find that the massless, electrically neutral, weakly interacting neutrino would interact with the massless, electrically neutral, electromagnetic interacting photon. Photon-neutrino interactions have been considered, in particular by [190,233,281] and others. *STCED* provides for their interaction via the force resulting from the interaction of their strain energy density, *i.e.* the interaction of screw dislocations and pure twist disclinations, which correspond to photon-neutrino interactions.

§18.4 Physical explanations of QED phenomena

As we have seen in previous sections, spacetime continuum dislocations and disclinations have fundamental properties that reflect those of phenomena at the quantum level. In particular, the improved understanding of the physical nature of interactions mediated by the strain energy density of the defects. Quantum Electrodynamics is a perturbative theory of the electromagnetic quantum vacuum [255], and the virtual particles are introduced as an interpretation of the propagators

which appear in the perturbation expansion of vacuum expectation values represented by Feynman diagrams. In *STCED*, the role played by virtual particles in Quantum Electrodynamics is replaced by the work done by the forces resulting from the defect stresses, and the resulting interaction of the strain energy density of the dislocations and disclinations. In the following sections, we examine the physical explanation of QED phenomena provided by this theory, including self-energy, vacuum polarization and mass renormalization. First we briefly recap the aspects of *STCED* that are relevant to these phenomena.

§18.4.1 Mass and wave-particle duality in the spacetime continuum

In *STCED*, energy propagates in the spacetime continuum (*STC*) as wave-like deformations which can be decomposed into *dilatations* and *distortions*. *Dilatations* involve an invariant change in volume of the spacetime continuum which is the source of the associated rest-mass energy density of the deformation. On the other hand, *distortions* correspond to a change of shape (shearing) of the spacetime continuum without a change in volume and are thus massless. Thus the deformations propagate in the continuum by longitudinal (*dilatation*) and transverse (*distortion*) wave displacements.

This provides a natural explanation for wave-particle duality, with the massless transverse mode corresponding to the wave aspects of the deformations and the massive longitudinal mode corresponding to the particle aspects of the deformations. The rest-mass energy density of the longitudinal mode is given by [238, see Eq.(32)]

$$\rho c^2 = 4\bar{\kappa}_0 \varepsilon \tag{18.58}$$

where ρ is the rest-mass density, c is the speed of light, $\bar{\kappa}_0$ is the bulk modulus of the *STC* (the resistance of the spacetime continuum to *dilatations*), and ε is the volume dilatation

$$\varepsilon = \varepsilon^{\alpha}{}_{\alpha} \tag{18.59}$$

which is the trace of the *STC* strain tensor obtained by contraction. The volume dilatation ε is defined as the change in volume per original volume $\Delta V/V$ [320, see pp. 149–152] and is an invariant of the strain tensor, as is the rest-mass energy density. Hence (see section §5.5.1)

$$mc^2 = 4\bar{\kappa}_0 \, \Delta V \tag{18.60}$$

where m is the mass of the deformation and ΔV is the dilatation change in the spacetime continuum's volume corresponding to mass m. This demonstrates that mass is not independent of the spacetime continuum, but rather mass is part of the spacetime continuum fabric itself.

§18.4.2 Energy in the spacetime continuum

In *STCED*, energy is stored in the spacetime continuum as strain energy [242]. As seen in section §5.2, the strain energy density of the spacetime continuum is separated into two terms: the first one expresses the dilatation energy density (the mass longitudinal term) while the second one expresses the distortion energy density (the massless transverse term):

$$\mathcal{E} = \mathcal{E}_{\parallel} + \mathcal{E}_{\perp} \tag{18.61}$$

where

$$\mathcal{E}_{\parallel} = \frac{1}{2}\,\bar{\kappa}_0 \varepsilon^2 \equiv \frac{1}{32\bar{\kappa}_0}\,\rho^2 c^4\,, \tag{18.62}$$

ρ is the rest-mass density of the deformation, and

$$\mathcal{E}_{\perp} = \bar{\mu}_0 e^{\alpha\beta} e_{\alpha\beta} = \frac{1}{4\bar{\mu}_0} t^{\alpha\beta} t_{\alpha\beta}\,, \tag{18.63}$$

with the strain distortion

$$e^{\alpha\beta} = \varepsilon^{\alpha\beta} - e_s g^{\alpha\beta} \tag{18.64}$$

and the strain dilatation $e_s = \frac{1}{4}\varepsilon^{\alpha}{}_{\alpha}$. Similarly for the stress distortion $t^{\alpha\beta}$ and the stress dilatation t_s. Then the dilatation (massive) strain energy density of the deformation is given by the longitudinal strain energy density (18.62) and the distortion (massless) strain energy density of the deformation is given by the transverse strain energy density (18.63).

The strain energy W of the deformation is obtained by integrating (18.61) over the volume V of the deformation to give

$$W = W_{\parallel} + W_{\perp} \tag{18.65}$$

where $W_{\parallel}$ is the (massive) longitudinal strain energy of the deformation given by

$$W_{\parallel} = \int_V \mathcal{E}_{\parallel}\,\mathrm{d}V \tag{18.66}$$

and $W_\perp$ is the (massless) transverse distortion strain energy of the deformation given by

$$W_\perp = \int_V \mathcal{E}_\perp \, \mathrm{d}V \tag{18.67}$$

where the volume element $\mathrm{d}V$ in cylindrical polar coordinates is given by $r\mathrm{d}r\,\mathrm{d}\theta\,\mathrm{d}z$ for a stationary deformation.

§18.4.3 Quantum particles from STC defects

In [245, 250, 254] and section §18.1, we show that quantum particles can be represented as defects in the spacetime continuum, specifically dislocations and disclinations. *Dislocations* are translational deformations, while *disclinations* are rotational deformations. In particular, we consider the simplest quantum particle defect given by the edge dislocation [250].

The strain energy density of a stationary edge dislocation is given by

$$W^E = W^E_\parallel + W^E_\perp \, . \tag{18.68}$$

The longitudinal strain energy of the edge dislocation $W^E_\parallel$ is given by [250, eq. (8)]

$$W^E_\parallel = \frac{\bar{\kappa}_0}{2\pi} \, \bar{\alpha}_0^2 \, b^2 \, \ell \, \log \frac{\Lambda}{b_c} \tag{18.69}$$

where

$$\bar{\alpha}_0 = \frac{\bar{\mu}_0}{2\bar{\mu}_0 + \bar{\lambda}_0} \, , \tag{18.70}$$

ℓ is the length of the dislocation, b_c is the size of the core of the dislocation, of order b_0, the smallest spacetime Burgers dislocation vector [246] and Λ is a cut-off parameter corresponding to the radial extent of the dislocation, limited by the average distance to its nearest neighbours. In (18.69), the edge dislocation is along the z-axis with Burgers vector b along the x-axis.

The transverse strain energy $W^E_\perp$ is given by [250, eq. (10)]

$$W^E_\perp = \frac{\bar{\mu}_0}{4\pi} \, \left(\bar{\alpha}_0^2 + 2\bar{\beta}_0^2 \right) b^2 \, \ell \, \log \frac{\Lambda}{b_c} \tag{18.71}$$

where

$$\bar{\beta}_0 = \frac{\bar{\mu}_0 + \bar{\lambda}_0}{2\bar{\mu}_0 + \bar{\lambda}_0} \tag{18.72}$$

and the other parameters are as defined previously.

§18.5 QED mass renormalization

The basic Feynman diagrams can be seen to represent screw dislocations as photons, edge dislocations as bosons, twist and wedge disclinations as fermions [250], and their interactions. The interaction of defects results from the overlap of the defects' strain energy densities. In QED, the exchange of virtual particles in interactions can be seen to be a perturbation expansion representation of the forces resulting from the overlap of the strain energy densities of the dislocations and disclinations.

Similarly, the phenomena of self-energy and vacuum polarization can be understood to result from the strain energy densities of individual defects. QED again represents this situation as a perturbation expansion of an interaction of a photon with the vacuum (photon self-energy also known as vacuum polarization) or of a particle such as an electron with its field (self-energy). In *STCED*, the perturbative expansions are replaced by finite analytical expressions for the strain energy density of individual screw dislocations as photons, edge dislocations as bosons, twist and wedge disclinations as fermions [250].

Quantum mechanics and QED only deal with the transverse component of spacetime continuum deformations as they are only concerned with the *wave* aspect of wave-particle duality (see [251] for a discussion of this topic). The energy terms used in QED thus correspond to the transverse strain energy $W^E_\perp$. Hence there is no equivalent dilatation massive longitudinal strain energy term ($W^E_\parallel$) used in QED, and no possibility of properly deriving the mass from the theory, as QED uses an incomplete description of particle energies at the quantum level.

The mass term used in the QED equations is external to and not derived from quantum equations. It is thus found to not correspond to the actual mass of the particle and is characterized instead as the bare mass m_0 [318]. To this mass is added the interaction of the particle with the medium or the field, δm, the result of which m_{qm} is "renormalized" (the value of m_0 and the field corrections are infinite) and replaced with the actual experimental mass m according to

$$m_{qm} = m_0 + \delta m \to m\,. \tag{18.73}$$

Comparing this equation with (18.68), we find that

$$\begin{aligned} m &= W^E \\ m_0 &= W^E_\parallel = \frac{\bar\kappa_0}{2\pi}\,\bar\alpha_0^2\, b^2\,\ell\,\log\frac{\Lambda}{b_c} \end{aligned} \tag{18.74}$$

$$\delta m = W_{\perp}^{E} = \frac{\bar{\mu}_0}{4\pi}\,\left(\bar{\alpha}_0^2 + 2\bar{\beta}_0^2\right) b^2\,\ell\,\log\frac{\Lambda}{b_c}\,.$$

The interaction of the particle with the medium or the field, δm, is the transverse strain energy present in the spacetime continuum (or vacuum), essentially a field energy.

We note that the bare mass (*i.e.* the massive longitudinal strain energy) and the field correction (*i.e.* the transverse strain energy) are both finite in this approach and there is no need for the subtraction of infinities as both terms are well-behaved. If integrated over all of spacetime, they would be divergent, with the divergence being logarithmic in nature. However, contrary to QED, the strain energies are bounded by the density of defects present in the spacetime continuum, which results in an upperbound to the integral of half the average distance between defects. As mentioned by Hirth [159], this has little impact on the accuracy of the results due to the logarithmic dependence. Hence including the longitudinal dilatation mass density term as derived in *STCED* along with the transverse distortion energy density term in the strain energy density provides the expression for the mass m and eliminates the need for mass renormalization as the theory is developed with the correct mass term.

Eq. (18.74) applies to massive bosons as shown in [250]. For electrons, we have

$$W^{\ell^3} = W_{\parallel}^{\ell^3} + W_{\perp}^{\ell^3}\,, \tag{18.75}$$

where the defect in this case is the ℓ^3 twist disclination [250] and where (18.74) is replaced with the following:

$$\begin{aligned} m &= W^{\ell^3} \\ m_0 &= W_{\parallel}^{\ell^3} = \frac{\bar{\kappa}_0}{6\pi}\,\bar{\alpha}_0^2\,\left(\Omega_x^2 + \Omega_y^2\right)\ell^3\log\frac{\Lambda}{b_c} \\ \delta m &= W_{\perp}^{\ell^3} = \frac{\bar{\mu}_0}{2\pi}\,\frac{\ell^3}{3}\,\Big[\,\left(\Omega_x^2 + \Omega_y^2\right)\left(\bar{\alpha}_0^2 + \tfrac{1}{2}\,\bar{\beta}_0^2\right) + \\ &\qquad + 2\,\Omega_x\Omega_y\left(\bar{\alpha}_0^2 - 2\bar{\beta}_0^2\right)\Big]\,\log\frac{\Lambda}{b_c} \end{aligned} \tag{18.76}$$

where Ω^μ is the spacetime Frank vector. The same considerations as seen previously for bosons apply to (18.76) due to the logarithmic dependence of the expressions.

For quarks, we have

$$W^{W} = W_{\parallel}^{W} + W_{\perp}^{W} \tag{18.77}$$

where the defect in this case is the wedge disclination [250]. In most cases $\Lambda \gg b_c$, and we have

$$\begin{aligned} m &= W^W \\ m_0 = W_{\parallel}^W &\simeq \frac{\bar{\kappa}_0}{2\pi}\,\Omega_z^2\,\ell\,\Lambda^2\,\Big[\bar{\alpha}_0^2\,\log^2\Lambda + \\ &\quad + \bar{\alpha}_0\bar{\gamma}_0\log\Lambda + \tfrac{1}{4}(\bar{\alpha}_0^2+\bar{\gamma}_0^2)\Big] \\ \delta m = W_{\perp}^W &\simeq \frac{\bar{\mu}_0}{4\pi}\,\Omega_z^2\,\ell\,\Lambda^2\,\Big[\bar{\alpha}_0^2\,\log^2\Lambda - \\ &\quad - \big(\bar{\alpha}_0^2 - 3\bar{\alpha}_0\bar{\beta}_0\big)\log\Lambda + \\ &\quad + \tfrac{1}{2}\,\big(\bar{\alpha}_0^2 - 3\bar{\alpha}_0\bar{\beta}_0 + \tfrac{3}{2}\,\bar{\beta}_0^2\big)\,\Big] \end{aligned} \tag{18.78}$$

where

$$\bar{\gamma}_0 = \frac{\bar{\lambda}_0}{2\bar{\mu}_0 + \bar{\lambda}_0}\,. \tag{18.79}$$

In this case, both the longitudinal strain energy $W_{\parallel}^W$ and the transverse strain energy $W_{\perp}^W$ are proportional to Λ^2 in the limit $\Lambda \gg b_c$. The parameter Λ is equivalent to the extent of the wedge disclination, and we find that as it becomes more extended, its strain energy is increasing parabolically. This behaviour is similar to that of quarks (confinement). In addition, as shown in [250, see eqs. (16) and (20)], as $\Lambda \to b_c$, the strain energy decreases and tends to 0, again in agreement with the behaviour of quarks (asymptotic freedom).

§18.6 Dislocation self-energy and QED self-energies

The dislocation self-energy is related to the dislocation self-force. The dislocation self-force arises from the force on an element in a dislocation caused by other segments of the *same* dislocation line. This process provides an explanation for the QED self-energies without the need to resort to the emission/absorption of virtual particles. It can be understood, and is particular to, dislocation dynamics as dislocations are defects that extend in the spacetime continuum [159, see p. 131]. Self-energy of a straight-dislocation segment of length L is given by [159, see p. 161]:

$$W_{self} = \frac{\bar{\mu}_0}{4\pi}\,\left((\mathbf{b}\cdot\boldsymbol{\xi})^2 + \frac{\bar{\mu}_0+\bar{\lambda}_0}{2\bar{\mu}_0+\bar{\lambda}_0}\,|(\mathbf{b}\times\boldsymbol{\xi})|^2\right) L\,\left(\ln\frac{L}{b} - 1\right) \tag{18.80}$$

where there is no interaction between two elements of the segment when they are within $\pm b$, or equivalently

$$W_{self} = \frac{\bar{\mu}_0}{4\pi} \left((\mathbf{b} \cdot \boldsymbol{\xi})^2 + \frac{\bar{\mu}_0 + \bar{\lambda}_0}{2\bar{\mu}_0 + \bar{\lambda}_0} |(\mathbf{b} \times \boldsymbol{\xi})|^2 \right) L \ln \frac{L}{eb} \tag{18.81}$$

where $e = 2.71828...$ is Euler's number. These equations provide analytic expressions for the non-perturbative calculation of quantum self energies and interaction energies, and eliminate the need for the virtual particle perturbative approach.

In particular, the pure screw (photon) self-energy

$$W^S_{self} = \frac{\bar{\mu}_0}{4\pi} (\mathbf{b} \cdot \boldsymbol{\xi})^2 L \left(\ln \frac{L}{b} - 1 \right) \tag{18.82}$$

and the pure edge (boson) self-energy

$$W^E_{self} = \frac{\bar{\mu}_0}{4\pi} \frac{\bar{\mu}_0 + \bar{\lambda}_0}{2\bar{\mu}_0 + \bar{\lambda}_0} |(\mathbf{b} \times \boldsymbol{\xi})|^2 L \left(\ln \frac{L}{b} - 1 \right) \tag{18.83}$$

are obtained from (18.81), while (18.81) is also the appropriate equation to use for the dual wave-particle "system".

We can relate (18.83) to (18.68) and (18.74) by evaluating W^E from (18.68) using (18.69) and (18.71):

$$W^E = \frac{b^2}{4\pi} \left[2\bar{\kappa}_0 \bar{\alpha}_0^2 + \bar{\mu}_0 \left(\bar{\alpha}_0^2 + 2\bar{\beta}_0^2 \right) \right] \ell \log \frac{\Lambda}{b_c} \,. \tag{18.84}$$

Substituting for $\bar{\kappa}_0$ from (2.3), for $\bar{\alpha}_0$ from (18.70) and for $\bar{\beta}_0$ from (18.72), the factor in square brackets in the above equation becomes

$$[] = \frac{\bar{\mu}_0}{(2\bar{\mu}_0 + \bar{\lambda}_0)^2} \left(4\bar{\mu}_0^2 + 6\bar{\mu}_0\bar{\lambda}_0 + 2\bar{\lambda}_0^2 \right) \tag{18.85}$$

which can be factored as

$$[] = \frac{2\bar{\mu}_0}{(2\bar{\mu}_0 + \bar{\lambda}_0)^2} (2\bar{\mu}_0 + \bar{\lambda}_0)(\bar{\mu}_0 + \bar{\lambda}_0) \,. \tag{18.86}$$

Substituting back into (18.84), we obtain

$$W^E_{self} = \frac{1}{2} W^E = \frac{\bar{\mu}_0}{4\pi} \frac{\bar{\mu}_0 + \bar{\lambda}_0}{2\bar{\mu}_0 + \bar{\lambda}_0} b^2 \ell \log \frac{\Lambda}{b_c} \,. \tag{18.87}$$

As noted in [39, see p. 178], the self-energy and the interaction energies are described by the same equations in the non-singular theory, except

that the self-energy is half of the interaction energy. We thus see that the above result (18.84) is essentially the same as (18.83) from Hirth [159, see p. 161] except that the log factors are slightly different, but similar in intent ($\log \Lambda/b_c$ compared to $\log \ell/eb$).

Dislocation self energies are thus found to be similar in structure to Quantum Electrodynamics self energies. They are also divergent if integrated over all of spacetime, with the divergence being logarithmic in nature. However, contrary to QED, dislocation self energies are bounded by the density of dislocations present in the spacetime continuum, which results in an upperbound to the integral of half the average distance between dislocations.

As seen previously in section §17.4.3, for a dislocation loop, as each element $d\mathbf{l}$ of the dislocation loop is acted upon by the forces caused by the stress of the other elements of the dislocation loop, the work done against these corresponds to the self-energy of the dislocation loop. The self-energy of a dislocation loop can be calculated from Eq. (4-44) of [159, see p. 110] to give

$$\begin{aligned} W_{self} &= \frac{\bar{\mu}_0}{8\pi} \oint_{C_1=C} \oint_{C_2=C} \frac{(\mathbf{b} \cdot d\mathbf{l_1})\,(\mathbf{b} \cdot d\mathbf{l_2})}{R} + \\ &+ \frac{\bar{\mu}_0}{4\pi} \frac{\bar{\mu}_0 + \bar{\lambda}_0}{2\bar{\mu}_0 + \bar{\lambda}_0} \oint_{C_1=C} \oint_{C_2=C} \frac{(\mathbf{b} \times d\mathbf{l_1}) \cdot \mathbf{T} \cdot (\mathbf{b} \times d\mathbf{l_2})}{R} \end{aligned} \tag{18.88}$$

where $\mathbf{T}$ is as defined in Eq. (4-44) of [159, see p. 110].

The photon self-energy also known as vacuum polarization is obtained from the strain energy density of screw dislocations. The longitudinal strain energy of the screw dislocation $W_{\parallel}^{S} = 0$ as given by [250, eq. (6)] *i.e.* the photon is massless. The photon self-energy is given by half the transverse strain energy of the screw dislocation $W_{\perp}^{S}$ given by [250, eq. (7)]

$$W_{self}^{S} = \frac{1}{2}\, W_{\perp}^{S} = \frac{\bar{\mu}_0}{8\pi}\, b^2\, \ell\, \log \frac{\Lambda}{b_c} \tag{18.89}$$

which again includes the $\log \Lambda/b_c$ factor. Comparing this expression with (18.82) and with (18.88), we find that (18.82) is likely off by a factor of 2, being proportional to $1/8\pi$ as per Hirth's (18.88) and (18.89), not $1/4\pi$ as given in Hirth's (18.80) and Hirth's (18.82).

§18.7 Disclination self-energy and QED self-energies

From dislocation self-energies, we can calculate the photon self-energy (also known as the vacuum polarization) and, in the general case, the

boson self-energy.

The fermion self-energies are calculated from the corresponding disclination self-energies, with the lepton self-energy calculated from the interaction energy W^{ℓ^3} of the ℓ^3 twist disclination, the neutrino self-energy calculated from the interaction energy W^{ℓ} of the ℓ twist disclination and the quark self-energy calculated from the interaction energy W^{W} of the wedge disclination, using the result that self-energy is half of the interaction energy as seen previously in Section 18.6.

§18.7.1 *The ℓ^3 twist disclination self-energy and lepton self-energies*

The lepton (electron) self-energy is calculated from the interaction energy W^{ℓ^3} of the ℓ^3 twist disclination by evaluating W^{ℓ^3} from (18.75) using $W_{\parallel}^{\ell^3}$ and $W_{\perp}^{\ell^3}$ from (18.76):

$$\begin{aligned} W^{\ell^3} = {} & \frac{\bar{\kappa}_0}{6\pi}\,\bar{\alpha}_0^2\,\left(\Omega_x^2+\Omega_y^2\right)\ell^3 \log\frac{\Lambda}{b_c} + \\ & + \frac{\bar{\mu}_0}{2\pi}\,\frac{\ell^3}{3}\,\Big[\,\left(\Omega_x^2+\Omega_y^2\right)\left(\bar{\alpha}_0^2+\tfrac{1}{2}\,\bar{\beta}_0^2\right) + \\ & + 2\,\Omega_x\Omega_y\left(\bar{\alpha}_0^2-2\bar{\beta}_0^2\right)\Big]\,\log\frac{\Lambda}{b_c}\,. \end{aligned} \tag{18.90}$$

Substituting for $\bar{\kappa}_0$ from (2.3), for $\bar{\alpha}_0$ from (18.70) and for $\bar{\beta}_0$ from (18.72), (18.90) becomes

$$\begin{aligned} W^{\ell^3} = {} & \frac{\ell^3}{6\pi}\,\frac{\bar{\mu}_0}{(2\bar{\mu}_0+\bar{\lambda}_0)^2}\times \\ & \times\Big[\,\left(\Omega_x^2+\Omega_y^2\right)\left(2\bar{\mu}_0^2+2\bar{\mu}_0\bar{\lambda}_0+\tfrac{1}{2}\bar{\lambda}_0^2\right) - \\ & - 2\,\Omega_x\Omega_y\left(\bar{\mu}_0^2+4\bar{\mu}_0\bar{\lambda}_0+2\bar{\lambda}_0^2\right)\Big]\,\log\frac{\Lambda}{b_c} \end{aligned} \tag{18.91}$$

which can be factored as

$$\begin{aligned} W^{\ell^3} = {} & \frac{\ell^3}{12\pi}\,\frac{\bar{\mu}_0}{(2\bar{\mu}_0+\bar{\lambda}_0)^2}\,\Big\{\,\left(\Omega_x^2+\Omega_y^2\right)\left(2\bar{\mu}_0+\bar{\lambda}_0\right)^2 - \\ & - 4\Omega_x\Omega_y\left[\left(\bar{\mu}_0+\bar{\lambda}_0\right)\left(\bar{\mu}_0+2\bar{\lambda}_0\right)+\bar{\mu}_0\bar{\lambda}_0\right]\Big\}\log\frac{\Lambda}{b_c}. \end{aligned} \tag{18.92}$$

The lepton self-energy is then given by

$$W^{\ell^3}_{self} = \frac{1}{2}\, W^{\ell^3} = \frac{\bar{\mu}_0}{24\pi} \Bigg\{ \left(\Omega_x^2 + \Omega_y^2\right) - \\ - 4\,\Omega_x\Omega_y\, \frac{\left(\bar{\mu}_0 + \bar{\lambda}_0\right)\left(\bar{\mu}_0 + 2\bar{\lambda}_0\right) + \bar{\mu}_0\bar{\lambda}_0}{(2\bar{\mu}_0 + \bar{\lambda}_0)^2} \Bigg\} \ell^3\, \log\frac{\Lambda}{b_c}\,, \tag{18.93}$$

where we have used the result that self-energy is half of the interaction energy as seen previously in Section 18.6.

§18.7.2 *The ℓ twist disclination self-energy and the neutrino self-energy*

The neutrino self-energy is calculated from the strain energy W^ℓ of the ℓ twist disclination. The longitudinal strain energy of the ℓ twist disclination $W^\ell_\parallel = 0$ as given by [250, eq. 33)] *i.e.* the neutrino is massless. In most cases $\Lambda \gg b_c$, and the strain energy W^ℓ of the ℓ twist disclination is given by the transverse strain energy $W^\ell = W^\ell_\perp$ given by [250, eq. (35)]:

$$W^\ell = \frac{\bar{\mu}_0}{2\pi}\, \ell\, \Lambda^2 \Bigg[\left(\Omega_x^2 + \Omega_y^2\right) \Big(\bar{\alpha}_0^2\, \log^2\Lambda + \bar{\alpha}_0\bar{\gamma}_0\, \log\Lambda - \\ - \tfrac{1}{2}\,\bar{\alpha}_0\bar{\gamma}_0 \Big) - 2\,\Omega_x\Omega_y \Big(\bar{\alpha}_0\,\bar{\beta}_0 \log\Lambda + \tfrac{1}{2}\,\bar{\beta}_0\bar{\gamma}_0 \Big) \Bigg]. \tag{18.94}$$

Substituting for $\bar{\alpha}_0$ from (18.70), for $\bar{\beta}_0$ from (18.72) and for $\bar{\gamma}_0$ from (18.79), (18.94) becomes

$$W^\ell = \frac{\bar{\mu}_0}{2\pi}\, \frac{\ell\,\Lambda^2}{(2\bar{\mu}_0 + \bar{\lambda}_0)^2} \Bigg\{ \left(\Omega_x^2 + \Omega_y^2\right) \Big[\bar{\mu}_0^2\, \log^2\Lambda + \\ + \bar{\mu}_0\bar{\lambda}_0 \left(\log\Lambda - \tfrac{1}{2}\right) \Big] - \\ - 2\,\Omega_x\Omega_y \left[\bar{\mu}_0 \left(\bar{\mu}_0 + \bar{\lambda}_0\right) \log\Lambda + \tfrac{1}{2}\,\bar{\lambda}_0 \left(\bar{\mu}_0 + \bar{\lambda}_0\right) \right] \Bigg\}. \tag{18.95}$$

The neutrino self-energy is then given by

$$W^\ell_{self} = \frac{1}{2}\, W^\ell = \frac{\bar{\mu}_0}{4\pi}\, \frac{\ell\,\Lambda^2}{(2\bar{\mu}_0 + \bar{\lambda}_0)^2} \times \\ \times \Bigg\{ \left(\Omega_x^2 + \Omega_y^2\right) \Big[\bar{\mu}_0^2\, \log^2\Lambda + \bar{\mu}_0\bar{\lambda}_0 \left(\log\Lambda - \tfrac{1}{2}\right) \Big] - \tag{18.96}$$

$$- \; 2\,\Omega_x\Omega_y \left(\bar{\mu}_0 + \bar{\lambda}_0\right)\left(\bar{\mu}_0 \log\Lambda + \tfrac{1}{2}\,\bar{\lambda}_0\right) \Bigg\}$$

where we have used the result that self-energy is half of the interaction energy as seen previously in Section 18.6.

§18.7.3 *The wedge disclination self-energy and quark self-energies*

The quark self-energy is calculated from the interaction energy W^W of the wedge disclination by evaluating W^W from (18.77) using $W^W_{\parallel}$ and $W^W_{\perp}$ from (18.78). In most cases $\Lambda \gg b_c$, and we have

$$\begin{aligned} W^W \simeq \frac{\bar{\kappa}_0}{2\pi}\,\Omega_z^2\,\ell\,\Lambda^2 \Big[&\bar{\alpha}_0^2\,\log^2\Lambda + \\ &+ \bar{\alpha}_0\bar{\gamma}_0 \log\Lambda + \tfrac{1}{4}(\bar{\alpha}_0^2 + \bar{\gamma}_0^2)\Big] + \\ &+ \frac{\bar{\mu}_0}{4\pi}\,\Omega_z^2\,\ell\,\Lambda^2 \Big[\bar{\alpha}_0^2\,\log^2\Lambda - \\ &- \left(\bar{\alpha}_0^2 - 3\bar{\alpha}_0\bar{\beta}_0\right)\log\Lambda + \\ &+ \tfrac{1}{2}\left(\bar{\alpha}_0^2 - 3\bar{\alpha}_0\bar{\beta}_0 + \tfrac{3}{2}\,\bar{\beta}_0^2\right)\Big]. \end{aligned} \tag{18.97}$$

Substituting for $\bar{\kappa}_0$ from (2.3), for $\bar{\alpha}_0$ from (18.70) for $\bar{\beta}_0$ from (18.72) and for $\bar{\gamma}_0$ from (18.79), (18.97) becomes

$$\begin{aligned} W^W \simeq \frac{\Omega_z^2}{2\pi}\,\frac{\ell\,\Lambda^2}{(2\bar{\mu}_0 + \bar{\lambda}_0)^2} \Big[&\bar{\mu}_0^2\left(\bar{\mu}_0 + \bar{\lambda}_0\right)\log^2\Lambda + \\ &+ \bar{\mu}_0\left(\bar{\mu}_0^2 + 2\bar{\mu}_0\bar{\lambda}_0 + \bar{\lambda}_0^2\right)\log\Lambda + \\ &+ \tfrac{1}{4}\,\bar{\lambda}_0\left(\bar{\mu}_0^2 + 2\bar{\mu}_0\bar{\lambda}_0 + \bar{\lambda}_0^2\right)\Big] \end{aligned} \tag{18.98}$$

which can be factored as

$$\begin{aligned} W^W \simeq \frac{\Omega_z^2}{2\pi}\,\frac{\ell\,\Lambda^2}{(2\bar{\mu}_0 + \bar{\lambda}_0)^2} \Big[&\bar{\mu}_0^2\left(\bar{\mu}_0 + \bar{\lambda}_0\right)\log^2\Lambda + \\ &+ \left(\bar{\mu}_0 + \bar{\lambda}_0\right)^2\left(\bar{\mu}_0\log\Lambda + \tfrac{1}{4}\,\bar{\lambda}_0\right)\Big]. \end{aligned} \tag{18.99}$$

The quark self-energy is then given by

$$W^{W}_{self} = \frac{1}{2}\, W^{W} \simeq \frac{\Omega_z^2}{4\pi}\, \frac{(\bar{\mu}_0 + \bar{\lambda}_0)^2}{(2\bar{\mu}_0 + \bar{\lambda}_0)^2}\, \ell\, \Lambda^2 \times \\ \times \left[\frac{\bar{\mu}_0^2}{\bar{\mu}_0 + \bar{\lambda}_0} \log^2 \Lambda + \bar{\mu}_0 \log \Lambda + \tfrac{1}{4}\, \bar{\lambda}_0 \right] \tag{18.100}$$

where we have used the result that self-energy is half of the interaction energy as seen previously in Section 18.6.

§18.7.4 *Summary*

In Sections §18.4 to §18.7, we have considered how the Elastodynamics of the Spacetime Continuum (*STCED*) explains the Quantum Electrodynamics (QED) phenomena of self-energy, vacuum polarization and mass renormalization. We have derived the strain energy equivalence for QED mass renormalization for bosons, leptons and quarks, and we have also derived the self-energy expressions for bosons including photons, leptons including neutrinos, and quarks.

It is important to note that

1. The expressions derived are for stationary (time independent) defects.
2. The case of time-dependent screw and edge dislocations moving with velocity v is covered in §16.1.2 and §16.2.2 of [254] respectively. The calculations involve integrals of the form

$$\int_y \frac{1}{\alpha y}\, \arctan\left(\frac{x - vt}{\alpha y} \right) \mathrm{d}y = \\ -\frac{i}{2} \left[\mathrm{Li}_2 \left(-i\, \frac{x - vt}{\alpha y} \right) - \mathrm{Li}_2 \left(i\, \frac{x - vt}{\alpha y} \right) \right] \tag{18.101}$$

where

$$\alpha = \sqrt{1 - \frac{v^2}{c^2}} \tag{18.102}$$

and where $\mathrm{Li}_n(x)$ is the polylogarithm function which arises in Feynman diagram integrals. For $n = 2$ and $n = 3$, we have the dilogarithm and the trilogarithm special cases respectively. This is a further indication that the interaction of strain energies are the physical source of quantum interaction phenomena described by Feynman diagrams as discussed in Section §18.5.

The results obtained are found to provide a physical explanation of QED phenomena in terms of the interaction resulting from the overlap of defect strain energies in the spacetime continuum in *STCED*.

§18.8 Nonlocality of quantum phenomena

Defects in the spacetime continuum give rise to nonlocal effects and nonlocal continuum field theories [112]. Discrete line defects extend in the spacetime continuum, and hence interact nonlocally, much as nonlocal interactions between distant atoms determine the properties of materials in solid-state physics.

§18.9 Entangled states in quantum physics

As noted in the previous section §18.5, the physical extension of defects in the spacetime continuum gives rise to nonlocal effects and to what are referred to as "entangled states" in quantum physics. Entangled states correspond to the overlap of defects in the spacetime continuum, overlaps that can extend between distant defects, and are characterized by the interaction of their strain energy densities. Entangled states are treated in detail in §13.5 and in particular in §13.5.3.

Chapter 19

Spacetime Continuum Fundamentals

§19.1 The spacetime Burgers dislocation constant b_0 and Planck's constant

In this section, we explore the relation between the spacetime Burgers dislocation constant b_0 and Planck's constant, and derive the value of the spacetime continuum constants.

Based on our identification of screw dislocations in the spacetime continuum with photons, we can determine the relation between the Burgers constant b_0 and Planck's constant h.

Even though the photon is massless, its energy is given by the strain energy density of the screw dislocation, equivalent to the transverse distortion energy density. As shown in [238, Eq. (147)],

$$\hat{p}^2 c^2 = 32 \bar{\kappa}_0 \, \mathcal{E}_\perp, \tag{19.1}$$

where $\hat{p}$ is the momentum density. For a screw dislocation, substituting for $\mathcal{E}_\perp$ from (9.22) in (19.1), we obtain

$$\hat{p}^2 c^2 = 32 \bar{\kappa}_0 \, \frac{\bar{\mu}_0 \, b^2}{8\pi^2} \, \frac{1}{r^2}. \tag{19.2}$$

The kinetic energy density $\hat{p}c$ has to be equivalent to the wave energy density $\widehat{h\nu}$ for the screw dislocation (photon):

$$\hat{p}c = \widehat{h\nu}. \tag{19.3}$$

The photon's energy is given by

$$h\nu = \int_V \widehat{h\nu} \, \mathrm{d}V = \widehat{h\nu} \, V \tag{19.4}$$

where V is the volume of the screw dislocation. We consider the smallest Burgers dislocation vector possible and replace b with the elementary Burgers dislocation vector b_0 and V with the smallest volume V_0 to derive Planck's constant. Combining (19.4), (19.3) and (19.2), (19.4) becomes

$$h = \sqrt{\frac{16 \bar{\kappa}_0 \, \bar{\mu}_0 \, {b_0}^2}{(2\pi r)^2}} \, \frac{V_0}{\nu}. \tag{19.5}$$

Using (15.7), the frequency $\nu = c/\lambda$ becomes $\nu = c/b_0$ for the smallest Burgers dislocation vector considered. Substituting into (19.5), the equation becomes

$$h = \frac{4\sqrt{\bar{\kappa}_0\,\bar{\mu}_0}\,b_0}{2\pi r}\,\frac{V_0 b_0}{c}. \tag{19.6}$$

The volume of one wavelength of the screw dislocation can be approximated by a cylinder and, using (15.7), written as

$$V = \pi r^2 \lambda = \pi r^2 b, \tag{19.7}$$

which in the limit as $b \to b_0$, becomes

$$V_0 = \pi r^2 b_0. \tag{19.8}$$

Substituting for V_0 into (19.6), the equation becomes

$$h = \frac{4\sqrt{\bar{\kappa}_0\,\bar{\mu}_0}\,b_0}{2\pi r}\,\frac{\pi r^2 b_0^2}{c}. \tag{19.9}$$

Simplifying,

$$h = \frac{2\sqrt{\bar{\kappa}_0\,\bar{\mu}_0}}{c}\,r b_0^3, \tag{19.10}$$

and in the limit as r approaches b_0, becomes

$$h = 2\frac{\sqrt{\bar{\kappa}_0\,\bar{\mu}_0}\,b_0^4}{c} \tag{19.11}$$

where the units of h are $[\mathrm{J}\cdot\mathrm{s}]$ as expected. This is the basic definition of Planck's constant h in terms of the Lamé spacetime constants and the Burgers spacetime dislocation constant b_0.

This relation can be further simplified using $\bar{\mu}_0 = 32\bar{\kappa}_0$ from [238, Eq. (150)]. Then

$$h = 8\sqrt{2}\,\frac{\bar{\kappa}_0\,{b_0}^4}{c} = \frac{1}{2\sqrt{2}}\,\frac{\bar{\mu}_0\,{b_0}^4}{c}. \tag{19.12}$$

Numerically,

$$\bar{\mu}_0\,{b_0}^4 = 2\sqrt{2}\,hc = 5.8\times 10^{-25}\,\mathrm{J\,m}. \tag{19.13}$$

The value of the spacetime shear modulus $\bar{\mu}_0$ is not a known physical constant, neither is the value of the spacetime bulk modulus $\bar{\kappa}_0$. However, Macken [223] has derived a value of $\bar{\kappa}_0 = 4.6\times 10^{113}\,\mathrm{J/m^3}$ which as

we will see in section §19.2.1 is expected to be a valid estimate. Using $\bar{\mu}_0 = 32\bar{\kappa}_0$ from Millette [238, Eq. (150)], this yields a value of

$$\bar{\mu}_0 = 1.5 \times 10^{115}\,\mathrm{J/m^3}. \tag{19.14}$$

Note that the units can be expressed equivalently as $[\mathrm{N}\cdot\mathrm{m}^{-2}]$ or as $[\mathrm{J}\cdot\mathrm{m}^{-3}]$. Substituting for $\bar{\mu}_0$ in (19.13), we obtain the value of the elementary Burgers vector

$$b_0 = 1.4 \times 10^{-35}\,\mathrm{m}. \tag{19.15}$$

This value compares very favorably with the Planck length 1.6×10^{-35} m. Given the approximations used in its derivation, this suggests that the elementary Burgers vector b_0 and the Planck length are equivalent.

§19.2 Spacetime continuum constants

With these constants, we are now in a position to calculate the remaining unknown spacetime constants, the density of the spacetime continuum $\bar{\rho}_0$ and the speed of longitudinal deformations c_l. Using the relation [238]

$$c = \sqrt{\frac{\bar{\mu}_0}{\bar{\rho}_0}}, \tag{19.16}$$

the density of the spacetime continuum is

$$\bar{\rho}_0 = 1.7 \times 10^{98}\,\mathrm{kg/m^3}. \tag{19.17}$$

This value is in the same ballpark as the vacuum energy density calculated by Carroll [52, see p. 173] ($\sim 10^{112}\,\mathrm{ergs/cm^3}$) from quantum mechanical considerations. From

$$c_l = \sqrt{\frac{2\bar{\mu}_0 + \bar{\lambda}_0}{\bar{\rho}_0}}, \tag{19.18}$$

(2.3) and (5.53), the speed of longitudinal deformations is given by

$$c_l = \frac{7}{4\sqrt{2}}\,c = 1.24\,c. \tag{19.19}$$

$$c_l = 3.7 \times 10^8\,\mathrm{m/s}. \tag{19.20}$$

Note that the speed of light is still the limiting speed in spacetime as discussed in [159, 245].

§19.2.1 *Analytic form of constants b_0 and $\bar{\kappa}_0$*

Blair [27, p. 3–4] writes Einstein's field equation as

$$\mathbf{T} = \frac{c^4}{8\pi G}\,\mathbf{G},$$

where $\mathbf{T}$ is the stress energy tensor, $\mathbf{G}$ is the Einstein curvature tensor and G is the universal gravitational constant. He notes the very large value of the proportionality constant. This leads him to point out that spacetime is an elastic medium that can support waves, but its extremely high stiffness means that extremely small amplitude waves have a very high energy density. He notes that the coupling constant $c^4/8\pi G$ can be considered as a modulus of elasticity for spacetime, and identifies the quantity c^3/G with the characteristic impedance of spacetime [27, p. 45].

From this, Macken [223] derives an "interactive bulk modulus of spacetime", which we identify with the spacetime continuum bulk modulus, given by

$$\bar{\kappa}_0 = \frac{c^7}{\hbar G^2}. \tag{19.21}$$

The result obtained for the numerical value of b_0 and its close correspondance to the Planck length suggests that the value of $\bar{\kappa}_0$ proposed in [223] is correct. From Millette [238, Eq. (150)] we then have

$$\bar{\mu}_0 = 32\frac{c^7}{\hbar G^2}. \tag{19.22}$$

From (19.13), we can write

$$b_0{}^4 = 2\sqrt{2}\,\frac{hc}{\bar{\mu}_0}. \tag{19.23}$$

Substituting from (19.22), this relation becomes

$$b_0{}^4 = \frac{\sqrt{2}\pi}{8}\,\frac{\hbar^2 G^2}{c^6} \tag{19.24}$$

and finally

$$b_0 = \left(\frac{\pi}{4\sqrt{2}}\right)^{\frac{1}{4}}\sqrt{\frac{\hbar G}{c^3}} = 0.86\,\ell_P \tag{19.25}$$

where ℓ_P is Planck's length, defined as [189]

$$\ell_P = \sqrt{\frac{\hbar G}{c^3}}. \tag{19.26}$$

Hence, as mentioned in section §19.1, this suggests that the elementary Burgers dislocation vector b_0 and the Planck length ℓ_P are equivalent within the approximations of the derivation.

§19.2.2 *Recommended constants*

Starting from the statement that the Burgers spacetime dislocation constant b_0 is equivalent to the Planck length ℓ_P, we derive the constant of proportionality of (19.11). We thus set

$$h = k\,\frac{\sqrt{\bar{\kappa}_0\,\bar{\mu}_0}\,b_0^4}{c} \tag{19.27}$$

where k is the improved constant of proportionality for the relation. Substituting for $\bar{\kappa}_0$ from (19.21), for $\bar{\mu}_0$ from (19.22), and setting $b_0 = \ell_P$ from (19.26), the equation becomes

$$h = k\,\sqrt{32}\,\frac{c^7}{\hbar G^2}\,\frac{1}{c}\,\frac{\hbar^2 G^2}{c^6} \tag{19.28}$$

from which we obtain

$$k = \frac{\pi}{2\sqrt{2}}. \tag{19.29}$$

Hence, with the Burgers spacetime dislocation constant b_0 equivalent to the Planck length ℓ_P, the basic definition of Planck's constant h in terms of the Lamé spacetime constants and the Burgers spacetime dislocation constant b_0 is given by

$$h = \frac{\pi}{2\sqrt{2}}\,\frac{\sqrt{\bar{\kappa}_0\,\bar{\mu}_0}\,b_0^4}{c}. \tag{19.30}$$

In terms of $\bar{\kappa}_0$, we have

$$h = 2\pi\,\frac{\bar{\kappa}_0\,b_0^4}{c} \tag{19.31}$$

or

$$\hbar = \frac{\bar{\kappa}_0\,b_0^4}{c} \tag{19.32}$$

and in terms of $\bar{\mu}_0$, we have

$$h = \frac{\pi}{16}\,\frac{\bar{\mu}_0\,b_0^4}{c}. \tag{19.33}$$

As stated, the Burgers spacetime dislocation constant b_0 is given by

$$b_0 = \ell_P = \sqrt{\frac{\hbar G}{c^3}} \tag{19.34}$$

and the spacetime continuum Lamé constants are as per (19.21) and (19.22):

$$\begin{aligned} \bar{\kappa}_0 &= \frac{c^7}{\hbar G^2} \\ \bar{\mu}_0 &= 32\frac{c^7}{\hbar G^2}. \end{aligned} \tag{19.35}$$

From (19.16) and the value of $\bar{\mu}_0$ above, the density of the spacetime continuum is given by

$$\bar{\rho}_0 = 32\frac{c^5}{\hbar G^2}\,. \tag{19.36}$$

It is recommended that the relations in this section be retained as the official definition of these constants.

§19.3 Action in the spacetime continuum

We consider (19.32) in greater details, viz.

$$\hbar = \frac{\bar{\kappa}_0\, b_0^4}{c}\,. \tag{19.37}$$

Interestingly enough, this equation can be considered to be a definition of Planck's reduced constant $\hbar$.

On the R.H.S. of the equation, we have the spacetime continuum bulk modulus constant $\bar{\kappa}_0$ in units of energy density $[\mathrm{J}\cdot\mathrm{m}^{-3}]$, that is energy per 3-D volume. We multiply $\bar{\kappa}_0$ by a 3-D volume to convert it to energy. However, $\bar{\kappa}_0$ is a spacetime continuum constant. We need a conversion in terms of the 4-D spacetime volume.

The R.H.S. of (19.37) also includes the term b_0^4 which can be taken to be the 4-D volume of a four-dimensional elementary hypercube of side $b_0 = 1.616\times10^{-35}\,\mathrm{m}$. This 4-D hypervolume has units of $[\mathrm{m}^4]$ while the four-dimensional spacetime continuum hypervolume consists of three space dimensions and one time dimension with units $[\mathrm{m}^3\cdot\mathrm{s}]$. This requires that one of the space elementary dimensions b_0 be divided by c to convert it to a time elementary dimension $t_0 = b_0/c = 5.39\times10^{-44}\,\mathrm{s}$ as seen in (19.37). Equation (19.37) can thus be written as

$$\hbar = \bar{\kappa}_0\, b_0^3\,\frac{b_0}{c} = \bar{\kappa}_0\, b_0^3\, t_0 = \bar{\kappa}_0\, V_0^{STC} \tag{19.38}$$

where V_0^{STC} is the four-dimensional elementary spacetime continuum hypervolume and $\hbar$ has units of $[\mathrm{J}\cdot\mathrm{s}]$ which are units of action $\mathcal{S}$.

Hence multiplying $\bar{\kappa}_0$ by a 3-D space volume converts it to energy, while multiplying it by a 4-D spacetime volume converts it to action. Energy applies to three-dimensional space, while action applies to four-dimensional spacetime. From (19.38), we see that Planck's reduced constant corresponds to an elementary quantum of action S_0:

$$\hbar = \bar{\kappa}_0 \, V_0^{STC} = S_0 \tag{19.39}$$

which has units of $[\mathrm{J} \cdot \mathrm{s}]$. Action units are the same as those of angular momentum, but this equivalence is accidental. The basic nature of $\hbar$ is an action, not an angular momentum. Calling $\hbar$ a "spin" quantity is an unfortunate misnomer from the early days of quantum mechanics. It needs to be called more appropriately an action quantity, *i.e.* a quantum of action.

We thus find that action is the fundamental four-dimensional spacetime scalar quantity corresponding to energy for three-dimensional space. This helps explain why equations of motion are determined by minimizing action, not energy, using the principle of least (or stationary) action given by

$$\delta \mathcal{S} = 0 \tag{19.40}$$

where the action $\mathcal{S}$ is expressed in terms of the Lagrangian L of the system as

$$\mathcal{S} = \int_{t_1}^{t_2} L \left(q(t), \dot{q}(t), t \right) \, dt \tag{19.41}$$

where $q = (q_1, q_2, ..., q_N)$ are the N generalized coordinates defining the configuration of the system and $\dot{q}$ denotes the time derivative of q.

In Lagrangian field theory, the action is written in terms of the Lagrangian density $\mathcal{L}$ specified in terms of one or more fields $\phi(x)$ and their derivatives $\partial_\mu \phi$ as [286, see p. 15ff]

$$\mathcal{S} = \int_{x_1}^{x_2} \mathcal{L} \left(\phi(x), \partial_\mu \phi \right) \, d^4 x \, . \tag{19.42}$$

The path integral formulation of quantum mechanics and quantum field theory is a generalization of the action principle of classical mechanics [280]. Interestingly enough, Feynman who developed this formulation [120]

> ... belie[ved] that the path integral captures the fundamental physics, and that hamiltonians and Hilbert space are merely mathematical methods for evaluating path integrals. [333, see p. 143]

In *STCED*, the path integral between two points x_1 and x_2 can be understood to be equivalent to the different possible wave paths between the two points.

The propagation amplitude $G(x_2; x_1)$ between the two points is determined from the path integral using the appropriate action for the system under consideration. One can see that since the contribution of a path is proportional to $e^{i\mathcal{S}/\hbar}$ [333, see p. 146], then, from (19.39), it is equivalent to $e^{i\mathcal{S}/S_0}$. In other words, the contribution of a path depends on the number of elementary quanta of action S_0 in the path.

§19.4 Volume dilatation and rest-mass energy density

In this section we explore in greater details the relation between the volume dilatation and rest-mass energy density. We recall the relation (2.24) between these quantities, *viz.*

$$\rho c^2 = 4\bar{\kappa}_0\, \varepsilon \tag{19.43}$$

which we rewrite as

$$\rho = \frac{4\bar{\kappa}_0}{c^2}\, \varepsilon\,. \tag{19.44}$$

Substituting for $\bar{\kappa}_0$ from (19.35),

$$\rho = \frac{4c^5}{\hbar G^2}\, \varepsilon \tag{19.45}$$

and numerically,

$$\rho = 2.06 \times 10^{97}\, \varepsilon \text{ kg/m}^3\,. \tag{19.46}$$

Since the dilatation $0 \leq \varepsilon \leq 1$, the range of values of the rest-mass density is $0 \leq \rho \leq \rho_{max}$, where $\rho_{max} = 2.06 \times 10^{97}\,\text{kg/m}^3$.

Recalling that the density of the spacetime continuum is given by (19.36), *viz.*

$$\bar{\rho}_0 = 32\frac{c^5}{\hbar G^2} \tag{19.47}$$

or numerically

$$\bar{\rho}_0 = 8\,\rho_{max} = 1.65 \times 10^{98}\,\text{kg/m}^3\,, \tag{19.48}$$

we see that the rest-mass density is always less than the spacetime continuum density which itself is a limiting density that applies only to massless distortion displacements. Dilatations result in a dilatation of the spacetime continuum, with a resulting reduction in its local density in the dilatation.

We define ρ_ε as the effective spacetime continuum density inside the dilatation. In the case of a massless transverse distortion displacement, then $\varepsilon = 0$ and the effective STC density ρ_ε in this case is the same as the density of the spacetime continuum $\bar{\rho}_0$, *i.e.* $\rho_\varepsilon = \bar{\rho}_0$. As the volume dilatation ε increases, the effective STC density becomes increasingly smaller than the density of the spacetime continuum $\bar{\rho}_0$. The maximum reduction in the effective STC density occurs for the maximum dilatation $\varepsilon = 1$ for which the effective STC density ρ_ε is equal to the density of the spacetime continuum $\bar{\rho}_0 = 8\,\rho_{max}$ minus the maximum rest-mass density ρ_{max}, *i.e.* $\rho_\varepsilon = \bar{\rho}_0 - \rho_{max}$. Hence the smallest effective STC density ρ_ε is equal to $7\,\rho_{max}$ and the range of effective STC density ρ_ε is given by

$$\bar{\rho}_0 - \rho_{max} \equiv 7\,\rho_{max} \leq \rho_\varepsilon \leq 8\,\rho_{max} \equiv \bar{\rho}_0 \tag{19.49}$$

for the dilatation in the range $1 \geq \varepsilon \geq 0$ respectively, or numerically,

$$1.44 \times 10^{98}\,\mathrm{kg/m^3} \leq \rho_\varepsilon \leq 1.65 \times 10^{98}\,\mathrm{kg/m^3}\,. \tag{19.50}$$

This is illustrated graphically in the following table.

Object	Dilatation ε	Rest-mass $\rho\,(\mathrm{kg/m^3})$	Effective STC $\rho_\varepsilon\,(\mathrm{kg/m^3})$
Massless distortion	0	0	1.65×10^{98} $(\bar{\rho}_0)$
...			
Classical electron	4.7×10^{-85}	9.72×10^{12}	1.65×10^{98} $(\Delta \text{ in } 85^{\text{th}} \text{ digit})$
...			
Theoretical maximum	1	2.06×10^{97} (ρ_{max})	1.44×10^{98} $(\bar{\rho}_0 - \rho_{max})$

Table 19.1: Relation between volume dilatation, rest-mass density and effective STC density.

As seen previously, Blair [27, p. 3–4] pointed out that spacetime is an elastic medium that can support waves, but its extremely high stiffness means that extremely small amplitude waves have a very high energy density. This results in extremely small values of ε and correspondingly very high values of rest-mass density from (19.46). The effective STC

density ρ_ε is itself in the range of the density of the spacetime continuum $\bar{\rho}_0$. It is important to note that this is applicable to elementary particles. For macroscopic bodies, one has to consider that they are composed of elementary particles, and that the applicable mechanics are those that govern the aggregate bodies.

For example, using the classical radius of the electron, 2.82×10^{-15} m, and assuming a sphere, one gets a rest-mass density of $9.72\times10^{12}\,\mathrm{kg/m^3}$ and an $\varepsilon = 4.7\times10^{-85}$ for an electron. The effective STC density ρ_ε inside the electron is essentially the same as the density of the spacetime continuum $\bar{\rho}_0$, with a reduction only in the 85^{th} digit of $\bar{\rho}_0$. A more point-like electron will have a smaller radius, a larger rest-mass density and a larger ε. Still, the values of ε are extremely small, reflecting the extremely high stiffness of the spacetime continuum. Macroscopic bodies are composed of elementary particles and are governed by the applicable existing physical laws and ultimately by the spacetime continuum methods of the General Theory of Relativity.

§19.5 Dark matter and dark energy

As mentioned previously in section §2.5.1, we now return to the question of dark matter and dark energy, which is a major concern to modern cosmologists.

One of the major drivers of the concept of dark matter, the hypothetical unseen matter in the universe, has been the missing mass of the galaxies inferred from the difference between the visual mass of galaxies estimated from luminosity measurements and that measured from the rotational speed of stars in the galaxies. Numerous theories have been proposed to explain the galactic rotational curve problem [25, 158, 225, 350], ranging from exotic non-baryonic matter to MOND, a modification of Newton's theory. The dark matter to visible matter ratio in the universe is estimated to be about 5.5 [158, 290], so the discrepancy is substantial.

Recently, Heymann [158] has proposed an elegant resolution to the missing dark matter problem based on basic physical theory. The Newtonian inverse square law of gravitation is known to apply between masses based on the distance between their barycenters, and similarly applies to bodies in the case of spherical geometry (known as the shell theorem). Heymann notes that the shape of spiral galaxies is better approximated by a disk and in that case a correction factor η_{disk} must be applied to Newton's law which he shows numerically to be about

7.44 ± 0.83 at a 99% confidence interval

$$F = \eta_{disk}\, G\, \frac{Mm}{R^2} \tag{19.51}$$

where the symbols have their usual significance and

$$\eta_{disk} = \frac{1}{\pi} \int_{u=0}^{1} \int_{\alpha=0}^{2\pi} \frac{u - u^2 \cos\alpha}{(u^2 + 1 - 2u\cos\alpha)^{\frac{3}{2}}}\, du\, d\alpha\,. \tag{19.52}$$

This model could be tweaked to account for the arms of spiral galaxies (instead of a disk) and for the density profile across a cross-section of a spiral galaxy. These corrections would reduce the value of η_{disk} which currently overestimates the assumed dark matter to visible matter ratio in our galaxy by $\sim 35\%$.

A recent 2012 study of the European Southern Observatory on the presence of dark matter in our solar neighbourhood concluded:

> The most accurate study so far of the motions of stars in the Milky Way has found no evidence for dark matter in a large volume around the Sun... The amount of mass that we derive matches very well with what we see – stars, dust and gas – in the region around the Sun. But this leaves no room for the extra material – dark matter – that we were expecting. Our calculations show that it should have shown up very clearly in our measurements. But it was just not there! ... Theories predict that the average amount of dark matter in the Sun's part of the galaxy should be in the range 0.4–1.0 kilograms of dark matter in a volume the size of the Earth. The new measurements find 0.00 ± 0.07 kilograms of dark matter in a volume the size of the Earth. [118, 260]

Fundamental questions are still being raised about dark matter and dark energy [267]. The question of dark matter is being discussed in this book in relation to *STCED* as the question has been raised whether *STCED* can provide an answer to the mystery of dark matter.

§19.5.1 *Cosmological constant energy density*

In section §2.5.1, we saw how the introduction of the cosmological constant term $+\Lambda g_{\mu\nu}$ in Einstein's field equations is equivalent to introducing additional rest-mass energy density in the spacetime continuum. In section §19.2, we derived the density of the spacetime continuum $\bar{\rho}_0 = 1.7 \times 10^{98}\,\mathrm{kg/m^3}$ and found this value to be in the same ballpark as the vacuum energy density calculated by Carroll [52, see pp. 173] ($\sim 10^{112}\,\mathrm{ergs/cm^3}$) from quantum mechanical considerations.

Carroll [52, see pp. 174,358] also calculates the vacuum energy density from the cosmological constant ($\approx 10^{-8}\,\text{ergs/cm}^3$) required by current cosmological observations. Comparing the two values, he points out, leads to "the origin of the famous discrepancy of 120 orders of magnitude between the theoretical and observational values of the cosmological constant." Hence any postulated cosmological constant vacuum energy density does not provide an explanation for the required source of dark matter.

§19.5.2 *Spacetime continuum energy density*

From the theory of *STCED* derived in this book, it is also evident that the spacetime continuum energy density (19.17) is not the source of dark matter. Notwithstanding the 120 orders of magnitude discrepancy, any source of dark matter would be embedded as deformations in the spacetime continuum itself, and manifest itself solely as rest-mass energy density associated with dilatations in the spacetime continuum as given by (2.24), not the *STC* itself. This rest-mass energy density does not provide the necessary source of dark matter.

Hence it would seem that the Elastodynamics of the Spacetime Continuum cannot shed any light on the subject of dark matter and dark energy. This in itself is not surprising as *STCED* does not deal with the cosmological scale, which is the sole domain of the Theory of General Relativity as covered in §2.5.

Chapter 20

A Work in Progress

§20.1 A new spacetime physics theory

This book lays the foundations of a new theory of spacetime physics. *STCED* (Spacetime Continuum Elastodynamics) is a natural extension of Einstein's Theory of General Relativity. Whereas General Relativity concentrates on the curvature of the spacetime continuum, *STCED* analyses the deformations of the spacetime continuum resulting in its curvature. This gives rise to an integrated theory of gravitation and electromagnetism. At the microscopic level, *STCED* leads to the analysis of defects in the spacetime continuum, which gives rise to quantum physics. *STCED* is thus found to be a spacetime physics theory of gravitation, electromagnetism and quantum physics. This book lays the theoretical foundations of the Elastodynamics of the Spacetime Continuum, allowing physicists to study and perform research in this new area of spacetime physics.

§20.2 Physical explanations

The theory presented in this book provides physical explanations for many of the phenomena that are currently unexplained or only partially explained in physics. This spacetime physics theory of gravitation, electromagnetism and quantum physics is based on a linear elastic theory of the Elastodynamics of the Spacetime Continuum for the analysis of the deformations of the spacetime continuum. Quantum physics is tied to defects in the spacetime continuum.

This book provides an integrated physical explanation derived from *STCED* of numerous currently unexplained phenomena including:

Nature and properties of the spacetime continuum. The spacetime continuum of Einstein's Theory of General Relativity, from the macroscopic to the microscopic, is not an empty canvas, but rather has physical properties of its own. One can always create an empty underlying mathematical structure used to "measure" the deviations of the spacetime continuum from a reference state, but there is no doubt that the spacetime continuum of physical theory is characterized by physical dynamic properties. Einstein himself published similar statements. See section §1.1.

Demonstration of strained spacetime. The presence of the energy-momentum *stress* tensor in Einstein's field equations implies that forces are being applied to the spacetime continuum by the energy-momentum present in its structure. From continuum mechanics, we know that the application of stresses to the spacetime continuum must result in strains in its structure, hence the terminology *strained spacetime*. The strains present in the spacetime continuum result in the displacement of the elements of the spacetime continuum from equilibrium, corresponding to spacetime continuum deformations. See sections §1.1.1 and §1.1.2. In section §1.2, we demonstrate from first principles that spacetime is indeed strained by the presence of mass.

Stress-strain relation of the spacetime continuum. The introduction of strains in the spacetime continuum as a result of the energy-momentum stress tensor leads us to derive the stress-strain relation of the spacetime continuum, which is found to be similar to Einstein's field equations in structure. The stress-strain relation is linear, implying a linear elastic continuum that obeys Hooke's law. One of the consequences of linearity is that the principle of superposition is applicable, as observed in physical laws. See section §2.2.

Decomposition of the metric tensor. We solve a long-standing problem of general relativity. There is no straightforward definition of local energy density of the gravitational field in general relativity. This arises because the spacetime metric tensor includes both the background spacetime metric and the local dynamical effects of the gravitational field. No natural way of decomposing the spacetime metric tensor into its background and dynamical parts is known. We obtain a natural decomposition of the spacetime metric tensor into its background and dynamical parts. The dynamical part corresponds to the strains generated in the spacetime continuum by the energy-momentum stress tensor. See section §1.2.

Decomposition of spacetime tensor fields of rank 2. The decomposition of spacetime tensor fields can be done in many ways. The application of continuum mechanics to the spacetime continuum offers a natural decomposition of tensor fields, in terms of dilatations and distortions. A *dilatation* corresponds to a change of volume of the spacetime continuum without a change of shape while a *distortion* corresponds to a change of shape of the spacetime continuum without a change in volume. This decomposition of spacetime tensor fields of rank 2 in terms of dilatation and distortion components allows us to also

decompose relations involving these tensor fields into separate dilatation and distortion relations. See section §1.3.

Decomposition of the Ricci tensor. The Ricci tensor used in general relativity is separated into dilatation and distortion components, by applying the natural decomposition of spacetime continuum tensor fields of rank 2 as seen previously. From this, we show that this results in a separation of the field equations of general relativity into a dilatation relation and a distortion relation. This shows that the geometry of the spacetime continuum used in general relativity is generated by the combination of all deformations present in the spacetime continuum. We then evaluate these equations in the weak field approximation to show that the longitudinal dilatation mass relation leads to Poisson's equation for a newtonian gravitational potential, and that the transverse distortion wave relation leads to the linearized field equation of gravity in the Transverse Traceless gauge. Hence the results derived in *STCED* also apply to general relativity. See section §2.4.

Wave-particle duality. Every excitation of the spacetime continuum can be separated into a transverse (distortion) and a longitudinal (dilatation) mode of propagation. This decomposition of spacetime continuum deformations into a massive dilatation ("particle") and a massless transverse wave distortion ("wave") provides a mechanism for wave-particle duality. This provides an explanation of why dilatation-measuring apparatus measure the massive "particle" properties of the deformation, while distortion-measuring apparatus measure the massless transverse "wave" properties of the deformation. See section §2.2, section §3.3 and Chapter 12, in particular section §12.4.

Nature of rest-mass energy. The longitudinal mode of propagation involves an invariant change in volume of the spacetime continuum. Rest-mass energy, and hence matter, arises from this invariant volume dilatation of the spacetime continuum. The rest-mass energy is equivalent to the energy required to dilate the volume of the spacetime continuum. It is a measure of the energy stored in the spacetime continuum that is perceived as mass. The volume dilatation is an *invariant*, as is the rest-mass energy density. Mass is thus part of the spacetime continuum fabric itself. In essence, matter does not warp spacetime, but rather, matter *is* warped spacetime (*i.e.* dilated spacetime). The universe consists of the spacetime continuum and energy-momentum that propagates in it by deformation of its (*i.e. STC*) structure. See sections §2.3 and §5.5.1.

Definition of mass. Another important consequence of this relation is that it provides a definition of mass. The definition of mass is still one of the open questions in physics, with most authors adopting an indirect definition of mass based on the ratio of force to acceleration. However, mass is one of the fundamental dimensions of modern systems of units, and as such, should be defined directly, not indirectly. This is a reflection of the current lack of understanding of the nature of mass in modern physics. *STCED* provides a direct physical definition of mass: *mass is the invariant change in volume of spacetime in the longitudinal propagation of energy-momentum in the spacetime continuum.* See section §2.3 and §5.5.2.

Point particles. The fact that the mass of a particle corresponds to a finite spacetime volume dilatation $V_{\varepsilon s}$ shows that a singular "point" particle is not physically valid. All particles occupy a finite volume, even if that volume can be very small. Problems arising from point particles are thus seen to result from the abstraction of representing some particles as point objects. Instead, particles need to be given a finite volume to give physically realistic results and avoid invalid results.. See section §5.5.3.

Mach's principle. Mach's principle, a terminology first used by Einstein [282, p. 287], was not explicitly stated by Mach, and hence various takes on its statement exist. One of the better formulation holds that one can determine rotation and hence define inertial frames with respect to the fixed stars [365, see pp. 86–88]. By extension, inertia would then be due to an interaction with the average mass of the universe [365, see p. 17]. The macroscopic description of the gravitational field in terms of the curvature of the spacetime continuum results from the combination of the many microscopic displacements of the spacetime continuum from equilibrium. The source of the inertia is thus in the massive dilatation associated with each deformation, and Mach's principle (or conjecture as it is also known) is seen to be incorrect. See sections §5.5.5.

Dynamics of the spacetime continuum. The dynamics of the spacetime continuum is described by the *displacement wave equation*, which includes the accelerations from the applied forces. This equation can be separated into longitudinal and transverse components, which correspond to wave and particle displacement equations respectively, and hence include wave-particle duality in their formulation. See section §2.2 and section §2.3.

Nature of the graviton. We recall that the transverse mode of propagation involves no volume dilatation and is thus massless. The strain wave equation is a nonhomogeneous symmetric tensor field equation. The quanta of this tensor field are equivalent to massless transverse waves of spin 2 and massive particles of spin 0. This explains wave-particle duality, with the spin 2 transverse mode corresponding to the wave aspects and the spin 0 longitudinal mode corresponding to the particle aspects. The massless transverse waves of spin 2 are the gravitational waves of General Relativity with the corresponding graviton quanta. See section §3.6, in particular section §3.6.4.

Electromagnetic potential four-vector. The theory provides a physical explanation of the electromagnetic potential, which arises from transverse (shearing) displacements of the spacetime continuum, in contrast to mass which arises from longitudinal (dilatational) displacements of the spacetime continuum. Sheared spacetime is manifested as electromagnetic potentials and fields. The constant of proportionality φ_0 between the electromagnetic potential A^ν and the transverse displacement (perpendicular to the direction of motion) $u^\nu_\perp$ is referred to as the "*STC electromagnetic shearing potential constant*", and it has units of $[\mathrm{V}\cdot\mathrm{s}\cdot\mathrm{m}^{-2}]$ or equivalently [T]. See section §4.1.

Current density four-vector. The theory provides a physical explanation of the current density four-vector, which arises from the spacetime volume dilatation current (the dilatation current) which is given by the 4-gradient of the volume dilatation of the spacetime continuum. A corollary of this relation is that massless (transverse) waves cannot carry an electric charge. See section §4.5.

Maxwell's equations. Maxwell's equations are derived from the theory, and a generalization is obtained when a volume force X^ν is present in the spacetime continuum. The current density four-vector is the only quantity affected by the volume force, with the addition of a second term proportional to the volume force. See section §4.2.

Lorenz condition. The Lorenz condition is obtained directly from the theory. The reason for the value of zero is that transverse displacements are massless because such displacements arise from a change of shape (distortion) of the spacetime continuum, not a change of volume (dilatation). See section §4.4.

Electromagnetic waves. The transverse mode of propagation involves no volume dilatation and is thus massless. Electromagnetic

waves are transverse waves propagating in the spacetime continuum itself. These massless transverse waves are solutions of the rotational wave equation which is a nonhomogeneous antisymmetric tensor field equation equivalent to a massless vector wave equation. The quanta of the vector field are equivalent to massless spin 1 transverse waves. See section §3.6, in particular section §3.6.3, sections §5.5.6 and §5.5.7, and section §12.1.

Speed of light. Energy propagates through the spacetime continuum as deformations of the continuum. The maximum speed at which the transverse distortions can propagate through the spacetime continuum is c, the speed of light. See section §3.2.2, section §9.2 and section §15.1.

Electromagnetic mass. From *STCED*, we see that the concept of electromagnetic mass that was pursued in the nineteenth century is not valid as electromagnetism is transverse and massless, and has no massive longitudinal component. The charge density is a manifestation of the spacetime fabric itself, however it does not depend on the volume dilatation ε, only on its gradient, and it does not contribute to inertial mass. The electromagnetic field contributes to the particle's total energy, but not to its inertial mass which *STCED* shows originates in the particle's dilatation energy density (the mass longitudinal term) which is zero for the electromagnetic field. See sections §5.5, §5.5.6 and §5.5.7.

Special relativistic quadratic energy relation. This relation is derived from the strain energy density which is separated into a dilatation energy density term (the "mass" longitudinal term) and a distortion energy density term (the "massless" transverse term), which are quadratic terms. The kinetic energy pc is carried by the distortion part of the deformation, while the dilatation part carries only the rest-mass energy. See section §5.2.

Mass of the photon. The longitudinal strain energy density (mass term) of the electromagnetic field is calculated and found to be equal to 0. Hence the rest-mass energy density of the photon is zero, *i.e.* the photon is massless. The transverse strain energy density (massless term) of the electromagnetic field is calculated and found to be proportional to the sum of the square of the electromagnetic field energy density and the square of the Poynting vector. See section §5.3.

Poynting four-vector. By analogy with the current density four-vector $j^\nu = (c\varrho, \boldsymbol{j})$, where ϱ is the charge density, and $\boldsymbol{j}$ is the current

density vector, we define the Poynting four-vector $S^\nu = (cU_{em}, \boldsymbol{S})$ where U_{em} is the electromagnetic field energy density, and $\boldsymbol{S}$ is the Poynting vector. Furthermore, S^ν satisfies $\partial_\nu S^\nu = 0$ and $S_\nu S^\nu$ is an invariant, confirming that S^ν as defined is a four-vector. See section §5.4.

Location of electromagnetic field energy. The indefiniteness of the location of the field energy referred to by Feynman [122, see p. 27-6] is resolved: the electromagnetic field energy resides in the distortions (transverse displacements) of the spacetime continuum. See section §5.4.

Nature of photons. The strain energy density of the electromagnetic field includes a longitudinal electromagnetic energy flux which is massless as it is due to distortion, not dilatation, of the spacetime continuum. However, because this energy flux is along the direction of propagation (*i.e.* longitudinal), it gives rise to the photon, the particle aspect of the electromagnetic field. See section §5.4 and sections §12.2 and §12.3.

Nature of the wavefunction. The quantum mechanical wavefunction describes wave propagations in the spacetime continuum. These can be, depending on the particular wave equation considered, either longitudinal wave propagations corresponding to the volume dilatation associated with the particle property of an object, or transverse wave propagations corresponding to the wave property of an object. In general, the appropriate physical interpretation of $|\Psi|^2$ is that it represents the physical intensity (energy density) of the transverse (*distortion*) wave, rather than the probability density of quantum theory. It corresponds to the transverse field energy of the deformation. It is not the same as the particle, which corresponds to the longitudinal (*dilatation*) wave displacement and is localized within the deformation via the massive volume dilatation. However, $|\Psi|^2$ can be normalized with the system energy and converted into a probability density, thus allowing the use of the existing probabilistic formulation of quantum theory. Additionally, the physical intensity waves of *STCED* help us understand the physics of wave-particle duality and resolve the paradoxes of quantum theory. See section §7.3 and Chapter 12, in particular section §12.4.

Klein-Gordon-like equation. The longitudinal wave equation derived from a quantum mechanically derived volume force corresponds to a Klein-Gordon-like equation with a source term corresponding to an interaction term of the form $\boldsymbol{A} \cdot \boldsymbol{j}$. This term is interpreted in electromagnetism as energy in the static magnetic induction field to establish

the steady current distribution. It is also the form of the interaction term introduced in the vacuum Lagrangian for classical electrodynamics. See section §7.3.1.

Magnetic torque density equation. The transverse wave equation derived from a quantum mechanically derived volume force is a new equation of the electromagnetic field strength $F^{\mu\nu}$, which includes an interaction term of the form $\boldsymbol{A} \times \boldsymbol{j}$. In electromagnetism, this term is the volume density of the magnetic torque (magnetic torque density), and is interpreted as the "longitudinal tension" between two successive current elements (Helmholtz's longitudinal tension), observed experimentally by Ampère (hairpin experiment). See section §7.3.2.

Proca-like equation. The displacement wave equation in the case of a quantum mechanically derived volume force is similar to a Proca-like vector field equation. See sections §4.8 and §7.3.5.

Quantum physics and defects in the spacetime continuum. Dislocation and disclination defects in the spacetime continuum represent the fundamental displacement processes that occur in its structure. These fundamental displacement processes correspond to basic quantum phenomena and provide a framework for the description of quantum physics in *STCED*. *Dislocations* are translational deformations, while *disclinations* are rotational deformations. These provide a description of basic quantum processes in the microscopic description of the spacetime continuum. See section §8.1.

Spacetime continuum quantization. At the quantum level, we assume that the spacetime continuum has a granularity characterized by a length b_0 corresponding to the smallest elementary Burgers dislocation-displacement vector possible in the spacetime continuum. The calculated value of b_0 is found to be equivalent to the Planck length ℓ_P within the approximations of the derivation. The existence of a shortest length in nature leads to a natural cut-off to generate finite integrals in QED. The smallest elementary Burgers dislocation-displacement vector thus provides a lower bound in QED calculations. See section §14.2 and sections §19.1 and §19.2.

Nature of bosons and fermions. We find that dislocations and disclinations have fundamental properties that reflect those of particles at the quantum level. Dislocations are translational displacements that commute, satisfy the superposition principle and behave as bosons. Disclinations, on the other hand, are rotational displacements that do

not commute, do not obey the superposition principle and behave as fermions. Dislocations, as translational processes, are found to correspond to bosons, while disclinations, as rotational processes, are found to correspond to fermions, based on their characteristics and symmetry transformations. See sections §14.1 and §14.4.

Quantum particles as spacetime continuum defects. We find that dislocations and disclinations have fundamental properties that reflect those of particles at the quantum level. Dislocations, as translational processes, are found to correspond to bosons, while disclinations, as rotational processes, are found to correspond to fermions, based on their characteristics and symmetry transformations. See sections §14.1 and §14.4.

Screw dislocations and photons. Screw dislocations are translational displacements that commute, satisfy the superposition principle and behave as bosons. Screw dislocations in the spacetime continuum are massless, transverse deformations, and are hence identified specifically with photons. The speed of the transverse displacement is c, the speed of light. The field $\omega^{\mu\nu}$ is of spin 1, and since it is massless, it does not have a spin 0 component. From section §9.2.3, the rest-mass density of the screw dislocation is $\rho = 0$, and from section §9.2.4, so is its charge density $\varrho = 0$ and its current density $j^{\nu} = 0$. See sections §3.6, §9.2, §15.1, §18.1.1 and §18.3.1.

Edge dislocations and bosons. Edge dislocations are translational displacements that commute, satisfy the superposition principle and behave as bosons. Edge dislocations are equivalent to massive longitudinal wave solutions propagating along the direction of motion and massless transverse wave solutions. The quanta of the longitudinal waves are spin 0 massive particles, while the quanta of the massless transverse waves are of spin 2. This explains wave-particle duality, with the spin 2 transverse mode corresponding to the wave aspects and the spin 0 longitudinal mode corresponding to the particle aspects. The massless transverse waves of spin 2 are the gravitational waves of General Relativity with the corresponding graviton quanta. The total strain energy of edge dislocations gives the total energy of the bosons, as the sum of the longitudinal particle aspect of the bosons and the wave aspect of the bosons. As seen in Chapter 12, the latter is associated with the wavefunction of the boson. The spin characteristics of these are seen to correspond to a combination of spin 0 (mass as deformation particle aspect) and spin-2 (deformation wave aspect) solutions. There are also

longitudinal and transverse wave solutions of a Proca-like vector field equation, of spin 0 and 1 respectively, in the case of a non-zero volume force as is expected at the quantum level. See sections §3.6, §**??**, §7.3.5, §9.3, §15.2 and §18.1.1.

Wedge disclinations and quarks. Wedge disclinations, as rotational processes, are found to correspond to fermions, based on their characteristics and symmetry transformations. Both the longitudinal strain energy and the transverse strain energy are proportional to Λ^2 in the limit $\Lambda \gg b_c$. The parameter Λ is equivalent to the extent of the wedge disclination, and we find that as it becomes more extended, its strain energy is increasing parabolically. This behaviour is similar to that of quarks (confinement) which are fermions. In addition, as $\Lambda \to b_c$, the strain energy decreases and tends to 0, again in agreement with the behaviour of quarks (asymptotic freedom). We thus identify wedge disclinations with quarks. See sections §10.6, §15.3 and §18.1.2.

ℓ^3 twist disclinations and leptons. Splay disclinations, as rotational processes, are found to correspond to fermions, based on their characteristics and symmetry transformations. The longitudinal (massive) strain energy of the splay disclination is proportional to $\ln \Lambda/b_c$, as are the screw dislocation (photon) and edge dislocation (bosons). However, the transverse (massless) strain energy does not have this simpler dependence, but a more complicated functional dependence. This, and the results of the next subsection, leads us to identify the splay disclinations with the charged leptons (electron, muon, tau) fermions, where the heavier muon and tau are expected to be excited states of the electron. See sections §10.7, §15.4 and §18.1.2.

ℓ twist disclinations and neutrinos. Pure twist disclinations, as rotational processes, are found to correspond to fermions, based on their characteristics and symmetry transformations. The longitudinal strain energy of the pure twist disclination is equal to zero and hence massless. Since the pure twist disclination is a massless fermion, this leads us to identify the pure twist disclination with the neutrino. It should be noted that even though the mass of the neutrino is currently estimated to be on the order of 10's of eV, this estimate is based on assuming neutrino oscillation between the currently known three lepton generations, to explain the anomalous solar neutrino problem. This is still a tentative explanation. Until the anomaly is fully understood, we can consider the pure twist disclination physical model where the mass of the neutrino is zero to be at least a first approximation of the neutrino

STC defect model, subject to refinement as the nature of the anomalous solar neutrino problem is better understood. See sections §10.7, §15.4 and §18.1.2.

Identification of quantum particles summary. The identification of the quantum particles based on their associated spacetime defects is summarized in the following table (see §18.1.3). See sections §18.1 and §18.1.3.

STC defect	Type of particle	Particles
Screw dislocation	Massless boson	Photon
Edge dislocation	Massive boson	Spin-0 particle
		Spin-1 Proca eqn
		Spin-2 graviton
Wedge disclination	Massive fermion	Quarks
ℓ^3 twist disclination	Massive fermion	Leptons
ℓ twist disclination	Massless fermion	Neutrino

Nature of QED interactions. Strain energy is the fundamental defining energy characteristic of defects and their interactions in the spacetime continuum. In *STCED*, the interaction of dislocations and disclinations is mediated through the interaction of their strain energy density. We find that this interaction of the strain energy density results from the overlap of the strain energy densities of defects, a process akin to the wavefunction overlap of quantum mechanics, which is physically explained by this process in *STCED*. The calculation of time-dependent dislocation strain energy involves polylogarithms which also arise in Feynman diagram integrals (and, in particular, in the computation of quantum electrodynamics corrections to the electron gyromagnetic ratio). This is a further indication that the interaction of strain energies are the physical source of quantum interaction phenomena described by Feynman diagrams. See section §14.5, sections §16.1.2 and §16.2.2 and section §17.1.

Nature of virtual particles. In *STCED*, the role played by virtual particles in quantum electrodynamics (QED) is replaced by the interaction of the strain energy density of the dislocations and disclinations. As stated by Weingard [366], "the question of the existence of

virtual particles is really the question of how to interpret the propagators which appear in the perturbation expansion of vacuum expectation values (scattering amplitudes)". The exchange of virtual particles in interactions can be seen to be a perturbation expansion representation of the forces resulting from the overlap of the defects' strain energy density. QED is a perturbative theory, and the virtual particles are introduced as an interpretation of the perturbative expansion represented by Feynman diagrams. See section §14.5.

Explanation of Feynman diagrams. The basic Feynman diagrams can be seen to represent screw dislocations as photons, edge dislocations as bosons, twist and wedge disclinations as fermions, and their interactions. More specifically, the external legs of Feynman diagrams that are on mass-shell representing real particles correspond to dislocations and disclinations, while the virtual off mass-shell particles are replaced by the interaction of the strain energy densities. The Feynman diagram propagators are replaced by the defect strain energy density interaction expressions. See section §18.2.

Explanation of photon-photon scattering. In QED, photon-photon interactions are known as photon-photon scattering and are thought to be mediated by virtual particles. This reflects the perturbative calculation used to evaluate the scattering, but as shown in this work, photon-photon interactions physically result from the overlap of their strain energy density, and can be calculated directly. See section §18.3.1.

Explanation of photon-neutrino interactions. It is surprising to find that the massless, electrically neutral, weakly interacting neutrino would interact with the massless, electrically neutral, electromagnetic interacting photon. *STCED* provides for their interaction via the force resulting from the interaction of the strain energy densities of screw dislocations and pure twist disclinations, which correspond to photon-neutrino interactions. See section §18.3.2.

QED self-energies. The dislocation self-energy is related to the dislocation self-force. The dislocation self-force arises from the force on an element in a dislocation caused by other segments of the *same* dislocation line. This process provides an explanation for the QED self-energies without the need to resort to the emission/absorption of virtual particles. It can be understood, and is particular to, dislocation dynamics as dislocations are defects that extend in the spacetime continuum. See section §18.5.

QED mass renormalization. Mass renormalization arises in QED due to the incomplete description of particle energies at the quantum level. In this book, we show that the strain energy density of an edge dislocation, which corresponds to a particle, consists of a longitudinal dilatation mass density term and a transverse distortion energy density term. QED, in its formulation, only uses the transverse distortion strain energy density in its calculations, which is referred to as the bare mass m_0. However, there is no dilatation mass density term used in QED, and hence no possibility of properly deriving the mass. The bare mass m_0 is thus renormalized by replacing it with the actual experimental mass m. Using the longitudinal dilatation mass density term provides the correct mass m and eliminates the need for mass renormalization. See sections §18.6 and §18.7.

Non-locality of quantum phenomena. Defects in the spacetime continuum give rise to nonlocal effects. Discrete line defects extend in the spacetime continuum, and hence interact nonlocally, much as nonlocal interactions between distant atoms determine the properties of materials in solid-state physics. See section §18.8.

Entangled states in quantum physics. As noted in §18.5, the physical extension of defects in the spacetime continuum gives rise to nonlocal effects and to what are referred to as "entangled states" in quantum physics. Entangled states correspond to the overlap of defects in the spacetime continuum, overlaps that can extend between distant defects, and are characterized by the interaction of their strain energy densities. See section §18.9 and in particular sections §13.5 and §13.6.

Spacetime continuum constants. Based on the identification of screw dislocations in the spacetime continuum with photons, the relation between the Burgers constant b_0 and Planck's constant h is determined. Planck's constant is expressed in terms of the spacetime continuum constants. The calculated value of b_0 is found to be equivalent to the Planck length ℓ_P within the approximations of the derivation. Numerical values of the spacetime constants are derived and a consistent set of analytical forms of the spacetime constants is proposed. See sections §19.1 and §19.2.

Nature of Action in the spacetime continuum. We elucidate the nature of Action in the spacetime continuum. Energy applies to three-dimensional space, while Action applies to four-dimensional spacetime, where it has a role in four-dimensional spacetime similar to energy in three-dimensional space. We thus find that Action is the fun-

damental four-dimensional spacetime scalar quantity corresponding to energy for three-dimensional space. This helps explain why equations of motion are determined by minimizing action, not energy, using the principle of least (or stationary) action. See section §19.3.

§20.3 Evolution of the theory

A solid foundation of a new theory of spacetime physics, the theory of the Elastodynamics of the Spacetime Continuum has been laid, from which further development can be achieved. This book lays the theoretical foundations of Spacetime Continuum Elastodynamics (*STCED*), to encourage physicists to study and perform research in this new area of spacetime physics.

The underlying principle of this theory is that the spacetime continuum is the source and the seat of all physical processes. The dynamics of the spacetime continuum is represented by the energy-momentum propagating as deformations in its structure. This thread is the guiding principle in the development of *STCED*.

Certainly much progress has been achieved towards this goal, but, however, more, much more, remains to be developed. Suggested future directions of investigation and areas of exploration to extend the theory include as candidates worthy of further study:

- Detailed application and calculations using the theoretical developments derived in this book.
- Exploration of alternative volume forces X^ν derived from other identifications of related physical results.
- Development of the theory in Einstein-Cartan spaces beyond the preliminary incorporation of torsion considered in this book, based on Élie Cartan's differential forms formulation.
- Further derivation of quantum electrodynamics results based on the presence of defects, such as dislocations and disclinations, in the spacetime continuum.
- Extension of the theory based on the evolution of Continuum Mechanics in the last one hundred years, including Eshelbian Mechanics [230] and the Mechanics of Generalized Continua [4].

Further development of *STCED* is expected to provide additional insight into the fundamental nature of the spacetime continuum and of physical theory.

Glossary of Physical Symbols

This book uses symbols across the fields of continuum mechanics, elasticity, general relativity, electromagnetism and quantum mechanics. The symbols used need to be applicable across these disciplines and be self-consistent. A glossary of the physical symbols is included below to facilitate the reading of this book.

α	Fine-structure constant.
α	Reciprocal of Lorentz gamma-factor.
α_l	Reciprocal of Lorentz longitudinal gamma-factor.
α_2	Reciprocal of Lorentz half-velocity gamma-factor.
$\bar{\alpha}_0$	Reduced $\bar{\mu}_0$ constant.
$\alpha^{\mu\nu}$	Dislocation density.
$\bar{\beta}_0$	Reduced $\bar{\mu}_0 + \bar{\lambda}_0$ constant.
$\beta^{\mu\nu}$	Distortion tensor.
${}^*\beta^{\mu\nu}$	Effective distortion tensor.
$\not{\beta}^{\mu\nu}$	Defect distortion tensor.
γ	Lorentz gamma-factor.
γ_l	Lorentz longitudinal gamma-factor.
γ_2	Lorentz half-velocity gamma-factor.
$\bar{\gamma}_0$	Reduced $\bar{\lambda}_0$ constant.
$\Gamma^{\lambda}{}_{\mu\nu}$	Connection coefficient.
$\Gamma_{\mu\nu\lambda}$	Modified connection coefficient.
$\delta^{\mu\nu}$	Kronecker delta.
$\epsilon^{\alpha\beta\mu\nu}$	Permutation symbol in four-dimensional spacetime.
ϵ_0	Electromagnetic permittivity of free space (STC).
ε	Volume dilatation.
$\varepsilon^{\mu\nu}$	Strain tensor.
${}^*\varepsilon^{\mu\nu}$	Effective strain tensor.
$\not{\varepsilon}^{\mu\nu}$	Defect strain tensor.
$\eta_{\mu\nu}$	Flat spacetime or Minkowski metric tensor.
$\theta^{\mu\nu}$	Disclination density.

$\Theta^{\mu\nu}$	Symmetric electromagnetic stress tensor.
$\bar{\kappa}_0$	Bulk modulus of the STC.
$\kappa^{\mu\nu}$	Bend-twist tensor.
${}^*\kappa^{\mu\nu}$	Effective bend-twist tensor.
$\not{\kappa}^{\mu\nu}$	Defect bend-twist tensor.
λ	Wavelength.
λ	Quantum mechanical hidden variable.
$\bar{\lambda}_0$	Lamé elastic constant of the STC.
λ_c	Compton wavelength of the electron.
Λ	Cutoff parameter corresponding to the extent of a defect.
$\bar{\mu}_0$	Shear modulus Lamé elastic constant of the STC.
μ_0	Electromagnetic permeability of free space (STC).
μ_B	Bohr magneton.
$\{\mu\nu, \lambda\}$	Christoffel symbol of the first kind.
$\left\{ {}_{\mu\ \nu}^{\lambda} \right\}$	Christoffel symbol of the second kind.
ν	Frequency.
ν	Poisson ratio.
(ξ, η, ζ)	Cartesian coordinates.
ξ^ν	Dislocation line direction.
ξ^ν	Dilatation current.
ρ	Rest-mass density.
$\bar{\rho}_0$	STC density.
ϱ	Charge density.
σ^{ij}	Cauchy stress tensor / Maxwell stress tensor.
$\sigma^{\mu\nu}$	Stress tensor.
υ	Dilatation/wavefunction proportionality constant.
ϕ	Electromagnetic scalar potential.
φ_0	STC electromagnetic shearing potential constant.
Φ	Static newtonian gravitational field.
ω^ν	Rotation or spin vector.
$\omega^{\mu\nu}$	Rotation tensor.
${}^*\omega^{\mu\nu}$	Effective rotation tensor.
$\not{\omega}^{\mu\nu}$	Defect rotation tensor.

Ω^{ν}	Frank vector.
Ω^{ν}	Reduced Frank vector.
$\Omega^{\mu\nu}$	Associated Frank rotation tensor.
ψ	Quantum mechanical wavefunction.
Ψ	Multi-component quantum mechanical wavefunction.
Ψ	Energy density of the transverse (*distortion*) wave.
$\boldsymbol{A}$	Vector potential.
A^{μ}	Four-vector potential.
$\underline{A}^{*\,\nu}$	Reduced four-vector potential..
b_0	*STC* elementary Burgers displacement vector.
b_c	Size of defect core.
b^{ν}	Burgers four-vector.
$\hbar^{\nu}$	Reduced Burgers vector.
b_{ij}	Eshelby stress tensor.
$\boldsymbol{B}$	Magnetic field.
c	Speed of light.
c_l	Speed of longitudinal waves.
c_t	Speed of transverse waves equivalent to the speed of light.
$\boldsymbol{D}$	Electric displacement field.
D_r	Disclinations (rotation) consisting of { Screw , Edge }.
D_t	Dislocations (translation) consisting of { Wedge , Twist }.
e	Electrical charge of the electron.
e_s	Strain scalar.
$e^{\mu\nu}$	Strain deviation tensor.
$e^{\alpha\beta\mu\nu}$	Covariant Levi-Civita pseudotensor.
$\boldsymbol{E}$	Electric field.
$\hat{E}$	Total energy density.
$\mathcal{E}$	Strain energy density.
$\mathcal{E}_{\parallel}$	Dilatation strain energy density.
$\mathcal{E}_{\perp}$	Distortion strain energy density.
$E^{\mu\nu\alpha\beta}$	Elastic moduli tensor of the *STC*.
$\boldsymbol{F}$	Interaction force.
$\mathbf{F}(\mathbf{r}, t)$	Riemann-Silberstein electromagnetic vector.

$F^{\mu\nu}$	Electromagnetic field strength tensor.
g^i	Momentum density vector.
$g_{\mu\nu}$	Metric tensor.
G	Gravitational constant.
$G^{\mu\nu}$	Einstein tensor in General Relativity.
$G^{\mu\nu}$	Einstein tensor in Riemann-Cartan space.
$\bar{G}_{\mu\nu}$	Einstein tensor in Riemann space.
h	Planck's constant.
$\hbar$	Reduced Planck's constant.
$h_{\mu\nu}$	Perturbation of the flat spacetime metric tensor.
H	Total energy density.
$i^{\mu\nu}$	Incompatibility tensor.
$\boldsymbol{j}$	Current density vector.
j^{μ}	Current density four-vector.
$\underline{j}^{*\nu}$	Reduced current density four-vector.
$\bar{k}_0$	Elastic force constant of the STC volume force.
k_L	STC longitudinal dimensionless ratio.
k_T	STC transverse dimensionless ratio.
$\boldsymbol{k}$	Wavevector.
k^{ν}	Wavevector four-vector.
$K^{\lambda}{}_{\mu\nu}$	Contortion tensor.
$K_{\mu\nu\lambda}$	Modified contortion tensor.
ℓ	Length of a defect.
ℓ_P	Planck length.
L	Disclination line (axis).
$\mathrm{Li}_n(x)$	Polylogarithm function.
L	Lagrangian.
$\mathcal{L}$	Lagrangian density.
m	Mass of the electron.
$\boldsymbol{p}$	Momentum 3-vector.
$\hat{p}$	Momentum density.
P^{ν}	Energy-momentum four-vector.
$\mathbb{P}$	Projection operator.

Q	Total charge.
(r, θ, φ)	Spherical polar coordinates.
(r, θ, z)	Cylindrical polar coordinates.
r_s	Ricci scalar.
$r^{\mu\nu}$	Ricci deviation tensor.
R	Contracted Ricci curvature tensor.
$\boldsymbol{R}$	Defect separation.
$R^{\mu\nu}$	Ricci curvature tensor.
$R^{\mu}{}_{\nu\alpha\beta}$	Curvature tensor.
s^j	Energy flux vector.
$\mathcal{S}$	Action.
S_0	STC elementary quantum of action.
$\boldsymbol{S}$	Poynting vector (electromagnetic field energy flux).
S^{μ}	Poynting four-vector.
$S^{\lambda}{}_{\mu\nu}$	Torsion tensor.
$S_{\mu\nu\lambda}$	Modified torsion tensor.
t_s	Stress scalar.
$t^{\mu\nu}$	Stress deviation tensor.
T	Contracted energy-momentum stress tensor.
$T^{\mu\nu}$	Energy-momentum stress tensor.
u^{μ}	Displacement four-vector.
$u_{\parallel}{}^{\mu}$	Longitudinal displacement four-vector.
$u_{\perp}{}^{\mu}$	Transverse displacement four-vector.
U_{em}	Electromagnetic field energy density.
$\boldsymbol{v}$	Velocity.
W	Strain energy.
$W_{\parallel}$	Dilatation strain energy.
$W_{\perp}$	Distortion strain energy.
W_{12}	Interaction strain energy.
(x, y, z)	Cartesian coordinates.
x^{μ}	Position four-vector.
X^{ν}	Volume (or body) force.
Z_0	Characteristic impedance of the vacuum (STC).

Bibliography

1. Achenbach J. D. Wave Propagation in Elastic Solids. Elsevier, Amsterdam, 1975.
2. Aharoni J. The Special Theory of Relativity, 2nd rev. ed. Dover Publications, New York, (1965) 1985, ch. 5.
3. Aharonov Y., Rohrlich D. Quantum Paradoxes: Quantum Theory for the Perplexed. Wiley-Vch, Weinheim, 2005.
4. Altenbach H., Maugin G. A., Erofeev V., eds. Mechanics of Generalized Continua. Springer-Verlag, Berlin, 2011.
5. Arndt M., Nairz O., Vos-Andreae J., Keller C., van der Zouw G., Zeilinger A. Wave-particle duality of C_{60} molecules. *Nature*, 1999, v. 401, 680–682.
6. Aspect A, Dalibard J. and Roger G. Experimental test of Bell's inequalities using time-varying analyzers. *Phys. Rev. Lett.*, 1982, v. 49, 1804–1807.
7. Aspect A. and Grangier P. *Hyp. Int.*, 1987, v. 37, 3.
8. Aspect A. In Miller A. I., ed. Sixty-Two Years of Uncertainty. Plenum, New York, 1990, pp. 45–59.
9. Auletta G. Foundations and Interpretation of Quantum Mechanics. World Scientific Publishing, Singapore, 2001.
10. Auyang S. Y. How is Quantum Field Theory Possible? Oxford University Press, Oxford, 1995.
11. Bailey J., Borer K., Combley F., Drumm H., Krienen F., Lange F., Picasso E., von Ruden W., Farley F. J. M., Field, J. H., Flegel, W., Hattersley P. M. Measurements of Relativistic Time Dilatation for Positive and Negative Muons in a Circular Orbit. *Nature*, 1977, v. 268, 301–305.
12. Ballentine L. E. Quantum Mechanics: A Modern Development. World Scientific Publishing, Singapore, 1998.
13. Balluffi R. W. Introduction to Elasticity Theory for Crystal Defects. Cambridge University Press, Cambridge, 2012.
14. Barut A. O. Electrodynamics and Classical Theory of Fields and Particles. Dover Publications, New York, 1980.
15. Barut A. O., van der Merwe A. and Vigier J.-P. Quantum, Space and Time – The Quest Continues. Cambridge University Press, Cambridge, 1983.
16. Basar Y., Weichert D. Nonlinear Continuum Mechanics of Solids: Fundamental Mathematical and Physical Concepts. Springer, Berlin, 2000.

17. Baylis W. E. Electrodynamics: A Modern Geometric Approach. Birkhäuser, Boston, 2002.
18. Bell J. S. Speakable and Unspeakable in Quantum Mechanics. Cambridge University Press, Cambridge, 1987.
19. Bell J. S. On the Einstein–Podolsky–Rosen Paradox. *Physics*, 1964, v. 1, 195–200. Reprinted in Bell J. S. Speakable and Unspeakable in Quantum Mechanics. Cambridge University Press, Cambridge, 1987, pp. 14–21.
20. Bell J. S. How to Teach Special Relativity. *Progress in Scientific Culture*, 1976, v. 1 (2). Reprinted in Bell J. S. Speakable and Unspeakable in Quantum Mechanics. Cambridge University Press, Cambridge, 1987, pp. 67–80.
21. Bell J. S. On the Impossible Pilot Wave. *Foundations of Physics*, 1982, v. 12, 989–999. Reprinted in Bell J. S. Speakable and Unspeakable in Quantum Mechanics. Cambridge University Press, Cambridge, 1987, pp. 159–168.
22. Belli S., Bonsignori R., D'Auria G., Fant L., Martini M. and Peirone S. Entangling macroscopic diamonds at room temperature: Bounds on the continuous-spontaneous-localization parameters. arXiv: quant-ph/1601.07927v3.
23. Berdichevsky V. L. Variational Principles of Continuum Mechanics I – Fundamentals. Springer-Verlag, Berlin, 2009.
24. Berdichevsky V. L. Variational Principles of Continuum Mechanics II – Applications. Springer-Verlag, Berlin, 2009.
25. Bergström L. Non-Baryonic Dark Matter: Observational Evidence and Detection Methods. *Reports on Progress in Physics*, 2000, v. 63 (5), 793–841. arXiv: hep-ph/0002126.
26. Bethe H. A. and Salpeter E. E. Quantum Mechanics of One- and Two-Electron Atoms. Plenum Publishing Corp., New York, NY, 1977.
27. Blair D. G., ed. The Detection of Gravitational Waves. Cambridge University Press, Cambridge, 1991.
28. Bohm D. A Suggested Interpretation of the Quantum Theory in Terms of "Hidden" Variables I, II. *Physical Review*, 1952, v. 85, 166-–179, 180–193.
29. Bohr N. Can Quantum Mechanical Description of Reality Be Considered Complete? *Phys. Rev.*, 1935, v. 48, 696.
30. Boi L. The Quantum Vacuum. The John Hopkins University Press, Baltimore, 2011.
31. Borzou A. and Sepangi H. R. Unification of Gravity and Electromagnetism Revisited. arXiv: gr-qc/0904.1363v3.
32. Bramm P. J. How Empty is the Vacuum? In Saunders S. and Brown H. R., eds. The Philosophy of Vacuum. Clarendon Press, Oxford, 2002, pp. 280–285.

33. Brans C. and Dicke R. H. Mach's Principle and a Relativistic Theory of Gravitation. *Physical Review*, 1961, vol. 124 (3), 925–935.
34. Brekhovskikh L. M., Goncharov V. Mechanics of Continua and Wave Dynamics, 2nd ed. Springer-Verlag, Berlin, 1994.
35. Brigham E. O. The Fast Fourier Transform. Prentice-Hall Inc., Englewood Cliffs, New Jersey, 1974.
36. Brown H. R. and Harré R. Philosophical Foundations of Quantum Field Theory. Clarendon Press, Oxford, 1988, p. 3.
37. Brown H. Physical Relativity: Spacetime Structure from a Dynamical Perspective. Oxford University Press, Oxford, 2005.
38. Bruno N., Martin A., Sekatski P., Sangouard N., Thew R. T. and Gisin N. Displacement of entanglement back and forth between the micro and macro domains. *Nature Physics Letters*, 2013, DOI: 10.1038/NPHYS2681, 1–4.
39. Bulatov V. V. and Cai W. Computer Simulation of Dislocations. Oxford University Press, Oxford, 2006.
40. Burgers J. M. *Proc. Kon. Ned. Akad. Wetenschap.*, 1939, v. 42, 293, 378.
41. Byalinicki-Birula I. Photon Wave Function. In Wolf E., ed. Progress in Optics XXXVI. Elsevier, Amsterdam, 1996, 245–294. arXiv: quant-ph/0508202v1.
42. Byalinicki-Birula I. On the Wave Function of the Photon. *Acta Physica Polonica A*, 1994, v. 86, 97–116.
43. Byalinicki-Birula I. *Acta Physica Polonica A*, 1995, v. 34, 885.
44. Byalinicki-Birula I. The Photon Wave Function. In Eberly J. H., Mandel L., Wolf E., eds. Coherence and Quantum Optics VII. Plenum, New York, 1996, 313–294.
45. Byalinicki-Birula I. Photon as a Quantum Particle. *Acta Physica Polonica B*, 2006, v. 37 (3), 935–946.
46. Callahan J. J. The Geometry of Spacetime: An Introduction to Special and General Relativity. Springer, New York, 2000.
47. Cao T. Y. Conceptual Developments of 20th Century Field Theories. Cambridge University Press, Cambridge, 1997.
48. Cao T. Y., ed. Conceptual Foundations of Quantum Field Theory. Cambridge University Press, Cambridge, 2004.
49. Cao T. Y. From Current Algebra to Quantum Chromodynamics: A Case for Structural Realism. Cambridge University Press, Cambridge, 2010.
50. Capusso V., Fortunato D. and Selleri F. Generic quantum nonlocality. *Int.J. Theor. Phys.*, 1973, v. 7, 319.
51. Carcione J. M. Wave Fields in Real Media: Wave Propagation in Anisotropic, Anelastic, Porous and Electromagnetic Media, 2nd ed. rev. and ext. Elsevier, Amsterdam, 2007.

52. Carroll S. M. Spacetime and Geometry: An Introduction to General Relativity. Addison Wesley, San Francisco, 2004.

53. Cartan É. On Manifolds with an Affine Connection and the Theory of General Relativity. Bibliopolis, Napoli, (1922,1955) 1986.

54. Cartwright M. Fourier Methods for Mathematicians, Scientists and Engineers. Ellis Norwood Ltd, London, 1990.

55. Chaikin P. M. and Lubensky T. C. Principles of Condensed Matter Physics. Cambridge University Press, Camvridge, 1995.

56. Chandrasekar N. Quantum Mechanics of Photons. *Adv. Studies Theor. Phys.*, 2012, v. 6 (8), 391–397.

57. Chandrasekharaiah D. S.. Debnath L. Continuum Mechanics. Academic Press, Boston, 1994.

58. Chang Y.-F. Unification of Gravitational and Electromagnetic Fields in Riemannian Geometry. arXiv: gen-ph/0901.0201v1.

59. Charap J. M. Covariant Electrodynamics: A Concise Guide. The John Hopkins University Press, Baltimore, 2011.

60. Chen X.-S., Zhu B.-C. Physical decomposition of the gauge and gravitational fields. arXiv: gr-qc/1006.3926v3.

61. Chen X.-S., Zhu B.-C. Tensor gauge condition and tensor field decomposition. arXiv: gr-qc/1101.2809v5.

62. Chernitskii A. A. On Unification of Gravitation and Electromagnetism in the Framework of a General-Relativistic Approach. arXiv: gr-qc/0907.2114v1.

63. Ciarlet P. G. An Introduction to Differential Geometry with Applications to Elasticity. Springer, Dordrecht, 2005.

64. Ciufolini I. and Wheeler J. A. Gravitation and Inertia. Princeton University Press, Princeton, 1995.

65. Combley F., Farley F. J. M., and Picasso E. The CERN Muon $(g-2)$ Experiments. *Physics Reports (Review Section of Physics Letters)*, 1981, v. 68 (2), 93–119.

66. Constantinescu A., Korsunsky A. Elasticity with Mathematica: An Introduction to Continuum Mechanics and Linear Elasticity. Cambridge University Press, Cambridge, 2007.

67. Cook D. M. The Theory of the Electromagnetic Field. Dover Publications, New York, 2002.

68. Corda C. The Mössbauer Rotor Experiment and the General Theory of Relativity. arXiv: gr-qc/1602.04212.

69. d'Espagnat B. Reality and the Physicist: Knowledge, Duration and the Qauntum World. Cambridge University Press, Cambridge, 1989.

70. d'Espagnat B. On Physics and Philosophy. Princeton University Press, Princeton, 2006.
71. Value for "dry air" from "Molecular number density" table in Wikipedia under entry "Number density", accessed 10 March 2018.
72. Dauxois T., Peyrard M. Physics of Solitons. Cambridge University Press, Cambridge, 2006.
73. Davies P. C. W. Quantum Mechanics. Routledge, London, 1984; quoted in Hughes R. I. G. The Structure and Interpretation of Quantum Mechanics. Harvard University Press, Cambridge, 1989.
74. Davis J. L. Mathematics of Wave Propagation. Princeton University Press, Princeton, 2000.
75. de Broglie L. Non-Linear Wave Mechanics. Elsevier Publishing, Amsterdam, 1960.
76. de Broglie L. Les incertitudes d'Heisenberg et l'interprétation probabiliste de la Mécanique Ondulatoire. Gauthier-Villars, Paris, 1982. Available in English: Heisenberg's Uncertainties and the Probabilistic Interpretation of Wave Mechanics. Kluwer Academic Publishers, Dordrecht, 1990.
77. deWit R. Linear Theory of Static Disclinations. in Simmons J. A. and deWit R., Bullough R, eds. Fundamental Aspects of Dislocation Theory, Conference Proceedings, National Bureau of Standards, April 21-25, 1969. National Bureau of Standards, Special Publication 317, Volume I, Washington, DC, 1970, pp. 651–673.
78. deWit R. Theory of Disclinations: II. Continuous and Discrete Disclinations in Anisotropic Elasticity. Journal of Research of the National Bureau of Standards – A. Physics and Chemistry, 1973, vol. 77A (1), pp. 49–100.
79. deWit R. Theory of Disclinations: III. Continuous and Discrete Disclinations in Isotropic Elasticity. Journal of Research of the National Bureau of Standards – A. Physics and Chemistry, 1973, vol. 77A (3), pp. 359–368.
80. deWit R. Theory of Disclinations: IV. Straight Disclinations. Journal of Research of the National Bureau of Standards – A. Physics and Chemistry, 1973, vol. 77A (5), pp. 607–658.
81. Deser S. Covariant decomposition of symmetric tensors and the gravitational Cauchy problem. *Annales de l'I.H.P., Section A*, 1967, vol. 7 (2), 149–188.
82. Diner S., Fargue D., Lochak G. and Selleri F. The Wave-Particle Dualism: A Tribute to Louis de Broglie on his 90th Birthday. D. Reidel Publishing, Dordrecht, 1984.
83. Dirac P. A. Lectures on Quantum Mechanics. Dover Publications, New York, (1964) 2001.

84. Dixon W. G. Special Relativity: The Foundation of Macroscopic Physics. Cambridge University Press, Cambridge, 1982, ch. 3.

85. Dodd R. K., Eilbeck J. C., Gibbon, J. D., Morris H. C. Solitons and Nonlinear Wave Equations. Academic Press, London, 1984.

86. Dolde F., Jakobi I., Naydenov B., Zhao N., Pezzagna N. Trautmann C., Meijer J., Neumann P., Jelezko F., and Wrachtrup J. Room-temperature entanglement between single defect spins in diamond. *Nature Physics Letters*, 2013, DOI: 10.1038/NPHYS2545, 139–143.

87. Doughty, N. A. Lagrangian Interaction: An Introduction to Relativistic Symmetry in Electrodynamics and Gravitation. Westview Press, Reading, MA, 1990.

88. Drumheller D. S. Introduction to Wave Propagation in Nonlinear Fluids and Solids. Cambridge University Press, Cambridge, 1998.

89. Duncan A. The Conceptual Framework of Quantum Field Theory. Oxford University Press, Oxford, 2012.

90. Dürr D., Teufel, S. Bohmian Mechanics: The Physics and Mathematics of Quantum Theory. Springer-Verlag, Berlin, 2009.

91. Eddington A. S. Space, Time & Gravitation. Cambridge University Press, Cambridge, (1920) 1987.

92. Eddington A. S. The Mathematical Theory of Relativity. Cambridge University Press, Cambridge, 1957.

93. Edelen, D. G. B. and Lagoudas D. C. Gauge Theory and Defects in Solids. North-Holland Publishing, Amsterdam, 1988.

94. Einstein A. Zur Electrodynamik bewegter Körper. *Annalen der Physik*, 1905, vol. 17. English translation (On the Electrodynamics of Moving Bodies) reprinted in Lorentz H. A., Einstein A., Minkowski H, and Weyl H. The Principle of Relativity: A Collection of Original Memoirs on the Special and General Theory of Relativity. Dover Publications, New York, 1952, pp. 37–65.

95. Einstein A. Ist die Trägheit eines Körpers von seinem Energiegehalt abhängig? *Annalen der Physik*, 1905, vol. 17. English translation (Does the Inertia of a Body Depend upon its Energy-Content?) reprinted in Lorentz H. A., Einstein A., Minkowski H, and Weyl H. The Principle of Relativity: A Collection of Original Memoirs on the Special and General Theory of Relativity. Dover Publications, New York, 1952, pp. 69–71.

96. Einstein A. Kosmologische Betrachtungen zur allgemeinen Relativitätstheorie. *Sitzungsberichte der Preussischen Akad. d. Wissenschaften*, 1917, vol. 17, pp. 142–152. English translation (Cosmological Considerations on the General Theory of Relativity) reprinted in Lorentz H. A., Einstein A., Minkowski H, and Weyl H. The Principle of Relativity: A Collection of Original Memoirs on the Special and General Theory of Relativity. Dover Publications, New York, 1952, pp. 175–188.

97. Einstein A. Die Grundlage der allgemeinen Relativitätstheorie. *Annalen der Physik*, 1916, vol. 49. English translation (The Foundation of the General Theory of Relativity) reprinted in Lorentz H. A., Einstein A., Minkowski H, and Weyl H. The Principle of Relativity: A Collection of Original Memoirs on the Special and General Theory of Relativity. Dover Publications, New York, 1952, pp. 109–164.

98. Einstein A. Dialog über Einwande gegen die Relativitätstheorie. *Die Naturwissenschaften*, 1918, vol. 6, pp. 697–702. English translation in Kostro L. Einstein and the Ether. Apeiron, Montreal, 2000, p. 76.

99. Einstein A. Relativity: The Special and the General Theory. Crown Publishers, New York, 1961.

100. Einstein A, Podolsky B. and Rosen N. Can Quantum-Mechanical Description of Physical Reality Be Considered Complete? *Phys. Rev.*, 1935, v. 47, 777–780.

101. Engelbrecht J. Nonlinear Wave Dynamics. Kluwer Academic Publishers, Dordrecht, 1997.

102. Roll P. G., Krotkov R., and Dicke R. H. The Equivalence of Inertial and Passive Gravitational Mass. *Annals of Physics*, 1964, vol. 26, 442–517.

103. Epstein M. The Geometrical Language of Continuum Mechanics. Cambridge University Press, Cambridge, 2010, pp. 323–335.

104. Eringen A. C., ed. Continuum Physics Volume I – Mathematics. Academic Press, New York, 1971.

105. Eringen A. C., ed. Continuum Physics Volume II – Continuum Mechanics of Single-Substance Bodies. Academic Press, New York, 1975.

106. Eringen A. C., ed. Continuum Physics Volume III – Mixtures and EM Field Theories. Academic Press, New York, 1976.

107. Eringen A. C., ed. Continuum Physics Volume IV – Polar and Nonlocal Field Theories. Academic Press, New York, 1976.

108. Eringen A. C., Suhubi, E. S. Elastodynamics Volume I – Finite Motions. Academic Press, New York, 1974.

109. Eringen A. C., Suhubi, E. S. Elastodynamics Volume II – Linear Theory. Academic Press, New York, 1975.

110. Eringen A. C., Maugin, G. A. Electrodynamics of Continua I – Foundations and Solid Media. Springer-Verlag, New York, 1990.

111. Eringen A. C., Maugin, G. A. Electrodynamics of Continua II – Fluids and Complex Media. Springer-Verlag, New York, 1990.

112. Eringen A. C. Nonlocal Continuum Field Theories. Springer-Verlag, New York, 2002.

113. Eshelby J. D. Elastic Inclusions and Inhomogeneities. *Progr. Solid Mechanics*, 1961, v. 2, 89–140.

114. Eshelby J. D. Energy Relations and the Energy-Momentum Tensor in Continuum Mechanics. in Kanninen M. F., Adler W. F., Rosenfield A. R. and Jaffee R. I., eds. Inelastic Behavior of Solids. McGraw-Hill, New York, 1970, pp. 77–115.

115. Eshelby J. D. The Elastic Energy-Momentum Tensor. *Journal of Elasticity*, 1975, v. 5, 321–335.

116. Eshelby J. D. The Energy-Momentum Tensor of Complex Continua. in Kröner, E. and Anthony K.-H., eds. Continuum Models of Discrete Systems. University of Waterloo Press, Waterloo, 1980, pp. 651–665.

117. Eshelby J. D. Aspects of the Theory of Dislocations. in Hopkins H. G. and Sewell M. J., eds. Mechanics of Solids – The Rodney Hill 60th Anniversary Volume.Pergamon Press, Oxford, 1982, pp. 185–225.

118. European Southern Observatory. Serious Blow to Dark Matter Theories? Press Release eso 1217, 18 April 2012.

119. Ferrarese G.; Bini D. Introduction to Relativistic Continuum Mechanics. Springer, New York, 2008.

120. Feynman R. P. Space-Time Approach to Non-Relativistic Quantum Mechanics. *Rev. Mod. Phys.*, 1948, v. 20, 367–387. Reprinted in Schwinger, J., ed. Selected Papers on Quantum Electrodynamics. Dover Publications, New York, 1958, pp 321–341.

121. Feynman R. P. The Concept of Probability in Quantum Mechanics. Lecture, 1951.

122. Feynman R. P., Leighton R. B., Sands M. Lectures on Physics, Volume II: Mainly Electromagnetism and Matter. Addison-Wesley Publishing Company, Reading, Massachusetts, 1964.

123. Feynman R. P., Leighton R. B., Sands M. Lectures on Physics, Volume III: Quantum Mechanics. Addison-Wesley Publishing Company, Reading, Massachusetts, 1965.

124. Feynman R. P., Morinigo R. B., Wagner W. G., Hatfield, B., ed. Feynman Lectures on Gravitation. Westview Press, Boulder, CO, 2003.

125. Fine A. The Shaky Game: Einstein Realism and the Quantum Theory, 2^{nd} ed. The University of Chicago Press, Chicago, 1996.

126. Flügge W. Tensor Analysis and Continuum Mechanics. Springer-Verlag, New York, 1972.

127. Frank F. C. *Disc. Faraday Soc.*, 1958, v. 25, 19.

128. Friedlander F. G. The Wave Equation on a Curved Space-Time. Cambridge University Press, Cambridge, 1975.

129. Friedman M. Foundations of Space-Time Theories: Relativistic Physics and Philosophy of Science. Princeton University Press, Princeton, 1983.

130. Fuchs C. A. Information Gain vs. State Disturbance in Quantum Theory. arXiv: quant-ph/9605014.

131. Pitalúa-García D. Quantum information causality. arXiv: quant-ph/1210.1943v3.

132. Georgi H. Tensor Lie Algebras in Particle Physics. Benjamin/Cummings, 1982.

133. Gisin N. Bell's inequality holds for all non-product states. *Phys. Lett. A*, 1991, v. 154, 201.

134. Goenner H. F. M. Mach's Principle and Theories of Gravitation. In Barbour J. B., Pfister, H., Eds. Mach's Principle: From Newton's Bucket to Quantum Gravity. Birkhäuser, Boston, 1995, pp. 442–457.

135. Goldstein S., Norsen T., Tausk D. V., Zanghi N. Bell's Theorem. *Scholarpedia*, 2011, v. 6 (10), 8378.

136. Goldstein S. Bohmian Mechanics. *The Stanford Encyclopedia of Philosophy*, 2013, http://plato.stanford.edu/archives/spr2013/entries/qm-bohm/.

137. Gouesbet G. Hidden Worlds in Quantum Physics. Dover Publications, New York, 2013, pp. 280–303.

138. Graff K. F. Wave Motion in Elastic Solids. Dover Publications, New York, 1975.

139. Grangier P., Roger G. and Aspect A. *Europhys. Lett.*, 1986, v. 1, 173.

140. Greenstein G. and Zajonc A. G. The Quantum Challenge, Modern Research on the Foundations of Quantum Mechanics. Jones and Bartlett Publishers, Sudbury, Mass., 1997.

141. Greiner W. Relativistic Quantum Mechanics: Wave Equations. Springer-Verlag, New York, 1994.

142. Griffiths R. B. Consistent Quantum Theory. Cambridge University Press, Cambridge, 2002, pp. 323–335.

143. Guo W. J., Fan D. H. & Wei L. F. Experimentally testing Bell's theorem based on Hardy's nonlocal ladder proofs. *Sci China-Phys Mech Astron*, 2015, v. 58, 024201-1–5.

144. Gurtin M. E. An Introduction to Continuum Mechanics. Academic Press, San Diego, 1981.

145. Hafele J. C. and Keating R. E. Around-the-World Atomic Clocks: Predicted Relativistic Time Gains. *Science*, 1972, v. 177, 166–168.

146. Hafele J. C. and Keating R. E. Around-the-World Atomic Clocks: Observed Relativistic Time Gains. *Science*, 1972, v. 177, 168–170.

147. Hansson J. On the Origin of Elementary Particle Masses. *Progress in Physics*, 2014, v. 10, 45–47.

148. Hardy L. Nonlocality for Two Particles without Inequalities for Almost All Entangled States. *Phys. Rev. Lett.*, 1993, v. 71, 1665–1668.

149. Harrison W. A. Electronic Structure and the Properties of Solids. Dover Publications, New York, 1989.

150. Hasselbach F. Recent Contributions of Electron Interferometry to Wave-Particle Duality. In Selleri F., ed. Wave-Particle Duality. Plenum, New York, 1992, 109–125.

151. Hayat A., Ginzburg P. and Orenstein, M. High-rate entanglement source via two-photon emission from semiconductor quantum wells. *Physical Review B*, 2001, v. 76, 035339.

152. Hayes W., Stoneham A. M. Defects and Defect Processes in Nonmetallic Solids. Dover Publications, New York, (1985) 2004.

153. Heinbockel J. H. Introduction to Tensor Calculus and Continuum Mechanics. Trafford Publishing, Victoria, BC, 2001.

154. Heisenberg W. Über den anschaulichen Inhalt der quantentheoretischen Kinematik und Mechanik. *Zeit. für Phys.*, 1927, v. 43, 172–98; quoted in Hughes R. I. G. The Structure and Interpretation of Quantum Mechanics. Harvard University Press, Cambridge, 1989.

155. Heitler W. The Quantum Theory of Radiation, 3rd ed. Dover Publications, New York, 1984.

156. Herbst T., Scheidl T., Fink M., Handsteiner J., Wittmann B., Ursin R. and Zeilinger A. Teleportation of Entanglement over 143 km. arXiv: quant-ph/1403.0009v3.

157. Hetnarski R. B., Ignaczak J. The Mathematical Theory of Elasticity, 2nd ed. CRC Press, Boca Raton, 2011.

158. Heymann Y. Dark Matter, the Correction to Newton's Law in a Disk. *Progress in Physics*, 2016, v. 12, 347–352.

159. Hirth R. M. and Lothe J. Theory of Dislocations, 2nd ed. Krieger Publishing Co., Florida, 1982.

160. Holland P. R. The Quantum Theory of Motion: An Account of the de Broglie-Bohm Causal Interpretation of Quantum Mechanics. Cambridge University Press, Cambridge, 1993.

161. Holzapfel G. A. Nonlinear Solid Mechanics: A Continuum Approach for Engineering. John Wiley & Sons, New York, 2000.

162. Home D. Conceptual Foundations of Quantum Physics, An Overview from Modern Perspectives. Plenum Press, New York, 1997.

163. Home D., Whitaker A. Einstein's Struggles with Quantum Theory, A Reappraisal. Springer, New York, 2007.

164. Home D. and Selleri F. *J. Phys. A*, 1991, v. 24, L1073.

165. Home D. and Selleri F. *Riv. Nuov. Cim.*, 1991, v. 14 (9), 1.

166. Horie K. Geometric Interpretation of Electromagnetism in a Gravitational Theory with Space–Time Torsion. arXiv: hep-th/9409018v1.

167. Hossenfelder S. Phenomenology of Space-time Imperfection I: Nonlocal Defects. arXiv: hep-ph/1309.0311.

168. Hossenfelder S. Phenomenology of Space-time Imperfection II: Local Defects. arXiv: hep-ph/1309.0314.

169. Hossenfelder S. Theory and Phenomenology of Spacetime Defects. arXiv: hep-ph/1401.0276.

170. Hudson J. A. The Excitation and Propagation of Elastic Waves. Cambridge University Press, Cambridge, 1980.

171. Hughes R. I. G. The Structure and Interpretation of Quantum Mechanics. Harvard University Press, Cambridge, 1989.

172. Hull D. and Bacon D. J. Introduction to Dislocations, 5^{th} ed. Elsevier Ltd., Amsterdam, 2011.

173. Hunter G., Jeffers S. and Vigier J.-P. Causality and Locality in Modern Physics. Kluwer Academic Publishers, Dordrecht, 1998.

174. Infeld E. and Rowlands G. Nonlinear Waves, Solitons and Chaos. Cambridge University Press, Cambridge, 1992.

175. Jabs A. Connecting Spin and Statistics in Quantum Mechanics. arXiv: quant-ph/0810.2300v4.

176. Jackson J. D. Classical Electrodynamics, 2^{nd} ed. John Wiley & Sons, New York, 1975.

177. Jaeger G. Entanglement, Information, and the Interpretation of Quantum Mechanics. Springer-Verlag, Berlin, 2009.

178. Jammer M. Concepts of Mass in Classical and Modern Physics. Dover Publications, New York, (1961) 1997.

179. Jammer M. Concepts of Space: The History of Theories of Space in Physics, 3^{rd} enlarged ed. Dover Publications, New York, 1993.

180. Jammer M. Concepts of Mass in Contemporary Physics and Philosophy. Princeton University Press, Princeton, 2000.

181. Jaramillo J. L., Gourgoulhon E. Mass and Angular Momentum in General Relativity. arXiv: gr-qc/1001.5429v2.

182. Jaynes E. T. Clearing Up Mysteries – The Original Goal. In Skilling J., ed. Proceedings Volume, Maximum Entropy and Bayesian Methods. Kluwer Academic Publishers, Dordrecht, 1989, pp. 1–27.

183. Jaynes E. T. Probability in Quantum Theory. In Zurek W. H., ed. Complexity, Entropy and the Physics of Information. Addison Wesley Publishing, Reading, MA, 1990.

184. Jaynes E. T., Bretthorst G. L. (ed.) Probability Theory; The Logic of Science. Cambridge University Press, Cambridge, 2003.

185. Jeffreys H. Scientific Inference. Cambridge University Press, Cambridge, 1931.

186. Jeffreys H. Theory of Probability. Oxford University Press, Oxford, 1939.

187. Joos E., Zeh H. D., Kiefer C., Giulini D., Kupsch J., Stamtescu I.-O. Decoherence and the Appearance of a Classical World in Quantum Theory, Second Edition. Springer-Verlag, Berlin, 2003.

188. Kadic A., Edelen D. G. B. A Gauge Theory of Dislocations and Disclinations. Springer-Verlag, Berlin, 1983.

189. Kaku M. Quantum Field Theory: A Modern Introduction. Oxford University Press, Oxford, 1993, p. 10.

190. Karl G., Novikov V. Photon-neutrino interactions. *Journal of Experimental and Theoretical Physics Letters*, 2005, v. 81 (6), 249–254. arXiv: hep-ph/04111746v1.

191. Kennard E. H. Zur Quantenmechanik einfacher Bewegungstypen. *Zeit. für Phys.*, 1927, v. 44, 326–352.

192. Kholmetskii A. L., Yarman T. and Missevitch O. V. Kündig's Experiment on the Transverse Doppler Shift Re-analyzed. *Phys. Scr.*, 2008, v. 77, 035302–035306.

193. Kholmetskii A. L., Yarman T., Missevitch O. V. and Rogozev B. I. A Mössbauer Experiment in a Rotating System on the Second-order Doppler Shift: Confirmation of the Corrected Result by Kündig. *Phys. Scr.*, 2009, v. 79, 065007.

194. Kholmetskii A. L., Yarman T., Missevitch O. V. and Rogozev B. I. Mössbauer Experiments in a Rotating System on the Time Dilation Effect. *Int. J. Phys. Sci.*, 2011, v. 6, 84–92.

195. Yarman T., Kholmetskii A. L., Arik M., Akku, B., Öktem Y., Susam A., Missevitch O. V. Novel Mössbauer Experiment in a Rotating System and the Extra Energy Shift Between Emission and Absorption Lines. arXiv: physics.gen-ph/1503.05853.

196. Yarman T., Kholmetskii A. L., Arik M. Mössbauer Experiments in a Rotating System: Recent Errors and Novel Interpretation. *The European Physical Journal Plus*, 2015, v. 130, 191.

197. Kholmetskii A. L., Yarman T., Yarman O., Arik M. Unabridged Response to "The Mössbauer Rotor Experiment and the General Theory of Relativity" by C. Corda: General Relativity Cannot Supply an Answer to the Extra Time Dilation in Rotor Mössbauer Experiments. arXiv: physics.gen-ph/1610.04219.

198. Kittel C. Introduction to Solid State Physics. John Wiley and Sons, New York, 1971.

199. Kleinert H. Gauge Fields in Condensed Matter, Vol. II Stresses and Defects. World Scientific Publishing, Singapore, 1989.

200. Kleinert H. Multivalued Fields in Condensed Matter, Electromagnetism, and Gravitation. World Scientific Publishing, Singapore, 2008.

201. Kleman M., Friedel J. Disclinations, Dislocations and Continuous Defects: A Reappraisal. arXiv: cond-mat.soft/0704.3055v1.

202. Kolsky H. Stress Waves in Solids. Dover Publications, New York, 1963.

203. Kosevich A. M. Crystal Dislocations and the Theory of Elasticity. in Nabarro F. R. N., ed. Dislocations in Solids, Volume I: The Elastic Theory. North-Holland Publishing Co., New York, 1979, pp. 33–141.

204. Kostro L. Einstein and the Ether. Apeiron, Montreal, 2000

205. Kreyszig E. Advanced Engineering Mathematics, 3rd ed. John Wiley and Sons, New York, 1972, pp. 134–146.

206. Kröner, E. Gauge Field Theories of Defects. Discussion Meeting, Max-Planck Institut für Festkoörperforschung und Metallforschung, Stuttgart, 1982.

207. Krupka D. The Trace Decomposition Problem. *Contributions to Algebra and Geometry*, 1995, vol. 36 (2), 303–315.

208. Kuhn T. S. The Structure of Scientific Revolutions, 2nd enlarged ed. Methuen & Co, London, 1971.

209. Kündig W. *Phys. Rev.*, 1963, v. 129, 2371.

210. Lamas-Linares A., Howell J. C. and Boowmeester, D. Stimulated emission of polarization-entangled photons. *Nature*, 2001, v. 412, 887–890.

211. Landau L. D., Lifshitz E. M., Kosevich A. M. and Pitaevskii L. P. Theory of Elasticity, 3rd ed., revised and enlarged. Butterworth-Heinemann, Oxford, 1986, pp. 108–132.

212. Lange M. An Introduction to the Philosophy of Physics: Locality, Fields, Energy, and Mass. Blackwell Publishing, Malden, MA, 2002.

213. La Rosa A. Introduction to Quantum Mechanics. Portland State University Lecture Notes, Portland, 2017, Chapter 12, Quantum Entanglement.

214. Lawden D. F. Tensor Calculus and Relativity. Methuen & Co, London, 1971.

215. Lazar M. Twist Disclination in the Field Theory of Elastoplasticity. arXiv: cond-mat.mtrl-sci/0304519v2.

216. Lazar M., Anastassiadis C. The Gauge Theory of Dislocations: Static Solutions of Screw and Edge Dislocations. arXiv: cond-mat.mtrl-sci/0802.0670v3.

217. Lee K. C., Sprague M. R., Sussman B. J., Nunn J., Langford N. K., Jin X. M., Champion T., Michelberger P., Reim K. F., England D., Jaksch D., Walmsley I. A. Entangling macroscopic diamonds at room temperature. *Science*, 2011, v. 334 (6060), 1253—1256.

218. Leinaas J. M. Non-Relativistic Quantum Mechanics. University of Oslo Lecture Notes, Oslo, 2003.

219. Loudon R. The Quantum Theory of Light, 3rd ed. Oxford University Press, Oxford, 2000.

220. Love A. E. R. A Treatise on the Mathematical Theory of Elasticity, 4th ed. Dover Publications, New York, 1944.

221. Lucas J. R. & Hodgson P. E. Spacetime & Electromagnetism: An Essay on the Philosophy of the Special Theory of Relativity. Clarendon Press, Oxford, 1990.

222. Lukin M. D. Nonlinear Optics and Quantum Entanglement of Ultra-Slow Single Photons. arXiv: quant-ph/9910094.

223. Macken J. A. The Universe is Only Spacetime, Rev. 7.1. Self-published, Santa Rosa, CA, 2013, p. 4-24.

224. Maluf J. W., Goya A. Space-Time Defects and Teleparallelism. arXiv: gr-qc/0110107.

225. Mannheim P. D. Alternatives to Dark Matter and Dark Energy. arXiv: astro-ph/0505266v2.

226. Margenau H. The Nature of Physical Reality. McGraw Hill, New York, 1950; quoted in Hughes R. I. G. The Structure and Interpretation of Quantum Mechanics. Harvard University Press, Cambridge, 1989.

227. Marklund M., Shukla P. K. Nonlinear Collective Effects in Photon–Photon and Photon–Plasma Interactions. *Rev. Mod. Phys.*, 2006, v. 78, 591–637. arXiv: hep-ph/0602123.

228. Marsden J. E. and Hughes T. J. R. Mathematical Foundations of Elasticity. Dover Publications, New York, (1983) 1994.

229. Maugin G. Material Inhomogeneities in Elasticity. Chapman & Hall / CRC, Boca Raton, 1993.

230. Maugin G. A. Configurational Forces: Thermomechanics, Physics, Mathematics, and Numerics. CRC Press, New York, 2011.

231. Maugin G. A. Nonlinear Waves in Elastic Crystals. Oxford University Press, Oxford, 1999.

232. Mehra J. Einstein, Physics and Reality. World Scientific Publishing, Singapore, 1999.

233. Meuren S., Keitel C. H. and Di Piazza A. Nonlinear neutrino-photon interactions inside strong laser pulses. arXiv: hep-ph/1504.02722v1.

234. Miklowitz J. The Theory of Elastic Waves and Waveguides. North-Holland Publishing, Amsterdam, 1978.

235. Miller J. P., de Rafael E., and Roberts B. L. Muon $(g-2)$: Experiment and Theory. *Rep. Prog. Phys.*, 2007, v. 70, 7953–881.

236. Millette P. A. and Varshni Y. P. New asymptotic expression for the average lifetime of hydrogenic levels. *Can. J. Phys.*, 1979, v. 57, 334–5.

237. Millette P. A. The Heisenberg Uncertainty Principle and the Nyquist-Shannon Sampling Theorem. *Progress in Physics*, 2013, v. 9 (3), 9–14. arXiv: quant-ph/1108.3135.

238. Millette P. A. Elastodynamics of the Spacetime Continuum. *The Abraham Zelmanov Journal*, 2012, vol. 5, 221–277.

239. Millette P. A. On the Decomposition of the Spacetime Metric Tensor and of Tensor Fields in Strained Spacetime. *Progress in Physics*, 2012, vol. 8 (4), 5–8.

240. Millette P. A. The Elastodynamics of the Spacetime Continuum as a Framework for Strained Spacetime. *Progress in Physics*, 2013, vol. 9 (1), 55–59.

241. Millette P. A. Derivation of Electromagnetism from the Elastodynamics of the Spacetime Continuum. *Progress in Physics*, 2013, vol. 9 (2), 12–15.

242. Millette P. A. Strain Energy Density in the Elastodynamics of the Spacetime Continuum and the Electromagnetic Field. *Progress in Physics*, 2013, vol. 9 (2), 82–86.

243. Millette P. A. Dilatation–Distortion Decomposition of the Ricci Tensor. *Progress in Physics*, 2013, vol. 9 (4), 32–33.

244. Millette P. A. Wave-Particle Duality in the Elastodynamics of the Spacetime Continuum (STCED). *Progress in Physics*, 2014, vol. 10 (4), 255–258.

245. Millette P. A. Dislocations in the Spacetime Continuum: Framework for Quantum Physics. *Progress in Physics*, 2015, vol. 11 (4), 287–307.

246. Millette P. A. The Burgers Spacetime Dislocation Constant b_0 and the Derivation of Planck's Constant. *Progress in Physics*, 2015, vol. 11 (4), 313–316.

247. Millette P. A. On the Applicability of Bell's Inequality. *Progress in Physics*, 2016, vol. 12 (3), 211–215.

248. Millette P. A. On Time Dilation, Space Contraction and the Question of Relativistic Mass. *Progress in Physics*, 2017, v. 13 (4), 200–203.

249. Millette P. A. On the Question of Acceleration in Special Relativity. *Progress in Physics*, 2017, vol. 13 (4), 215–219.

250. Millette P. A. Bosons and Fermions as Dislocations and Disclinations in the Spacetime Continuum. *Progress in Physics*, 2018, vol. 14 (1), 10–18.

251. Millette P. A. On the Classical Scaling of Quantum Entanglement. *Progress in Physics*, 2018, vol. 14 (3), 121–130.

252. Millette P. A. QED Mass Renormalization, Vacuum Polarization and Self-Energies in the Elastodynamics of the Spacetime Continuum (STCED). *Progress in Physics*, 2018, vol. 14 (4), 197–202.

253. Millette P. A. The Origin of Inertia in the Spacetime Continuum. *Progress in Physics*, 2019, vol. 15 (2), 86–91.

254. Millette P. A. Elastodynamics of the Spacetime Continuum: A Spacetime Physics Theory of Gravitation, Electromagnetism and Quantum Physics. American Research Press, Rehoboth, NM, 2017.

255. Milonni P. W. The Quantum Vacuum: An Introduction to Quantum Electrodynamics. Academic Press, San Diego, 1994.

256. Milton K A. The Casimir Effect: Physical Manifestations of Zero-Point Energy. World Scientific Publishing, Singapore, 2001.

257. Minkowski H. Space and Time. 80^{th} *Assembly of German Natural Scientists and Physicians*. Cologne, 21 September 1908. English translation reprinted in Lorentz H. A., Einstein A., Minkowski H, and Weyl H. The Principle of Relativity: A Collection of Original Memoirs on the Special and General Theory of Relativity. Dover Publications, New York, 1952, pp. 73–91.

258. Misner C. W., Thorne K. S., Wheeler J. A. Gravitation. W.H. Freeman and Company, San Francisco, 1973.

259. Mohr P. J. Solutions of the Maxwell Equations and Photon Wave Functions. *Annals of Physics*, 2010, v. 325, 607–663.

260. Moni Bidin C.; Carraro G.; Méndez R.A.; Smith R. Kinematical and Chemical Vertical Structure of the Galactic Thick Disk. II, A Lack of Dark Matter in the Solar Neighborhood. *Astrophysical Journal*, 2012, v. 751, 30.

261. Morse M. M., Feshback H. Methods of Theoretical Physics, Part I. Feshback Publishing, Minneapolis, (1953) 1981, pp.322–323.

262. Müller-Kirsten H.W. Electrodynamics: An Introduction Including Quantum Effects. World Scientific Publishing, Singapore, 2004.

263. Nabarro F. R. N., ed. Dislocations in Solids, Volume I: The Elastic Theory. North-Holland Publishing Co., New York, 1979.

264. Nabarro F. R. N., ed. Dislocations in Solids, Volume V: Disclinations. North-Holland Publishing Co., New York, 1980.

265. Nabarro F. R. N. Theory of Crystal Dislocations. Dover Publications, New York, 1987.

266. Nairz O., Arndt M., and Zeilinger A. Quantum interference experiments with large molecules. *American Journal of Physics*, 2003, v. 71, 319—325.

267. Nielsen J. T., Guffanti A. & Sarkar S. Marginal Evidence for Cosmic Acceleration from Type Ia Supernovae. *Scientific Reports*, 2016, Art. no. 35596, DOI 10.1038.

268. Nolan P.J. The Fundamentals of the Theory of Relativity. Farmingdale State College, New York, pp. 7-2, 7-13.

269. Novozhilov V. V. Foundations of the Nonlinear Theory of Elasticity. Dover Publications, New York, (1953) 1999.

270. Oas G. On the Abuse and Use of Relativistic Mass. arXiv: physics.ed-ph/0504110v2.

271. Oas G. On the Use of Relativistic Mass in Various Published Works. arXiv: physics.ed-ph/0504111.

272. Ogden R. W. Non-linear Elastic Deformations. Dover Publications, New York, (1984) 1997.

273. Okun L. B. The Concept of Mass. *Physics Today*, 1989, v. 42 (6), 31–36.

274. Okun L. B. The Einstein Formula: $E_0 = mc^2$. "Isn't the Lord Laughing?". *Physics–Uspekhi*, 2008, v. 51 (5), 513–527. arXiv: physics.hist-ph/0808.0437.

275. Okun L. B. Energy and Mass in Relativity Theory. World Scientific, New Jersey, 2009.

276. Omnès R. The Interpretation of Quantum Mechanics. Princeton University Press, Princeton, 1994.

277. Oppenheim A. V. and Willsky A. S., Signals and Systems. Prentice-Hall Inc., Englewood Cliffs, New Jersey, 1983.

278. Orowan E. *Z. Phys.*, 1934, v. 89, 605, 634.

279. Padmanabhan T. Gravitation, Foundations and Frontiers. Cambridge University Press, Cambridge, 2010.

280. Padmanabhan T. Quantum Field Theory: The Why, What and How. Springer, Cham, 2016.

281. Patwardhan A. V. Neutrino-photon interactions in vacuum and material media. University of California at San Diego, Paper 2013S-215C-Patwardhan-Amol, 2013.

282. Pais A. 'Subtle is the Lord...': The Science and the Life of Albert Einstein. Oxford University Press, Oxford, 1982.

283. Pauli W. The Connection Between Spin and Statistics. *Phys. Rev.*, 1940, v. 58, 716–722. Reprinted in Schwinger, J., ed. Selected Papers on Quantum Electrodynamics. Dover Publications, New York, 1958, pp 372–378.

284. Pawlowski M., Paterek T., Kaszlikowski D., Scarani V., Winter A. and Zukowski M. Information causality as a physical principle. *Nature Letters*, 2009, vol. 461, doi:10.1038/nature08400, T101–104.

285. Penrose R. and Isham C. J. Quantum Concepts in Space and Time. Clarendon Press, Oxford, 1986.

286. Peskin M. E., Schroeder D. V. An Introduction to Quantum Field Theory. Westview Press, Boulder, CO, 1995.

287. Petkov V. Relativity and the Nature of Spacetime, 2nd ed. Springer, New York, 2009, pp. 111–114.

288. Petkov V. Inertia and Gravitation: From Aristotle's Natural Motion to Geodesic Worldlines in Curved Spacetime. Minkowski Institute Press, Montreal, 2012, pp. 78–82.

289. Hubbell J. H. Photon Cross-Sections, Attenuation Coefficients, and Energy Absorption Coefficients from 10 keV to 100 GeV. Nat. Bur. Stand. (US) Report NSRDS-NBS-29, Washington DC, 1969, pp. 45–46.

290. Planck collaboration. Planck 2013 results. I. Overview of products and scientific results. *Astronomy and Astrophysics*, 2014, v. 571, Table 10.

291. Polanyi M. *Z. Phys.*, 1934, v. 89, 660.

292. Polyanin A. D. Handbook of Linear Partial Differential Equations for Engineers and Scientists. Chapman & Hall/CRC, New York, 2002.

293. Popescu S. and Rohrlich D. Generic quantum nonlocality. *Phys. Lett. A*, 1992, v. 166, 293.

294. Popper K. R. Quantum Theory and the Schism in Physics. Rowan and Littlefield, Totowa, NJ, 1982; quoted in Hughes R. I. G. The Structure and Interpretation of Quantum Mechanics. Harvard University Press, Cambridge, 1989.

295. Poruchikov V. B. Methods of the Classical Theory of Elastodynamics. Springer-Verlag, Berlin, 1993.

296. Powell J. L., Crasemann B. Quantum Mechanics. Addison-Wesley Publishing, Reading, MA, 1961.

297. Puntigam R. A., Soleng H. H. Volterra Distortions, Spinning Strings, and Cosmic Defects. *Class. Quantum Grav.*, 1997, v. 14, 1129–1149. arXiv: gr-qc/9604057.

298. Rabounski D. A Theory of Gravity Like Electrodynamics. *Progress in Physics*, 2005, v. 1 (2), 15–29.

299. Rabounski D. Declaration of Academic Freedom (Scientific Human Rights). *Progress in Physics*, 2006, v. 2 (1), 57–60.

300. Rapp D. Quantum Mechanics. Holt, Rinehart and Winston, New York, 1971.

301. Raymer M. G., Smith B. J. The Maxwell Wave Function of the Photon. *Proc. SPIE*, 2005, v. 5866, 293. arXiv: quant-ph/0604169.

302. Smith B. J., Raymer M. G. Two-Photon Wave Mechanics. *Phys. Rev. A* 2006, v. 74 062104. arXiv: quant-ph/0605149v3.

303. Smith B. J., Raymer M. G. Photon Wave Functions, Wave-Packet Quantization of Light, and Coherence Theory. *New Journal of Physics*, 2007, v. 9, 414. arXiv: 0708.0831.

304. Reichenbach H. The Philosophy of Space & Time. Dover Publications, New York, (1927) 1957.

305. Reddy J. N. Principles of Continuum Mechanics: A Study of Conservation Principles with Applications. Cambridge University Press, Cambridge, 2010, p. 151.

306. Ringbauer M., Fedrizzi A., Berry D. W. and White A. G. Information Causality in the Quantum and Post-Quantum Regime. arXiv: quant-ph/1406.5034v2.

307. Rousseaux G. On the interaction between a current density and a vector potential: Ampère force, Helmholtz tension and Larmor torque. hal.archives-ouvertes.fr/docs/00/08/19/19/DOC/Larmor4.doc, 2006.

308. Royer D., Dieulesaint E. Elastic Waves in Solids I: Free and Guided Propagation. Springer, Berlin, 2000.

309. Rugiero M. L., Tartaglia A. Einstein-Cartan theory as a theory of defects in space-time. arXiv: gr-qc/0306029.

310. Sabbata V. de, Sivaram C. Spin and Torsion in Gravitation. World Scientific, Singapore, 1994.

311. Sadd M. H. Elasticity: Theory, Aplications, and Numerics. Elsevier Butterworth-Heinemann, Burlington, MA, 2005.

312. Sakharov A. D. Vacuum Quantum Fluctuations in Curved Space and the Theory of Gravitation. *Soviet Physics–Doklady*, 1968, vol. 12, 1040–1041.

313. Sartori L. Understanding Relativity: A Simplified Approach to Einstein's Theories. University of California Press, Berkley, 1996, pp. 151–201.

314. Saunders, S. and Brown, H. R., eds. The Philosophy of Vacuum. Clarendon Press, Oxford, 2002.

315. Schrödinger E. Die gegenwaertige Situation in der Quantenmechanik. *Die Naturwissenschaften*, 1935, v. 23, 807; Discussion of probability relations between separated systems. *Proc. Cambridge Philos. Soc.*, 1935, v. 32, 446.

316. Schrödinger E. Space-Time Structure. Cambridge University Press, Cambridge, (1950) 1985.

317. Schürmann T. and Hoffman I. A closer look at the uncertainty relation of position and momentum. *Found. of Phys.*, 2009, v. 39, 958–63.

318. Schweber S. S. An Introduction to Relativistic Quantum Field Theory. Dover Publications, Mineola, NY, (1962), 2005, pp. 510–511.

319. Schwinger, J., ed. Selected Papers on Quantum Electrodynamics. Dover Publications, New York, 1958.

320. Segel L. A. Mathematics Applied to Continuum Mechanics. Dover Publications, New York, 1987.

321. Selleri F., ed. Quantum Mechanics Versus Local Realism: The Einstein-Podolsky-Rosen Paradox. Plenum, New York, 1988.

322. Selleri F. Quantum Paradoxes and Physical Reality. Kluwer Academic Publishers, Dordrecht, 1990.

323. Selleri F., ed. Wave-Particle Duality. Plenum, New York, 1992.

324. Shahverdiyev S. S. Unification of Electromagnetism and Gravitation in the Framework of General Geometry. arXiv: gen-ph/0507034v1.

325. Sidharth B. G. The Unification of Electromagnetism and Gravitation in the Context of Quantized Fractal Space Time. arXiv: gen-ph/0007021v1.

326. Simmons J. A. and de Wit R., Bullough R, eds. Fundamental Aspects of Dislocation Theory, Conference Proceedings, National Bureau of Standards, April 21-25, 1969. National Bureau of Standards, Special Publication 317, Volume I, Washington, DC, 1970.

327. Simmons J. A. and de Wit R., Bullough R, eds. Fundamental Aspects of Dislocation Theory, Conference Proceedings, National Bureau of Standards, April 21-25, 1969. National Bureau of Standards, Special Publication 317, Volume II, Washington, DC, 1970.

328. Sipe J. E. Photon Wave Functions. *Phys. Rev. A*, 1995, v. 52, 1875–1883.

329. Sklar L. Space, Time, and Spacetime. University of California Press, Berkeley, 1977.

330. Sklar L. Philosophy and Spacetime Physics. University of California Press, Berkeley, 1985.

331. Steeds J. W. Introduction to Anisotropic Elasticity Theory of Dislocations. Clarendon Press, Oxford, 1973.

332. Stone A. D. Einstein and the Quantum: The Quest of the Valiant Swabian. Princeton University Press, Princeton, 2013.

333. Stone M. The Physics of Quantum Fields. Springer-Verlag, New York, 2000.

334. Straumann N. Proof of a decomposition theorem for symmetric tensors on spaces with constant curvature. arXiv: gr-qc/0805.4500v1.

335. Styer D. F., Balkin M. S., Becker K. M., Burns M. R., Dudley C. E., Forth S. T., Gaumer J. S., Kramer M. A., Oertel D. C., Park L. H., Rinkoski M. T., Smith C. T. and Wotherspoon T. D. Nine formulations of quantum mechanics. *Am. J. Phys.*, 2002, v. 70 (3), 288–297.

336. Svensson B. E. Y. Pedagogical Review of Quantum Measurement Theory with an Emphasis on Weak Measurements. *Quqnta*, 2013, vol. 2 (1), 18–49.

337. Szabados L. B. Quasi-Local Energy-Momentum and Angular Momentum in GR: A Review Article. *Living Rev. Relativity*, 2004, v. 7, 4.

338. Talpaert Y. R. Tensor Analysis and Continuum Mechanics. Kluwer Academic Publishers, Dordrecht, 2002.

339. Tamir B. and Cohen E. Introduction to Weak Measurements and Weak Values. *Quqnta*, 2013, vol. 2 (1), 7–17.

340. Tartaglia A. Defects in Four-Dimensional Continua: a Paradigm for the Expansion of the Universe? arXiv: gr-qc/0808.3216.

341. Tartaglia A. A Strained Space-time to Explain the large Scale Properties of the Universe. *International Journal of Modern Physics: Conference Series*, 2011, vol. 3, 303–311.

342. Tartaglia A., Radicella N., Sereno M. Lensing in an elastically strained space-time. *Journal of Physics: Conference Series*, 2011, 283 012037.

343. Taylor G. I. *Proc. Roy. Soc.*, 1934, v. A145, 362.

344. Taylor E. F., Wheeler J. A. Spacetime Physics: Introduction to Special Relativity, 2nd ed. Freeman, New York, 1992.

345. Teller P. An Interpretive Introduction to Quantum Field Theory. Princeton University Press, Princeton, 1995.

346. Tolman R. C. Relativity, Thermodynamics and Cosmology. Dover Publications, New York, (1934) 1987, pp. 42–58.

347. Torretti R. Relativity and Geometry. Dover Publications, New York, (1984) 1996.

348. Torretti R. The Philosophy of Physics. Cambridge University Press, Cambridge, 1999.

349. Townsend R. H. D. Stellar Astrophysics. University of Wisconsin-Madison Lecture Notes, Madison, 2008, Section 10, Radiation & Matter.

350. Trimble V. Existence and Nature of Dark Matter in the Universe. *Ann. Rev. Astron. Astrophys.*, 1987, v. 25, 425–472.

351. Truesdell C. Continuum Mechanics I – The Mechanical Foundations of Elasticity and Fluid Dynamics. Gordon and Breach Science Publishers, New York, 1966.

352. Truesdell C., ed. Continuum Mechanics II – The Rational Mechanics of Materials. Gordon and Breach Science Publishers, New York, 1965.

353. Truesdell C., ed. Continuum Mechanics III – Foundations of Elasticity Theory. Gordon and Breach Science Publishers, New York, 1965.

354. Truesdell C., ed. Continuum Mechanics IV – Problems of Non-Linear Elasticity. Gordon and Breach Science Publishers, New York, 1965.

355. Truesdell C. and Noll, W. The Non-Linear Field Theories of Mechanics, 3rd ed. Springer-Verlag, Berlin, 2004.

356. Unzicker A. Teleparallel Space-Time with Defects yields Geometrization of Electrodynamics with quantized Charges. arXiv: gr-qc/9612061.

357. Unzicker A. What can Physics learn from Continuum Mechanics?. arXiv: gr-qc/0011064.

358. Vaidman L. Weak Value and Weak Measurements. arXiv: quant-ph/0706.1348.

359. Vaidman L. Weak Value Controversy. arXiv: quant-ph/1703.08870.

360. Volterra V. Sur l'équilibre des corps élastiques multiplement connexes. *Ann. Éc. Norm. Sup.*, 1907, v. 24, 401–517.

361. von Neumann J. Mathematical Foundations of Quantum Mechanics. Princeton University Press, Princeton, (1932) 1996.

362. Wald R. M. General Relativity. The University of Chicago Press, Chicago, 1984.

363. Wanas M. I. and Ammar S. A. Space-Time Structure and Electromagnetism. arXiv: gr-qc/0505092v2.

364. Weertman J. and Weertman J. R. Elementary Dislocation Theory. Oxford University Press, Oxford, 1992.

365. Weinberg S. Gravitation and Cosmology: Principles and Applications of the General Theory of Relativity. John Wiley & Sons, New York, 1972.

366. Weingard R. Virtual Particles and the Interpretation of Quantum Field Theory. in Brown H. R. and Harré R. Philosophical Foundations of Quantum Field Theory. Clarendon Press, Oxford, 1988, pp. 43–58.

367. Weisstein E. MathWorld. http://mathworld.wolfram.com/FourierTransform.html.

368. Weisstein E. World of Physics. http://scienceworld.wolfram.com/physics/Wavenumber.html.

369. Weyl H. Space–Time–Matter. Dover Publications, New York, (1920) 1952.

370. Weyl H. Philosophy of Mathematics and Natural Science. Princeton University Press, Princeton, (1949) 2009.

371. Ciufolini I. and Wheeler J. A. Gravitation and Inertia. Princeton University Press, Princeton, NJ, 1995.

372. Whitaker A. Einstein, Bohr and the Quantum Dilemma: From Quantum Theory to Quantum Information, 2nd ed. Cambridge University Press, Cambridge, 2006.

373. Whitham G. B. Linear and Nonlinear Waves. John Wiley & Sons, New York, 1999.

374. Williams L. P. The Origins of Field Theory. University Press of America, Lanham, MD, 1980.

375. Woit P. Not Even Wrong; The Failure of String Theory and the Search for Unity in Physical Law. Basic Books, NewYork, 2006.

376. Wolfram Mathematica Online Integrator. integrals.wolfram.com, June 2015.

377. Wolfram MathWorld Polylogarithm. mathworld.wolfram.com/Polylogarithm.html, June 2015.

378. Woodside D. A. Uniqueness theorems for classical four-vector fields in Euclidean and Minkowski spaces. *Journal of Mathematical Physics*, 1999, vol. 40, 4911—4943.

379. Wu N. Unification of Electromagnetic Interactions and Gravitational Interactions. arXiv: hep-th/0211155v1.

380. Xiao S. M., Herbst T., Scheldt T., Wang D., Kropatschek S., Naylor W., Wittmann B., Mech A., Kofler J., Anisimova E., Makarov V., Jennewein Y., Ursin R and Zeilinger A. Quantum teleportation over 143 kilometres using active feed-forward. *Nature Letters*, 2012, v. 489, 269–73.

381. Zhao H. L. On Bell's Joint Probability Distribution Assumption and Proposed Experiments of Quantum Measurement. arXiv: physics.gen-ph/0906.0279v4.

382. Ziman J. M. Principles of the Theory of Solids, 2nd ed. Cambridge University Press, Cambridge, 1979.

383. Zubov L. M. Nonlinear Theory of Dislocations and Disclinations in Elastic Bodies. Springer-Verlag, Berlin, 1997.

Index

About the Author

Pierre A. Millette did his graduate studies on atomic physics and astrophysics research of stellar atmospheres at the Department of Physics of the University of Ottawa under Dr. Yatendra P. Varshni, a prominent physicist in atomic physics (the Varshni potential functions) and the physics of Quasi-Stellar Objects (the Plasma Laser Star model), and an accomplished philosopher and historian of science. Pierre Millette subsequently worked in geophysics and in the high-technology sector in communication systems (optical networks and SATCOM), while pursuing an independent research program on the Elastodynamics of the Spacetime Continuum (STCED). He has published more than 20 scientific publications on atomic physics, stellar astrophysics, the foundation of quantum mechanics, special and general relativity, and STCED. In 2013, he joined the editorial board of the American journal of physics, *Progress in Physics*. He is currently continuing his scientific research work as an independent researcher.

Elastodynamics of the Spacetime Continuum

A Spacetime Physics Theory of Gravitation, Electromagnetism and Quantum Physics

by Pierre A. Millette

This book lays the foundations of a new theory of spacetime physics. STCED (Spacetime Continuum Elastodynamics) is a natural extension of Einstein's Theory of General Relativity. Whereas General Relativity concentrates on the curvature of the spacetime continuum, STCED analyses the deformations of the spacetime continuum resulting in its curvature. This gives rise to an integrated theory of gravitation and electromagnetism. At the microscopic level, STCED leads to the analysis of defects in the spacetime continuum, which gives rise to quantum physics. STCED is thus found to be a spacetime physics theory of gravitation, electromagnetism and quantum physics. This book lays the theoretical foundations of the Elastodynamics of the Spacetime Continuum, allowing physicists to study and perform research in this new area of spacetime physics.

ISBN 978-1-59973-987-8
American Research Press
Printed in the USA